GARTEUR GROUP FOR AERONAUTICAL RESEARCH AND TECHNOLOGY IN EUROPE

FRANCE· GERMANY· THE NETHERLANDS· SPAIN · SWEDEN· UNITED KINGDOM

GARTEUR TP 115

ORIGINAL : ENGLISH

GARTEUR SM/AG19 TP115

APRIL 1999

GARTEUR LIMITED

GROUND VIBRATION TEST TECHNIQUES

compiled by

A. Gravelle (ONERA, Châtillon)

GARTEUR aims at stimulating and co-ordinating co-operation between Research Establishments, Industry and Academia in the areas of Aerodynamics, Flight Mechanics, Helicopters, Structure & Material and Propulsion Technology.

DISTRIBUTION

Executive Committee

Mrs D Nouailhas
ONERA BP 72
29, avenue de la Division Leclerc,
F-92322 Châtillon CEDEX, France

Mr P Garcia Samitier
INTA
Carretera de Ajalvir km 4
E-28850 Torrejón de Ardoz
Madrid, Spain

Mr A Gustafsson
FFA
Box 11021
S - 161 11 BROMMA, Stockholm, Sweden

Dr D E Mowbray
Assistant Director Civil & International Programmes
A8 Building, Room 1005
DERA Farnborough
Hampshire GU14 0LX

Prof. Ir. J.W. Sloof
NLR
PO Box 90502
NL - 1006 BM Amsterdam, Netherlands

Dr R. Haupt
DLR/PD-L
D - 51170 Köln

GARTEUR Secretary

Dr O K Sodha (Secretary)
Manager Civil & International Programmes
A8 Building, Room 1005
DERA Farnborough
Hampshire GU14 0LX

Structures & Materials Group of Responsables

Dr H Ansell
Saab AB
Future Products and Technology
S - 58188 Linköping

Dr A Blom
FFA
Box 11021
S - 161 11 BROMMA

Dr-Ing. Bühlmeier
Daimler Benz Aerospace AG
Dornier Luftfarht GmbH
Postfach 1103
D - 82230 Wessling

Prof. P. Curtis
DRA Farnborough
Structural Materials Centre
Farnborough
UK - Hants GU14 6TD

Ir. F. Holwerda
Head Structures & Materials Division
NLR
PO Box 153
NL - 8300 AD Emmeloord

Mr T. Khan
ONERA BP 72
29, avenue de la Division Leclerc
F-92322 Châtillon CEDEX, France

Dr. R Ohayon
ONERA BP 72
29, avenue de la Division Leclerc
F-92322 Châtillon CEDEX, France

Mr H Price
Bae Airbus Ltd
Chester Road
Woodford
UK - Cheshire SK7 1QR

Dr K. Rohwer
DLR
Inst. Für Strukturmechanik
Postfach 3267
D - 38022 Braunschweig

M. E. van Teeseling
Fokker Services BV
Dept Engineering/TE
MS/S S055-11
PO Box 75047
NL - 1117 ZN Schiphol

Mr B Palmberg (Secretary)
FFA
Box 11021
S - 161 11 BROMMA

Action Group

Dr T. Abrahamson
Saab Scania AB
Structural Dynamics Dpt
S-581 88 Linköping

Mr L.P. Bugeat
Intespace
B.P. 4356
F -31029 Toulouse cedex

Dr J. Cooper
Manchester University
Engineering Dpt, Simon Bldg.
Manchester, M13 9PL - Grande-Bretagne

Mr M. Degener
DLR
Bunsenstrasse 10
D - 37073 Gottingen

M. J.P. Esauerre
Aérospatiale A/DET-EG-ST
316, route de Bayonne,
F - 31060 Toulouse Cedex 03

M. A. Gravelle
ONERA - DDSS
B.P.72
F - 92322 Châtillon Cedex

Mme N. Henriet
CNAM - Chaire de Mécanique
LMSS
2, rue Conté,
F - 75003 Paris

M. R. Lemonde
SOPEMEA
BP 48
F - 78142 Vélizy Cedex

Mr A.J. Persoon
NLR AE
PO Box 90502
NL - 1006 BM Amsterdam

Dr A. Robb
Imperial College
Mechanical Engineering Dpt.
Exhibition Road
UK - London SW7 2BX

Dr G.W. Skingle
DRA
Materials and Structures Dpt.
Farnborough
UK - Hampshire - GU14 6TD

CONTENTS

1 INTRODUCTION

Within the frame of the aircraft certification, the Ground Vibration Tests (GVTs) play an important role in order to validate or to update the structural dynamic numerical model of the airplanes which are necessary to insure the aeroelastic stability facing the flutter risks.
The GVTs consist in performing the identification of the structure modal parameters according to the different vibration modes, i.e. eigen frequencies, mode shapes and modal masses. Additionnally the damping factors are also estimated.The objectives of the GARTEUR Action Group SM-AG19 were to have comparative tests on a same testbed performed by different european laboratories in order to evaluate the efficiency of different test methods as well as parameter identification methods.
A similar round robin had been realised in the late 70's, beginning of the 80's by a previous european group [1],[2] showing rather large discrepancies in the measurement results by themselves as well as in the modal identification results.
A part of the experience accumulated in this occasion was used in order to avoid the major difficulties of the exercise such as to insure a correct reliability of the test structure along the whole exercise time.
The main features to be evaluated through this activity were, as described in Annex 1 (Proposal for the formation of a GARTEUR Action Group on Ground Vibration Test Techniques) :
- the effect of different test methods (number and location of exciters, nature of excitation signals, measuring instrumentation),
- the effect of using different parameter identification methods (phase resonance or different phase separation methods).

2 TEST ARTICLE

The test article was designed and manufactured by Onera after having been approved by the whole AG19 group. It was a rather simple structure which was for a few points dynamically representative of an airplane structure. It was composed of several beams simulating a fuselage with wings and tail. Wing tip drums allowed to adjust bending and torsion frequencies similarly to airplane ones, with some very close modal frequencies.
The overall dimensions were relatively small, within 2 meters by 2 meters, in order to be easily moved around the test facilities of all the participants. Special attention had been paid to the connection between the removable parts in order to get the best repeatability of the structural characteristics.
The documentation note for the testbed is given in Annex 2, section 5 of which showing detailed geometrical characteristics.

3 TEST SET UP VALIDATION

After the final adjustments done at Onera,the whole test set up was validated by means of a first Ground Vibration Test performed by SOPEMEA. SOPEMEA had to provide all the participants with a reference set of data consisting in a 2x2 matrix of transfer functions between vertical excitations and responses at the two wing tips.
The test procedure as well as the transfer function results and the modal results from these validation tests are given in Annex 3.

A special test was also asked to all the participants. This test consisted in verifying the eigen frequency and the damping ratio of the rotation mode of the fuselage so-called hereafter the reference mode. As a matter of fact, those modal parameters were the most influenced by the connection conditions between the wings and the fuselage, so that a good correlation on them gives a warranty of a good test article assembly.

4 TEST RESULTS AND COMPARISONS

4.1 Test results

The tests were successfully performed by all the participants according to an actual time schedule (from april 1995 to june 1996), very close to the planned one (from april 1995 to march 1996). After the first test performed by SOPEMEA in april, 1995, the following ones took place.

The NLR tests conducted in cooperation with Fokker Aircraft B.V. were realised in may, 1995. The results given in Annex 4 showed a very good agreement between SOPEMEA measurements, some previous Onera measurements and the NLR ones, as far as the reference transfer functions (2 by 2 matrix at the wing tip drums) and the reference mode were concerned.

The DLR tests were performed in june, 1995. Both phase resonance and phase separation methods were applied at the DLR vibration test facility. The test conditions and the main test results as well as comparisons with the other participants are given in Annex 15.

The tests at Imperial College were carried out in august, 1995. The results, given in Annex 5 (full contribution), show significant differences with those of the previous participants, due to differences in the test set up (shakers configuration, drum tip mass, suspension).

Then tests were performed successively by DRA and Manchester University in the DRA facilities at Farnborough in october, 1995, using the same suspension conditions. The results, given in Annex 6 for DRA (without appendices) and 7 for Manchester University were in a reasonable agreement with those obtained by SOPEMEA.

The results of the tests performed by Onera in november 1995 are the subject of Annex 8, by Aerospatiale in january1996 of Annex 9, by SAAB in february of Annex 10, by CNAM in march 1996 of Annex 11 and by Intespace in june 1996 of Annex 12.

4.2 Comparisons

a) Reference mode frequency and damping

Participant	Sopemea	NLR	DLR	Imp. Colleg.	DRA	Manch Un.
Frequency	16.08	16.14	16.10	16.21	16.45	16.40
Damping %	1.36	1.54	1.30	2.66	1.14	1.28

Participant	Onera	Aerosp.	SAAB	CNAM	Intespace
Frequency	16.25	16.00	16.33	16.16	16.30
Damping %	1.18	1.34	1.38	1.42	1.15

The scattering on the resonance frequency is within +-1.4 %.while the damping was measured between 1.14% and 1.54% except for one participant. This low scattering reveals that the fuselage

rotation mode, choosen as a reference mode, which is representative of the test bed assembly, seems quite independent of the suspension conditions.

b) Reference transfer functions

The reference transfer functions at the wing tips compare fairly well as shown on figure 6 of Annex 13, except for participants B (NLR), D (Imperial College) and J (CNAM) due to unappropriate drum tip masses, and H (Aerospatiale) due to some measurement difficulty.

c) Modal parameters

The comparisons between the modal parameters, as far as the modal frequencies, the modal damping ratios, the mode shapes were concerned are given for the three critically close modes on figure 11, Annex 13. The modal frequencies values are very close for the first two modes, particularly if participants B, D, J and K (Intespace) are excepted. The scattering is higher for the third mode frequency and reaches +- 20 % for the damping ratios. The mode shape shown as Modal Assurance Criterium (MAC) compare very well except for participant B.

Generally speaking, the scattering on the modal frequencies is in the range +- 2% while values close to +- 20% are observed for the damping ratios of all the identified modes, as shown on figure 10, Annex 13. The largest variations in the modal frequency parameter seem to be due to differences in the suspension system, some of the participants having connected directly the bungees suspension provided with the testbed to a rigid frame while most of the other ones used an additionnal pendulum system with different lengths.

The modeshapes compare very well in most of the cases, as demonstrated by the very good values of the Modal Assurance Criterium given figure 12, Annex 13, by reference to participant C (DLR).

The table 3 of Annex 13 gives the variation, in %, of the modal masses as well as of the damping coefficients for the participants A (Sopemea), E (Manchester University), F (DRA) and G (Onera), by reference again to participant C. In most of the cases, the modal mass variations are much lower than the damping coefficient variations.

Some other comparisons concerning the modeshapes and the generalised masses values are shown in Annexes 14 and 15.

d) Comparison between the 2 Onera tests

A last test were performed by Onera after the completion of the tests by all the participants in order to check the reliability of the structural characteristics of the testbed. The comparison of the results of this test and the previous Onera test, given on figure 6, shows a very good consistancy in the dynamic behaviour of the testbed, as far as the wing tip transfer function were concerned.

5 CONCLUSIONS

The present exercise showed the results which can be obtained using up-to-date vibration test methods on a "similar to airplane" but relatively simple structure.
The frequency response measurement results show a must better consistency between the participants than the ones obtained in the previous similar exercise, beginning of the 80's.

The repeatability of the tests, although the necessity to disassemble and reassemble the testbed at each step of the round robin, was checked and satisfactorily demonstrated.

Although the methods as well as the test conditions (shakers location and number, measurement pick-ups, suspension frame...) were different, the modal frequencies identification results compare reasonably well as far as the correct mass configuration was respected. Nevertheless some suspension effect (suspension modes) due to the pendulum length seems to alter some of the modes.
Larger discrepancies, as far as generalised masses and especially damping ratio are concerned, remain.
The phase resonance methods and phase separation methods used both by several of the participants and for different excitation configurations led to very similar modal identification.

The structure under test was representative of a real aircraft structure, having airplane type mode shapes, very coupled low frequency modes and relatively high damping coefficients. However this structure was simpler than an airplane and didn't present the same level of non-linearity. Higher discrepancies would be expected between the different kind of methods (phase separation and phae resonance methods) as well as between different excitation configurations in case of realistic non-linearities.
For those reasons, it appears that, in the case of actual aircraft Ground Vibration Tests, great attention must always be paid to the test conditions. The use of the phase resonance method remains necessary in order to identify, at least, difficult modes, as far as non-linearity and/or very close coupling are present. Phase separation methods may be used in the context of a faster GVT process to identify more isolated or linear modes.
For the case of distributed non-linearities, phase separation methods are still in development, some of them using stochastic approach. Such methods will have to be tested on complex structures in the near future. They should be efficient particularly in the case of slightly non-linear, strongly coupled modes.

6 BIBLIOGRAPHY

[1] Ewins, D.J.Griffin, J., "A State of the Art Assesment of Mobility Measurement Techniques - Results for the mid-range structures (30-3000 HZ)", JSV, 1981, 78-2, pp. 197-222.

[2] Ewins, D.J., "State of the Art Assessment of Mobility Measurement Techniques (SAMM) - Summary of results", SEE Journal, march 1981.

[3] Balmès, E., "GARTEUR group on ground vibration testing. Results from the test of a single structure by 12 laboratories in Europe", IMAC, Orlando, FL, february 3-6,1997.

[4] Persoon, A.J., Balmès, E., "A ground vibration test on the GARTEUR SM AG-19", IMAC, Tokyo, Japan, september 1-4, 1997.

[5] Degener M., "Ground Vibration Tests on an aircraft model performed as part of a Eropean round robin exercise", International Forum on Aeroelasticity and Structural Dynamics, Roma, Italy, july 1997.

Annex 1

PROPOSAL FOR THE FORMATION OF A GARTEUR ACTION GROUP ON GROUND VIBRATION TEST TECHNIQUES

GARTEUR - SM-EG 20

PROPOSAL FOR THE FORMATION OF A GARTEUR ACTION GROUP ON GROUND VIBRATION TEST TECHNIQUES

1 INTRODUCTION

Within the frame of certification procedure, aircraft manufacturers have to prove for each new airplane, or each significant structural modification of an airplane, the aeroelastic stability in an extended flight domain. For that purpose, different possible mixtures of numerical and experimental methods are used: structural dynamics calculation by means of finite element methods, Ground Vibration Test (GVT), unsteady aerodynamics computation and measurement in windtunnel, flutter calculation, flight vibration test. The gathering of results issued from these different methods allows to comply with regulations.

GVTs play a key role in the certification process by allowing flutter predictions based on the experimental modal basis and/or allowing a verification and update of analytical structural models. Since, facing the flutter risk, the highest level of security and reliability has to be achieved, the quality of GVT results is very important.

The phase resonance method is generally used to perform GVTs. Phase separation techniques have proved to be convenient for identification of smaller structures, and the manufacturers and institutes performing aircraft GVTs are trying to use them on large aircraft coupled or not with the phase resonance methods. The proposed GARTEUR activity, issued from the work of the SM-EG20 exploratory group, deals with the identification methods by themselves as well as their implementation during the Ground Vibration Tests.

2 OBJECTIVES

Within the proposed GARTEUR Action Group, it is expected to make comparative tests on a common testbed by means of different GVT methods.

The main objectives of these comparative tests are:

- to evaluate the efficiency and the reliability of different test methods: i.e. to evaluate the effect of using different excitation signals (broadband or sinusoidal), different excitation points (phase resonance or phase separation),
- to evaluate the efficiency and the reliability of different phase separation methods: i.e. to compare the modal parameters issued from different identification methods (time or frequency domain) applied to a same set of measured data,
- to evaluate and analyse the discrepancies between the modal parameters estimated by means of different test set-ups and analysis methods.

A critical review of the different test and analysis methods, more than the selection of the "best" method, is to be performed. The aim will be to define the application field of each one, and evaluate both the accuracy of results and the easiness of implementation.

3 STATEMENT OF ACTIVITIES

The activities described below in more details are proposed for this future Action Group.

Design and construction of a common testbed

It is necessary to design and manufacture a test article which will be representative of aircraft structures. This test article must also be easily moved around the test facilities of the different participants and ensure a perfect structural repeatability.

For that purposes, the following design requirements are proposed:

- general shape: beams assembly representing a fuselage with wings and tail,
- dimensions of 2 by 2 meters and mass in the 50 to 100 kg range
- frequency range 5 to 50 Hz
- joints: only the wing to fuselage joint will be removable; the repeatability after assembly-disassembly has to be proved
- damping treatment by means of constrained viscoelastic layers in order to get damping coefficients as high as those encountered on aircraft
- non linearity: no specific non linear elements, this could be the object of possible further activity
- very low frequency (under 1 Hz) suspension as a part of the testbed in order to eliminate the surroundings effect
- vibration modes constraint: the testbed has to present at least 3 modes within 1 Hz frequency band in order to simulate the difficulty encountered on aircraft.

Construction of a data base of results

A common data base has to be constituted in order to know the structural design and to be able to make comparative analysis using different methods on the same measurement set. This common data base must contain:

- analytical modeling results (frequencies, modeshapes)
- Multi Input Multi Output (MIMO) frequency responses for a 2 points excitation configuration (wing tips) by means of different excitation signals: sinusoidal, broadband...

Furthermore, a full set of time and frequency domain measurements will be available for participants to test their own analysis method to unique measurement results. The modal parameters: frequency, damping ratio, modeshape and modal mass, can be identified and compared.

GVTs of the testbed

A GVT will have to be performed by each participant in his own test facility and using his own instrumentation. A common set of results to be obtained by all will be defined and distributed in a common test plan. It will include:

- measurement of a selected set of frequency responses functions (2x2 matrix),
- identification of the modal parameters: frequency,

damping ratio,
mode shape,
modal mass,

in the 5 - 50 Hz frequency range.

Analysis of the results

The results obtained by all the participants will be gathered and compared. The analysis of their scattering will be conducted according to the test or analysis method used.

4 COMMITMENTS

The different contributions of research institutes and industrial partners are listed in the following table, on the basis of a 2 years duration (commitments for the whole period):

	manpower (menmonths)	expenses (kEcu)
Aérospatiale	2	
CNAM	2	
DLR	6	10
DRA	1	
FOKKER	4	
Imperial College	1	
Intespace	2 - 3	
Manchester University	1	
NLR	4	
ONERA	6	10
SAAB	1 - 2	
SOPEMEA	2 - 3	

5 DISTRIBUTION OF TASKS

The involvement of the partners in the different tasks will be as following:

- design and construction of the testbed: ONERA
- qualification tests SOPEMEA
- construction of a data base of results MANCHESTER and/or ONERA
- analysis of the common data base ALL
- GVT of the testbed ALL
- analysis of the results ALL

6 MEMBERSHIP AND MANAGEMENT

The representatives of the different research institutes and industries are listed in the following table:

Dr Jonathan E. COOPER Manchester University Engineering Dpt., Simon Bldg. Manchester, M13 9PL Grande Bretagne Phone: (44) 61 275 4337 Fax: (44) 61 275 3844 E-mail:	Jean Paul ESQUERRE Aérospatiale A/DET-EG-ST 316 route de Bayonne 31060 TOULOUSE Cedex 03 France Phone: (33) 61 93 84 64 Fax: (33) 61 93 52 92 E-mail:	Manfred DEGENER DLR Bunsenstrasse 10 37073 GOTTINGEN Allemagne Phone: (49) 551 709 2349 Fax: (49) 551 709 2862 E-mail:
Peter SCHIPPERS Fokker Aircraft BV Dpt. EDAA S029-32 PO Box 7600 NL 1117 ZJ SCHIPHOL Pays Bas Phone: (31) 20 605 2187 Fax: (31) 20 605 4780 E-mail:	Graham W. SKINGLE DRA Materials and Structures Dpt. Farnborough Hampshire GU14 6TD Grande Bretagne Phone: (44) 25 239 5629 Fax: (44) 25 237 6372 E-mail:	Thomas ABRAHAMSON Saab Scania AB Structural Dynamics Dpt S-581 88 LINKOPING Suède Phone: (46) 13 185 429 Fax: (46) 13 181 802 E-mail: thoab@weald.air.saab.se
Alain GRAVELLE ONERA OR B.P. 72 92322 Chatillon Cedex France Phone: (33) 1 46 73 46 49 Fax: (33) 1 46 73 41 43 E-mail: gravelle@onera.fr	Robert LEMONDE SOPEMEA BP 48 78142 Vélizy Cédex France Phone: (33) 1 46 30 22 74 Fax: (33) 1 46 30 54 06 E-mail:	Albert J. PERSOON NLR AE PO Box 90502 1006 BM AMSTERDAM Pays-Bas Phone: (31) 20 511 3448 Fax: (31) 20 511 3210 E-mail:
A. ROBB Imperial College Mechanical Engineering Dpt. Exhibition Road LONDON SW7 2BX Grande Bretagne Phone: (44) 71 594 7072 Fax: (44) 71 584 1560 E-mail: d.ewins@ic.ac.uk	L.P. BUGEAT Intespace B.P. 4356 31029 Toulouse Cedex France Phone: (33) 61 28 12 65 Fax: (33) 61 28 11 12 E-mail:	Nicole HENRIET CNAM Chaire de Mécanique LMSS 2 rue Conté 75003 Paris France Phone: (33) 1 40 27 26 42 Fax: (33) 1 40 27 27 16 E-mail:

Mr. Alain Gravelle from ONERA is prepared to assume the chairmanship while Mr. Albert J. Persoon of NLR will accept the vice-chairmanship.

Dr. Roger Ohayon will act as Monitoring Responsable.

7 TIME SCHEDULE

The proposed activity can be performed according to the following time schedule:

Task	1995	1996
testbed design	—	
testbed construction	——	
qualification	—	
data base constr.	—	
data base analysis	———	
GVTs	———	———
results analysis		———

8 REPORTING PUBLICATIONS

Progress reports will be produced for the GoR meetings. The final report will be edited by the chairman. The classification of the final report will be "GARTEUR open".
Members will be free to report their own work in accordance with their national and company policies.

9 SECURITY AND INTELLECTUAL PROPERTY RIGHTS

Background and foreground information will be treated according to Appendix A to MoU: Rules for the Protection and Use of Intellectual Property in GARTEUR Co-operation.

Table of contents

3 Checkup

3.1 SUMMARY

This section gives a summary of the operations that you should perform. Please make sure that you do perform all of them.

- ❑ Call the person who will be testing when you are done and arrange for shipping of the testbed.
- ❑ Before you send the testbed to the next participant grease the connection plates and check the packing list.

- ❑ Degrease the connection plates, assemble wing and fuselage, and apply specified torque to connection screws.
- ❑ Suspend the structure as shown in figure 1 and record length of suspension assembly.
- ❑ Place the 24 common accelerometers at the specified locations.
- ❑ Log accelerometer characteristics.
- ❑ Machine and attach complement masses for the drum tip shakers and take a picture of the drum tips.
- ❑ Log shaker characteristics.
- ❑ Check the fuselage rotation mode at 16.06 Hz (mode 2 at 13.16 Hz of the design FE model). Log frequency and damping and send it to ONERA rapidly so that we can track changes.
- ❑ Take pictures or film your set up (see details in section 3.6).
- ❑ Measure the four common FRFs (to/from drum tips).
- ❑ If practical, keep the time signals used for the generation of the 4 transfer functions provided above.
- ❑ Measure modes in the 4 to 65 Hz range. Provide shape, frequency, damping, and generalized mass.

These last points should be done after your testing period in preparation for the discussion that we will have after everybody has finished testing.

- ❑ Indicate how to reconstruct the FRFs based on the modes provided.
- ❑ Write a comparison of your results with the reference set given by SOPEMEA.
- ❑ Send your results to ONERA so that we can update the global comparison.

3.2 PACKING LIST

❑ The testbed box comes with a number of elements. Before you send the testbed to the next participant check the packing list.

- 1wing assembly
- 1 fuselage/tail assembly
- 4 wing/fuselage connection screws, 2 bolts and 2 hooks.
- 2 reference complement masses with 2 screws, 2 bolts, 2 washers (total of 200g each). These masses should be used for hammer testing.
- 1 suspension connection piece (one hook for user, three hooks for bungee cords)
- 1 set of 3 bungee cords (a new set will be send to each participant)
- 1 copy of the test documentation (this document)

3.3 SETTING UP THE TESTBED

The testbed comes in two pieces (wing/drum and fuselage/tail). The connection is done through two black steel plates centered by two pins and a four screws (for a figure of the assembly see section 5.1). The two front nuts are standard, the two back nuts are hooks used to attach the suspension bungee cords.

❑ Degrease the two steel connection plates before the assembly and regrease them before you send the testbed to the next participant.

❑ The four connection screws should be loaded with a torque of 1.6 m/kg. Do not use a higher value

❑ Suspend the structure as shown in figure 1. Please make sure that you do suspend the testbed as shown and record the length of the resulting pendulum.

Initial tests have shown that you are quite likely to find suspension modes (translations of the attachment hook, etc.). Please make sure that these modes do not perturb you measurements of structural modes too much. As a safety check you are encouraged to place sensors on the suspension.

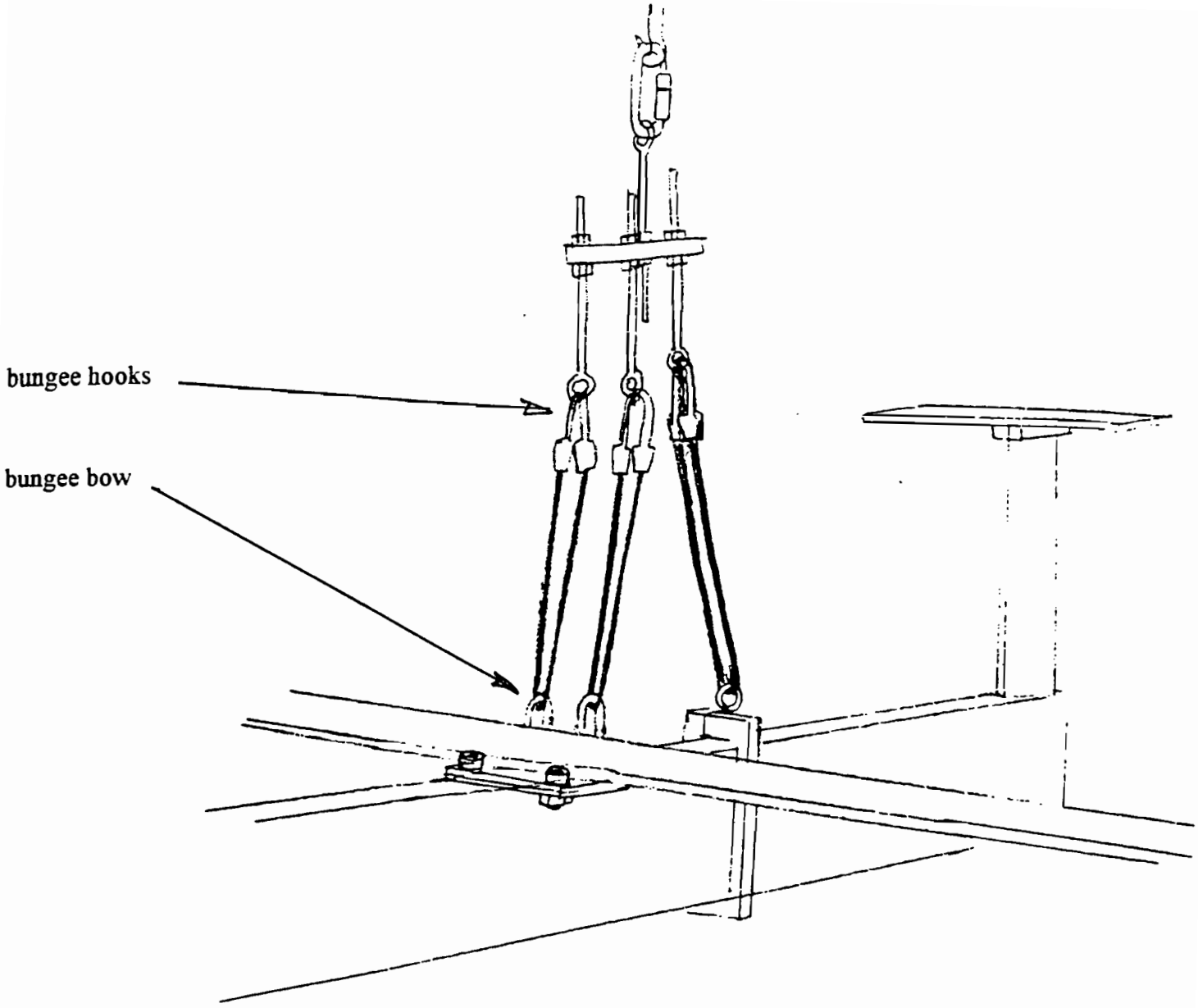

Figure 1: Suspension setup. The three bungees are identical. The hooks are connected to the suspension connection piece. The rear bungee is more stretched than the others.

3.4 DETAILS OF THE EXPERIMENTAL SETUP

All participants should provide results at 24 common accelerometer locations shown below (see also the geometry section 5.1). On the structure, a point marks the exact location of the 24 common accelerometers and a sticker recalls the identifiers used in figure 2. You may add any number of accelerometers (and you are encourage to place two of them on the suspension) but comparisons will be made on the basis of these accelerometers only.

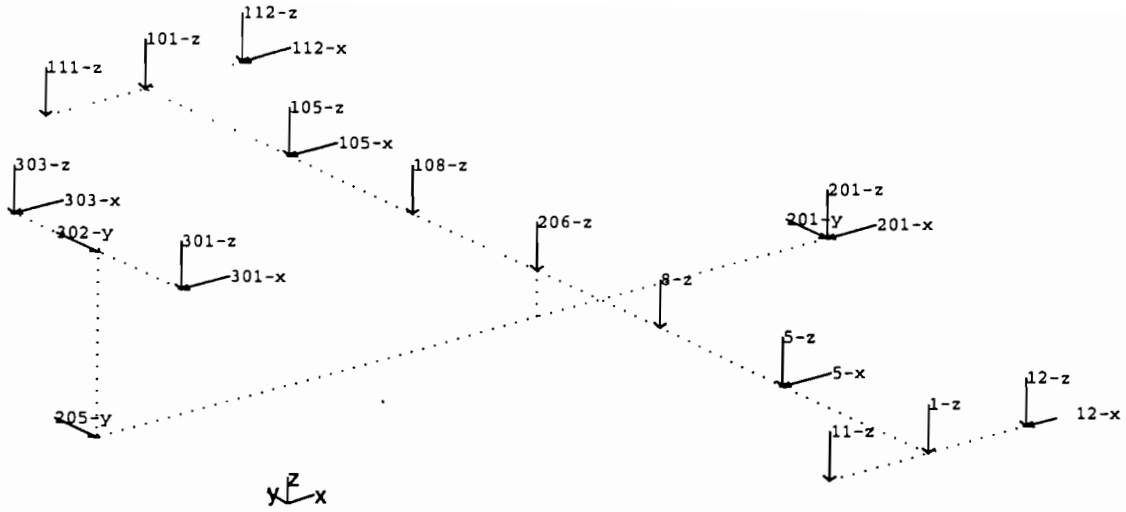

Figure 2: Locations and directions of the 24 common accelerometers. See the marks on the structure and blueprints for mode details.

❑ At this point you should log the properties of your accelerometers

Accelerometers, Type, Weight

❑ At this point you should log the properties of your shakers

Excitation, Type, Weight and stiffness of moving part

❑ Machine and attach complement masses for the drum tip shakers and take a picture of the drum tips.

Only two common shaker locations at the drum front tips are required for the common measurement of FRFs. The sensitivity of the wing torsion modes to the moving mass of the shaker is quite large so that you need to adjust the total mass present at the drum tips. The total of the mass added to the tips should be 200g. This total should include all masses linked to your shakers (moving mass, stinger, load cell, accelerometer, etc.) and you should manufacture a **complement mass** such that the weight of the complement mass (and screw) plus the excitation masses add up to 200g.

❑ In your answer you need to include a section on the approach you have used to measure the force input to your structure.

3.5 CHECK OF PROPER EXPERIMENTAL SETUP

As a check of your experimental setup you should verify that the frequency of the global fuselage rotation mode is found at 16.17 Hz with a damping ratio of 1.45 %. The mass normalized modeshape at the 24 reference sensors was identified at ONERA and is shown in table 1.

Table 1: Reference mass normalized modeshape results for the second flexible mode at 16.06 Hz (with 1.66% damping).

DOF	FE model	Test		FE model	Test
11-z	-1.9425e-01	-2.1084e-01	201-x	7.9818e-12	4.1935e-05
1-z	-2.0671e-01	-2.2120e-01	201-y	1.9049e-02	-4.3013e-03
12-x	1.0018e-01	6.8343e-02	201-z	-4.0715e-12	-1.4436e-03
12-z	-2.2274e-01	-2.4736e-01	206-z	-2.3427e-12	-1.9260e-03
5-x	6.2270e-02	3.8283e-02	205-y	-1.2461e-01	-8.8705e-02
5-z	2.2410e-02	8.7033e-02	302-y	4.4911e-01	4.3956e-01
8-z	1.0906e-01	1.7198e-01	301-x	1.9686e-02	7.7945e-02
111-z	1.9425e-01	1.9867e-01	301-z	3.7794e-01	3.6447e-01
101-z	2.0671e-01	2.3346e-01	303-x	-1.9686e-02	-1.7355e-02
112-x	-1.0018e-01	-3.5782e-02	303-z	-3.7794e-01	-4.3194e-01
112-z	2.2274e-01	2.4969e-01			
105-x	-6.2270e-02	-3.9193e-02			
105-z	-2.2410e-02	-8.0323e-02			
108-z	-1.0906e-01	-1.7049e-01			

Note for the mass normalized mode given here, the generalized mass at a given sensor is linked to the modeshape at this sensor $c\phi_j$ by

$$MG_{Cj} = \frac{1}{\left(c\phi_j\right)^2} \tag{1}$$

Thus the generalized mass at sensor *112 z* is 20.1 m^2Kg for the FE model and 16.0 m^2Kg for the test. If you can easily provide mass normalized modes please do so.

3.6 PICTURES

❑ Take pictures or film your set up.

To help in the comparisons, you are asked to take a number of pictures. These should at least include a global view and close-ups of the suspension, the excitation equipment at the drum tips (and elsewhere if any), the tail (showing the tail sensors).

3.7 REQUIRED MEASUREMENT OF TRANSFER FUNCTIONS

❑ Each participant is required to provide a 2 by 2 set transfer functions corresponding to excitation and response at the drum front tips (vertical excitation at nodes 12 and 112). Two of these FRFs are collocated, the other two are cross transfers.

The frequency band of interest is 4-65 Hz. The comparison will be easier if you can use 2048 frequency points evenly spaced between 4 and 65 Hz. Your answer should indicate the method used to estimate the transfer functions, the amount and type of signal processing used.

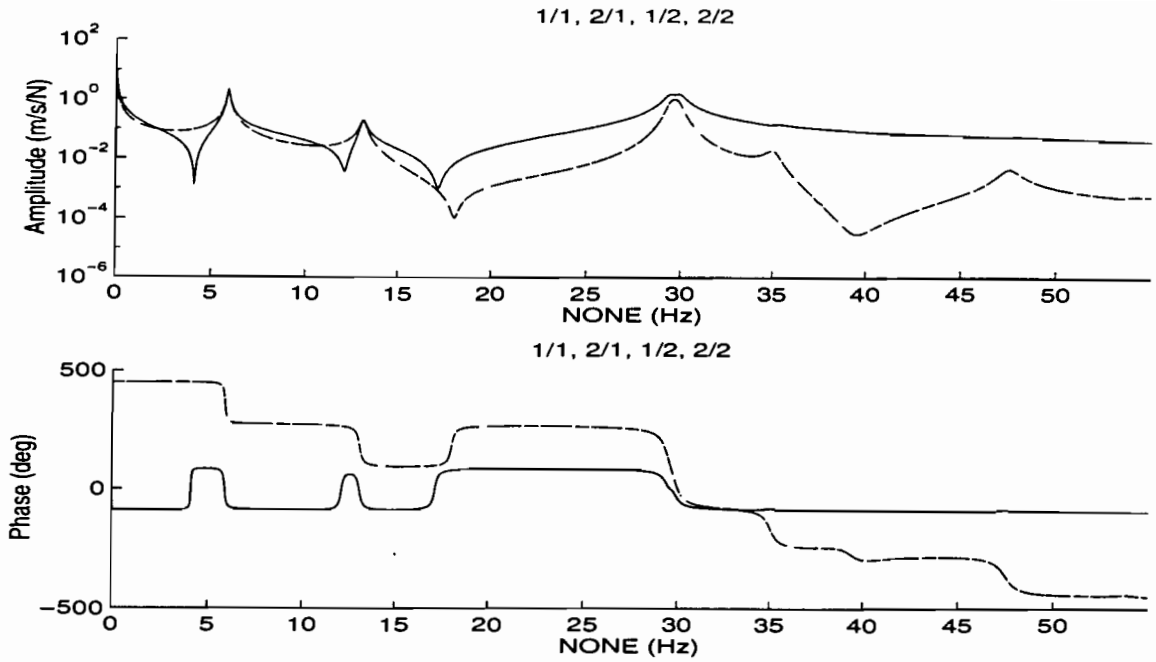

Figure 3: Typical plot of the required transfer functions. This result is based on the design FE model (initial test results look somewhat the same).

❑ If practical it may be interesting to keep the time signals used for the generation of the 4 transfer functions provided above.

3.8 REQUIRED CHARACTERIZATION OF MODES

❑ Your answer must contain estimates by one or more method of a number of modes in the 5-50 Hz range. A mode is characterized by a shape, frequency, damping ratio, and modal mass.

You are expected to provide estimates of the modes below 60 Hz (see section 6 for an initial guess of these modes based on a simple FE model). These modeshapes should be given at the 24 reference accelerometers (see figure 2 and table 1). If you can easily provide mass normalized modes please do so.

❑ If you are identifying your modes based on measured FRFs, provide an explanation on how your modes allow a reconstruction of the measured transfer functions. If residual terms and/or computational modes should be added please provide them.

3.9 COMPARISON OF YOUR RESULTS WITH THE SOPEMEA SET

Once you are done with the testing ask Etienne Balmès to send you a copy of the SOPEMEA test results, which contains

- a description of their test procedure
- the four required transfer functions (in the universal file xxx)
- the modes they have tested (in the universal file xxx)

❑ You are asked to provide a comparison of your results with those of this sample set.

Since asking everybody to do a global comparison does not seem practical, these comparisons with a sample set will provide a good idea of the approaches used to compare different test results.

4 General Information

4.1 CURRENT SCHEDULE

time	task	Participants
3/95	design/manufacturing	ONERA
4/95	testing	SOPEMEA
5/95		NLR-Fokker
6/95		DLR
7/95		
8/95	↕	Imperial College
9/95		Manchester U.
10/95		ONERA
11/95		Aérospatiale
12/95		Intespace
1/96	testing	CNAM
2/96	group meeting	All

All efforts will be made to have all the current members test by February 1996 so that we can have a meeting and start discussing results at that time. Please call ONERA if you have any problem with this schedule.

5 Testbed characteristics

5.1 GEOMETRY

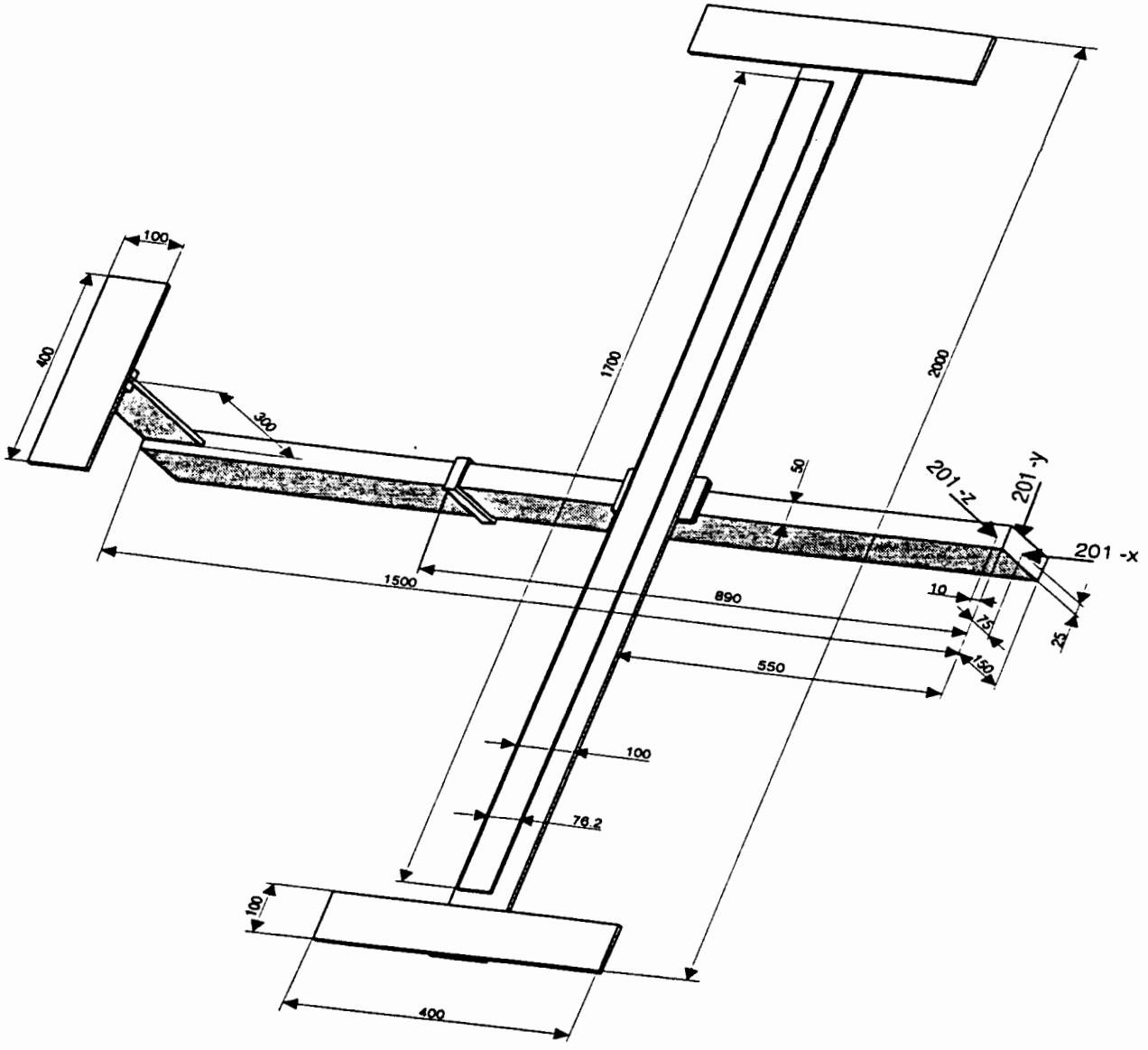

The figures (global view, left drum, left wing, and tail) given in the next pages show details on the testbed geometry and required sensor positions. If you have questions before you get the testbed please send questions to ONERA.

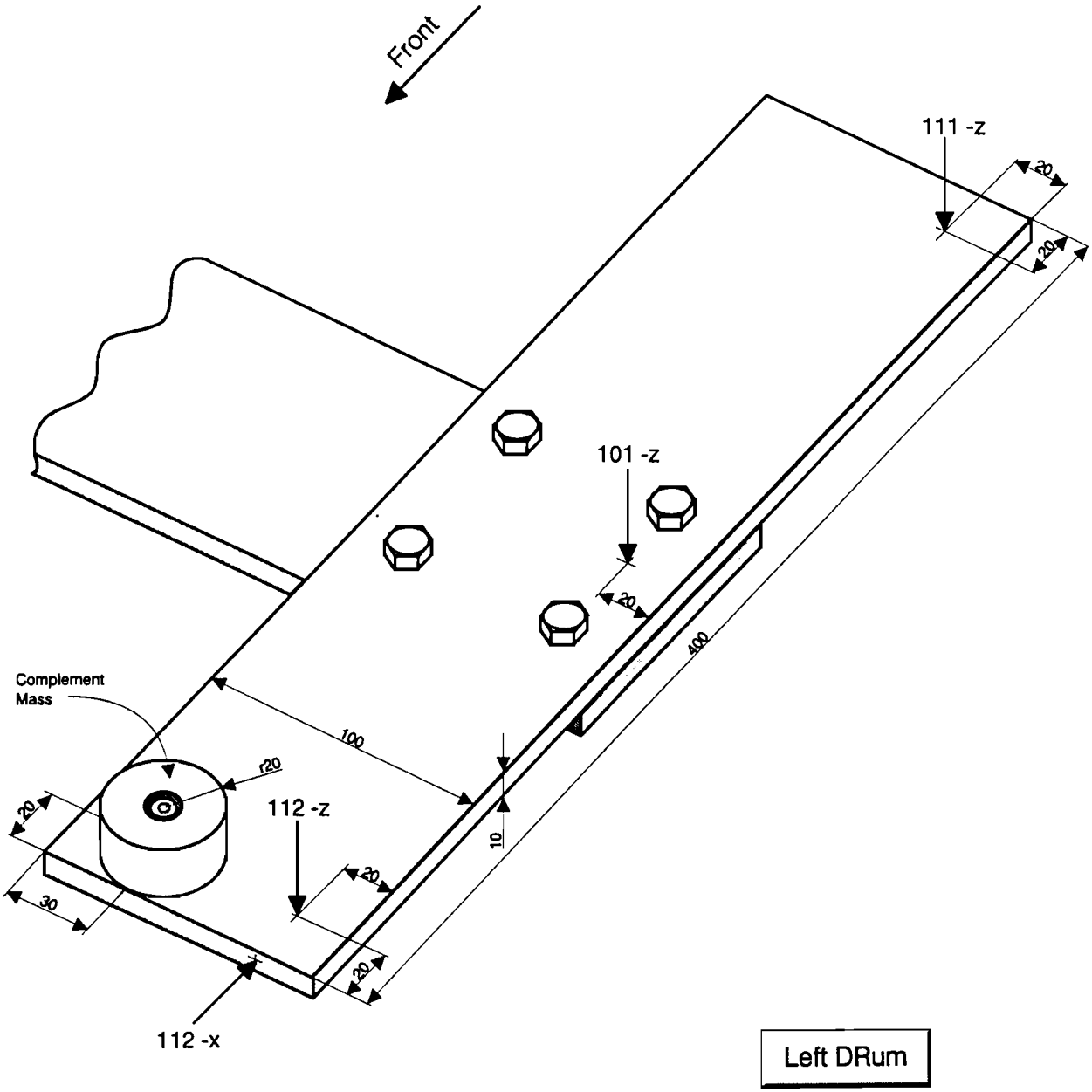
Front
111 -z
20
20
101 -z
20
400
Complement
Mass
100
r20
112 -z
20
20
10
20
30
112 -x
Left DRum

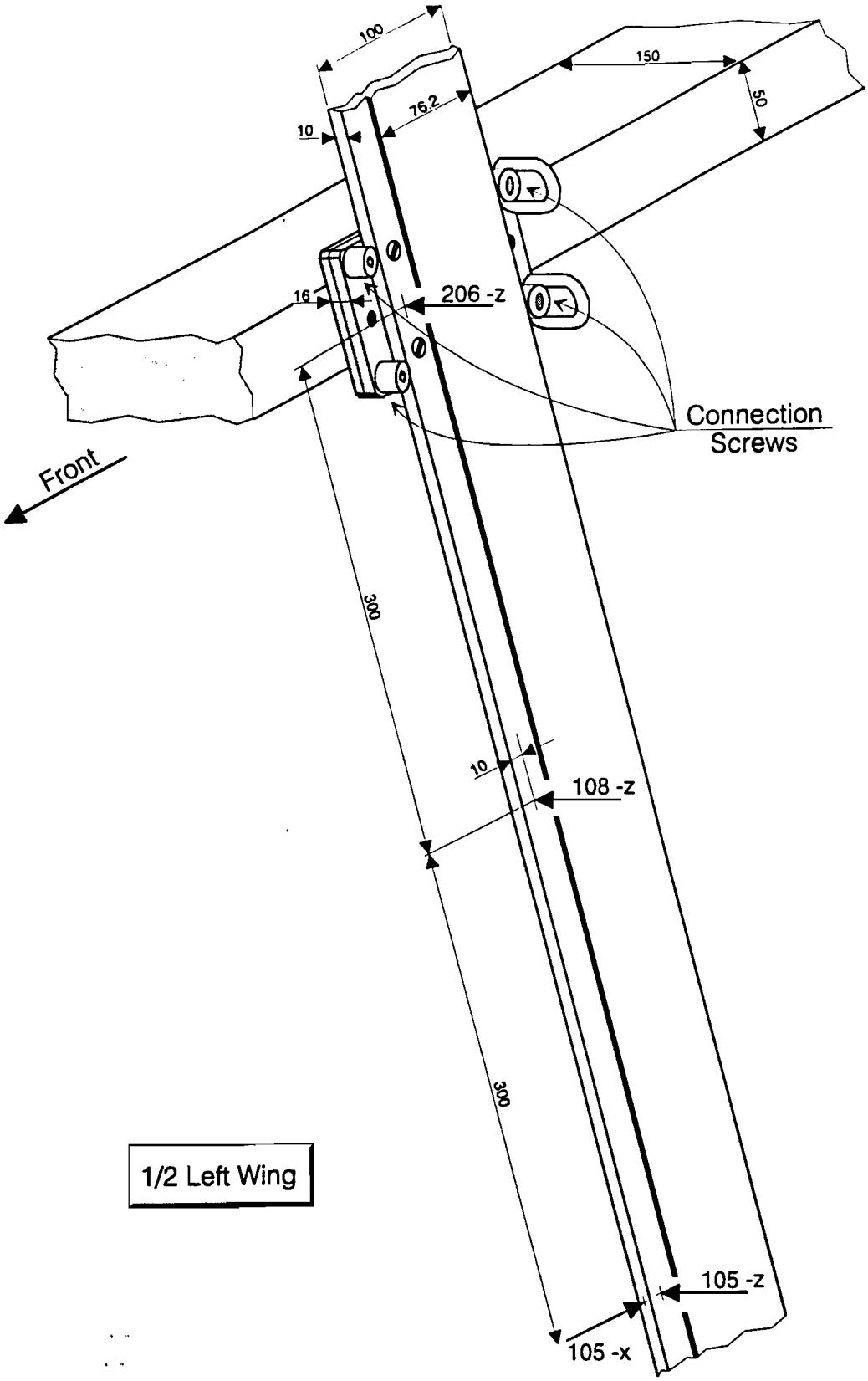
100
150
50
76.2
10
16
206 -z
Connection
Screws
Front
300
10
108 -z
300
105 -z
105 -x
1/2 Left Wing

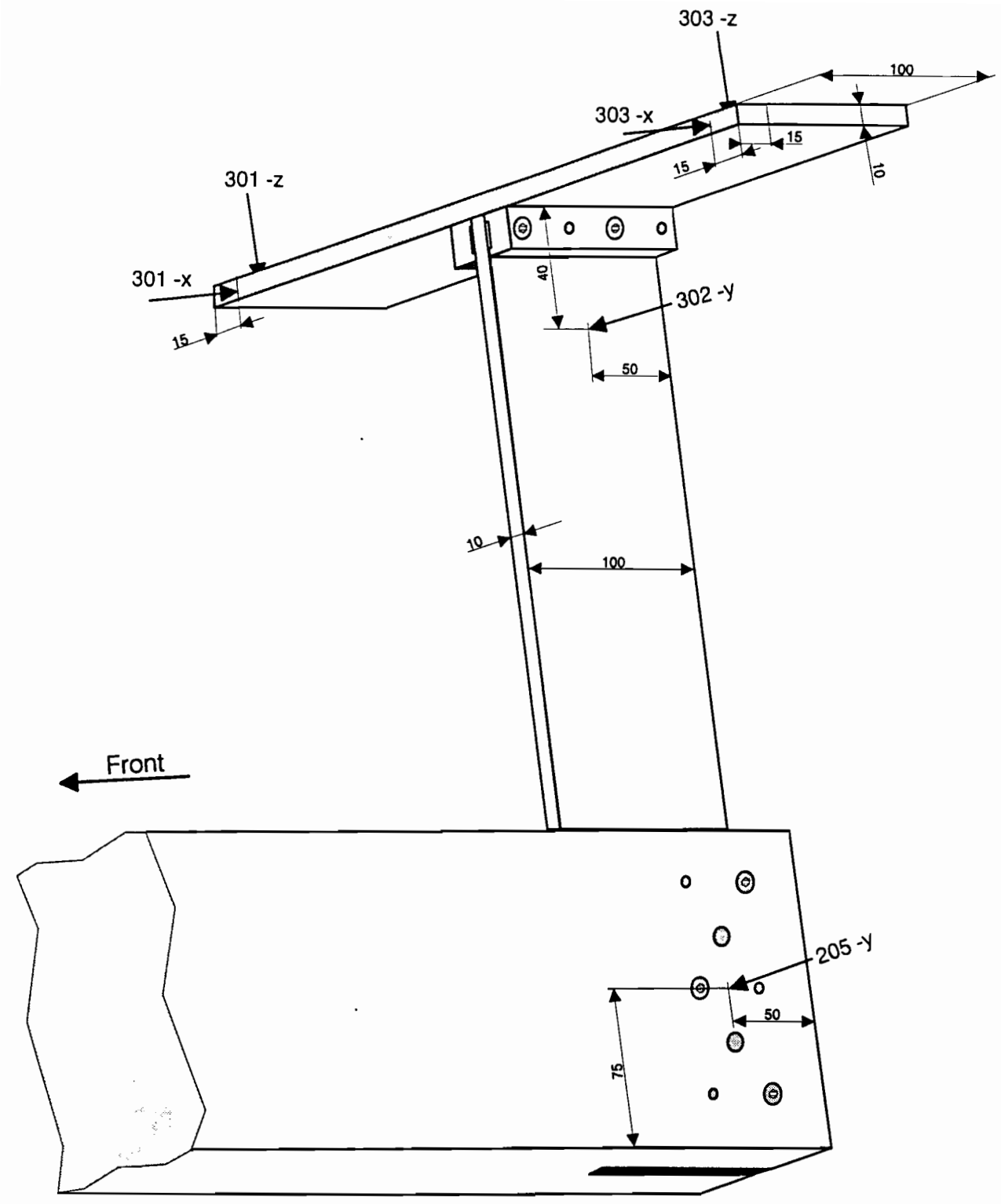
303 -z
303 -x
301 -z
301 -x
302 -y
205 -y
Front
100
15
15
10
40
50
10
100
50
75

5.2 DAMPING TREATMENT

Sufficient damping levels are obtained through the use of a viscoelastic layer with an aluminum constraining layer.

The viscoelastic used is the 3M acrylic viscoelastic polymer ISD 112 in the form of a 76 mm by 50 μm roll. A sample roll (Ref: SJ 2015 Type 1202) was provided to us by 3M Laboratories (Europe), Hansastr. 9, 41453 Neuss, Germany. This viscoelastic is particularly well suited for the testbed operating range of 5-50 Hz and 20 C where it operates near its peak loss factor of 0.9.

Significant levels of shear strain are obtained in the viscoelastic through the use of a 1.1 x 76.2 x 170 mm constraining layer covering the complete viscoelastic treatment. The ISD 112 being pressure sensitive, the bonding was obtained easily and 3M has confirmed that only extreme conditions should damage it. As a safety rule however you should **not do anything that might damage the viscoelastic bonding** (such as trying to lift the constraining layer or gluing anything to the constraining layer).

Damping levels in a wing only test increased significantly with the added damping treatment. From 0.28% to 1.1% in bending (at 9 Hz) and from 0.15% to 0.86% in torsion (at 27 Hz). Tests done on different days gave very similar results.

6 Design FE model

A finite element model was created to help in the testbed design process. Although this model uses simple beam elements, the predictions obtained are quite good. To give an initial common basis for analytical studies, the characteristics of this model are given here. It is not implied that this model should be used as a starting point for FE model update studies.

```
% Garteur testbed FE model Updated March 27, 1995
%
% Structural Dynamics Toolbox for MATLAB

node = [
% Right wing
1       0 0 0           0       -95     0
2       0 0 0           0       -90     0
3       0 0 0           0       -80     0
4       0 0 0           0       -70     0
5       0 0 0           0       -60     0
6       0 0 0           0.      -50     0
7       0 0 0           0       -40     0
8       0 0 0           0       -30     0
9       0 0 0           0       -20     0
10      0 0 0           0       -10     0
11      0 0 0           -20     -95     0
12      0 0 0           20      -95     0
% left wing
101     0 0 0           0       95      0
102     0 0 0           0       90      0
103     0 0 0           0       80      0
104     0 0 0           0       70      0
```

```
105     0 0 0           0       60      0
106     0 0 0           0       50      0
107     0 0 0           0       40      0
108     0 0 0           0       30      0
109     0 0 0           0       20      0
110     0 0 0           0       10      0
111     0 0 0           -20     95      0
112     0 0 0           20      95      0
% fuselage
201     0 0 0           60      0       -9.60
202     0 0 0           0       0       -9.60
203     0 0 0           -40     0       -9.60
204     0 0 0           -75     0       -9.60
205     0 0 0           -90     0       -9.60
206     0 0 0           0       0       0
% tail
301     0 0 0           -90     -20     28.5
302     0 0 0           -90     0       28.5
303     0 0 0           -90     20      28.5
99      0 0 0           0       0       1
];node(:,5:7) = node(:,5:7)/100;
```

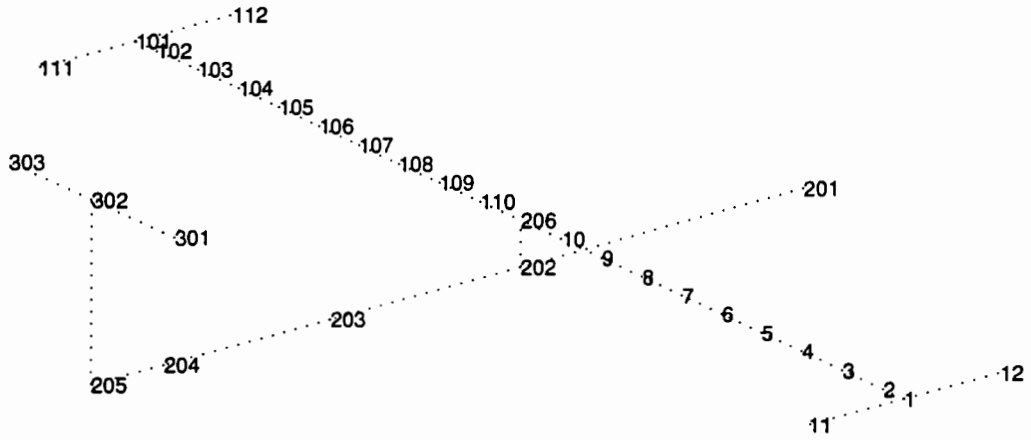

Figure 4: Node numbers in the design finite element model. These node numbers are also used to designate common sensor positions in the test.

```
% elements
elt = [Inf abs('beam1')
        1       2       1       1       12 0
        2       3       1       1       12 0
        3       4       1       1       12 0
        4       5       1       1       12 0
        5       6       1       1       12 0
        6       7       1       1       12 0
        7       8       1       1       12 0
        8       9       1       1       12 0
        9       10      1       1       12 0
        10      206     1       1       12 0


        1       11      1       1       112 0
        1       12      1       1       112 0

        101     102     1       1       12 0
        102     103     1       1       12 0
        103     104     1       1       12 0
        104     105     1       1       12 0
        105     106     1       1       12 0
        106     107     1       1       12 0
```

```
        107     108     1       1       12 0
        108     109     1       1       12 0
        109     110     1       1       12 0
        110     206     1       1       12 0

        101     111     1       1       12 0
        101     112     1       1       12 0

        201     202     1       2       302 0
        202     203     1       2       302 0
        203     204     1       2       302 0
        204     205     1       2       302 0

        202     206     1       4       302 0

        205     302     1       1       201 0
        301     302     1       3       205 0
        302     303     1       3       205 0
        ];elt = [elt zeros(size(elt,1),1)];

pl = [ % aluminum
  1 1 7.2000e+10   3.0000e-01   2.7000e+03 72e9/2/1.3          0];

b1=0.10; h1 = 0.01; b2=0.15; h2 = 0.05; b3 = 0.01; h3 = 0.10;
il =[
        1 1 (b1*h1^3)*0.312 b1*h1^3/12  b1^3*h1/12 b1*h1 0
        2 1 (b2*h2^3)*0.263 h2*b2^3/12  h2^3*b2/12 b2*h2 0
        3 1 (h3*b3^3)*0.312 b3*h3^3/12  b3^3*h3/12 b3*h3 0
        4 1 (b2*h2^3)*0.263 h2*b2^3/12  h2^3*b2/12 b2*h2 0
    ];

il(1,3:4)=il(1,3:4)*1.1;     % correction for constraining layer stiffness

a = (1/2700)^(1/3); m =[1 1 1 a^6/12 a^6/12 a^6/12];
elt = [elt;Inf abs('mass1') 0;
        302     m*1.6
         12     m*.200
        112     m*.200];

[FEm,FEk,mdof] = fe_mk(node,elt,pl,il);
[mode,freq] = fe_eig(FEm,FEk,[0 20 1e3 1]);
```

Table 2: Names and computed frequencies for the first 10 normal modes (in Hz).

6.02	Two node bending	47.57	Four node bending
13.16	Global fuselage rotation	55.01	Symmetric in plane bending
32.54	First symetric wing torsion	57.01	Second fuselage rotation mode
33.40	First antisymetric wing torsion	66.30	Tail torsion
35.58	Three node bending	69.79	Five node bending

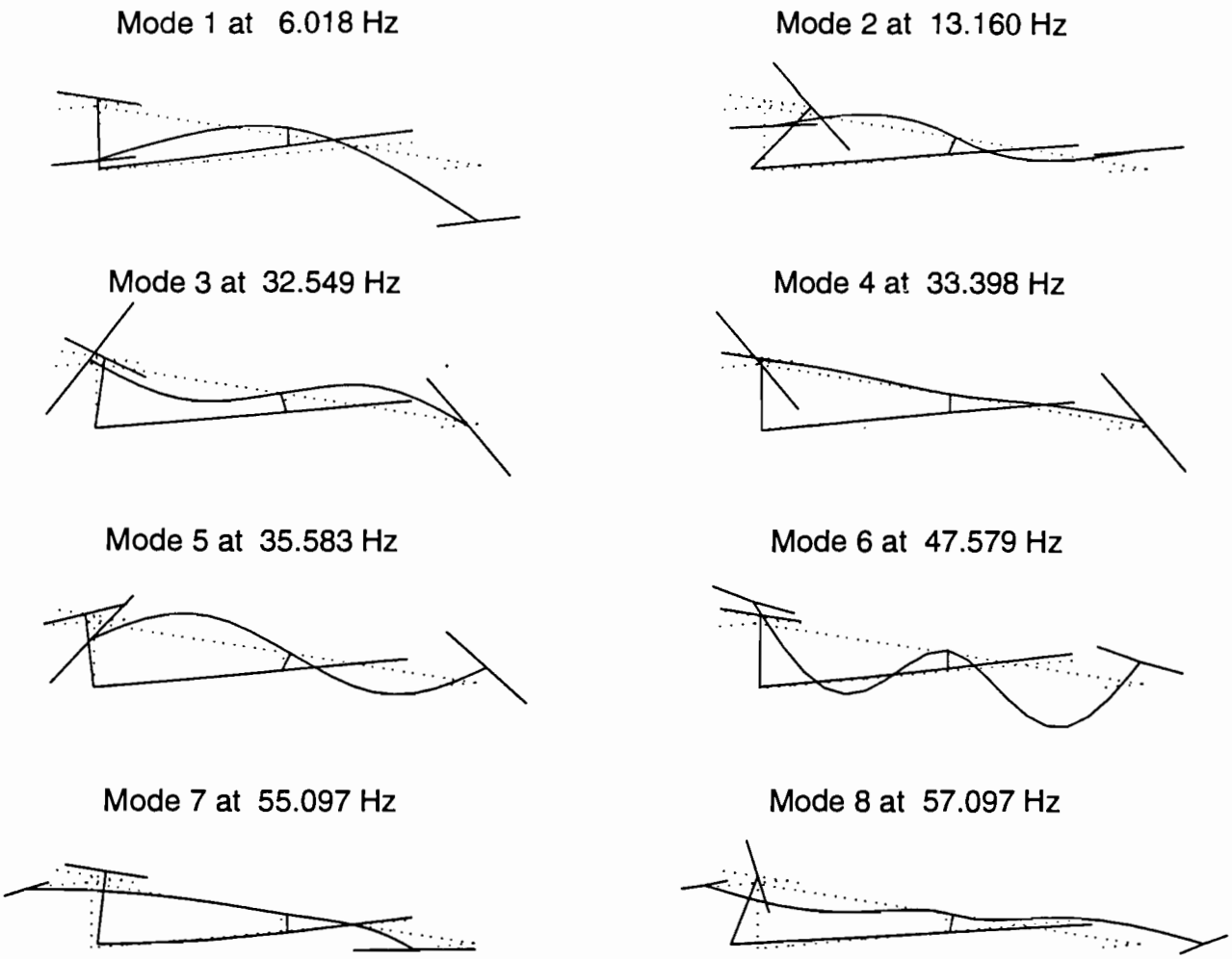

Figure 5: First 8 modes of the design FE model given for reference.

7 References

[ewi8] Ewins, D.J., Griffin, J., "A State of the Art Assessment of Mobility Measurement Techniques – Results for the Mid-Range Structures (30-3000 Hz)," *Journal of Sound and Vibration*, 1981, **78**-2, pp. 197-222

[ewi9] Ewins, D.J., "State of the Art Assessment of Mobility Measurement Techniques (SAMM) – Summary of results," *SEE Journal*, March 1981

Annex 3

SOPEMEA REFERENCE RESULTS

Reference results from SOPEMEA

1 Introduction

As planned during our meetings, the members of the group are asked to submit a comparison of their own results with those of a reference set of data taken by SOPEMEA as they were the first to test. The objective of this comparison is not to see whether some results are better than other but rather to understand the criteria that you use to evaluate the relative quality of two sets of data.

The present document gives an English summary of relevant information in the preliminary report given by SOPEMEA, relevant comments and a description of the two universal files (`sopmode.uf` and `sopfrf.uf`) which you have received by e-mail or DOS formatted floppy.

If you can return to ONERA a set of FRFs and modes similar to the data described here this will be appreciated as it will allow global comparisons of all results.

2 Test equipment

The data included was acquired using a system with a large capacity in measurement channels including analog and digital hardware capable of acquiring and treating 768 accelerometer channels in appropriated sine mode and 256 filtered channels in sine, random or transient mode with transfer function computations.

The structure was instrumented using the 24 reference channels indicated in the testbed documentation plus 20 others which are not included in the data you have received.

Wilcoxon accelerometers associated with an integrating amplifier delivering a velocity signal of 3.8 V efficient per m/s.

PRODERA electrodynamic shakers with power amplifiers were used. Their frequency range is 0--200 Hz and maximum force 10N. Shaker 101 has a force factor of 7.4 N/A and a longitudinal stiffness of 980 N/m. Shaker 104 has a force factor of 7.2 N/A and a longitudinal stiffness of 650 N/m.

The shaker/structure links are done using an assembly with

- a threaded rod linked to the shaker moving mass
- an intermediate universal joint
- for wing tip excitation, a threaded rod linked to the structure (the threaded rod of the additional masses). Note that this excitation is in the z direction but does not exactly correspond to nodes 12 and 112 which are supposed to be excited.
- for other excitation locations a threaded rod glued to the structure (with an intermediate double faced scotch tape).

For excitation by the wings the initial complement masses were replaced by 76 g masses. The mass linked to excitation (moving mass of the shaker: coil and spider) and connection (threaded rod, universal joint, nut) was of 124 g.

3 FRF data

Results of a stepped sine sweep are given here. In this type of sweep the excitation is driven using a discrete frequency sine signal. For each point of stabilized frequency, measurement and excitation signals are acquired in real time. The frequencies are spaced using a logarithmic law function of initial and final frequencies.

The results included here come from two tests. Test 1 corresponds to a symmetric excitation at points E1 (shaker 101) and E2 (shaker 104). Test 2 corresponds to an antisymmetric excitation at points E1 (shaker 101) and E2 (shaker 104). The data given `sopfrf.uf` reconstructs the expected tests input at E1 and input at E2 by taking the sum and difference of test 1 and test 2 and dividing by 2 (the extent of effects linked to the position of E1 and E2 is not known).

The analysis of responses is done using a Fourier series decomposition with extraction of amplitude and phase of the fundamental. Response and inputs are stored and FRFs are reconstructed by dividing all the outputs by the input level. For test 1 the levels are 0.6N from 5 to 9 Hz, 2 N from 9 to 46 Hz, 10 N from 46 to 60 Hz. For test 2, the levels are 2N from 5 to 40 Hz and 10 N from 40 to 60 Hz. For test 2 near 40 Hz, the force measurement are probably not very accurate as the resulting FRFs are not continuous. As the given data correspond to linear combinations of test 1 and 2, these erroneous points appear in most FRFs.

Finally the data was given in m/s. For easier comparisons with standard accelerometer data, it was transformed to acceleration by multiplying by $j\omega$ (ω in rad/s).

The data sent to ONERA were not in the universal file format and the transformations detailed above were performed to present data in the appropriate format. A significant effort was done to fill the universal file headers appropriately but please tell E. Balmès about errors you may still find.

Figures 1 and 2 show the given data for the 2 by 2 set of transfer functions that were required in the testbed documentation (up to 60 and not the specified 65 Hz).

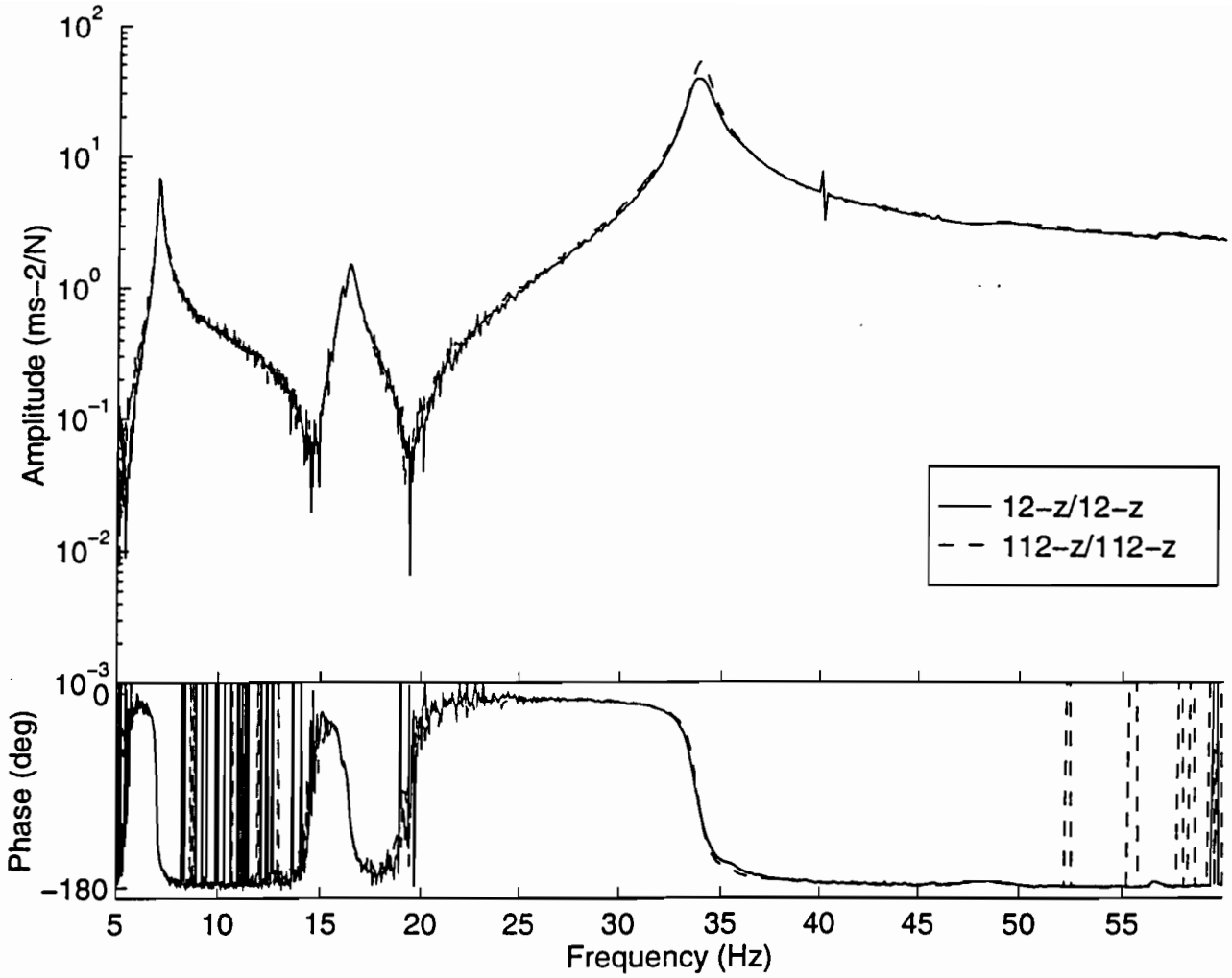

Figure 1. Superposition of the left and right collocated transfer functions (—) 12-z/12-z and (- - -) 112-z/112-z

4 Modal data

Modes were identified using the appropriation method were one excites the structure with a sine and a combination of inputs such that one only measures the response of one mode.

For each mode, SOPEMEA gives a modeshape (corresponding to the real part of the measured velocity response), a phase plot (to see if the mode is well appropriated) and an impedance plot (dependence of the modeshape and frequency on amplitude). The reference data set which you have received only contains the real part (modeshape). A table in annex A gives a summary of properties of the measured modes (some of which are measured more than one time). The modes to be retained are numbered 101 to 109 and are shown in figure 3 below.

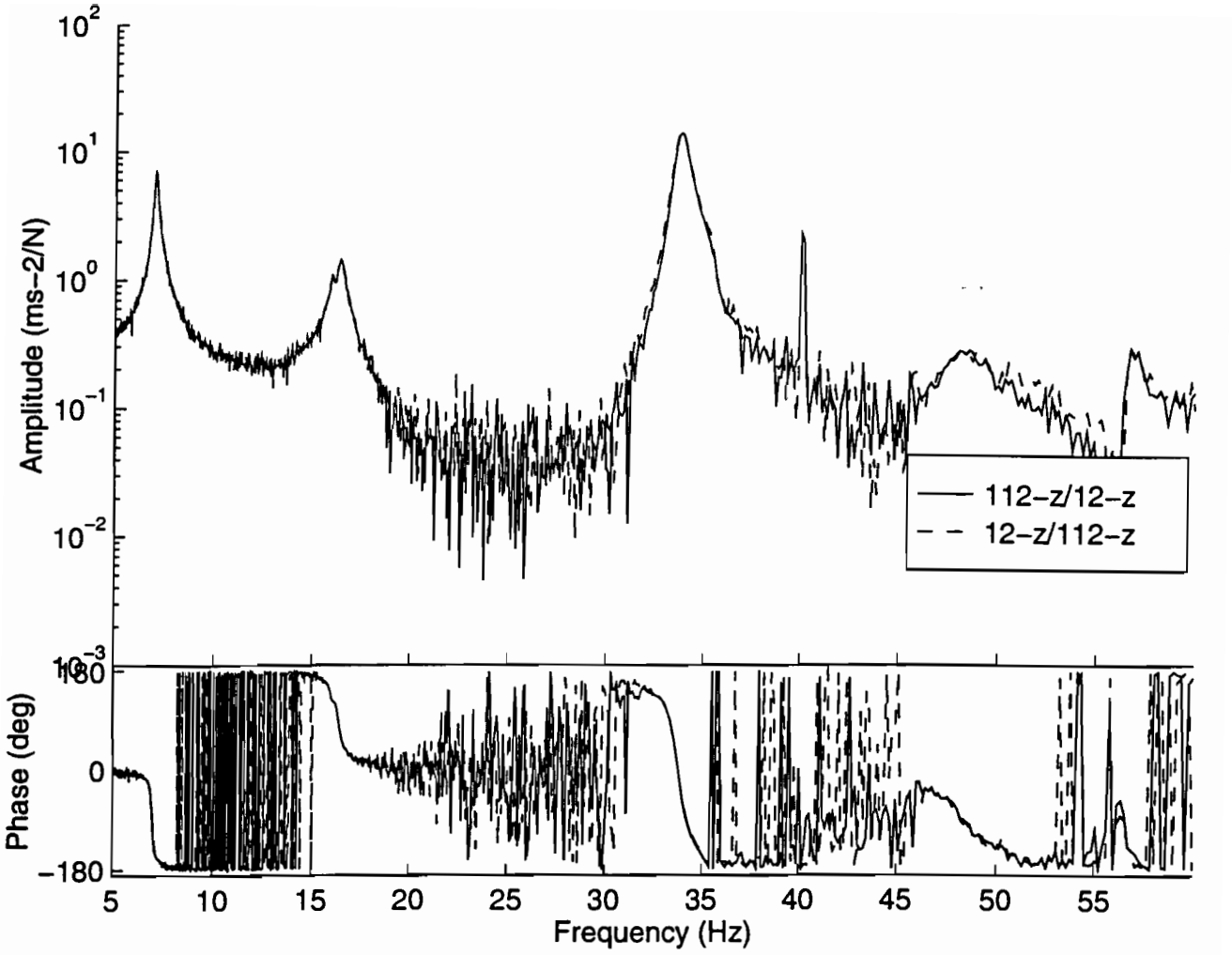

Figure 2. Superposition of the reciprocal transfer functions (—) 112-z/12-z and (- - -) 12-z/112-z

SOPEMEA made the following comments these results.

The results to be retained are modes 101 to 109.

Mode 201 was measured with excitation in the middle of the fuselage with a 50 N shaker. Even though the appropriation is correct, one sees that an excitation without compensation of the mass added by the shaker, in particular the frequency that goes from 6.373 Hz for 6.974 by the wing tips E1 and E2. The renormalized and recomputed generalized mass is 4.29 kgm2 which is close to mode 101.

Modes 301, 302, 303 were measured after switching the shakers for E1 and E2. One sees a large difference on frequencies and generalized parameters when compared to modes 101, 102 and 103, which can be attributed to the different stiffness of the shaker moving parts (980 and 650 N/m). One can thus conclude that mass compensation is not sufficient for this type of test with the equipment used and stiffness compensation would also be needed.

Similarly, in order to favor a good appropriation quality led to the use of other excitation points than the wing tips. This poses the question of homogeneity and quality of measures in appropriated sine.

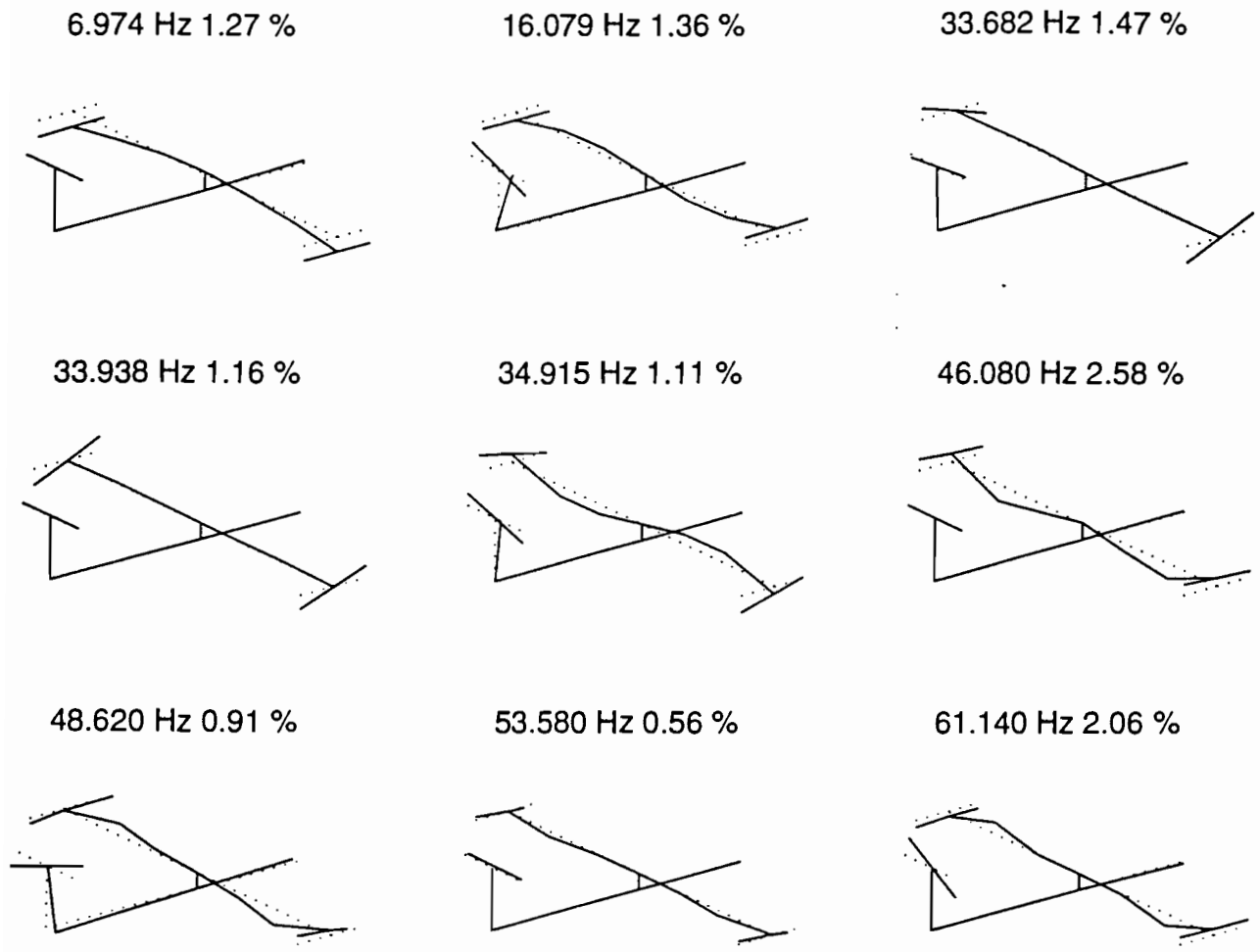

Figure 3. Measured set of modes.

The `sopmode.uf` file gives mass normalized modes $c_l\phi_j$ such that the transfer function from force at location *l1* to displacement at location *l2* is given by

$$[\alpha_{l1l2}(s)] = \sum_{j=1}^{N} \frac{\{c_{l2}\phi_j\}\{c_{l1}\phi_j\}^T}{s^2 + 2\zeta\omega s + \omega^2}$$

which also corresponds to the fact that the generalized mass of mode j at a sensor l is given by

$$mg_{lj} = \frac{1}{(c_l\phi_j)^2}$$

It is unclear whether this corresponds to the usual normalization of the universal file format.

Annex 4

NLR CONTRIBUTION

NLR TECHNICAL REPORT

TR 95439 L

GROUND VIBRATION TESTS ON THE GARTEUR SM AG19 TESTBED

Part I: Measurement of a reference set of transfer functions

by

A.J. Persoon, C.S.G. Dogger

and P. Schippers*

This investigation was carried out in the framework of the GARTEUR activity (SM AG19): "Ground Vibration Test Techniques".

* Fokker Aircraft B.V.

Division : Fluid Dynamics
Prepared : AJP/ CSGD/ PS/
Approved : RJZ/

Completed : 950904
Order number : 524.502
Typ. : PA

1 Introduction

Within the framework of certification of a new aircraft, a ground vibration test (GVT) plays an important role for the verification or updating of analytical models, allowing more accurate aeroelastic (flutter) predictions. Facing the risk of flutter, a high level of quality and reliability of GVT results has to be achieved in obtaining the dynamical characteristics of the airplanes's structure.

The present GARTEUR activity has the major objective to compare a number of current measurement and identification techniques in application to a common testbed. This testbed (Fig. 1) was designed and constructed by ONERA (France) and will be investigated by various research institutes and industrial partners (Tab. 1). More specifically, the objectives of the GVT tests (Ref. 1) are to evaluate the efficiency and reliability of test methods, to compare modal parameters extracted from different identification techniques and to evaluate discrepancies between data or modal parameters using different test setups and experimental analysis methods.

The data from these experiments might be used in a later stage for model updating techniques.

Each participant has been requested to provide at least a 2 X 2 set of transfer functions (reference set) corresponding to excitation and response of the left and right wing tip body (again Fig. 1) in a frequency band of 4 to 65 Hz, using two electrodynamic shakers. Hereafter the participants are free to perform an additional ground vibration test following their own view to identify the number of modes in this frequency band characterized by the mode shape, frequency, damping factor and modal mass.

This report (Part I) deals with the measurements of the required set of transfer functions and the comparison with test results obtained by ONERA (France). Further, the report should inform ONERA in an early stage of the activity as a final report will be made after all participants (Tab. 1) have performed their experiments. Also the test setup and instrumentation are described briefly.

The complete modal survey carried out on the testbed with various shaker positions and different testing techniques as commonly applied at NLR and Fokker on a real aircraft, will be reported in part II.

2 The reference set of transfer functions

In order to be able to compare the results from a specific measurement (and appropriate data reduction), all participants were requested to measure a set of transfer functions using the multiple input/multiple output (MIMO) technique, based on a two-point excitation. A vertical excitation was prescribed at nodes 12 and 112 (Fig. 2a, 2b) being the wing tip body front positions (right and left). With the accelerations concerned (12Z and 112Z), a 2 X 2 matrix of transfer functions is obtained by which two FRF's are the driving points transfers, the other two are cross-transfers. The frequency band of interest is 4 to 65 Hz and a blocksize of 2048 spectral lines was applied (4096 time samples).

The results obtained by NLR/Fokker and a comparison with results of ONERA are discussed in chapter 5.

3 Description of the test setup

3.1 Support and instrumentation of the testbed

The aluminium testbed was elastically supported in bungees (Fig. 3a), according to the recommendations of ONERA. The rigid body motions and their frequencies were determined (heave: f=1,88Hz). With the measured stiffness of the bungees, the mass of the testbed was calculated and compared with the result from a weighting.

The model excitation was realized by two electrodynamic shakers (type: Goodman V50Mk1, moving mass: 81 gr, maximum force: 108 N). Each shaker was connected to the front position of wing tip body by a plastic rod, a piezo-electric loadcell (PCB, type 7900, ± 2.5 mV/N) and an additional mass of 46 gr. as compensation for the 200 gr mass (Ref. 2).

On the testbed 24 accelerometers were mounted (type: kulite GY-280, 10 gr) according to the prescribed positions and directions (Fig. 2). The accelerometers were of a piezo-resistive type with a nominal sensitivity of about 5 mV/g (range: 20g) to be used from DC up to 300 Hz. As will be discussed later, the amount of accelerometers was not enough to animate all the vibration modes clearly, but it was agreed by the participants before the test campaign that data reduction and analysis would be based on the prescribed 24 accelerometer positions.

3.2 Measuring equipment

Use was made of a multi-channel measuring system of NLR (AE-2), consisting of a SCADAS front-end (DIFA, The Netherlands) and a workstation of Hewlett Packard (HP 9000/382 controller) with CADA-X software of Leuven Measurement System (LMS, Belgium) for data acquisition and advanced modal analysis. This 40-channel system is a stripped version of NLR's 128-channel system which, in combination with the NLR conditioners (MCCU's) for piezo-resistive transducers, is easy to use at the site. A dual-channel structural dynamics analyzer (HP 3562A) served as a real-time monitoring device in case of sinus excitation of the testbed by which the 90 deg phase criterium was applied. Miscellaneous equipment consisted of amplifiers for the shakers, a signal generator, oscilloscopes and a laser printer as a hard copy device.

A block diagram of the instrumentation setup is shown in figure 4.

4 Check on proper connection of wing/fuselage

Before starting the actual measurements of the required set of transfer functions first a check of the testbed setup was carried out based on data given by ONERA (Ref. 2). Each participant should verify the frequency and damping ratio of the fuselage rotation mode measured by SOPEMEA (also France) being f=16.172 Hz with a damping ratio of 1,452 % (c/cr*100), see figure 5a. This measurement should verify that mounting the wing to the fuselage (by connection bolts torqued to 1.6 kgm) was done in a correct way.

Results of the check performed by NLR/Fokker agree very well (Fig. 5b). A frequency of f=16.14 Hz was found and a damping ratio of 1,54 % using a least squares complex exponential curve-fitter (LSCE) on the data. The animated motion of the horizontal tail does not correspond with the vertical tail motion because of the absence of accelerometers measuring in Y-direction. This representation should therefore be adjusted in a later stage (only for presentation purposes).

After ONERA was informed about these results, NLR/Fokker proceeded with the ground vibration tests.

5 Transfer functions

As already mentioned, use was made of two electro-dynamic shakers. Uncorrelated noise was applied within the bandwidth of 4 to 65 Hz (2048 spectral lines). The number of averages was 30 with 50 % overlapping of data blocks, resulting in a measuring time of around 16 minutes. Within that time, the FRF's were fully stabilized in amplitude and phase.

5.1 Presentation of results by NLR/Fokker

The requested set of transfer functions is presented in figures 6.1 and 6.2. The vertical scale of the magnitude (ms^{-2}/N) is plotted as a logaritmic scale; the scale of the phase angle is linear.

A number of resonance frequencies occurs in the transfer functions, belonging to symmetric and anti-symmetric vibration modes. At about 35 Hz three neighbouring frequencies were found. The mode shapes and related modal parameters were determined. The different excitation and analysis techniques as applied, will be one of the objectives to be reported separately (Part II).

5.2 Comparison with results of ONERA

The reference set of transfer functions was measured by ONERA before shipping the testbed to NLR. The results are presented in figure 7.

A comparison with the NLR/Fokker results shows a very good agreement, both in amplitude and phase. Only small differences appeared at the frequency of 35 Hz: the NLR/Fokker results show more clearly the presence of closely spaced modes.

6 Concluding remarks

1 The suspension of the model by bungees introduced sufficiently low rigid body frequencies.

2 A check on proper mounting of the wing to fuselage showed identical reference results of ONERA and NLR/Fokker.

3 The reference set of transfer functions as obtained by NLR/Fokker agrees very well with the ONERA results.

4 The measured data can be used for model updating techniques.

5 Further analysis towards mode shapes, damping factors and modal masses using the excitation techniques as commonly applied by NLR/Fokker will be reported separately.

7 References

1 Garteur: Proposal for the formation of a GARTEUR action group on ground vibration test techniques; ONERA document 30.201/OR., november 1994.

2 Balmès, E., Documentation for the Garteur SM AG19 testbed, test documentation 0405/95.

3 Fourier Monitor/DIFA SCADAS, manual of LMS, revision 3.2.

Table 1 Participants in the Garteur activity SM AG19

a) Time schedulle

April 1995	SOPEMEA
May 1995	NLR-FOKKER
June 1995	DLR
July 1995	
August 1995	Imperial College
September 1995	DRA-Manchester University
October 1995	ONERA
November 1995	Aérospatiale
December 1995	Intespace
January 1996	CNAM
February 1996	SAAB

b) Representatives

Company	Representative
Aérospatiale	Mr. J.P. ESQUERRE
DLR	Mr. M. DEGENER
DRA	Dr. G.W. SKINGLE
FOKKER	Mr. P. SCHIPPERS
Imperial College	Dr. D. ROBB
Intespace	Mr. L.P. BUGEAT
Manchester University	Dr. J.E. COOPER
NLR	Mr. A.J. PERSOON
ONERA	Mr. A. GRAVELLE
SAAB	Dr. T. ABRAHAMSON
SOPEMEA	Mr. B. CARRE

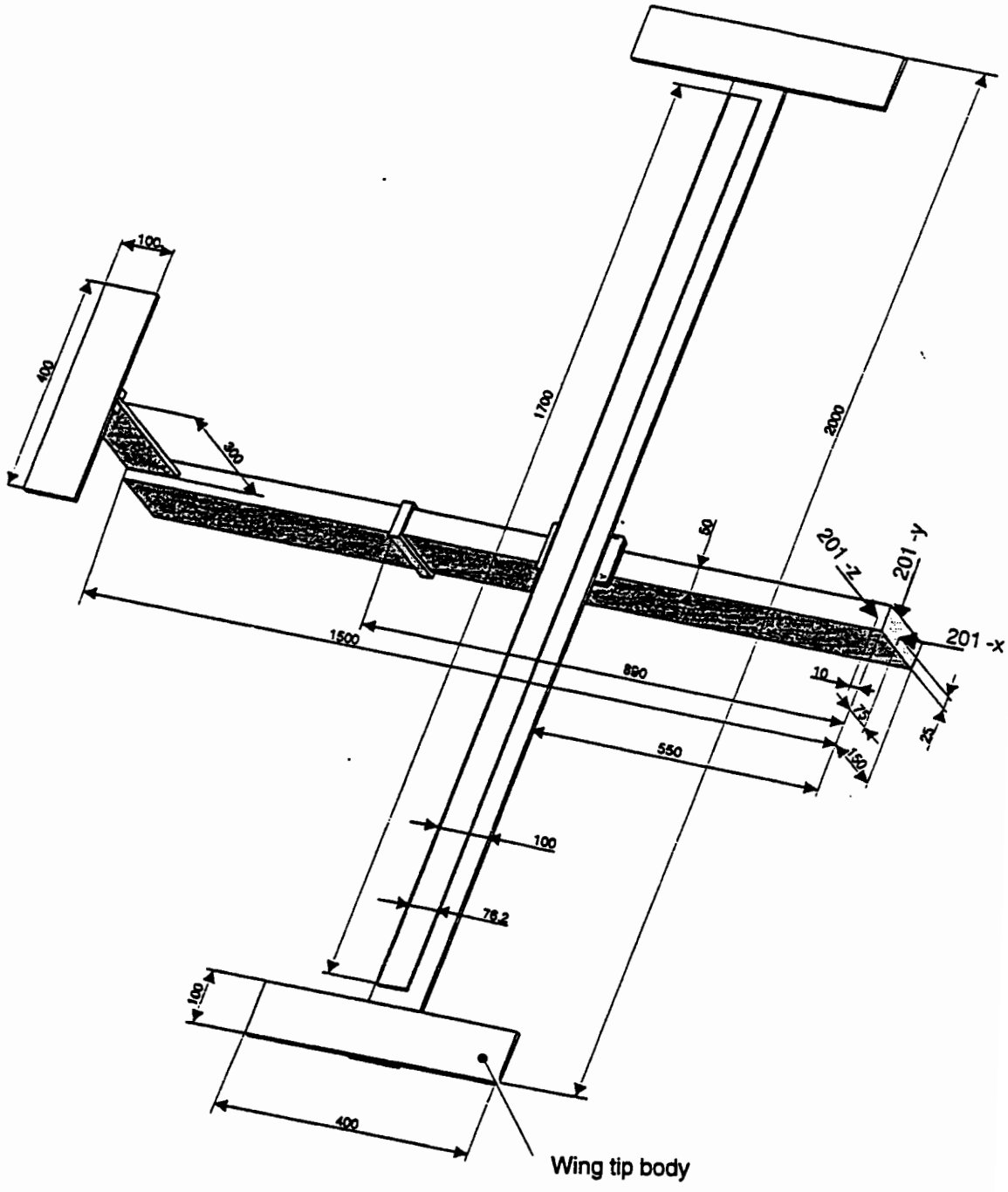

Fig. 1 Sketch of the testbed with dimensions

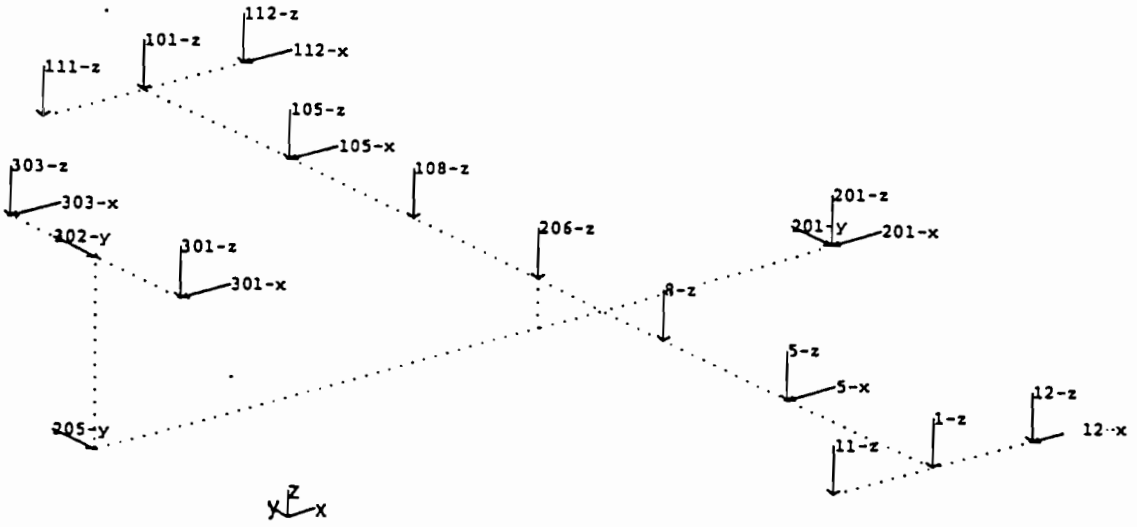

a) Proposed by ONERA

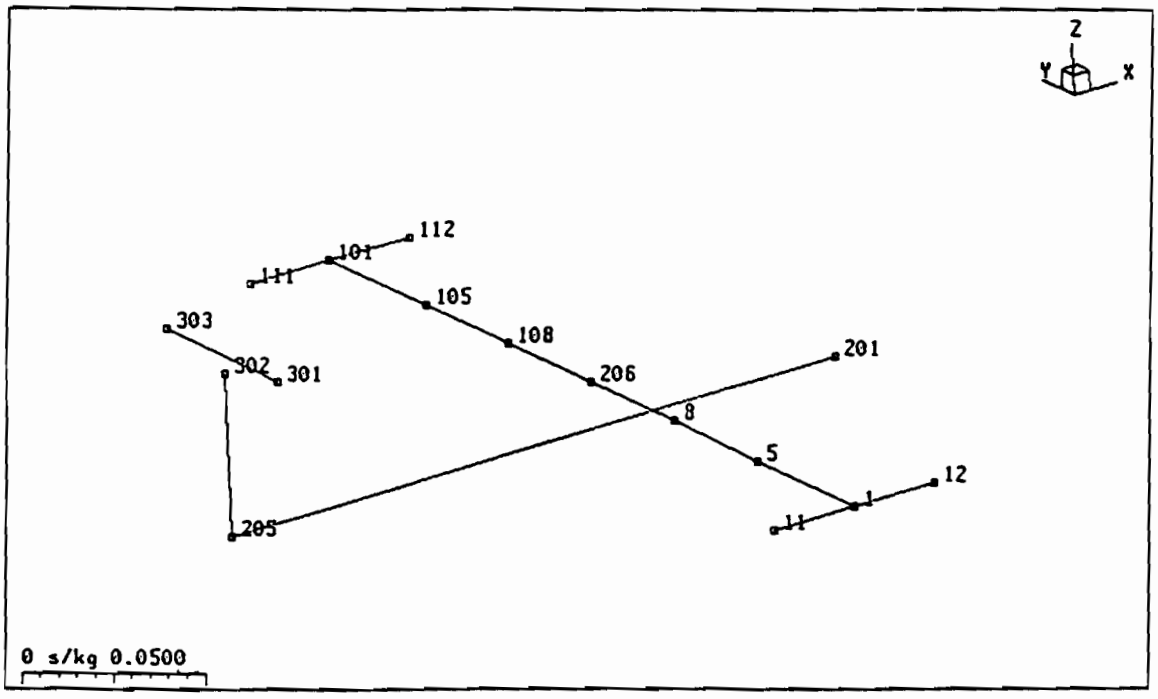

b) The wire frame for mode shape animation (NLR/Fokker)

Fig. 2 Locations and directions of the 24 accelerometers to be used

a) The testbed supported by bungees

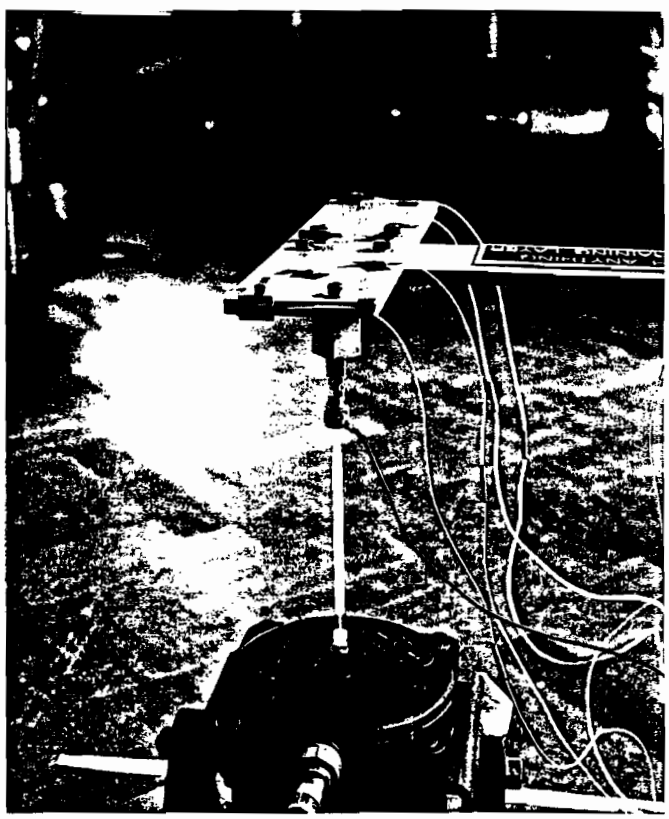

b) Shaker connection to the testbed

Fig. 3 Test setup for the SM-AG19 testbed at NLR

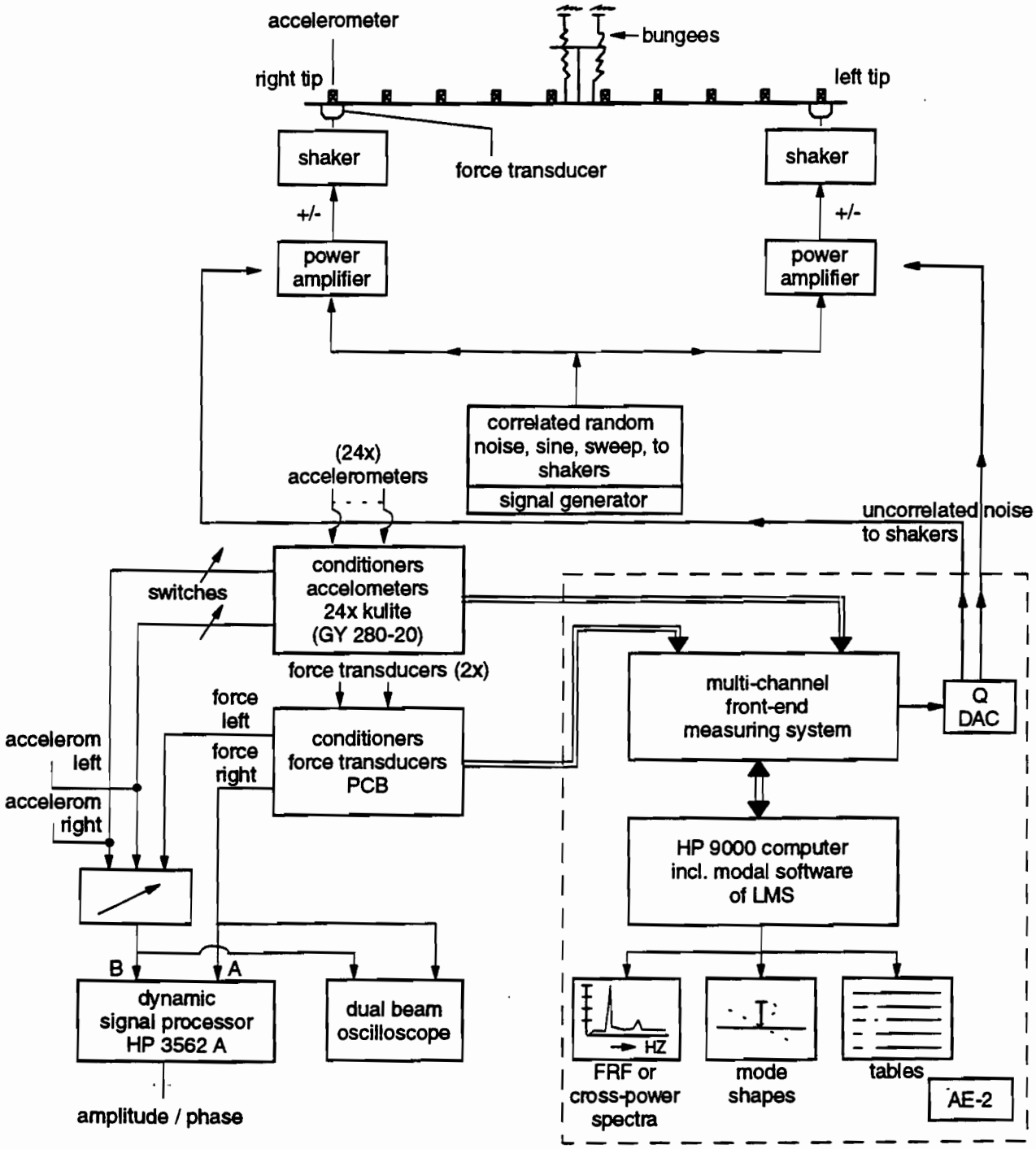

Fig. 4 Schematic view of test setup

Measured by SOPEMEA : f = 16.17 Hz, b = 1.45%
ONERA : f = 16.06 Hz, b = 1.66%

Calculated by ONERA:

Mode 2 at 13.160 Hz

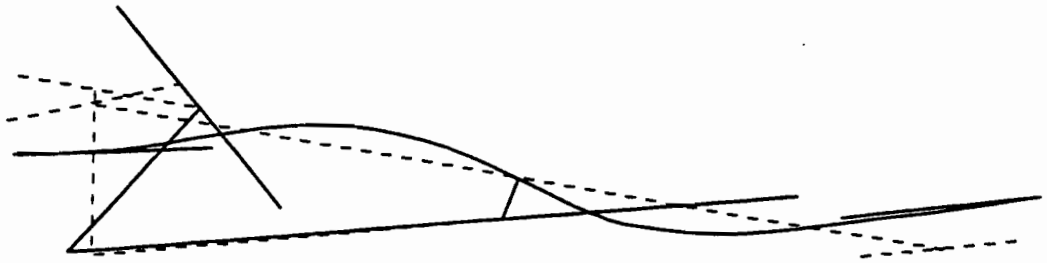

a) By ONERA/SOPEMEA

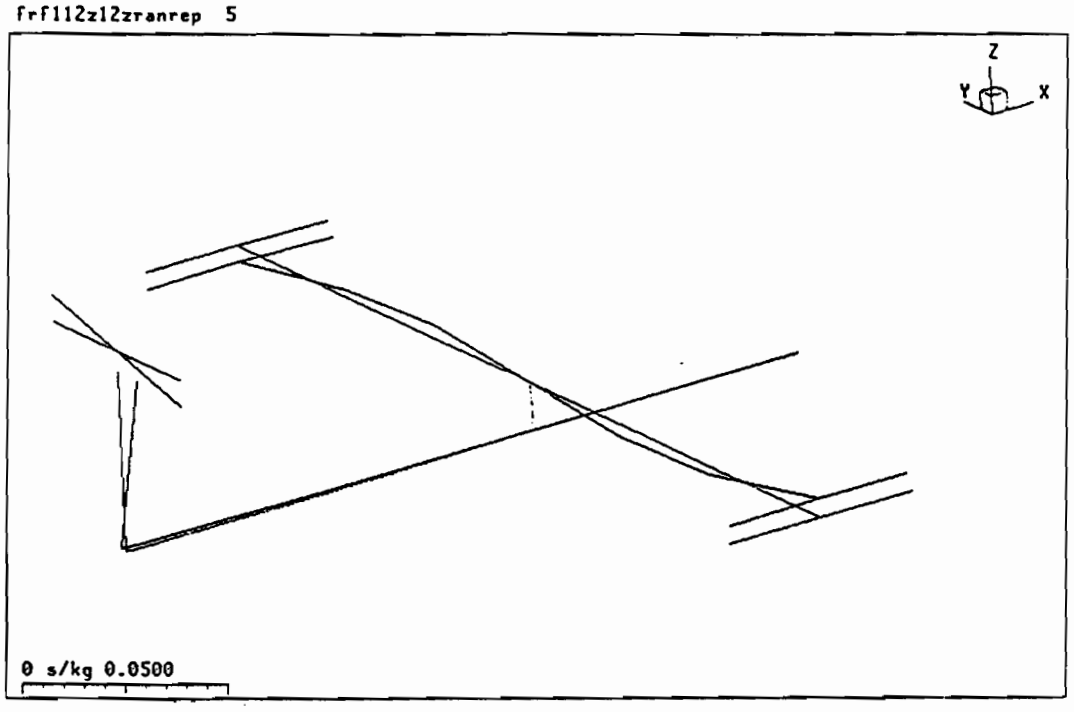

b) By NLR/Fokker
(note: vertical tail/stabilizer motion, see chapter 4)

Fig. 5 Verification of the fuselage rotation mode

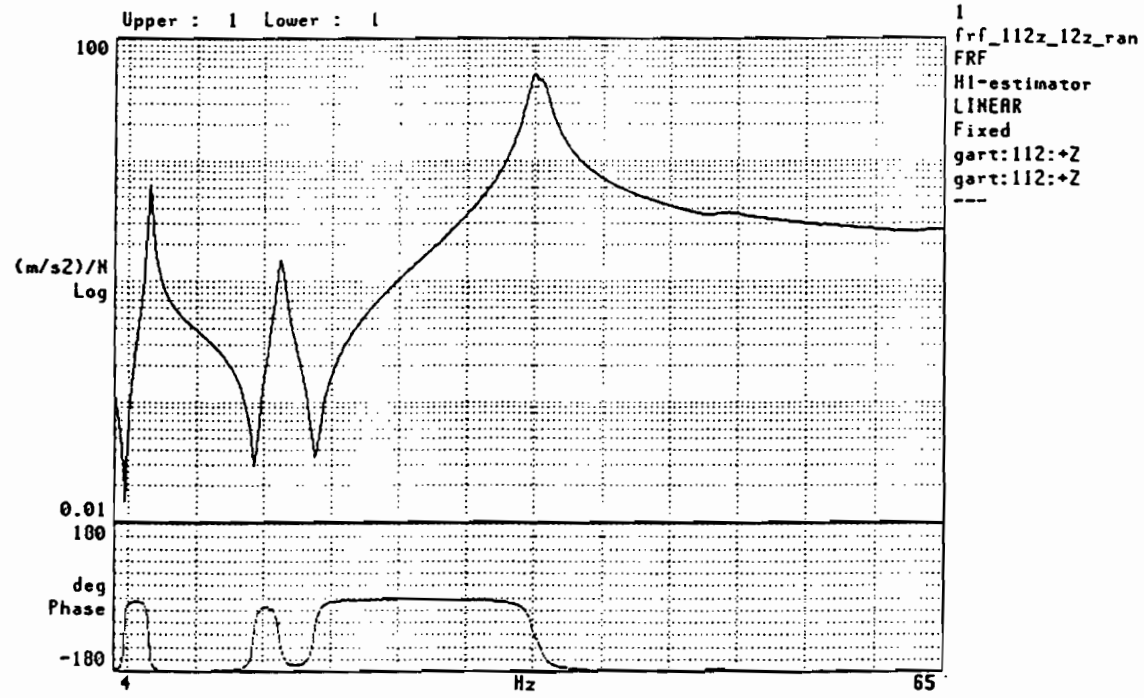

a) Driving point FRF (112/112)

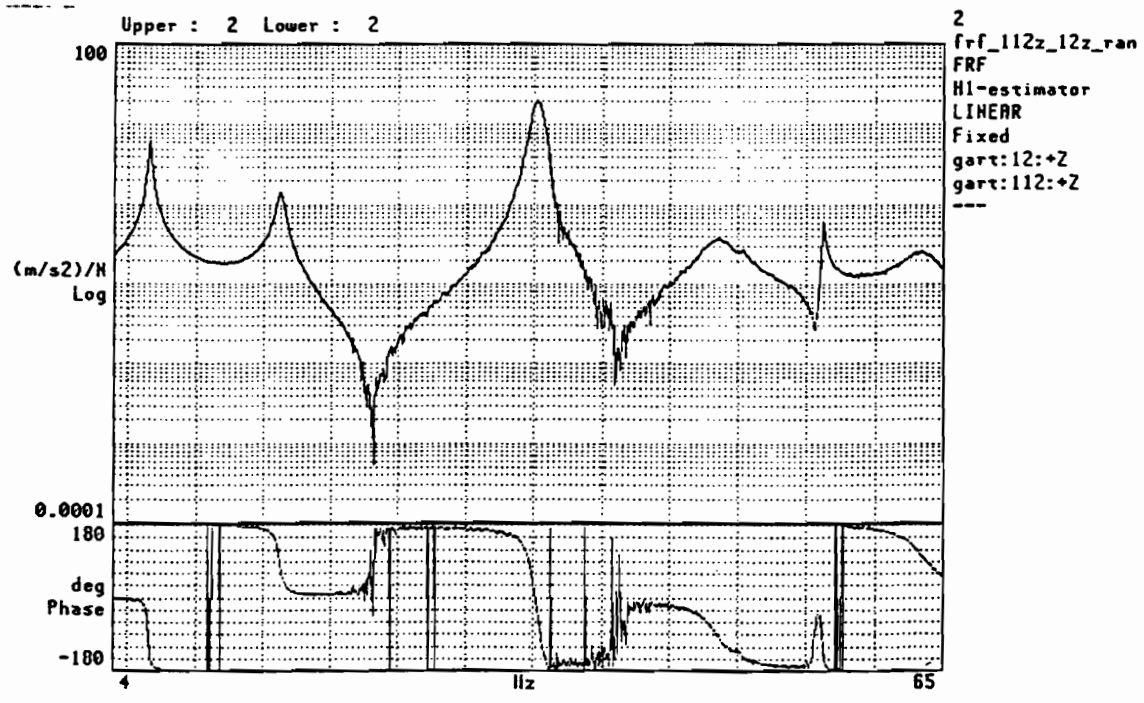

b) Cross-transfer (12/112)

Fig 6.1 Transfer functions measured with uncorrelated noise at position 112 and 12 (z-direction)

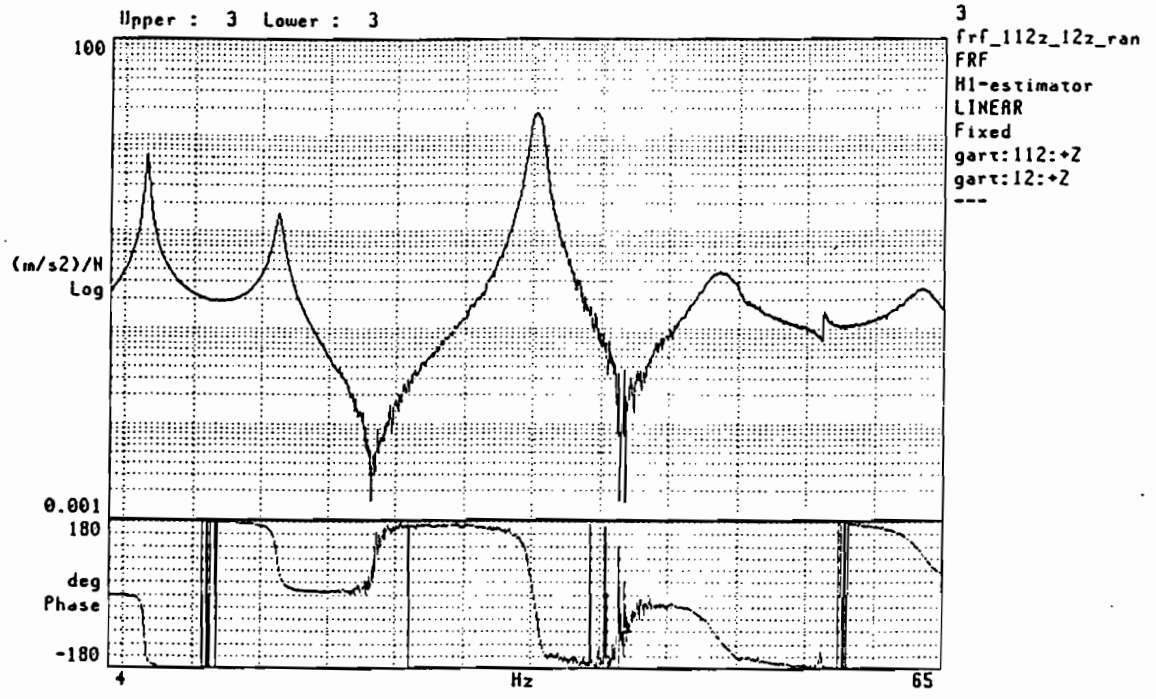

a) Cross-transfer (112/12)

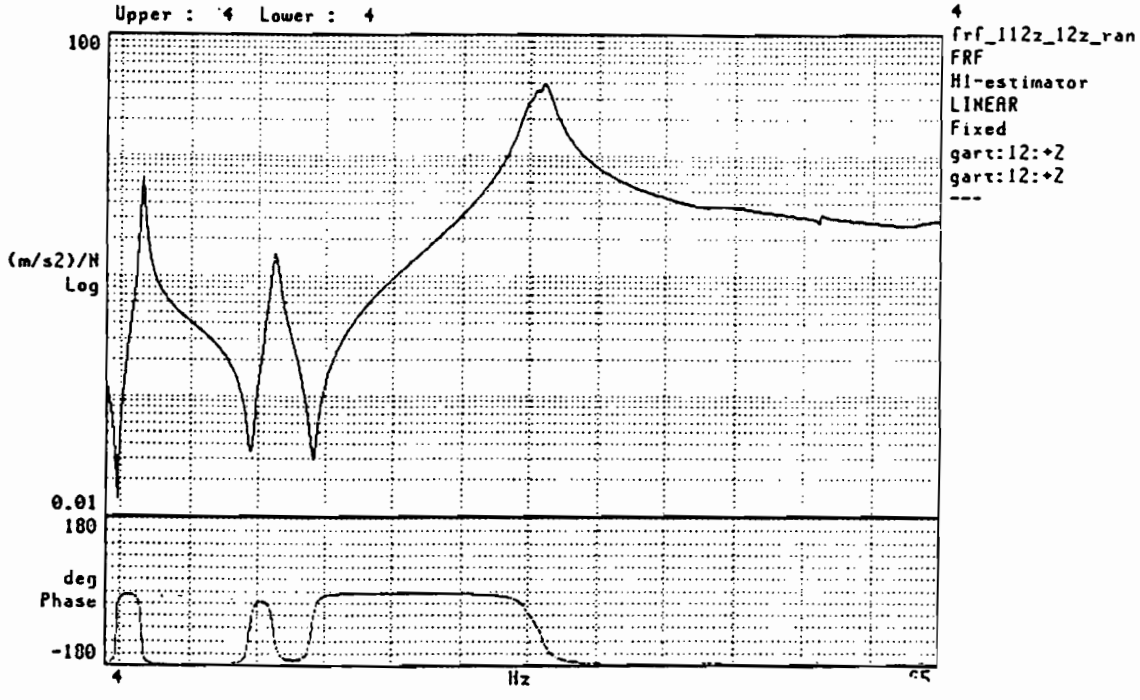

b) Driving point FRF (12/12)

Fig 6.2 Transfer functions measured with uncorrelated noise at position 112 and 12 (z-direction) -Concluded-

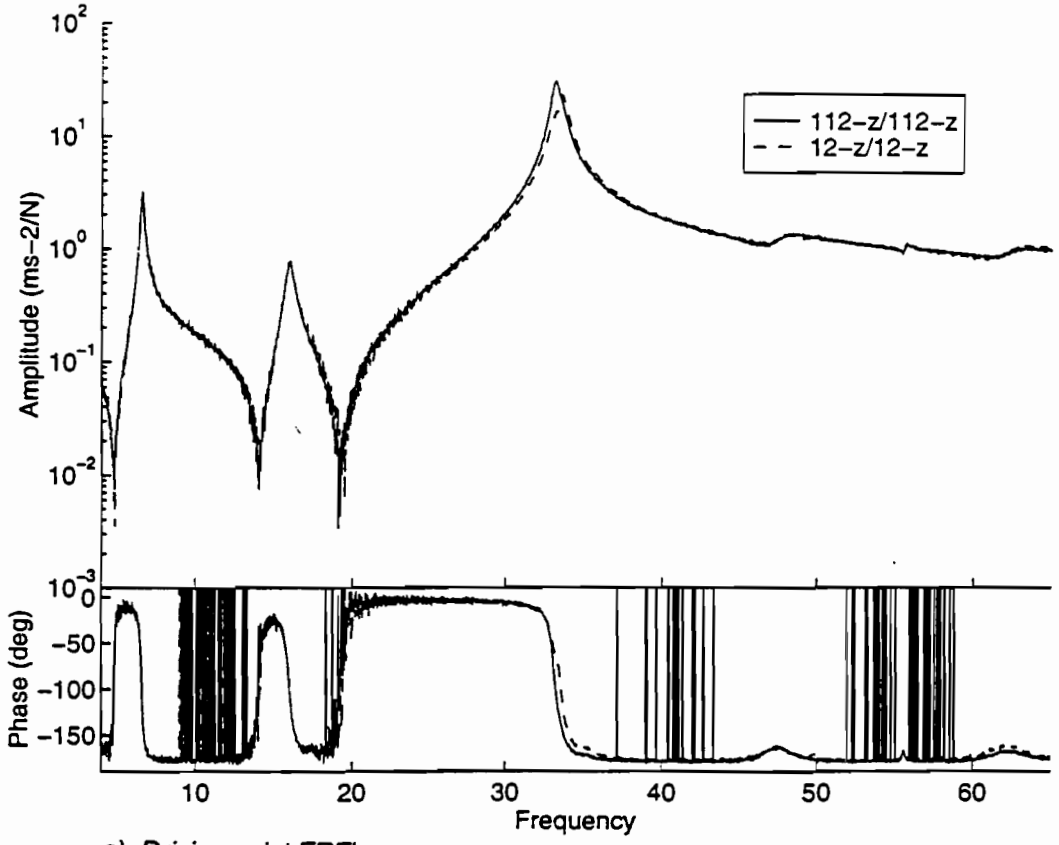

a) Driving point FRF's

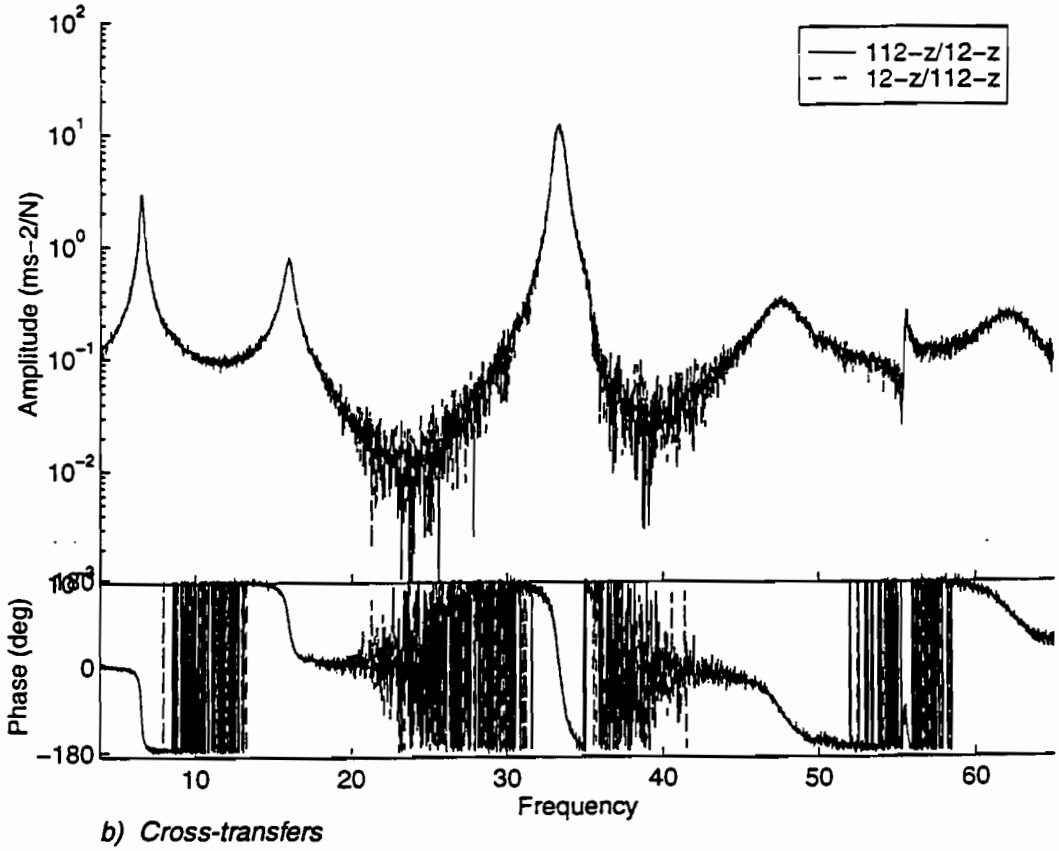

b) Cross-transfers

Fig. 7 Transfer functions measured by ONERA (Uncorrelated noise, position 112 and 12)

Annex 5

IMPERIAL COLLEGE CONTRIBUTION

MODAL TESTING ON GARTEUR SM-AG19 TEST BED

W Liu , D A Robb and D J Ewins

Dynamics Section, Department of Mechanical Engineering
Imperial College of Science, Technology and Medicine
London SW7 2BX U K

I. Introduction

The round-robin modal testing on GARTEUR SM-AG19 test bed organised by ONERA was carried out in Imperial College in August, 1995. The tasks listed in the documentation for the test were accomplished and the results are presented here for further discussion and reference. This report consists of five sections. Section II describes the system set-up, including a description of the test bed and an introduction of the excitation and measurement system. In section III the method of analysis is introduced and the experimental results are presented. Section IV demonstrates the process and results of FE model analysis, and the last section, section V presents comparisons between the different results.

II. System Set-up

The system for the test consists of three sub-systems: the test bed, excitation and measurement. The set-up for each sub-system is described individually in the following.

1). Test bed

The test bed came in two pieces, wing/drum and fuselage/tail. The connection was done through four screws with a torque of 1.6 mkg.

The structure was then suspended with three bungee cords and the hooks in the suspension connection piece were adjusted to keep the structure in a horizontal plane.

Due to the limitation of the number of available channels in the analysers, which was four for the measurement system, the condition of measuring at 24 points simultaneously was imitated by providing dummy masses at the corresponding points. Each dummy mass possesses the same weight as a common accelerometer used, i.e. 18 grams.

The two reference compliment masses were not used.

The set-up of the model is demonstrated in Fig. 1. and Fig. 2.

2). Excitation

The model was excited by both stepped sine sweep and random force. The random signal generated by SOLARTRON 1220 analyser and stepped sine sweep signal generated by SOLARTRON 1254 were used to drive a shaker through a power amplifier. A single shaker used here to excite the structure at the coordinate 112z has the specification:

TYPE	V400
MOVING MASS	200 g
SUSPENSION STIFFNESS	12.3 N/mm.

A push-rod was used to connecte the shaker and the structure. A force gauge screwed at one end to the top of the push-rod was screwed at the other end to an aluminium nut which was stuck right at the point 112z (under the drum front tip) by super glue. The mass of the push-rod and force gauge together is 37 grams.

The assembly of the excitation sub-system is shown in Fig. 3.

3). Measurement

The analyser of SOLARTRON 1220 (4 channels) was employed to measure FRFs of the test bed for random test and the analyser of SOLARTRON 1254 (4 channels) was employed for sine-sweep test. The accelerometers used were B&K's with the sensitivity:

Series No.	4383-293(ch. 2)	4382-611(ch. 3)	4383-088(ch. 4)
Sensitivity	3.20 pC/ ms^{-2}	3.25 pC/ ms^{-2}	3.10 pC/ ms^{-2}.

Force gauge was B&K 8200, Sensitivity 4.00 pC/N;

Charge amplifiers were B&K 2626.

The system was calibrated before test, using a 10 kg mass block.

The complete measuring system was set up and examined by testing the reciprocity. The reciprocity test result is shown in Fig. 4 and Fig. 5 in the form of amplitude/phase.

III. Result

The measured FRFs were analysed using GLOBAL-M in MODENT of ICATS (Imperial College, Analysis, Testing and Software).

GLOBAL-M is based on a complex SVD of a system matrix expressed in terms of measured FRF properties and then on a complex eigensolution which extracts the required modal properties. An advantage of GLOBAL-M lies in its ability to detect very close modes.

The result required, including natural frequencies, damping (in the form of loss factors) and mode shapes are shown in Fig. 6 through Fig. 10.

IV. Finite element model analysis

A finite element model given in the test documentation was analysed using ANSYS5.0. The structure of the test bed was modelled using simple beam elements (BEAM4) which is acceptable in the sense of engineering.

It is noticeable that the result produced by ANSYS5.0 is different from that obtained using MATLAB structural dynamics toolbox, which was given in the test documentation, even though the input data were exactly the same. Table 1 shows the results.

In the discussion of the next section, It will be indicated that the FE result produced by ANSYS5.0 is better than that produced by MATLAB toolbox by calculating MAC values (modal assurance criterion) of the FE results versus experimental results. Therefore, the FE analysis for the other test bed set-ups were carried on by using ANSYS5.0.

Table 1: Natural frequencies and mode shape description of two FE results

MATLAB	ANSYS5.0	Mode shape
6.02	6.014	Two node bending
13.16	12.933	Global fuselage rotation
32.54	31.473	First symmetric wing torsion
33.40	33.000	First antisymmetric wing torsion
35.58	34.060	Three node bending
47.57	47.291	Four node bending
---	49.526	Fuselage swinging in plane
55.09	55.603	Symmetric in plane bending
57.09	61.775	Second fuselage rotation mode
66.30	63.563	Tail torsion
69.79	---	Five node bending
---	95.542	Tail bending

V. Discussions on the results

a. Comparison with SOPEMEA Results

The SOPEMEA results, two sets of FRFs and one set of modal data, came with a document describing the reference results. It is noticeable that some differences exist between the test models that we set up here and that SOPEMEA used.

1. The test bed we used had no any reference compliment mass mounted at the two drum tips because it was mentioned in the test instruction (page 4, section 3.2: Packing List) that 'these masses should be used for hammer testing'. SOPEMEA's test bed had these two masses mounted at the two drum tips, and each of them weights 76g to make up the 200g moving mass.

2. We measured excitation force using a force gauge, which was screwed at the drum tip and connected to a shaker through a threaded rod. Therefore, the moving mass (moving mass of shaker and the mass of connections) had no effect to the structure. While SOPEMEA did not use a force gauge and the mass linked to the excitation (124g) might cause the change of the natural characters of the structure.

Due to the differences in the set up of the test bed, the results that we obtained are quite different from that of SOPEMEA. Table 2 shows the comparison of natural frequencies and Table 3 demonstrates the comparison of damping parameters.

Cases A, B and C correspond to (A), the results in this report, (B), the results of SOPEMEA, and (C) the results of mis-assembled test bed mentioned in Appendix A. Case D

was obtained from the two sets of FRFs given by SOPEMEA by analysing them using ICATS modal analysis system.

The presented damping parameters of case B are viscous damping ratio, and the damping parameters of A, C and D are loss factors of structural damping model.

The mode shape comparisons expressed using MAC between A and B is shown in Fig. 11. MAC between B and C is shown in Fig. 12.

b. Comparisons between FE model analysis and experiments

Three cases were carried out in FE model analysis using ANSYS5.0. Each of them is corresponding to a case of assembly of the test bed, A, B and C as mentioned above. To make the description clear, the definition of each case is listed as follow:

case A: a correct assembly without the two supplement masses;
case B: a correct assembly with the two supplement masses;
case C the wings were assembled in the way around with the two supplement masses.

For each case, the natural frequencies of FE model and experiment as well as MACs are presented from table 4 to table 6. The MAC values are expressed by set 1 versus set 2, where set 1 and set 2 are FE modes and test modes respectively.

The best correlation between test and FE modal analysis is in case B(table 4).

The MAC values of mode 4 and 5 in case A (table 5) are low, 52.2% and 17.7% respectively. This unsatisfactory is believed due to the test error because only one shaker was used here rather than two shakers used in case B. One single shaker exciting the structure at one end of the wing resulted in that the response level at the other end (drum tips) apart from the excitation side was much lower.

The poorest MAC values exist in case C (table 6), where the values of MAC are 0.2 and 0.3 for mode 6 and 7 respectively. The most significant difference of natural frequency exist at mode 6 as well. The reason is still unclear.

Table 2. Comparison of natural frequencies (Hz)

No.of mode	case A	case B	case C	case D
1	6.623	6.974	6.278	6.988
2	16.210	16.079	15.946	16.386
3	35.420	33.862	32.134	33.700
4	37.177	33.938	32.490	33.849
5	37.464	34.915	35.652	35.496
6	48.421	46.080	35.714	47.508
7	50.712	48.620	48.821	50.462
8	57.054	53.580	54.671	56.690
9	63.452	61.140	62.700	
10	64.829			

Table 3. Comparison of damping parameters

No.of mode	A	B	C	D
1	.295000E-01	1.27000e-02	.191000E-01	.246000E-01
2	.266000E-01	1.36000e-02	.240000E-01	.319000E-01
3	.173000E-01	1.47000e-02	.218000E-01	.235000E-01
4	.195000E-01	1.16000e-02	.214000E-01	.287000E-01
5	.970000E-02	1.11000e-02	.174000E-01	.224000E-01
6	.438000E-01	2.58000e-02	.137000E-01	.456000E-01
7	.640000E-02	9.10000e-03	.780000E-02	.141000E-01
8	.260000E-02	5.60000e-03	.170000E-02	.062000E-01
9	.383000E-01	2.06000e-02	.357000E-01	
10	.132000E-01			

Table 4. Comparison between FE model analysis and experiment results of case A

Mode	fr (Hz)		MAC values(%)									
No.	FE	Test (A)		→ *set 1(FE)*								
1	6.317	6.623		**99.6**	0.0	0.0	0.0	0.0	14.7	0.0	0.0	0.0	0.0
2	13.109	16.210		0.0	**97.6**	2.3	0.0	0.0	0.0	0.0	0.0	41.2	0.2
3	32.788	35.420		0.0	1.8	**80.4**	2.3	5.2	0.2	12.7	0.0	2.8	0.0
4	40.276	37.177		0.0	0.0	0.1	**52.2**	47.3	0.2	0.0	0.1	0.0	0.0
5	40.341	37.464		2.7	0.5	12.3	26.9	**17.7**	10.3	4.4	0.0	12.5	0.0
6	47.487	48.421		18.0	0.1	0.0	0.1	0.2	**86.9**	0.0	0.0	0.0	0.0
7	51.030	50.712		1.2	0.9	10.2	1.0	0.1	2.1	**91.4**	0.8	2.7	9.6
8	58.790	57.054	↓	0.0	0.0	0.1	0.0	1.0	0.1	0.8	**95.0**	0.1	0.1
9	62.372	63.452	*set 2*	0.4	24.8	7.5	0.0	0.0	0.2	7.9	0.1	**94.3**	23.6
10	63.637	64.829	*(test)*	0.0	0.1	0.6	0.0	0.0	0.0	8.2	0.0	16.6	**98.2**

Table 5. Comparison between FE model analysis and experiment results of case B

Mode No.	fr (Hz) FE	fr (Hz) Test (B)	MAC values(%) → set 1(FE)								
1	6.014	6.974	**99.6**	0.0	0.0	1.7	0.0	12.3	0.0	0.0	3.0
2	12.933	16.079	0.0	**97.2**	0.3	0.0	0.6	0.0	0.2	0.0	46.0
3	31.473	33.862	0.0	0.5	**76.5**	2.6	69.6	0.4	0.0	0.0	3.9
4	33.000	33.938	0.6	0.0	0.4	**97.5**	0.7	12.9	0.0	0.1	0.0
5	34.060	34.915	0.0	0.1	1.5	0.0	**59.4**	0.0	14.1	0.0	10.9
6	47.291	46.080	19.3	0.0	0.0	1.8	0.0	**95.4**	0.1	0.0	0.0
7	49.526	48.620	*set 2* 0.3	0.1	1.6	0.0	8.7	1.3	**96.3**	0.0	0.3
8	55.603	53.580	*(test)* 0.2	0.0	0.0	3.2	0.0	2.0	0.0	**95.1**	0.0
9	61.775	61.140	0.0	43.1	0.4	0.0	2.4	1.0	5.4	0.0	**92.7**

Table 6. Comparison between FE model analysis and experiment results of case C

Mode No.	fr (Hz) FE	fr (Hz) Test (C)	MAC values(%) → set 1(FE)								
1	5.988	6.278	**99.2**	0.0	0.0	1.5	0.0	10.2	0.0	0.0	0.1
2	12.941	15.946	0.0	**87.1**	0.7	0.0	1.6	0.0	1.8	0.0	42.4
3	31.426	32.134	0.0	0.8	**68.0**	0.1	81.4	0.0	0.0	0.0	5.7
4	33.065	32.490	1.4	0.0	0.7	**95.5**	1.3	17.0	0.0	0.1	0.2
5	34.023	35.652	1.1	1.2	0.1	1.6	**57.1**	0.1	36.7	0.1	0.0
6	47.238	35.714	6.8	8.8	19.6	5.5	0.8	**0.2**	0.2	0.4	44.3
7	49.270	48.821	*set 2* 0.9	5.1	11.7	0.1	3.3	3.0	**0.3**	0.0	0.1
8	55.603	54.671	*(test)* 0.6	0.0	0.0	2.5	0.0	2.3	0.1	**85.5**	0.1
9	61.945	62.700	0.1	30.9	0.7	0.0	4.7	0.1	1.0	0.0	**89.7**

Appendix A. Results of mis-assembled test bed

The wings of the test bed was assembled at first in the way around by mistake (Fig. 13). Tests on the mis-assembled test bed were accomplished using both sine-sweep and random excitations with the two reference compliment masses of 200 grams each at the tips of the drum. All dummy masses were used and the set-up of the excitation and measurement systems were the same as mentioned above.

The figures in this appendix (Fig. 14 to Fig. 18) present the modal data in the case of random excitation.

The result of sine-sweep is almost the same with that of random excitation. However, they are not comparable due to the fact that the signs of FRFs at 12x, 5x, 105x and 112x obtained using sine-sweep are opposite to those obtained using random excitation.

Appendix B. Discussion on the effect of moving mass

The concept of *moving mass* mentioned in the test instruction is ambiguous. So called *moving mass* here, which consists of the mass of accelerometer, force gauge, push rod as well as the moving part of the shaker, has no effect at all on the testing result using the measurement set up mentioned in section I. If the input force was derived from measuring input current to the shaker, case is different. The *moving mass* is required in the deriving process as an important parameter. Actually, measuring input force directly using force gauge is more precise and practical.

To investigate the effect of *moving mass*, hammer test was carried out at some measured points of the test bed. It shows that natural frequencies obtained either from hammer test or sine-sweep have no obvious differences. For instance, the most sensitive mode to this *moving mass* is 6.597 Hz obtained from hammer test (without the two reference complement masses) while it has the value of 6.6094 Hz from sine-sweep and 6.6099 Hz from random test respectively.

Fig. 1 Set-up of the test bed

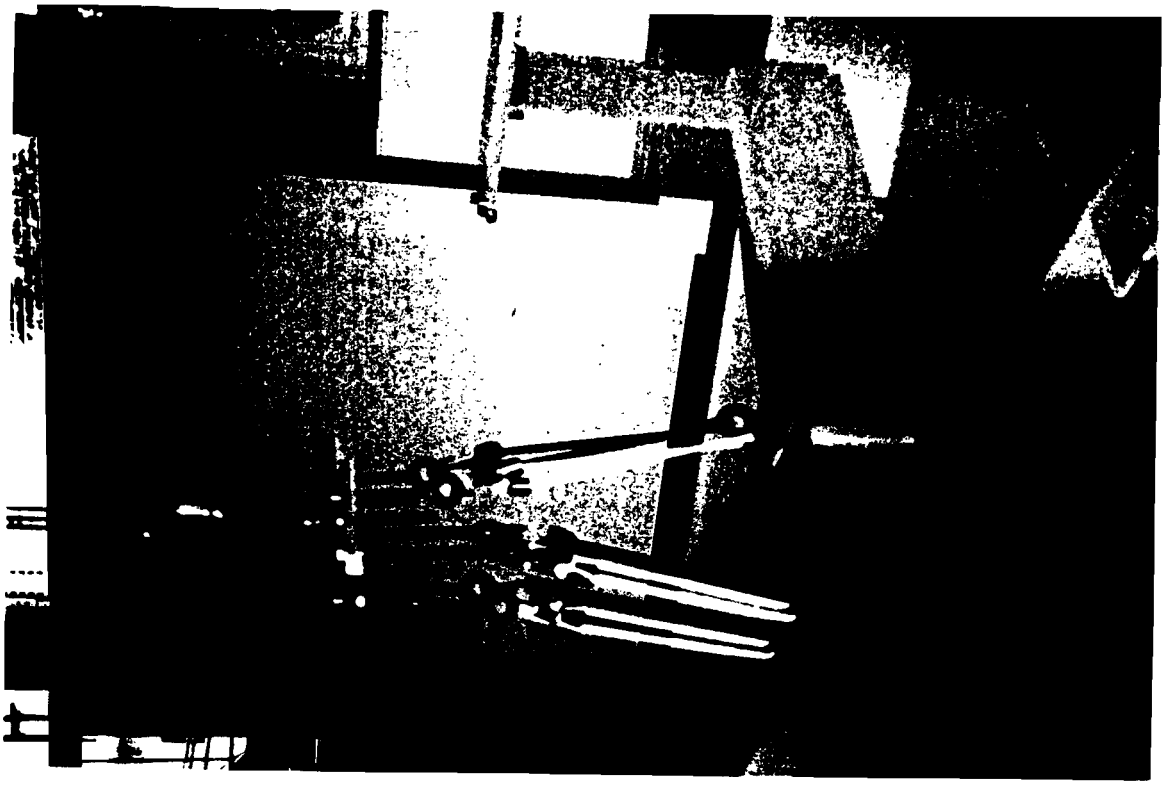

Fig. 2 Set-up of the test bed

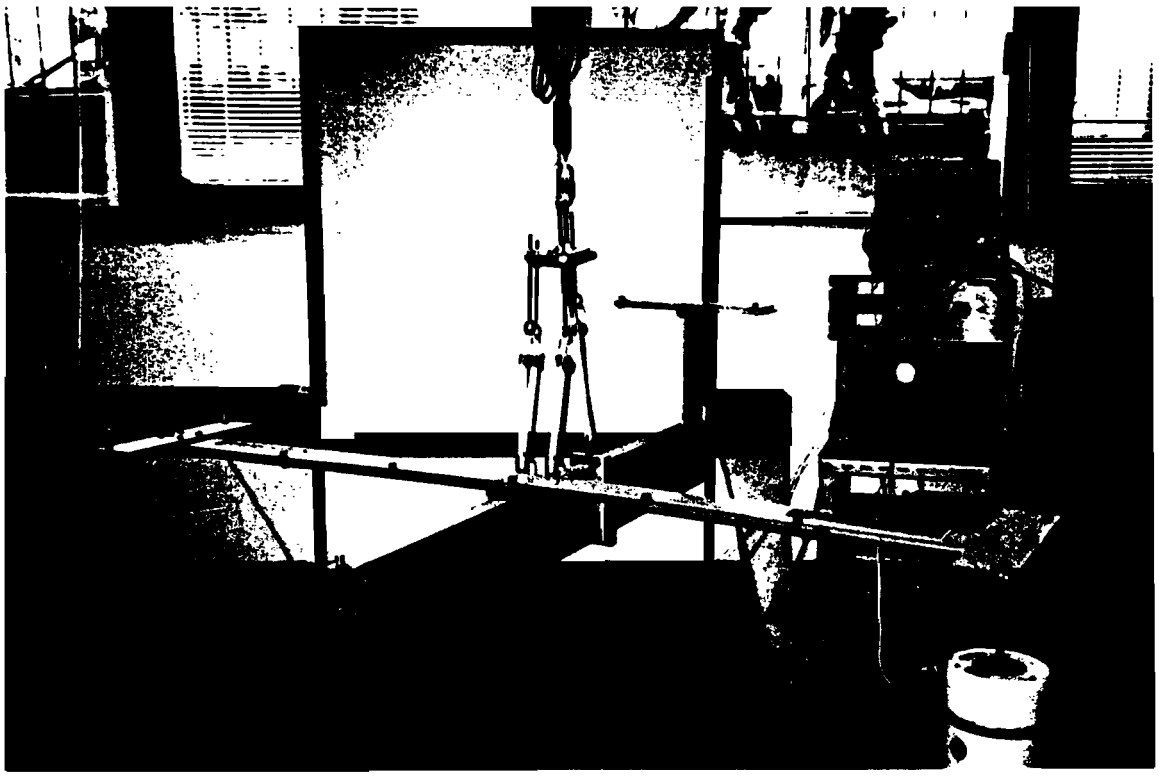

Fig. 3 The assembly of the excitation equipment

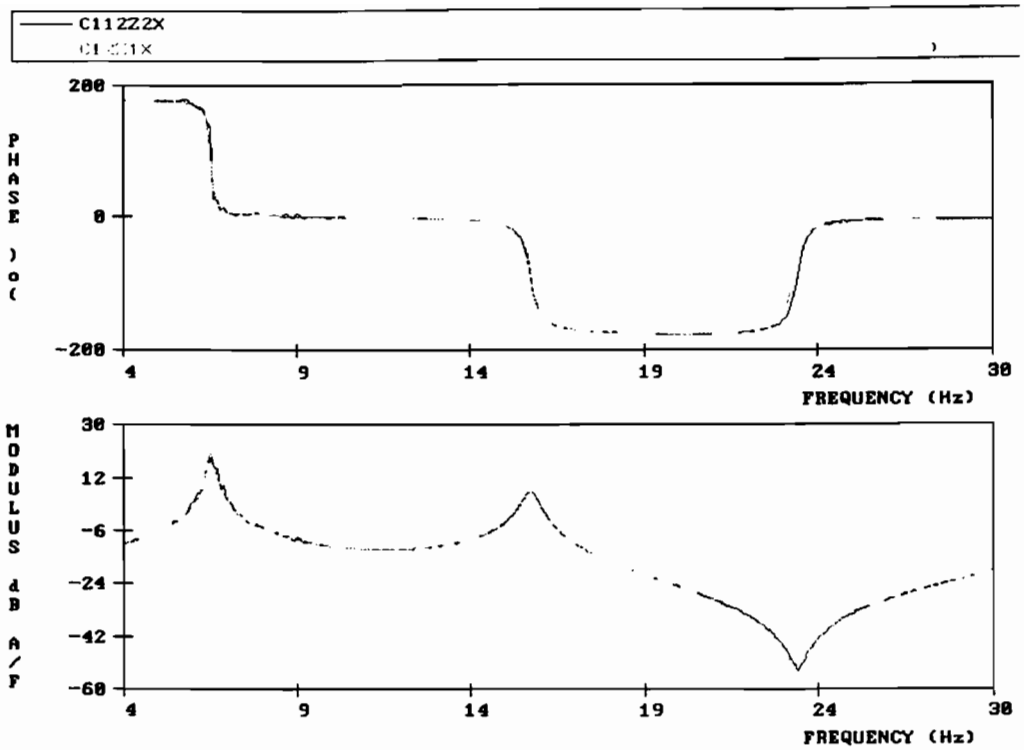

Fig. 4 Reciprocity test FRFs overlaid of case A (4 ~ 30 Hz)

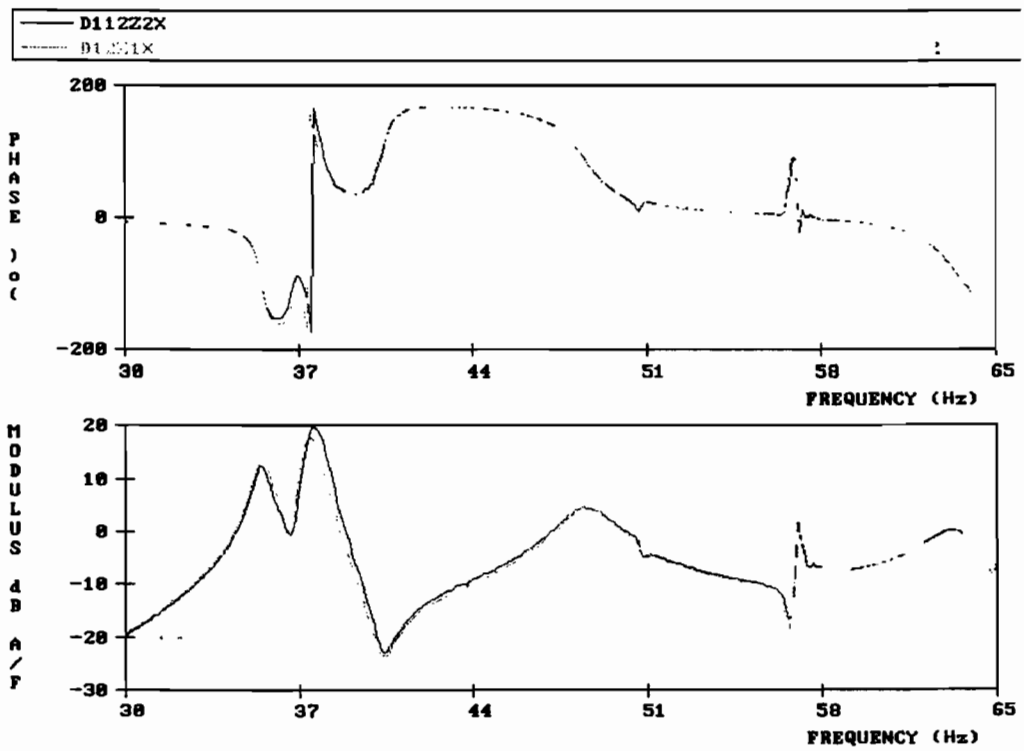

Fig. 5 Reciprocity test FRFs overlaid of case A (30 ~ 65 Hz)

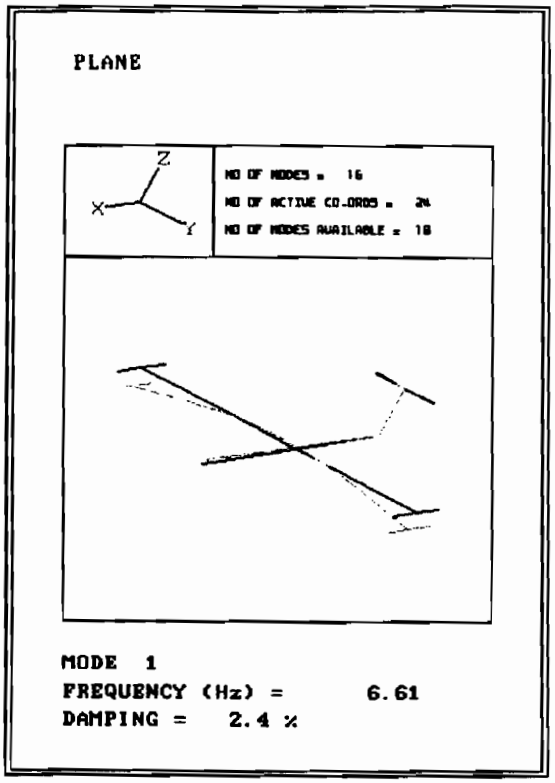

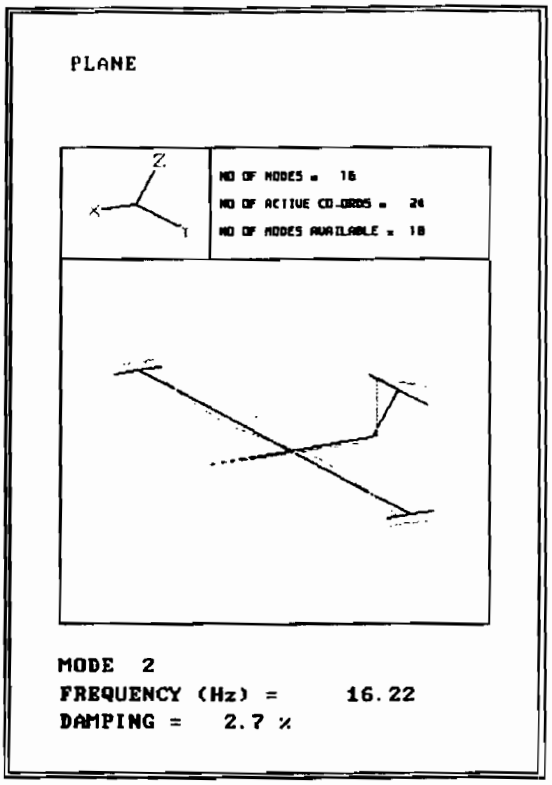

Fig. 6 Modal test result of case A: mode 1 and mode 2

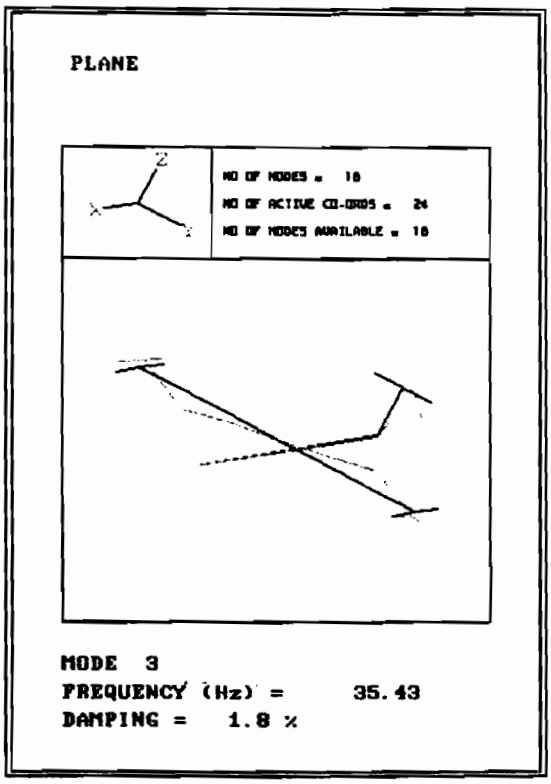

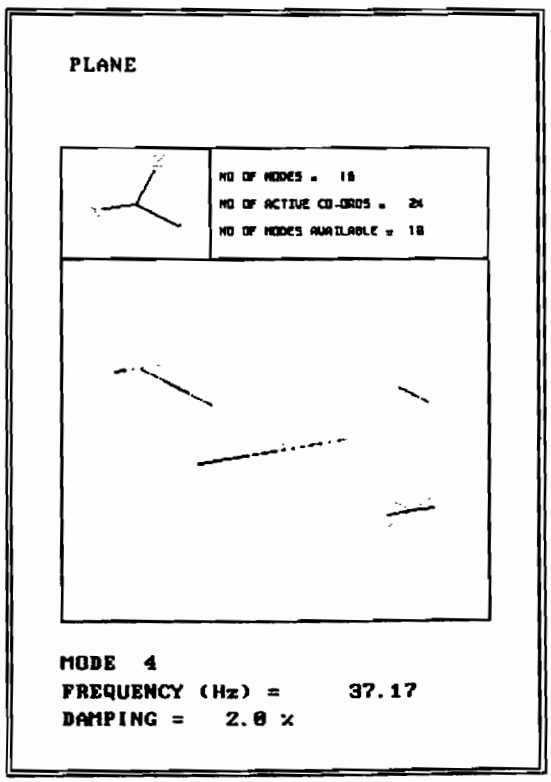

Fig. 7 Modal test result of case A: mode 3 and mode 4

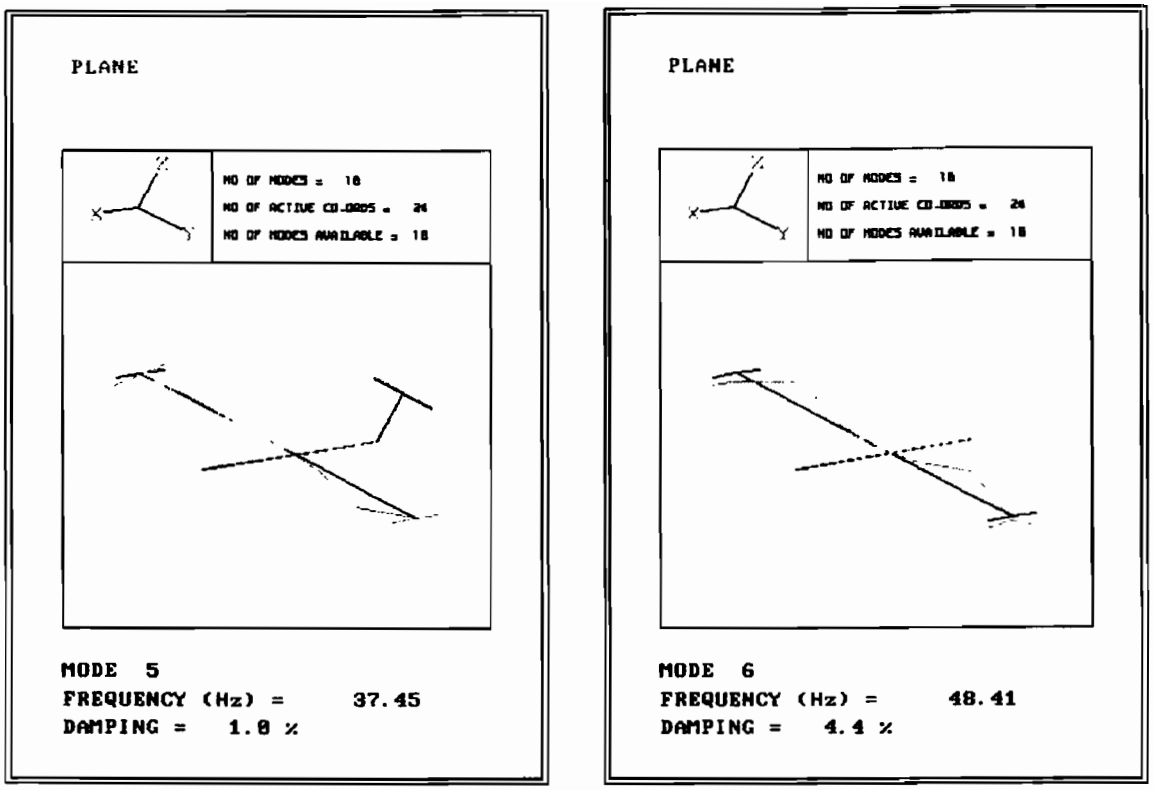

Fig. 8 Modal test result of case A: mode 5 and mode 6

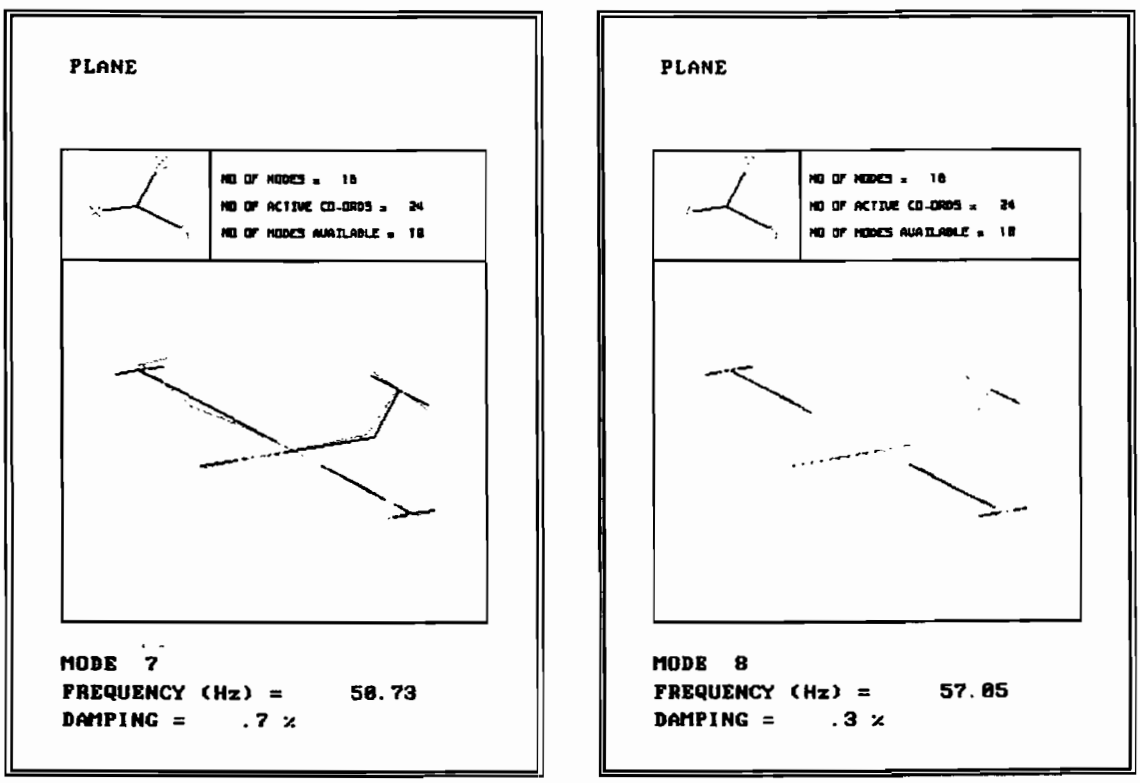

Fig. 9 Modal test result of case A: mode 7 and mode 8

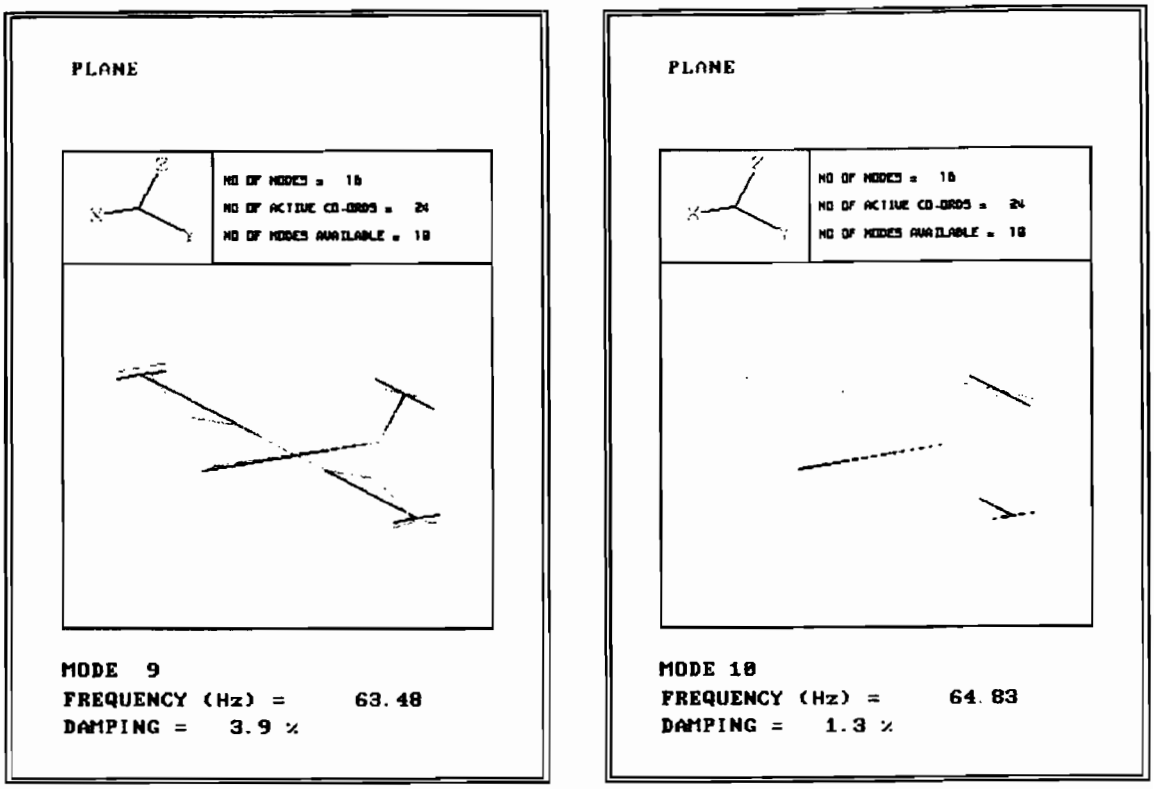

Fig. 10 Modal test result of case A: mode 9 and mode 10

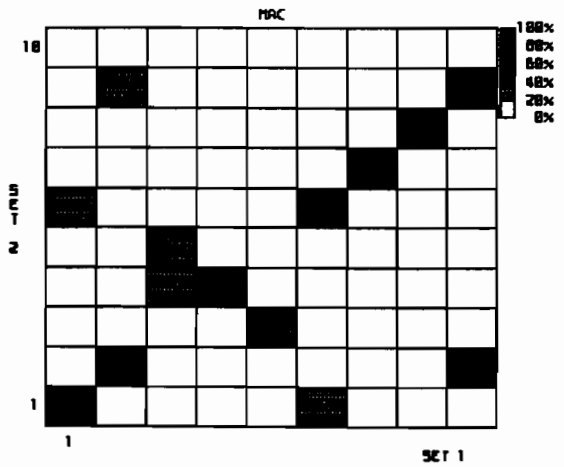

Fig. 11 MAC between case A and case B

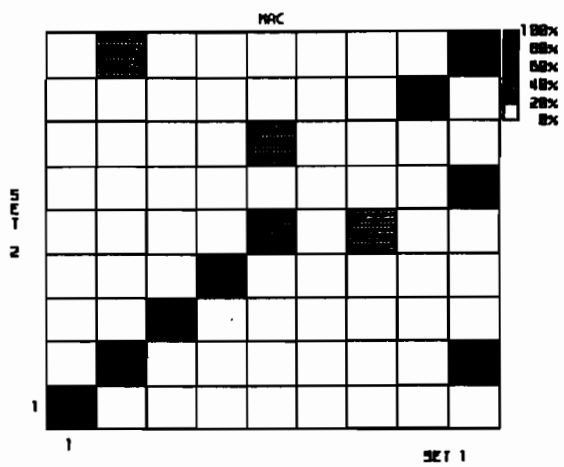

Fig. 12 MAC between case B and case C

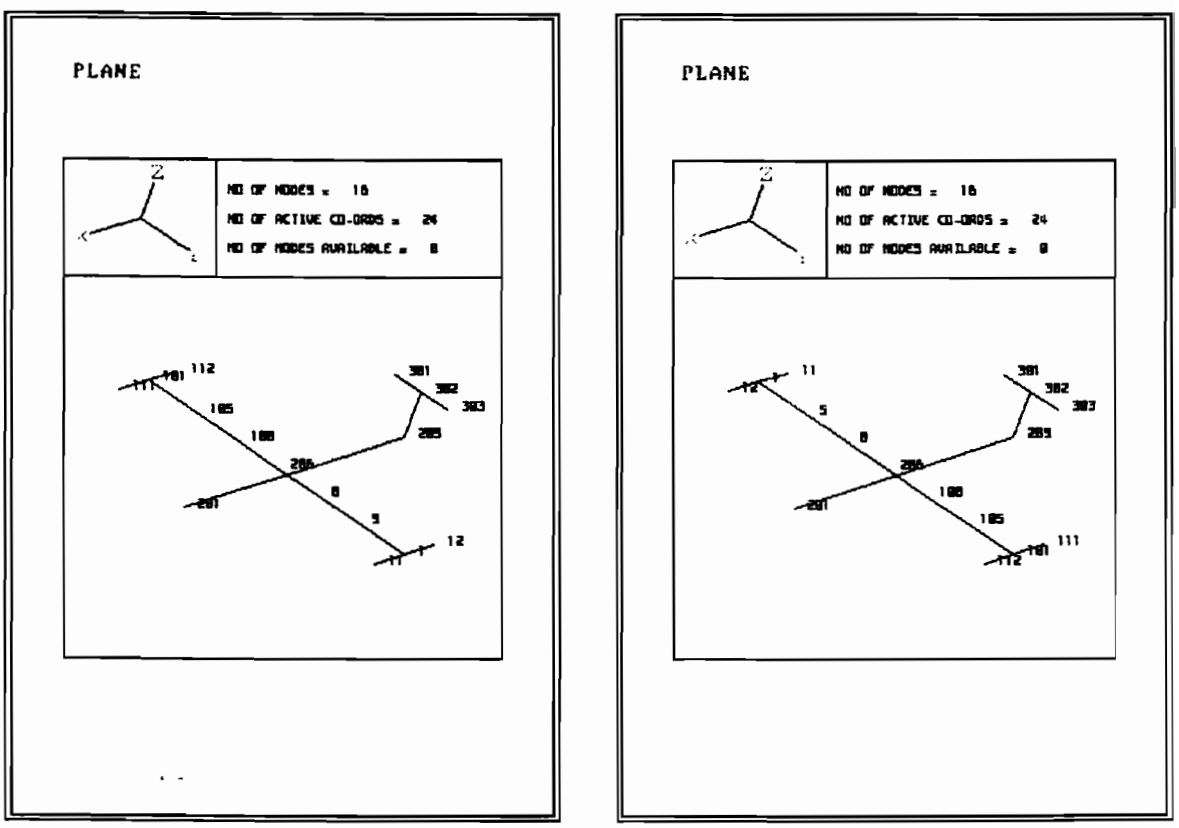

Fig. 13 Left: Mis-assembled test bed (case C) and right: correct assembly (case A)

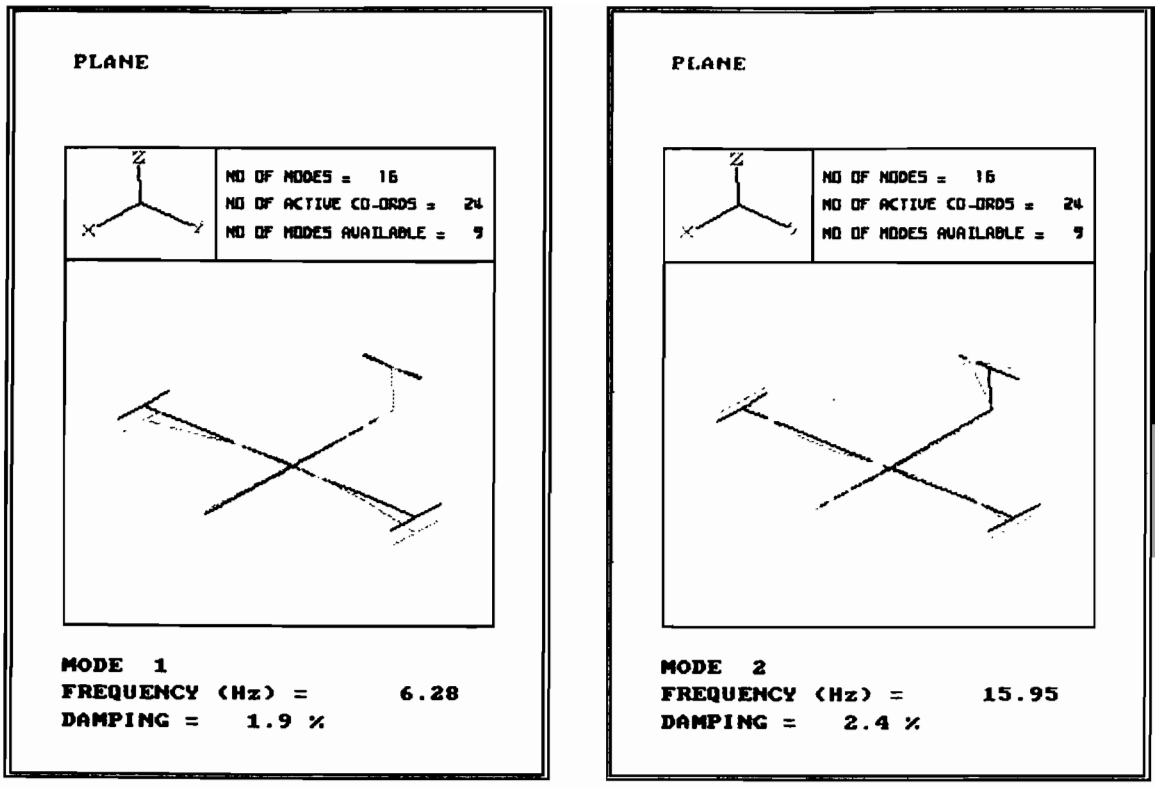

Fig. 14 Modal testing result of case C: mode 1 and mode 2

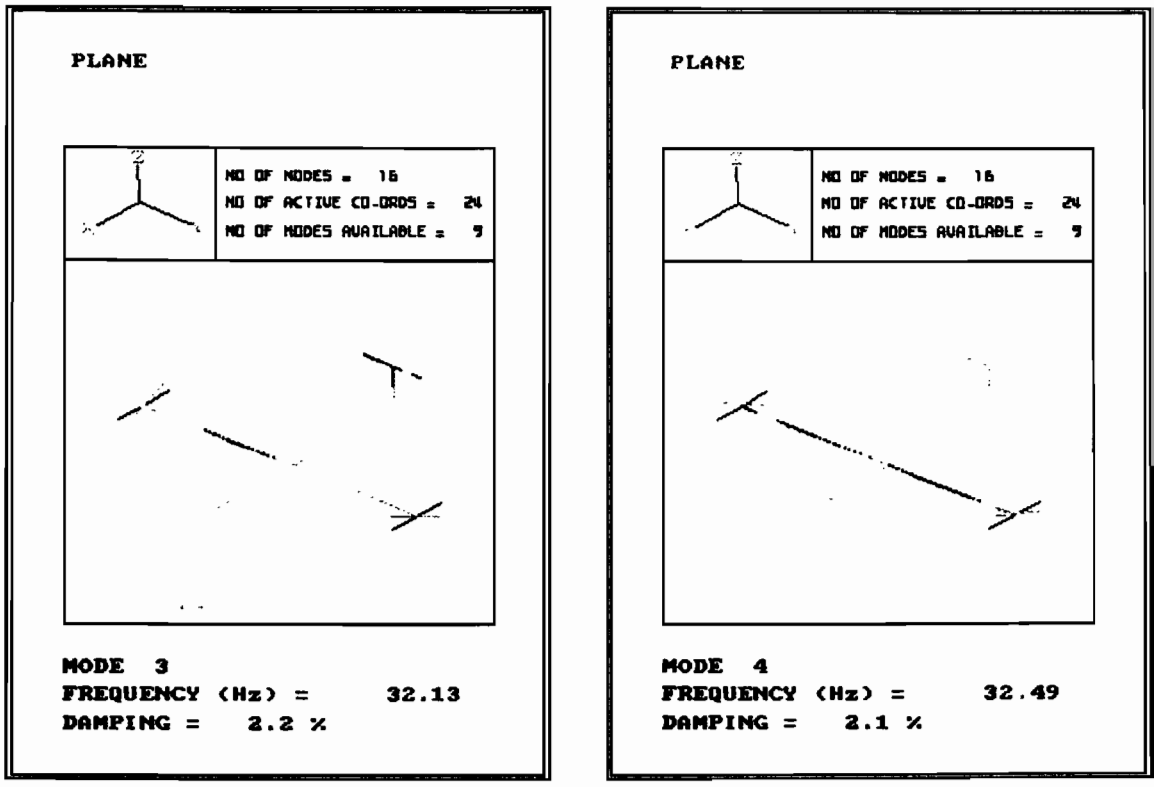

Fig. 15 Modal testing result of case C: mode 3 and mode 4

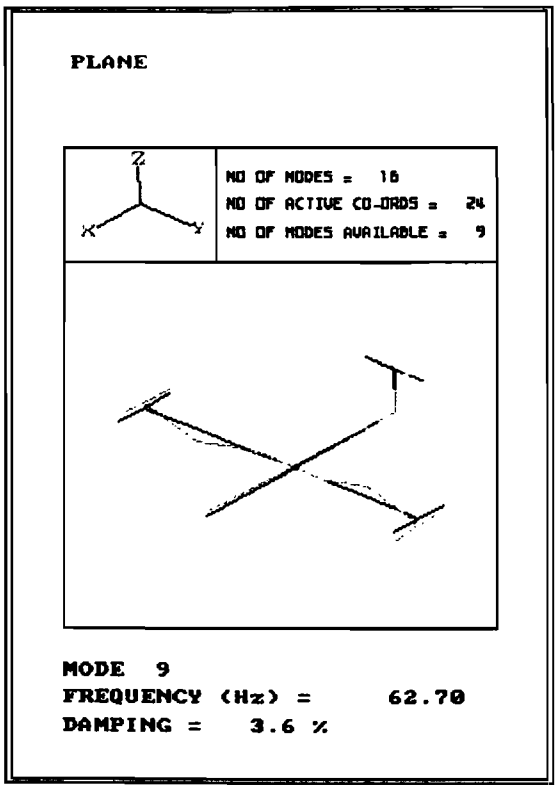

Fig. 18 Modal testing result of case C: mode 9

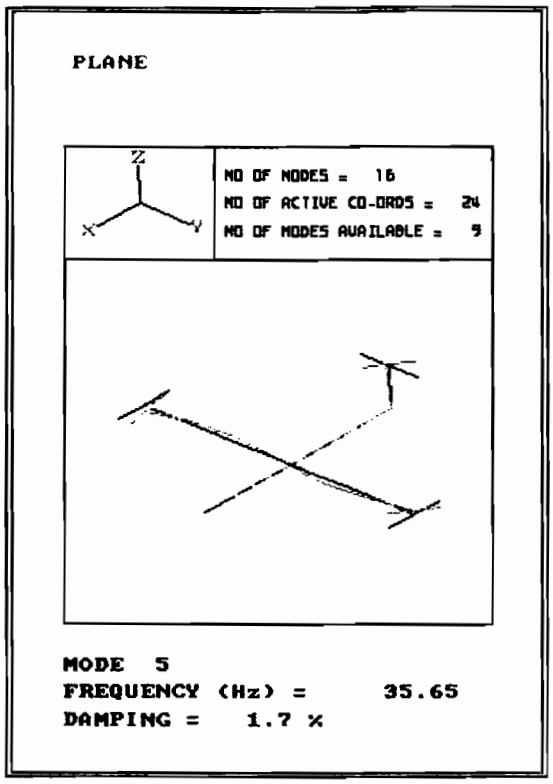

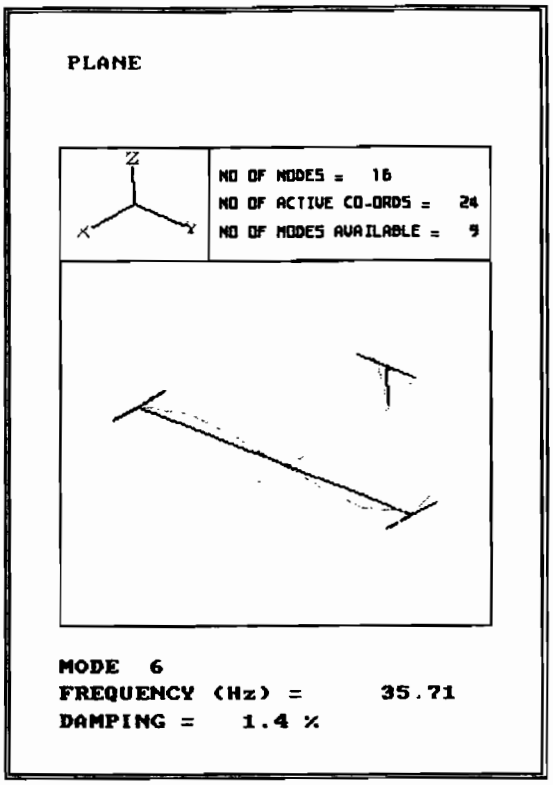

Fig. 16 Modal testing result of case C: mode 5 and mode 6

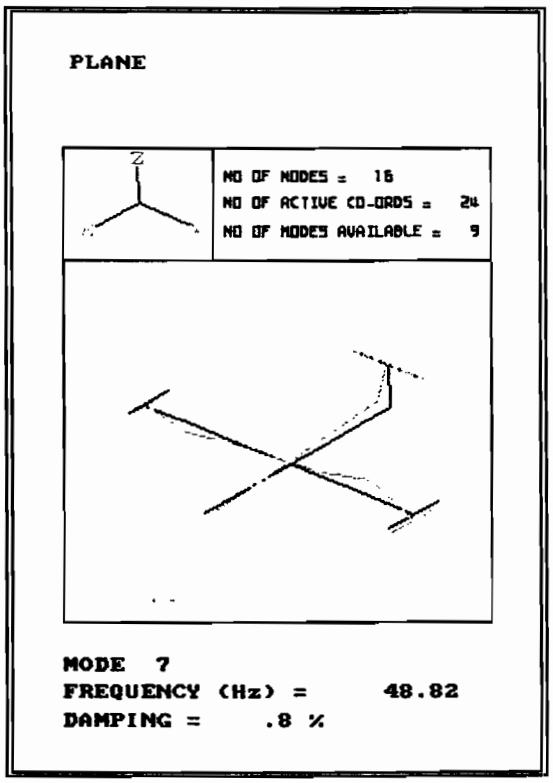

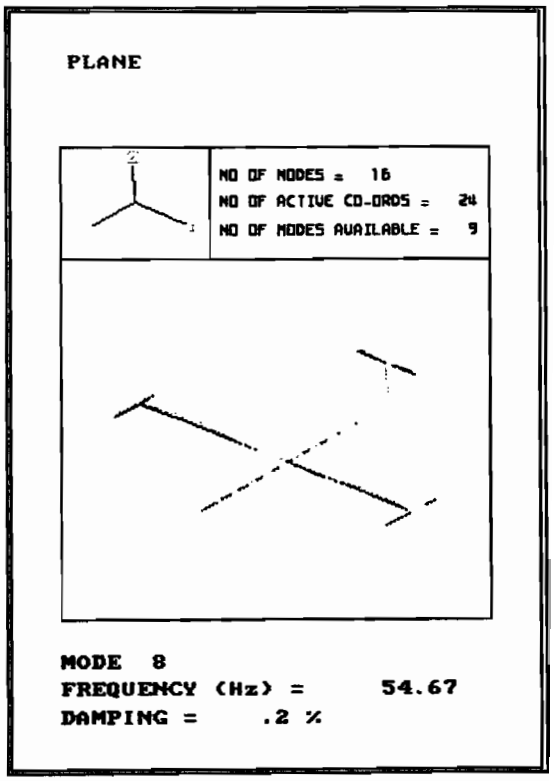

Fig. 17 Modal testing result of case C: mode 7 and mode 8

Annex 6

DRA CONTRIBUTION

Measurement and Analysis of Vibration Test Data for the GARTEUR SM-AG19 Testbed

DRA/AS/ASD/TR96062/1

Cover + iii + 90 pages

June 1996

DRA

Defence Research Agency
Farnborough
Hampshire
GU14 6TD

Authorisation

Prepared by	Graham Skingle
Title	
Signature	G.W. Skingle.
Date	26/06/96
Address	DRA Farnborough
Telephone	01252 395629
Authorised by	Dr. M Nash
Title	Technology Leader (Structures)
Signature	M. Nash.
Date	26/06/96

Principal Authors

Name	Graham Skingle
Appointment	
Location	DRA Farnborough
Telephone	01252 395629

Executive summary

This report is an account of the measurement and analysis of vibration test data for the GARTEUR SM-AG19 testbed structure carried out at the DRA in Farnborough. The experimental set-up of the model and the dynamic testing performed are described in detail. The results from several tests are presented and discussed. Theoretical predictions of the effects of a simple modification are shown to agree well with that actually measured.

Some results from SOPEMEA for tests on the same model have been included. A brief comparison of the DRA results with those from SOPEMEA has been made. The two sets of results had a reasonable level of agreement.

List of contents

1. Introduction

As part of the certification procedure for all new aircraft, and indeed, major modifications to existing aircraft, vibration tests are required to provide data used in assessments of the aeroelastic stability of the aircraft. Ground Vibration Tests (GVTs) as the tests are commonly known, can be extensive and costly to perform. For this reason, the amount of testing is kept to a minimum. It is rare for GVTs to be repeated by another independent group as a check on the quality and validity of the measured data. It is important to distinguish between the terms 'quality' and 'validity'. A measured data set may be of exceptionally high quality, but be completely invalid because of some systematic error in the test set-up. Systematic errors may not come to light unless tests are performed by a completely independent group, using a different set of equipment and analysis methods.

The purpose of this GARTEUR Action Group was to assess the variability in the measurements and analysis results for a single structure passed to a number of participants throughout Europe.

Some considerable thought was devoted to the design of the testbed structure in an attempt to highlight potential difficulties in the test and analysis methods to be used; several closely spaced modes was one criterion in the design. A practical limitation on the size of the model was that it should be relatively easy to transport between the participants with a minimum of assembly and disassembly. In the resulting testbed structure there were only two separate parts; a wing component and a fuselage component, see Figure 1. The joint between these components was designed to try and ensure that the coupling conditions were repeatable between different tests and when assembled by different participants. Tests were undertaken to prove the repeatability of assembly before the structure was released to the participants.

Another obvious source of discrepancies between the tests of different participants was identified as the method of suspension of the structure. For this reason, a simple suspension system was devised and supplied as part of the testbed kit. Tests were also undertaken to prove the repeatability of the suspension set-up before release of the structure.

All measurement locations were defined in the documentation and etched into the model itself. The attachment of transducers and excitation systems was left to the participants.

This page intentionally blank

2. Receipt and Set-Up of GARTEUR Model at DRA Farnborough

Upon receipt of the model, the component parts were removed from the transport box and inspected. Wax, double-sided tape and excess glue (used for the attachment of transducers) were cleaned off the component parts, together with some old excitation attachment blocks. The wing to fuselage attachment plates were degreased and cleaned. There was some evidence of edge damage to these plates where 'implements' had been used to separate them.

The model was then assembled. A torque of 1.6 m/kg was specified in the documentation for the wing to fuselage bolts. This torque figure was taken to mean 1.6 kgm, that is 15.7 Nm. Despite the fact that this was a very small torque, the bolts were tightened to this value. A spring balance and socket wrench were used to tighten the bolts. The nuts were too close to the fuselage to allow the use of a ring spanner or a socket. Therefore, the torque was applied to the bolt heads via an Allen key adapter for the socket wrench.

A small aluminium excitation attachment block (3.2 g) was bonded (using Rapid Araldite) beneath each wing tip at the points defined as 12:Z and 112:Z. Scribed crosses marking the response measurement points were extended with pencil lines. Double sided (Tessa) tape pieces were then placed over the scribed transducer location points and pressed firmly onto the structure.

At this point, the complete model (without transducers, or suspension system) was weighed using a balance beam. The model was found to have a mass of 44.05 kg.

The bungee cords and suspension plate were then attached to the model and the whole structure suspended on a steel hawser 1.64 m below a gantry frame. Including the bungee suspension system, the top of the model fuselage was 2.295 m below the point of attachment to the gantry, Figure 2. Originally, it had been proposed that each participant should use a new set of bungee suspension cords. However, there were no new bungees in the transport box and the set previously used by NLR have been re-used for these tests.

When not connected to the shakers, the model was supported on a wooden block, thereby unloading the bungee suspension cords. This was done in an attempt to prevent long-term creep of the bungee throughout the duration of the test period.

The effect of the constrained damping layer on the model wing was quite obvious. When the wing was tapped, it sounded dull and did not ring. In contrast, when the tailplane, which did not have any damping treatment, was struck it sounded bright and rang for a considerable time.

As part of the basic documentation, details were given of a finite element model of the testbed structure. This model was reproduced in NASTRAN, see Appendix A. The mass of the NASTRAN model was 44.55 kg, which compared very well with the measured value for the actual structure (44.05 kg). Results from the finite element analysis were useful in showing modes of the structure not excited particularly well when using two shakers acting in the vertical direction at the wing tips.

This page intentionally blank

3. Experimental Equipment and Test Set-Up

3.1. Measurement of Responses

In total, 26 Entran EGA 125F accelerometers were used for measurement of the responses at the defined points on the model. Another single accelerometer was attached to the suspension plate to check for any troublesome suspension modes. The measurement locations and directions can be seen in Figure 3. All the accelerometers were attached to the structure using double-sided 'Tessa' tape. Each accelerometer wire was taped to the model close to the transducer and then taken away, suspended on strings, to the signal conditioning equipment. Efforts were made to ensure the accelerometer wires had as little restraining effect on the model as possible. Another general photograph of the complete model set-up can be seen in Figure 4.

The accelerometer response signals were conditioned and amplified by Vishay strain gauge bridge monitoring equipment. The amplified signals were then sent to the Difa SCADAS analogue to digital converters (ADCs) as a front-end to the HP computer and LMS Cada-X software.

3.2. Measurement of Forces

PCB type 208B piezoelectric force transducers were used for measurement of the excitation forces applied to the structure. Each force gauge was mounted directly on the shaker platform, as shown in Figure 5. A wire pushrod was then used to connect each force gauge to the attachment point on the model. The force gauges were mounted 'Base' towards the model and 'Top' towards the shaker. This arrangement of the force gauges differs from that normally recommended. It is usual to mount the force gauge on the structure ('base-side' towards structure) and then to connect the top of the force gauge to a shaker with a pushrod link. The conventional arrangement was not used in this case because of concerns over the mass loading effect of the force gauge. A force gauge is constructed to have as little mass on the 'base-side' of the sensing element as possible. The 'live-side' mass is kept as small as possible to minimise the modification to the structure. However, what is minimised is the mass modification to the structure *in the sensing direction of the force transducer*. The full mass of the force transducer modifies the structure in directions perpendicular to the sensing direction. By locating the transducer on the shaker, only the pushrod and fixture mass modify the structure in all degrees-of-freedom, plus the small 'live-side' mass of the transducer in the sensing direction only. In this case, the pushrod and fixture mass was significantly smaller than the mass of the whole force transducer, so the overall modification effect was less. Furthermore, there was a much smaller difference between the modification effect in the sensing direction and that in the transverse directions. A detailed photograph of the force transducer and its connection to the model can be seen in Figure 5.

The following masses were measured for the constituent parts on the 'live-side' of the transducer sensing element;

pushrod carrier on model	3.2 g
pushrod and nuts	6.6 g
pushrod carrier on force transducer	2.0 g
live-side mass of force transducer (assumed)	5.0 g
(Total mass of force transducer = 25 g)	
TOTAL	16.8 g

As specified in the set-up documentation, wing tip 'drum' masses had to be manufactured such that the total added drive point mass was 200 g. Since the attachment bolt and nut had a mass of 15.6 g, the 'drum' masses were made to be 167.6 g.

A supplementary advantage of this arrangement of the force transducers was that the micro-dot cables (which are relatively stiff and massive compared with the Entran accelerometer wires) also had less influence on the model.

In all cases, the pushrods used were the same; 0.75 mm diameter piano wire with an active length of 95 mm.

For the majority of the tests, only two excitation inputs were used. However, some tests used three or four excitations.

The force signals were passed through PCB signal conditioning equipment to the Difa SCADAS ADCs.

3.3. Excitation of the Model

Ling V409 electromagnetic shakers were used to excite the model. For excitation in the vertical direction (z-direction) at the wing tips, the shakers were placed on stands on the floor. For tests involving excitation in the x-direction, the shakers were either placed on larger floor stands or attached to a 100 kg reaction mass and suspended from a crane. In all cases, care was taken to align each shaker perpendicular to the surface to which it was attached. The photographs in Figures 2 and 4 show two shakers set for vertical excitation at the wing tips.

The excitation signals were all generated in the digital to analogue (DAC) section of the Difa SCADAS. These signals were then fed through Kemo high-pass filters set at 2 Hz, and amplified, using DRA MAMA power amplifiers, to drive the shakers. These power amplifiers are constant current amplifiers and so provide very little inherent damping.

4. Experimental Measurement Survey

4.1. Preliminary Measurement of the Model

A series of preliminary measurements on the model was made to deduce an appropriate excitation level, burst length and the frequency resolution required for good definition of the Nyquist modal circles.

Before each test in this survey, the Vishay bridge amplifiers were balanced and then an auto-range procedure was started on all the SCADAS acquisition channels. The auto-range display was then checked to see that a significant number of 12 bits available were used in the analogue-to-digital conversion for every channel.

4.1.1. Measurement of Time Data

With a shaker attached to each wing tip and acting in the vertical direction, measurements of the response time history at each of the measurement locations were made. Burst random excitation was used and responses for two burst durations (75% and 50%) were recorded. The responses for a burst duration of 75% can be seen in Figure 6 and those for the 50% burst duration are given in Figure 7. It can be seen from these Figures that the X-direction responses are generally much less well damped than responses measured in the other directions. This is shown clearly in Figure 6 by the X-direction wing tip responses (12X and 112X) that 'ring on' well beyond the end of the acquisition block when a 75% burst duration is used. For the same burst duration responses in the Z-direction have decayed to zero before the end of the acquisition block. When a 50% burst length excitation was used, the X-direction responses (Figure 7) had almost decayed to zero before the end of the acquisition block.

From these measured responses it was concluded that the constrained layer damping treatment was effective in dissipating energy from the modes with motion predominantly in the Z-direction, but relatively ineffective for modes in the X-direction.

Although reducing the excitation burst length ensured that more of the responses had decayed to zero before the end of the acquisition block, it also reduces the 'signal-to-noise' ratio. Assuming that the noise is constant, halving the burst duration halves the signal-to-noise ratio.

4.2. Multi-Point Random Measurements using 2 Shakers

For this series of measurements, two shakers were attached to the structure to provide excitation in the vertical direction at the front of the wing tips. Based on experience gained from the preliminary measurements, a blocksize of 4096 frequency lines was used to cover a baseband frequency range up to 128 Hz. A burst random excitation strategy was selected to avoid the problems associated with the use of a Hanning window function. From the mode shapes given in the documentation, it could be seen that there were not too many modes in the X-direction, so it was decided to sacrifice the accuracy of these X-direction modes for improved signal-to-noise ratio for all the response points. An excitation burst length of 75% was used therefore, for all these measurements and 16 averages were taken.

Some typical FRFs from this test (defined as test A6) are shown in Figures 8 and 9. It can be seen that the majority of the modes are well spaced, but that there are two groups of closely spaced modes around 33 and 50 Hz. The 33 Hz group of modes was intentional, but no mention of a group around 50 Hz was given in the 'Documentation for the GARTEUR SM-AG19 Testbed'. The two reciprocal FRF terms are plotted together with their vector difference in Figure 10. This plot shows the measured reciprocity to be exceptionally good across virtually the whole of the frequency range from 4 to 80 Hz. The difference between the FRF terms is approximately an order of magnitude less than the FRFs themselves everywhere except at the anti-resonances.

Measurements were also made using half the nominal excitation level to provide a crude indication of any non-linear behaviour of the structure (test A8). The two point FRFs are shown in Figure 11 and the reciprocal FRFs are given in Figure 12.

As a further check on the repeatability of the measurements, another test was performed at the original excitation level (test C1). Then a mass modification consisting of a 198.2 g brass cylinder was bolted to the right-hand wing tip (point 12). Another set of measurements (defined as test C2) was made for this 'modified model'.

4.3. Multi-Point Random Measurements using 4 Shakers

By comparison of the results obtained using two shakers in the vertical direction at the wing tips with the finite element results, it was found that the X-direction modes were not excited at all well by these two shakers. Therefore, 2 extra shakers were added, one at each wing tip, acting in the X-direction. Each force gauge was again mounted directly on the shaker, with the 'top' towards the shaker and connected to the structure by a 95 mm pushrod. Because fore-aft response of the wings was now excited to a much greater degree, it was necessary to reduce the excitation burst length to 50% in order to allow the response to decay sufficiently before the end of the block.

The four drive-point FRFs are shown in Figures 13 to 16 and these FRFs all show the classic resonance anti-resonance characteristics. In comparison with the FRFs measured with excitation in the Z-direction only, it can be seen that the quality of these FRFs is relatively poor. This is especially evident around the first flexural mode of the structure. A series of Nyquist plots (Figures 17 to 20) has been made for the point FRF (112Z+) shown in Figure 13. The poor quality of the measured FRF in the frequency range 6 to 8 Hz can be seen in Figure 17. Part of the problem can be attributed to insufficient frequency resolution. However, the quality of the FRF in this frequency range is reduced by the additional 'noise' resulting from the X-direction excitations applied at the wing tips. Progressing up through the frequency range (Figures 18 to 20) it can be seen that the quality of the measured FRF increases substantially as the frequency resolution becomes better suited to the frequency and damping properties of the modes. The modes are shown as clear and very well defined circles in the Nyquist plots of Figures 18 and 19.

For a four input test, there are 6 reciprocal FRF pairs and plots of these FRFs together with their vector differences can be seen in Figures 21 to 26. The first two reciprocal plots (Figures 21 and 22) are for 'in-plane' excitation and response directions; in the remaining four reciprocal plots the excitation and response directions are perpendicular to one another. The reciprocity shown by the in-plane terms is considerably better than that by the others. The in-plane reciprocity exhibited by this 4 shaker test is similar to that obtained in the 2 shaker test (Figure 10). For perpendicular excitation and response directions, the reciprocity is not as good; the vector difference is often very similar to the constituent FRFs. Once again, this is particularly evident for the frequency range up to about 10 Hz.

This page intentionally blank

5. Modal Analysis Results

5.1. Analysis Results from 2 Point MPR Measurements

The standard frequency domain MDoF method of analysis available within the LMS software was used on the data sets for this 2 point excitation MPR test configuration. The analyses were made assuming that the modes would be 'complex'. This avoided an initial assumption of 'real' modes, the validity of which could only then be checked by performing a 'complex' analysis. Separate analyses covering small frequency ranges around the individual modes or groups of modes were performed. Low-frequency and high-frequency residual terms were also generated to account for modes outside the overall frequency range of interest. These residual modes have only been used in the synthesis of FRFs from the modal database.

5.1.1. Analysis of Measurements on the Basic Model

Measurement data from the three separate tests on the basic model have been analysed; tests A6, A8 and C1. The frequency and damping results for these tests can be seen in Table 1. Mode shape results for the analysis of test A6 data can be seen in Figures 27 to 35. The shapes from analyses of tests A8 and C1 data were almost identical to those from test A6.

The 'extra mode' at 2.7 Hz, Figure 36, identified in the C1 analysis is a rigid body vertical bounce of the whole structure on the bungee suspension. The reason for its appearance in this set of data is that the reconstruction filtering on the excitation signals was reduced for these measurements, resulting in the excitation of this mode.

Test ID	A6			A8			C1		
Mode	Freq. (Hz)	Damp (%)	Modal Mass (Kg)	Freq. (Hz)	Damp (%)	Modal Mass (Kg)	Freq. (Hz)	Damp (%)	Modal Mass (Kg)
							2.70	2.80	29.7 (111:Z)
1	6.50	0.93	4.27 (11:Z)	6.50	0.96	4.46 (11:Z)	6.49	0.92	4.30 (11:Z)
2	16.45	1.14	3.79 (302:Y)	16.47	1.12	3.86 (302:Y)	16.41	1.19	3.80 (302:Y)
3	33.49	1.06	0.70 (111:Z)	33.47	1.03	0.69 (111:Z)	33.42	0.87	0.70 (111:Z)
4	33.97	1.35	0.66 (11:Z)	33.97	1.33	0.66 (11:Z)	33.87	1.14	0.67 (11:Z)
5	36.34	0.77	3.42 (11:Z)	36.38	0.73	3.51 (11:Z)	36.26	0.81	3.48 (11:Z)
6	49.85	1.96	2.15 (105:Z)	49.84	1.97	2.19 (5:Z)	49.55	2.12	2.10 (105:Z)
7	50.48	0.33	94.2 (11:Z)						
8	56.08	0.09	3.85 (12:X)	56.09	0.07	3.83 (12:X)	56.07	0.10	3.37 (112:X)
9	64.56	1.83	3.69 (303:Z)	64.62	1.79	3.68 (303:Z)	64.29	1.88	3.67 (303:Z)
10				69.52	0.34	0.40 (301:X)	69.31	0.31	0.69 (301:X)

Analysis Results for 2 Point MPR Tests

Table 1

The fundamental vertical bending mode of the wings occurred at 6.5 Hz, Figure 27. It is a symmetrical mode of the wings on the fuselage. Because there was some vertical motion of the support point in this mode, the stiffness of the bungee cords may have had an influence on the exact mode frequency.

The next mode was found at a frequency of 16.45 Hz. It can be seen from Figure 28 that this is the first anti-symmetric wing bending mode. There is a nodal point at the fuselage attachment (model support point) and the tail unit rocks in sympathy with the wings; the fin remains perpendicular to the centre of the wing.

Three closely spaced modes were found at 33.49 Hz, 33.97 Hz and 36.34 Hz, Figures 29 to 31. The first two modes of this group are very similar; torsion of the wings and wing tip plates. In the first mode (33.49 Hz, mode 3) the two wing tip plates move out-of-phase. In the second mode (33.97 Hz, mode 4), however, the wing tip plates move in-phase. Owing to some slight non-symmetry in the model construction or the test equipment and set-up, the magnitude of each wing tip motion is not the same. In mode 3, the starboard wing tip motion is much less than that shown by the port wing tip; and vice versa for mode 4. Nevertheless, the spatial orthogonality of these two modes can still be observed.

The fifth mode, at 36.34 Hz (Figure 31), is a coupled anti-symmetric wing bending and torsion mode. As for mode 2, there is a node point at the joint with the fuselage. The coupled bending and torsion of the wings in this mode produce very little vertical motion at the front of the wing tip plates. In contrast to mode 2, the fin and tailplane now move out-of-phase with the wing attachment point.

Another group of modes, Figures 32 and 33, was found around 50 Hz; one at 49.86 Hz (mode 6) and one at 50.49 Hz (mode 7). It can be seen that mode 6 is the second symmetric wing bending mode in which there is also some slight torsion of the wing tips. The second of these two modes was particularly lightly damped, had an uncharacteristically high modal mass and the scatter plot, Figure 42, indicated a poor quality 'non-real' mode. These characteristics were probably due to some spurious 50 Hz mains frequency interference on the measured FRFs.

The fundamental fore-aft bending mode of the wings (mode 8) was found at a frequency of 56.08 Hz, Figure 34. The tailplane behaves in a similar fashion to the wing, but out of phase. This mode is not driven at all well by the excitation set-up used for these measurements (two exciters attached in the vertical direction, one at each wing tip).

The next mode at 64.57 Hz would appear to be (Figure 35) the second anti-symmetric vertical bending mode of the wings. There is also considerable bending and torsion of the tail unit in this mode. The distribution of measurement points on the wings is not really sufficient to define this mode shape properly; only three of the five node points normally associated with a second anti-symmetric bending mode are shown.

Scatter plots of the mode shapes derived from analysis of the A6 test data are shown in Figures 37 to 45. From these Figures it can be seen that all the modes are predominantly 'real', except for the spurious 'mode' at 50.49 Hz, probably caused by mains interference. For each mode, the eigenvector points are grouped closely about the real axis. The low scatter of the points around the real axis indicates a good and consistent data and analysis set.

Comparison of the mode frequencies obtained from the A6 and A8 (half the nominal excitation level) measurement sets (Table 1) shows little evidence of amplitude dependent non-linearities. Also, comparison of the A6 and C1 results shows a high level of repeatability between measurements performed on different days and involving detachment of the shakers overnight. Figure 46 shows a drive point FRF from test A6 and the same one from test C1 together with the vector difference between the two. The very high degree of repeatability attained for these measurements can be seen clearly from this plot.

The full mode shape results from test A6 are tabulated in Appendix B.

The modal database obtained from test C1 data was used in a prediction of the effect of adding a mass of 198.3 g to the front right-hand wing tip (point 12). This modal modification was accomplished using the LMS modal design program from the Cada-X software suite. The mass was added in all three translational degrees-of-freedom at point 12. No effect was, or could be, taken regarding the added rotational inertia. Only the ten modes in the C1 modal database shown in Table 1 were used in the prediction of the modified modal properties. The results of this modification prediction can be seen in Table 2, together with the measured modal properties of both the unmodified and the modified systems.

5.1.2. Analysis of Measurements on the Modified Model and Comparison with Predicted Results

The measured FRFs from the model with the mass attached to the right-hand wing tip (test C2) have been analysed in exactly the same way as was used for analysis of the base model FRFs; the standard frequency domain MDoF method applied over small frequency ranges around individual modes or groups of modes. Frequency and damping modal properties for this modified model can be seen in Table 2. A MAC comparison of these measured unmodified and modified systems has shown the mode shapes to have a very high degree of similarity; see Appendix C, Table C1. The largest differences occur in the exact nature of the mode shapes for modes 4 and 5. Mode 4 also exhibits the largest change in frequency, -8.8%.

Test ID	C1 (Unmodified) Measured		C2 (Modified) Measured		Difference; Unmodified - Modified	Modified **prediction** using C1 data		Difference; Measured - Predicted
Mode	Freq. (Hz)	Damp (%)	Freq. (Hz)	Damp (%)	Freq. (Hz)	Freq. (Hz)	Damp (%)	Freq. (Hz)
1	2.70	2.80	2.72	2.70	-0.02	2.69	2.90	0.03
2	6.49	0.92	6.38	0.95	0.11	6.36	0.92	0.02
3	16.41	1.19	16.33	1.20	0.08	16.30	1.20	0.03
4	33.42	0.87	30.47	1.10	2.95	30.33	1.10	0.14
5	33.87	1.14	33.46	0.83	0.41	33.46	0.84	0.00
6	36.26	0.81	36.15	0.77	0.11	36.20	0.80	-0.05
7	49.55	2.12	49.43	2.08	0.12	49.44	2.10	-0.01
8	56.07	0.10	55.09	0.11	0.98	54.71	0.17	0.38
9	64.29	1.88	63.84	1.90	0.45	64.15	1.90	-0.31
10	69.31	0.31	69.43	0.32	-0.12	69.38	0.31	0.05

Comparison of Measured and Predicted Results for the Modified Structure

Table 2

A MAC comparison of the measured and predicted modes for the modified structure is presented in Table 3. The high level of agreement between the measured and predicted results for this simple modification to the structure indicates that the modal model of the basic structure is a good representation of the dynamic characteristics.

	2.719	6.384	16.33	30.47	33.46	36.15	49.44	55.09	63.85	69.43
2.693	**0.99**	0.45	0.00	0.02	0.00	0.04	0.01	0.00	0.00	0.00
6.360	0.45	**1.00**	0.00	0.02	0.01	0.04	0.20	0.00	0.00	0.00
16.30	0.00	0.00	**1.00**	0.01	0.00	0.00	0.00	0.00	0.48	0.00
30.33	0.01	0.02	0.01	**0.99**	0.00	0.03	0.05	0.01	0.03	0.00
33.46	0.00	0.01	0.00	0.00	**1.00**	0.07	0.05	0.01	0.01	0.00
36.20	0.00	0.00	0.00	0.08	0.06	**0.95**	0.00	0.00	0.06	0.00
49.44	0.01	0.19	0.00	0.08	0.05	0.00	**0.99**	0.02	0.00	0.00
54.71	0.00	0.00	0.00	0.01	0.00	0.00	0.01	**0.97**	0.00	0.00
64.15	0.00	0.00	0.47	0.05	0.01	0.06	0.00	0.00	**1.00**	0.02
69.38	0.00	0.00	0.00	0.00	0.00	0.00	0.00	0.00	0.01	**1.00**

Mode Ordering:

Row no:	1.0	2.0	3.0	4.0	5.0	6.0	7.0	8.0	9.0	10.0
Column no:	1.0	2.0	3.0	4.0	5.0	6.0	7.0	8.0	9.0	10.0
% freq. difference:	-0.9	-0.4	-0.2	-0.5	0.0	0.1	0.0	-0.7	0.5	-0.1

MAC Matrix Comparison of Measured and Predicted Results for the Modified Structure (Rows: Predicted, Cols: Measured)

Table 3

5.2. Analysis Results from 4 Point MPR Measurements

The FRFs from the 4 point MPR measurements have been analysed in exactly the same way as for the previous 2 point excitation. Results for this analysis can be seen in Table 5. Comparison of this set of modal properties with those for the 2 point MPR results shows there to be very little difference. Indeed, most of the mode shapes are almost indistinguishable and this is also corroborated by the MAC comparison shown in Appendix C, Table C2. The largest difference in the mode frequencies obtained from the two sets of measurements was for mode 1. With 4 point MPR excitation, the first mode frequency was found to be approximately 3% higher than when measured using 2 point MPR excitation. As this is the fundamental symmetric vertical bending mode of the wings there is considerable motion of the wing tips, just where the shakers are connected. Attachment of the X-direction shakers could have added some transverse stiffness (from the pushrods) that has caused the frequency of this mode to be increased. The frequencies of all the other correlated mode frequencies all match to within 1.2%.

It can be seen from Table C2 that mode 7 from the 2 point MPR test (50.49 Hz) and mode 7 from the 4 point MPR test (49.98 Hz) do not correlate with each other or with any other mode. However, mode 7 from the 4 point MPR test has a sensible modal mass compared

with that for mode 7 of test A6. Furthermore, the scatter plot for this mode from this test (Figure 47) again shows the high quality 'real' characteristic found for all the other modes. It can be seen that this mode exhibits considerable out-of-phase X-direction motion of the wing tips, balanced by out-of-phase Y-direction motion of the fuselage nose and tail, Figure 48. The vertical motion of the wings is anti-symmetric.

Test ID	F1		
Mode	Freq. (Hz)	Damp (%)	Modal Mass (Kg)
1	6.70	2.30	3.27 (11:Z)
2	16.36	1.30	3.55 (302:Y)
3	33.57	0.83	0.79 (111:Z)
4	33.95	0.98	0.69 (11:Z)
5	36.17	0.75	3.04 (11:Z)
6	49.26	2.26	2.14 (105:Z)
7	49.98	0.55	7.89 (112:X)
8	55.59	0.20	4.71 (112:X)
9	64.01	2.00	3.53 (303:Z)
10	69.34	0.31	0.51 (301:X)

Analysis Results for 4 Point MPR Test

Table 4

5.3. Comparison of Results with Finite Element Model Results

A finite element model of the structure (A001) was created and analysed; see Appendix A. The calculated mass of the FE model was only 1% greater than the mass of the actual model, 44.05 kg. The first 10 elastic mode frequencies predicted by the FE analysis are shown in Table 5. Mode shape plots are also given in Appendix A.

From the table of results it can be seen that the frequencies obtained from measured data are generally higher than those from the FE model. This implies that the FE model is slightly too flexible. This is unusual because small FE models with a coarse distribution of elements are often too stiff. The results from test F1 (4 point MPR excitation) show all the modes predicted by the FE model, except for that at 58.12 Hz. As the frequency increases, the measured and predicted frequencies match more closely.

The availability of a FE model was of great benefit during the testing phase of the work. It provided guidance for the location of shakers to excite all the modes and confirmation that there were modes around 50 Hz that should not be dismissed as mains interference.

Model ID	A001 (FE)	A6	F1
Mode	Freq. (Hz)	Freq. (Hz)	Freq. (Hz)
7	6.377	6.50	6.70
8	13.123	16.45	16.36
9	30.250	33.49	33.57
10	30.836	33.97	33.95
11	32.946	36.34	36.17
12	49.269	49.85	49.26
13	49.648		49.98
14	55.971	56.08	55.59
15	58.142		
16	64.213	64.56	64.01
			69.34

Finite Element Model Analysis Results and MPR Test Results (6 rigid-body modes omitted)

Table 5

5.4. Comparison of Results with those from SOPEMEA

Test ID	SOPEMEA Results		DRA Results Test A6		DRA Results Test F1	
Mode	Freq. (Hz)	Damp (%)	Freq. (Hz)	Damp (%)	Freq. (Hz)	Damp (%)
1	6.97	1.27	6.50	0.93	6.70	2.30
2	16.07	1.36	16.45	1.14	16.36	1.30
3	33.68	1.47	33.49	1.06	33.57	0.83
4	33.94	1.16	33.97	1.35	33.95	0.98
5	34.92	1.11	36.34	0.77	36.17	0.75
6	46.08	2.56	49.85	1.96	49.26	2.26
7	48.62	0.91	50.48	0.33	49.98	0.55
8	53.58	0.56	56.08	0.09	55.59	0.20
9	61.14	2.06	64.56	1.83	64.01	2.00

Analysis Results from SOPEMEA Compared with those from DRA

Table 6

The DRA modal analysis results are shown in Table 6 alongside a set from SOPEMEA. It is interesting that the measured results for the first four modes compare with one another much more closely than with the FE models. In contrast to the trend found in comparison of the measured results with those from the FE model the comparison of the measured results with those from SOPEMEA becomes less good as the frequency increases. Above mode 4, the SOPEMEA mode frequencies are always less than those measured at DRA. Despite these discrepancies between the frequencies for the higher modes the general level of agreement for the two sets of data is reasonable considering the following;

(i) that the model has been assembled and dismantled several times between the tests,

(ii) the tests span a significant period of time,

(iii) the tests were not conducted under specified and controlled conditions of temperature and humidity,

(iv) different transducers have been used,

(v) different excitation equipment has been used,

(vi) different test and analysis techniques have been used,

(vii) different support bungee cords have been used, and

(viii) different suspension set-ups have been used.

The comparison of results from all participants in the exercise will be most interesting and instructive.

6. Concluding Remarks

The GARTEUR testbed structure was received at DRA Farnborough in a slightly less than satisfactory condition; glue, double-sided tape and attachments remained from previous participants. No new bungee suspension cords were supplied. In all other respects the model was complete and the wing mated well with the fuselage. Following suspension of the model and preliminary checks, several sets of vibration tests were performed. In setting the model up for the tests, great care was taken to try and ensure that the measuring equipment had as little effect on the structure as possible. To this end, the force transducers were mounted at what would normally be considered to be the 'wrong' end of the pushrods. A bandlimited random type testing method was used. Separate tests with two and four simultaneous excitation sources were made. Although the four-point excitation test produced a better response for some of the modes than that with the two-point excitation test, the quality of the FRFs was, perhaps, not quite so good. It has been suggested that this was due to the lower signal-to-noise ratio for the four-point excitation. Nevertheless, the results obtained from the two sets of tests correlated very well.

No problems were encountered with testing the structure. Having a finite element model available was helpful for the choice of excitation locations and confirmation of the modes measured.

One of the modal databases from the tests was used in a prediction of the effect of a very simple mass modification to the structure. The same modification was made to the structure and the dynamic characteristics measured. It was found that the predicted dynamic characteristics matched those measured for the modified structure very well, thus providing further confidence in the accuracy of the modal database for the original structure.

Modal properties obtained at the DRA Farnborough for the GARTEUR structure have been compared with a set obtained by SOPEMEA. Although not identical, the sets of results do have a resaonable level of agreement considering the differences in methods and equipment for testing and analysis and the fact that the model has been assembled and dismantled several times between the tests.

Comparisons of results and experiences from all of the participants involved in testing this structure should be most interesting and informative.

This page intentionally blank

7. Figures

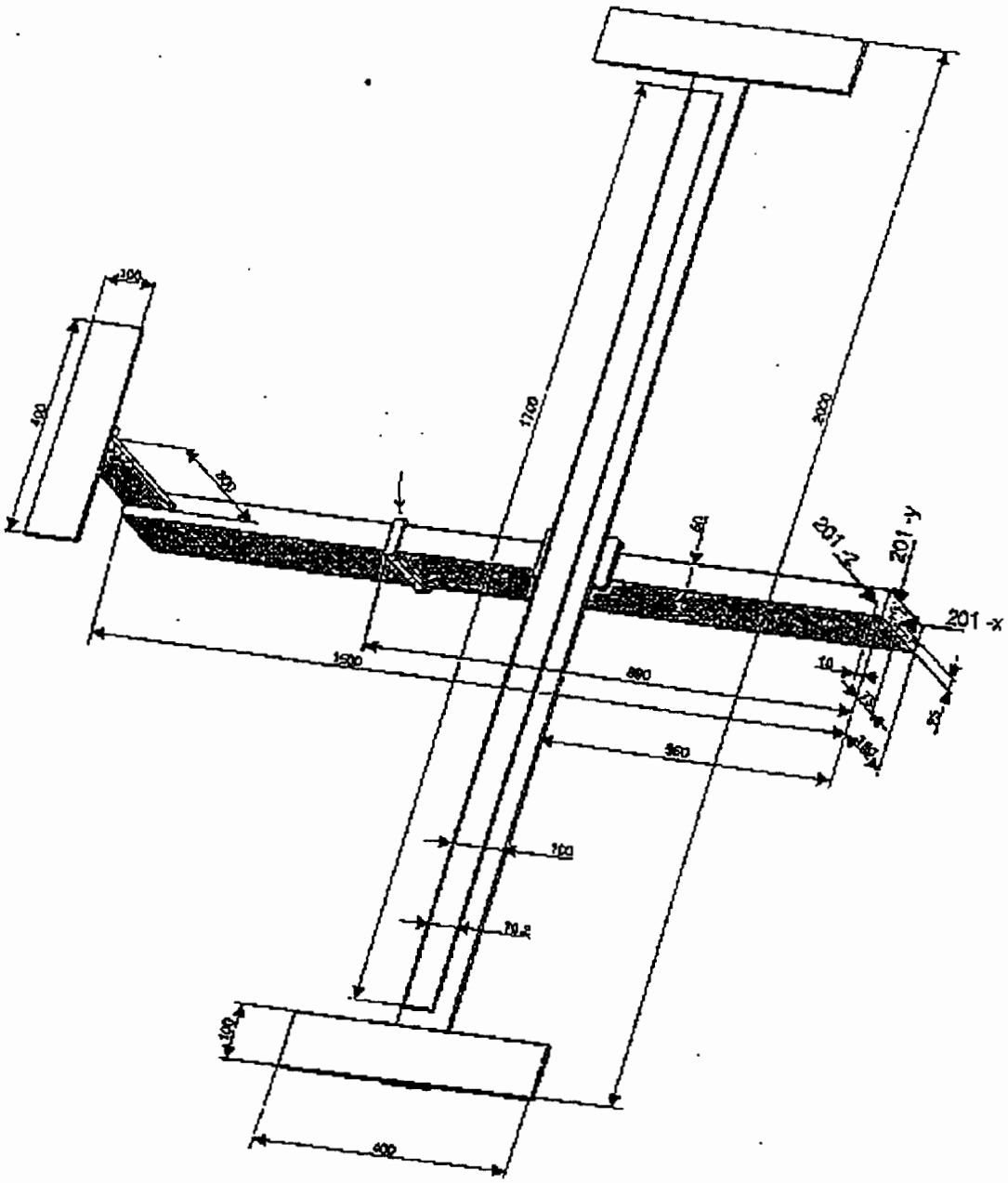

Sketch of the GARTEUR SM-AG19 Testbed

Figure 1

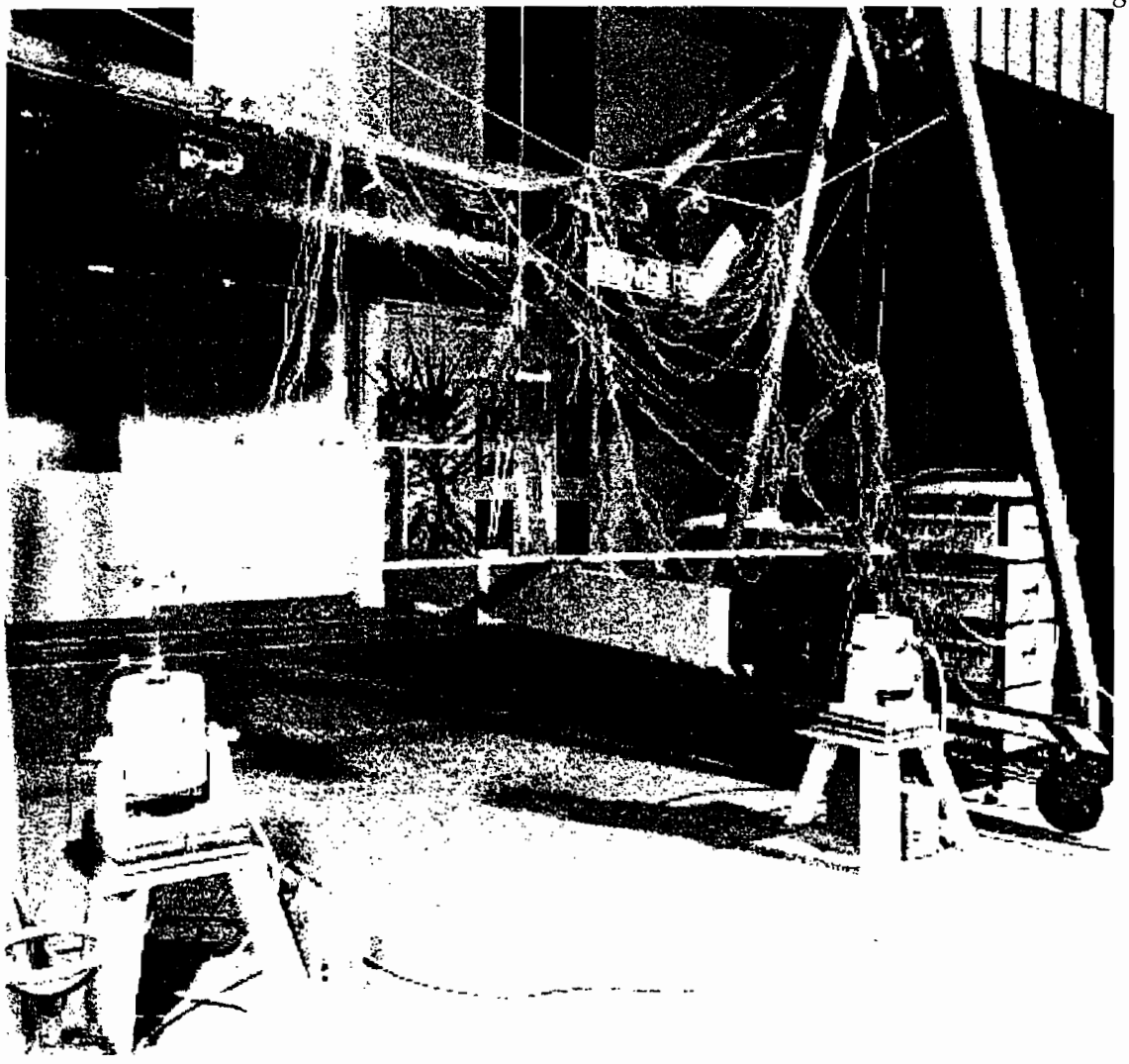

Photograph of the Overall Test Set-up

Figure 2

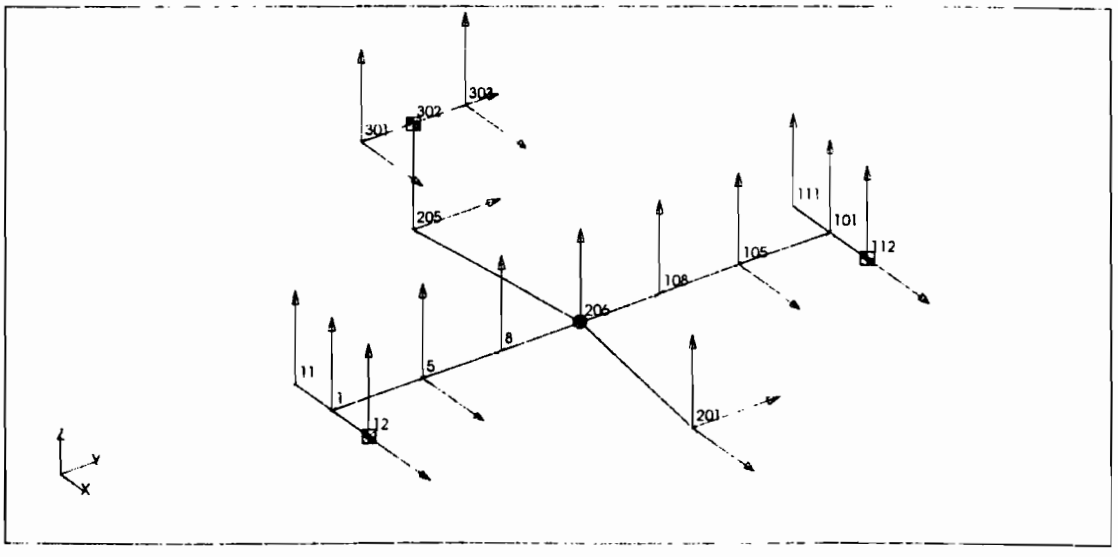

Response Measurement Locations and Directions

Figure 3

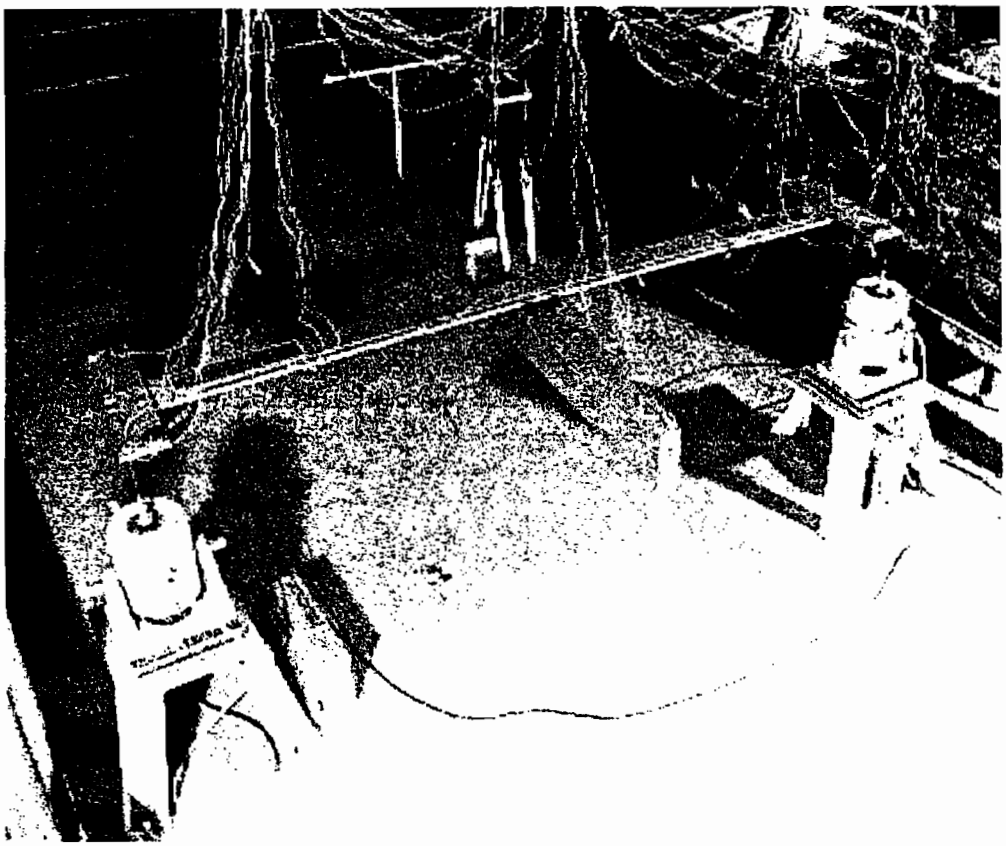

Photograph of the Complete Model Test Set-up

Figure 4

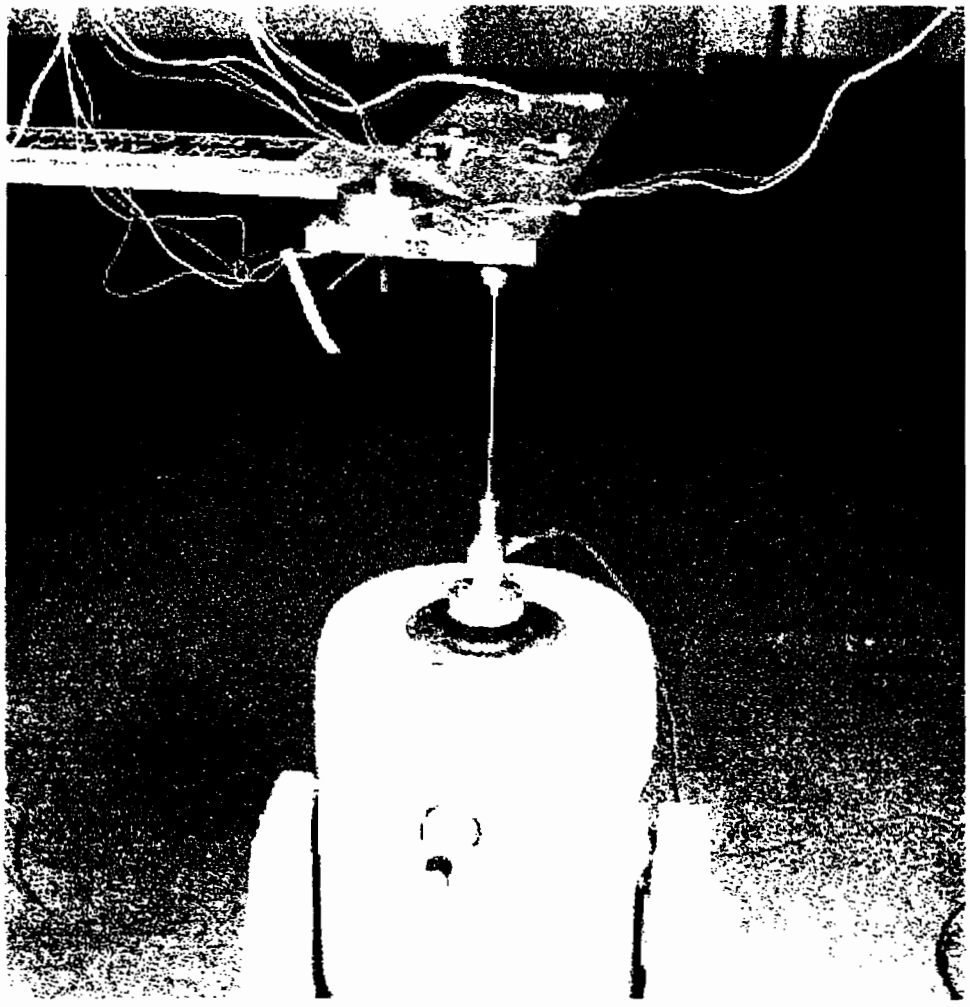

Detail Photograph of the Force Transducer Position and Attachment

Figure 5

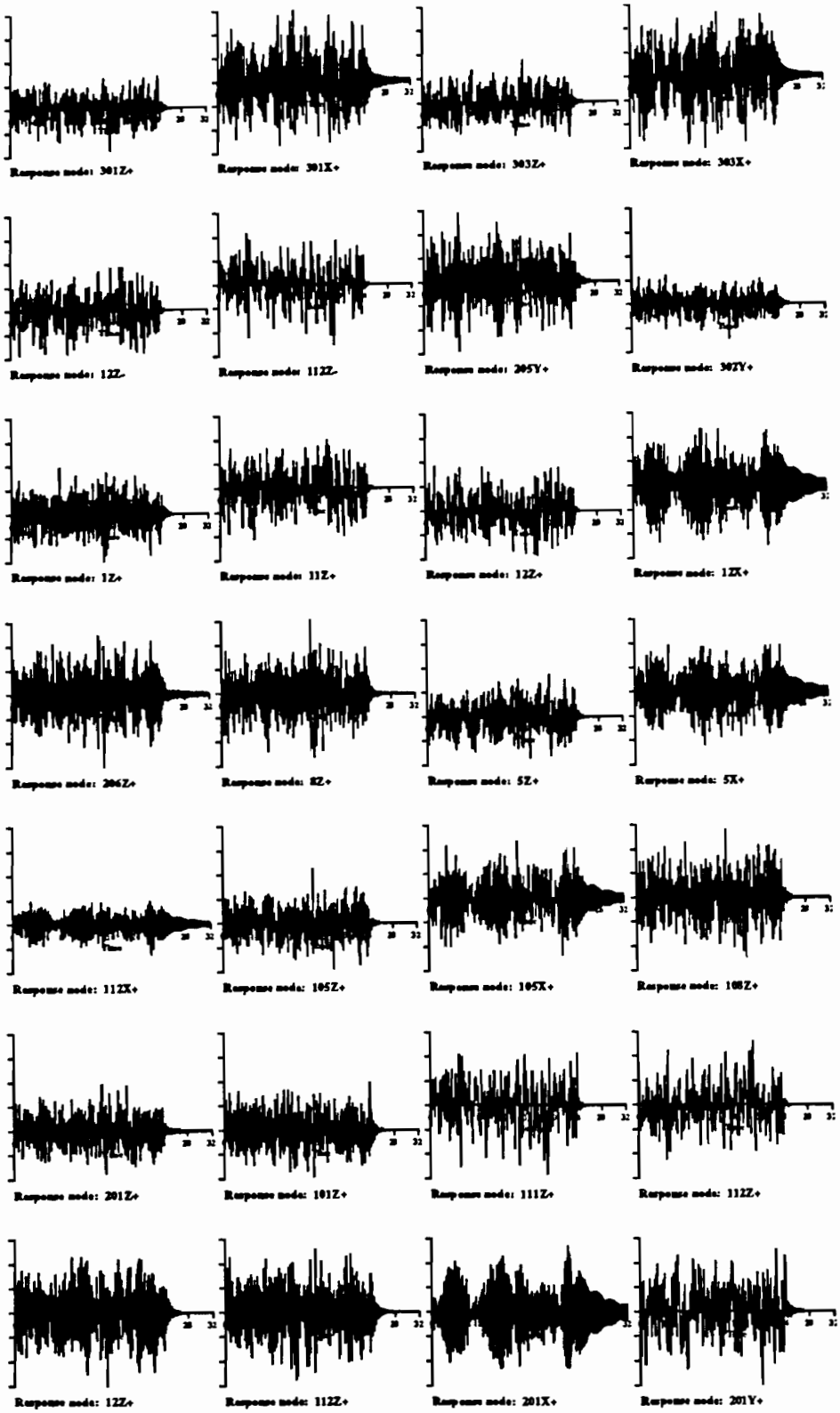

Response Time Data for 75% Excitation Burst Length

Figure 6

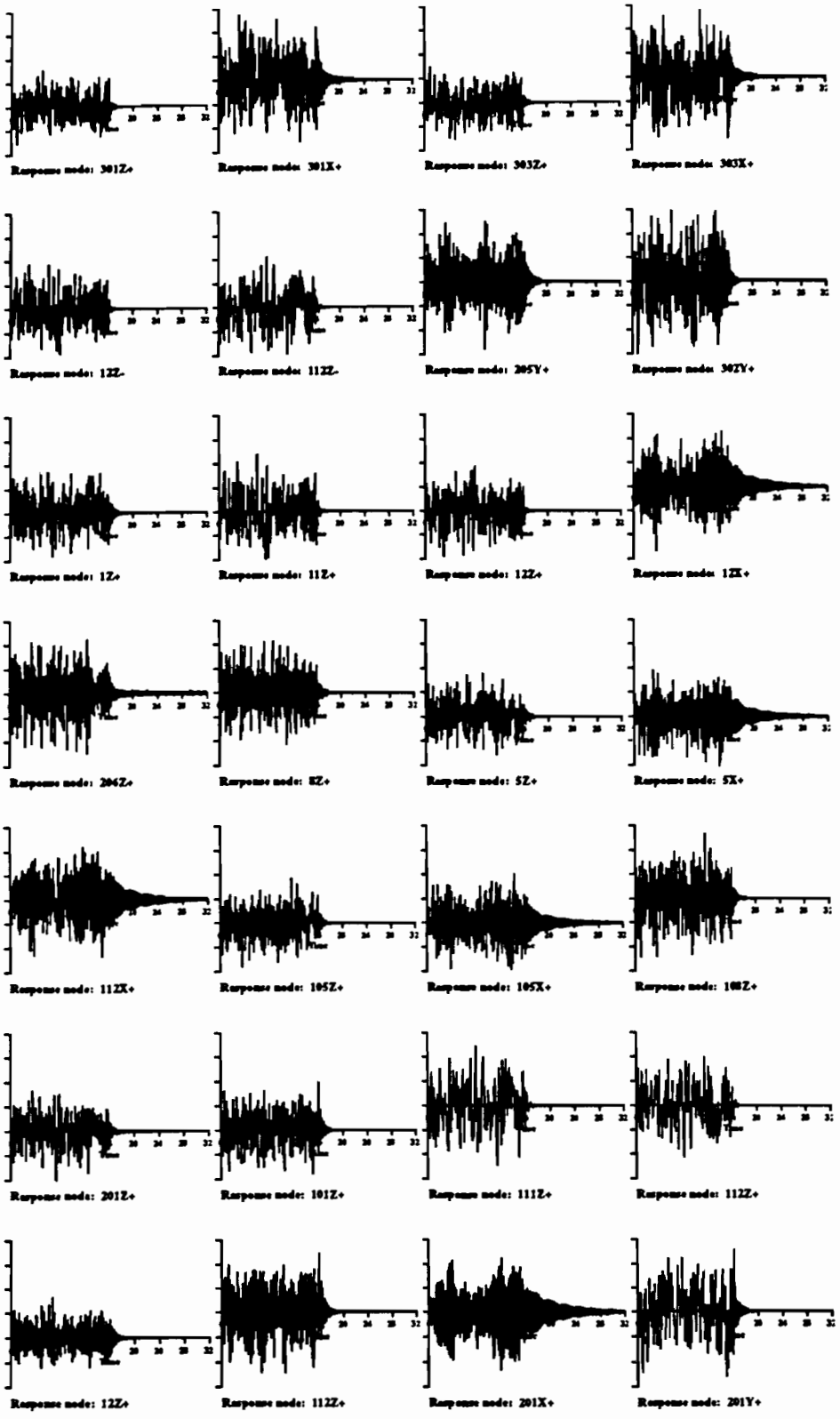

Response Time Data for 50% Excitation Burst Length

Figure 7

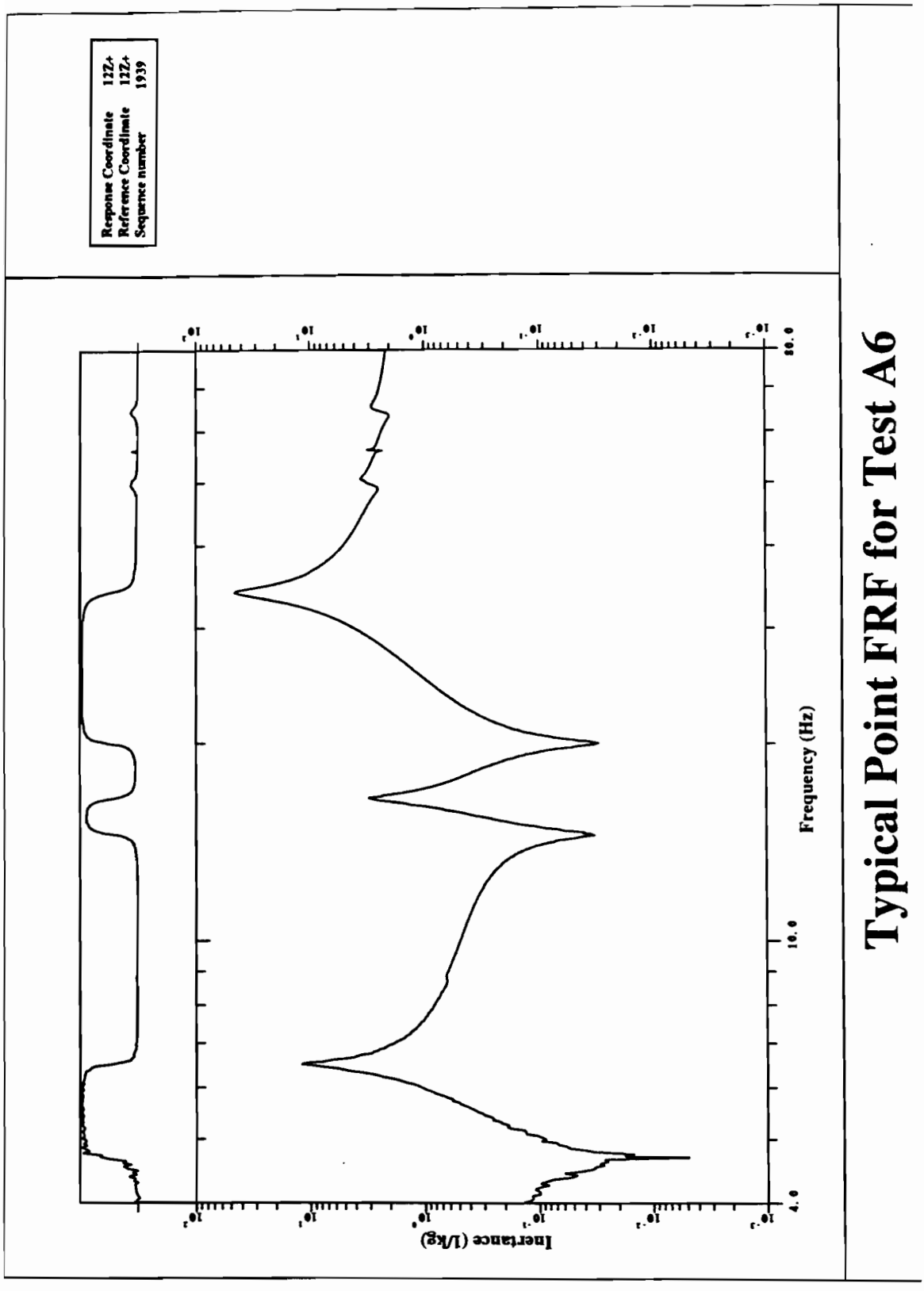

Typical Point FRF for Test A6

Figure 8

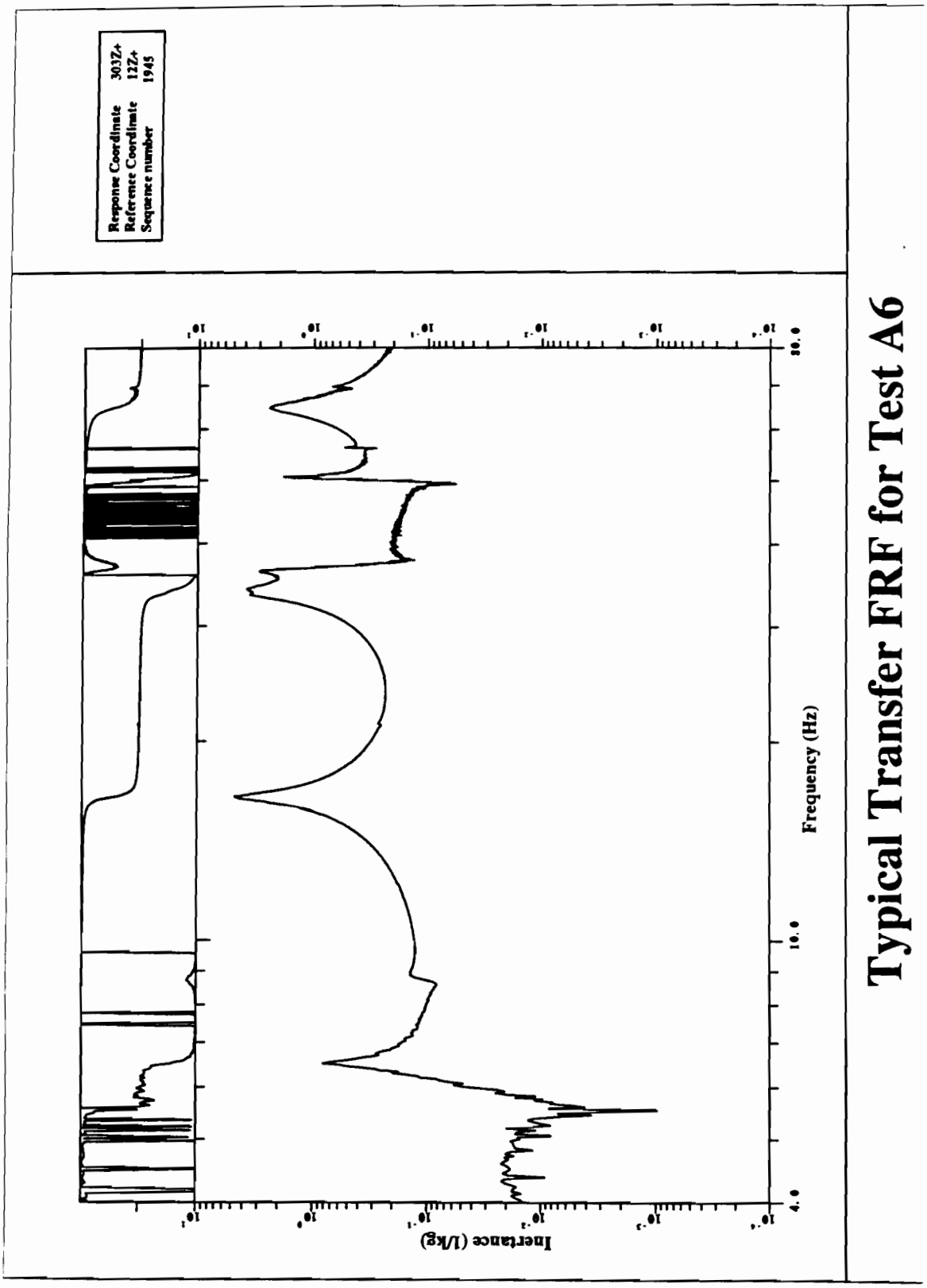

Typical Transfer FRF for Test A6

Figure 9

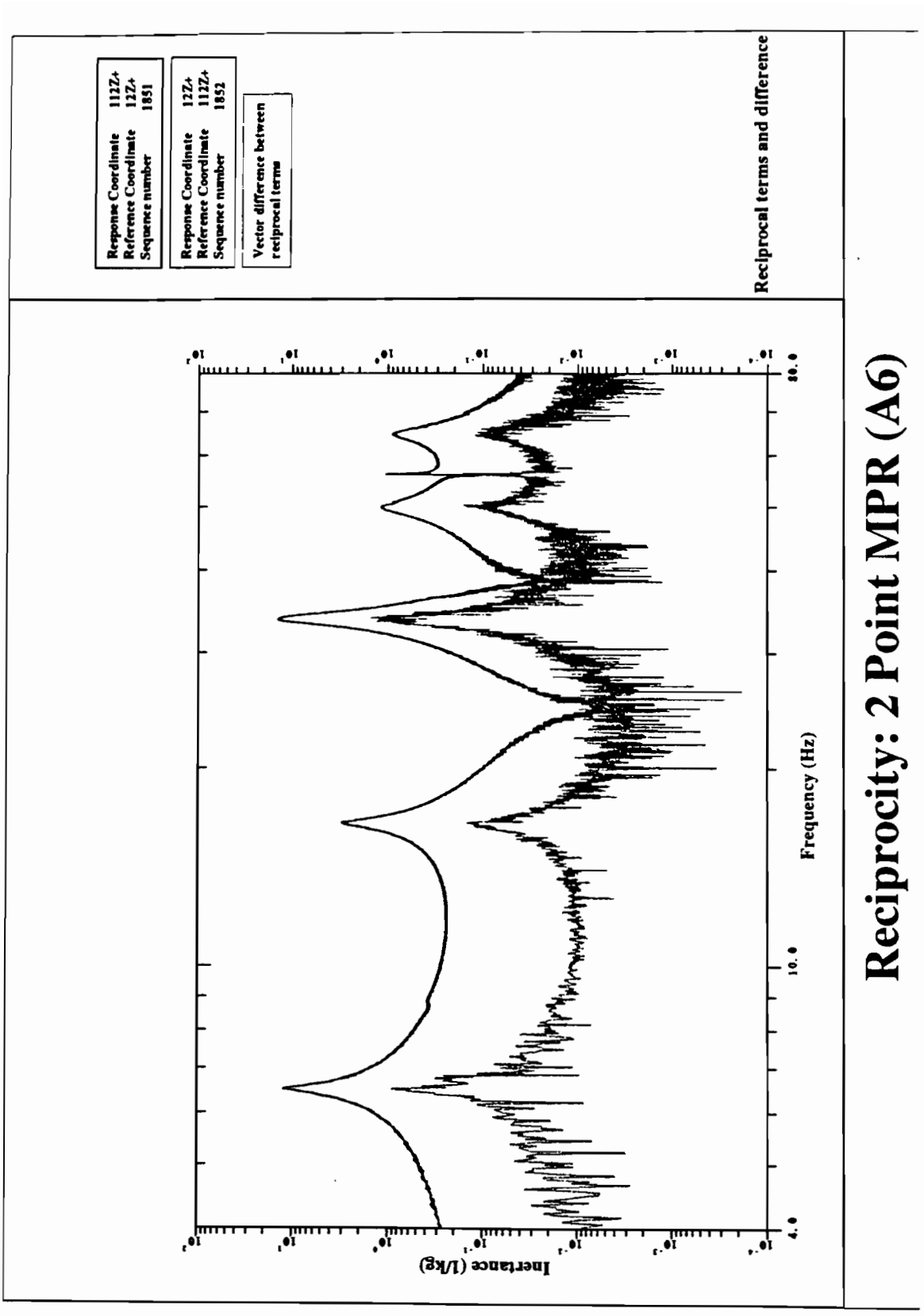
Reciprocity: 2 Point MPR (A6)
Reciprocal terms and difference
Response Coordinate 112Z+
Reference Coordinate 12Z+
Sequence number 1851
Response Coordinate 12Z+
Reference Coordinate 112Z+
Sequence number 1852
Vector difference between reciprocal terms
Inertance (1/kg)
Frequency (Hz)
4.0
10.0
80.0

Figure 10

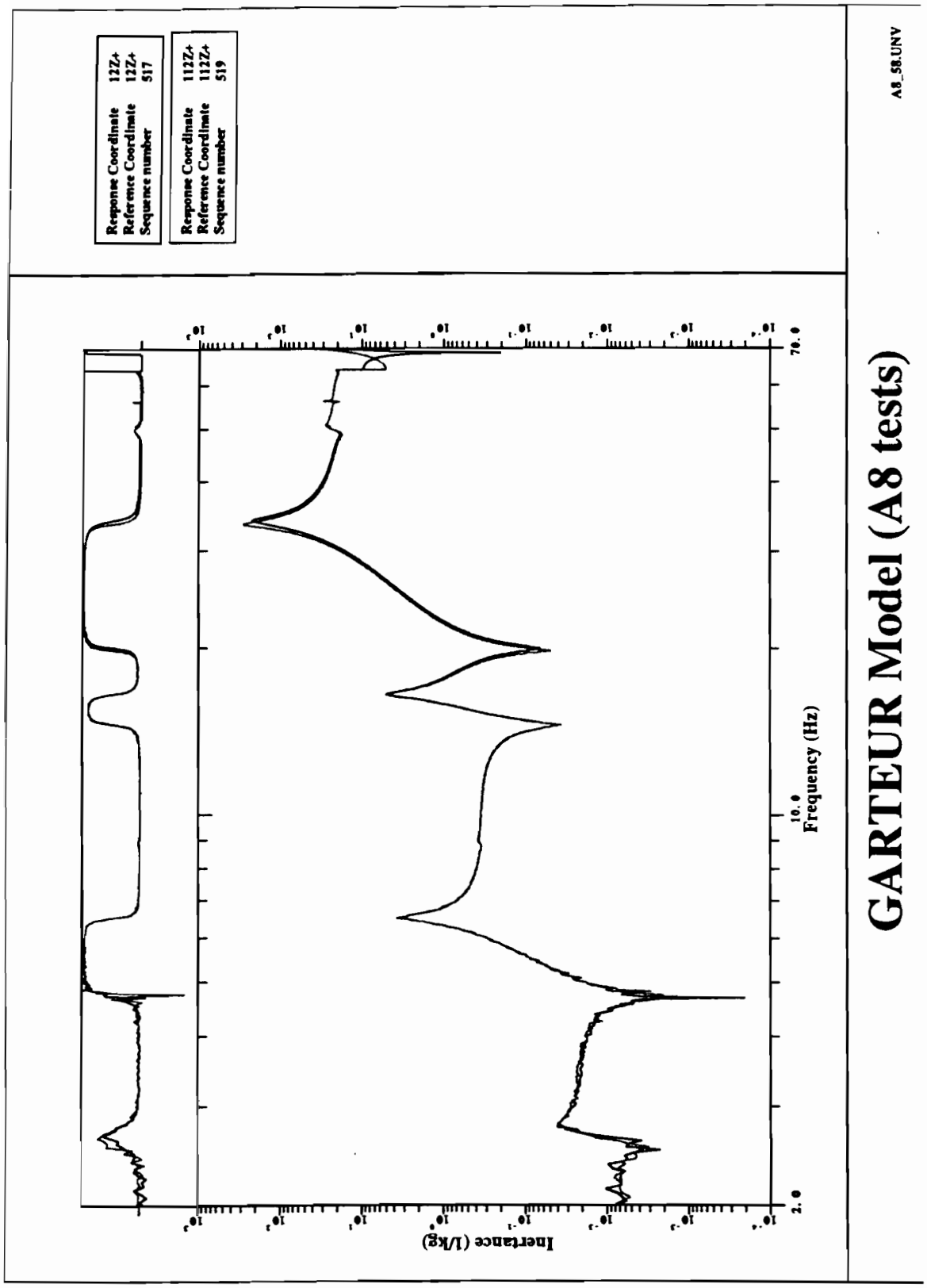
GARTEUR Model (A8 tests)
A8_58.UNV
Response Coordinate 12Z+
Reference Coordinate 12Z+
Sequence number 517
Response Coordinate 112Z+
Reference Coordinate 112Z+
Sequence number 519
Inertance (1/kg)
Frequency (Hz)
2.0
10.0
70.0

Figure 11

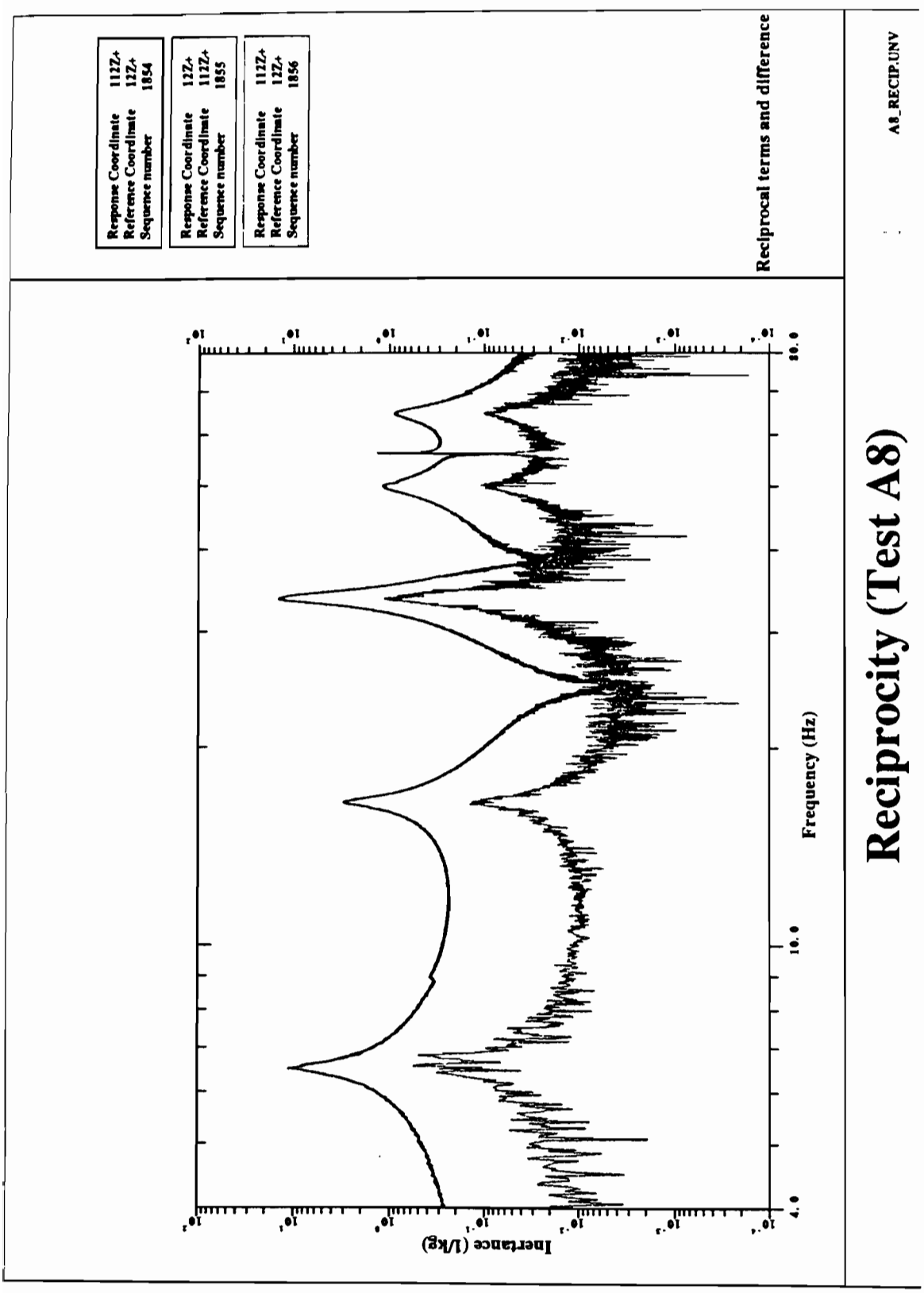
Reciprocity (Test A8)
Reciprocal terms and difference
A8_RECIP.UNV
Response Coordinate 112Z+
Reference Coordinate 12Z+
Sequence number 1854
Response Coordinate 12Z+
Reference Coordinate 112Z+
Sequence number 1855
Response Coordinate 112Z+
Reference Coordinate 12Z+
Sequence number 1856
Inertance (1/kg)
Frequency (Hz)
4.0
10.0
80.0

Figure 12

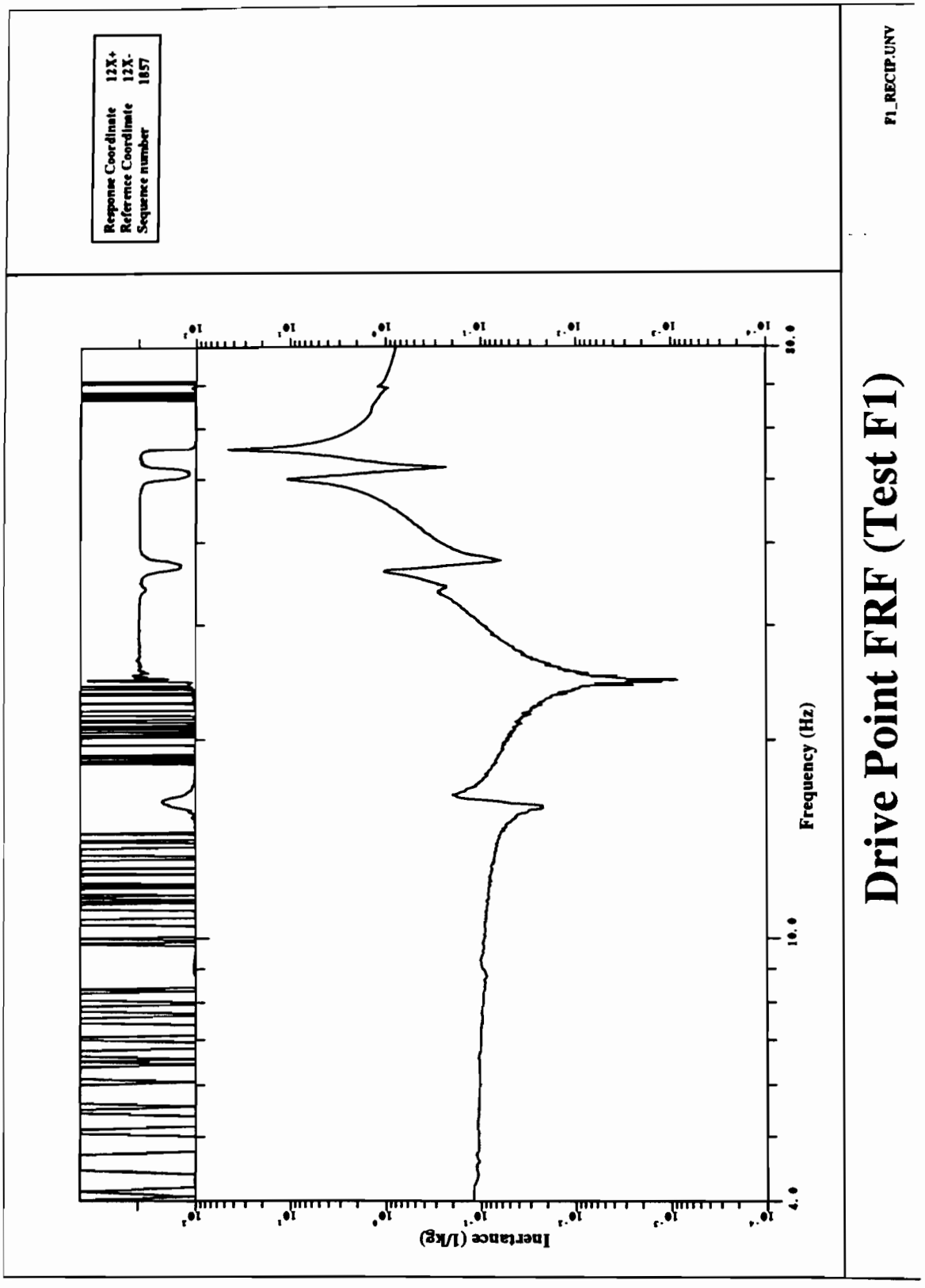
Response Coordinate 12X+
Reference Coordinate 12X-
Sequence number 1857
F1_RECIP.UNV
Drive Point FRF (Test F1)
Inertance (1/kg)
Frequency (Hz)
4.0
10.0
80.0

Figure 13

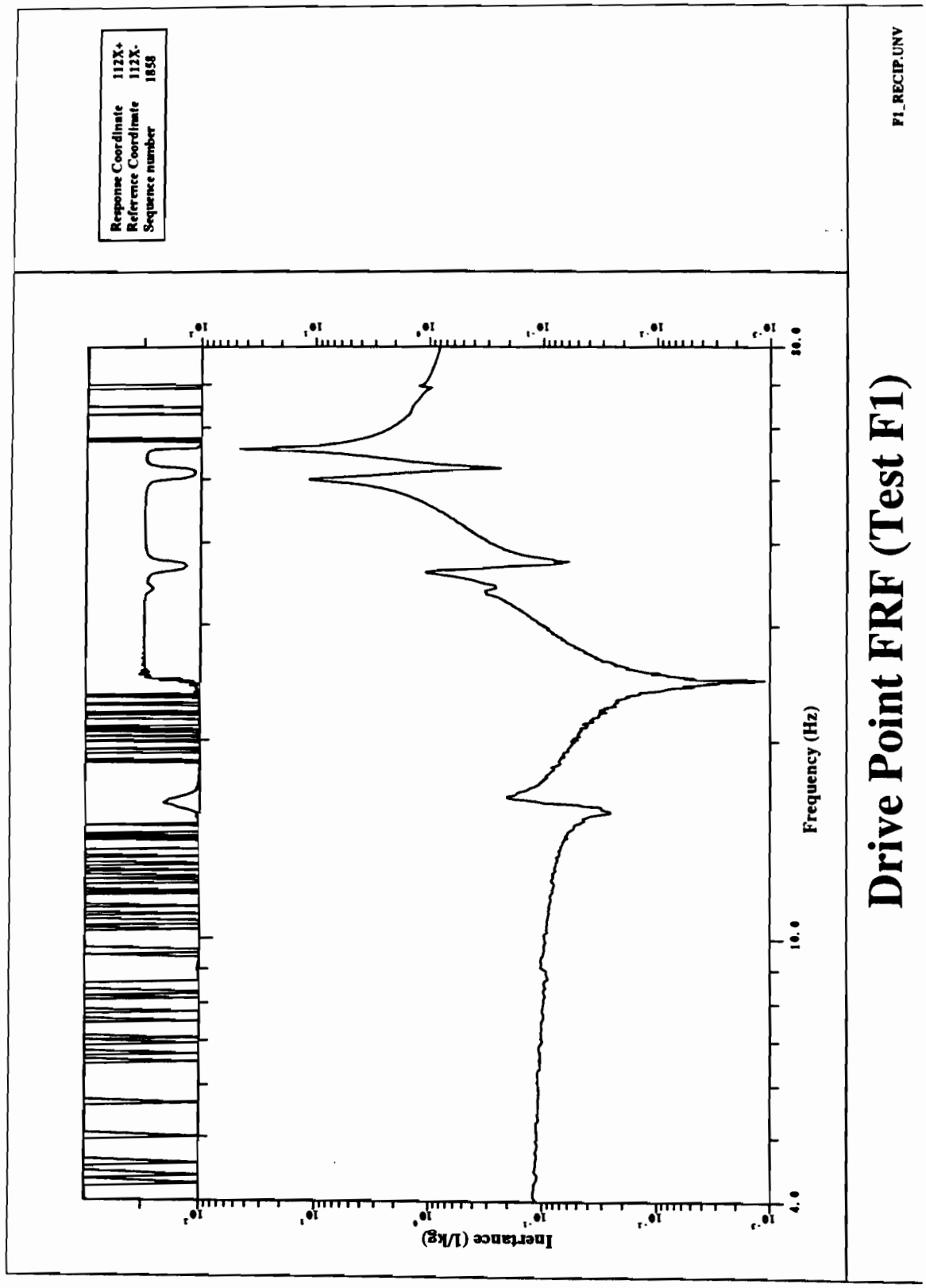
Response Coordinate 112X+
Reference Coordinate 112X-
Sequence number 1858
F1_RECIP.UNV
Drive Point FRF (Test F1)
Inertance (1/kg)
Frequency (Hz)
4.0
10.0
80.0

Figure 14

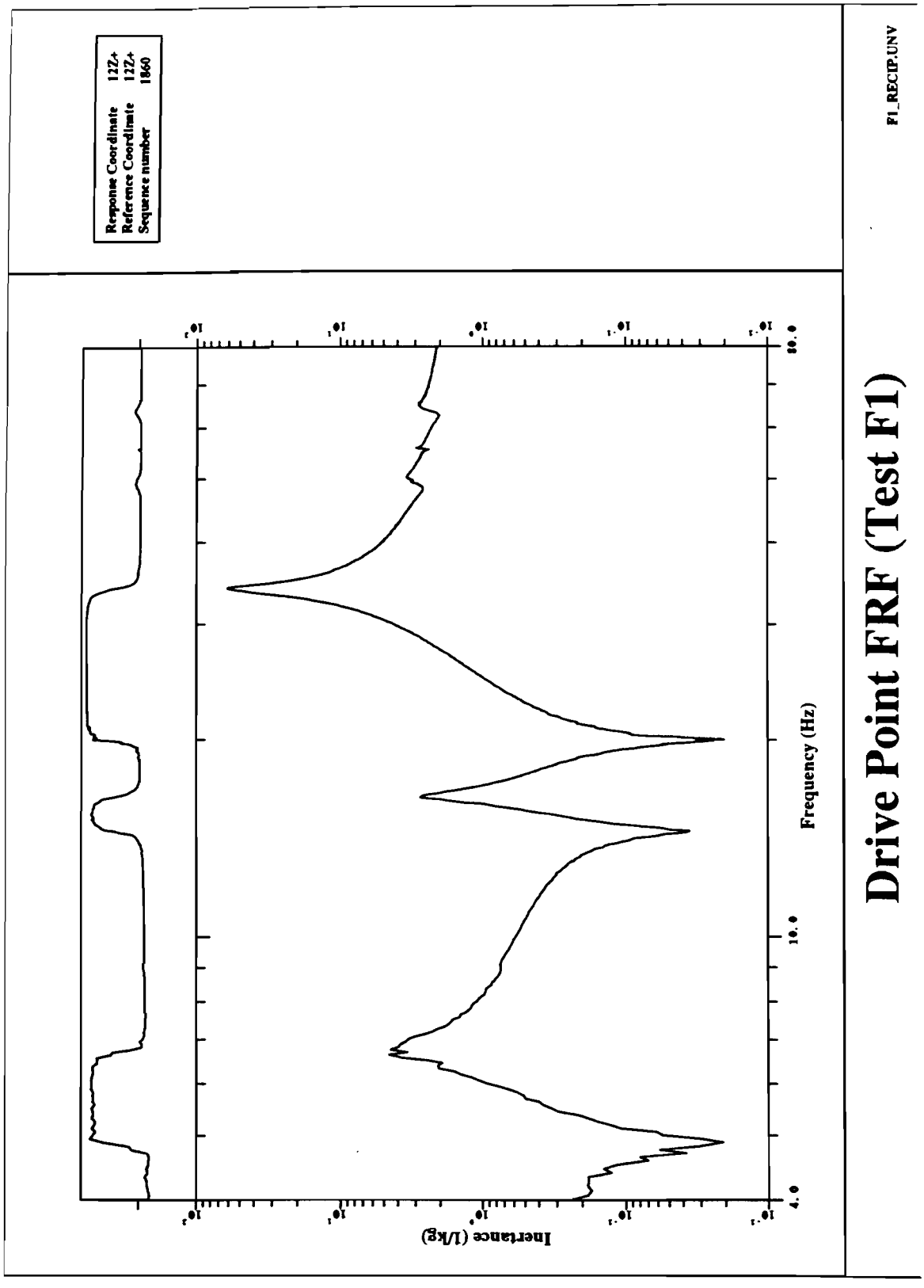
Response Coordinate 12Z+
Reference Coordinate 12Z+
Sequence number 1860
F1_RECIP.UNV
Drive Point FRF (Test F1)
Inertance (1/kg)
Frequency (Hz)
4.0
10.0
80.0

Figure 15

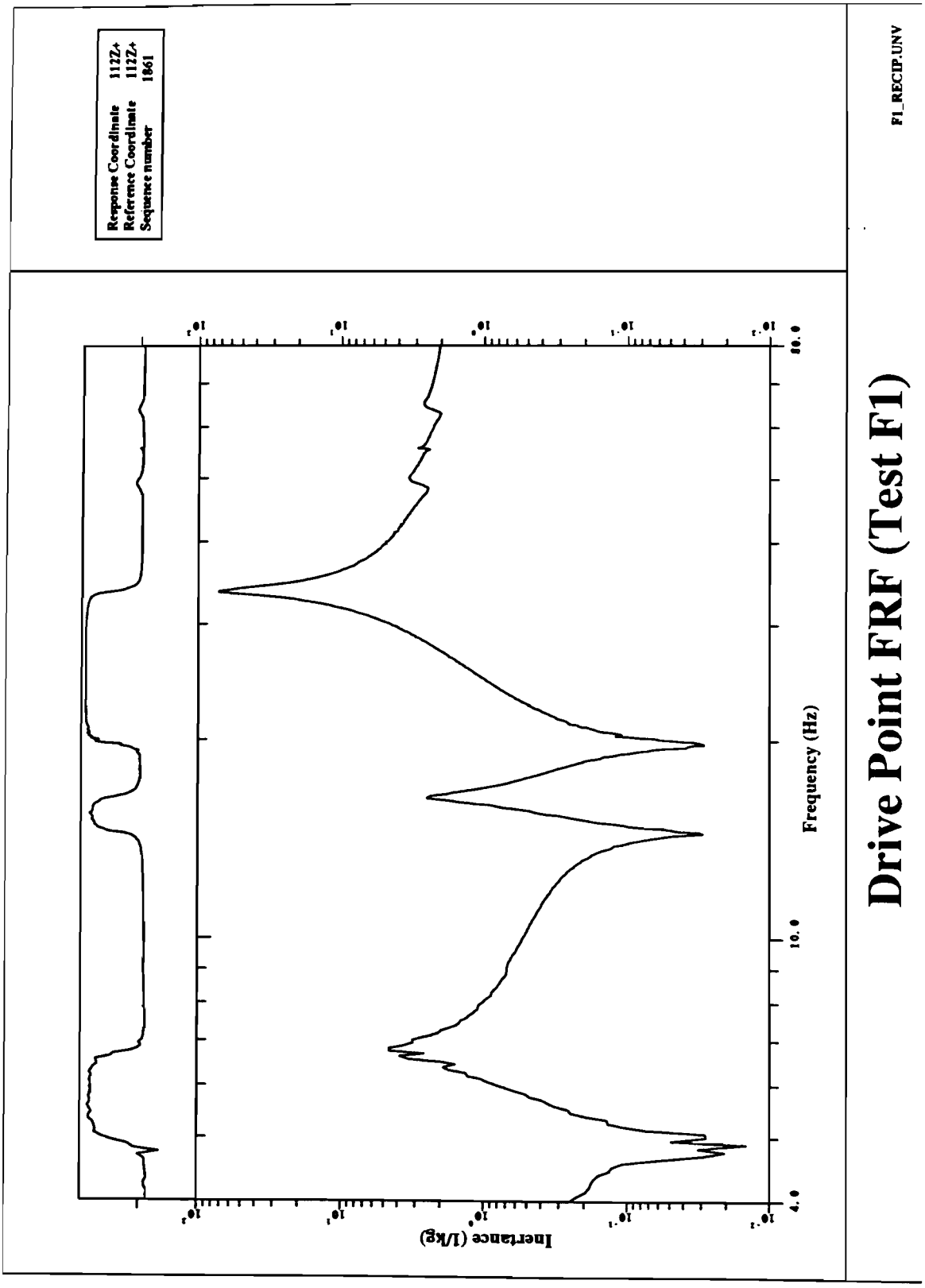
Response Coordinate 112Z+
Reference Coordinate 112Z+
Sequence number 1861
F1_RECIP.UNV
Drive Point FRF (Test F1)
Inertance (1/kg)
Frequency (Hz)
4.0
10.0
80.0

Figure 16

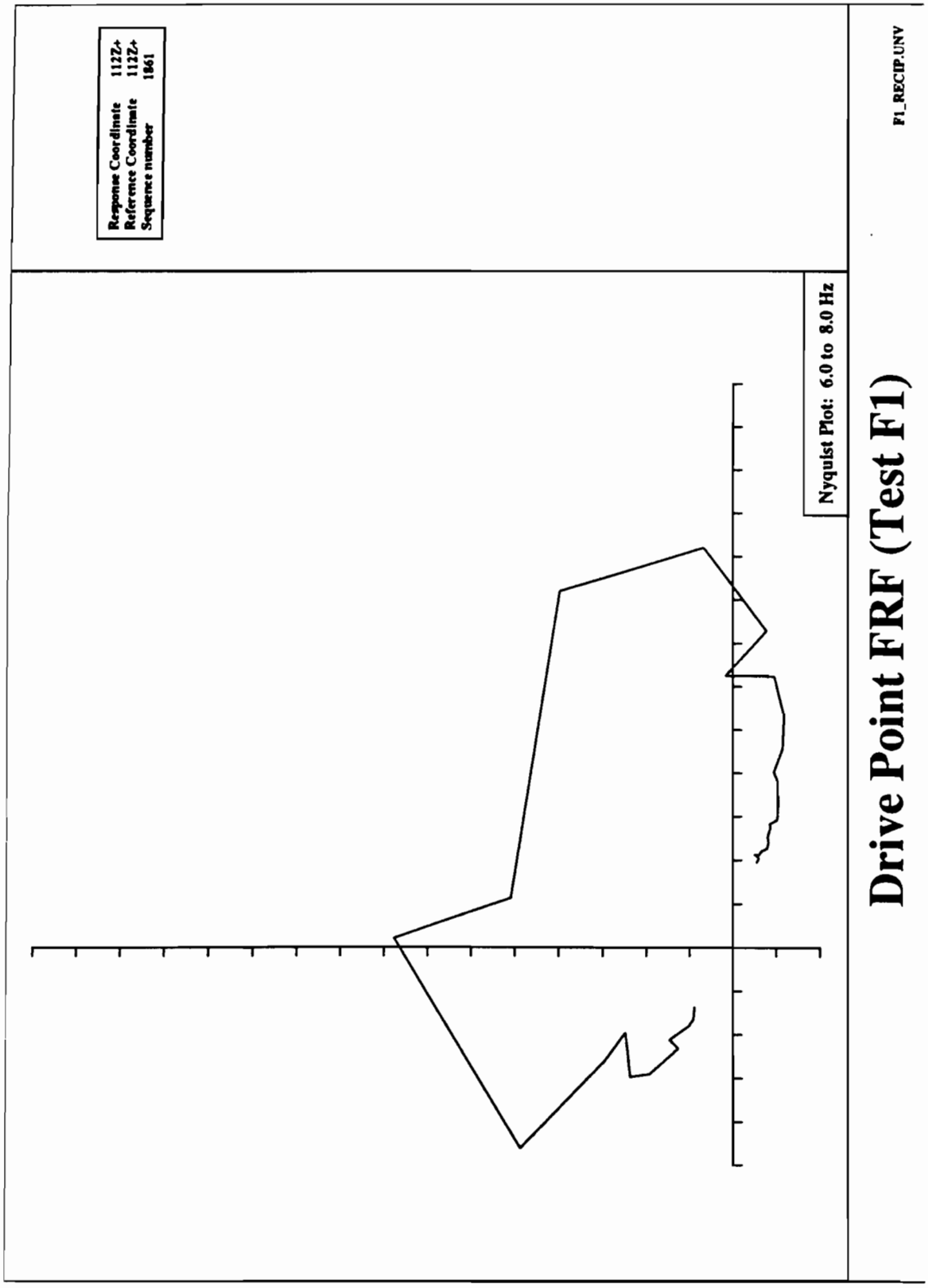
Response Coordinate 1122+
Reference Coordinate 1122+
Sequence number 1861
Nyquist Plot: 6.0 to 8.0 Hz
Drive Point FRF (Test F1)
F1_RECIP.UNV

Figure 17

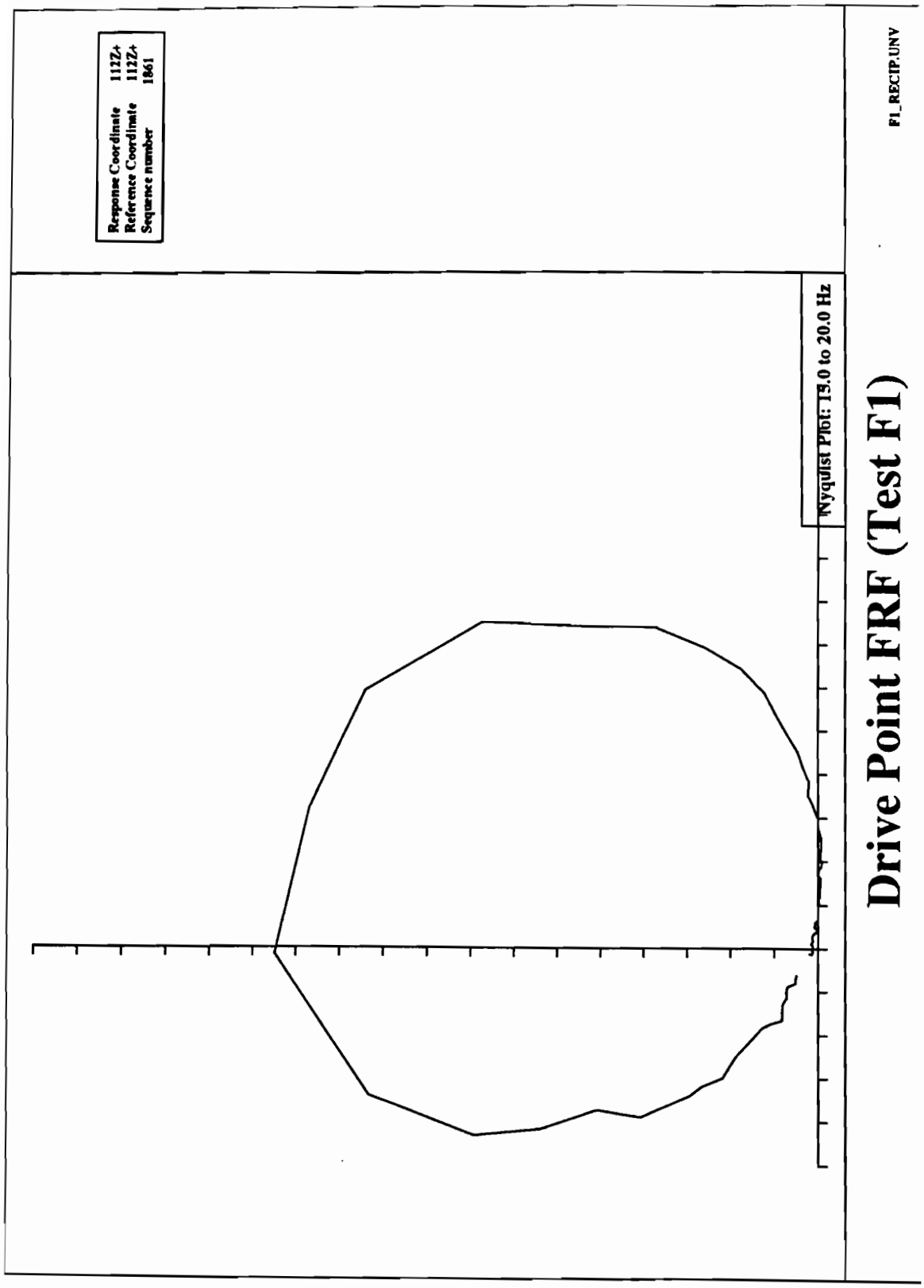
Response Coordinate 112Z+
Reference Coordinate 112Z+
Sequence number 1861
Nyquist Plot: 13.0 to 20.0 Hz
Drive Point FRF (Test F1)
F1_RECIP.UNV

Figure 18

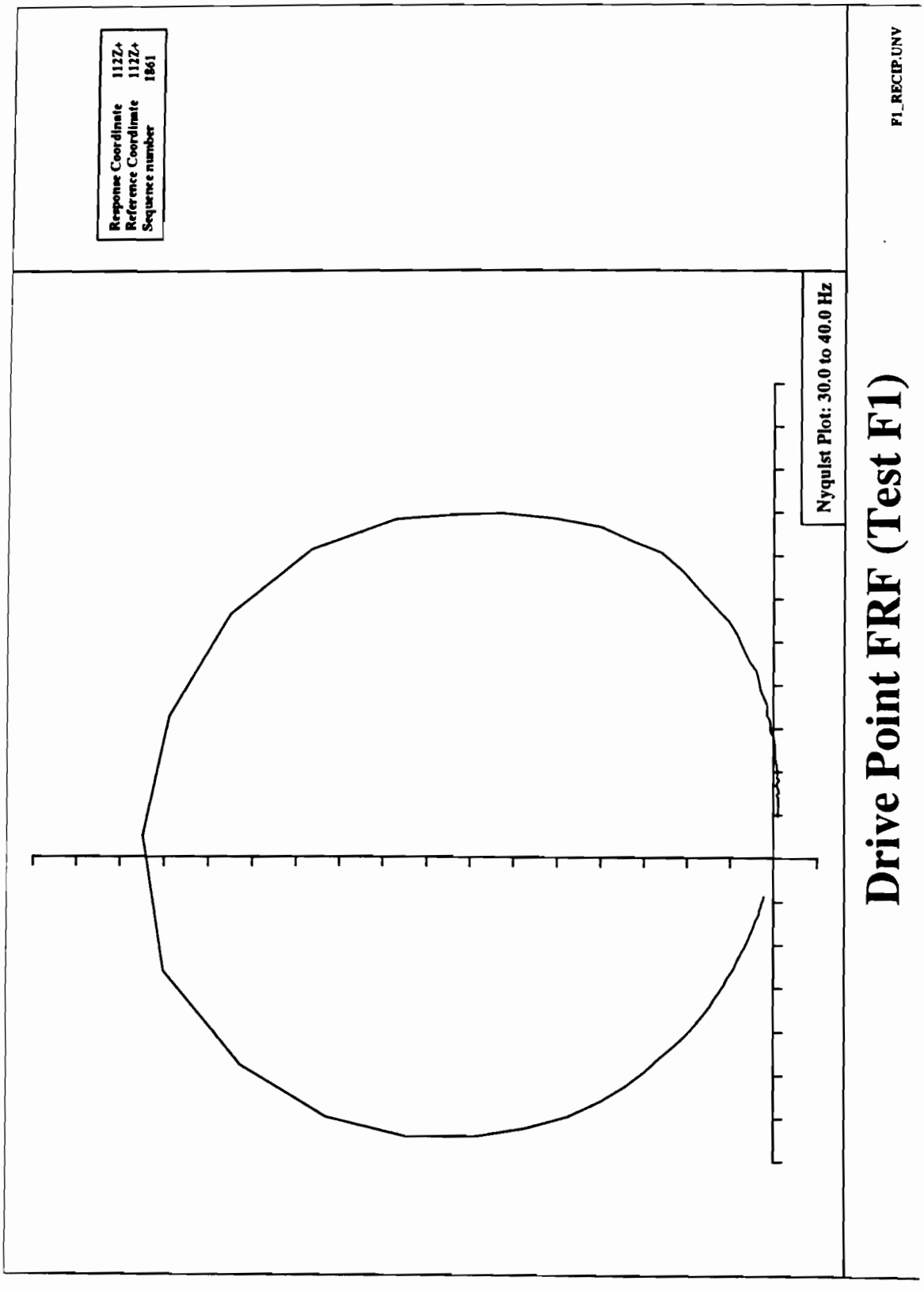
Response Coordinate 1122+
Reference Coordinate 1122+
Sequence number 1861
Nyquist Plot: 30.0 to 40.0 Hz
Drive Point FRF (Test F1)
F1_RECIP.UNV

Figure 19

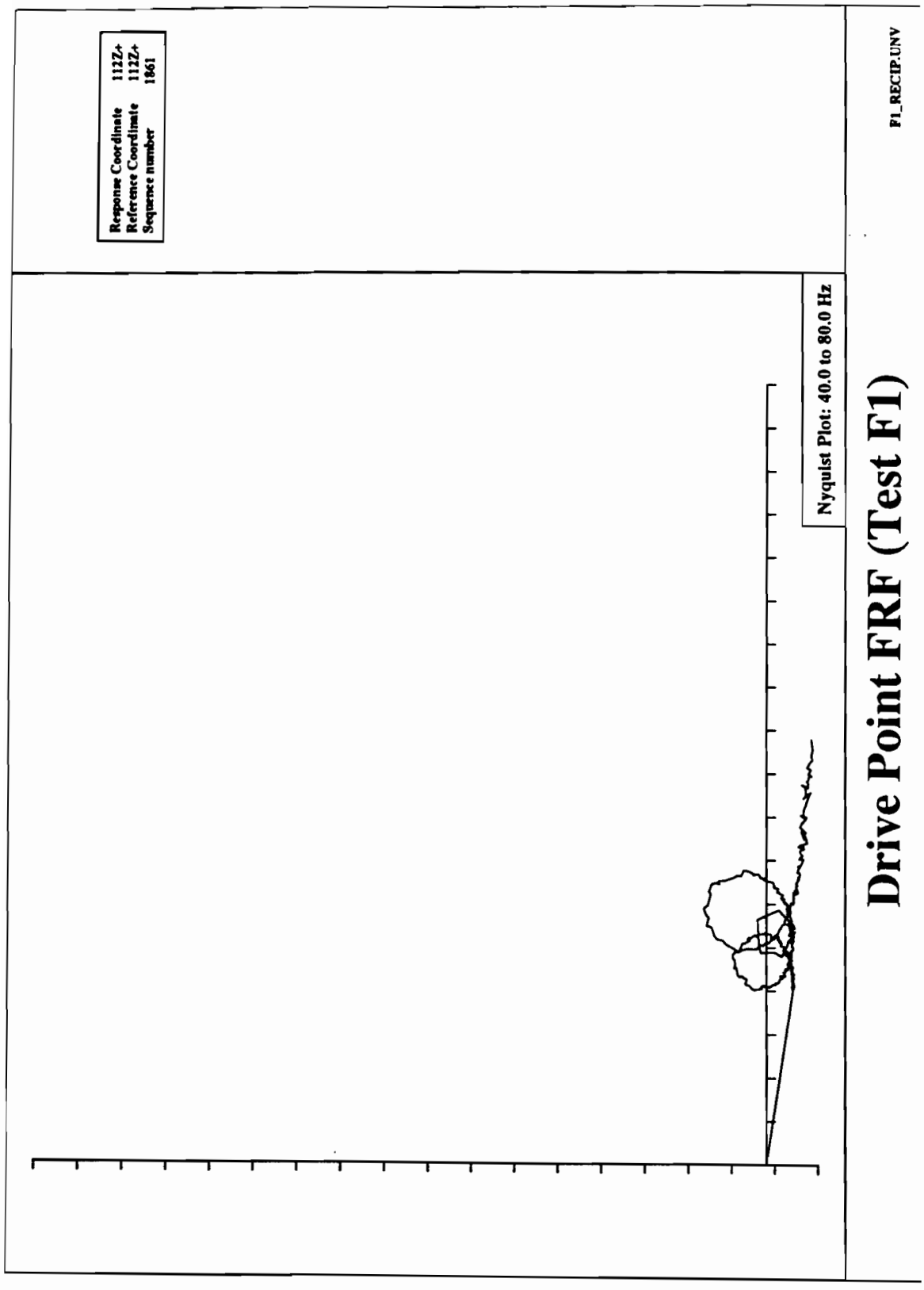
Response Coordinate 112Z+
Reference Coordinate 112Z+
Sequence number 1861
F1_RECIP.UNV
Drive Point FRF (Test F1)
Nyquist Plot: 40.0 to 80.0 Hz

Figure 20

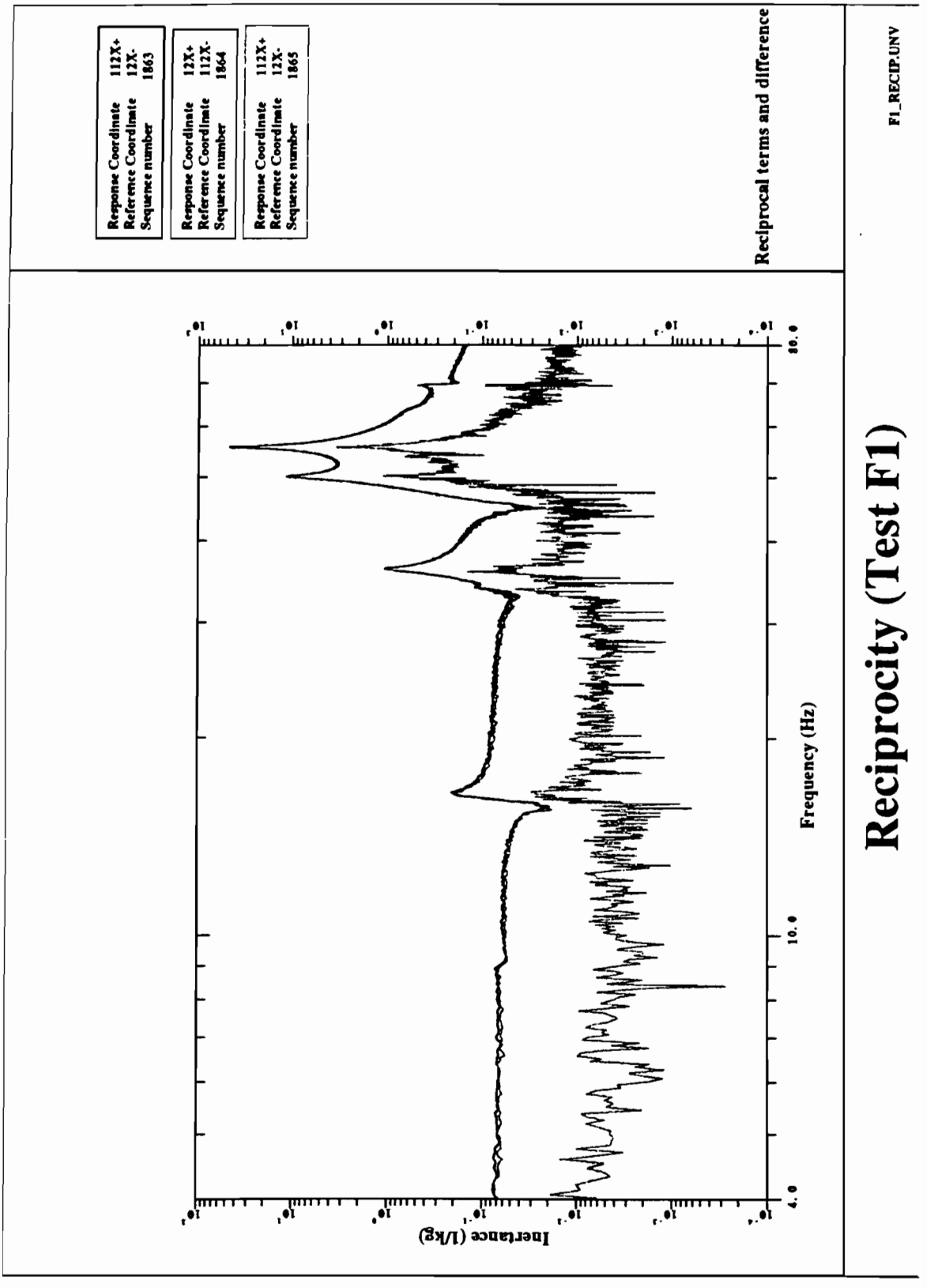
Response Coordinate 112X+
Reference Coordinate 12X-
Sequence number 1863
Response Coordinate 12X+
Reference Coordinate 112X-
Sequence number 1864
Response Coordinate 112X+
Reference Coordinate 12X-
Sequence number 1865
Reciprocal terms and difference
F1_RECIP.UNV
Reciprocity (Test F1)
Inertance (1/kg)
Frequency (Hz)
4.0
10.0
10.0

Figure 21

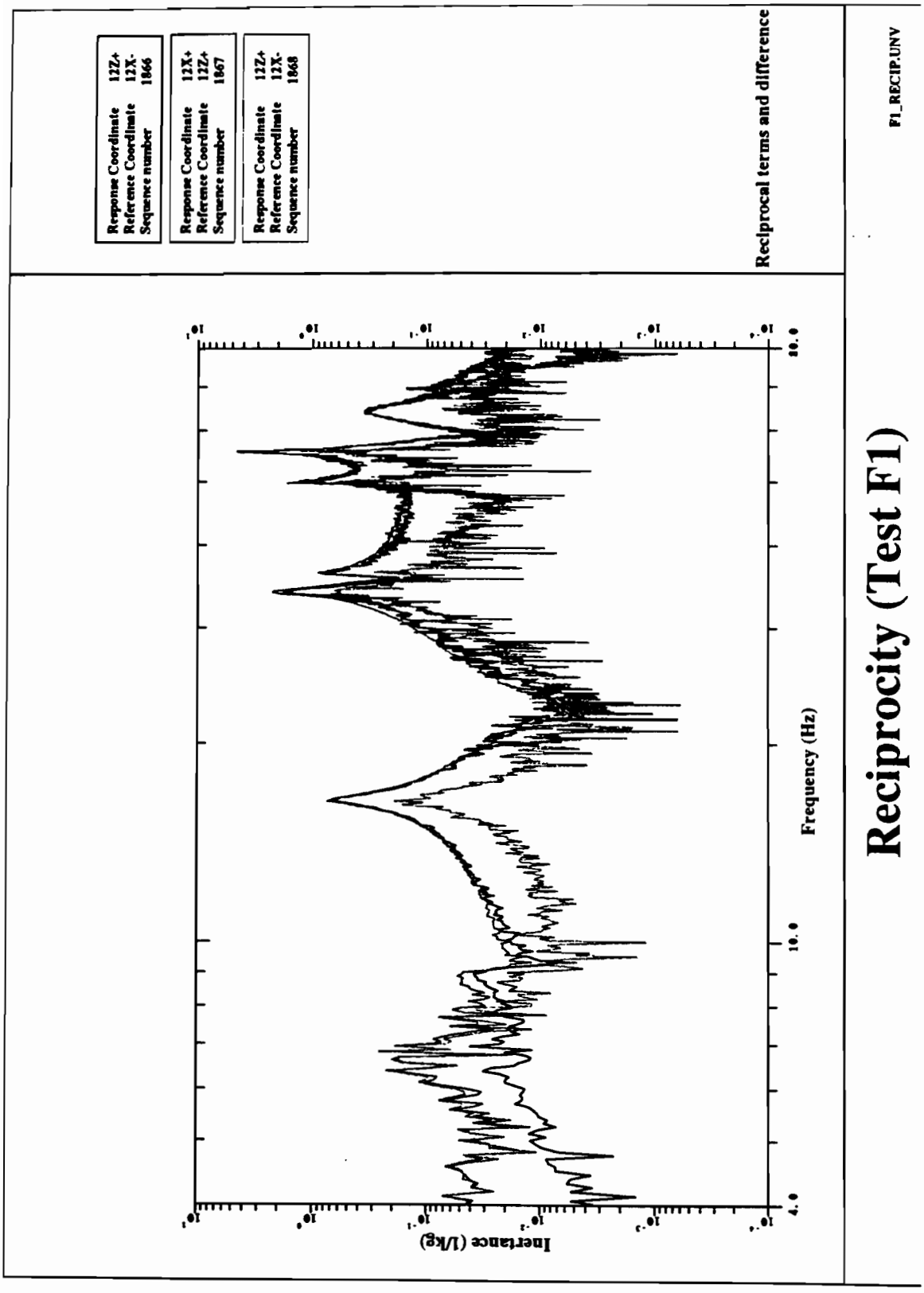
Reciprocity (Test F1)
Reciprocal terms and difference
F1_RECIP.UNV
Response Coordinate 12Z+
Reference Coordinate 12X-
Sequence number 1866
Response Coordinate 12X+
Reference Coordinate 12Z+
Sequence number 1867
Response Coordinate 12Z+
Reference Coordinate 12X-
Sequence number 1868
Inertance (1/kg)
Frequency (Hz)
4.0
10.0
80.0

Figure 22

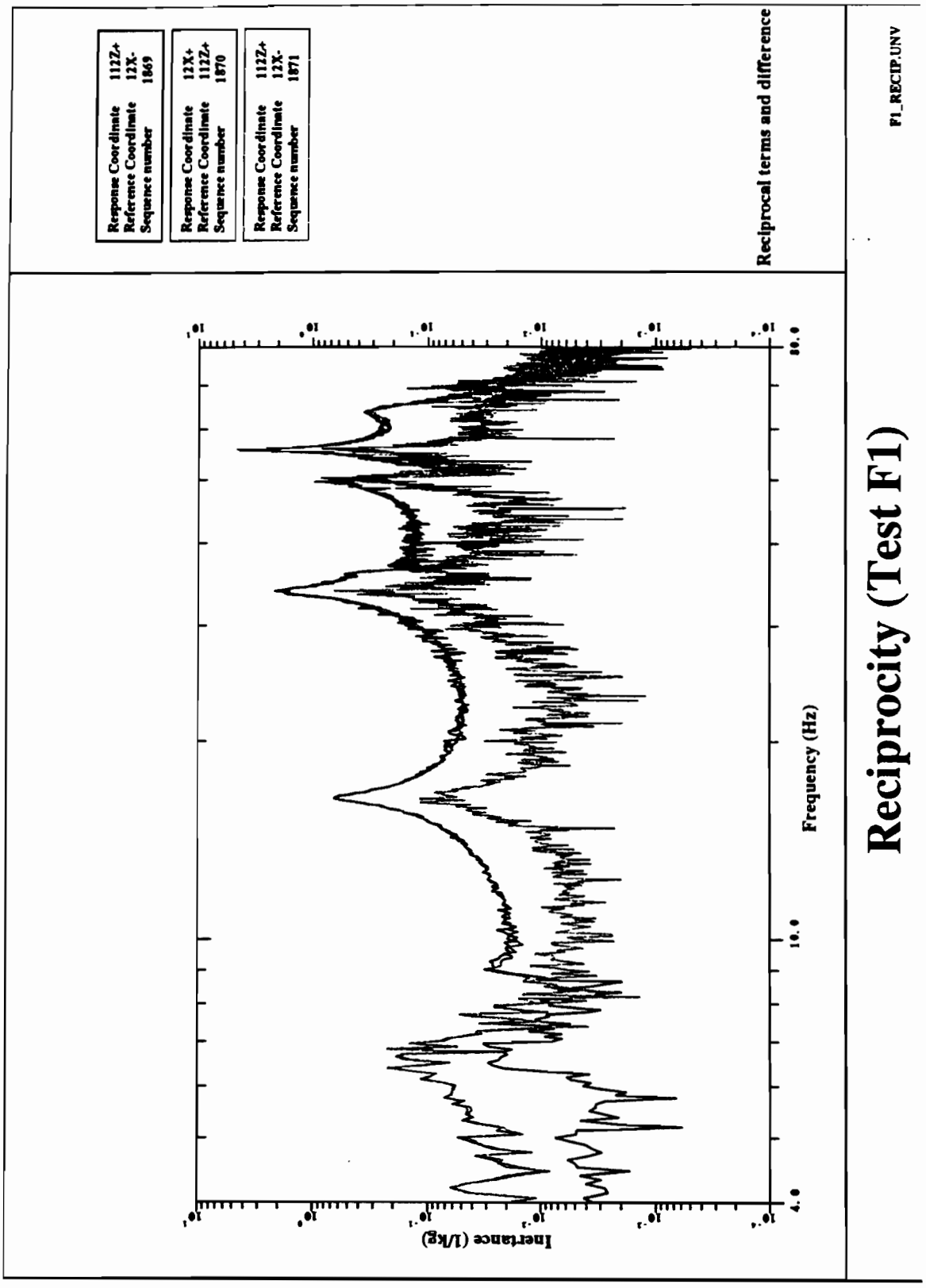
Response Coordinate 1122Z+
Reference Coordinate 12X-
Sequence number 1869
Response Coordinate 12X+
Reference Coordinate 1122Z+
Sequence number 1870
Response Coordinate 1122Z+
Reference Coordinate 12X-
Sequence number 1871
Reciprocal terms and difference
F1_RECIP.UNV
Reciprocity (Test F1)
Inertance (1/kg)
Frequency (Hz)
4.0
10.0
80.0

Figure 23

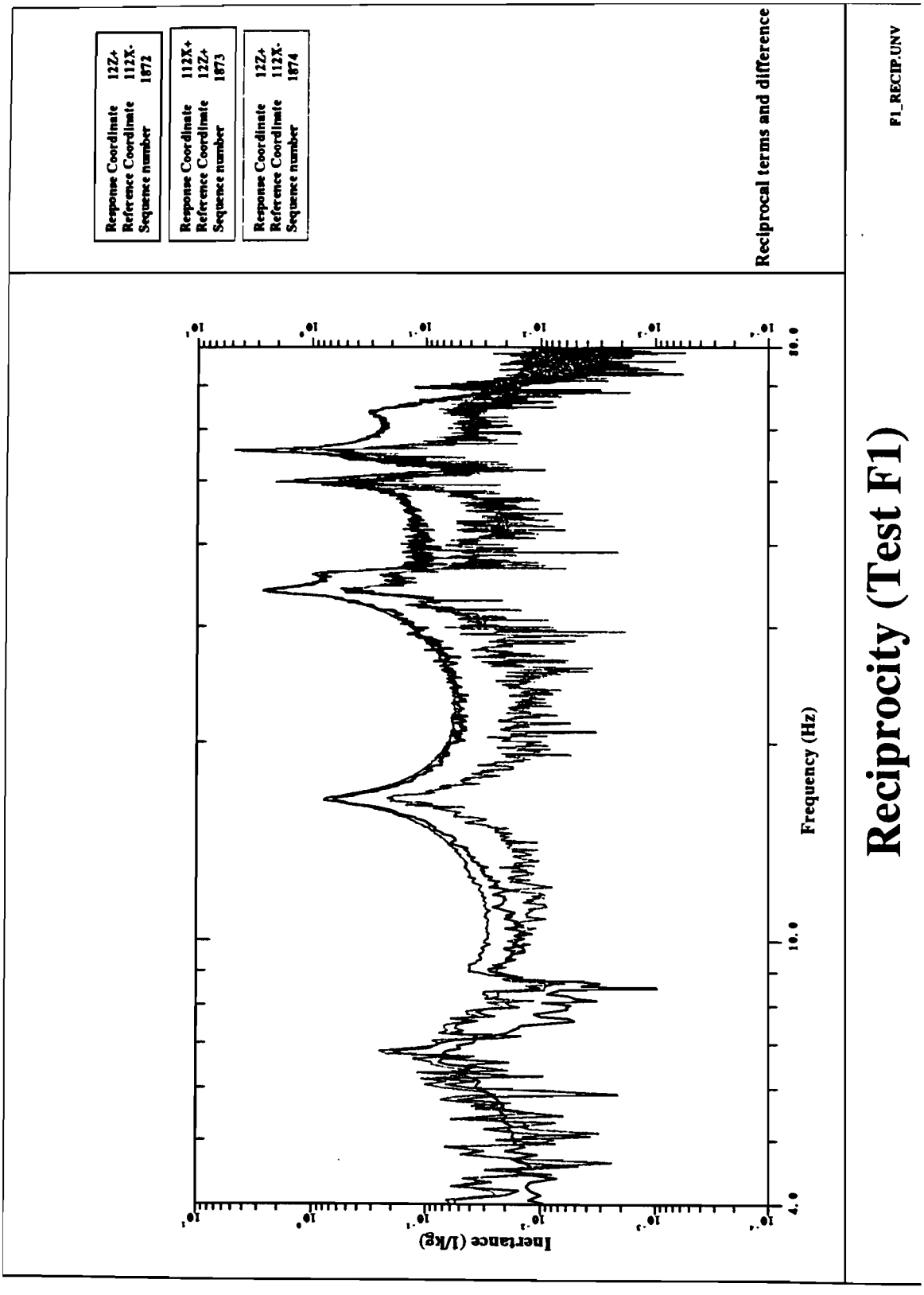
Response Coordinate 122+
Reference Coordinate 112X-
Sequence number 1872
Response Coordinate 112X+
Reference Coordinate 122+
Sequence number 1873
Response Coordinate 122+
Reference Coordinate 112X-
Sequence number 1874
Reciprocal terms and difference
F1_RECIP.UNV
Reciprocity (Test F1)
Inertance (1/kg)
Frequency (Hz)
4.0
10.0
20.0

Figure 24

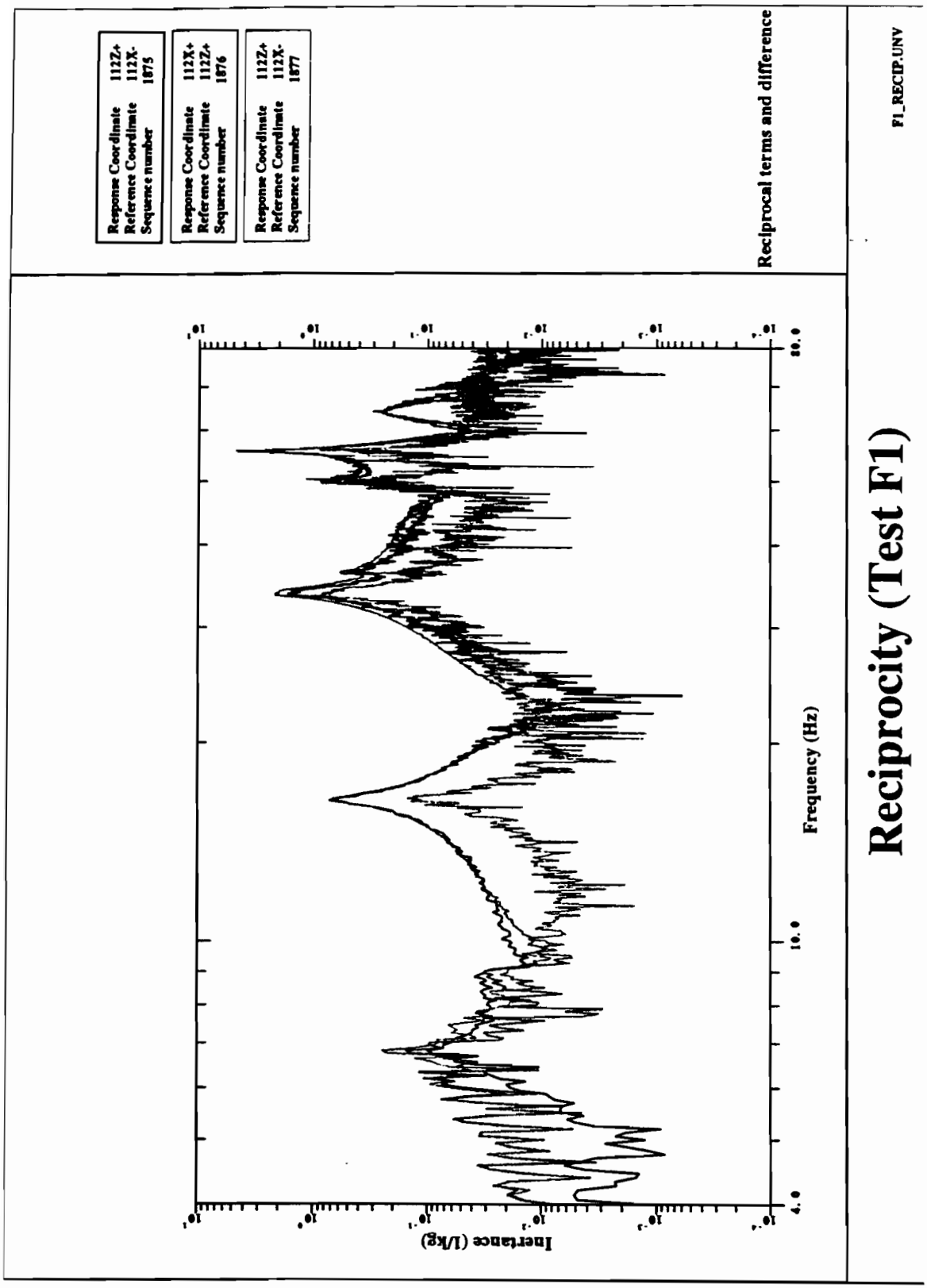
Response Coordinate 1122+
Reference Coordinate 112X-
Sequence number 1875
Response Coordinate 112X+
Reference Coordinate 1122+
Sequence number 1876
Response Coordinate 1122+
Reference Coordinate 112X-
Sequence number 1877
Reciprocal terms and difference
F1_RECIP.UNV
Reciprocity (Test F1)
Inertance (1/kg)
Frequency (Hz)
4.0
10.0
80.0

Figure 25

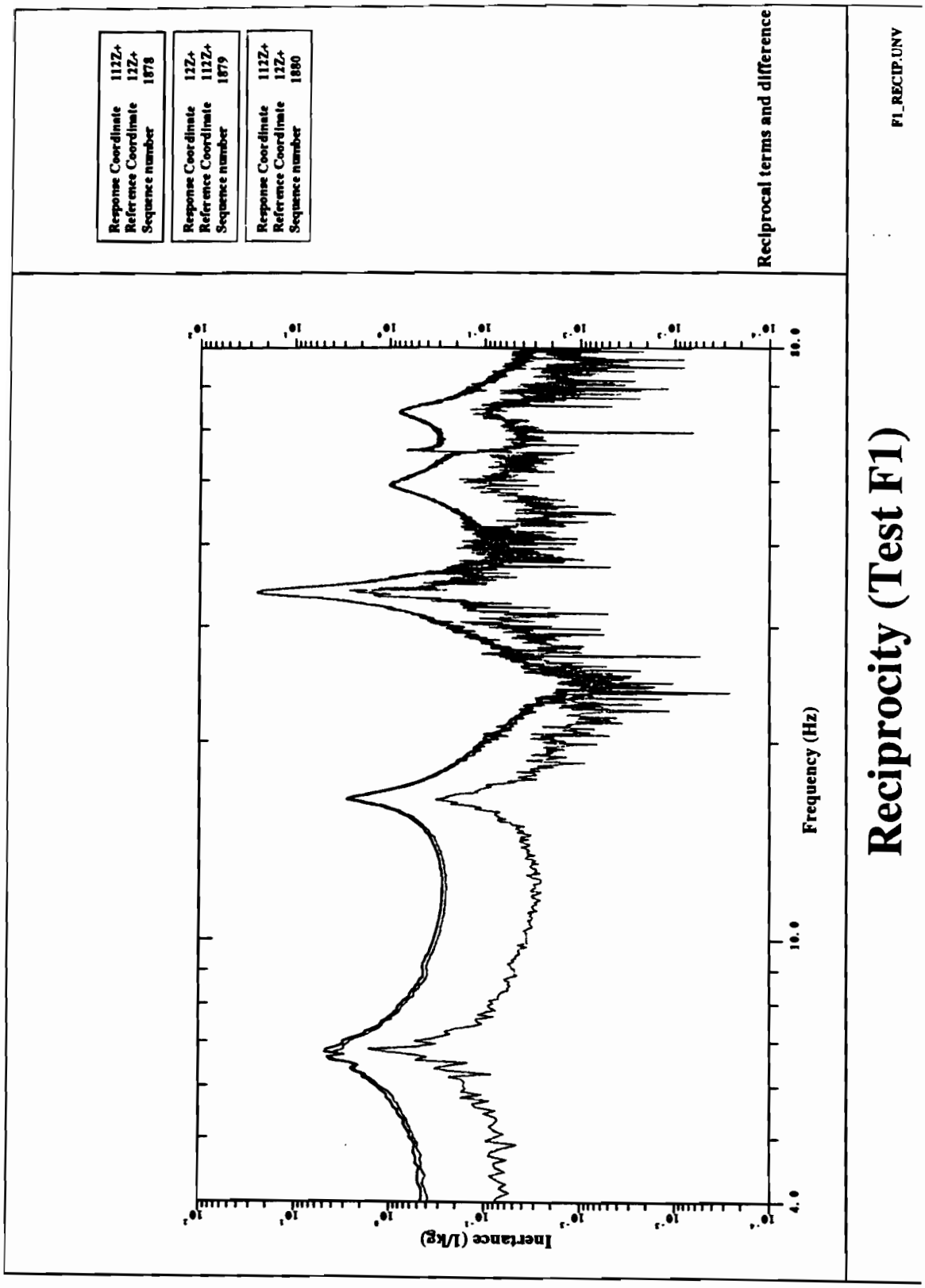
Response Coordinate 112Z+
Reference Coordinate 12Z+
Sequence number 1878
Response Coordinate 12Z+
Reference Coordinate 112Z+
Sequence number 1879
Response Coordinate 112Z+
Reference Coordinate 12Z+
Sequence number 1880
Reciprocal terms and difference
F1_RECIP.UNV
Reciprocity (Test F1)
Inertance (1/kg)
Frequency (Hz)
4.0
10.0
10.0

Figure 26

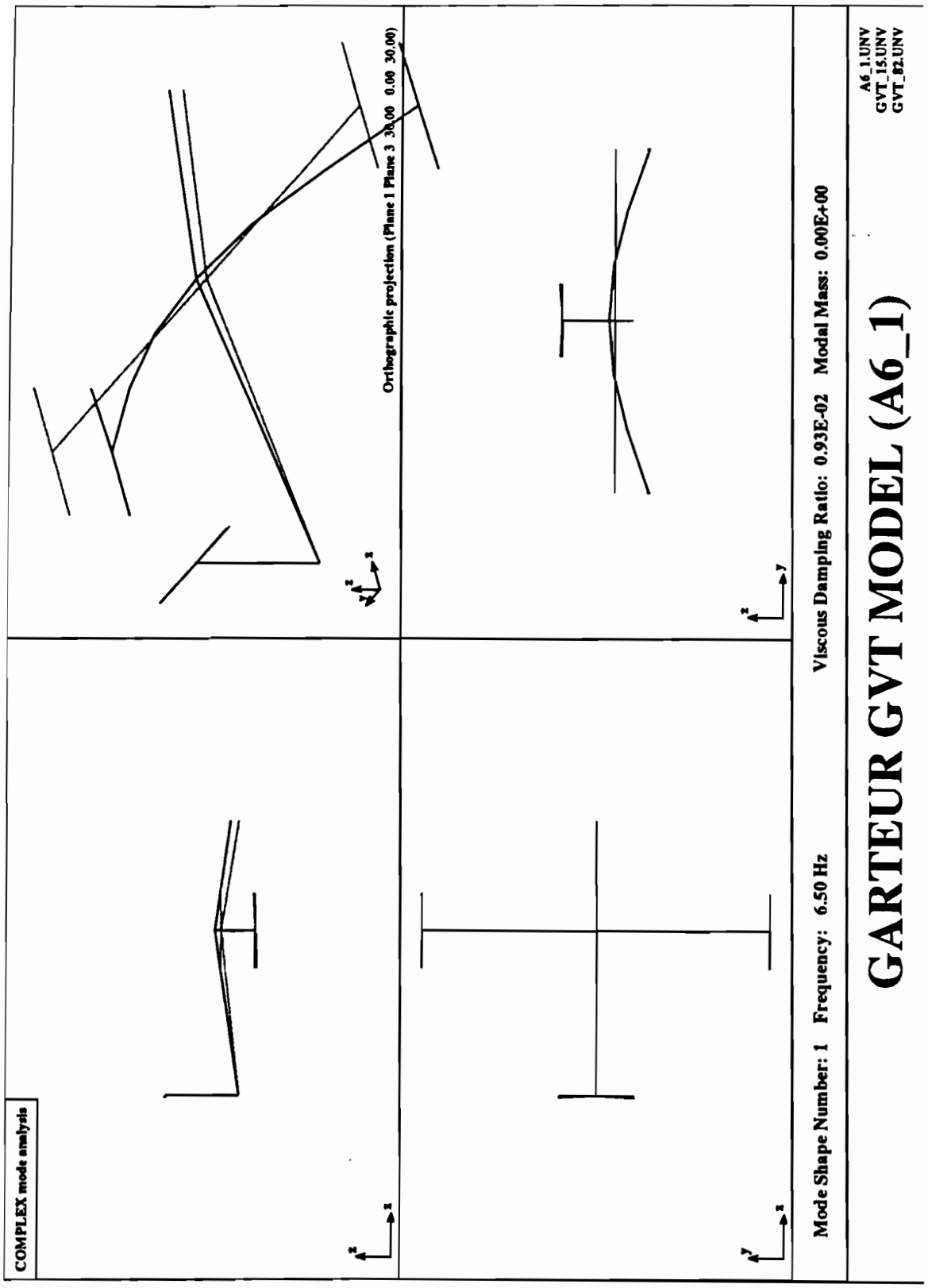
COMPLEX mode analysis
Orthographic projection (Plane 1 Plane 3 30.00 0.00 30.00)
Mode Shape Number: 1 Frequency: 6.50 Hz
Viscous Damping Ratio: 0.93E-02 Modal Mass: 0.00E+00
GARTEUR GVT MODEL (A6_1)
A6_1.UNV
GVT_15.UNV
GVT_82.UNV

Figure 27

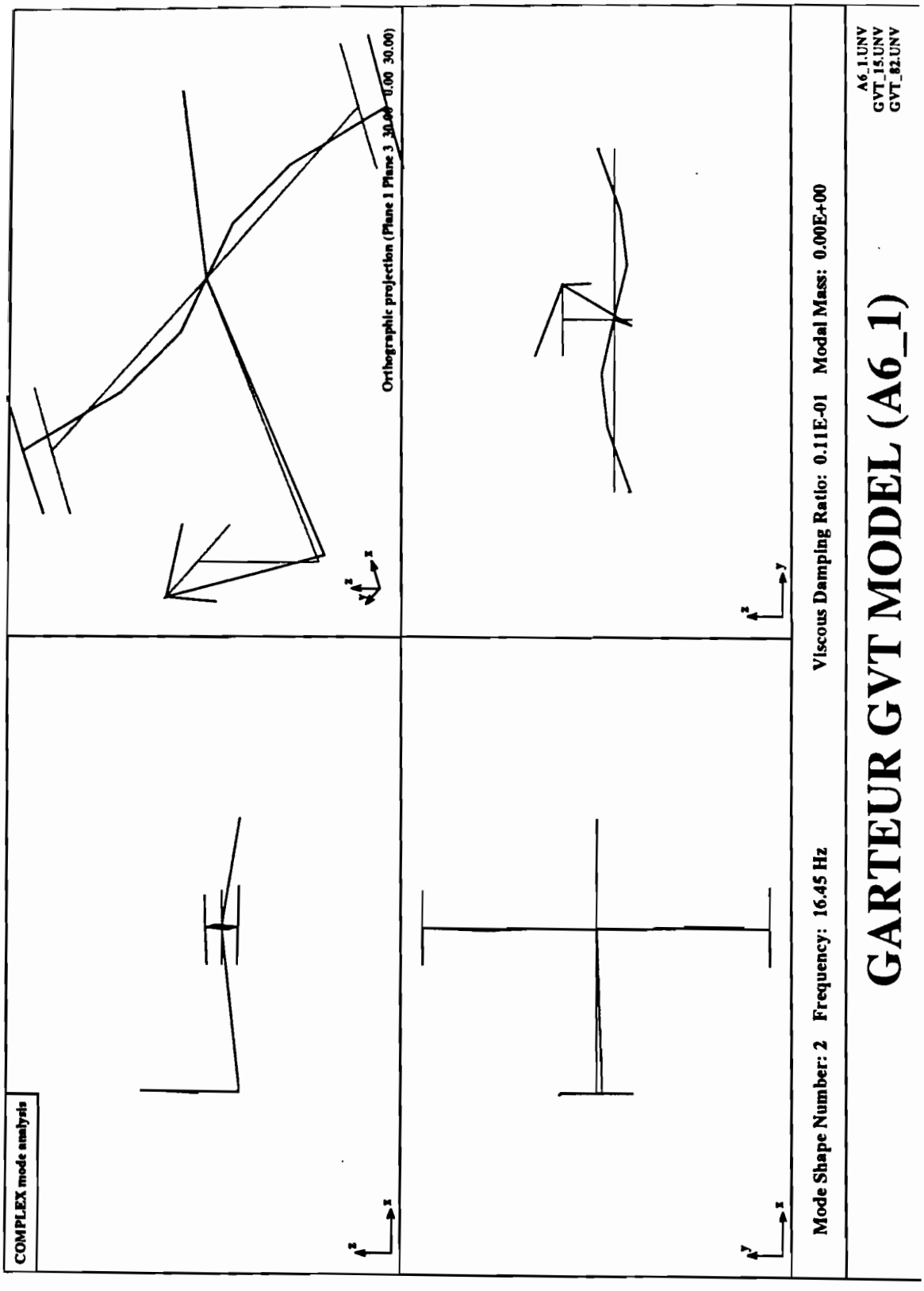
COMPLEX mode analysis
Orthographic projection (Plane 1 Plane 3 30.00 0.00 30.00)
Mode Shape Number: 2 Frequency: 16.45 Hz
Viscous Damping Ratio: 0.11E-01 Modal Mass: 0.00E+00
GARTEUR GVT MODEL (A6_1)
A6_1.UNV
GVT_15.UNV
GVT_82.UNV

Figure 28

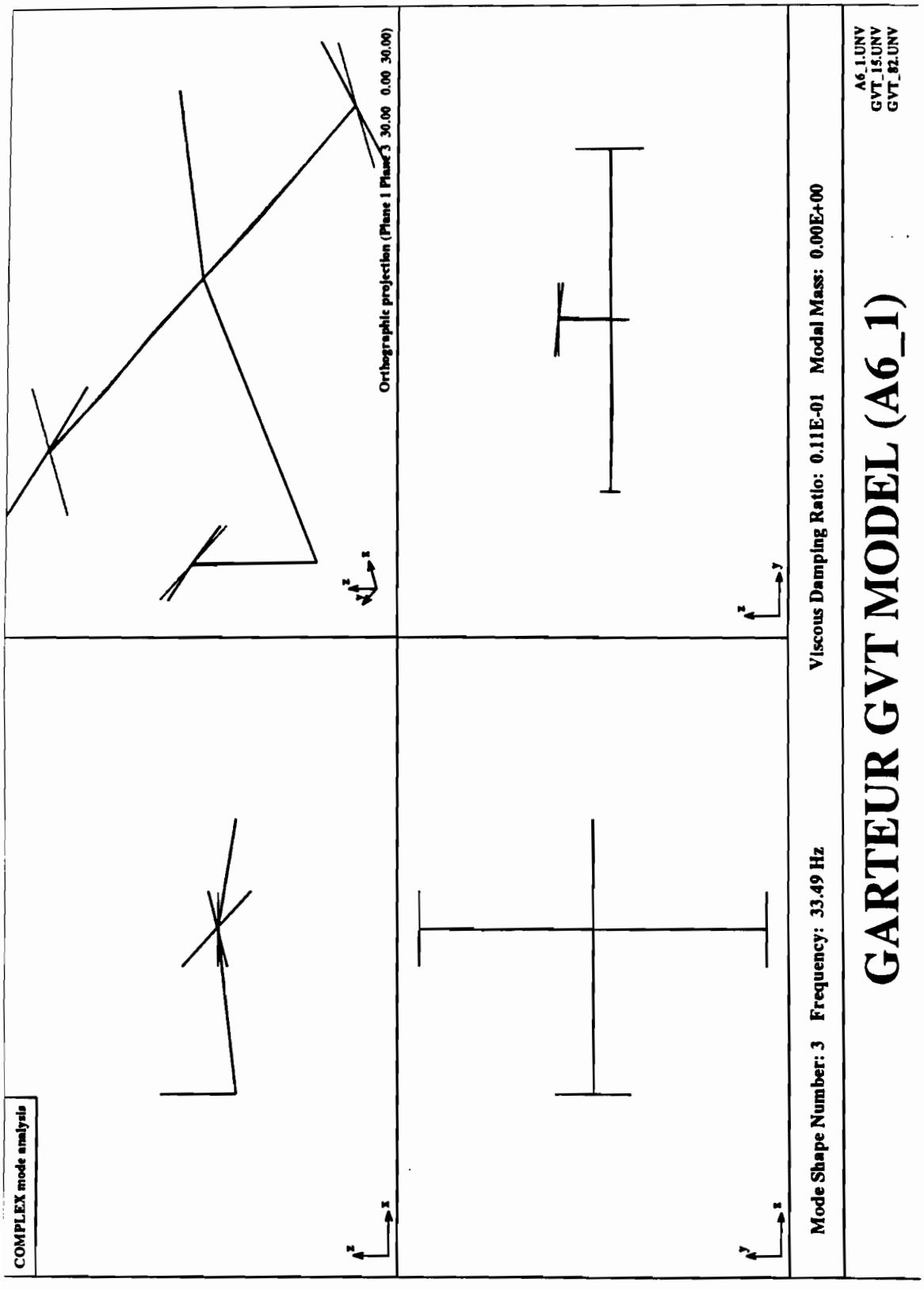
COMPLEX mode analysis
Orthographic projection (Plane 1 Plane 3 30.00 0.00 30.00)
Mode Shape Number: 3 Frequency: 33.49 Hz
Viscous Damping Ratio: 0.11E-01 Modal Mass: 0.00E+00
GARTEUR GVT MODEL (A6_1)
A6_1.UNV
GVT_15.UNV
GVT_82.UNV

Figure 29

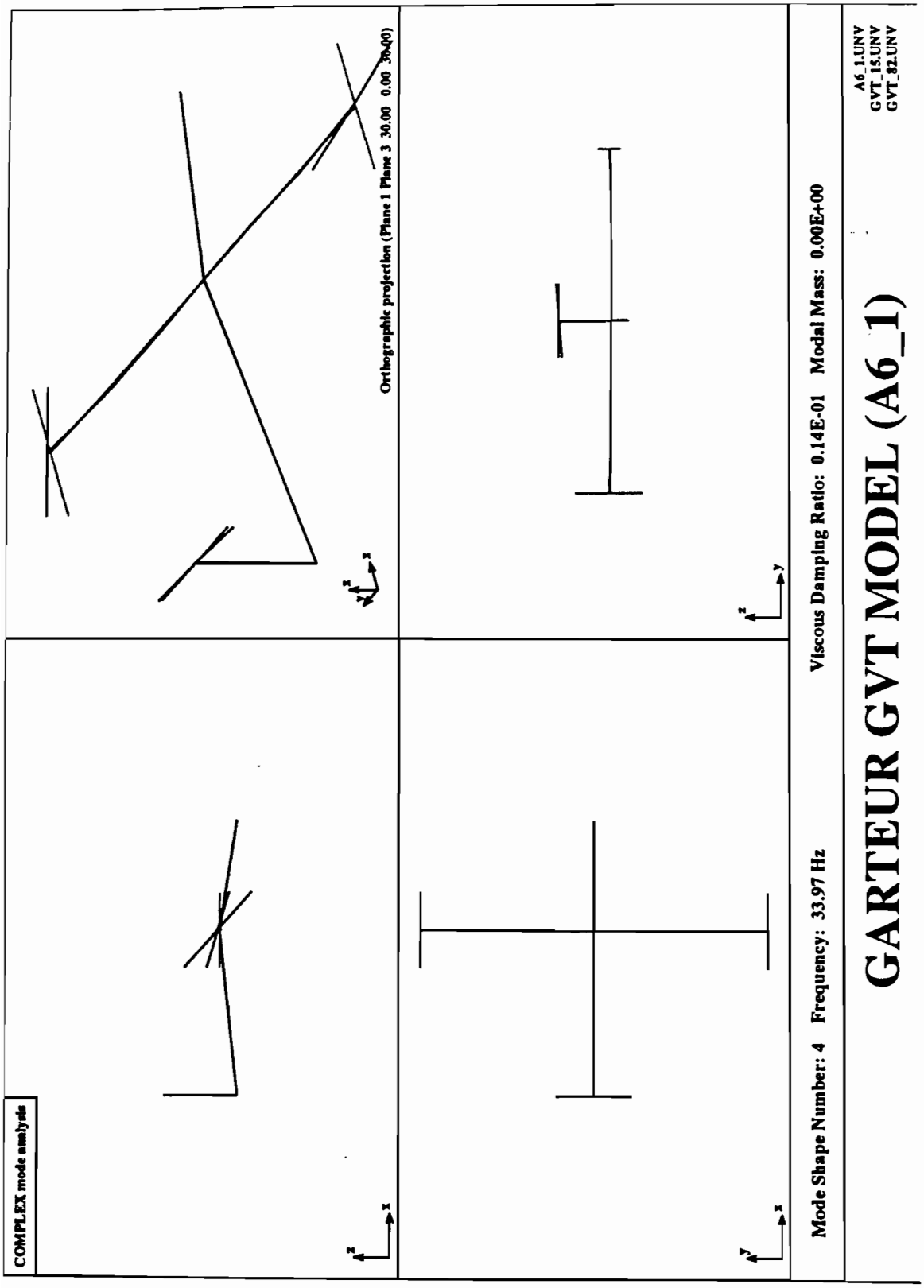
COMPLEX mode analysis
Orthographic projection (Plane 1 Plane 3 30.00 0.00 30.00)
Mode Shape Number: 4 Frequency: 33.97 Hz
Viscous Damping Ratio: 0.14E-01 Modal Mass: 0.00E+00
GARTEUR GVT MODEL (A6_1)
A6_1.UNV
GVT_15.UNV
GVT_82.UNV

Figure 30

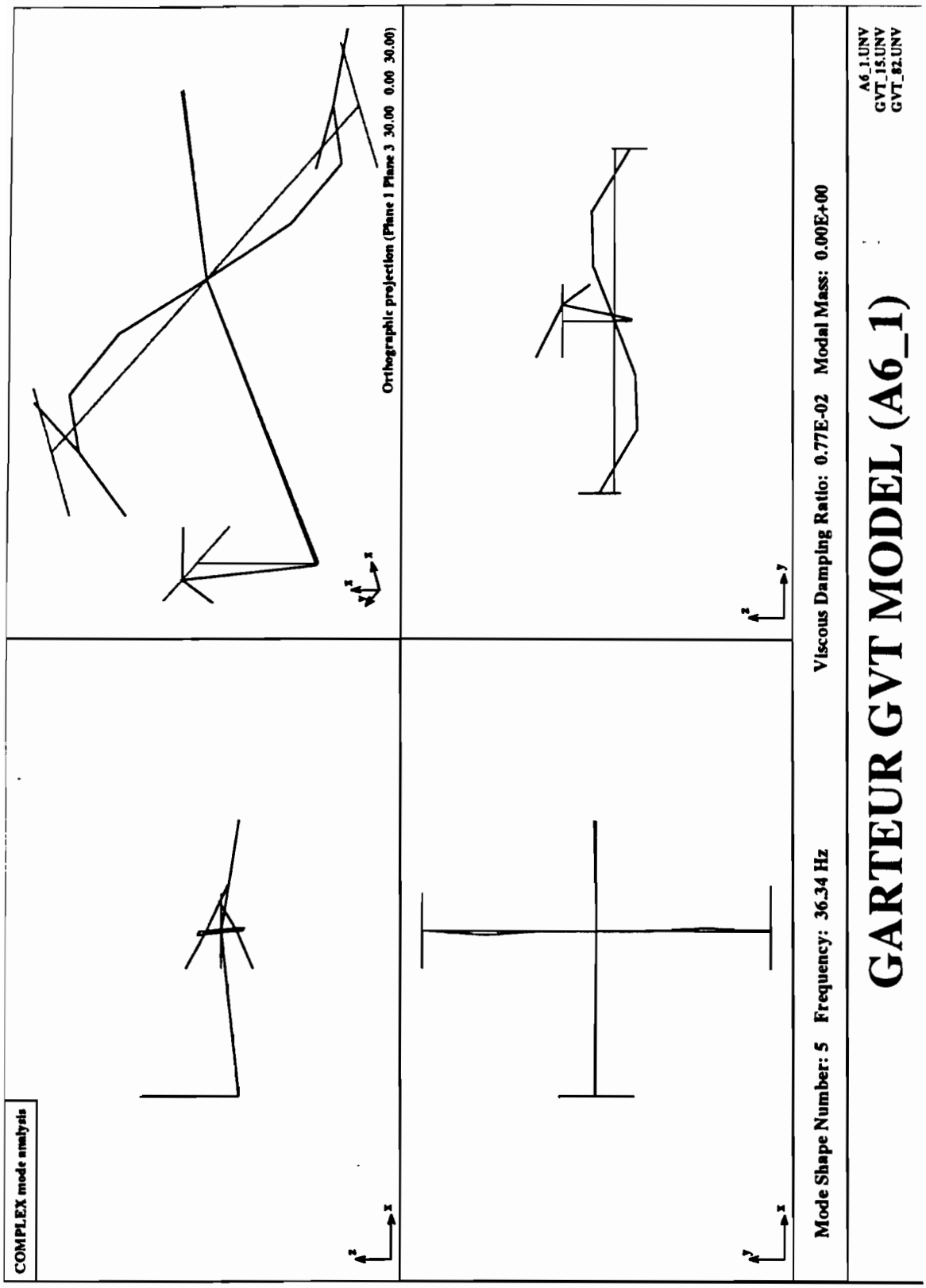
COMPLEX mode analysis
Orthographic projection (Plane 1 Plane 3 30.00 0.00 30.00)
Mode Shape Number: 5 Frequency: 36.34 Hz
Viscous Damping Ratio: 0.77E-02 Modal Mass: 0.00E+00
GARTEUR GVT MODEL (A6_1)
A6_1.UNV
GVT_15.UNV
GVT_82.UNV

Figure 31

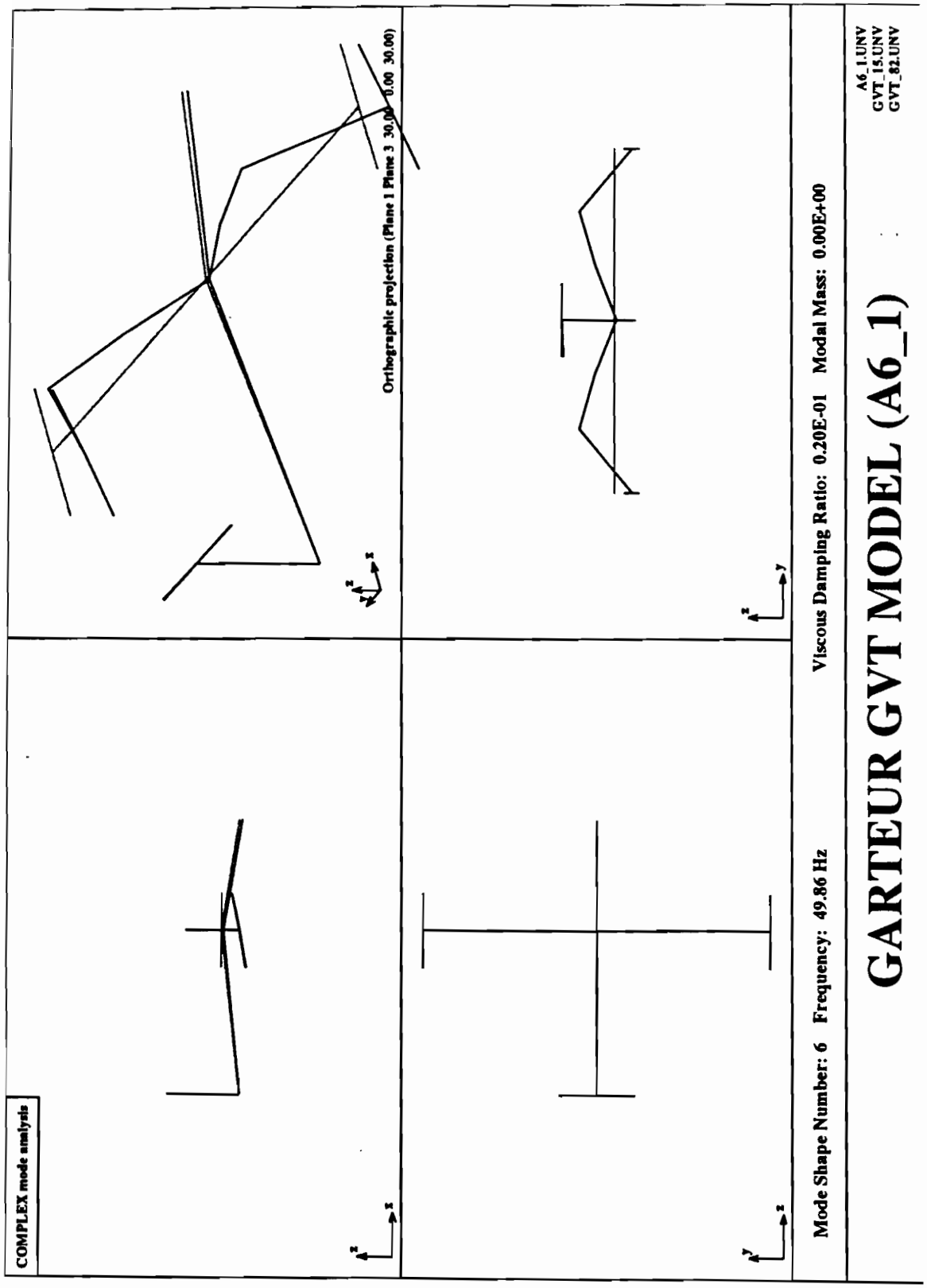
COMPLEX mode analysis
Orthographic projection (Plane 1 Plane 3 30.00 0.00 30.00)
Mode Shape Number: 6 Frequency: 49.86 Hz
Viscous Damping Ratio: 0.20E-01 Modal Mass: 0.00E+00
GARTEUR GVT MODEL (A6_1)
A6_1.UNV
GVT_15.UNV
GVT_82.UNV

Figure 32

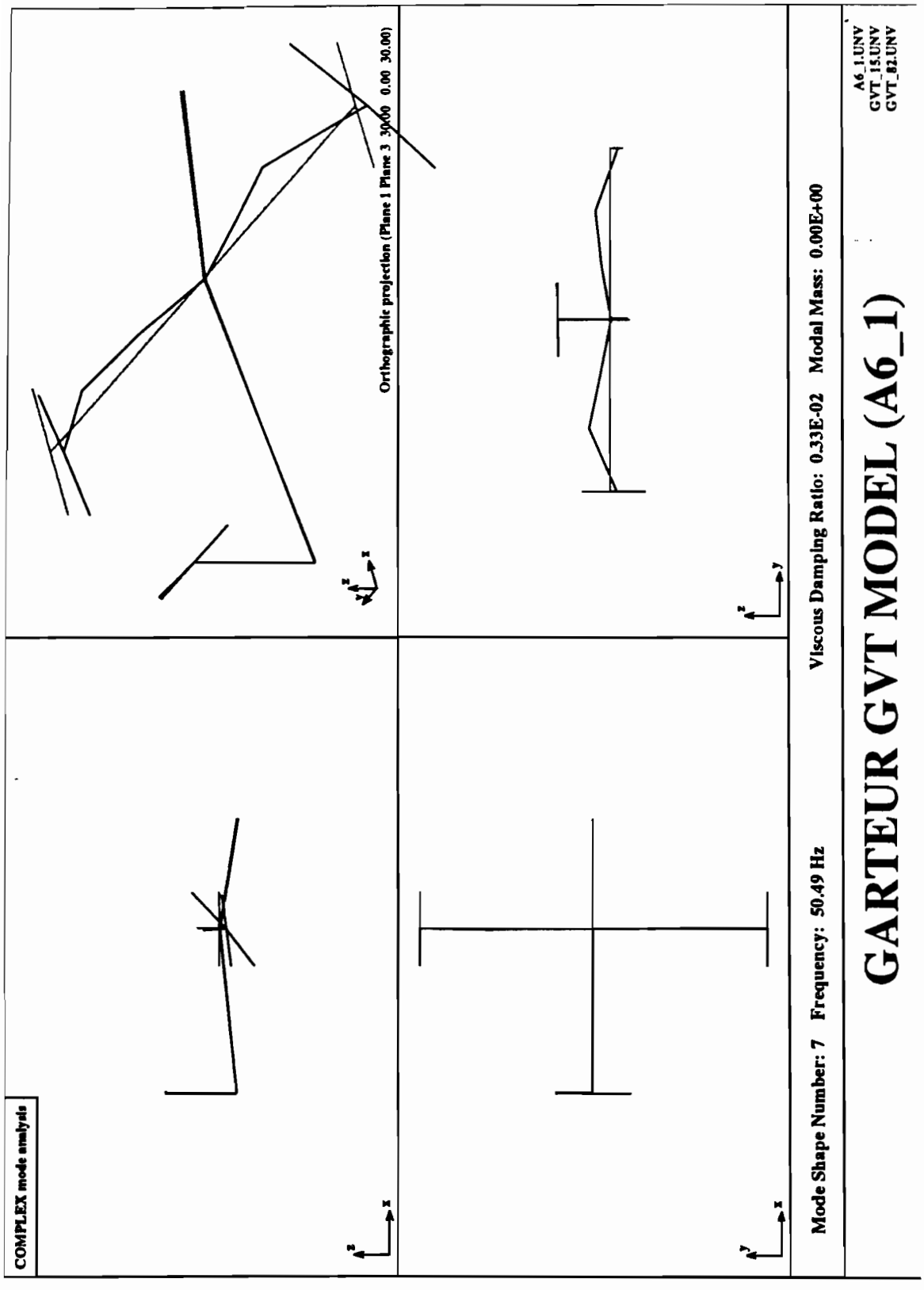
COMPLEX mode analysis
Orthographic projection (Plane 1 Plane 3 30.00 0.00 30.00)
Mode Shape Number: 7 Frequency: 50.49 Hz
Viscous Damping Ratio: 0.33E-02 Modal Mass: 0.00E+00
GARTEUR GVT MODEL (A6_1)
A6_1.UNV
GVT_15.UNV
GVT_82.UNV

Figure 33

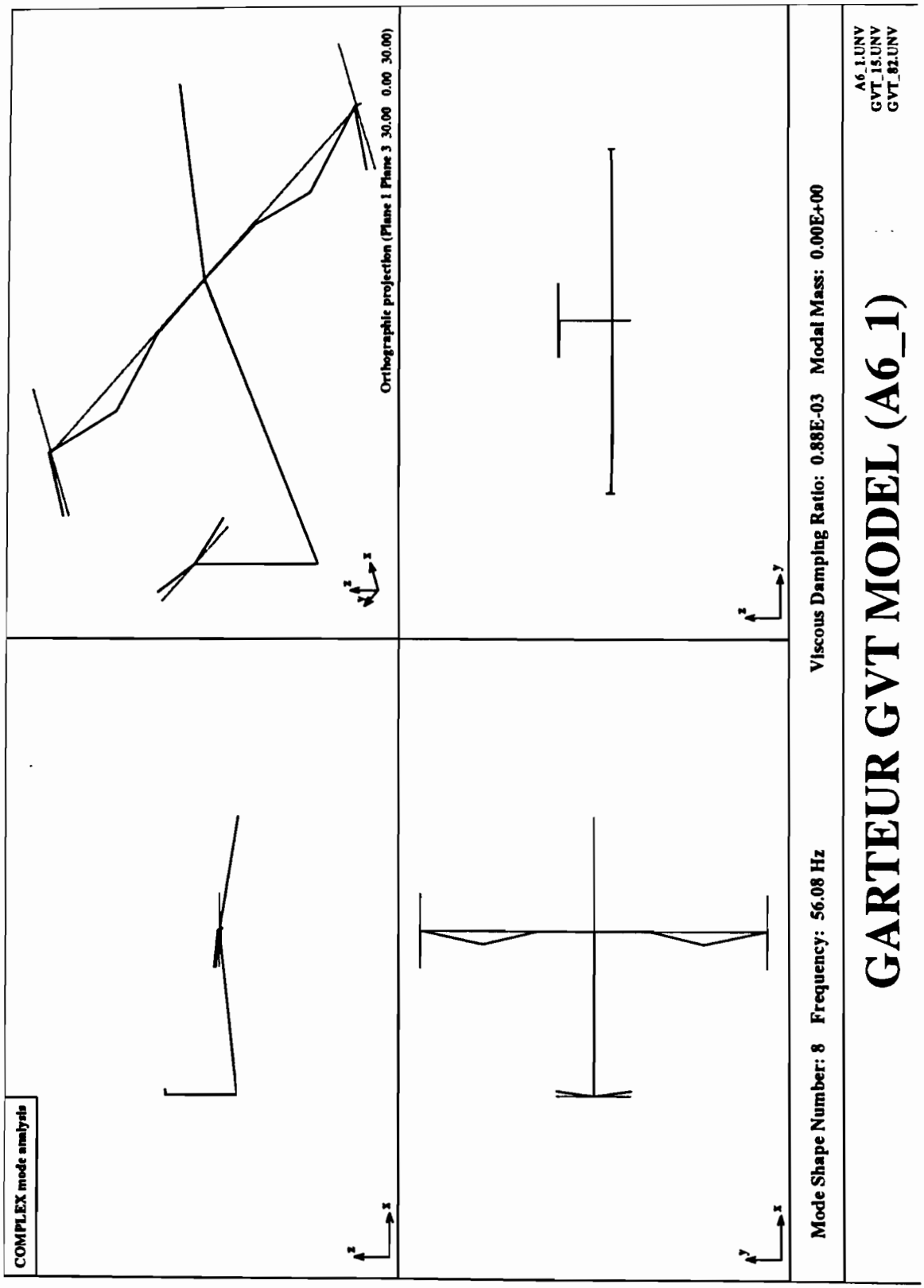
COMPLEX mode analysis
Orthographic projection (Plane 1 Plane 3 30.00 0.00 30.00)
Mode Shape Number: 8 Frequency: 56.08 Hz
Viscous Damping Ratio: 0.88E-03 Modal Mass: 0.00E+00
GARTEUR GVT MODEL (A6_1)
A6_1.UNV
GVT_15.UNV
GVT_82.UNV

Figure 34

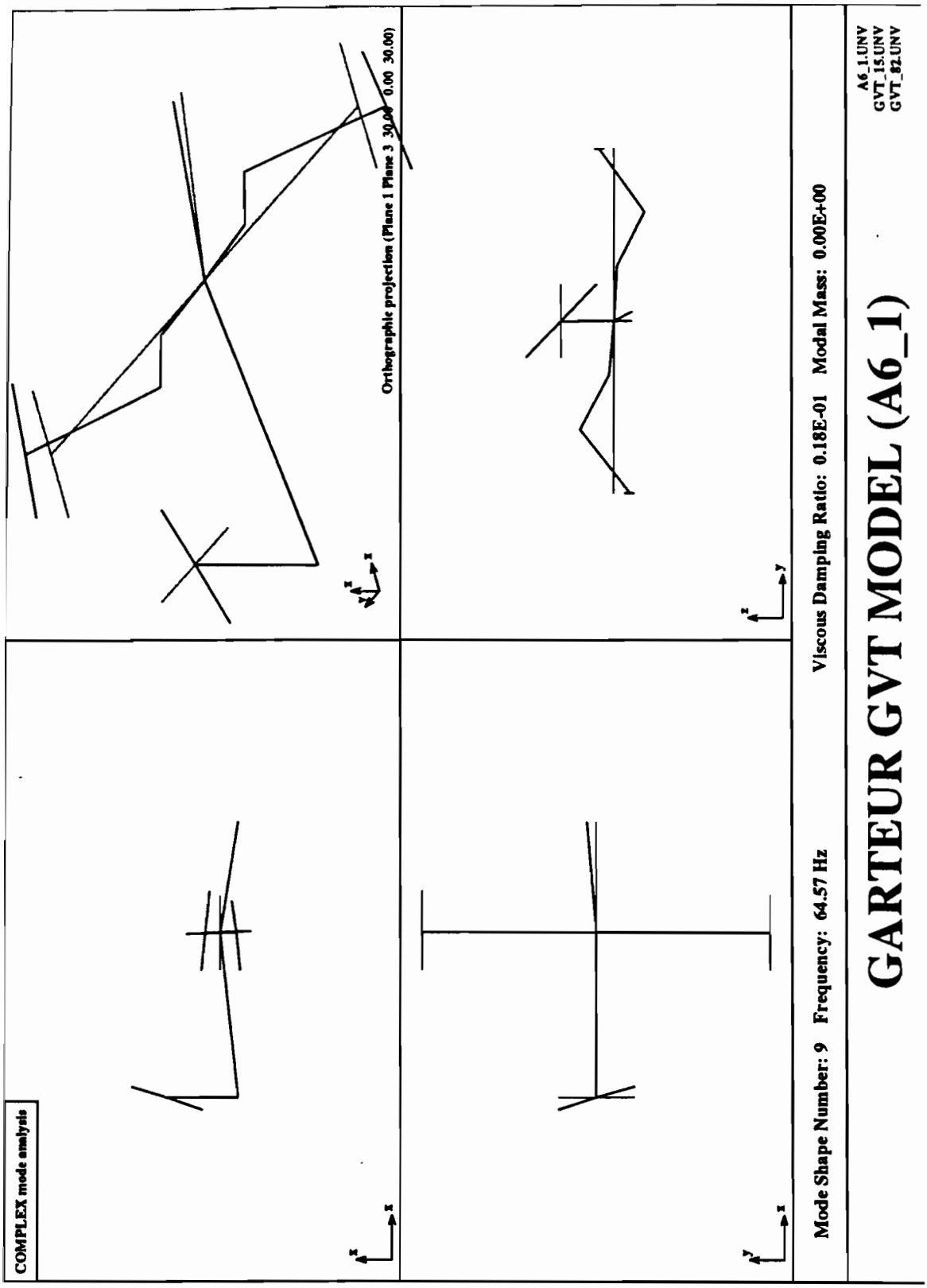
COMPLEX mode analysis
Orthographic projection (Plane 1 Plane 3 30.00 0.00 30.00)
Mode Shape Number: 9 Frequency: 64.57 Hz
Viscous Damping Ratio: 0.18E-01 Modal Mass: 0.00E+00
GARTEUR GVT MODEL (A6_1)
A6_1.UNV
GVT_15.UNV
GVT_82.UNV

Figure 35

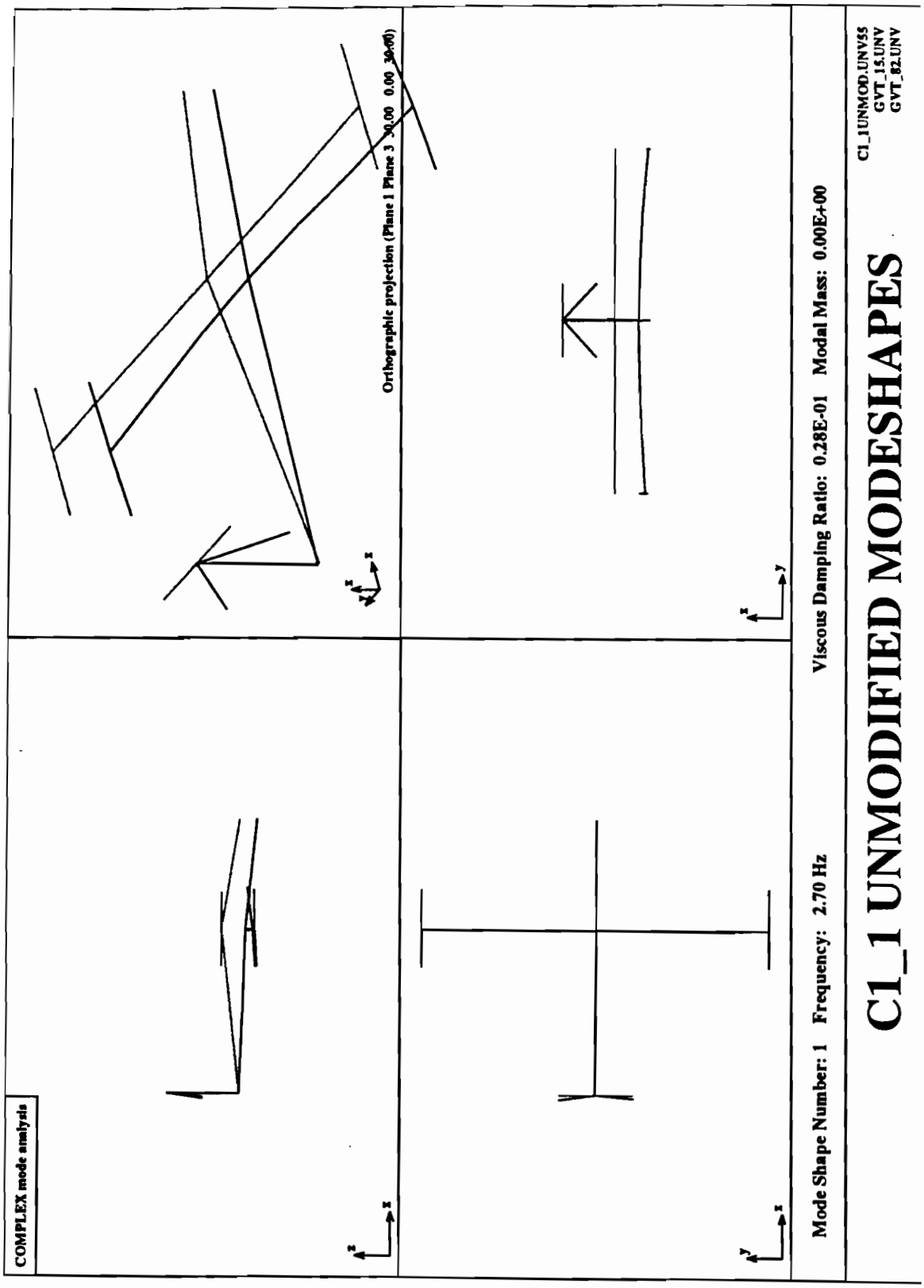
COMPLEX mode analysis
Orthographic projection (Plane 1 Plane 3 30.00 0.00 30.00)
Mode Shape Number: 1 Frequency: 2.70 Hz
Viscous Damping Ratio: 0.28E-01 Modal Mass: 0.00E+00
C1_1UNMOD.UNV55
GVT_15.UNV
GVT_82.UNV
C1_1 UNMODIFIED MODESHAPES

Figure 36

Mode number 3

Frequency = 6.497 Hz
Damping = 0.9254 %
Generalised Mass = 4.272 Kg
Scaling point and direction: 11 3

A6_1.UNV35
A6_1
Analysis data universal file, CADA-X project "mpr_1"
95-Nov-30 15:02.19
MODE NO. 3, FREQUENCY 6.497020(Hz), DAMPING 0.009254

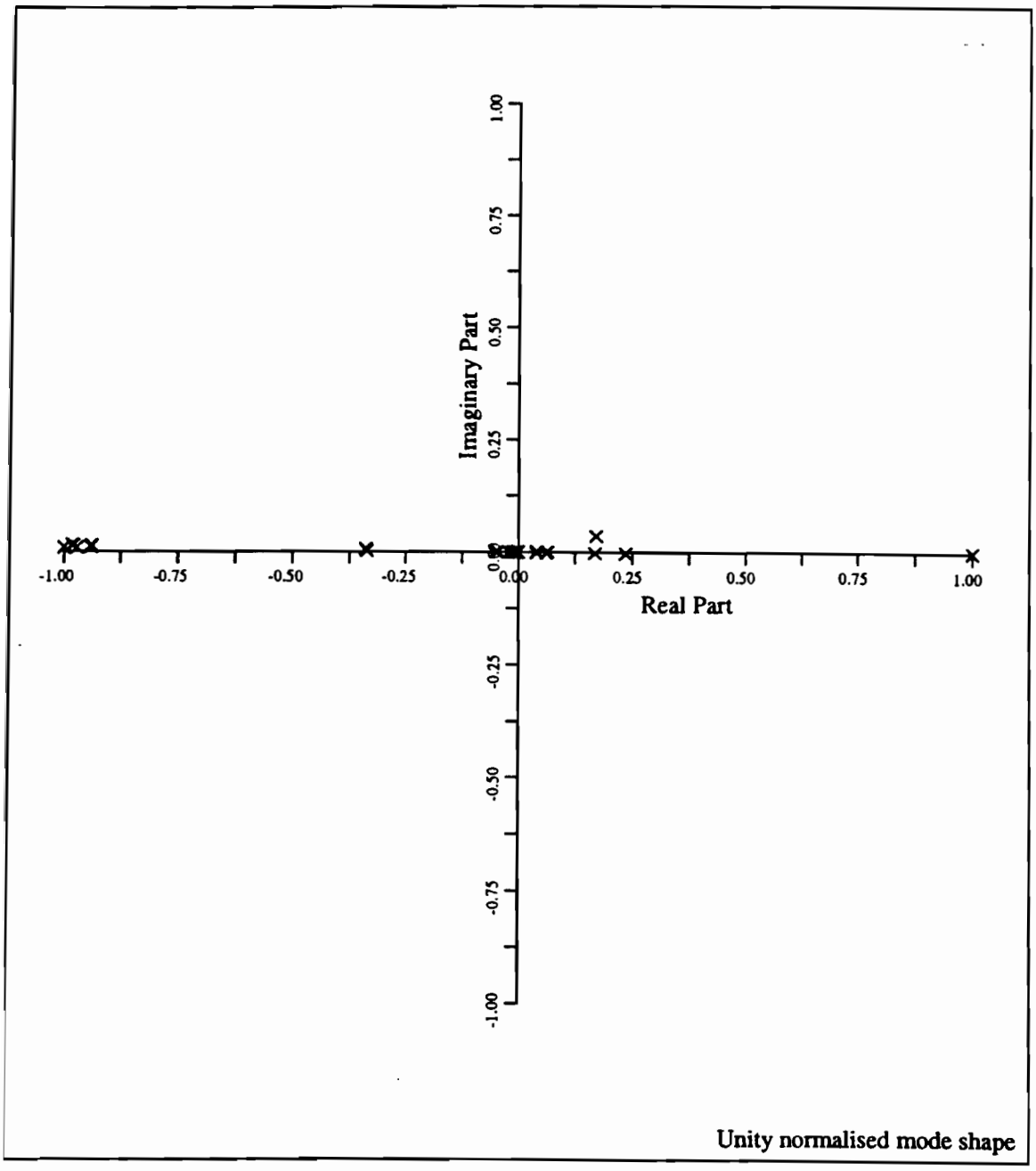

Scatter Plot for 6.50 Hz Mode

Figure 37

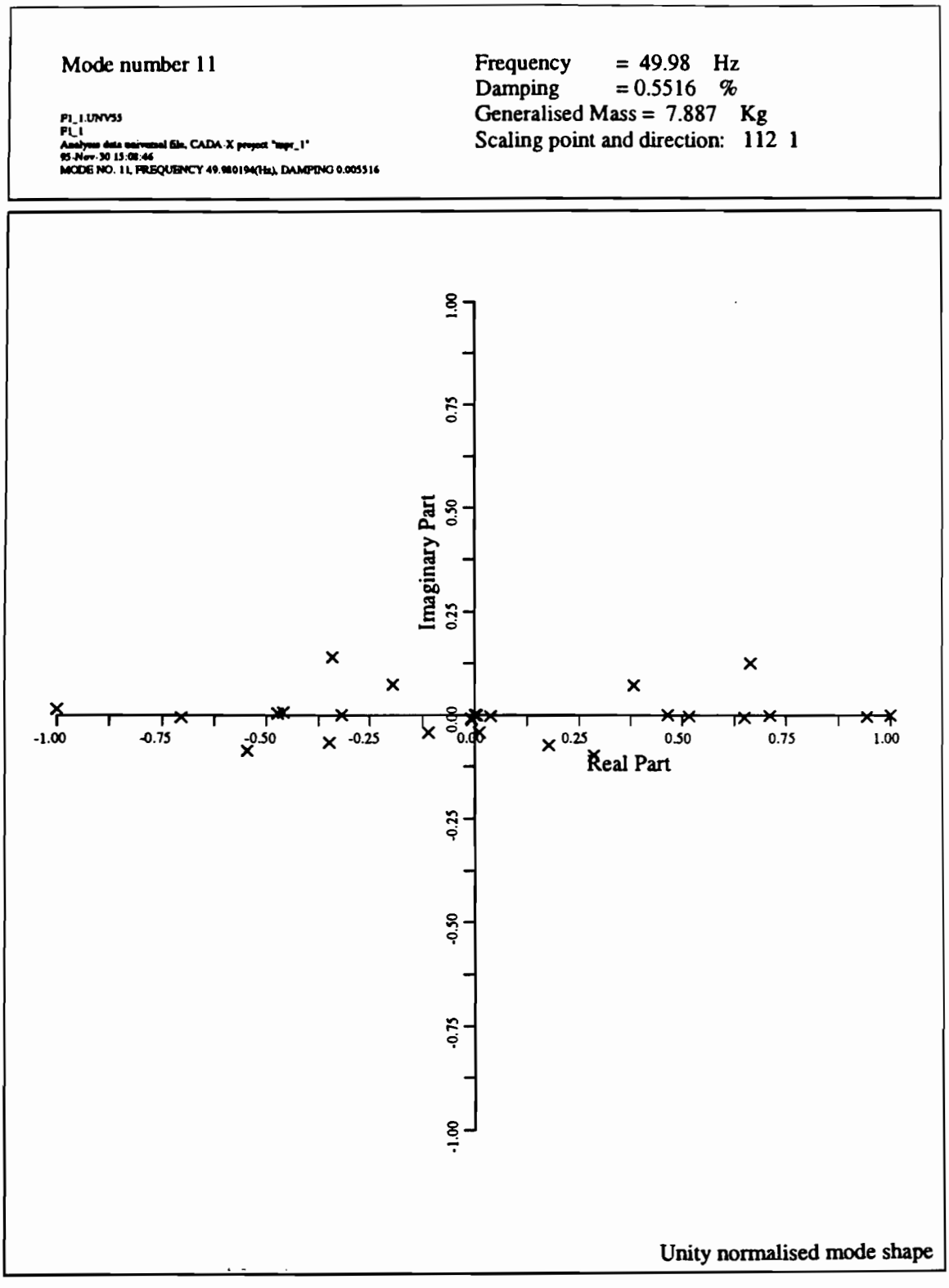

Scatter Plot for 49.98 Hz Mode

Figure 47

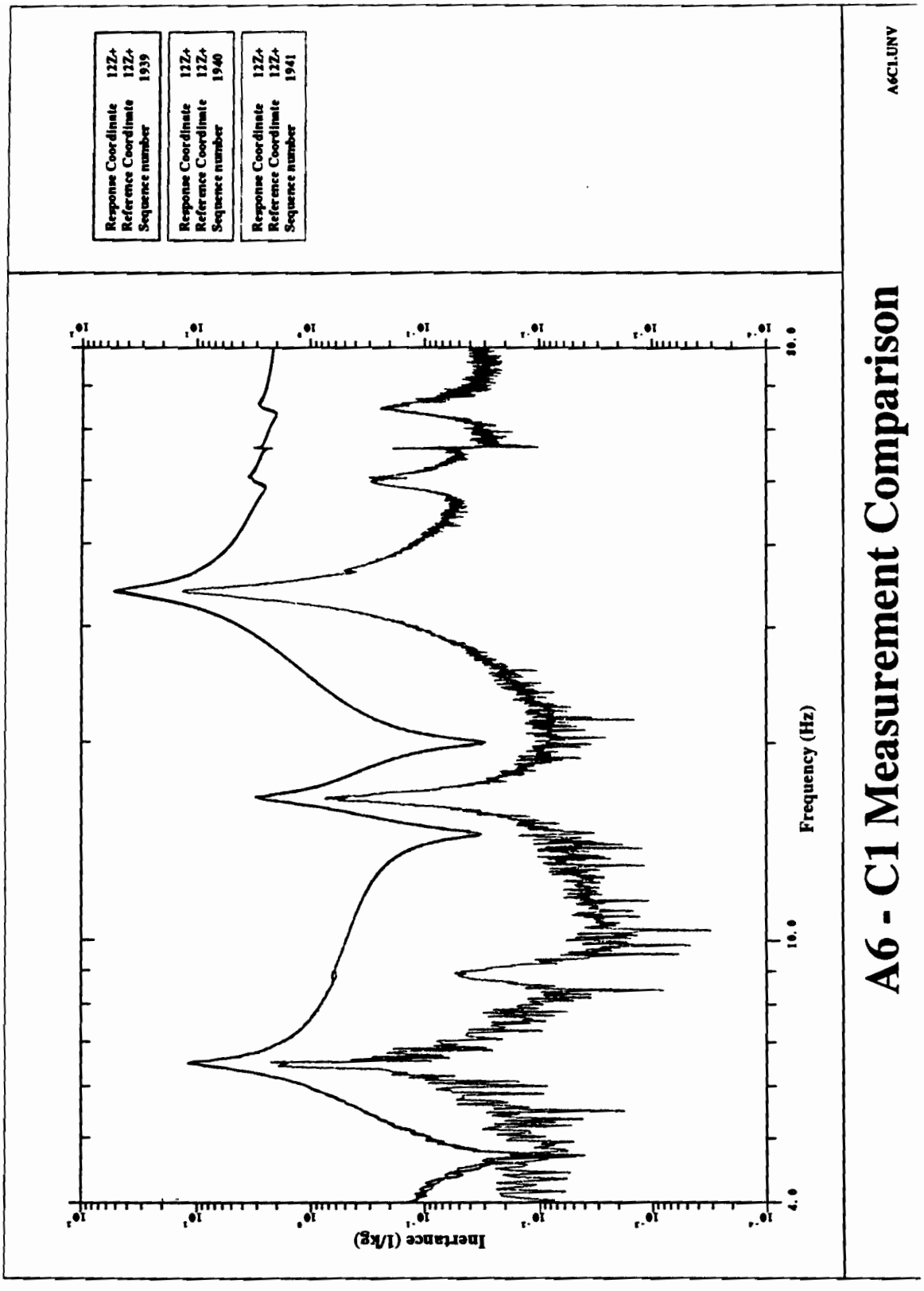
A6 - C1 Measurement Comparison
A6C1.UNV
Response Coordinate 12Z+
Reference Coordinate 12Z+
Sequence number 1939
Response Coordinate 12Z+
Reference Coordinate 12Z+
Sequence number 1940
Response Coordinate 12Z+
Reference Coordinate 12Z+
Sequence number 1941
Inertance (1/kg)
Frequency (Hz)
4.0
10.0
20.0

Figure 46

Mode number 11

Frequency = 64.57 Hz
Damping = 1.826 %
Generalised Mass = 3.686 Kg
Scaling point and direction: 303 3

A6_1.UNV55
A6_1
Analysis data universal file, CADA-X project "mpr_1"
95-Nov-30 15:02:20
MODE NO. 11, FREQUENCY 64.555473(Hz), DAMPING 0.018259

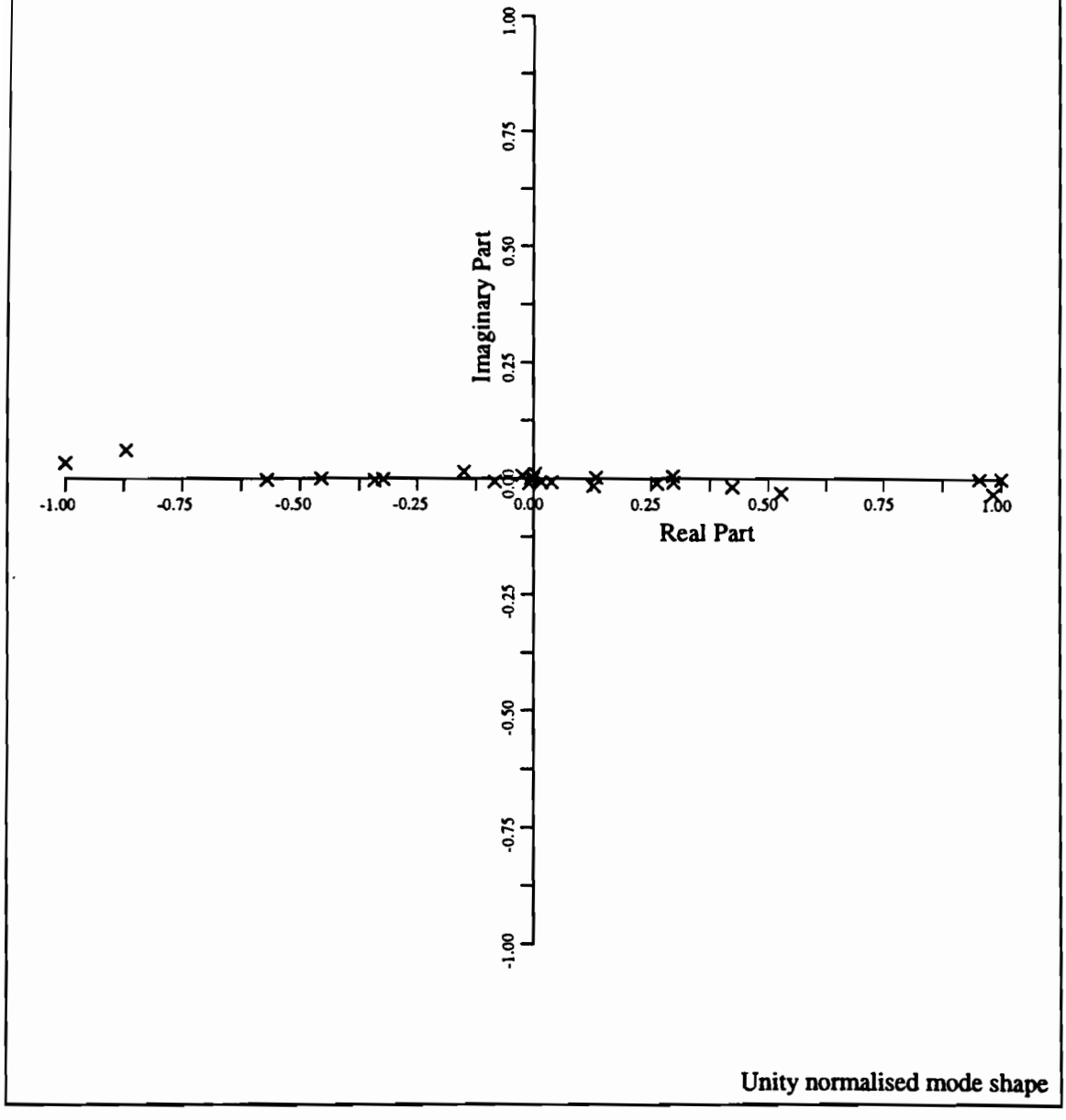

Scatter Plot for 64.57 Hz Mode

Figure 45

Mode number 10

Frequency = 56.08 Hz
Damping = 0.8806E-01%
Generalised Mass = 3.851 Kg
Scaling point and direction: 12 1

A6_1.UNV55
A6_1
Analysis data universal file, CADA-X project "mpr_1"
95-Nov 30 15:02:20
MODE NO. 10, FREQUENCY 56.075478(Hz), DAMPING 0.000881

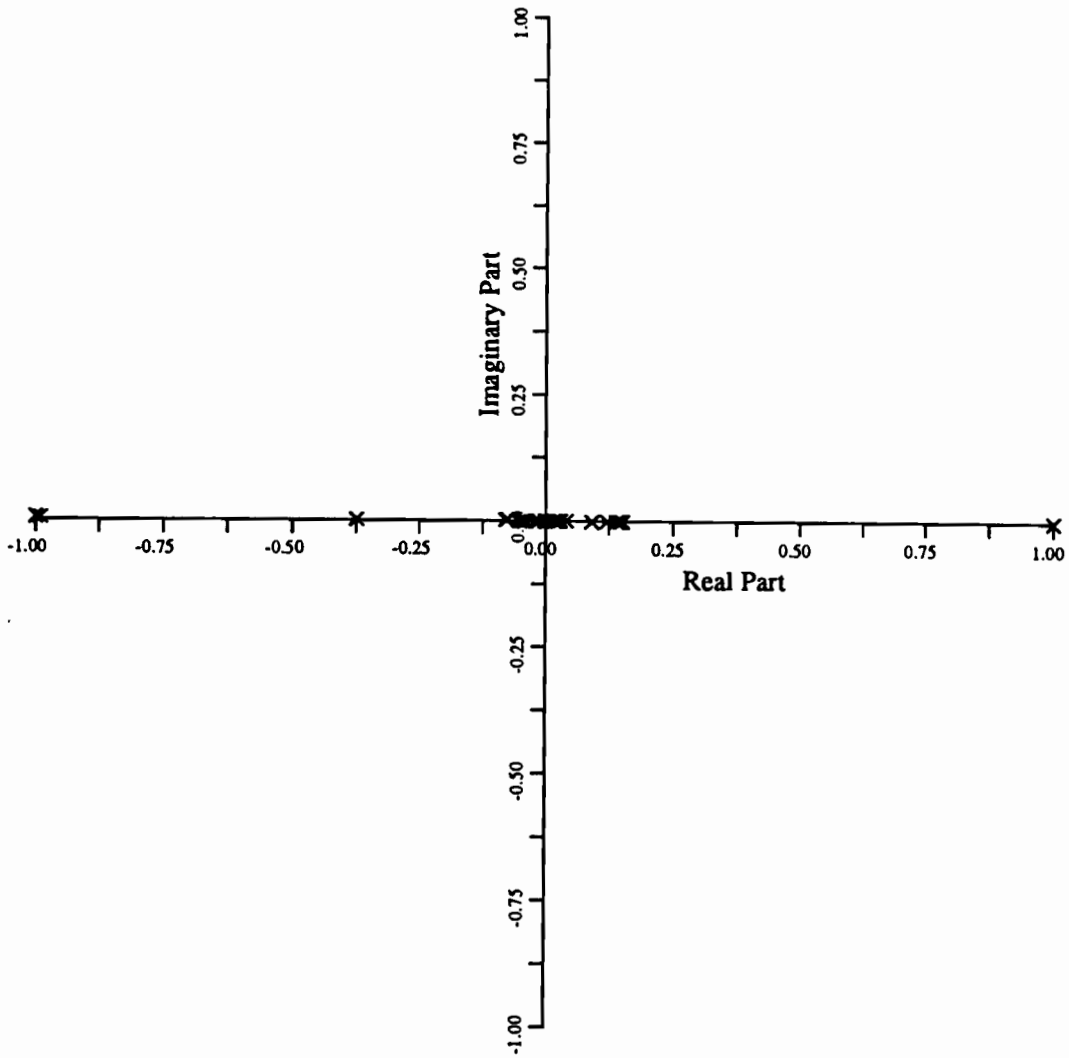

Unity normalised mode shape

Scatter Plot for 56.08 Hz Mode

Figure 44

Mode number 9

Frequency = 50.49 Hz
Damping = 0.3335 %
Generalised Mass = 94.24 Kg
Scaling point and direction: 11 3

A6_1.UNV55
A6_1
Analysis data universal file, CADA-X project "mpr_1"
95-Nov-30 15:02:20
MODE NO. 9, FREQUENCY 50.484779(Hz), DAMPING 0.003335

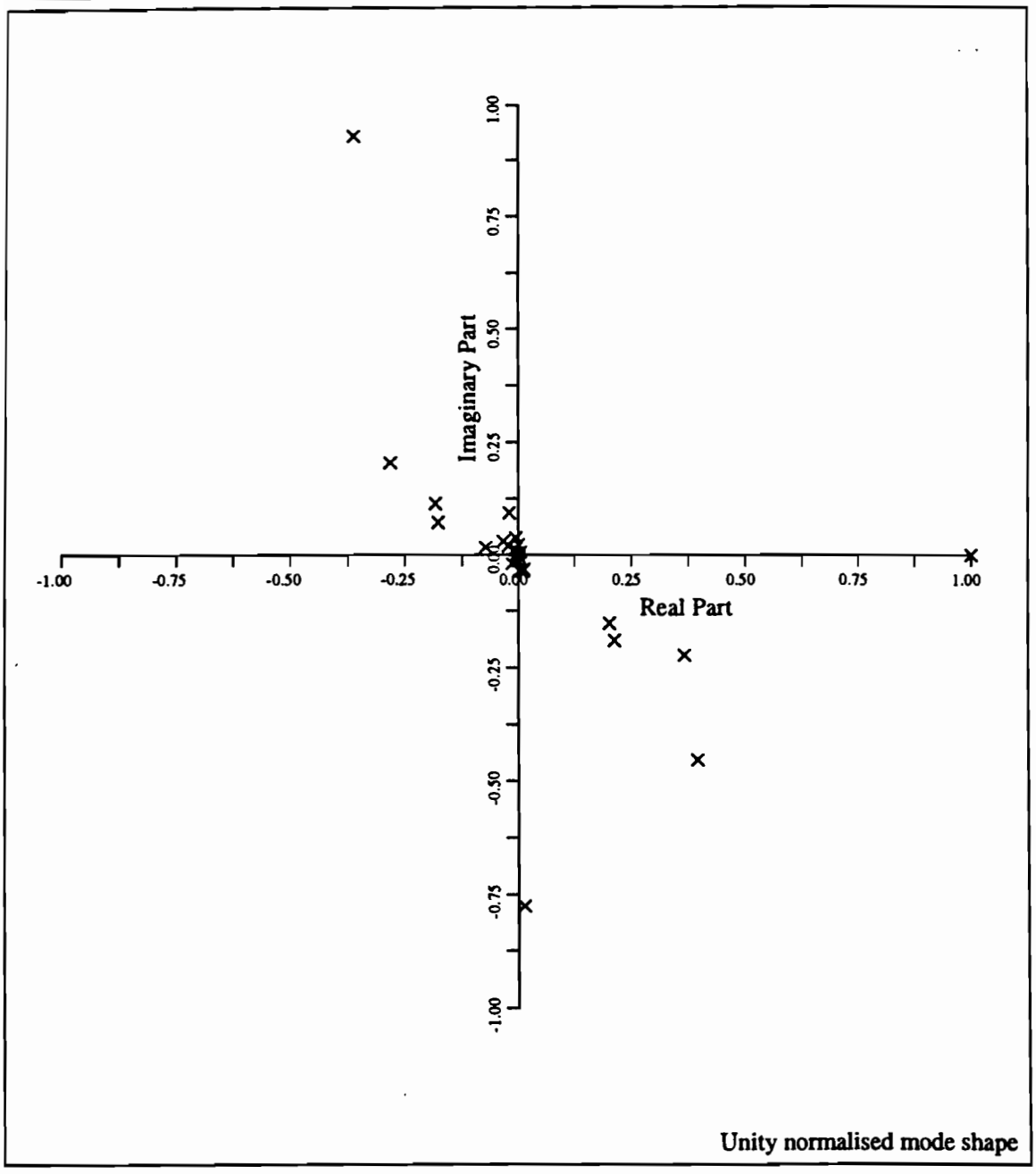

Scatter Plot for 50.49 Hz Mode

Figure 43

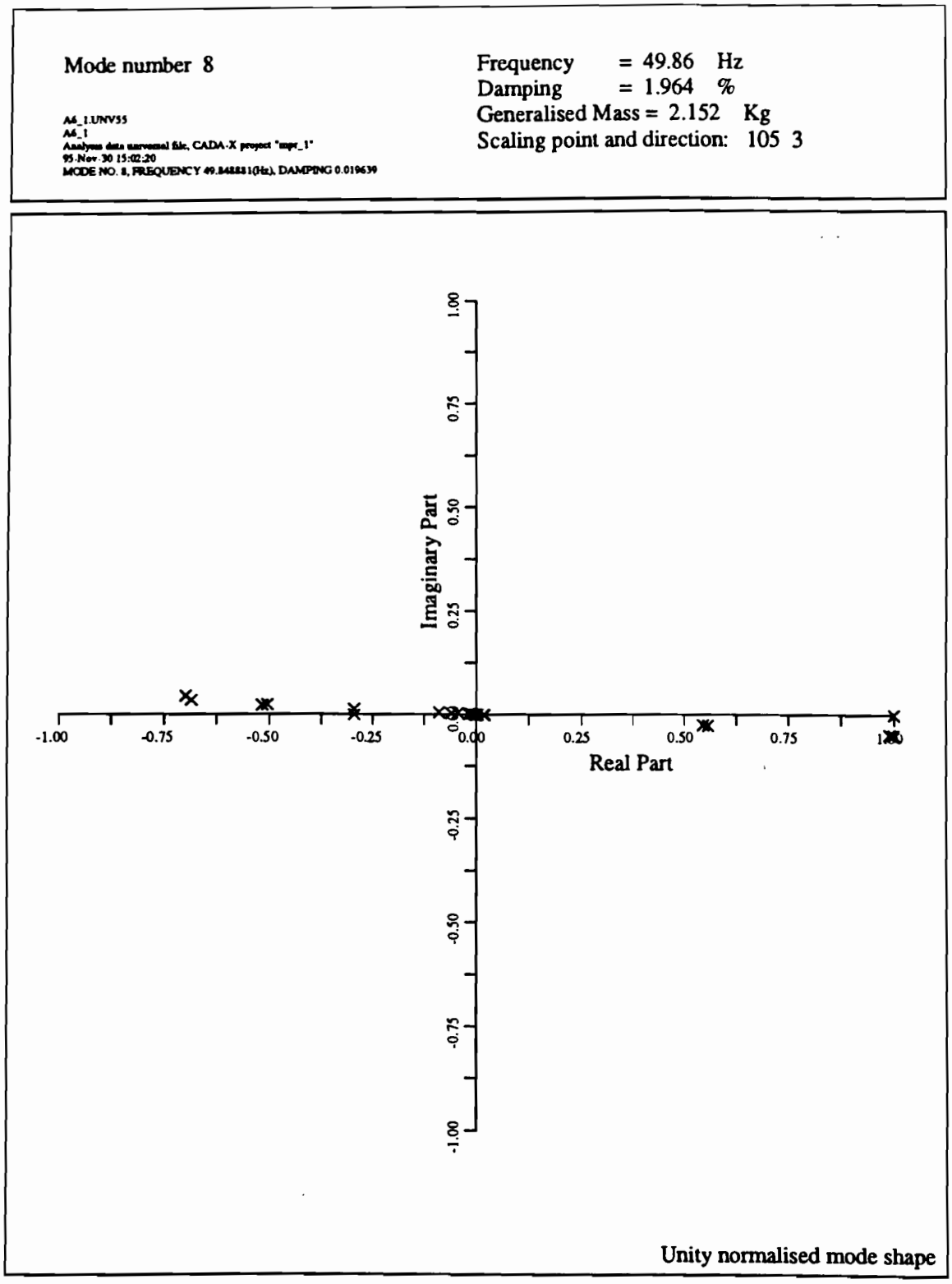

Scatter Plot for 49.86 Hz Mode

Figure 42

Mode number 7

Frequency = 36.34 Hz
Damping = 0.7665 %
Generalised Mass = 3.417 Kg
Scaling point and direction: 11 3

A6_1.UNV55
A6_1
Analysis data universal file, CADA-X project "mpr_1"
95-Nov-30 15:02:20
MODE NO. 7, FREQUENCY 36.335117(Hz), DAMPING 0.007664

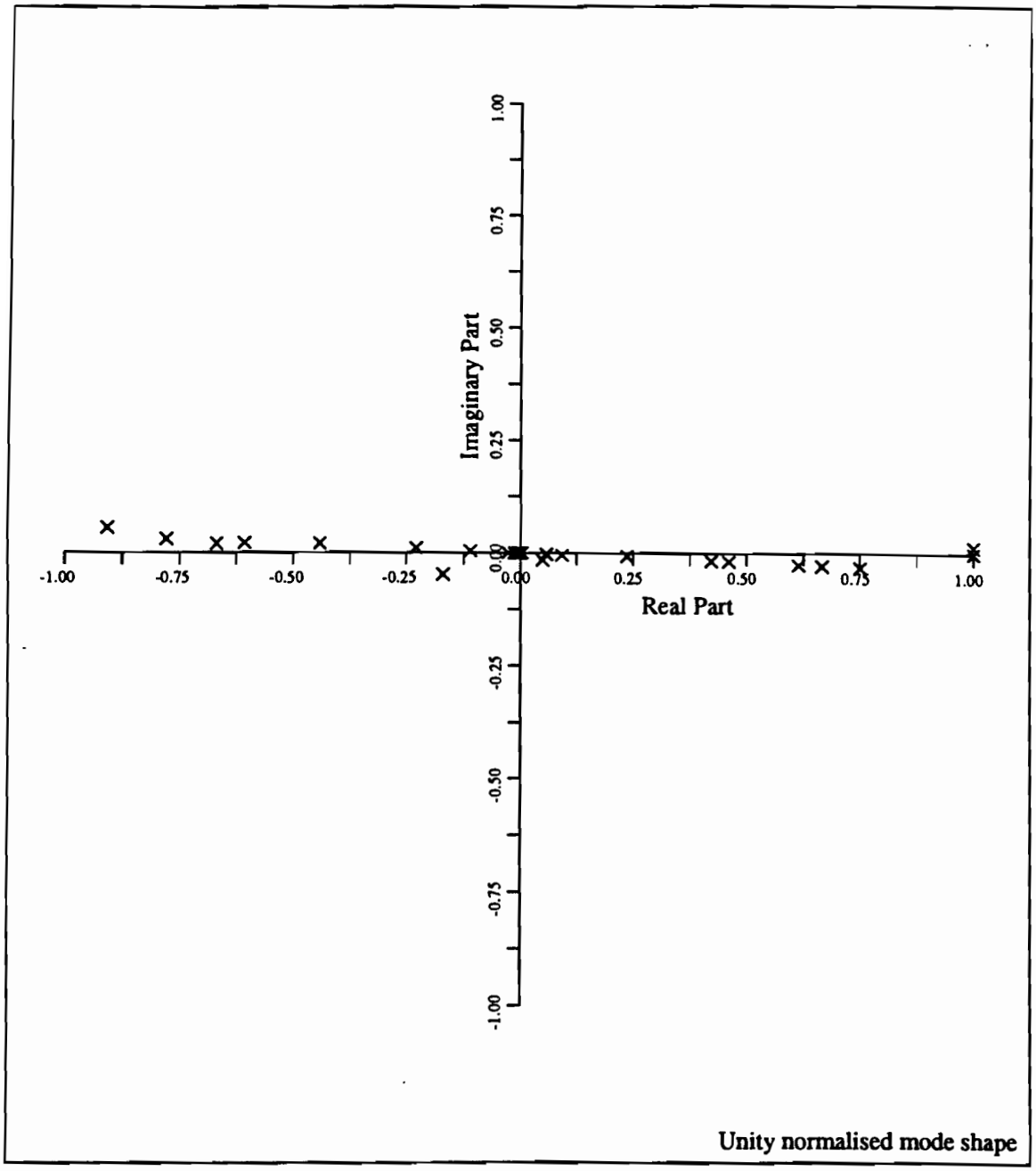

Scatter Plot for 36.34 Hz Mode

Figure 41

Mode number 6

Frequency = 33.97 Hz
Damping = 1.353 %
Generalised Mass = 0.6638 Kg
Scaling point and direction: 11 3

A6_1.UNV55
A6_1
Analysis data universal file, CADA-X project "mpr_1"
95-Nov-30 15:02:20
MODE NO. 6, FREQUENCY 33.971516(Hz), DAMPING 0.013533

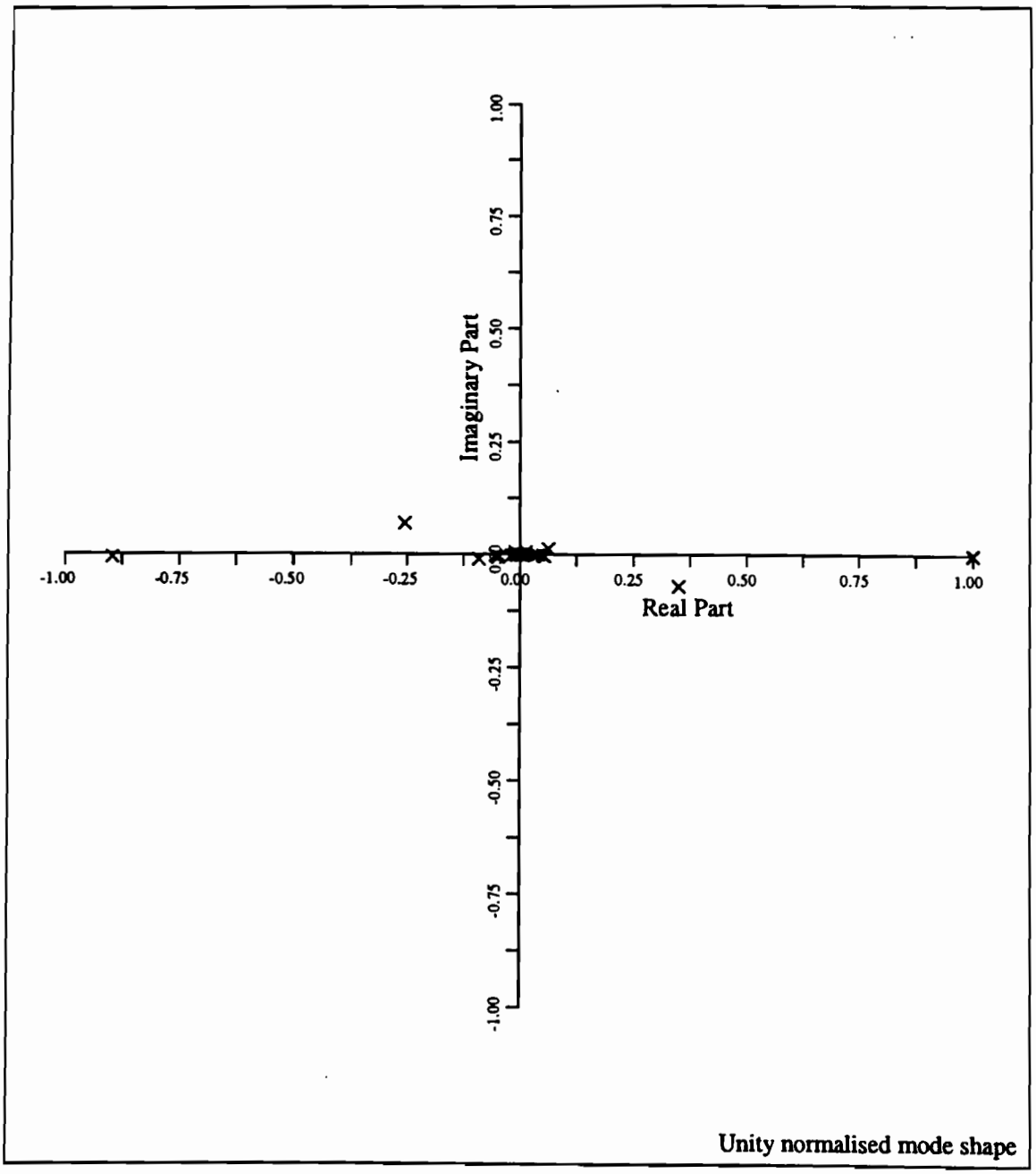

Scatter Plot for 33.97 Hz Mode

Figure 40

Mode number 5

Frequency = 33.49 Hz
Damping = 1.062 %
Generalised Mass = 0.7025 Kg
Scaling point and direction: 111 3

A6_1.UNV55
A6_1
Analysis data universal file, CADA-X project "supr_1"
95-Nov-30 15:02:20
MODE NO. 5, FREQUENCY 33.484715(Hz), DAMPING 0.010621

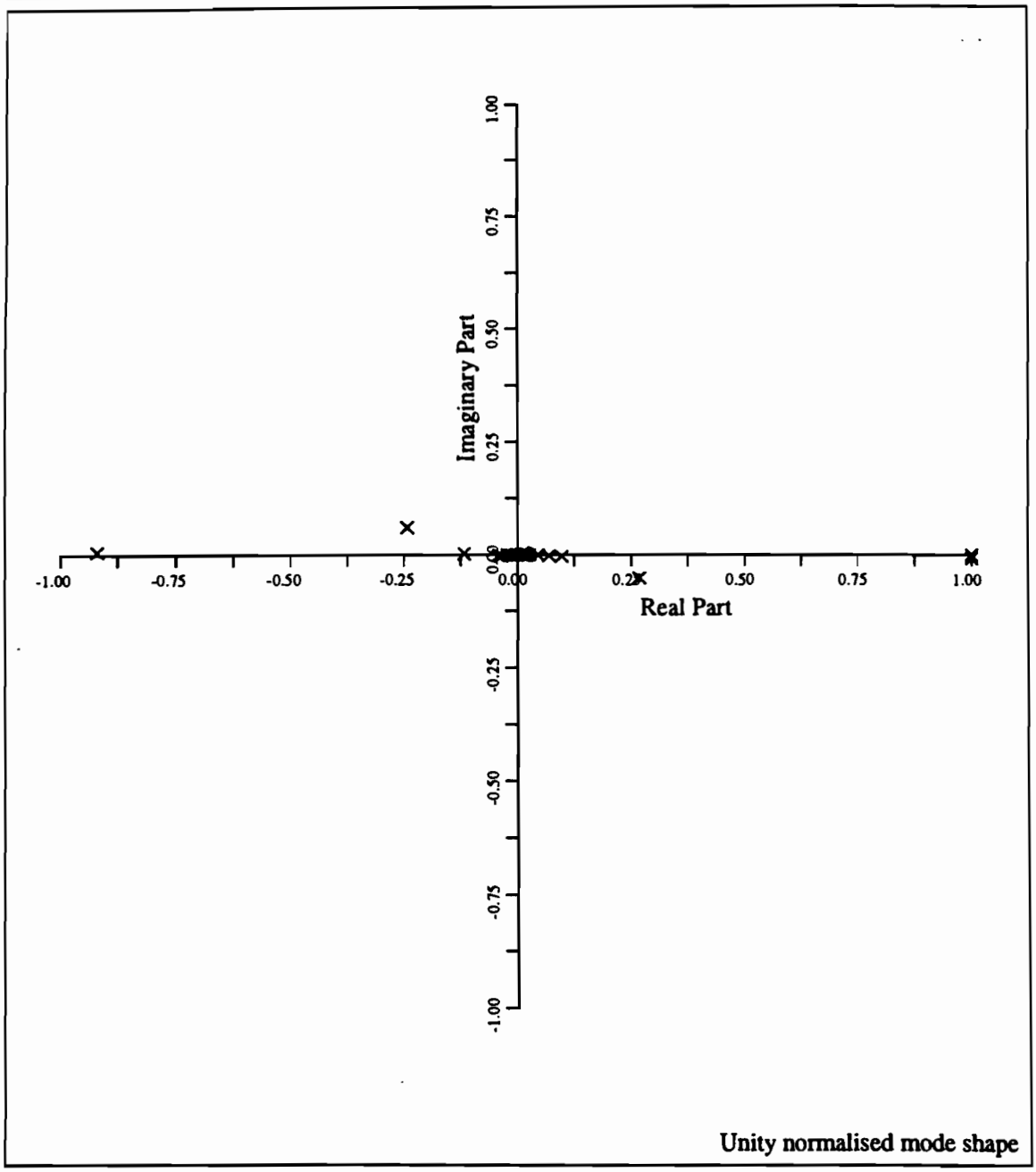

Scatter Plot for 33.49 Hz Mode

Figure 39

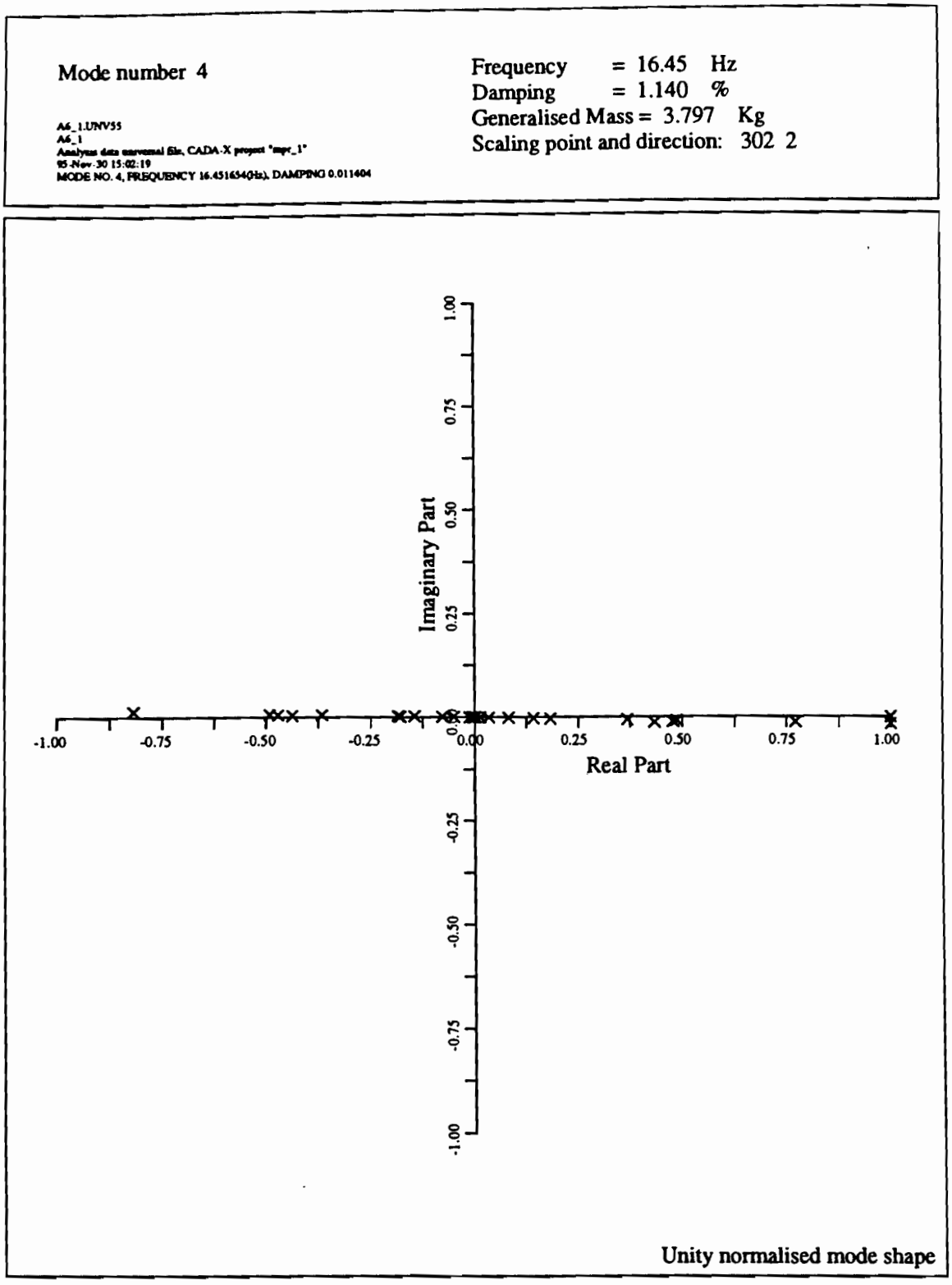

Scatter Plot for 16.45 Hz Mode

Figure 38

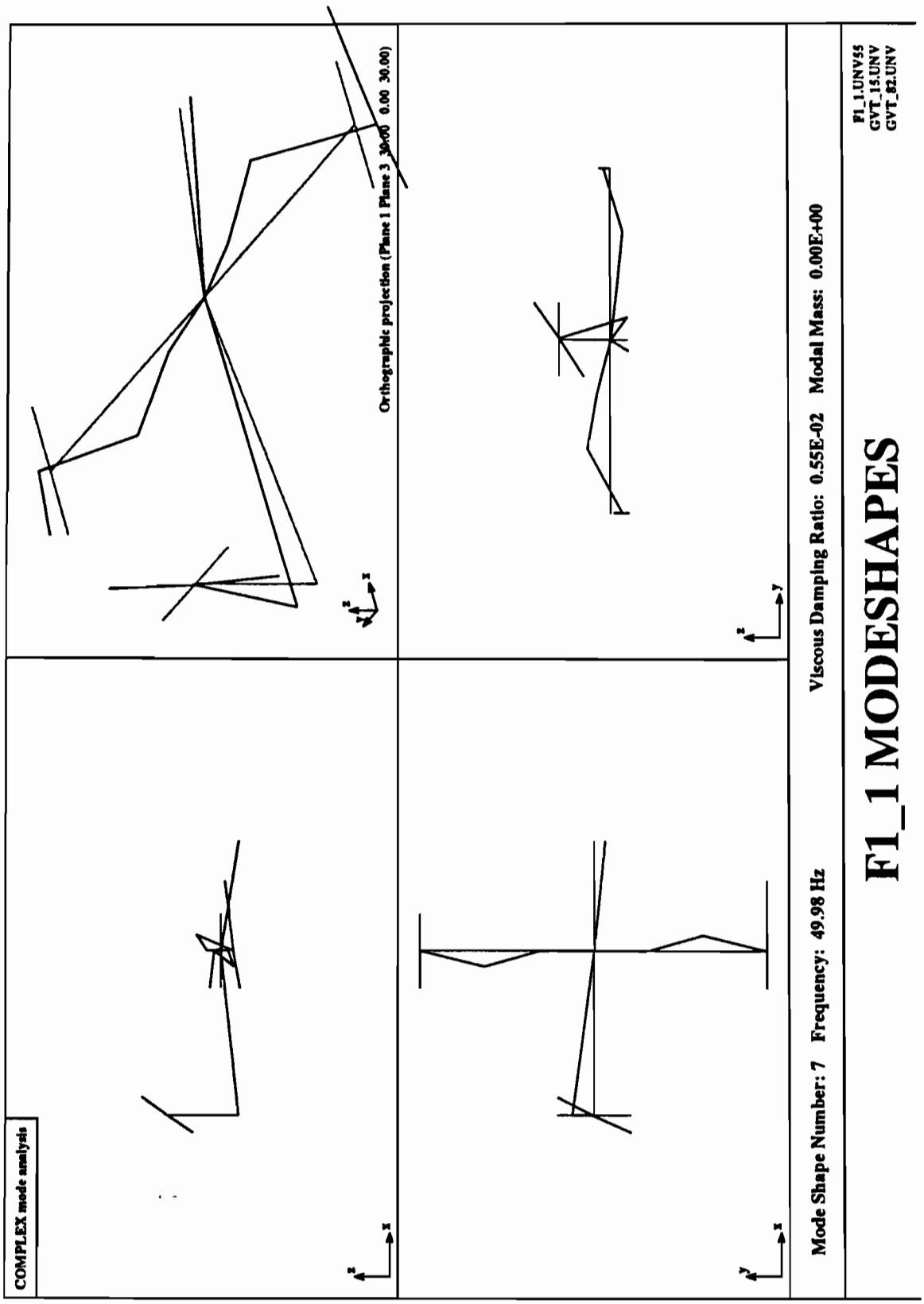
COMPLEX mode analysis
Orthographic projection (Plane 1 Plane 3 30.00 0.00 30.00)
Mode Shape Number: 7 Frequency: 49.98 Hz
Viscous Damping Ratio: 0.55E-02 Modal Mass: 0.00E+00
F1_1.UNV55
GVT_15.UNV
GVT_82.UNV
F1_1 MODESHAPES

Figure 48

Annex 7

MANCHESTER UNIVERSITY CONTRIBUTION

Dynamics and Control Research Group
School of Engineering
University of Manchester

Garteur SM-AG19 - University of Manchester Results

Report No. DCRG/96/1
23nd January 1996

Author: P.S.Holmes

Approved by: Dr. J.R.Wright

Circulation: P.S.Holmes (U of M)
J.E.Cooper (U of M)
J.R.Wright (U of M)
G.W.Skingle (DRA)
M.Nash (DRA)
E.Balmes (ONERA)

Summary

This report gives details of the University of Manchester tests carried out on the Garteur SM-AG19 testbed and the major results obtained.

Contents

1 Introduction

This report gives a summary of the main results from the University of Manchester normal mode tests on the Garteur SM-AG19 testbed, carried out during the period 9^{th} to 12^{th} October 1995. A fuller account of the methods used and results obtained can be found in [1]. A brief comparison is made with the results of corresponding tests performed independently by SOPEMEA.

2 Test Set Up

2.1 Equipment

The acquisition and processing of test data were controlled by an HP 300 Series Workstation running LMS CADA-X [2]/University of Manchester [3] dynamic test software interfacing a DIFA Scadas II 48 channel data acquisition system.

The excitation signals were amplified by HH S500-D constant voltage power amplifiers before being passed to up to four Ling V409 electrodynamic exciters (peak uncooled force 22.3 N, peak to peak displacement 8.8 mm). Each exciter was attached to the structure by a thin steel drive rod and a PCB 208B force transducer (mass 27.5 g). Signals from the force transducers were conditioned by PCB 483A multi-channel transducer amplifiers before acquisition.

The response levels of the structure were measured by 24 Entran EGA-125F-100D strain gauge type acceleration transducers (mass 3.0 g each). Signals from the acceleration transducers were conditioned by Vishay strain gauge amplifiers before acquisition.

2.2 Garteur Arrangement

The Garteur structure was suspended in the horizontal plane from a rigid support frame by a steel cable and three elastic cords, giving a nominally free-free test configuration.

The locations of the 24 acceleration transducers and position numbering convention is shown in Fig 1.

Three exciter configurations were used during the tests. Exciter Configuration 1 has two

exciters in the vertical z-direction at positions 12 and 112, while Exciter Configuration 2 has exciters at the same positions in the horizontal x-direction. Exciter Configuration 3 has four exciters in the vertical z-direction at positions 11, 12, 111 and 112.

The effective added mass of the force transducers is $\frac{1}{3}^{rd}$ of their total mass, therefore complementary masses of 191 g were attached at positions 12 and 112 to satisfy the requirement that 200 g be added at these positions.

3 Test Procedure

Exciter Configuration 1 was used to measure the required FRFs (drive point and transfer FRFs for positions $12z$ and $112z$) using multiple exciter uncorrelated bandlimited random excitation for the frequency range 4 to 80 Hz, using a 70% burst and a uniform window. FRF data were acquired using a resolution of 2048 frequency points over the frequency range 0 to 80 Hz.

The first 8 flexible modes of the Garteur structure were measured individually using the normal mode force appropriation (phase resonance) technique. Estimates of the undamped natural frequencies and corresponding appropriated force vectors (patterns) required to excite the undamped normal modes were obtained via the Modified MMIF [4] method of force appropriation. The undamped normal modes were excited by applying in turn each monophase sinusoidal appropriated force vector to the structure at the corresponding estimate of the undamped natural frequency and adjusting the frequency until a reference force and acceleration were in quadrature. The measured response then yielded the undamped normal mode shape and the corresponding frequency was the undamped natural frequency.

Undamped normal modes 1 to 4 were measured using Exciter Configuration 1, modes 5 and 6 were measured using Exciter Configuration 3, while modes 7 and 8 were measured using Exciter Configuration 2.

Modal masses and damping ratios were estimated using the Rades method [5].

4 Results

4.1 Required FRFs

Fig 2 shows the required drive point FRFs for positions $12z$ (solid trace) and $112z$ (dotted trace) overlaid, while Fig 3 shows the transfer FRFs corresponding to these positions overlaid. As would be expected for a nominally linear structure, the transfer FRFs overlay almost perfectly indicating that reciprocity is satisfied. The drive point FRFs indicate, rather surprisingly, that the response of the structure is non-symmetrical around the resonance peaks in the 34 Hz region (wing torsion modes).

4.2 Undamped Normal Modes

Fig 4 shows the Modified MMIF analysis of FRFs acquired using Exciter Configuration 1. The 8 minima of the primary MMIF eigenvalues (upper plot) indicate the first 8 undamped natural frequencies, while the MMIF eigenvector (lower plot) corresponding to a MMIF eigenvalue minimum yields the appropriated force vector required to excite the undamped normal mode. The primary MMIF eigenvalue minima for modes 4 to 8 do not drop close to zero thus indicating that the chosen exciter configuration is unsuitable for exciting these modes; hence different exciter configurations should be used. Exciter Configurations 2 and 3 yielded MMIF results that were considerably better for these 4 modes.

The first 8 measured undamped normal modes, measured with the most suitable exciter configuration are presented as raw mode shape data in Tables 1 and 2. Note that each mode shape is normalised such that the largest element of the part of the response in quadrature with the excitation (imaginary) is unity. The mode shapes are also shown in Figs 5 to 12 at the instant of maximum defection and as a phase scatter diagram. Note that the phase scatter diagram shows the part of the response in-phase with the excitation plotted along the horizontal axis, while the part of the response in quadrature with the excitation is plotted along the vertical axis. Thus, a perfect undamped normal mode has a phase scatter diagram with all responses lining up vertically, indicating a monophase response in quadrature with the excitation.

The undamped natural frequencies, modal masses, damping ratios and normal mode purities corresponding to the first 8 undamped normal modes are presented in Table 3. Note that

the scaling of the modal masses is consistent with the scaling of the mode shapes in Tables 1 and 2. The normal mode purity [6] is a value that varies between zero and unity that relates the degree of deviation of the responses of a normal mode from being in quadrature with the excitation. A normal mode purity of unity indicates a perfect undamped normal mode. However, in practice a value of above 0.90 indicates an acceptable result, while a value of above 0.95 represents a good quality undamped normal mode.

The results show that good quality undamped normal modes have been identified for modes 1, 2, 3, 4 and 8. Modes 5, 6 and 7 are of a slightly lower quality, but nonetheless acceptable.

It should be noted that for clarity of animation, slave degrees-of-freedom (dof) in the horizontal x-direction were used for positions 1, 8 and 12 (starboard wing) and 101, 108 and 111 (port wing) for modes 7 and 8 (Figs 11 and 12).

4.3 Comparison with SOPEMEA Results

Figs 13 to 16 show the four required FRFs (presented previously in Figs 3 and 4) obtained by the University of Manchester tests (dotted trace) overlaid with the corresponding results from the SOPEMEA tests (solid trace). In all cases there is a 180° phase difference between the results from the two tests, presumably because of different orientation of the sensors. It would be expected for acceleration data that the phase of the phase for drive point FRFs would be in the range 0° to 180°, as showm in the University of Manchester data. In the case of the two drive point FRFs (see Figs 13 and 14), the traces overlay fairly well. However, the comparison is not as good for the two transfer FRFs (see Figs 15 and 16), the SOPEMEA results being highly contaminated by noise.

The identified mode shapes, natural frequencies and damping ratios supplied by SOPEMEA are shown in Fig 17. If these results are compared with the corresponding results from the University of Manchester tests (see Figs 5 to 12 and Table 3), it can be seen that the general agreement is quite good. The most notable differences occur in the identified natural frequencies of modes 5 to 8 and the mode shapes for modes 3 and 4 (wing torsion). The significantly lower natural frequencies of SOPEMEA modes 4 to 8 suggests that there is a greater added instrumentation mass for the SOPEMEA tests. SOPEMEA mode shapes 3 and 4 appear very symmetrical in amplitude, whereas the corresponding University of Manchester mode shapes are highly unsymmetrical. The remainder of the mode shapes appear very similar. Note that no slave dof are used in the animation of SOPEMEA modes 7

and 8.

5 Conclusions

Normal mode force appropriation was successfully used to identify the first 8 undamped normal modes of the Garteur SM-AG19 testbed with two or four exciters employed. A comparison with the corresponding results from the SOPEMEA tests revealed general agreement.

References

[1] Holmes P.S., *Advanced Applications of Normal Mode Testing*, Ph.D. Thesis, School of Engineering, University of Manchester, 1996.

[2] LMS International, *LMS CADA-X Basic Concepts Manual (Revision 3.1)* Interleuvenlaan 68, 3001 Heverlee (Leuven), Belgium, 1991.

[3] Burrows A., *Ground Vibration Test Suite Documentation (Release 3.0)*, Dynamics and Control Research Group, Department of Engineering, University of Manchester, 1994.

[4] Nash M., "A Modification for the Multivariate Mode Indicator Function Employing Principal Force Vectors," *Proceedings of the* 9^{th} *International Modal Analysis Conference*, pp. 688-693, 1991.

[5] Rades M., "On Modal Analysis of Structures With Non-Proportional Damping," *Revue Roumane Des Sciences Techniques Serie Mechanique Applique Vol. 26, No. 4*, pp. 605-622, 1981.

[6] Breitbach E., "A Semi-Automatic Modal Survey Test Technique for Complex Aircraft and Spacecraft Structures," *Proceedings of the* 3^{rd} *ESRO Testing Symposium*, pp. 519-528, 1973.

Response	Mode 1	Mode 2	Mode 3	Mode 4
201:X	-0.001+0.003i	0.000+0.000i	0.000-0.001i	0.000-0.002i
201:Y	-0.001+0.003i	0.000+0.017i	0.000+0.011i	0.000-0.008i
201:Z	0.008-0.212i	0.000+0.006i	0.000+0.007i	0.000+0.012i
101:Z	-0.001+0.927i	-0.064-0.594i	-0.008+0.050i	-0.001+0.048i
111:Z	-0.002+0.911i	-0.109-0.539i	-0.008+1.000i	-0.006+0.334i
112:Z	-0.003+0.910i	-0.014-0.636i	-0.006-0.929i	0.005-0.244i
112:X	0.000-0.004i	0.001+0.177i	0.000+0.029i	0.000+0.038i
105:Z	0.003+0.308i	-0.021+0.214i	0.002-0.010i	-0.003-0.052i
105:X	0.000+0.007i	0.002+0.094i	0.000-0.021i	0.000+0.009i
108:Z	0.003-0.046i	-0.001+0.446i	0.002+0.016i	-0.001-0.044i
206:Z	0.005-0.157i	0.000-0.002i	0.000+0.001i	0.000+0.002i
8:Z	0.004-0.021i	0.010-0.448i	0.000-0.037i	-0.001+0.010i
5:Z	0.001+0.353i	0.031-0.218i	0.000-0.031i	-0.004-0.016i
5:X	-0.003+0.013i	-0.001-0.098i	0.000+0.016i	0.000-0.018i
1:Z	-0.006+0.974i	0.063+0.588i	0.002+0.011i	-0.007+0.052i
11:Z	-0.001+1.000i	0.117+0.548i	-0.002-0.203i	-0.011+1.000i
12:Z	-0.007+0.957i	0.008+0.637i	0.005+0.228i	-0.002-0.901i
12:X	0.006+0.010i	0.000-0.168i	-0.001+0.016i	0.001+0.033i
205:Y	-0.002+0.002i	0.000+0.225i	0.000-0.005i	0.000+0.003i
302:Y	0.000+0.002i	0.000-0.122i	0.000+0.006i	0.000-0.005i
301:Z	0.003-0.066i	0.000-0.937i	-0.002+0.086i	0.002-0.086i
301:X	-0.001+0.037i	0.000-0.015i	0.000-0.003i	0.000-0.011i
303:Z	0.003-0.088i	-0.002+1.000i	0.003-0.109i	-0.001+0.059i
303:X	-0.001+0.031i	0.001+0.058i	0.000-0.013i	0.000-0.005i

Table 1: Garteur Modes 1-4 - Undamped Normal Mode Shapes

Response	Mode 5	Mode 6	Mode 7	Mode 8
201:X	0.000+0.002i	0.000+0.002i	0.001-0.009i	-0.001 -0.125i
201:Y	-0.002-0.071i	0.008+0.102i	-0.009+0.299i	0.002+0.000i
201:Z	-0.014-0.004i	0.003-0.077i	-0.008+0.003i	0.001+0.020i
101:Z	0.124+0.520i	-0.091-0.529i	-0.060-0.197i	-0.004-0.038i
111:Z	-0.073+0.497i	0.044-0.597i	-0.083-0.313i	-0.011-0.113i
112:Z	0.313+0.567i	-0.222-0.466i	-0.037-0.035i	0.007+0.094i
112:X	-0.003+0.259i	0.033+0.319i	0.040+1.000i	0.061+1.000i
105:Z	0.109-0.804i	0.002+1.000i	0.127+0.384i	0.009+0.055i
105:X	0.006+0.147i	0.009+0.146i	0.023+0.457i	0.029+0.380i
108:Z	0.026-0.755i	0.013+0.544i	0.048+0.214i	0.003+0.045i
206:Z	-0.009+0.003i	0.003-0.050i	-0.005+0.005i	0.000+0.013i
8:Z	0.062+0.740i	-0.033+0.367i	0.056-0.333i	-0.008+0.044i
5:Z	0.133+0.786i	-0.058+0.642i	0.072-0.589i	-0.014+0.052i
5:X	0.001-0.126i	-0.008-0.142i	-0.009-0.436i	-0.004+0.376i
1:Z	0.016-0.519i	0.002-0.354i	-0.040+0.303i	0.008-0.041i
11:Z	-0.008-0.859i	0.000-0.425i	-0.056+0.492i	0.009-0.147i
12:Z	0.029-0.212i	0.012-0.313i	-0.027+0.094i	0.006+0.100i
12:X	-0.001-0.278i	-0.012-0.337i	-0.017-0.886i	-0.008+0.957i
205:Y	0.000-0.074i	-0.008-0.220i	0.002-0.621i	-0.009-0.006i
302:Y	0.000-0.059i	0.000-0.002i	-0.001-0.004i	0.000+0.000i
301:Z	-0.003-0.951i	0.023+0.189i	-0.049+0.663i	0.004-0.020i
301:X	0.001+0.018i	0.007+0.172i	0.003+0.450i	0.008-0.148i
303:Z	0.001+1.000i	-0.023-0.229i	0.047-0.674i	-0.004-0.025i
303:X	0.005+0.035i	-0.011-0.151i	0.004-0.500i	-0.010-0.152i

Table 2: Garteur Modes 5-8 - Undamped Normal Mode Shapes

Mode	Frequency/[Hz]	Modal Mass/[kg]	Damping Ratio/[%]	Mode Purity
1	6.71	3.56	1.05	0.996
2	16.40	5.88	1.28	0.950
3	33.46	0.67	0.77	0.991
4	33.94	0.72	1.14	0.991
5	36.12	4.38	0.81	0.909
6	49.65	2.47	2.10	0.921
7	50.26	6.02	0.76	0.933
8	55.41	6.13	0.31	0.961

Table 3: Garteur Modes 1-8 - Undamped Natural Frequencies, Modal Masses, Damping Ratios and Normal Mode Purities

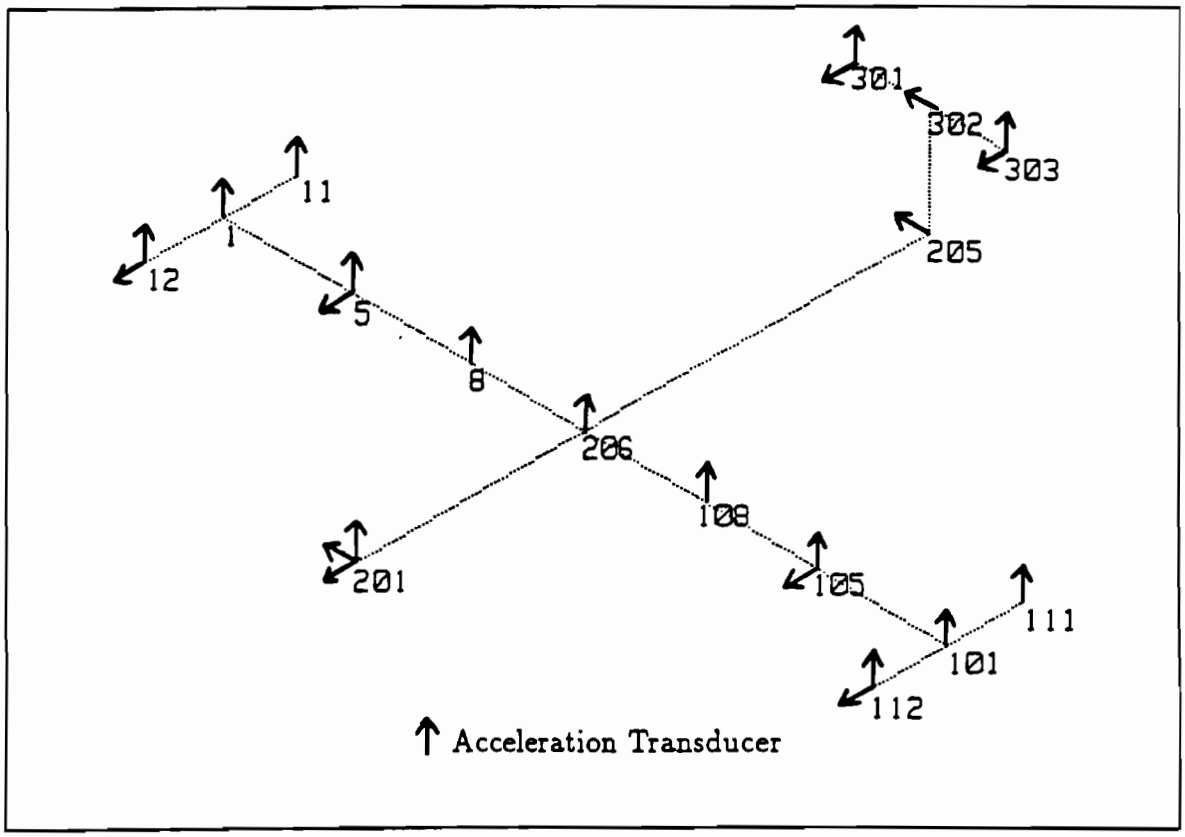

Figure 1: Garteur - Response Positions

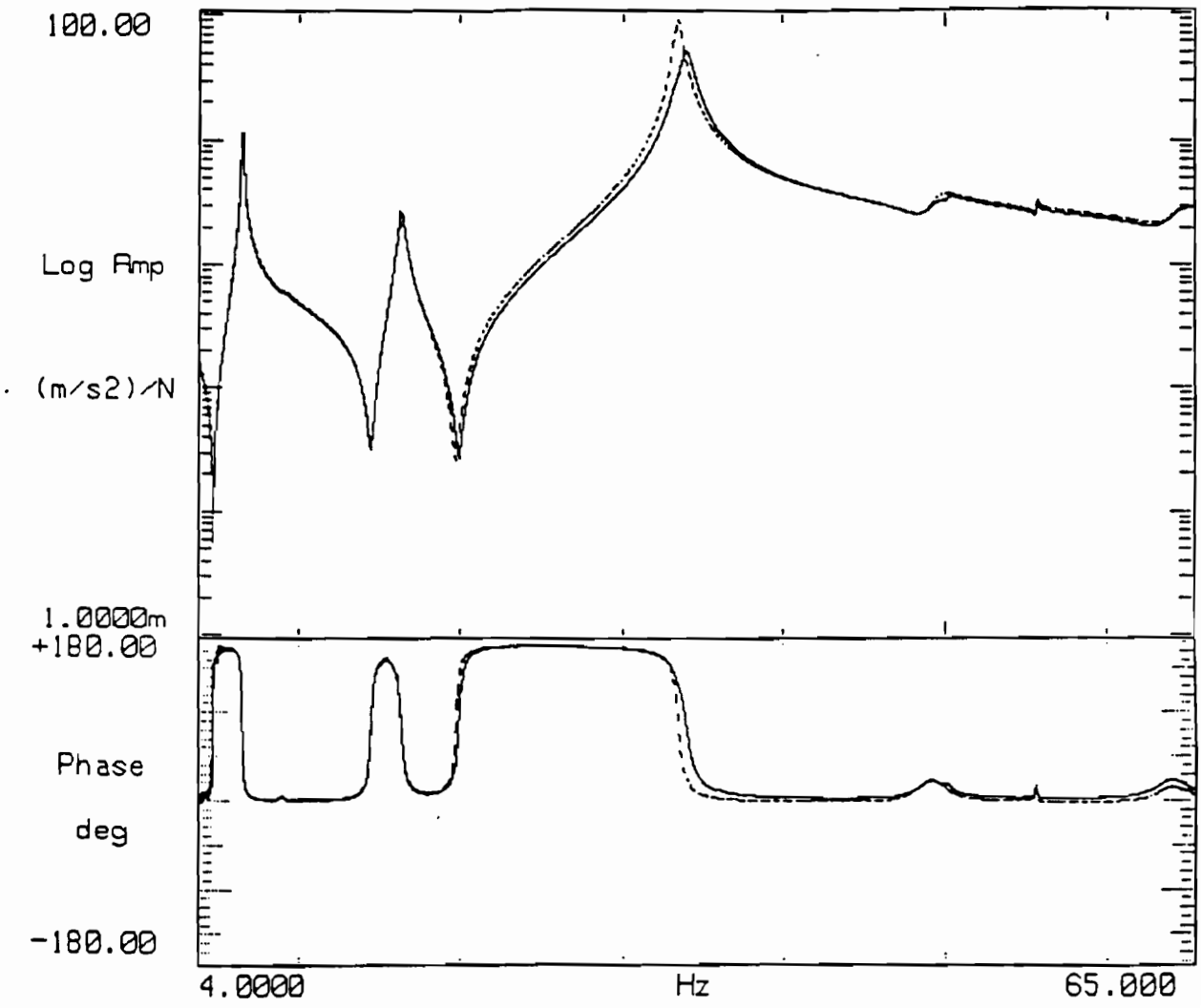

Figure 2: Garteur - Drive Point 12z and 112z FRFs

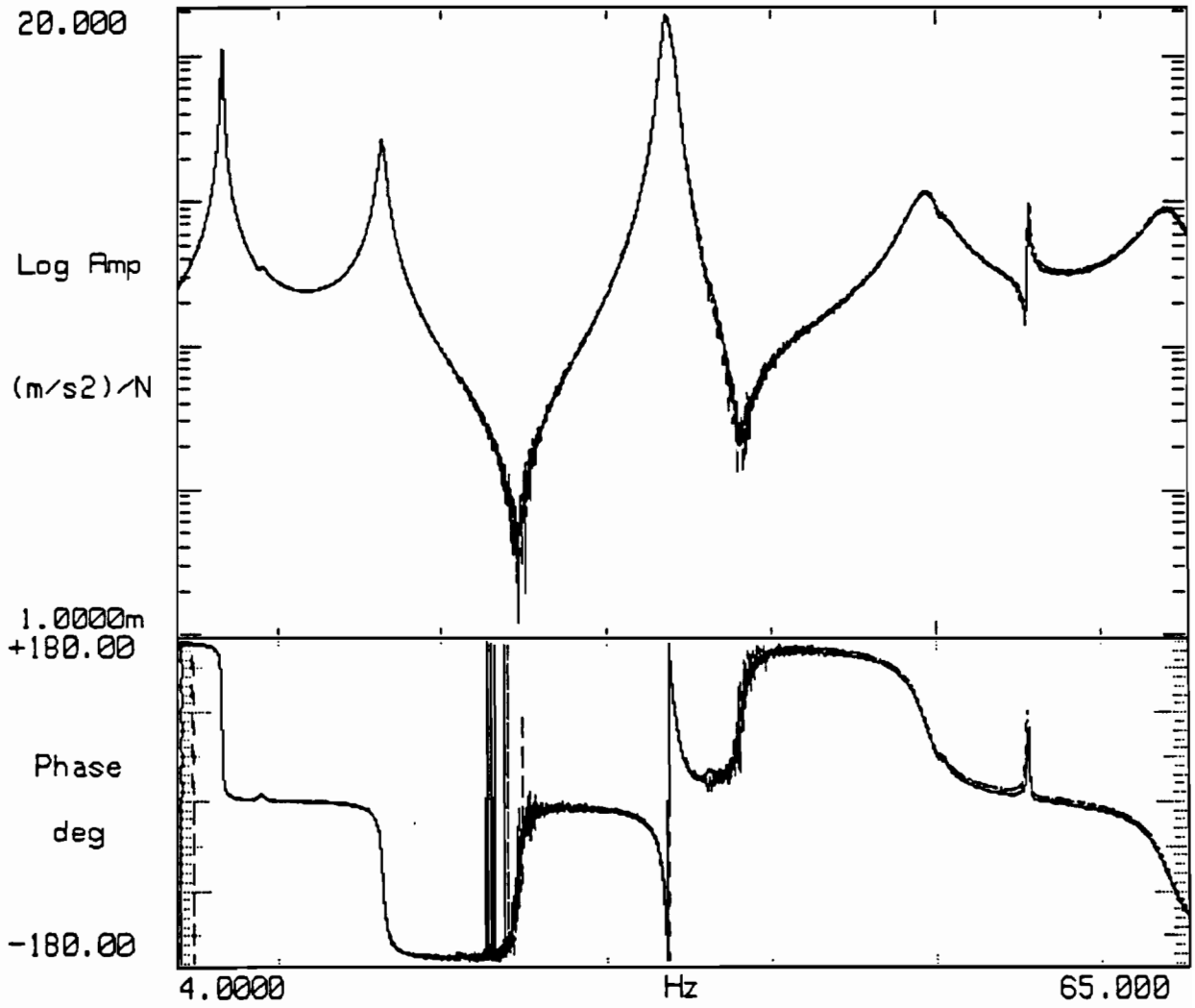

Figure 3: Garteur - Transfer FRFs Between Positions $12z$ and $112z$

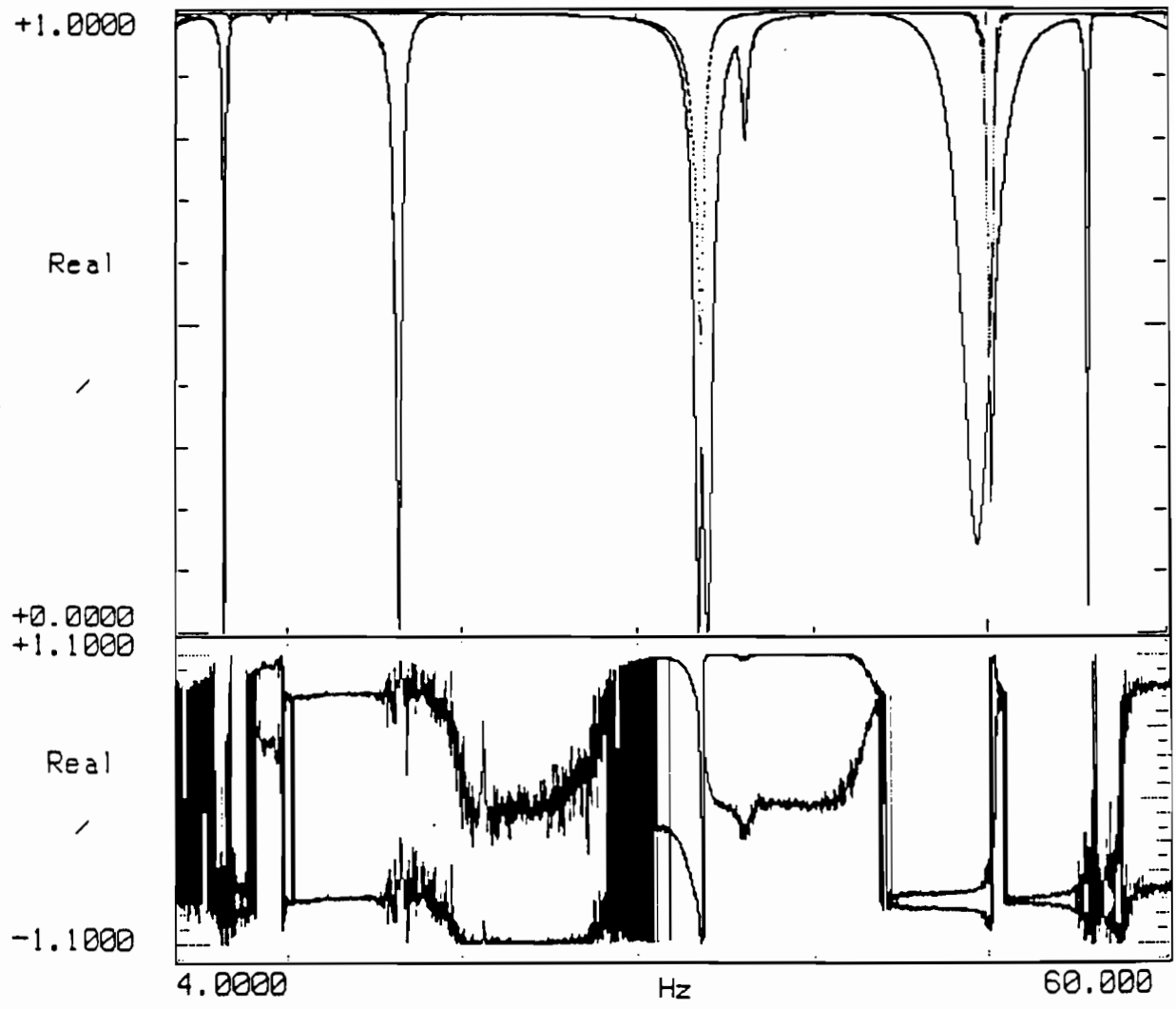

Figure 4: Garteur - Exciter Configuration 1 Modified MMIF

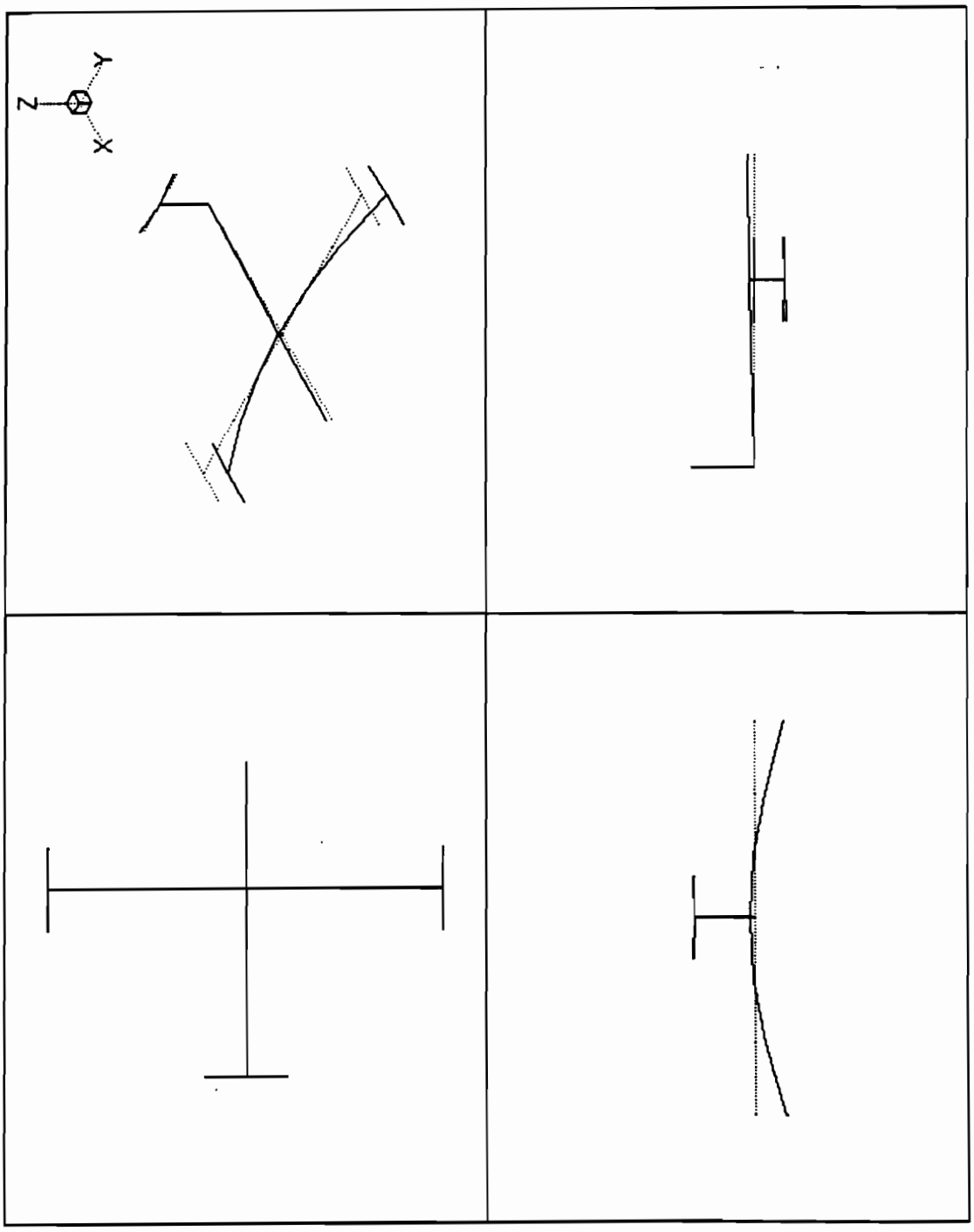

Figure 5: Garteur - Undamped Normal Mode 1, Freq=6.71 Hz, Mode Purity=0.996

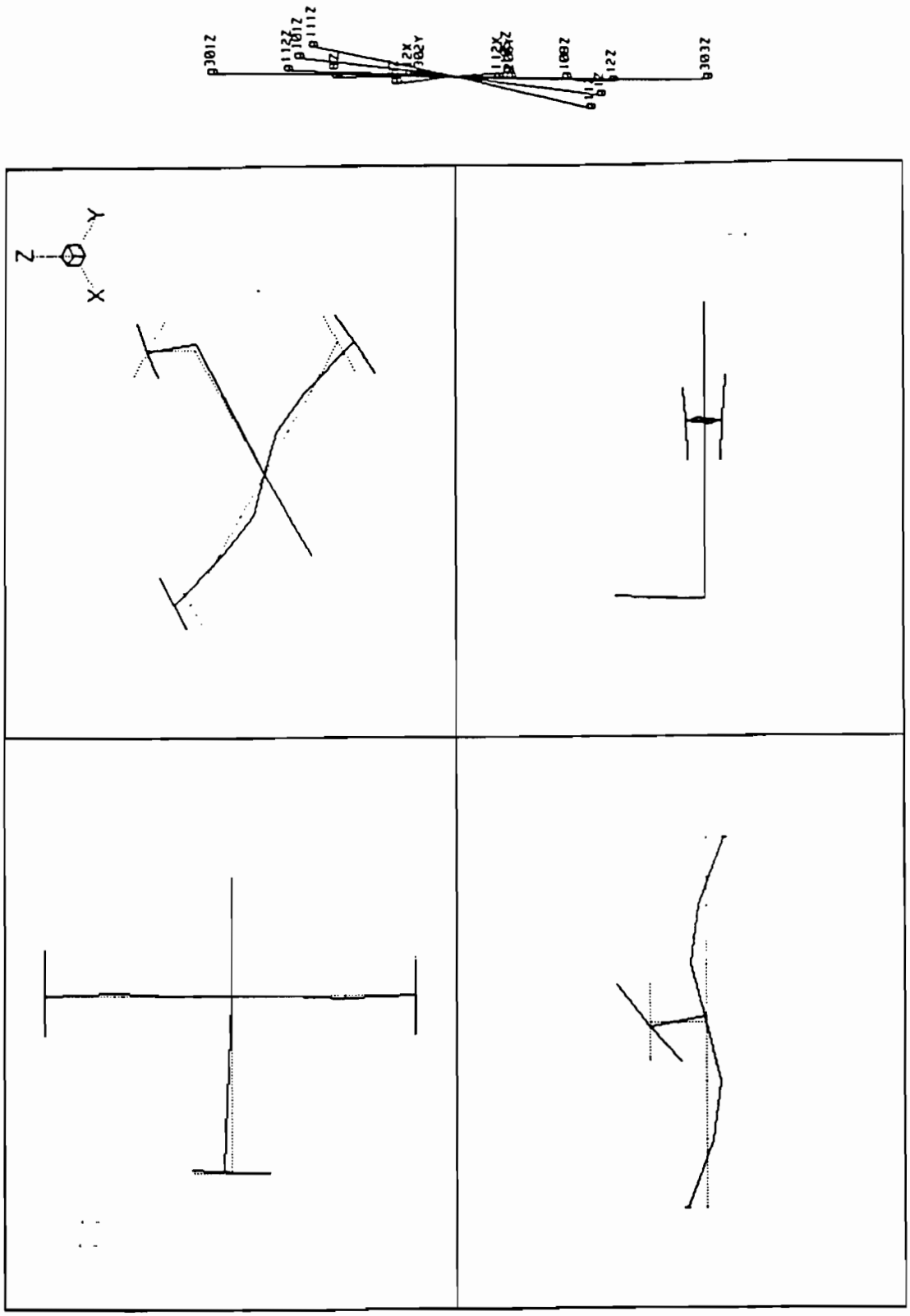

Figure 6: Garteur - Undamped Normal Mode 2, Freq=16.40 Hz, Mode Purity=0.950

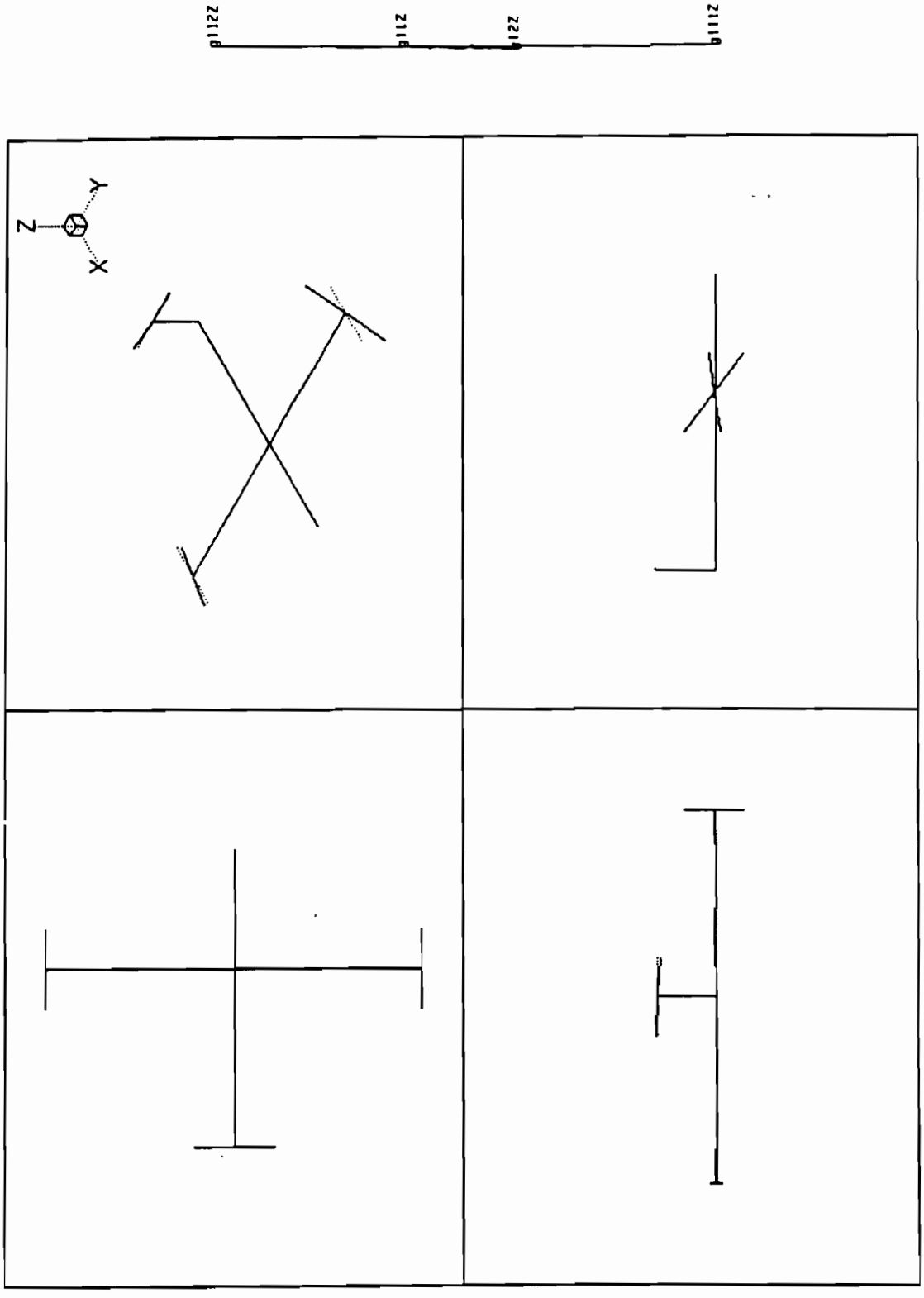

Figure 7: Garteur - Undamped Normal Mode 3, Freq=33.46 Hz, Mode Purity=0.991

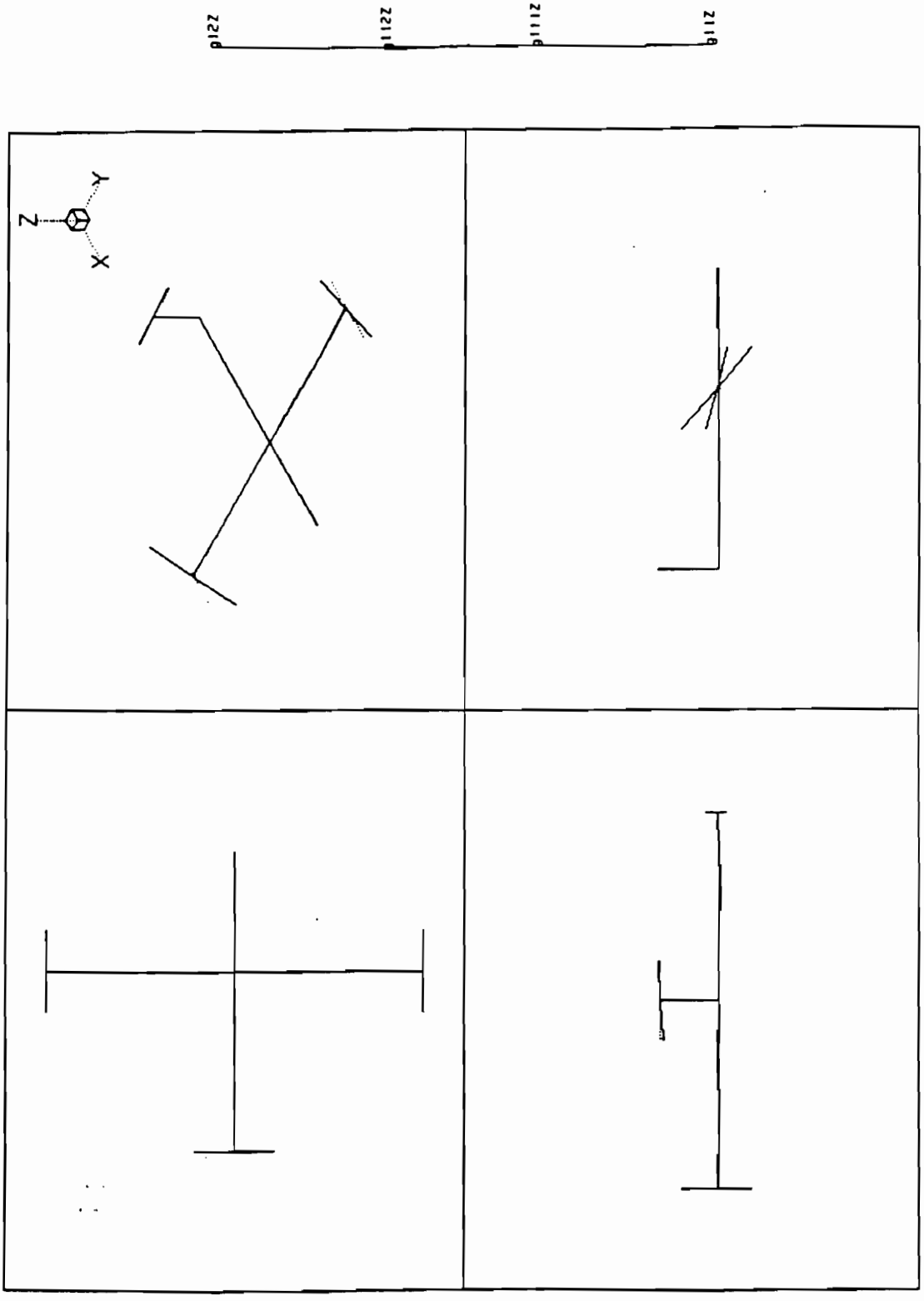

Figure 8: Garteur - Undamped Normal Mode 4, Freq=33.94 Hz, Mode Purity=0.991

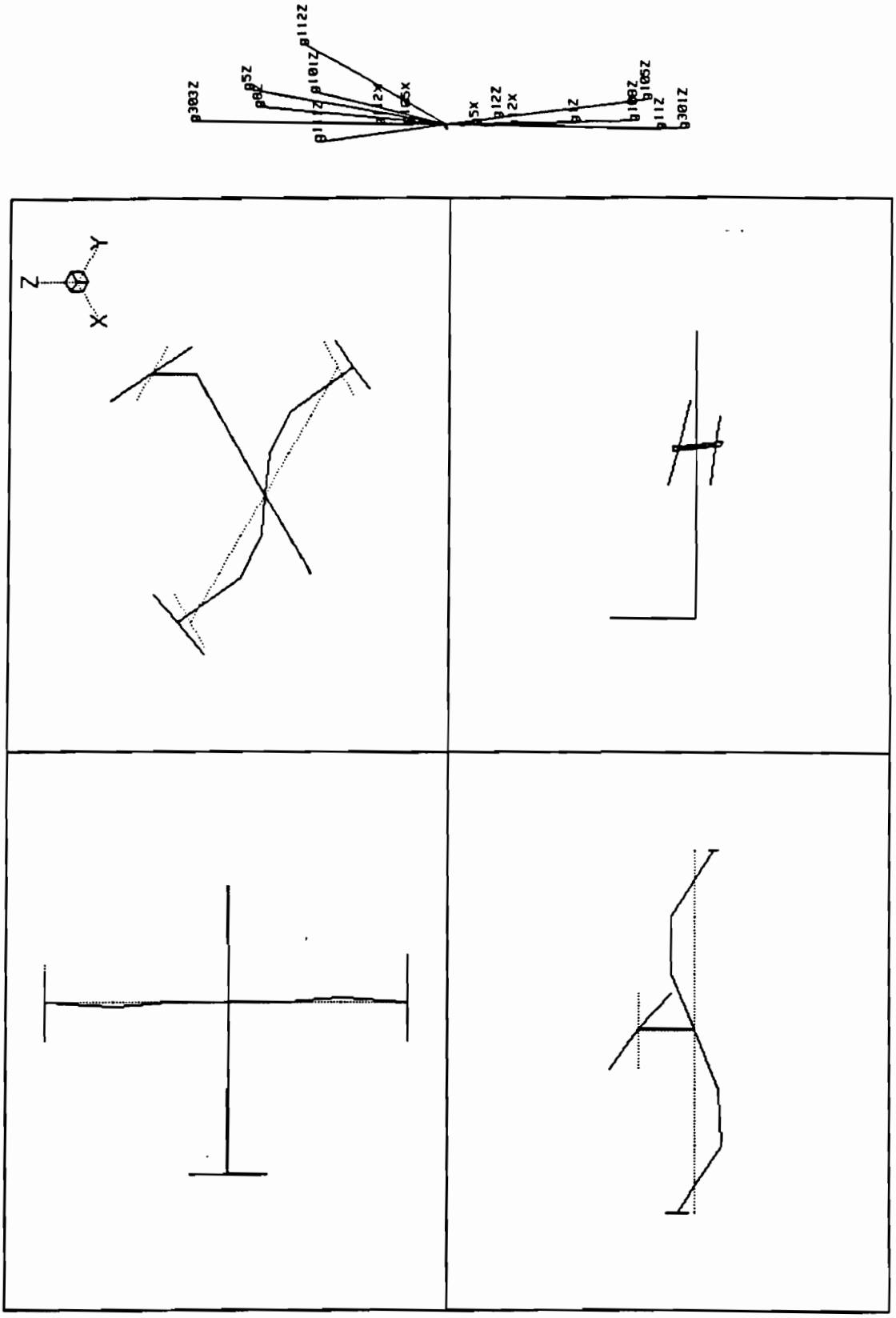

Figure 9: Garteur - Undamped Normal Mode 5, Freq=36.12 Hz, Mode Purity=0.909

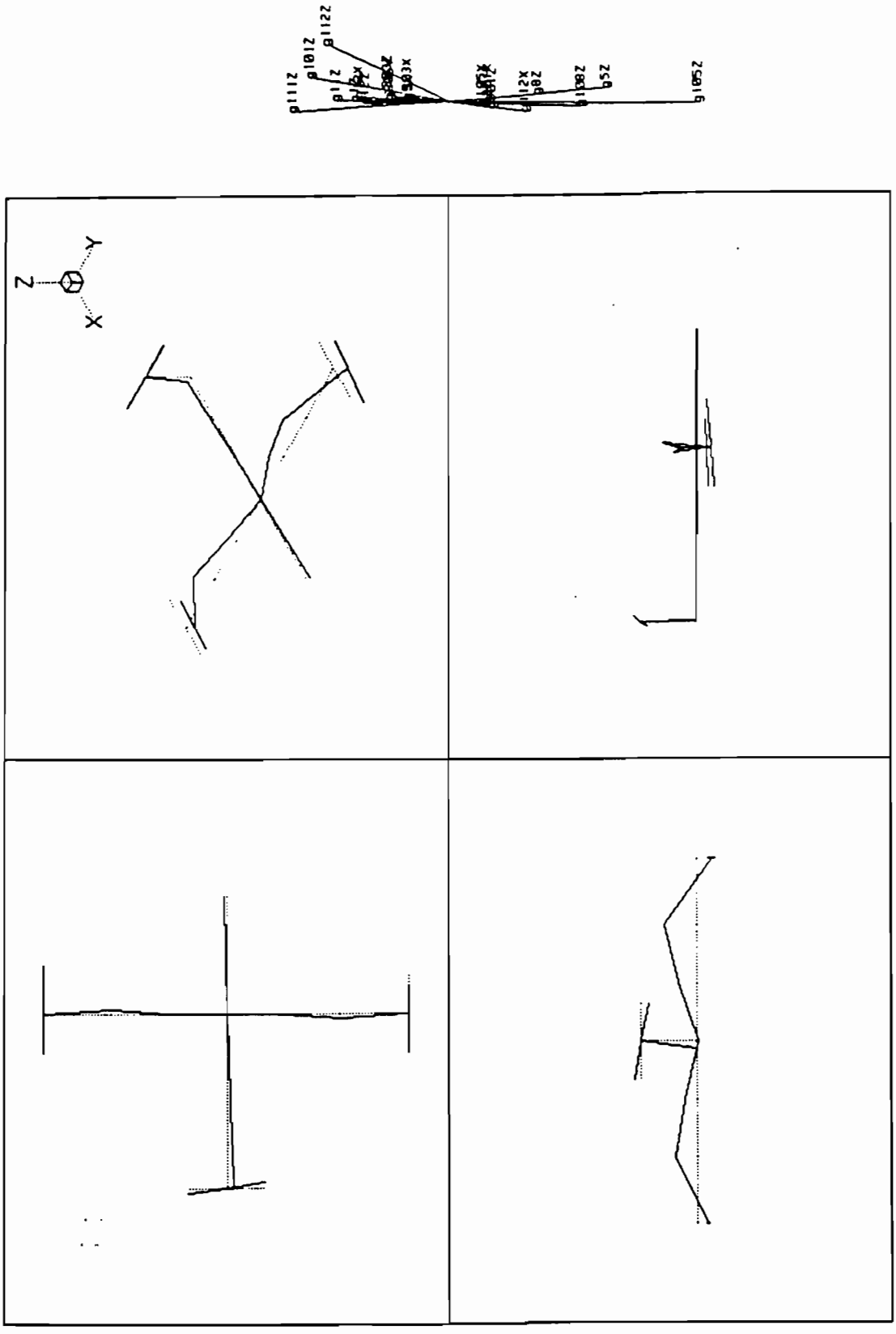

Figure 10: Garteur - Undamped Normal Mode 6, Freq=49.65 Hz, Mode Purity=0.921

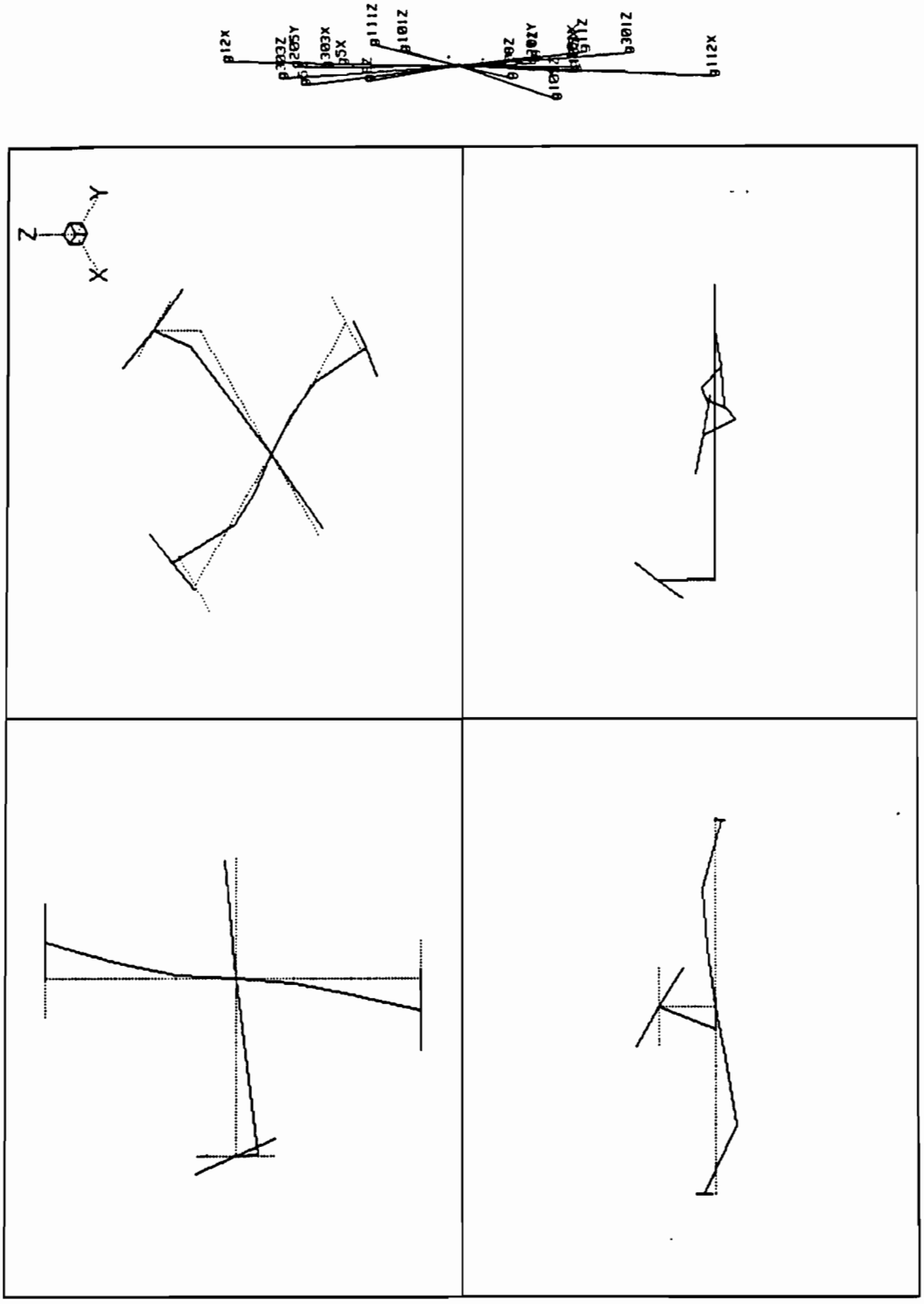

Figure 11: Garteur - Undamped Normal Mode 7, Freq=50.26 Hz, Mode Purity=0.933

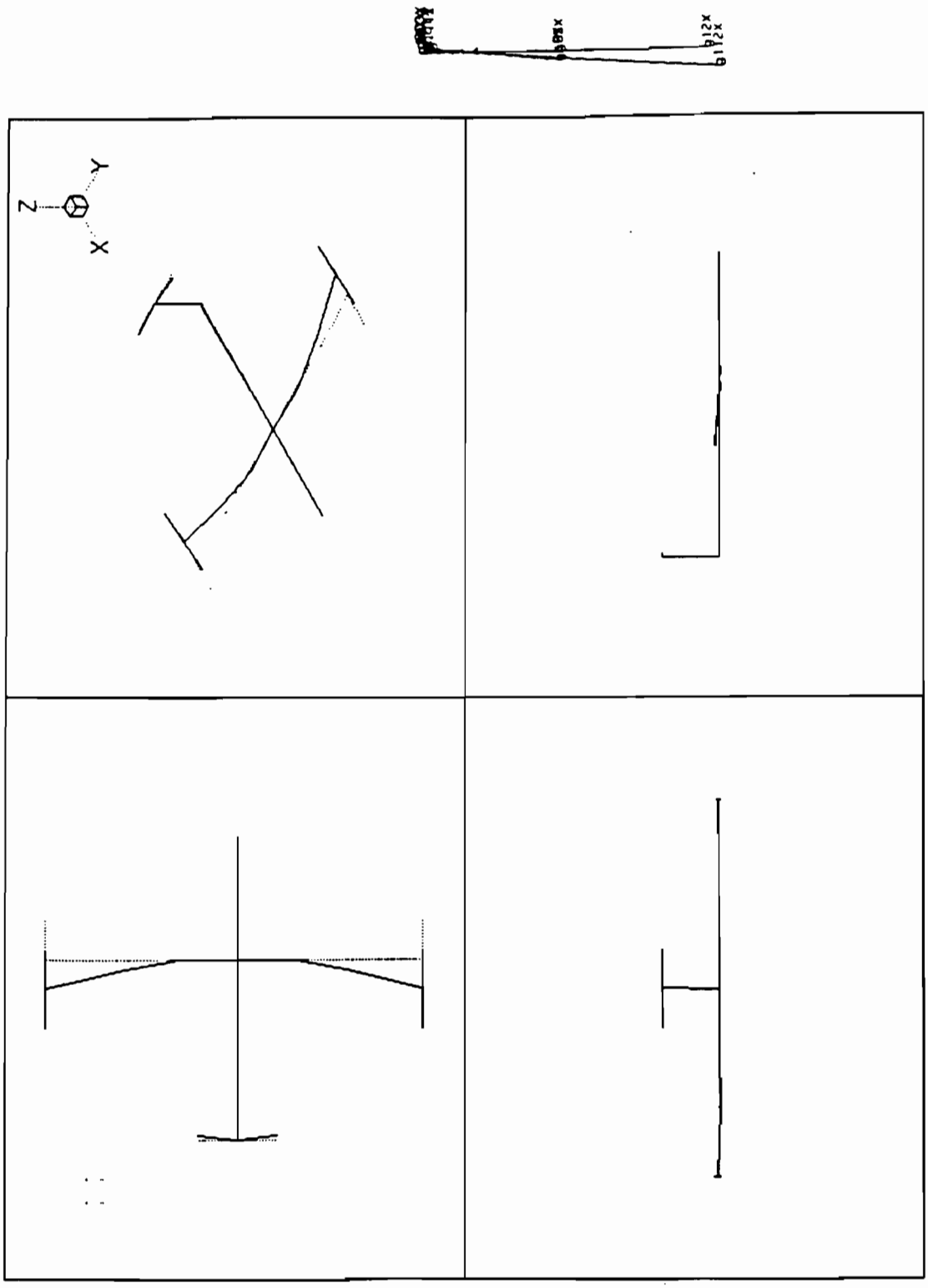

Figure 12: Garteur - Undamped Normal Mode 8, Freq=55.41 Hz, Mode Purity=0.961

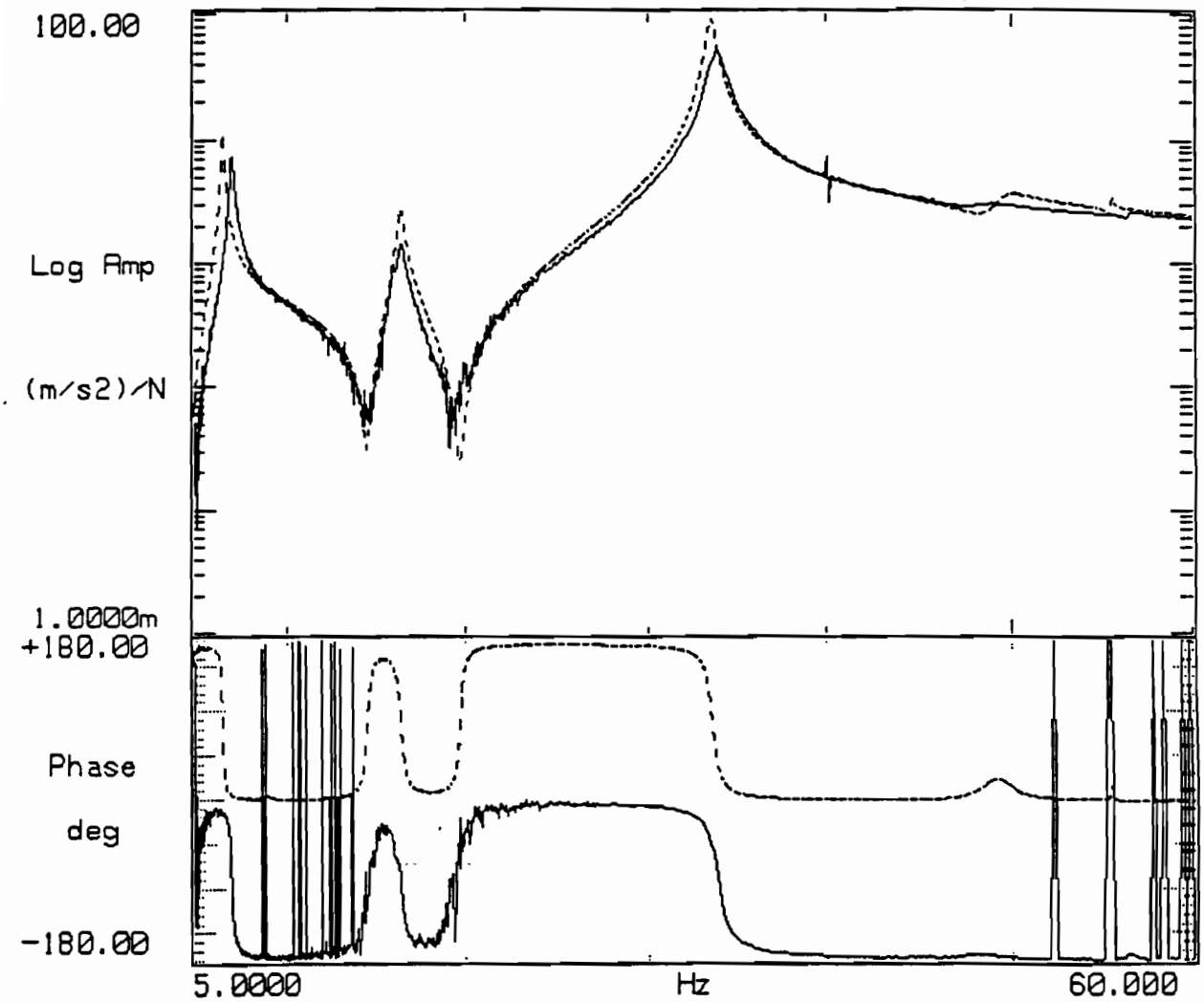

Figure 13: Garteur - Comparison of U of M and SOPEMEA Drive Point 12z FRFs

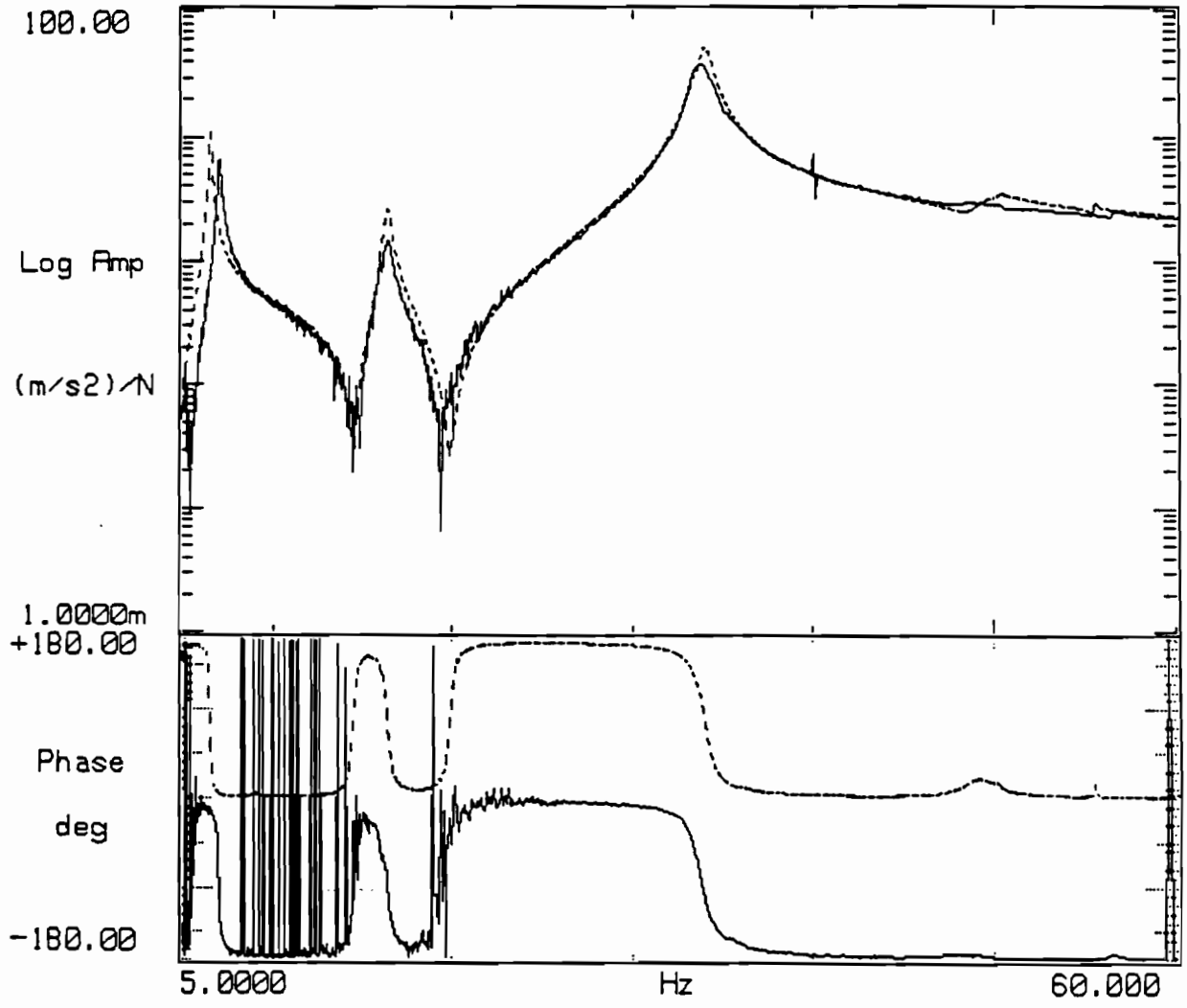

Figure 14: Garteur - Comparison of U of M and SOPEMEA Drive Point 112z FRFs

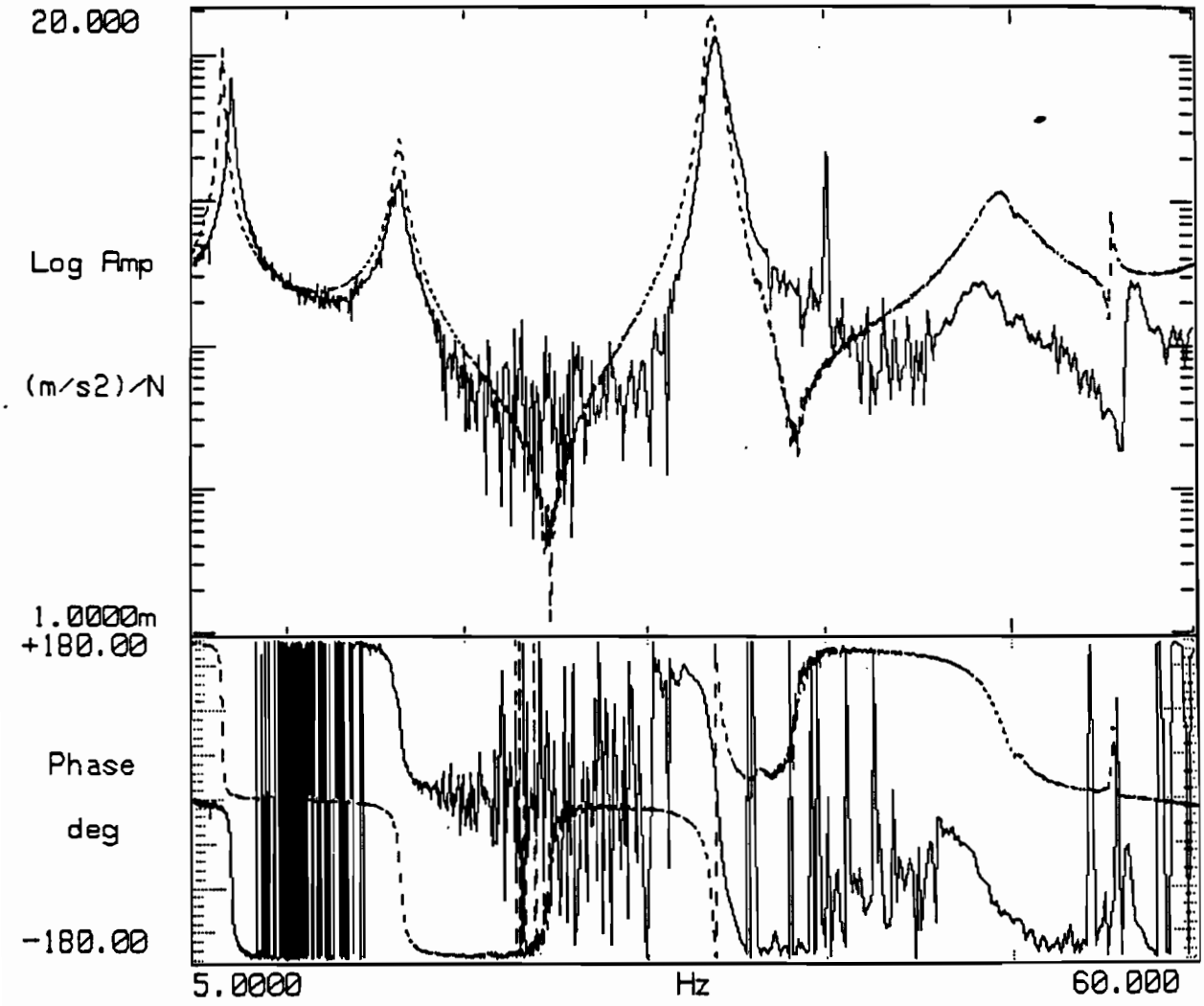

Figure 15: Garteur - Comparison of U of M and SOPEMEA Transfer FRF $H_{112z,12z}$

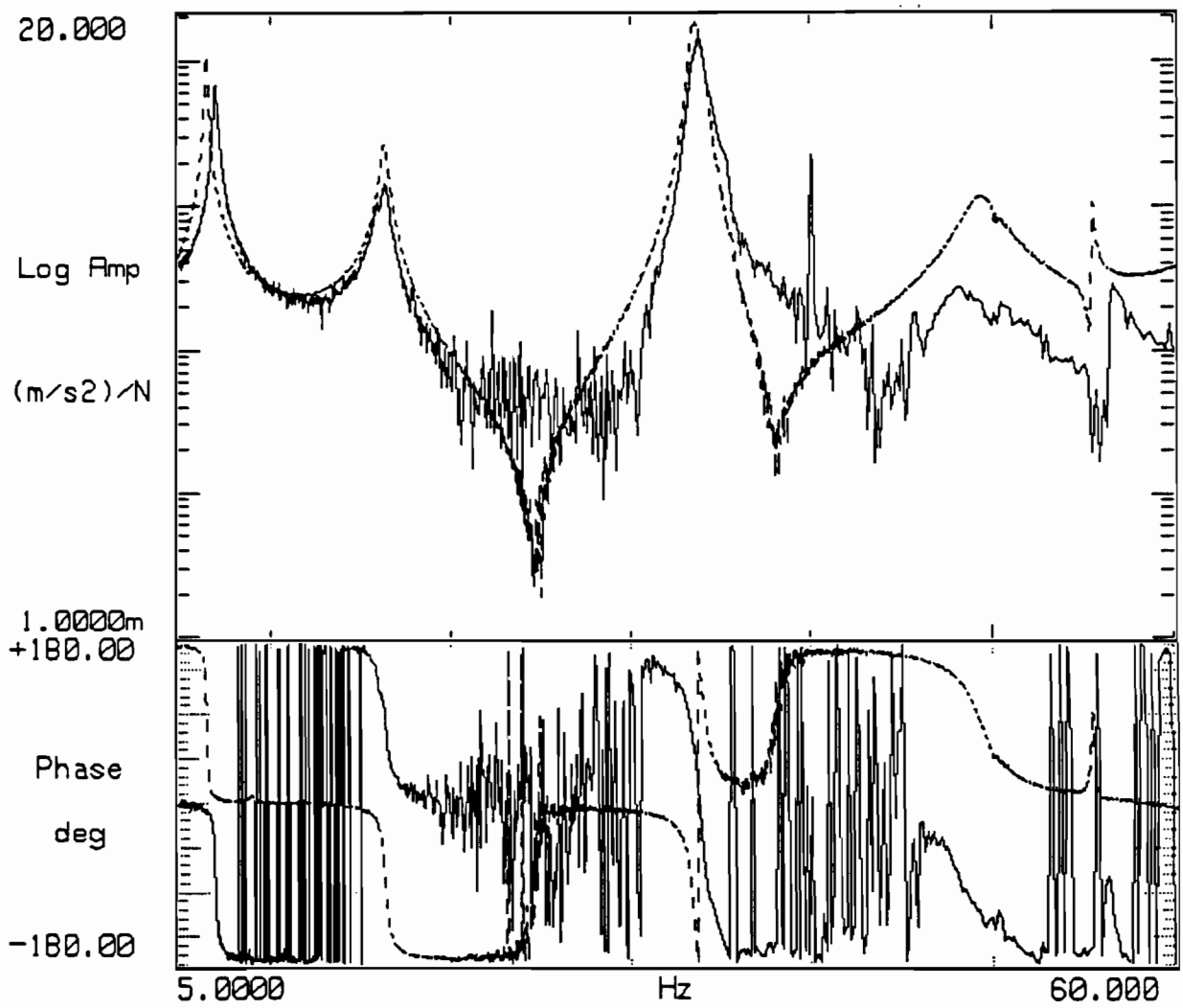

Figure 16: Garteur - Comparison of U of M and SOPEMEA Transfer FRF $H_{12z,112z}$

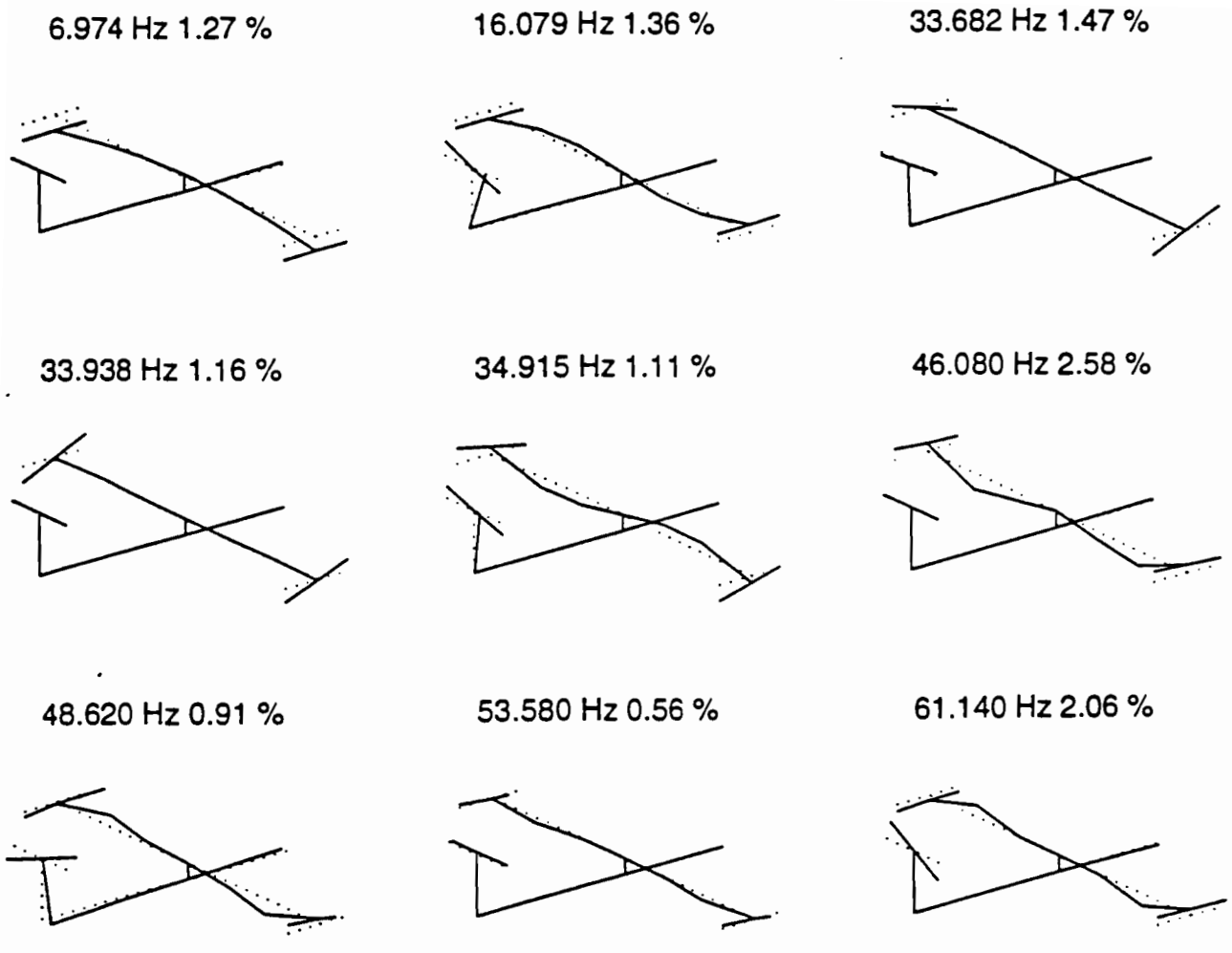

Figure 17: Garteur - SOPEMEA Natural Frequencies, Mode Shapes and Damping Ratios

Annex 8

ONERA CONTRIBUTION

OFFICE NATIONAL D'ETUDES ET DE RECHERCHES AEROSPATIALES

29, avenue de la Division Leclerc, 92320 CHATILLON - FRANCE

STRUCTURES DEPARTMENT

Technical Report N° RT 31/1677 RN

May 1996

GARTEUR group on GVT methods. Results from ONERA

Written by :

Ph. Fargette

Verified by :

A. Morvan, Head of the Structures Dynamic Identification Division

Approved by :

Scientific Director

Structures Department

R. Labourdette

INTENTIONALLY BLANK

CONTENTS

Sans texte

1. INTRODUCTION

Within the certification process of an aircraft, analytical models are used to make aeroelastic predictions and evaluate flutter risks.

In this process, ground vibrations test plays an important role for the updating and/or verification of numerical models.

The present GARTEUR activity has the major objectives to compare the modal testing techniques and identification methods used by the participants through a common application. A testbed with particular characteristics was designed and made by ONERA (France). To increase the challenge, the model was adjusted to obtain three neighbouring modes. The test request is described in document ref. [1].

At first, each participant is requested to provide at least a 2 by 2 transfer functions matrix corresponding to excitation and response at left and right front tip drums in a 4 to 65Hz frequency range. After that, members are invited to estimate the dynamic characteristics of the first 9 modes by one or more method and to provide a comparison of those results with the SOPEMEA reference set [4].

After NLR / FOKKER, DLR, Imperial College, Manchester U., DRA, ONERA performed the GVT in November 1995. The schedule of the GARTEUR activity is listed at the end of this report.

2. DETAILS OF THE EXPERIMENTAL SETUP

2.1. Testbed geometry and instrumentation

The testbed is composed of two aluminium substructures (wing/drum and fuselage/tail). The connection beetwen the two sub-systems is done through two steel plates centered by two pins and fixed by four bolts. A set of views in figures 6 to 9 shows details of the geometry.

Significant damping levels are obtained through the use of a 50 µm thick acrylic viscoelastic layer (ref ISD 112 made by 3M) covered by a thin aluminium contraining layer (1.1 mm thick). This composite is glued on the wing.

The structure is suspended with three bungees as shown in picture 2 giving a 2 Hz heave mode frequency.

According to the request (see locations and directions in figures 10-11), the testbed is equipped with 24 accelerometers plus two sensors on the suspension. These pick-ups made by ONERA are piezo-capacitive type with a common sensibility of 80 mV/ms^{-2} and 10 g mass (see characteristics in figure 12).

Because the test was not dedicated for FEM updating or flutter analysis and because the sensitivity of the structure to the additionnal masses, we choose to limit the pick-up instrumentation to the request which is sufficient to distinguish all modes in the interesting frequency band.

Four electrodynamic shakers were used for the excitation. The main characteristics of these actuators are listed below.

	Force maxi	stroke pick-pick	coil weight	stiffness and resonance frequency (unloaded coil)		force-current coefficient	shaker weight
I.S. units	6 N	20 mm	0,037 kg	228 N/m	12,5 Hz	0,45 N/A	13 kg
G.B. units	*1,3 lbf*	*0,79 inch*	*0,08 lb*	*1,30 lbf/inch*	*12,5 Hz*	*2,00 lbf/A*	*28 lb*

figure 1: principal characteristics of the 6N Onera electrodynamic shaker

The exciter is driven by a current controlled amplifier with a built in shunt connected in series with the output. The current is measured across this shunt and it is used to calculate the input force level.

Two additionnal masses were added at nodes 12 and 112 to obtain a total moving mass of 200 g. The connection is done through a flexible steel shaft as shown in picture 3.

2.1. Testing facilities

To evaluate reliability of measurements, ONERA choose to use two data acquisition systems.

The mobile laboratory usually used for GVT on large aircraft was used to obtain results for stepped sine excitation and force appropriation normal mode testing. This equipment consists of two HP workstations,

- ▷ one HP 9000/433s including private software for synchronous acquisition and
- ▷ one HP 9000/730 risc workstation which implements Matlab(TM) environnement for post-processing and analyses.

This system allows up to 1024 measuring channels and provides up to 12 outputs for simultaneous excitations.

A second system linked to the vibro-acoustic laboratory ORION was used to performed impact and broadband MIMO tests. This 54 channels acquisition system is built on two master/slave SCADAS front-end and driven by a HP9000/380 and LMS(TM) Cada-X software. For the broadband test, two HP generators and Kemo filters have been used for generating a band limited noise with an infinite period.

3. TRANSFER FUNCTIONS

3.1. Stepped sine sweep

This procedure (based on a synchrone analysis) is really simple in fact. A common harmonic reference is used for both excitation control and for signal processing allowing a direct estimation of the frequency responses.

More specifically, the measurement consists in applying, at discrete frequency points, a sinusoïdal set of forces (with constant amplitudes) and to measure the first harmonic of the associated stationnary response.

This approach was performed through two experiments (shaking at 12-z and 112-z) providing the reference set of transfer functions. The interesting band was [4 Hz,66 Hz] with 2441 frequency points evenly spaced resulting in a measuring time of 58 mn. During the tests, the temperature was 18°C and a pair of electodynamic shakers were always connected at the drum front tips. As previously mentioned, the required moving mass at the drum tips was obtained with two complement masses of 150g. The results of these tests are presented in figure 13.

Except for the [54Hz, 56Hz] frequency band which contains lightly damped mode, the spectral resolution of 0.025Hz appears sufficient.

One notes that the collocated FRF superimposed in fig. 13a, do not exactly overlay. That means that the testbed is not really symetric. Similarly, figure 13b shows that the cross-transfers overlay quite well implying that reciprocity is verified.

3.2. Broadband MIMO test

Experience using the FRF estimation with broadband uncorrelated MIMO excitation have generally given good results. Some limitations are however expected for structures with significant non-linearities, which most aircrafts are.

In our case, use was made of two uncorrelated inputs (gaussian white noise). To obtain the results presented in figure 14, one used the H1 estimator, 50 averages, 4096 spectral lines implying a recording time of around 40 mn.

Figure 15 shows a comparison of results for sine and broadband excitation. The most noticeable differences are slight frequency shifts of the modes. It appears also a surprising resonance due to the suspension that didn't appear in the initial sine measurements.

3.3. Comparison with the SOPEMEA reference set

Despite a contraining test setup, plots of SOPEMEA reference set of FRFs in figure 17 show significant differences with our test results.

SOPEMEA set indicates the presence of significant noise in measured signal and an important attenuation which increases with frequency.

One also notes that resonances which appear in transfer functions are always pointed at higher frequencies in SOPEMEA set than ONERA measurements excepted for the mode around 16.3Hz. These shifts may be due both to distinct characteristics of shakers (mass and stiffness) and to stiffness introduces by the connection with the structure.

Finally, SOPEMEA reference set shows a mode at 40 Hz that might be due to the suspension.

4. Testbed modes

4.1. Identification using the appropriation method

For identifying the nine flexible modes below 65 Hz, ten different sites for excitation were used. In complement with the 24 displacements requested, the four suspension modes appearing in the interesting frequency band were also measured.

All results which include resonance frequency, damping factor, generalized mass and other parameters are listed in figure 18.

To estimate the quality of the appropriation, the *"appropriation criterion" C.a.* is computed:

$$C.a. = 1 - \frac{\sum imag(V) * \|V\|}{\sum \|V\|^2}$$

where V represents the velocity response. So, when the mode is isolated, the response V is modulo π in phase with the reference and the criterion tends to 1.

Since the number of measurement points is not large enough to provide a realistic wire-frame animation of each mode shape, the eigenvector is presented through an arrow distribution.

Damping factor and generalized mass parameters are evaluated through two useful identification methods:

- force in quadrature
- complex power method

For each mode, one also archives the evolution of the resonance frequency and eigenvector with the level of the excitation so called impedance. These data which are plotted in the same figure as the mode shapes are used to evaluate the linearity of the structure.

The sensitivity of wing modes to the complement mass is quite large so that we need sometimes to limit the number of exciters connected to the testbed. In particular, the 5th mode (3n wing bending) is not really well isolated as indicated by the value of *C.a.=0.772*. One could improve the appropriation by adding a shaker at node 5-z. But the moving mass of the shaker would load the wing thus implying a lower resonance frequency and a very different eigenvector due to stronger coupling with the torsion modes.

4.2. Comparison with results of SOPEMEA

Resonance frequencies measured by Onera are lightly lower than those measured by Sopemea for the first four flexible modes and they are higher for the last five modes.

Except for the case of first symetric wing torsion mode, damping ratios measured by Onera are always lower than Sopemea measurements.

Although M.A.C. results which are equivalent to a normalized scalar product indicate that identified modeshapes (eigenvectors) are generally similar, some large differences still appear for the torsion modes.

Figure 27 lists our results and the Sopemea reference set (see ref. [4]).

4.3. Frequency domain identification using a pole / residue model

To obtain the first nine flexible modes of the testbed, the L.I.S.A. ref [2] and I.D.R.C. ref.[3] algorithms were performed on the two experimental sets of FRF's (sine and broadband measuring results).

The L.I.S.A. method provide a linear optimization in the base of eigenvectors. The principle of the I.D.R.C. algorithm is to optimize (non-linear optimization) the poles of a pole/residue model while recomputing the residues at each step.

As shown in figure 28, identifications based on sine set of transfer functions generally give satisfactory results. Comparing to the appropriation data, one notes however some small differences.

For the 3n bending mode, the I.D.R.C. method based on a broadband model (a single model for the whole frequency range) gives a poor M.A.C. (0.573). If a narrow frequency band is considered (35.6 Hz to 36.8 Hz), results improve tremendously (MAC of 0.963). The L.I.S.A. software which uses narrow bands gives good results from the start. The poor prediction of the broadband I.D.R.C. model is linked to assymptotic contributions of modes external to the tested frequency range which are difficult to represent for this structure (this might be due to the viscoelastic material).

Similarly, the I.D.R.C. results for the wing yaw mode can be improved by the use of a narrow band identification.

narrowband I.D.R.C. fit using a very lightly damped pole at 50 Hz, gives an estimated mode at 49.90 Hz and an associated MAC of 0.998.

5. CONCLUSION

The suspension of the testbed by bungees gives acceptable low rigid body modes.

Nevertheless more tests have been necessary to obtain a configuration (distance between the clamped point and the middle hook) where suspension modes (translations of the attachment hook) do not disturb the flexible modes of the model.

The implementation of a new stabilization process in case of harmonic input allows shorter measuring time and best accuracy.

Comparisons of our results with the Sopemea test datas sometimes show large differences. These gaps can be due to various excitation materials to a great extent.

6. REFERENCES

[1] Balmès E.,
Documentation for the GARTEUR SM AG19 testbed,
test documentation 04/05/95.

[2] Balmès E.,
Structural Modeling Toolbox Version 2.0
(A toolbox for MATLAB™, Scientific Software Group (france))

[3] Lepart M.,
"Méthode de lissage de réponses fréquentielles en coordonnées généralisées",
ONERA RT n° 24/1677 RN 002 R, 12-1993.

[4] GARTEUR SM-AG19,
"the reference set of results from SOPEMEA",
September 1995.

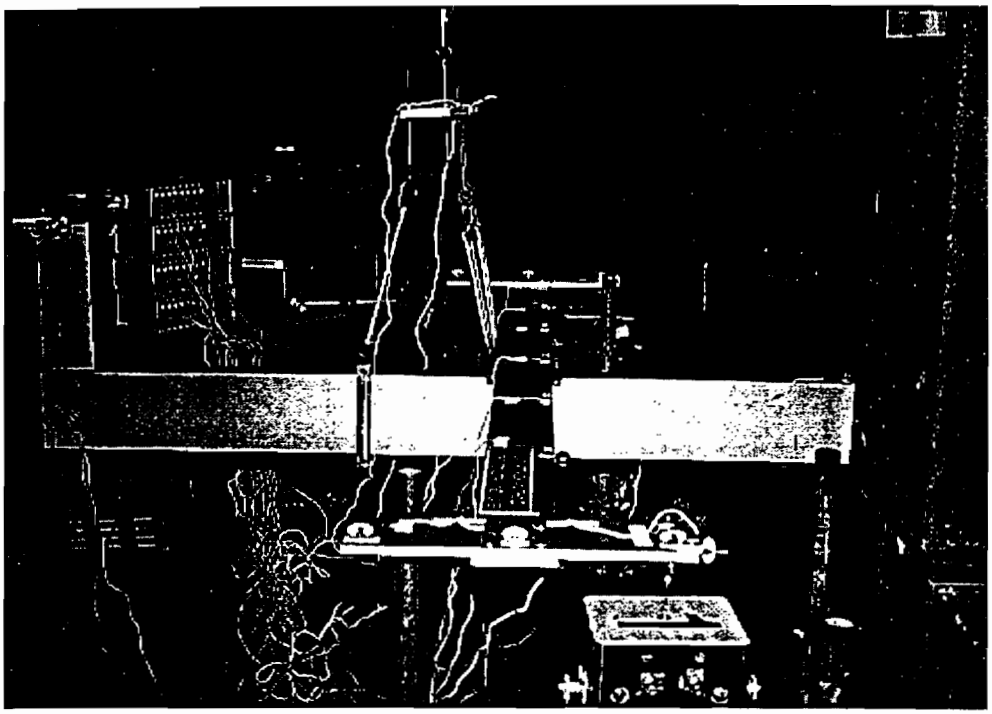

2.a: Global view of the GVT

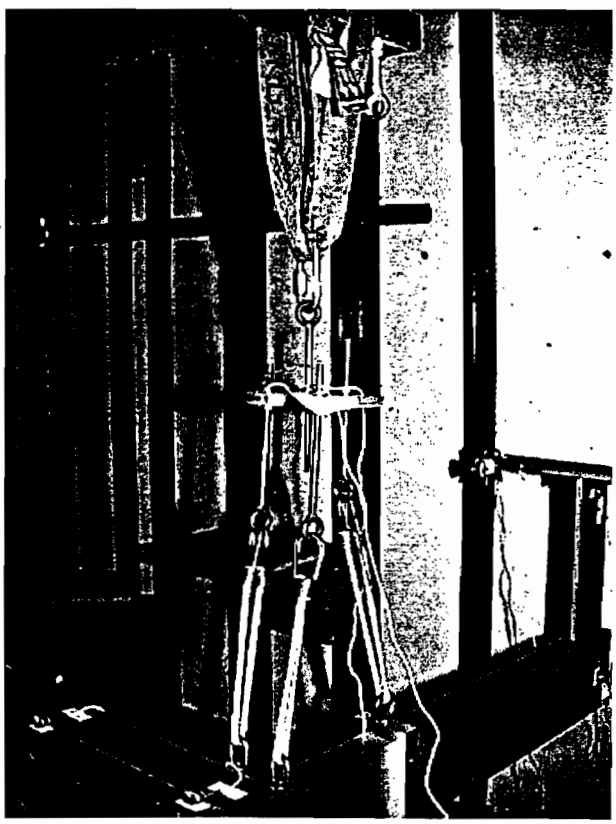

2.b: Details of the suspension

figure 2: Test setup for the SM-AG19 testbed

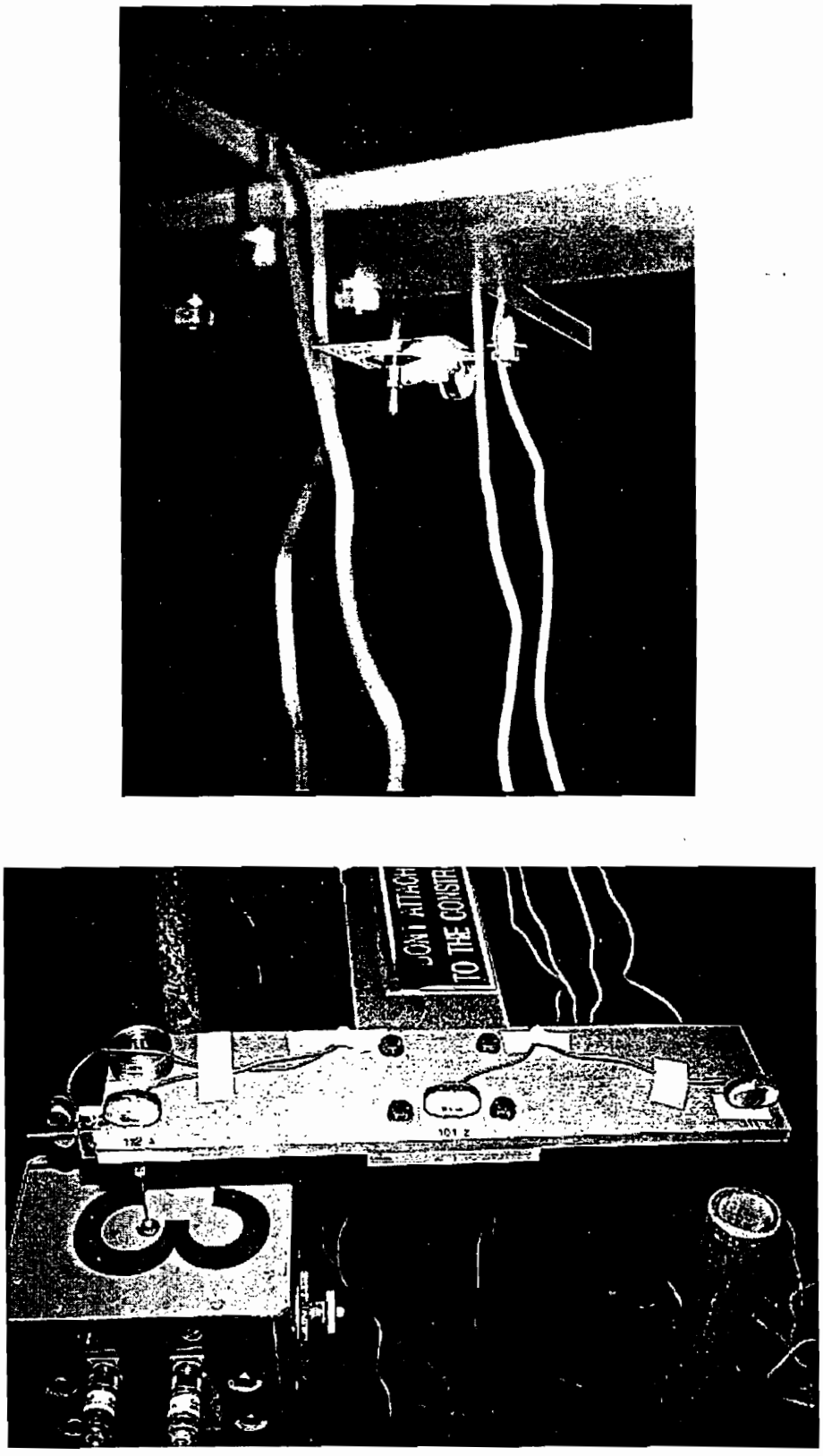

Figure 3: Shaker connection to the SM-AG19 testbed

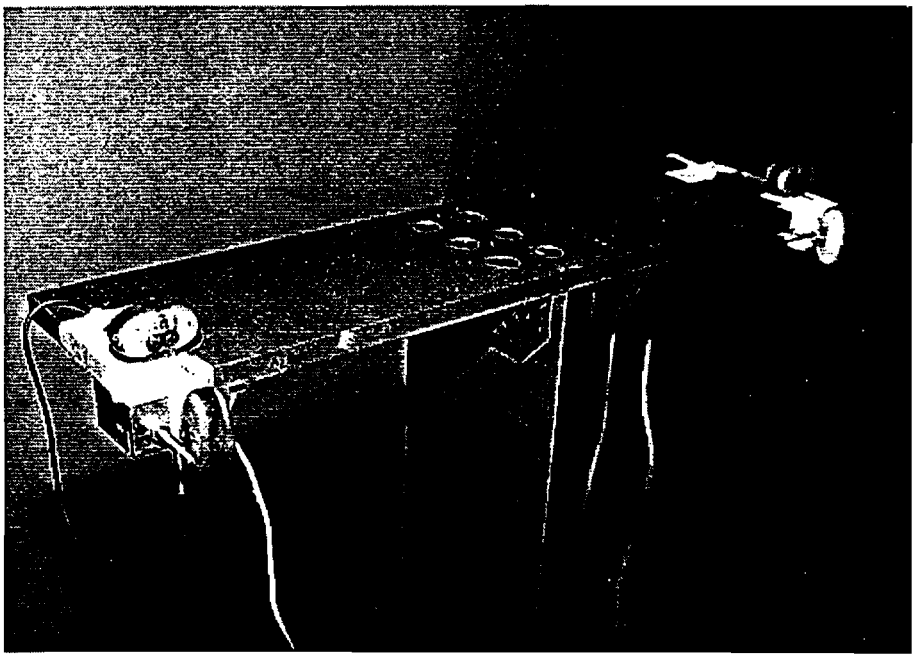

Figure 4: zoom of the tail

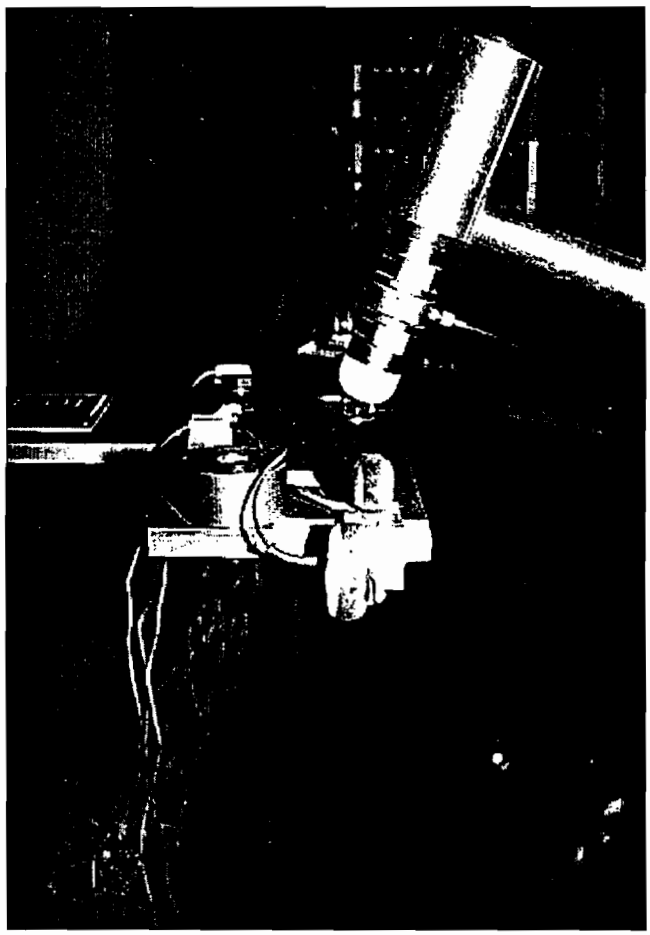

Figure 5: Impact test setup for the SM-AG19 testbed

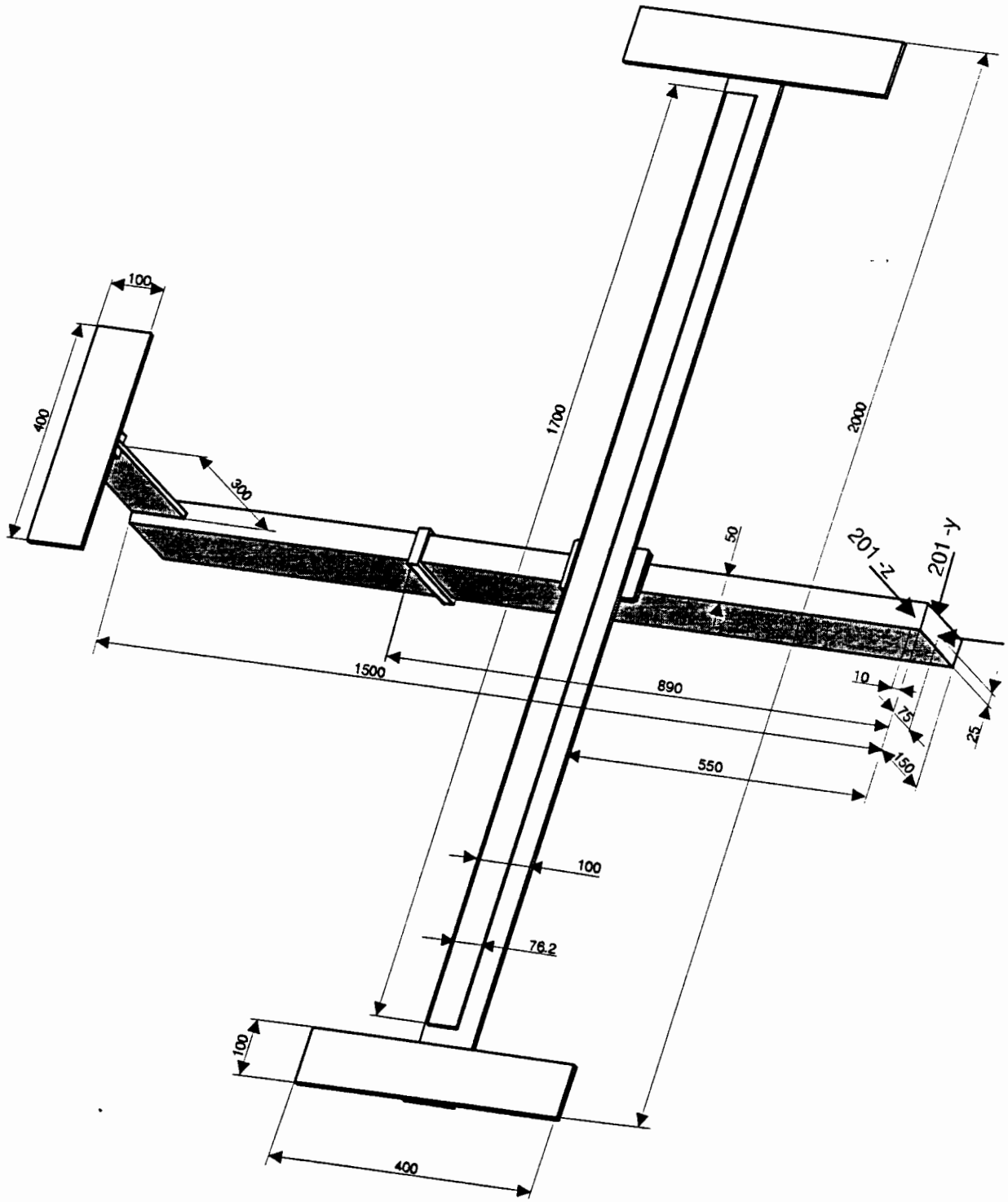

Figure 6: global view showing the testbed geometrie and sensor locations

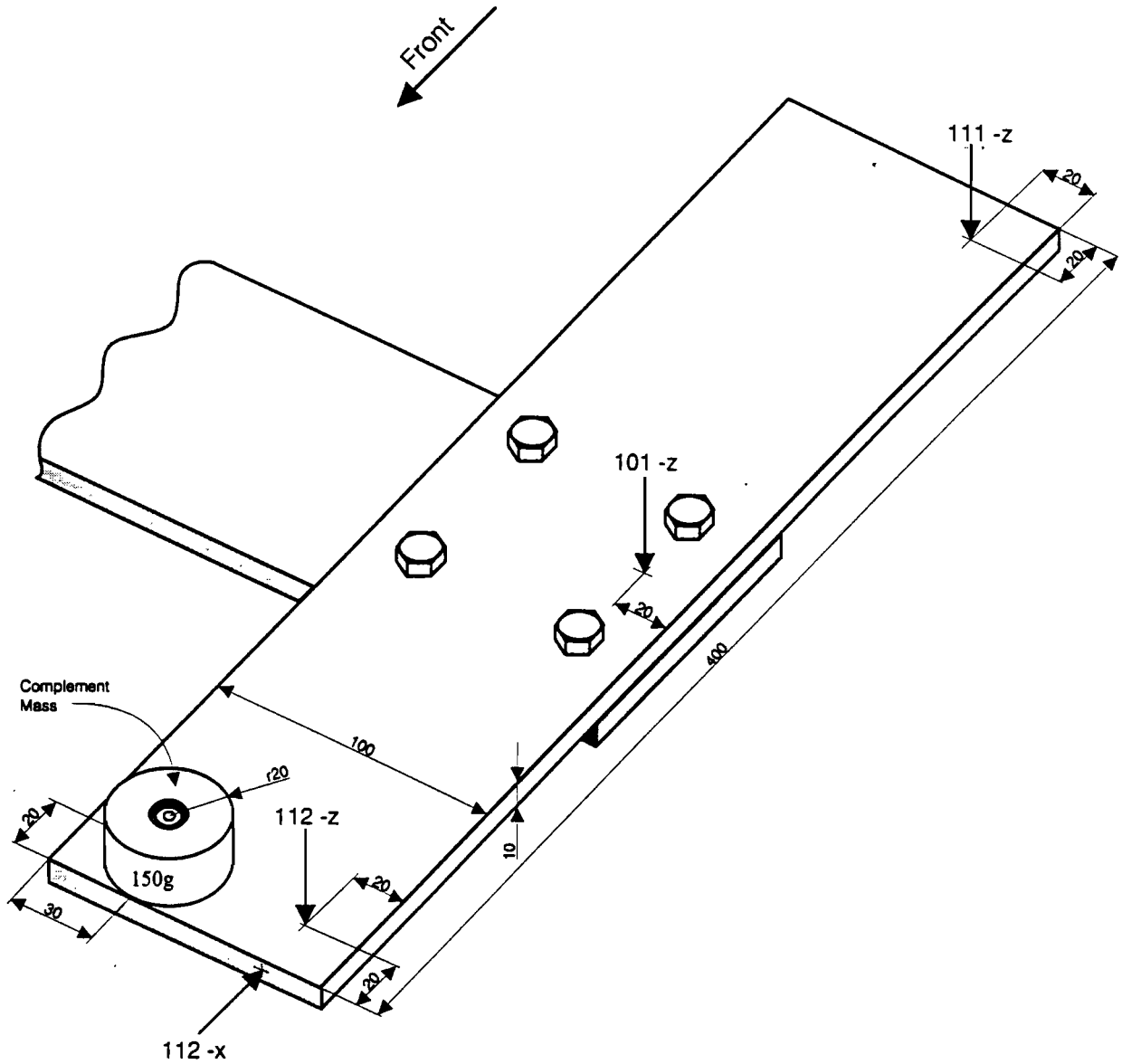

Figure 7: details of the left drum

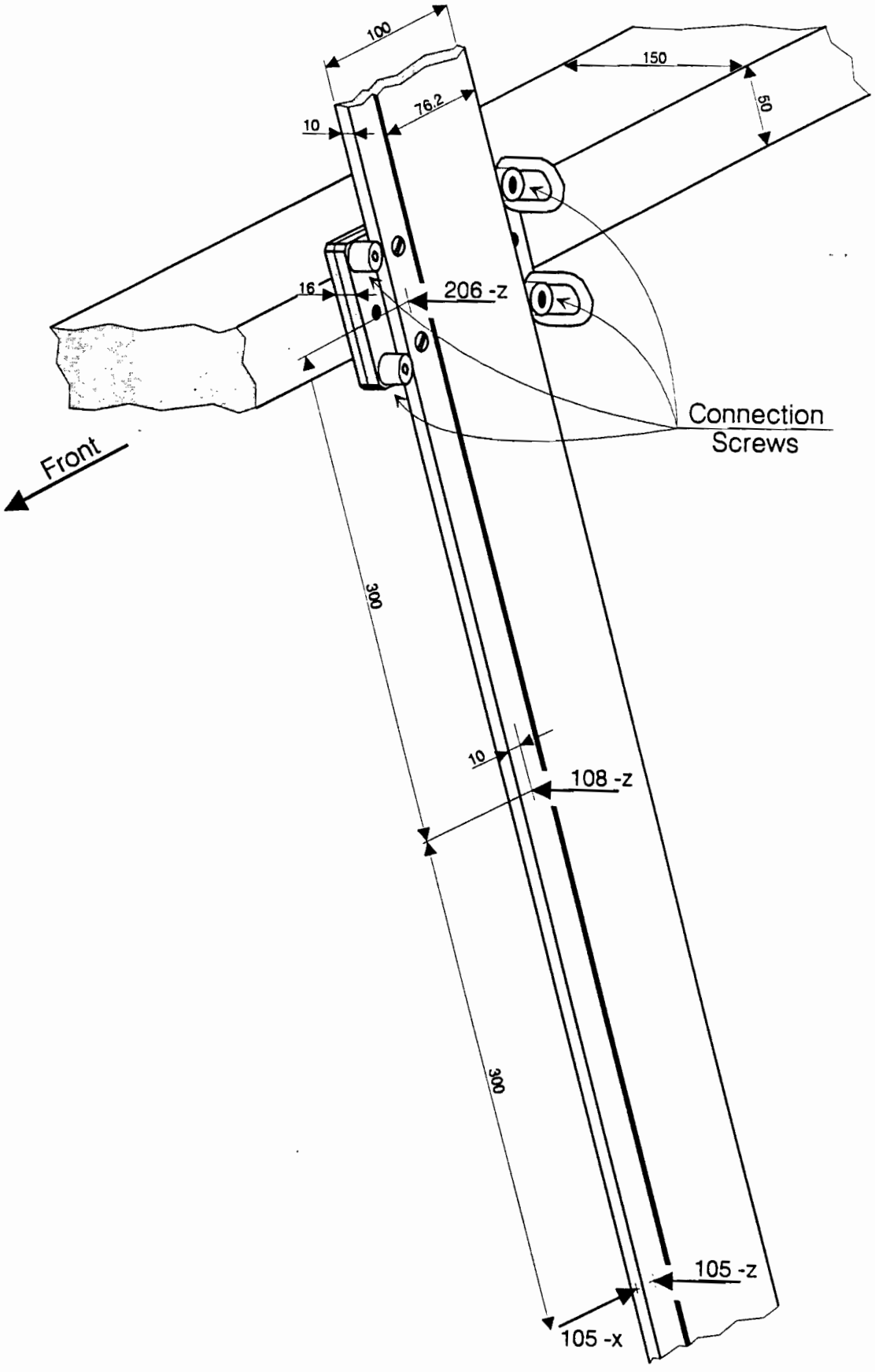

Figure 8: connection beetwen the wings and the fuselage

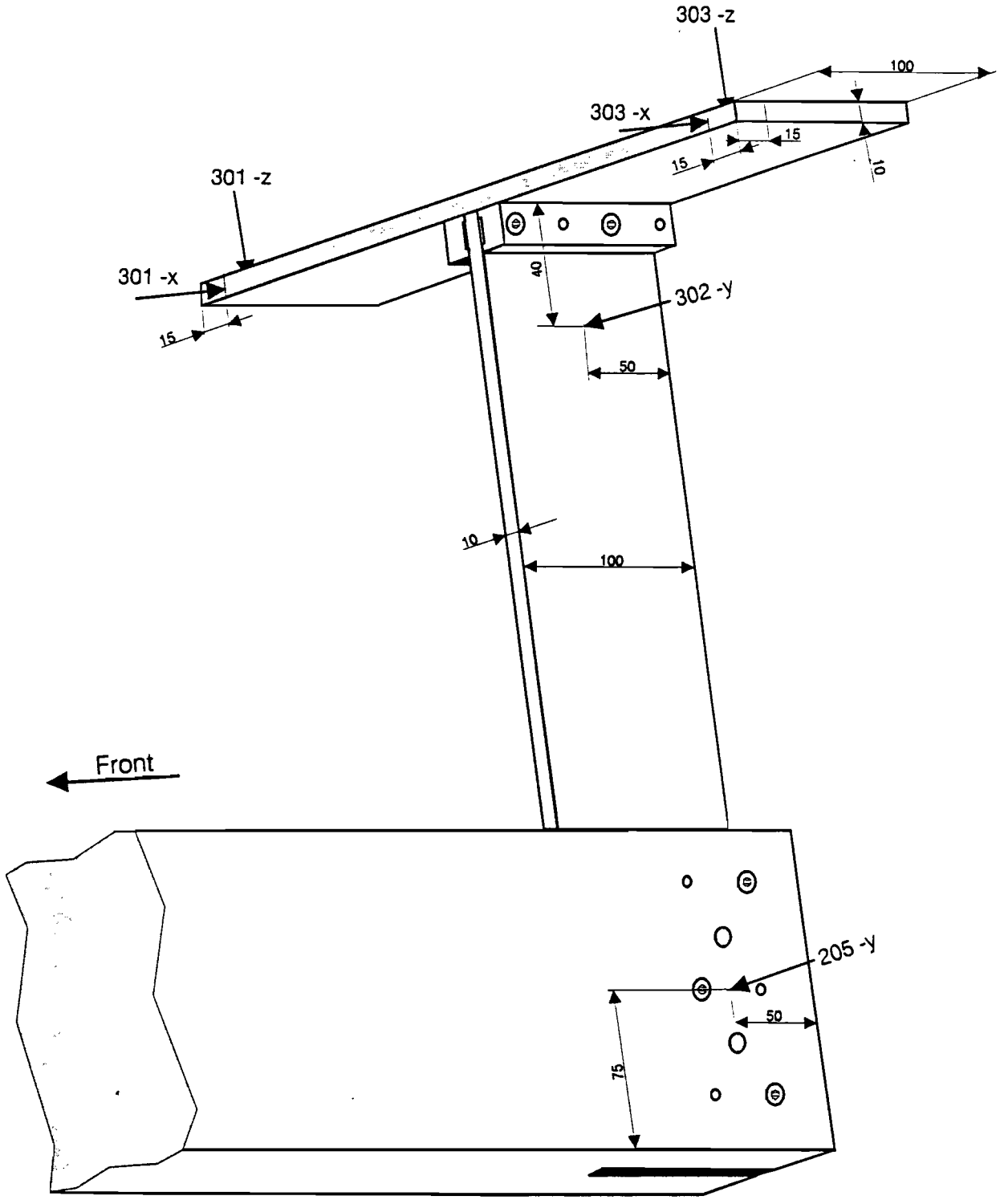

Figure 9: zoom of the tail

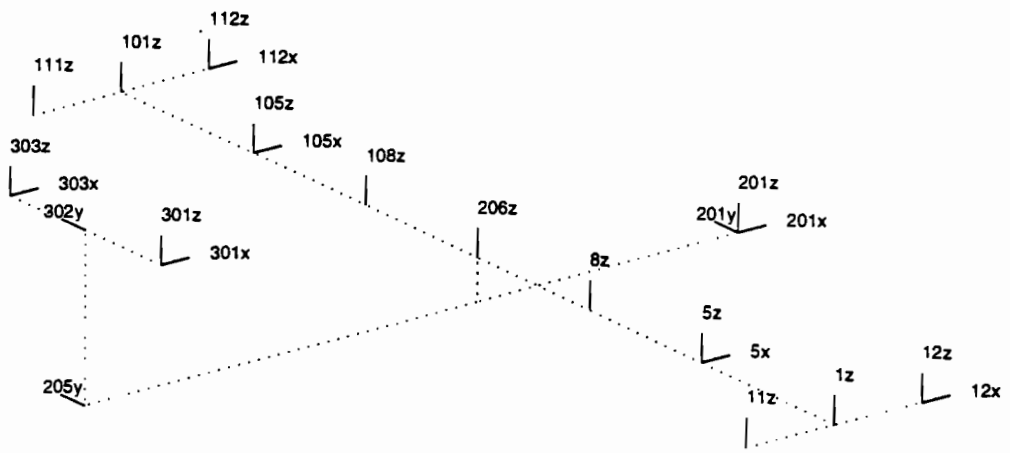

Figure 10: locations and directions of the 24 required accelerometers

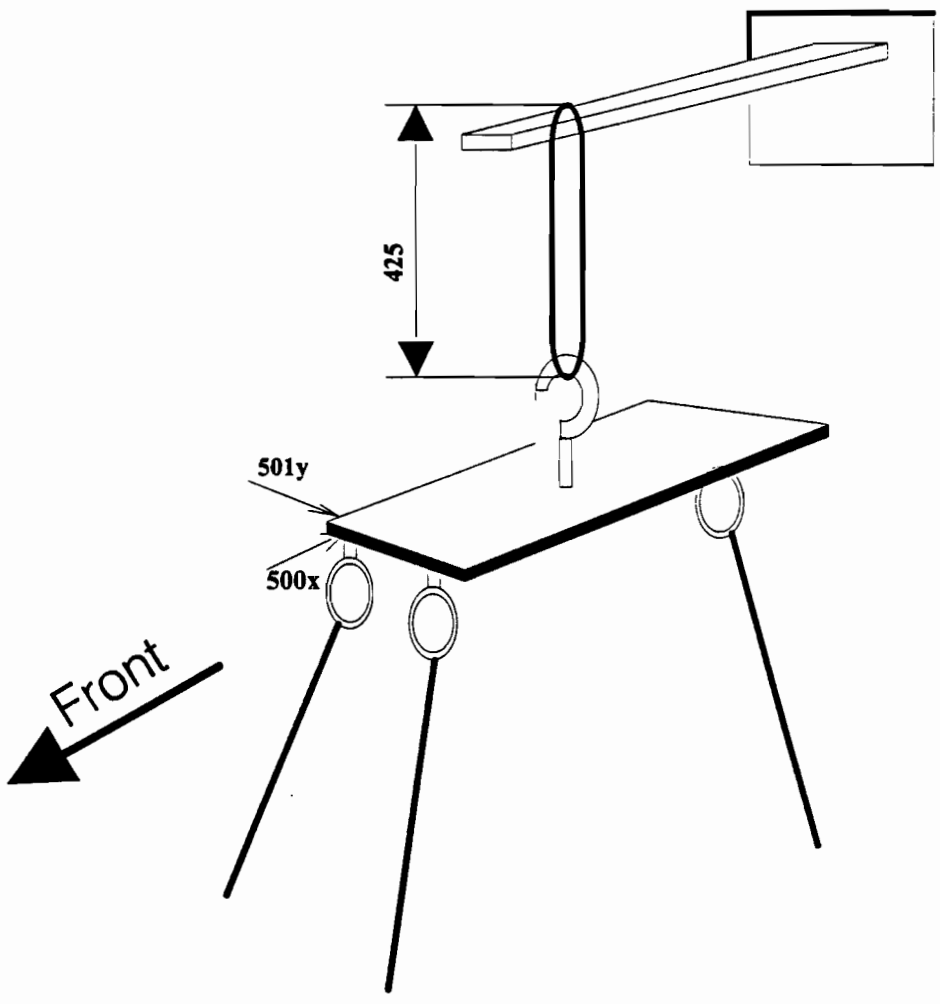

figure 11: Position of the two accelerometers placed on the suspension

Channel I.D.	D.O.F.	Position (mm)			Sensor characteristics			
		x	y	z	type	serial number	calibration (mV/ms^{-2})	weight (g)
1	11-z	-200	-950	0	P.C.A.*	180	80	10
2	1-z	0	-950	0	P.C.A.*	181	80	10
3	12-x	200	-950	0	P.C.A.*	182	80	10
4	12-z	200	-950	0	P.C.A.*	183	80	10
5	5-x	0	-600	0	P.C.A.*	184	80	10
6	5-z	0	-600	0	P.C.A.*	185	80	10
7	8-z	0	-300	0	P.C.A.*	186	80	10
8	111-z	-200	950	0	P.C.A.*	187	80	10
9	101-z	0	950	0	P.C.A.*	190	80	10
10	112-x	200	950	0	P.C.A.*	191	80	10
11	112-z	200	950	0	P.C.A.*	192	80	10
12	105-x	0	600	0	P.C.A.*	193	80	10
13	105-z	0	600	0	P.C.A.*	194	80	10
14	108-z	0	300	0	P.C.A.*	195	80	10
15	201-x	600	0	-96	P.C.A.*	196	80	10
16	201-z	600	0	-96	P.C.A.*	197	80	10
17	201-y	600	0	-96	P.C.A.*	210	80	10
18	206-z	0	0	0	P.C.A.*	211	80	10
19	205-y	-900	0	-96	P.C.A.*	212	80	10
20	302-y	-900	0	285	P.C.A.*	213	80	10
21	301-x	-900	-200	285	P.C.A.*	214	80	10
22	301-z	-900	-200	285	P.C.A.*	215	80	10
23	303-x	-900	200	285	P.C.A.*	216	80	10
24	303-z	-900	200	285	P.C.A.*	217	80	10
25	500-x				P.C.A.*	220	80	10
26	501+y				P.C.A.*	221	80	10

P.C.A.*: piezo capacitive accelerometer made by O.N.E.R.A.

figure 12: Characteristics of the accelerometers used for the test

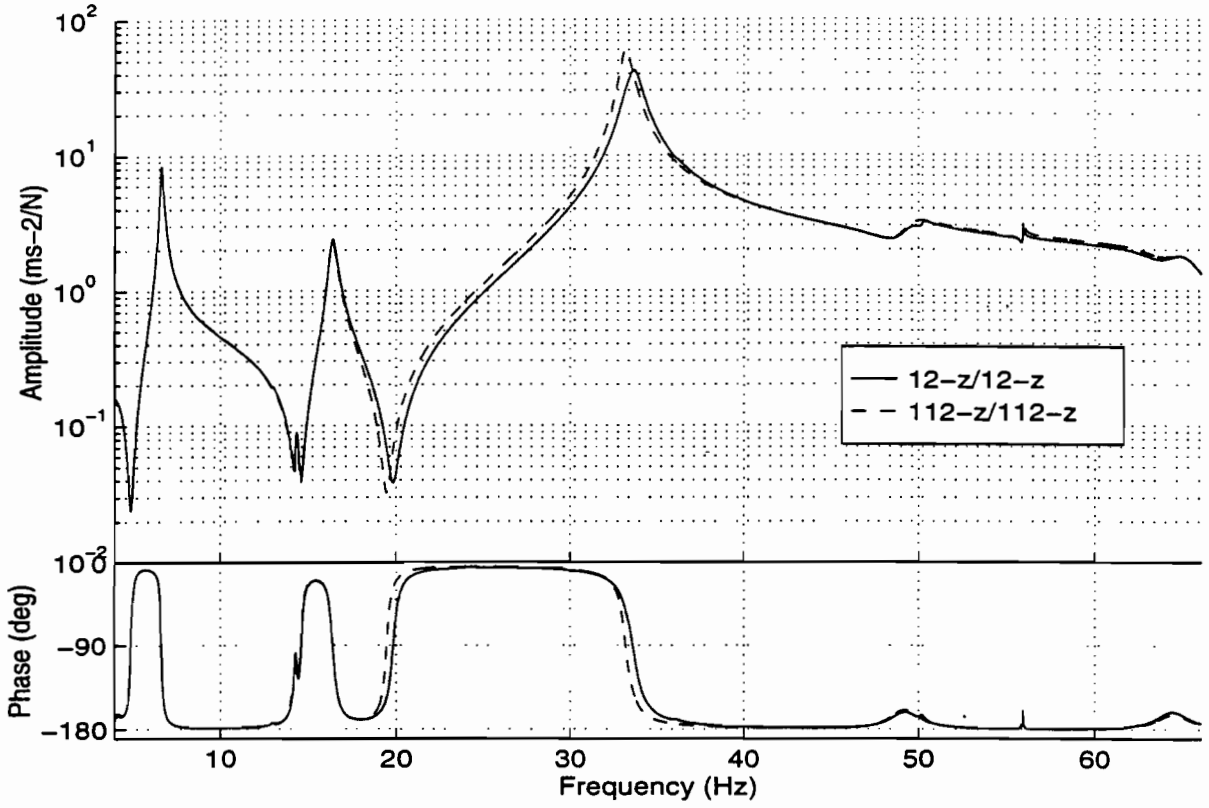

a) Collocated FRF's

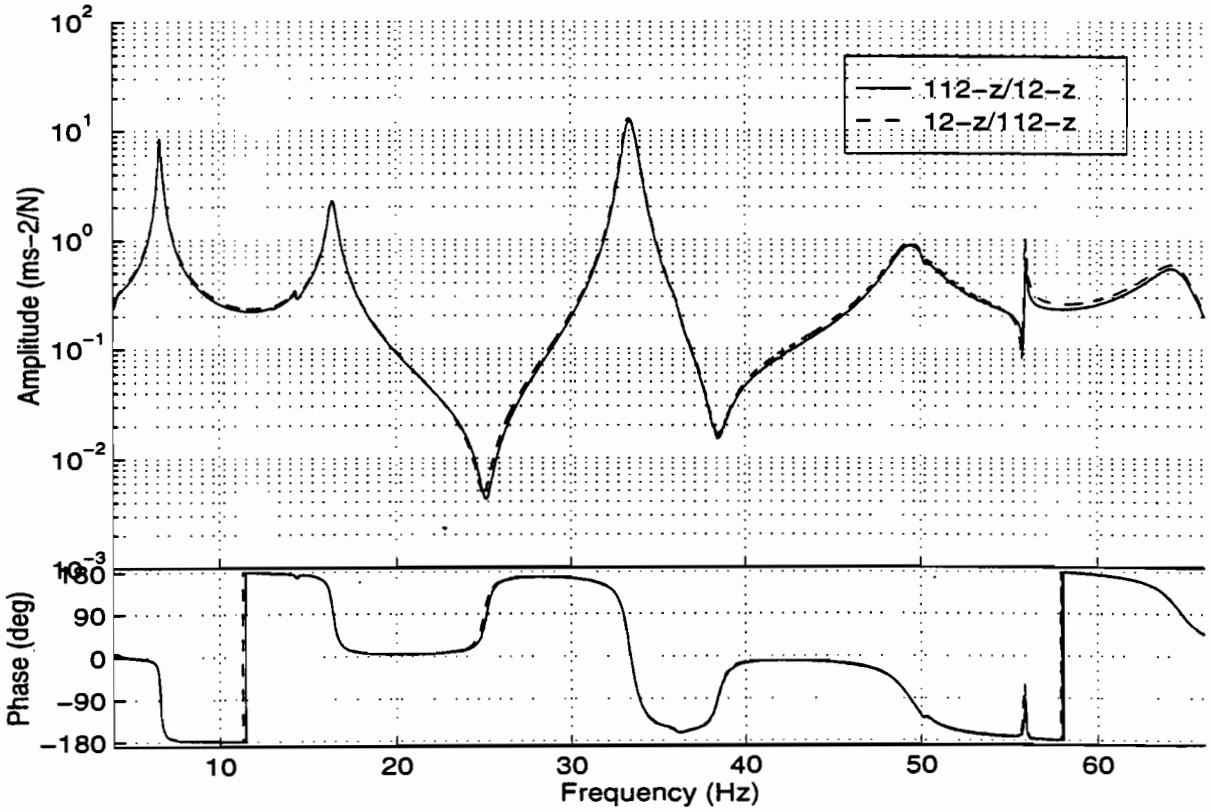

b) Cross-transfers

Figure 13: Transfer functions measured with harmonic inputs at nodes 12-z and 112-z

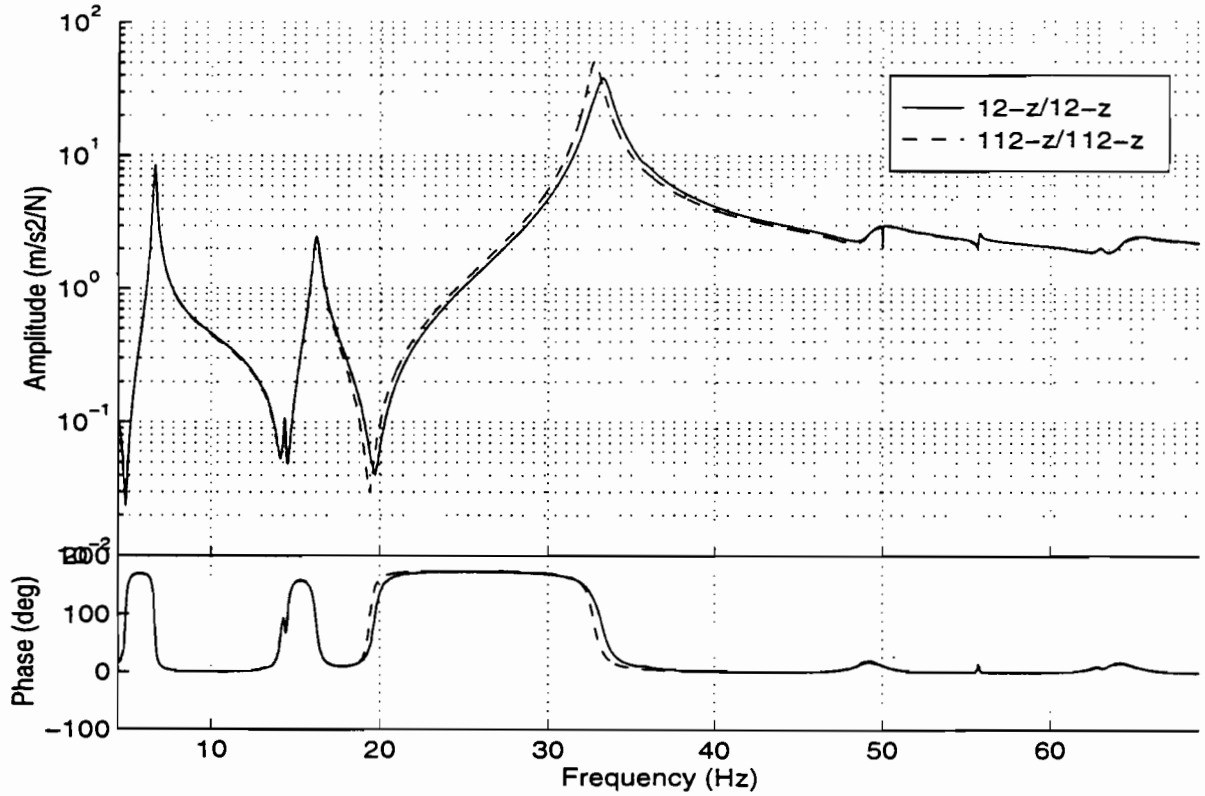

a) Collocated FRF's

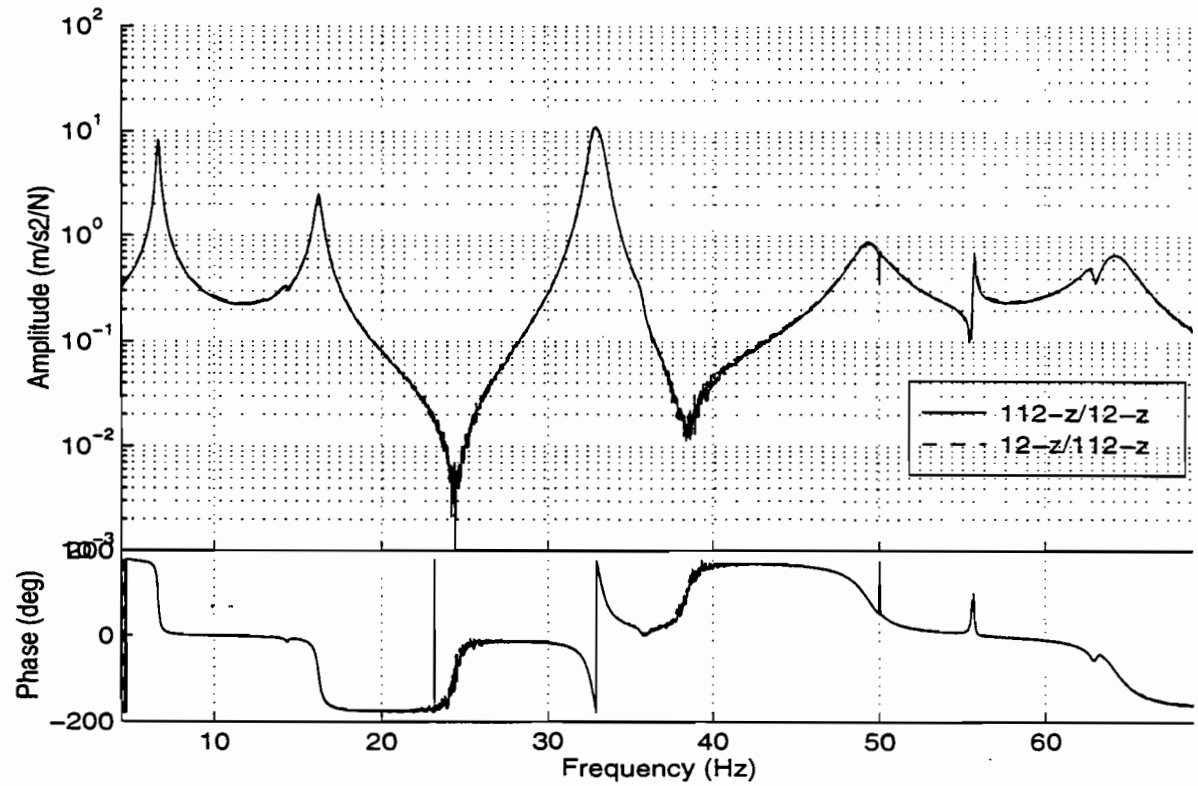

b) Cross-transfers

Figure 14: Transfer functions measured with uncorrelated, Gaussian noise inputs at nodes 12-z and 112-z

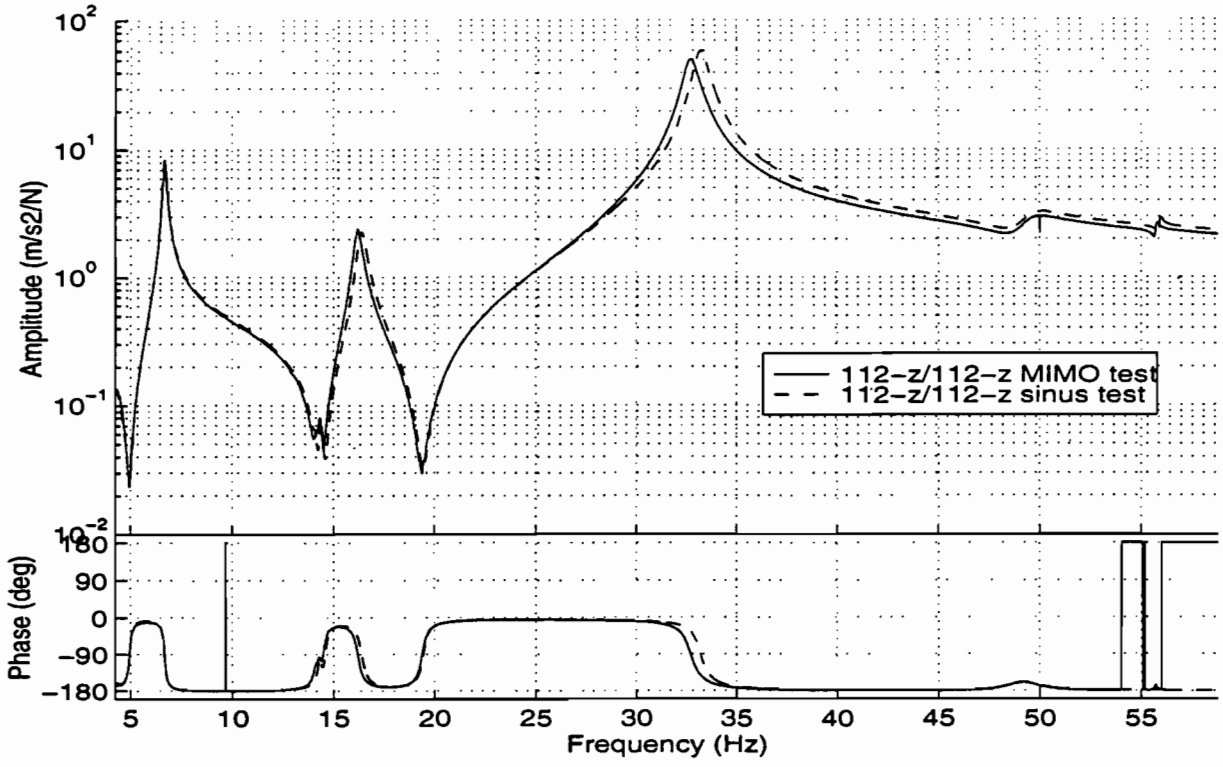

a) Collocated FRF's

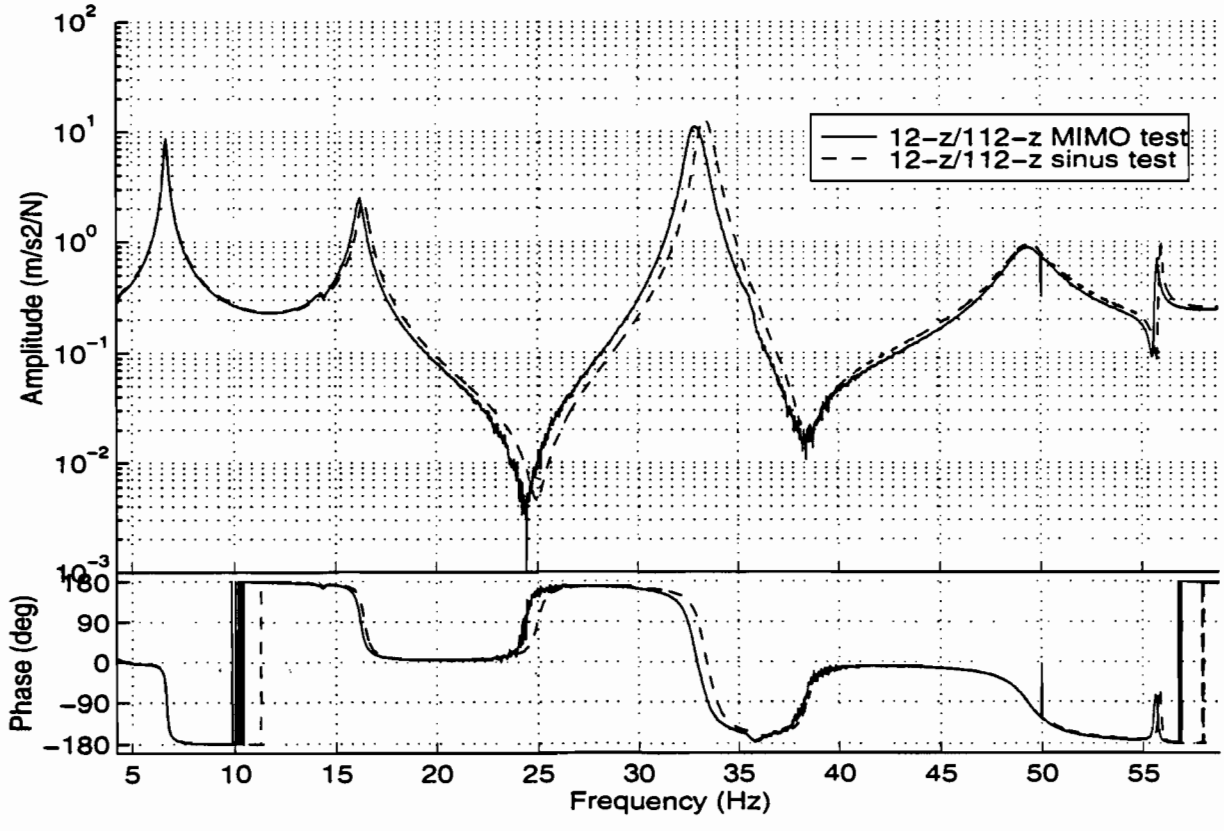

b) Cross-transfers

Figure 15: Superimposition of the measured sine and broadband noise sets of FRF

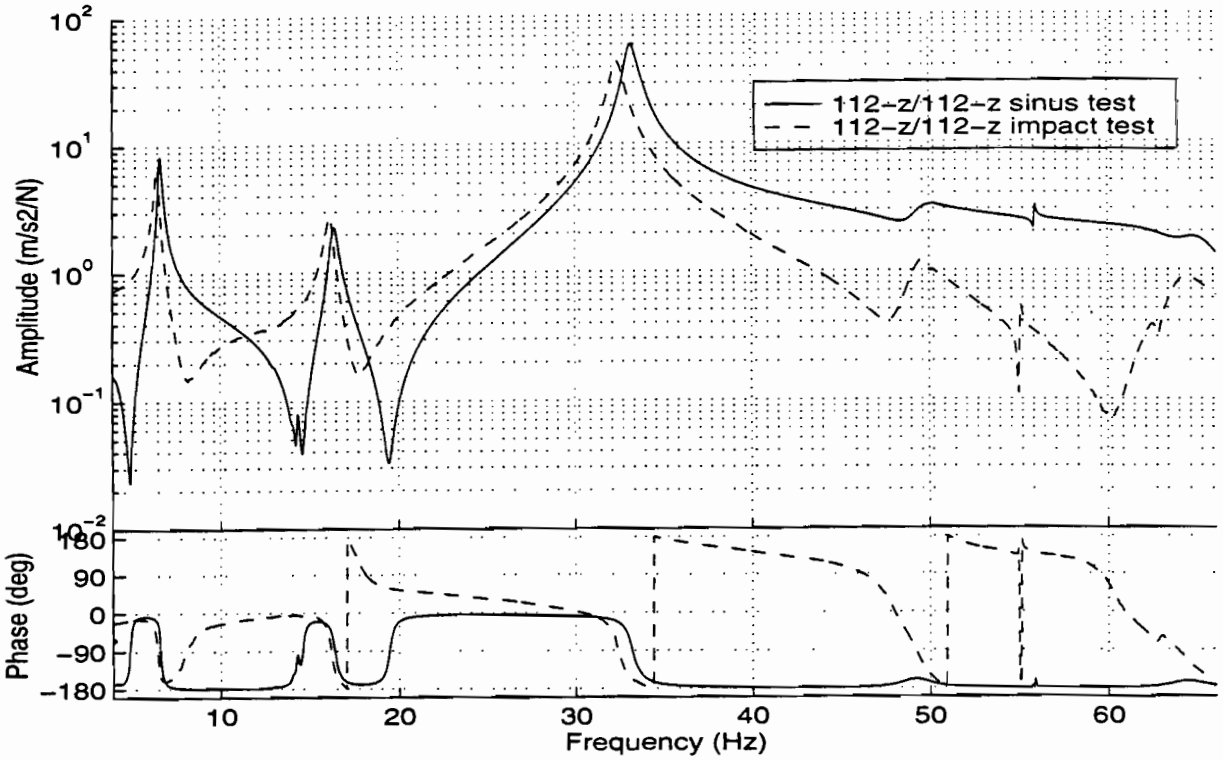

a) Collocated transfer functions

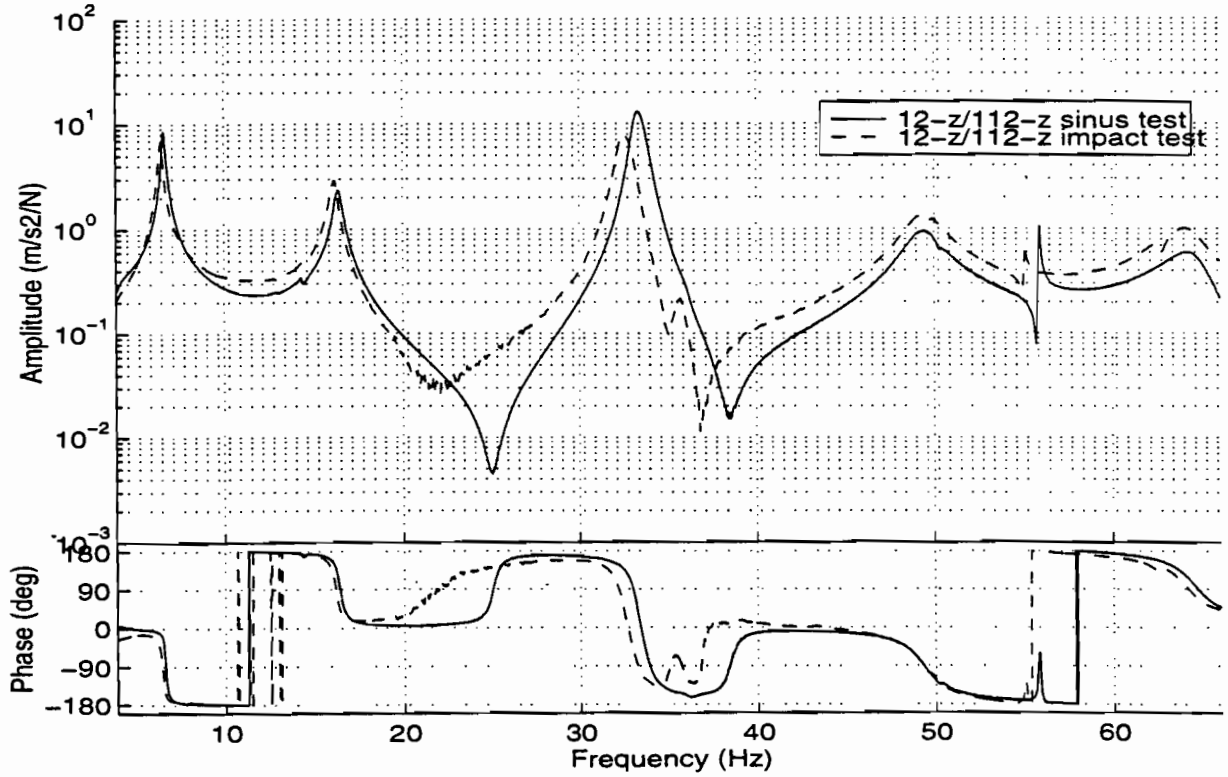

b) Cross-transfers

figure 16: Plots of transfer functions measured by an impact test (the sine set is also plot as reference)

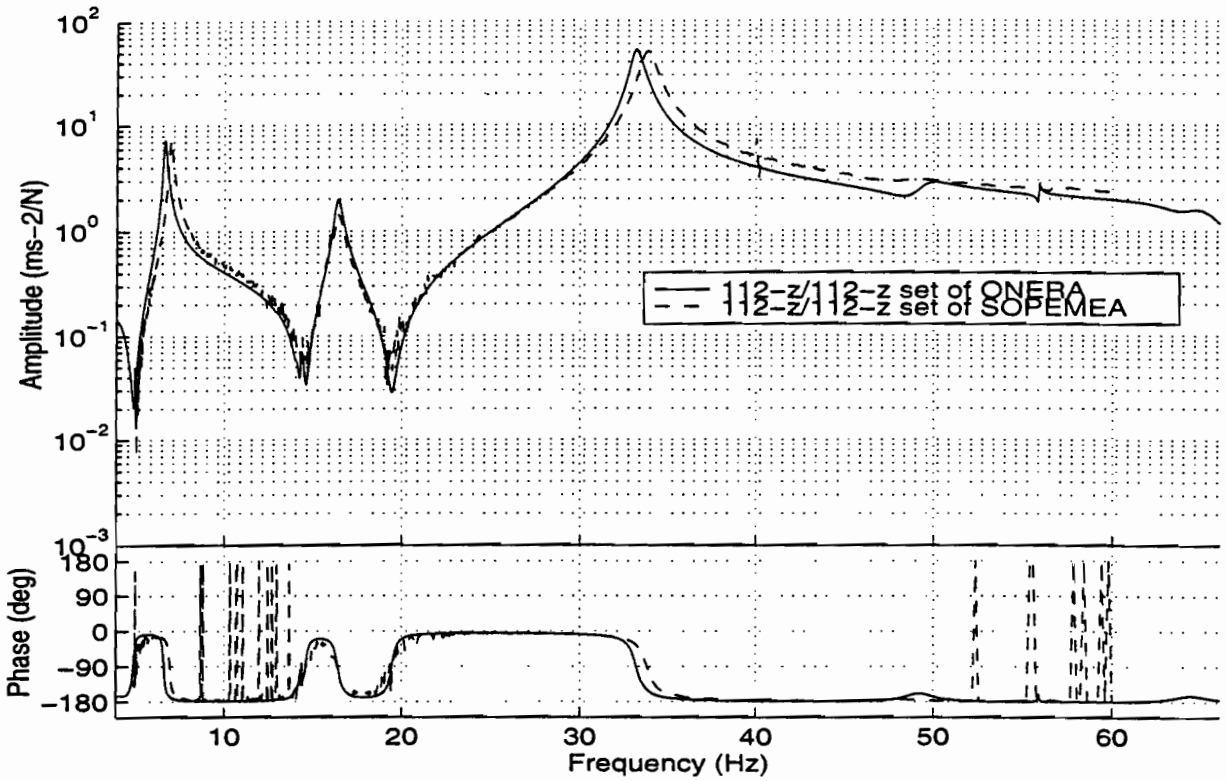

a) Collocated transfer functions

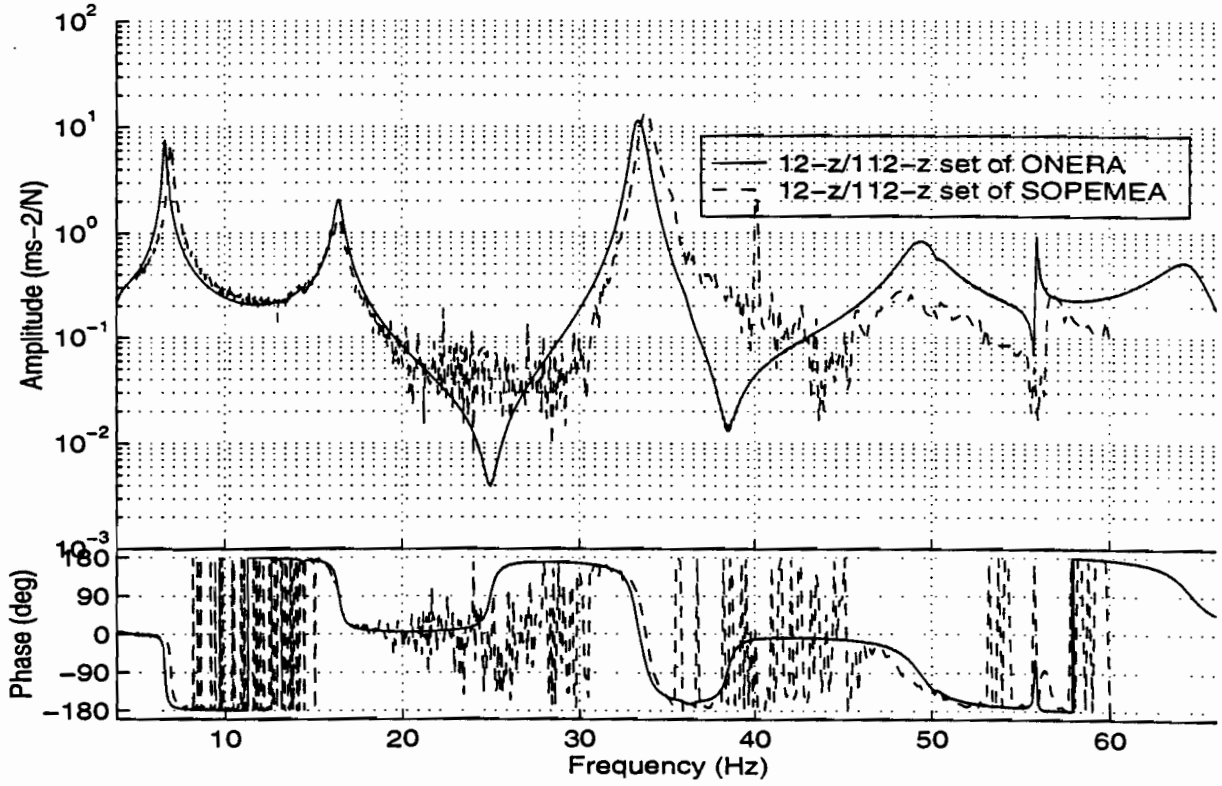

b) Cross-transfers

Figure 17: Comparison of FRF's measured by ONERA with the reference set given by SOPEMEA (both sets are measured with harmonic inputs)

DOF Id.	Nature	frequency (Hz)	Damping factor ξ	Norm. point	Response (m/s^2)	Amp. (mm)	Acc (g)	μ (m^2kg)	C.a.	θ (°C)
1	2 n wing	**6,63**	1,231E-02	11-z	1,171E+01	6,75	1,19	3,68E+00	0,992	16
2	fin bending	**16,25**	1,181E-02	302-y	8,540E+00	0,82	0,87	5,17E+00	0,991	16
3	first antisymetric wing torsion	**33,16**	1,059E-02	111-z	1,148E+02	2,64	11,70	7,86E-01	0,989	16
4	first symetric wing torsion	**33,57**	1,283E-02	11-z	6,310E+01	1,42	6,43	6,56E-01	0,991	16
5	3 n wing	**35,36**	8,450E-03	11-z	3,326E+01	0,67	3,39	6,43E+00	0,772	17
6	4 n wing	**48,62**	2,115E-02	105-z	1,402E+01	0,15	1,43	2,75E+00	0,894	17
7	wing yaw	**48,79**	6,370E-03	12-x	3,800E+01	0,40	3,87	7,73E+00	0,921	15
8	2 n wing fore & aft bending	**54,88**	2,300E-03	12-x	6,144E+01	0,52	6,26	4,01E+00	0,992	15
9	HTP yaw	**63,82**								14

a) First flexible modes of the GARTEUR SM-AG19 testbed

DOF Id.	Nature	frequency (Hz)
101	lateral dof	**12,99**
102	fore&aft dof	**14,07**
103	lateral dof	**14,39**
104	lateral dof	**61,70**

b) Suspension dof's in the 4 to 65 Hz frequency band

Figure 18: Characterization of the testbed by the appropriation method (sine excitation coupled with a 0° phase criterion)

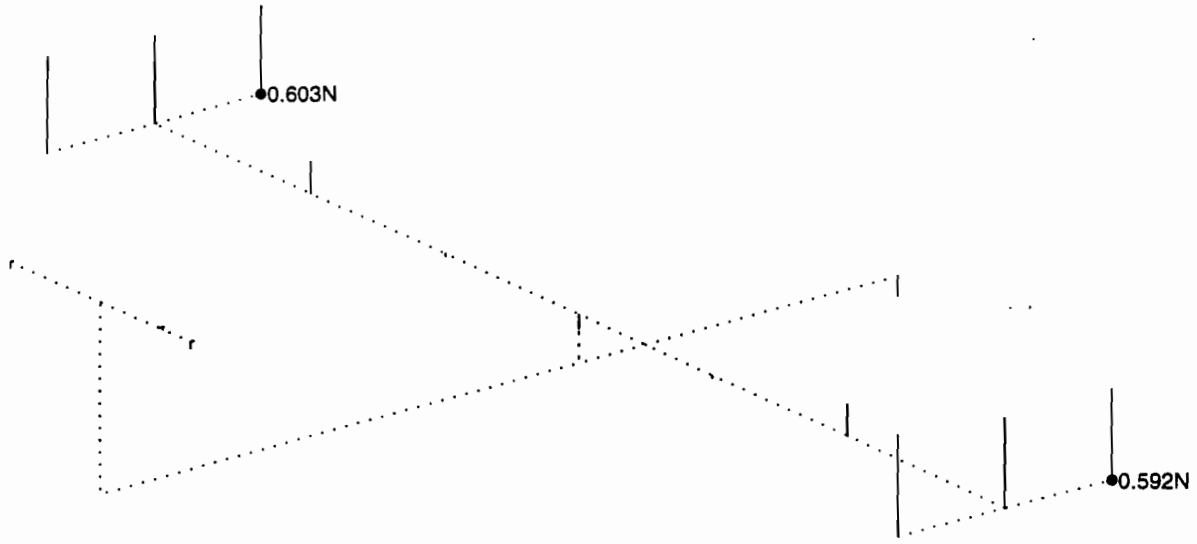

a) modeshape plot

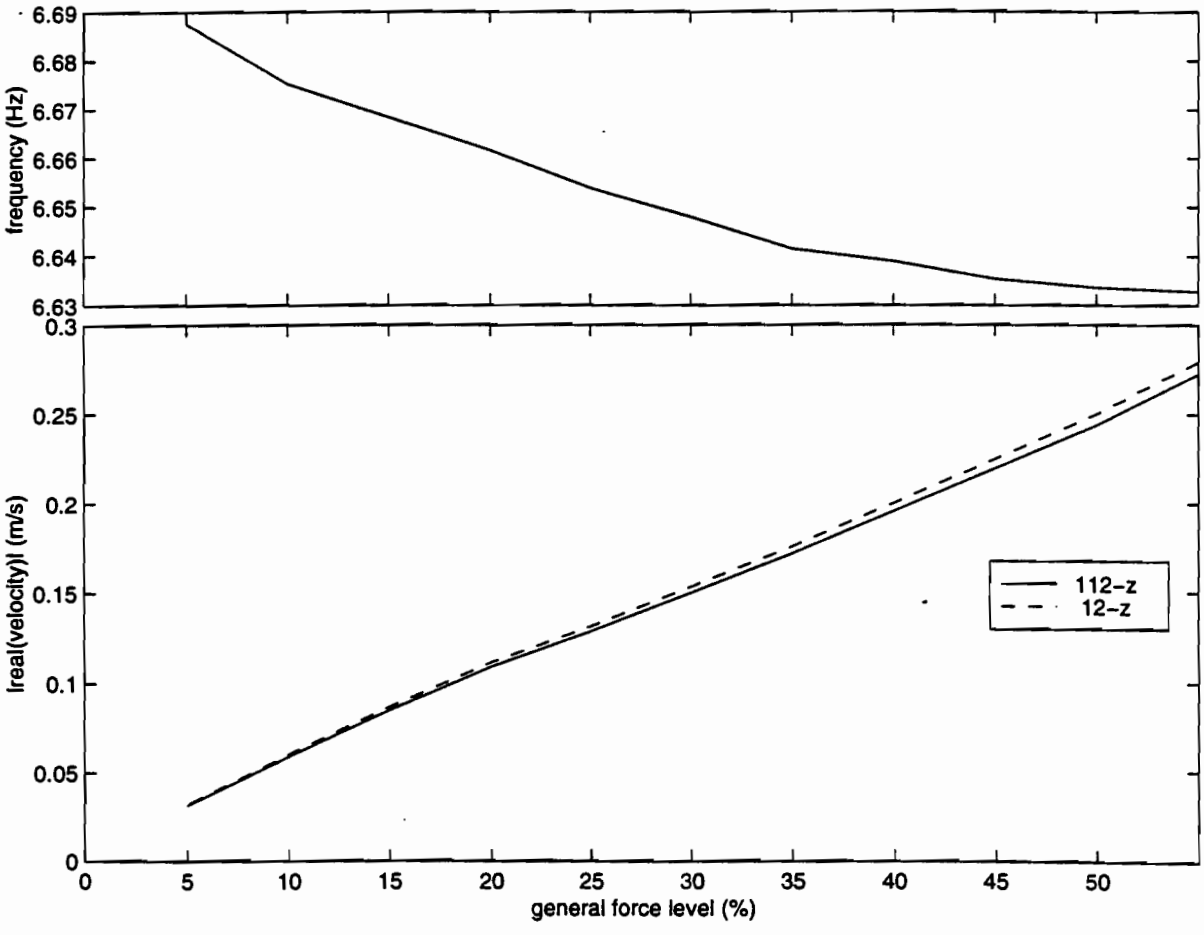

b) Impedance plot

Figure 19: Characterization of the 1st mode by appropriation- 2 nodes wing bending at 6,63Hz -

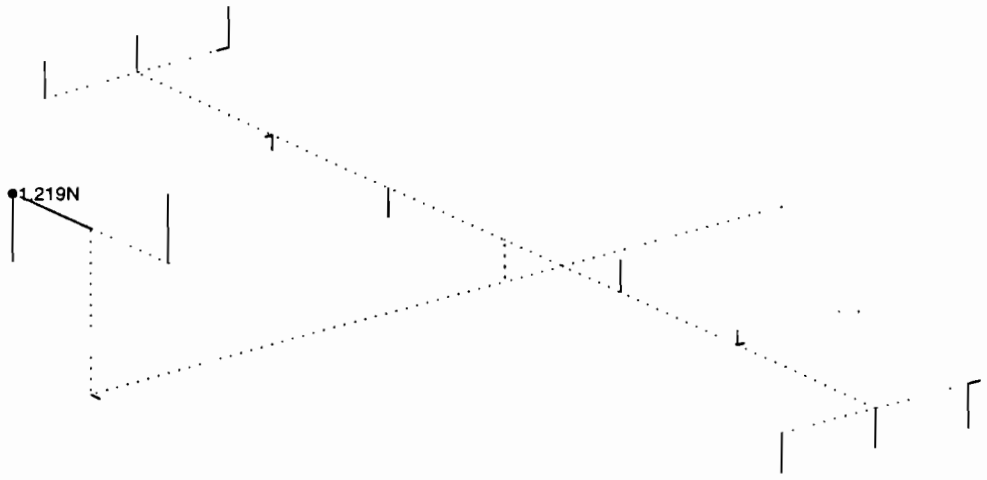

a) modeshape plot

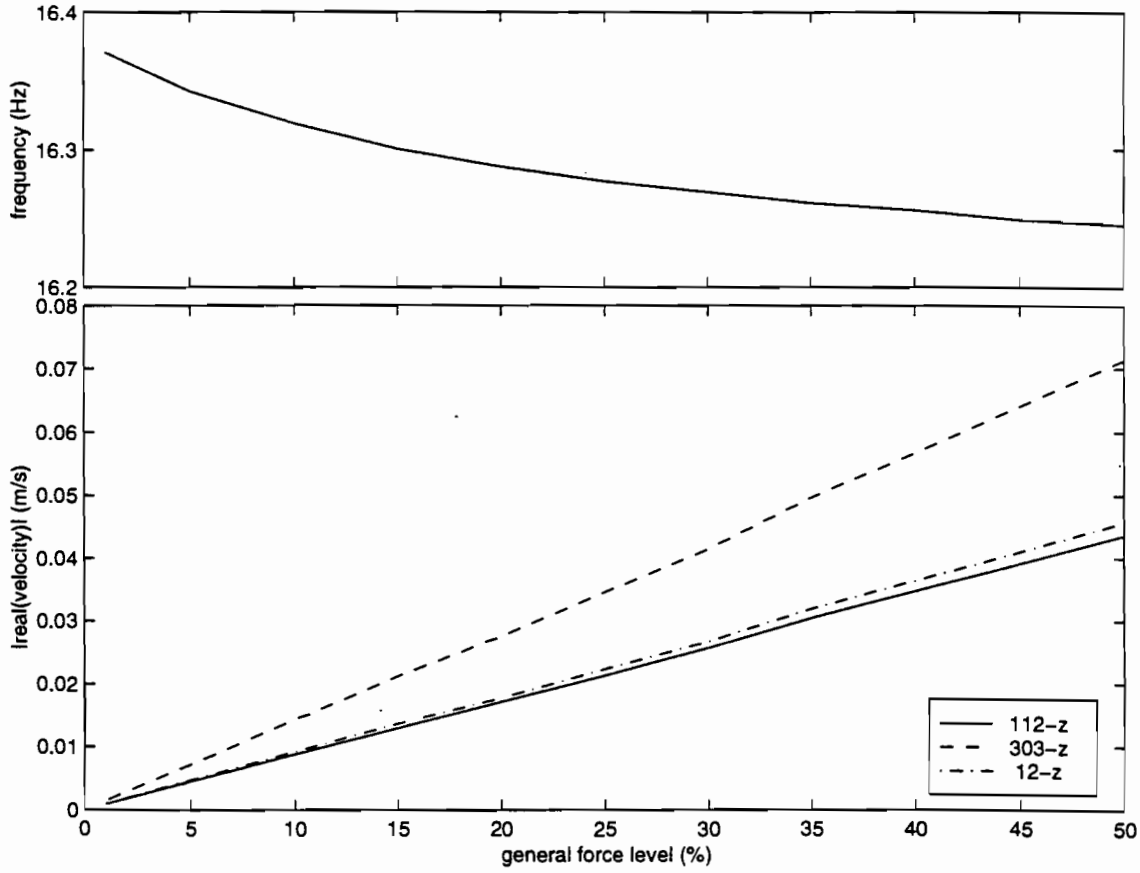

b) Impedance plot

Figure 20: Characterization of the 2nd mode by appropriation - fin bending at 16,25Hz -

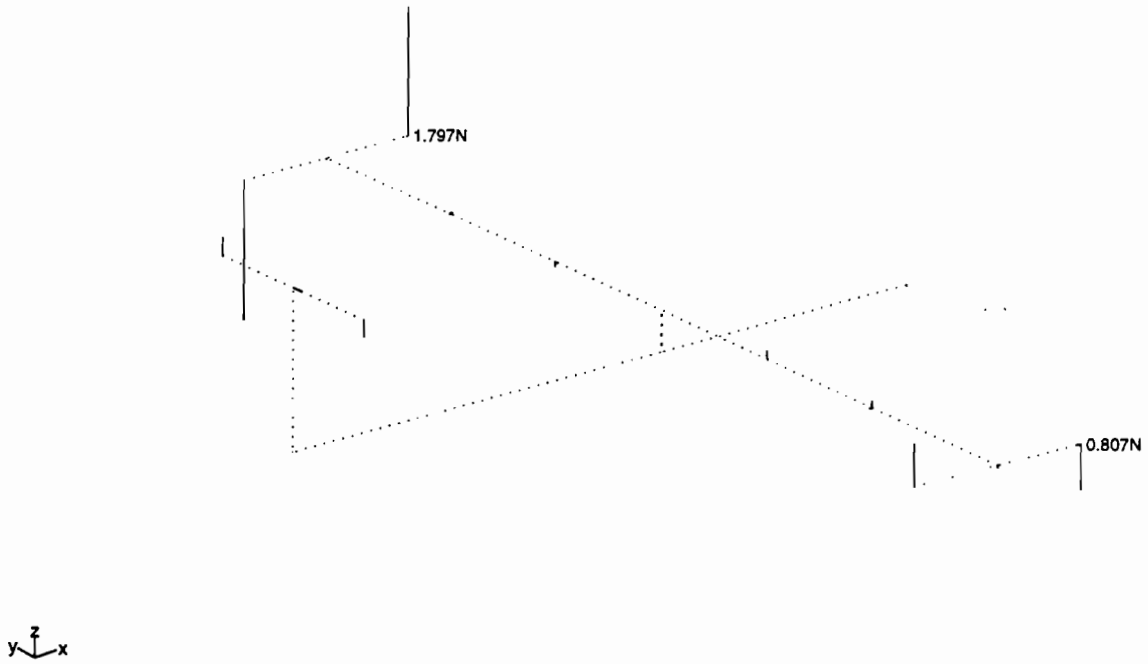

a) modeshape plot

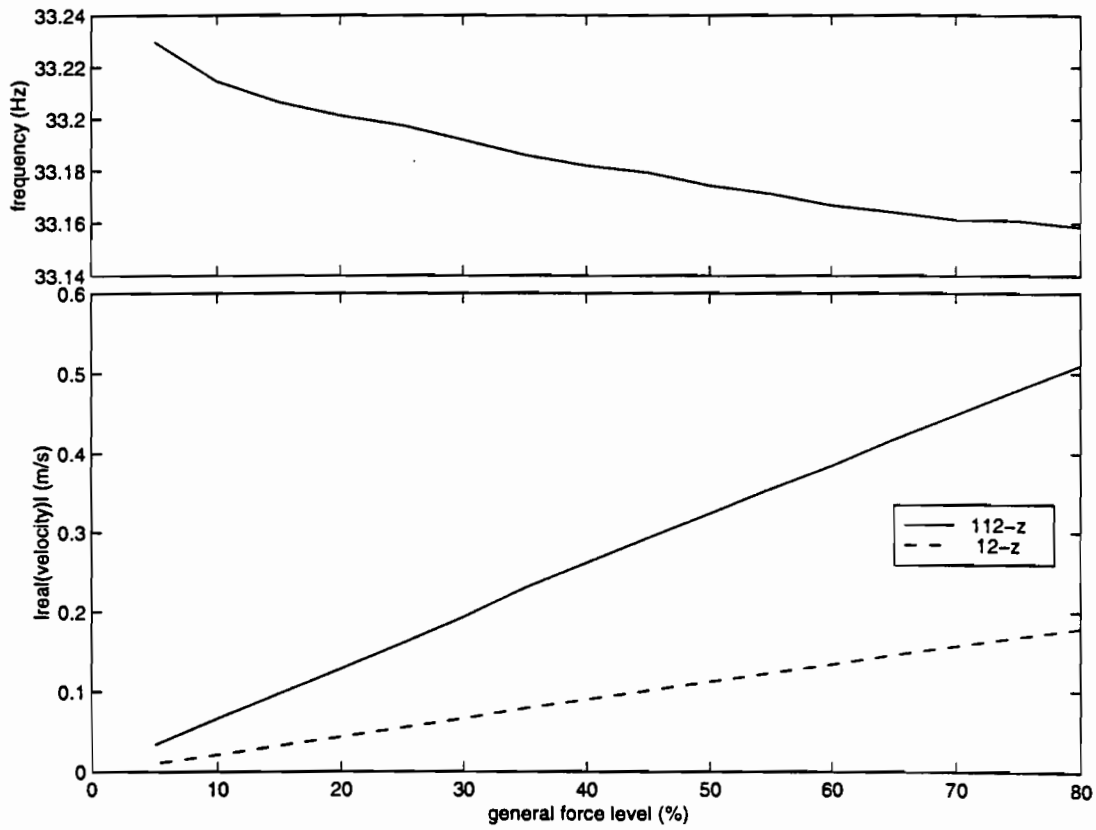

b) Impedance plot

Figure 21: Characterization of the 3rd mode by appropriation - first antisymetric wing torsion at 33,16Hz -

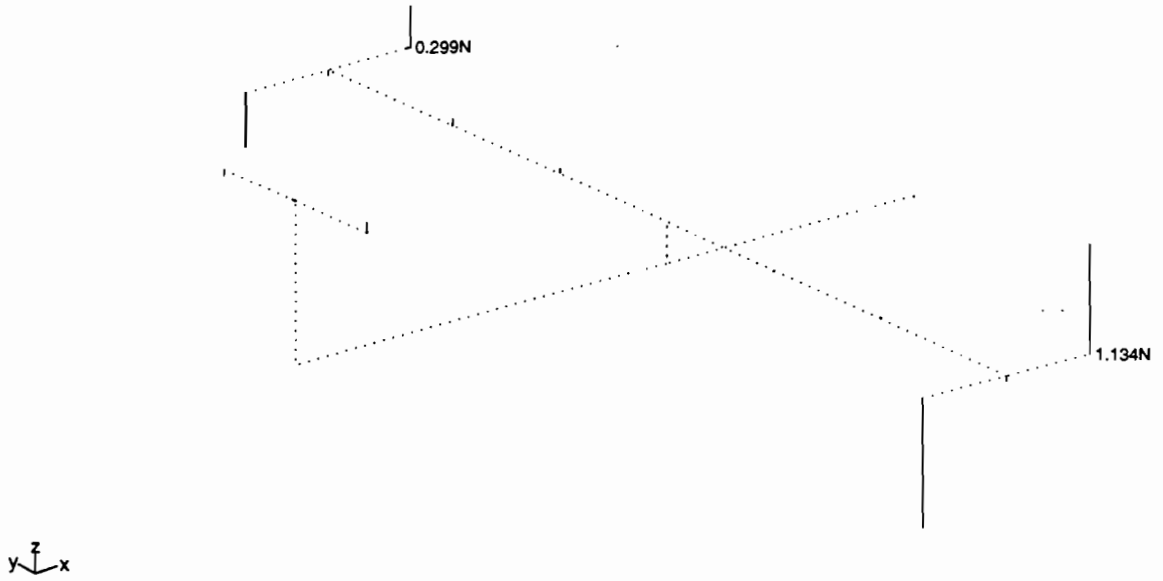

a) modeshape plot

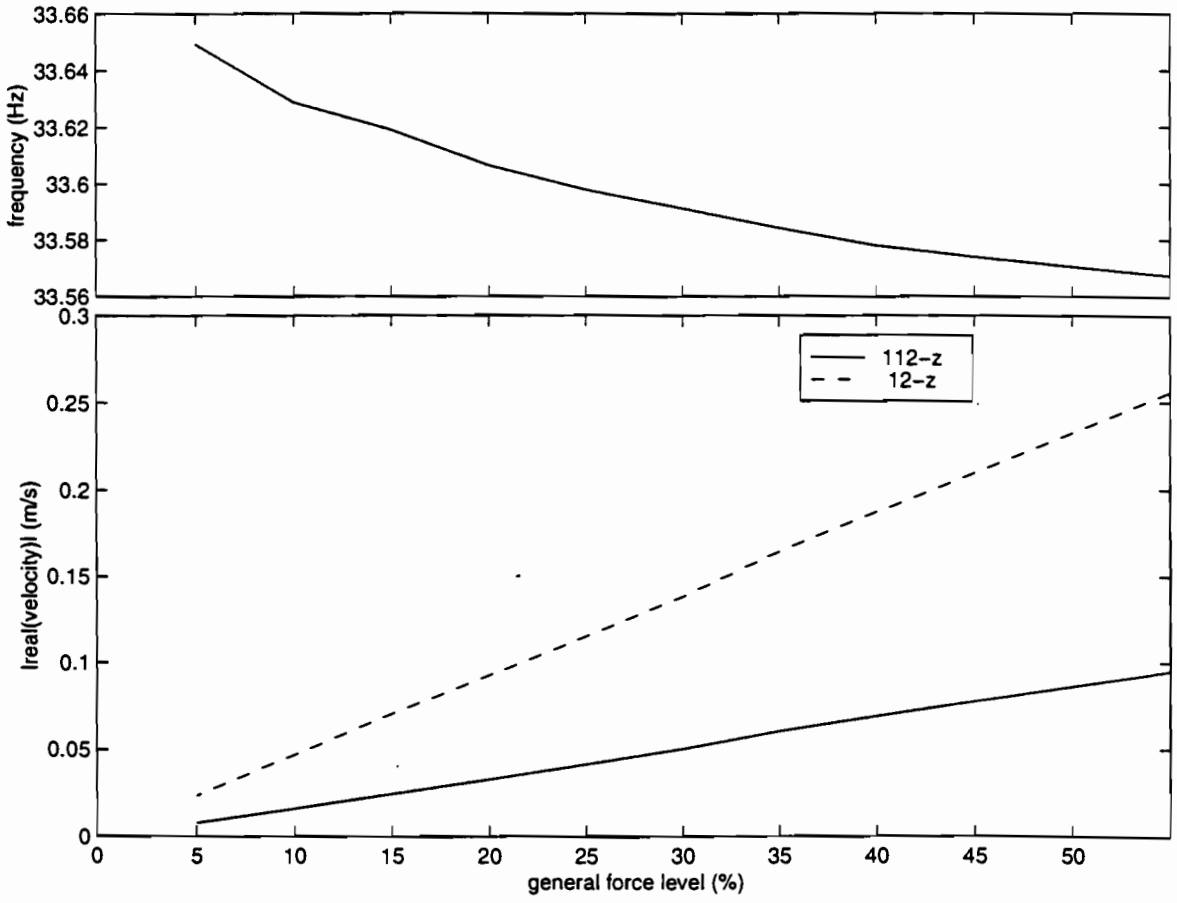

b) Impedance plot

Figure 22: Characterization of the 4th mode by appropriation

- first symetric wing torsion at 33,57Hz -

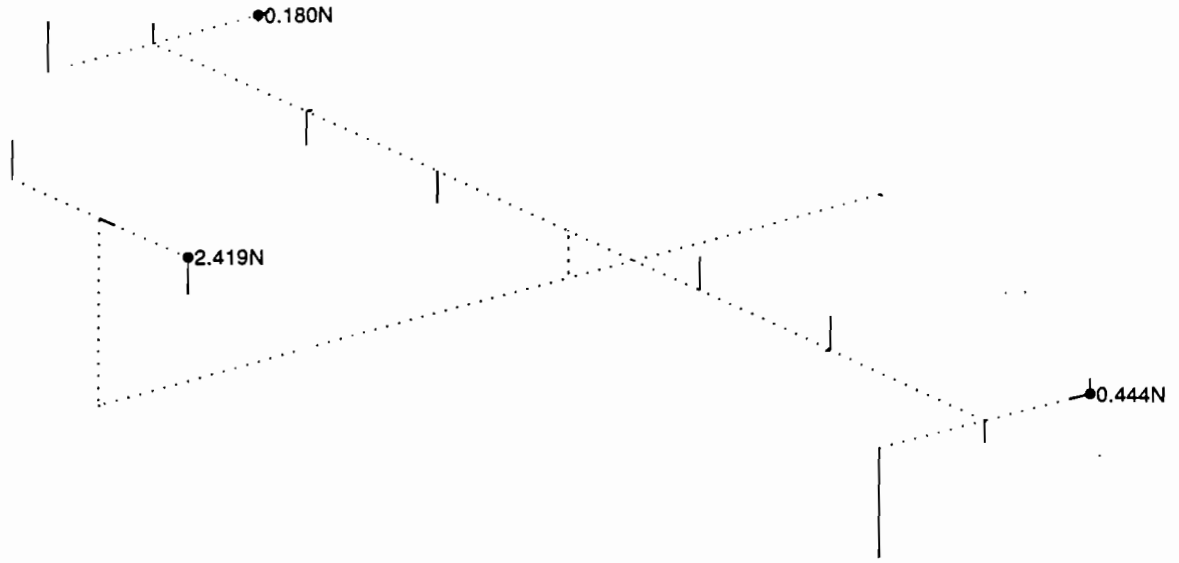

a) modeshape plot

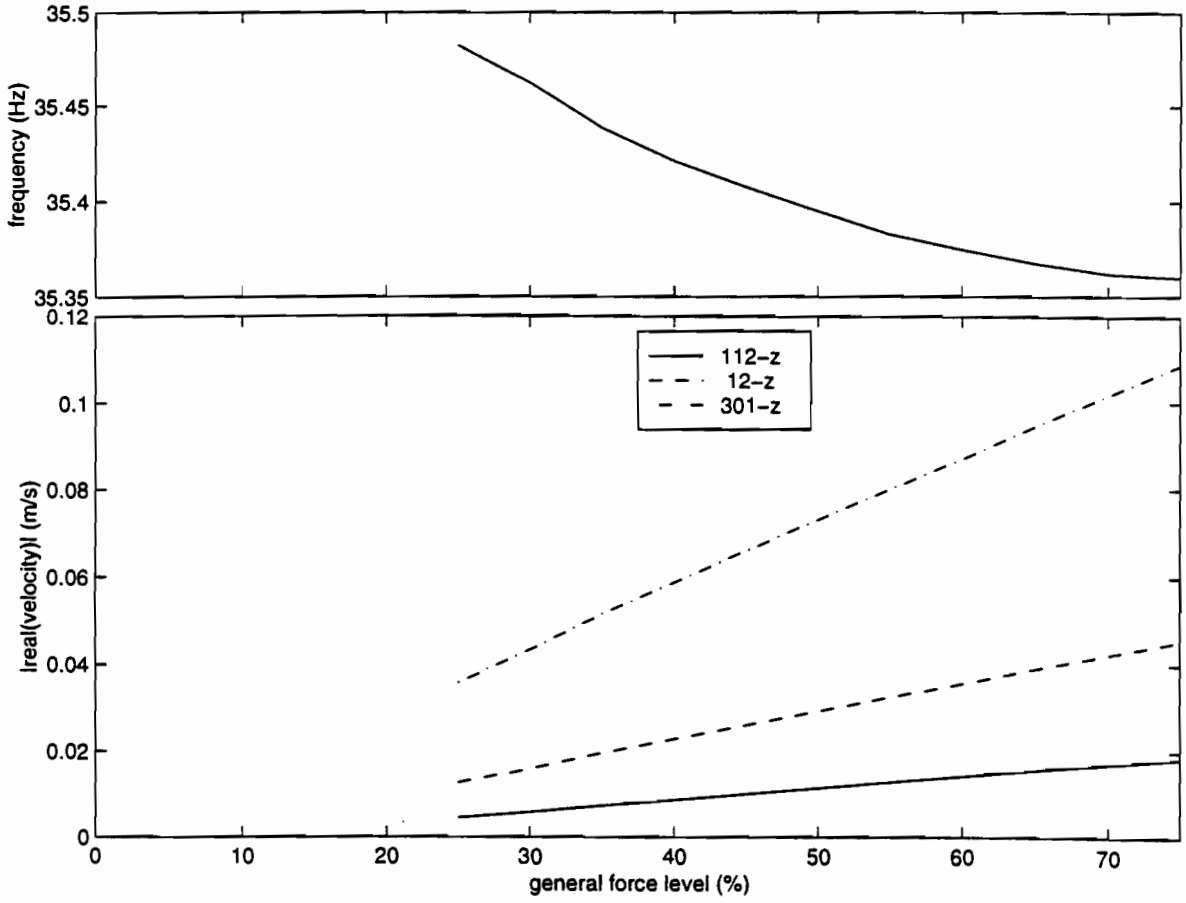

b) Impedance plot

Figure 23: Characterization of the 5th mode by appropriation

- 3 nodes wing bending at 35,36Hz -

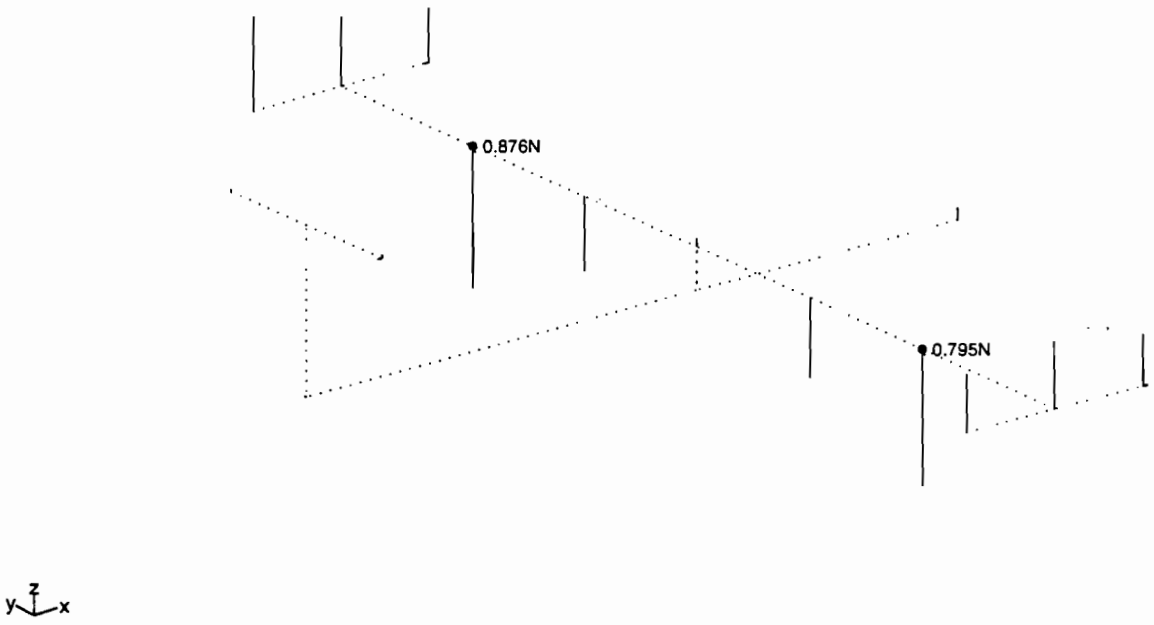

a) modeshape plot

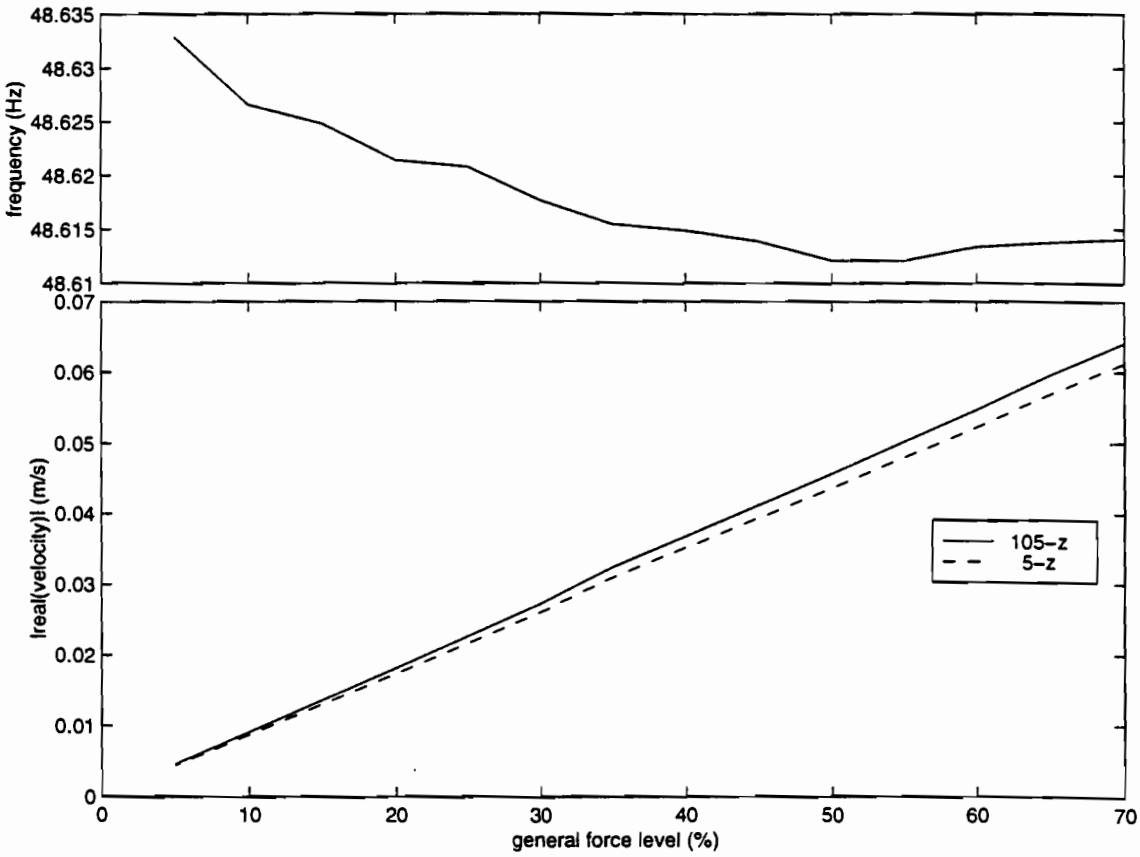

b) Impedance plot

Figure 24: Characterization of the 6th mode by appropriation

- 4 nodes wing bending at 48,62Hz -

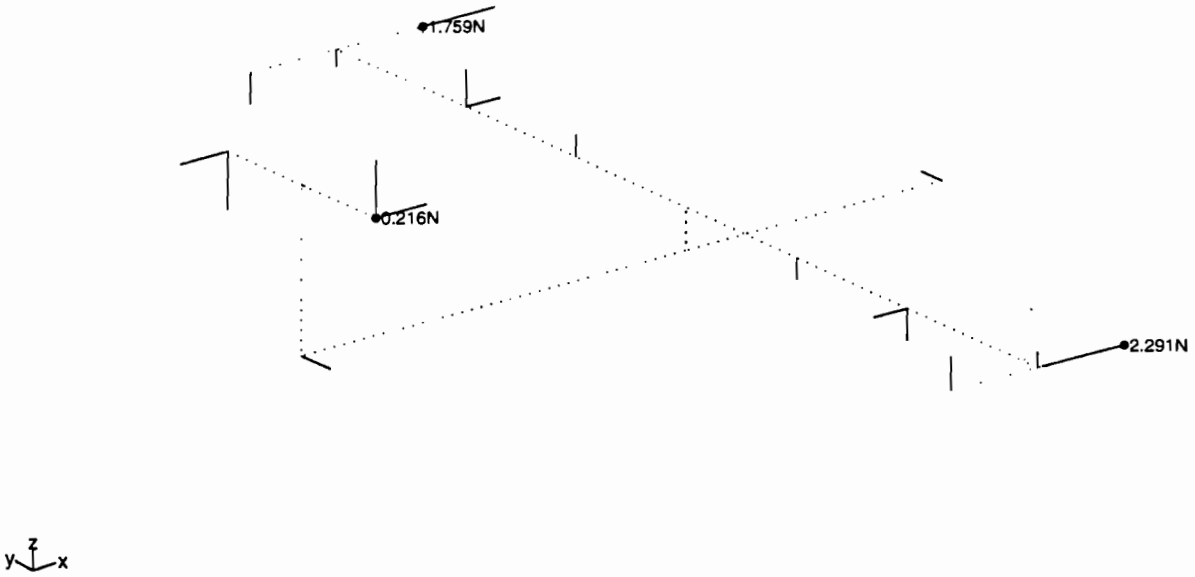

a) modeshape plot

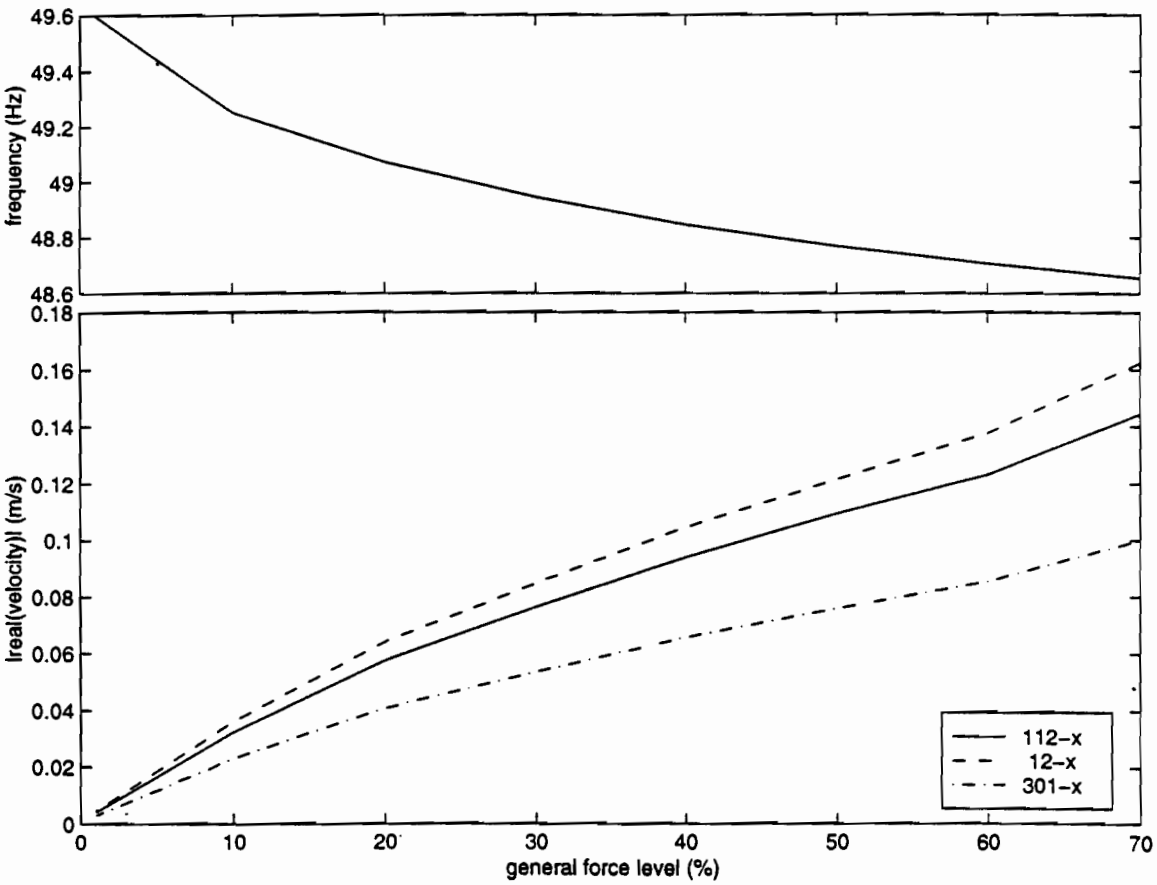

b) Impedance plot

Figure 25: Characterization of the 7th mode by appropriation

- wing yaw at 48,79Hz -

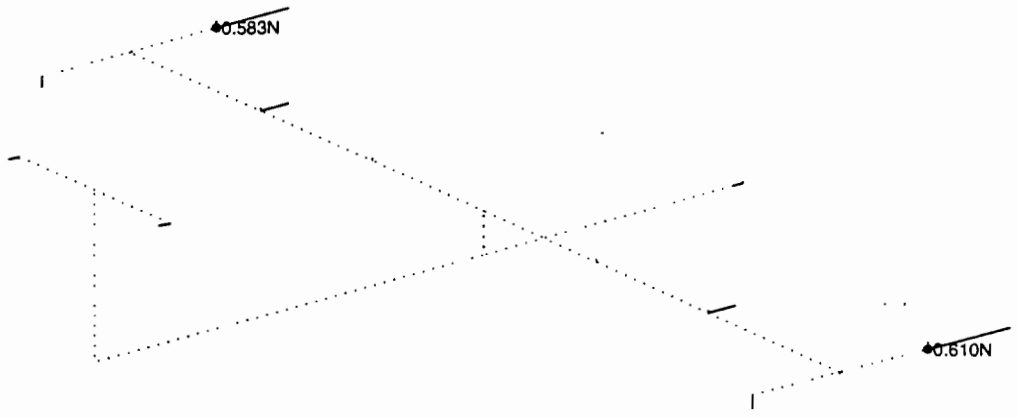

a) modeshape plot

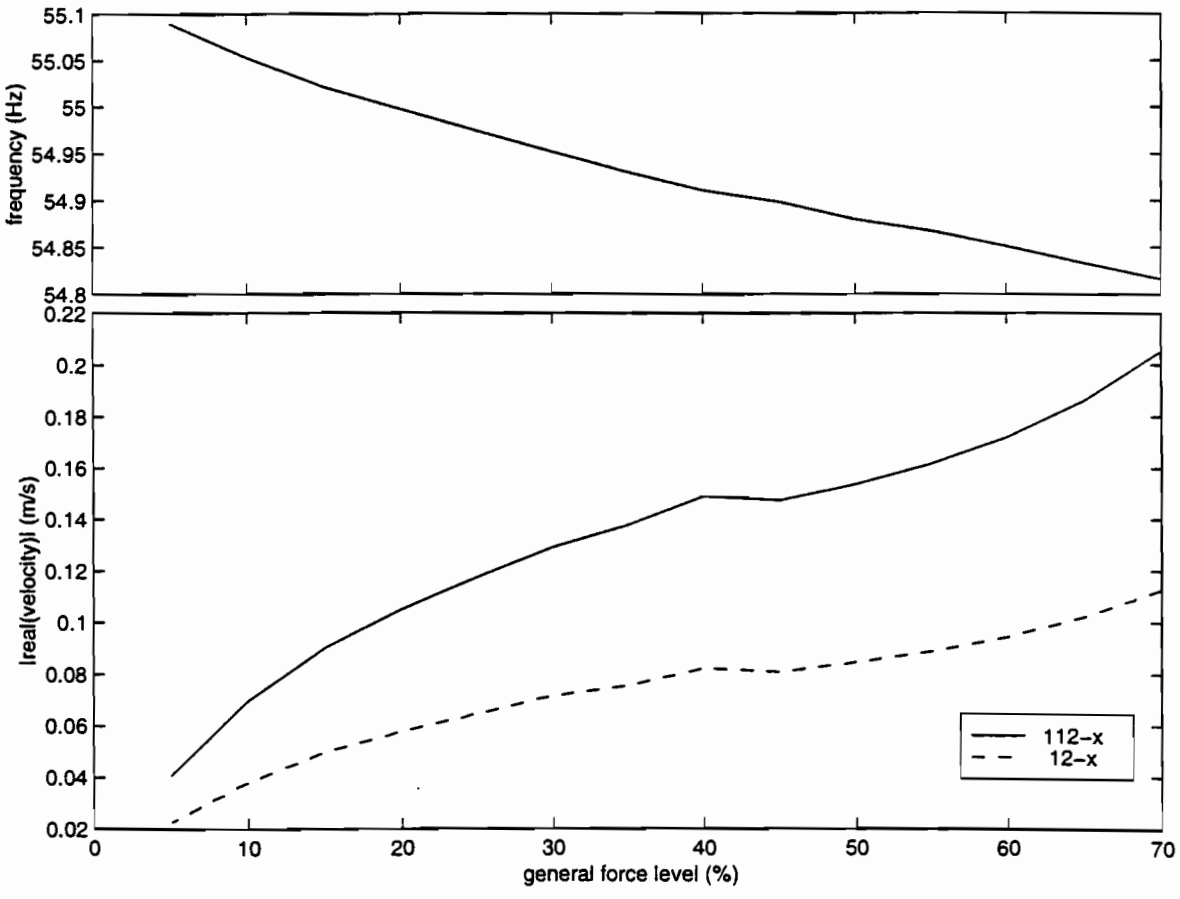

b) Impedance plot

Figure 26: Characterization of the 8th mode by appropriation

- 2 nodes fore & aft wing bending at 54,88Hz -

D.O.F. ID	NATURE	SOPEMEA set (Appropriation results)		ONERA set (Appropriation results)		
		Frequency (Hz)	Damping factor ζ	Frequency (Hz)	Damping factor ζ	M.A.C.
1	2n wing bending	6,97	1,270E-02	6,63	1,231E-02	0,994
2	fin bending	16,08	1,360E-02	16,25	1,181E-02	0,998
3	first antisymetric wing torsion	33,68	1,470E-02	33,16	1,059E-02	0,654
4	first symetric wing torsion	33,94	1,160E-02	33,57	1,283E-02	0,773
5	3n wing bending	34,92	1,110E-02	35,36	8,450E-03	0,973
6	4n wing bending	46,08	2,580E-02	48,62	2,115E-02	0,984
8	2n wing fore & aft bending	53,58	5,600E-03	54,88	2,300E-03	0,992
9	H.T.P. yaw	61,14	2,060E-02	63,82		

Figure 27: Comparison of the appropriation results measured by Onera with the reference set Sopemea

D.O.F. ID	NATURE	Appropriation result (Spera set)		G.C. method			I.D.R.C method		
		Frequency (Hz)	Damping factor ζ	Frequency (Hz)	Damping factor ζ	M.A.C. (appro. ref)	Frequency (Hz)	Damping factor ζ	M.A.C. (appro. ref)
1	2n wing bending	6,63	1,231E-02	6,65	1,269E-02	1,000	6,65	1,214E-02	1,000
2	fin bending	16,25	1,581E-02	16,40	1,330E-02	1,000	16,40	1,330E-02	1,000
3	first antisymétric wing bending	33,16	1,059E-02	33,19	9,770E-03	0,994	33,18	9,850E-03	0,994
4	first symetric wing torsion	33,57	1,283E-02	33,61	1,415E-02	0,997	33,71	1,486E-02	0,994
5	3n wing bending	35,36	8,450E-03	36,13	8,390E-03	0,965	36,13	9,180E-03 *(8,92E-03)**	0,573 *(0,963)**
6	4n wing bending	48,62	2,115E-02	49,32	2,139E-02	0,977	49,40	2,210E-02	0,979
7	wing yaw	48,79	6,370E-03	50,26	3,150E-03	0,974	50,31 *(50,25)**	2,710E-03 *(3,34E-03)**	0,596 *(0,941)**
8	2n wing fore & aft bending	54,88	2,300E-03	55,91	7,400E-04	0,999	55,91	8,300E-04	1,000
9	H.T.P. yaw	63,82		64,52	1,822E-02		64,49	1,790E-02	

(*) narrowband IDRC fit

Figure 28: Estimate of the first 9 modes using the measured sine set of FRF's by the G.C. and I.D.R.C. methods

D.O.F. ID	NATURE	Approximation result (MIMO) Frequency (Hz)	Damping factor ζ	G.C. method Frequency (Hz)	Damping factor ζ	M.A.C. (appro. ref)	I.D.R.C method Frequency (Hz)	Damping factor ζ	M.A.C. (appro. ref)
1	2n wing bending	6,63	1,13E-02	6,68	1,246E-02	0,999	6,68	1,247E-02	0,999
2	fin bending	16,25	1,181E-02	16,21	1,234E-02	1,000	16,20	1,252E-02	0,999
3	first antisymetric wing bending	33,16	1,050E-02	32,70	1,120E-02	0,989	32,71	1,139E-02	0,995
4	first symetric wing torsion	33,57	1,245E-02	33,09	1,342E-02	0,958	33,19	1,464E-02	0,985
5	3a wing bending	35,66	7,450E-03	35,66	7,730E-03	0,974	35,72	8,830E-03	0,954
6	4a wing bending	48,62	2,115E-02	49,37	1,751E-02	0,940	49,27	1,553E-02	0,967
7	wing yaw	48,79	6,370E-03	50,26			50,23 *(49,90)**	2,500E-04 *(6,00E-03)**	0,384 *(0,998)**
8	2n wing fore & aft bending	55,68	2,300E-03	55,72	1,240E-03	0,999	55,72	1,210E-03	0,998
9	H.T.P. yaw	64,63	1,502E-02	64,17	1,502E-02		64,33	1,815E-02	

(*) narrowband IDRC fit

figure 29: Estimate of the first 9 modes using the MIMO set of FRF's by the G.C. and I.D.R.C. methods

Annex 9

AEROSPATIALE CONTRIBUTION

AEROSPATIALE
AERONAUTIQUE

Etablissement de Toulouse

316, route de Bayonne
31060 Toulouse Cedex 03 France
Tél : 16 61 93 55 55
Telex : AISPA 531 546 F

ONERA OR

BP 72
92322 CHATILLON CEDEX

A l'Attention de Mr Alain GRAVELLE

TOULOUSE, le 8 août 1996
MP/DL/NF N° 450.0182/96

OBJET : GARTEUR SM-AG19

Please find attached the "RESULTS OF MODAL ANALYSIS AND FRF MEASUREMENTS PERFORMED ON GARTEUR SM-AG19 TESTBED".

Best regards.

M. PEVROL

1) Goal of the test

The aim of this test is to compare the test means and methods (hardware & software) of many laboratories in Europe by performing ground vibration test on the same testbed and to compare results. Test program is joined as annex at the end of this document.

2)Description of testbed and AEROSPATIALE test means

The pictures here after show the test installation and acurate views of shaker positions on the testbed.

To perform this test, three different methods of modal analysis were used by AEROSPATIALE :
- modal phase resonance (or appropriation) method with harmonic sine excitation,
- global curve fitting method applied to FRF[1] measured with a random shaker excitation,
- global curve fitting method applied to FRF measured with an impulse excitation.

To have an easier way of work, the locations of accelerometers are named differently than in test program. The accelerometers numbers correspondance is indicated in following array :

Test program	Global method	Phase resonance method
1Z	1Z	143
5Z	2Z	144
5X	2X	163
8Z	3Z	145
206Z	4Z	146
108Z	5Z	147
105Z	6Z	148
105X	6X	164
101Z	7Z	149
112Z	8Z	150
112X	8X	161
111Z	9Z	151
11Z	11Z	153
12Z	10Z	152
12X	10X	162
201X	12X	160
201Y	12Y	159
201Z	12Z	154
301Z	13Z	155
301X	13X	165
303Z	14Z	156
303X	14X	166
302Y	15Y	157
205Y	16Y	158

Position of accelerometers is given on page 2.

[1]FRF : Frequency Response Function

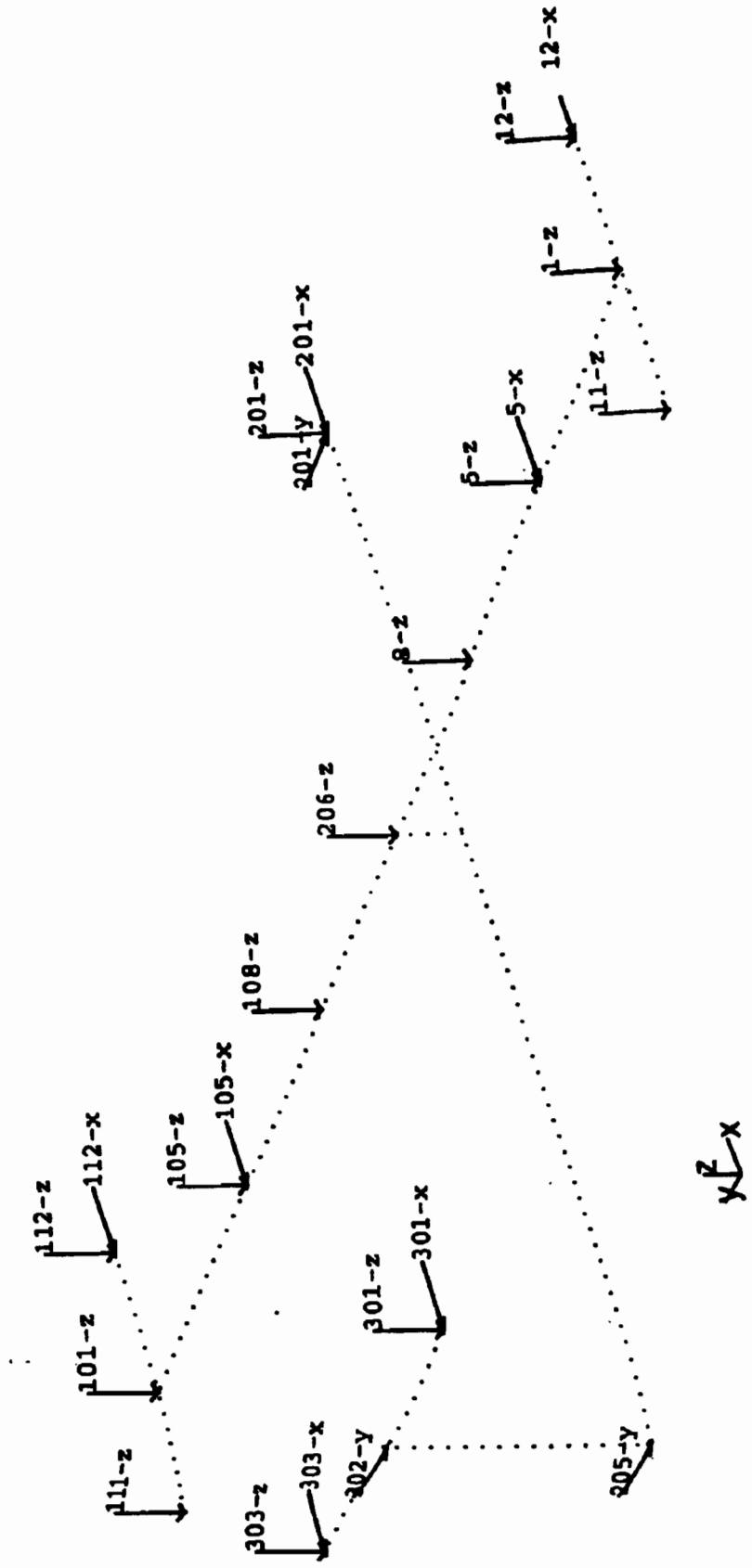

Position of accelerometers on testbed

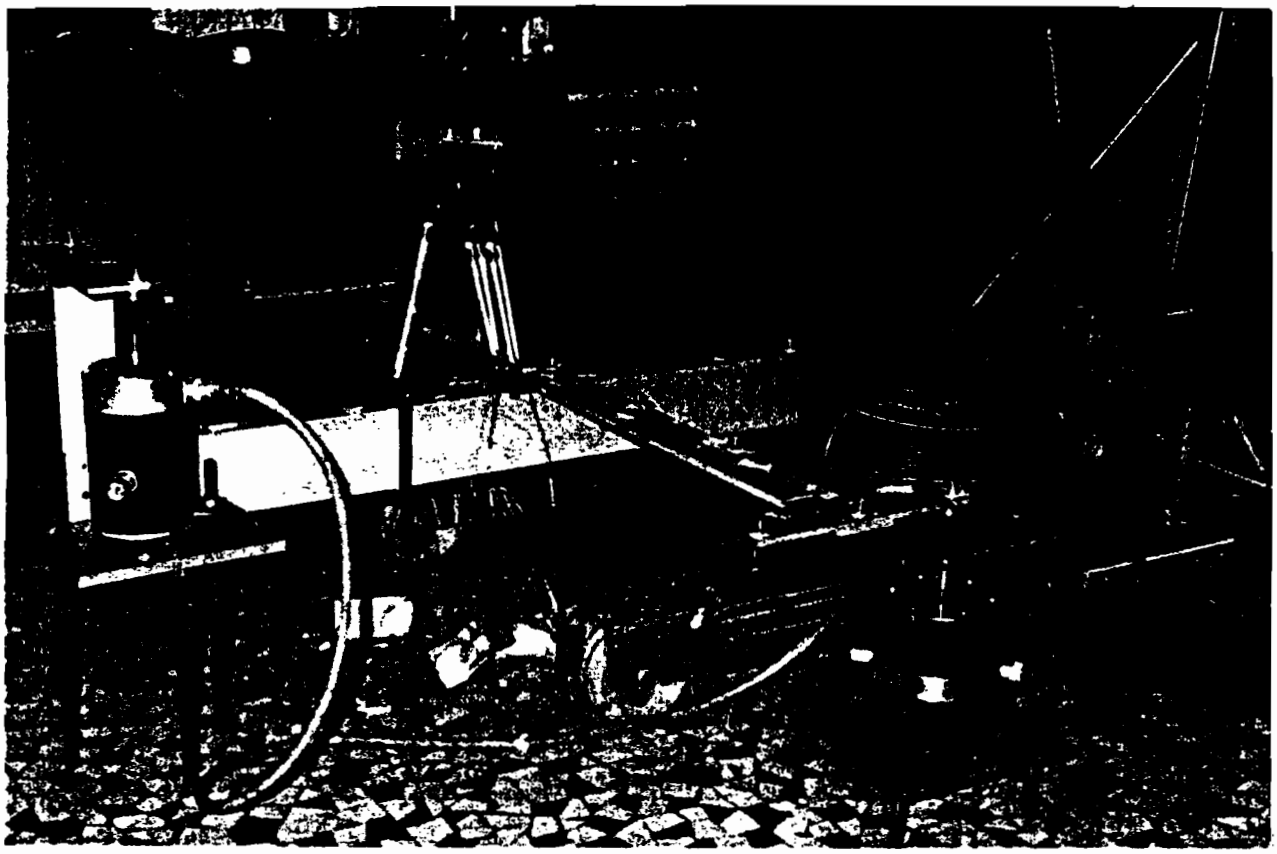

Figure 1 : View of test installation

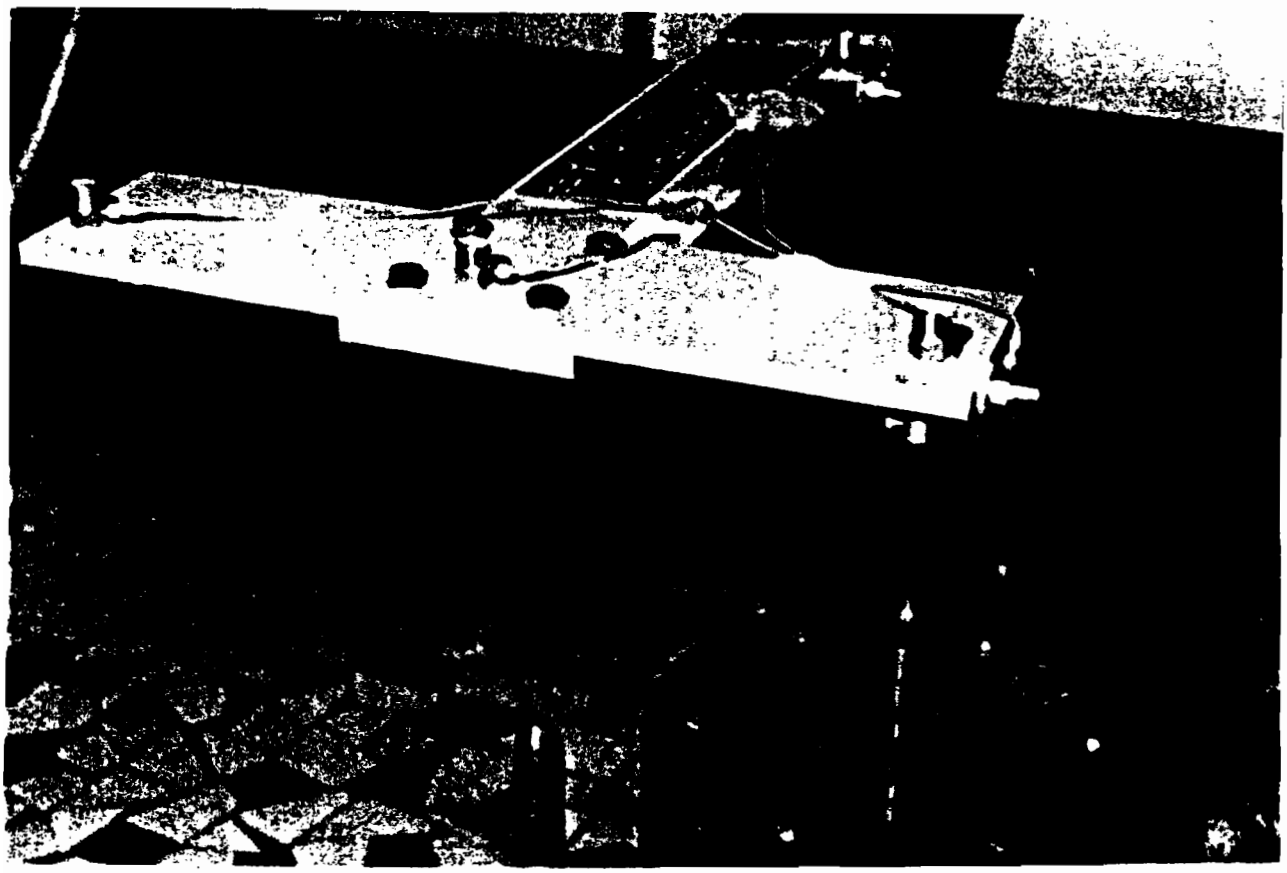

Figure 2 : detailed view of shaker (phase resonance configuration)

3)Description of test methods

3.1) Harmonic sine phase resonance method

- Frequency sweep acquisition
- Isolation and appropriation of each mode
- Measurement of modal parameters with complex power method and quadrature force method

Accelerometers TYPE : DJB A120 / VL2 Weight : 14 g

Exciters : at point 12Z and 112Z : PRODERA 20 JE 20 C , Weight of moving part : 190 g

Stiffness of moving part : 1000 N/m

Computer : Concurent Computer Corporation 7500 fitted with 256 acquisition channels and 8 excitation channels.

Software : Specific software written by SYMINEX based on AEROSPATIALE specification.

3.2) Global curve fitting method, shaker excitation

- FRFs acquisition, no correlation between the two exciters (2 different random noise generators)
- Global curve fitting of FRFs with Multiple Input, Multiple Output (MIMO) method
- Calculation of eigen frequency, damping and mode shapes.

Accelerometers TYPE : DJB A120 / VL2 Weight : 14 g

Exciters : at point 12Z and 112Z : PRODERA 20 JE 20 C , Weight of moving part : 190 g

Stiffness of moving part : 1000 N/m

Computer : PC 486 DX compatible coupled with TEKTRONIX 2630 spectrum analyser for FRF acquisition.

Software : SMS GENRAD STAR MODAL Version 5.1

3.3) Global curve fitting method, impulse excitation

- FRFs acquisition
- Curve fitting of FRFs with Single Degree Of Freedom (SDOF) method (polynomial or global least square, depending of mode coupling)
- Calculation of eigen frequency, damping and mode shapes
- Global curve fitting of FRFs with Single Input, Multiple Output (SIMO) method
- Calculation of eigen frequency, damping and mode shapes.

Accelerometers TYPE : DJB A120 / VL2 Weight : 14 g

Exciter : Impulse Hammer type PCB 086C03

Computer : PC 486 DX compatible coupled with TEKTRONIX 2630 spectrum analyser for FRF acquisition.

Software : SMS GENRAD STAR MODAL Version 5.1

4) Nominal Transfer functions

4.1) Sine swept excitation signal

The reference signal (force introduced in the structure) is given by measuring the current in the moving coil of the exciter and the response signal is the acceleration at the considered point (12Z or 112Z). Acquisition is done step by step in the bandwidth from 4 to 65 Hz by 29.8 e^{-3} Hz (2048 points).

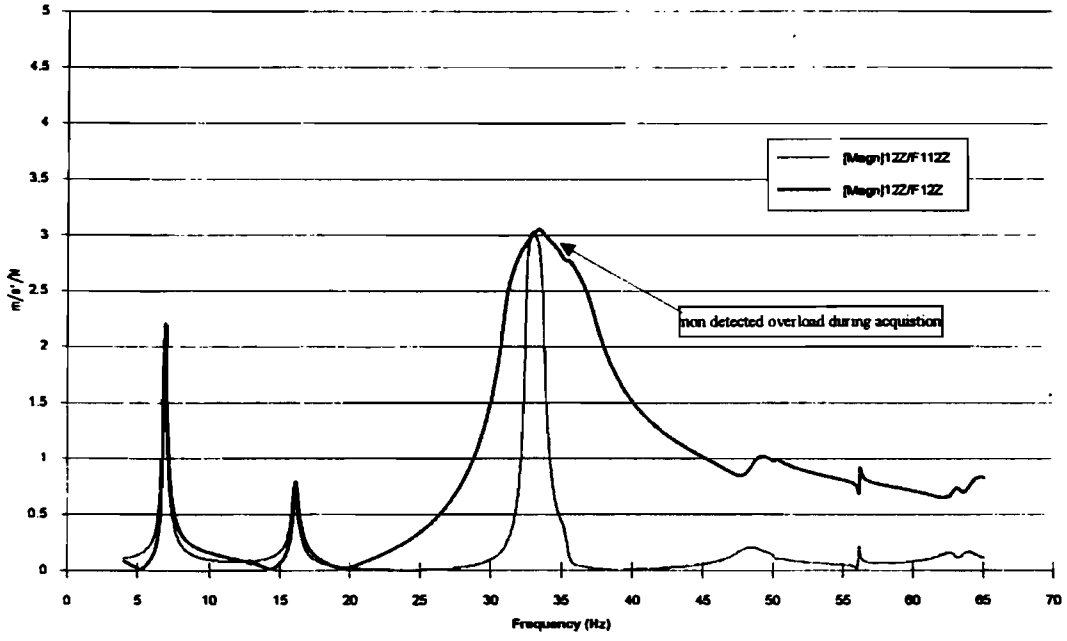

Figure 3 . Magnitude of transfer functions 12Z/F112Z and 12Z/F12Z

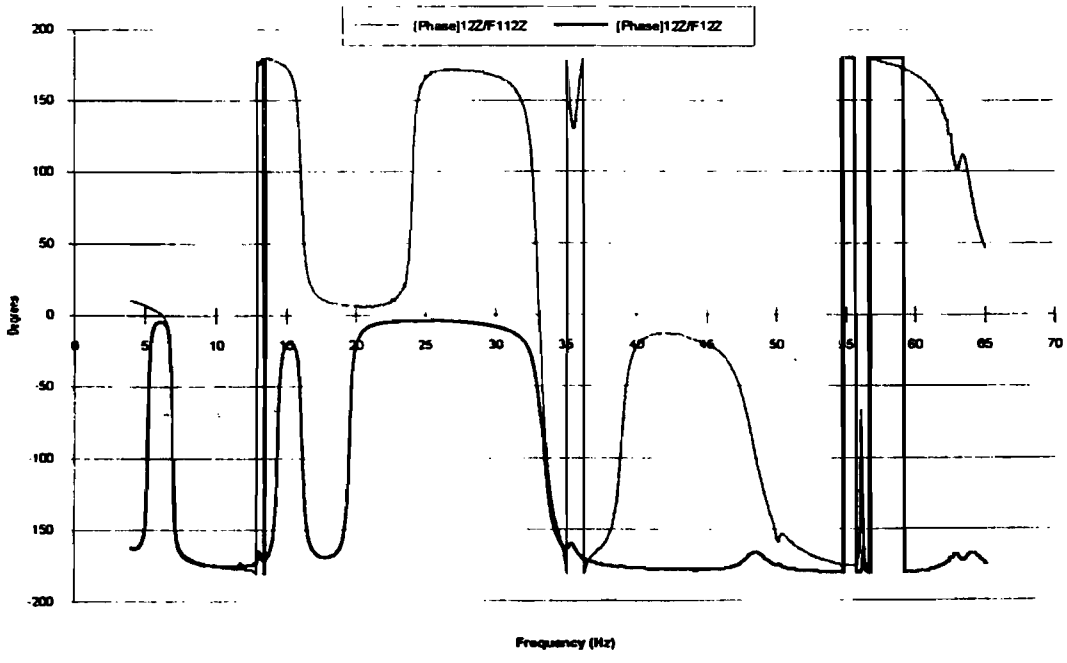

Figure 4 : Phase of transfer functions 12Z/F112Z and 12Z/F12Z

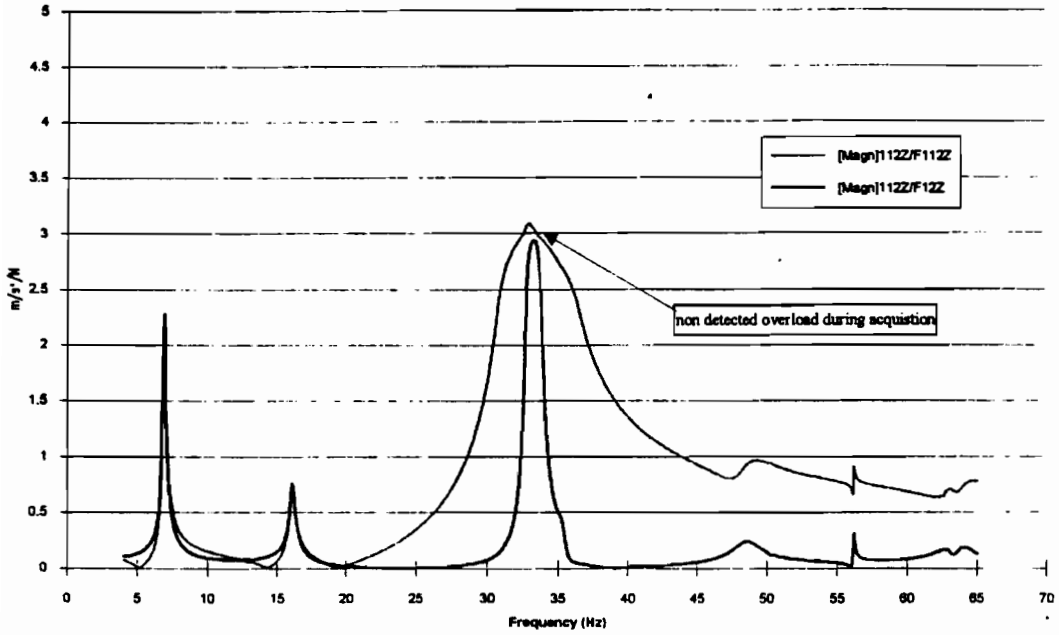

Figure 5 : Magnitude of transfer functions 112Z/F112Z and 112Z/F12Z

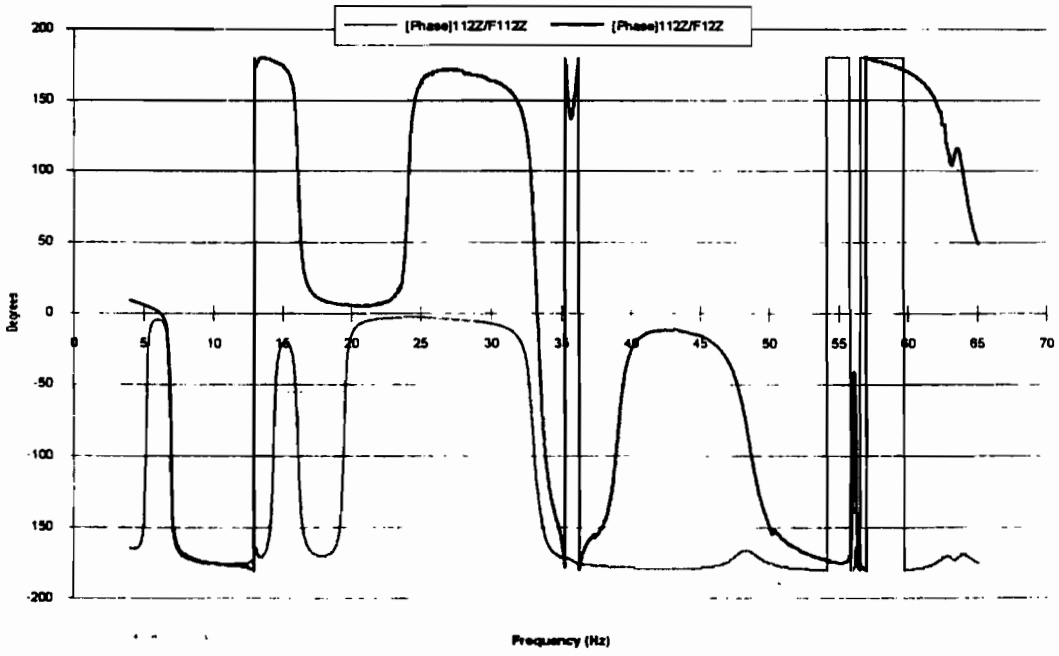

Figure 6 : Phase of transfer functions 112Z/F112Z and 112Z/F12Z

3.1) Random noise excitation signal

The reference signal (force introduced in the structure) is given by a force cell placed between the exciter and the structure, the response signal is the acceleration at the considered point (12Z or 112Z). The transfer functions presented here are the result of FFT[2] averaging of the global signal analysed in the bandwidth from 4 to 65 Hz by 29.8 e^{-3} Hz (2048 points).

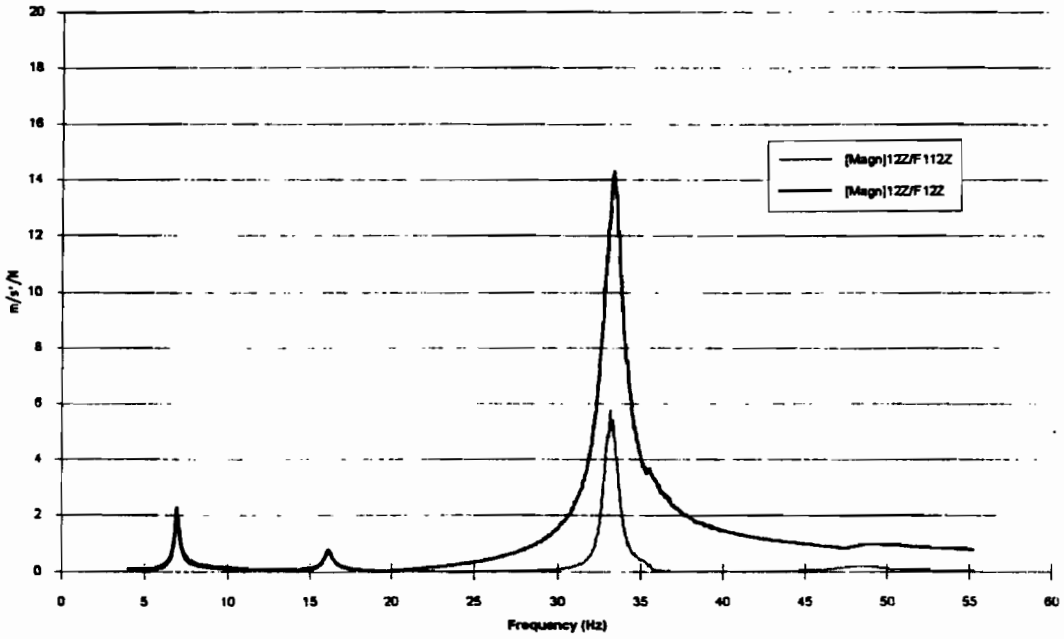

Figure 7 . Magnitude of transfer functions 12Z/F112Z and 12Z/F12Z

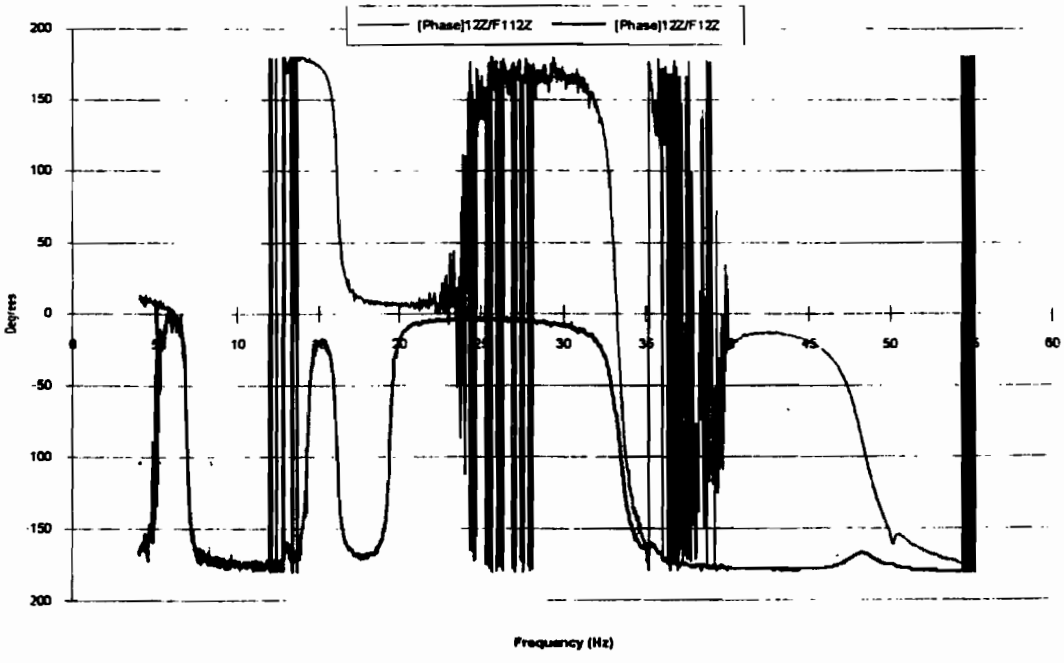

Figure 8 : Phase of transfer functions 12Z/F112Z and 12Z/F12Z

[2]FFT : Fast Fourier Transform

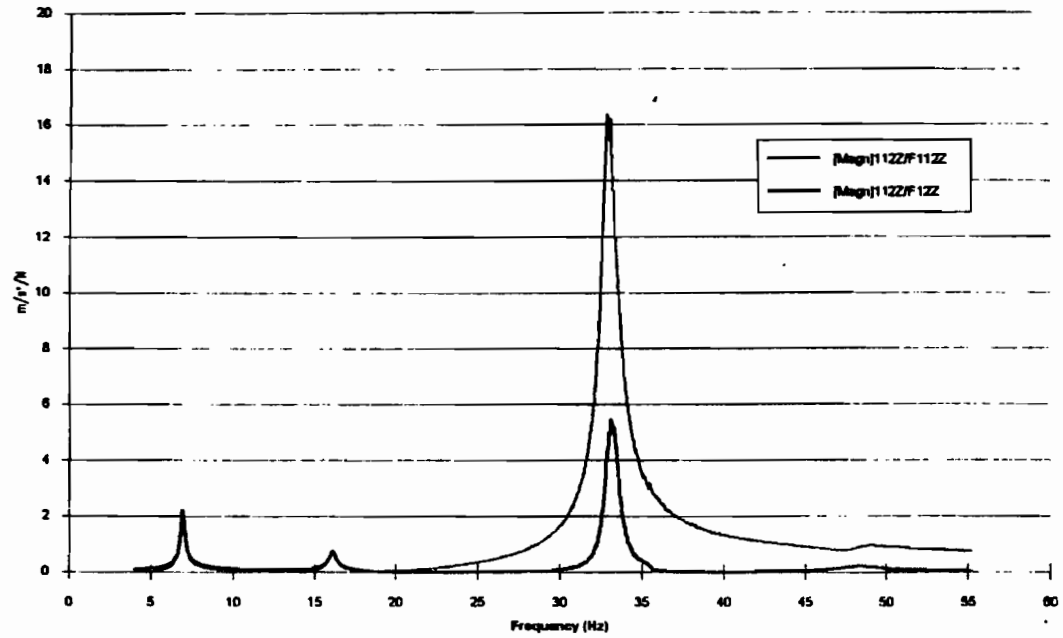

Figure 9 : Magnitude of transfer functions 112Z/F112Z and 112Z/F12Z

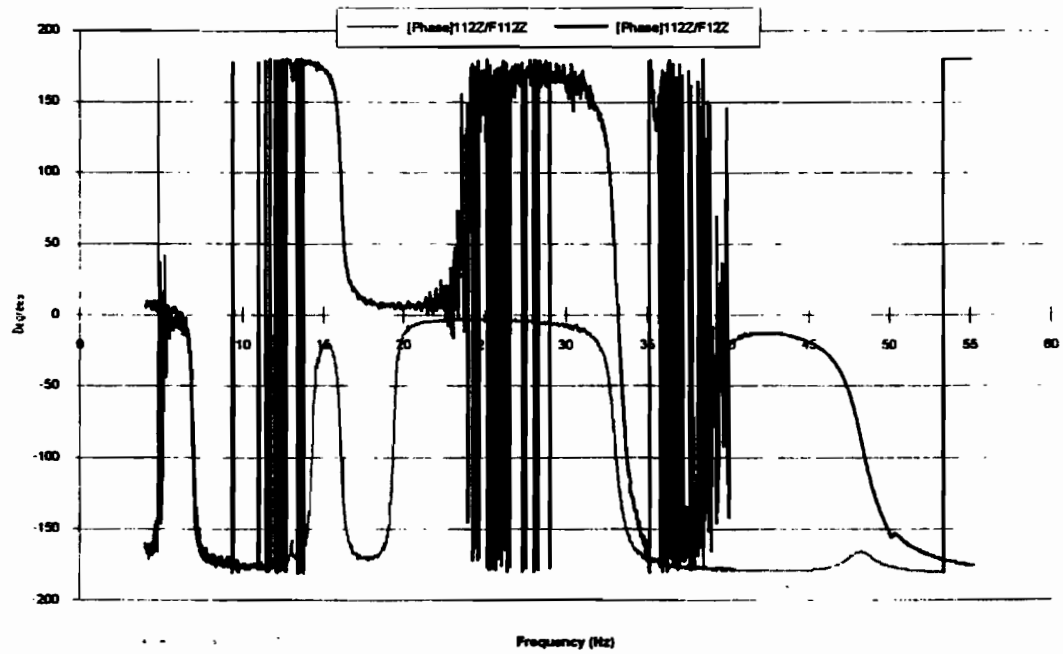

Figure 10 : Phase of transfer functions 112Z/F112Z and 112Z/F12Z

The comparison of the FRFs acquired with the two methods shows that results are close together in term of frequency and amplitude for the two first peaks (6 & 16 Hz). For the third frequency (34 Hz), gap in amplitude is due to overload problem of input amplifier not detected during acquisition.

A more noisy signal is acquired in cross FRF with random excitation due to a loss of coherence during acquisition.

5) Modes results

Frequencies and structural damping of measured modes by the three method are given below. Generalized mass were only obtained with the phase resonance method.

Sinusoidal excitation
Phase resonance method

Mode n°	Frequency (Hz)	Damping (%)		Gen. mass (m^2Kg)	
		PC[3]	FQ[4]	PC	FQ
1 S[5]	2.628	###[6]	###	###	###
2 A[7]	2.675	###	###	###	###
3 S	6.949	1.65	1.18	3.84	4.47
4 A	15.996	1.39	1.34	12.1	12.5
5 A	32.867	1.06	0.96	0.69	0.76
6 S	33.375	1.65	1.27	0.65	0.8
7 A	34.726	1.03	0.80	15.6	20.2
8 S	48.07	2.38	2.12	9.14	10.3
9 A	49.276	0.54	0.53	92	94.1
10	###	###	###	###	###
11 A	62.443	2.08	1.56	18.6	26.2
12 A	63.888	0.74	###	38.1	###

Random noise excitation
MDOF extraction method

Mode n°	Frequency (Hz)	Damping (%)
1 S	###	###
2 A	2.01	29.24
3 S	6.92	1.15
4 A	16.09	1.29
5 A	32.96	1.01
6 S	33.48	1.19
7 A	35.33	1.1
8 S	48.41	2.37
9 A	50.07	1.14
10	56.17	0.19977
11 A	63.15	0.3352
12 A	63.34	1.03

Hammer excitation
SDOF extraction method

Mode n°	Frequency (Hz)	Damping (%)
1 S	3.01	6.94
2 A	###	###
3 S	6.4	2.23
4 A	16.01	1.74
5 A	31.92	1.3
6 S	34.66	1.89
7 A	35.13	1.08
8 S	48.49	2.52
9 A	49.28	0.50577
10	54.43	0.2847
11 A	62.9	1.72
12 A	63.29	0.92621

Hammer excitation
MDOF extraction method

Mode n°	Frequency (Hz)	Damping (%)
1 S	3.02	8.01
2 A	###	###
3 S	6.39	2.36
4 A	15.98	1.79
5 A	31.84	1.49
6 S	32.33	7.83
7 A	35.12	1.13
8 S	48.47	2.51
9 A	49.25	5.55E-01
10	54.42	2.97E-01
11 A	63.01	1.47
12 A	64.74	10.61

Modes n° 1 & 2 are rigid modes of the testbed on its suspension.

---

[3] PC : Complex Power method
[4] FQ : Force Quadrature method
[5] S : Symmetrical mode
[6] ### : Data not measured in this configuration
[7] A : Antisymmetrical mode

5.1) Comments on obtained results

-Sinusoidal excitation, Phase resonance method
The two values for damping are obtained with complex power method for the first one and quadrature force method for the other one.

Modes n° 1 & 2 : rigid symetric and antisymetrical modes, calculation of modal parameters was not performed

Mode n° 10 : this mode was not acquired because the shakers were not in the good position to isolate this mode

Mode n° 12 : only complex power method was applied to calculate modal parameters

- Random noise excitation MDOF extraction method

Mode n° 1 : not enough definition at this frequency to extract correctly this mode (too high coupling with mode n°2)

- Hammer excitation SDOF & MDOF extraction methods

Mode n° 2 : same problem as explained above for random excitation.

5.2) Methods comparison

Following tables compare the frequencies and damping of structural modes for three other cases versus phase resonance method results.

	Phase Resonance	Random MDOF	Hammer SDOF	Hammer MDOF
Mode n°	Freq. (Hz)	Delta	Delta	Delta
3	6.949	-0.42%	-7.90%	-8.04%
4	15.996	0.59%	0.09%	-0.10%
5	32.867	0.28%	-2.88%	-3.12%
6	33.375	0.31%	3.85%	-3.13%
7	34.726	1.74%	1.16%	1.13%
8	48.07	0.71%	0.87%	0.83%
9	49.276	1.61%	0.01%	-0.05%
10	###	###	###	###
11	62.443	1.13%	0.73%	0.91%
12	63.888	-0.86%	-0.94%	1.33%

	Phase Resonance	Random MDOF	Hammer SDOF	Hammer MDOF
Mode n°	Damping (%)	Delta	Delta	Delta
3	1.18	-2.54%	88.98%	100.00%
4	1.34	-3.73%	29.85%	33.58%
5	0.96	5.21%	35.42%	55.21%
6	1.27	-6.30%	48.82%	516.54%
7	0.8	37.50%	35.00%	41.25%
8	2.12	11.79%	18.87%	18.40%
9	0.53	115.09%	-4.57%	4.72%
10	###	###	###	###
11	1.56	-78.51%	10.26%	-5.77%
12	###	###	###	###

We notice close results between phase resonance method and random noise excitation MDOF method.More discrepancies for mode n°3 frequency and mainly for damping values of all modes are obtained with the 2 methods using hammer excitation.

These results were expected due to the lack of energy introduced in structure by hammer impact.

To complete this test, no particular problems were encountered to measure the modes of the testbed with the phase resonance method. But, for the modes n° 5, 6 & 7, which frequencies are close together, the results of the phase resonance test which was performed before the phase separation test were very helpfull to extract these three modes and so improve the comparison.

6) Modes shapes

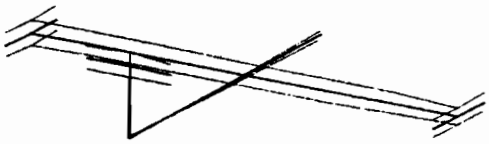

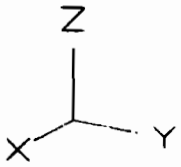

Sine phase resonance
Frequency : 2.628 Hz
Damping : ### / ### %
generalised mass : ### / ### m²Kg

(Mode not measured)
Random MDOF
Frequency : ### Hz
Damping : ### %

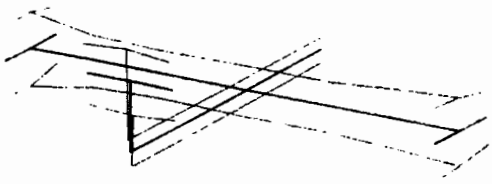

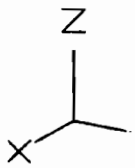

Hammer SDOF
Frequency : 3.01 Hz
Damping : 6.94 %

Hammer MDOF
Frequency : 3.02 Hz
Damping : 8.01 %

Mode n°1 (rigid mode)

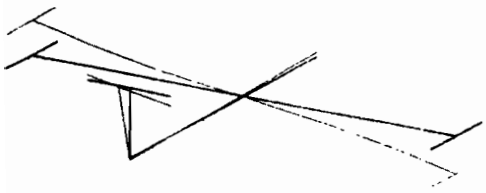

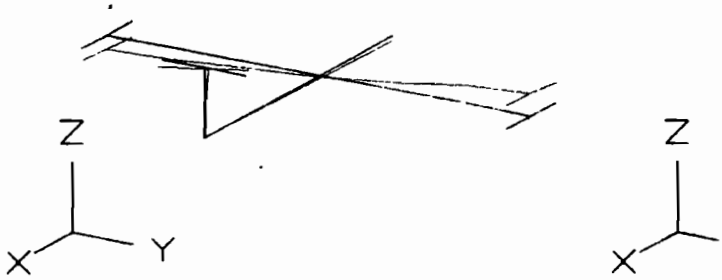

Sine phase resonance
Frequency : 2.675 Hz
Damping : ### / ### %
generalised mass : ### / ### m²Kg

Random MDOF
Frequency : 2.01 Hz
Damping : 29.24 %

Mode n°2 (rigid mode)

Sine phase resonance
Frequency : 6.949 Hz
Damping : 1.65 / 1.18 %
generalised mass : 3.84 / 4.47 m²Kg

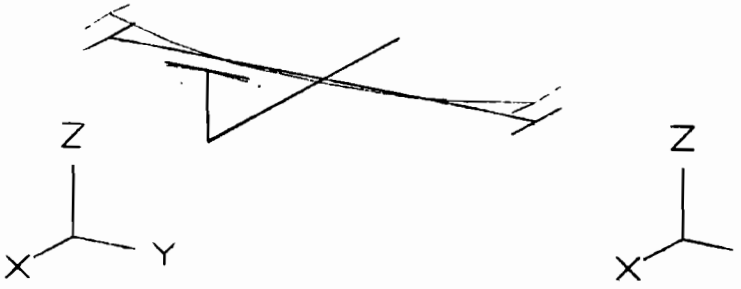

Random MDOF
Frequency : 6.92 Hz
Damping : 1.15 %

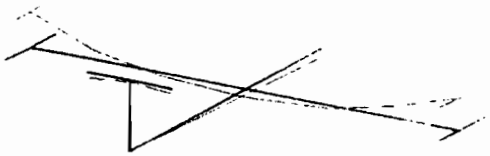

Hammer SDOF
Frequency : 6.4 Hz
Damping : 2.23 %

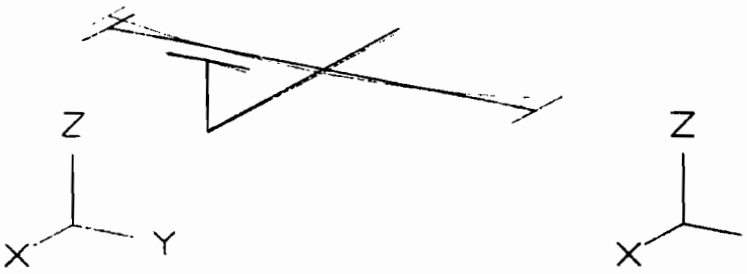

Hammer MDOF
Frequency : 6.39 Hz
Damping : 2.36 %

Mode n°3

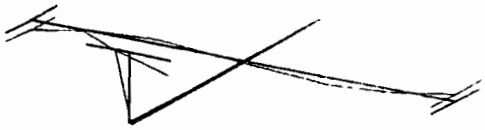

Sine phase resonance
Frequency : 15.996 Hz
Damping : 1.39 / 1.34 %
generalised mass : 12.1 / 12.5 m²Kg

Random MDOF
Frequency : 16.09 Hz
Damping : 1.29 %

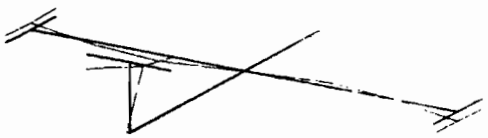

Hammer SDOF
Frequency : 16.01 Hz
Damping : 1.74 %

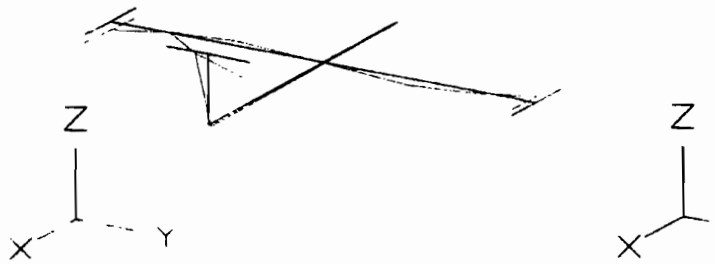

Hammer MDOF
Frequency . 15.98 Hz
Damping : 1.79 %

Mode n°4

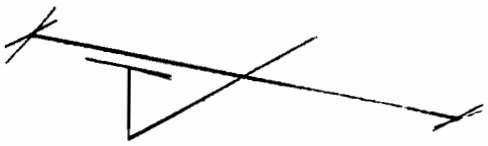

Sine phase resonance
Frequency : 32.867 Hz
Damping : 1.06 / 0.96 %
generalised mass : 0.698 / 0.766 m²Kg

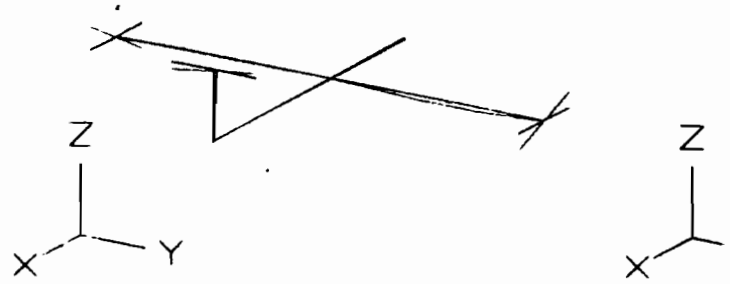

Random MDOF
Frequency : 32.96 Hz
Damping : 1.01 %

Hammer SDOF
Frequency : 31.92 Hz
Damping 1.3 %

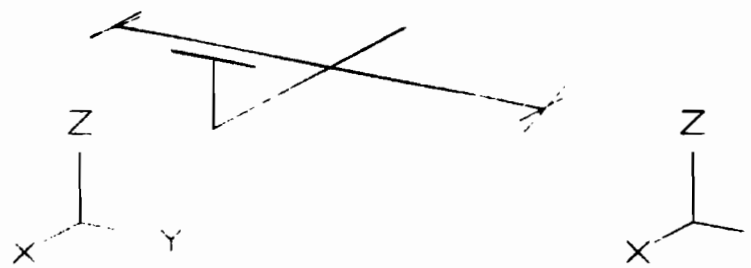

Hammer MDOF
Frequency : 31.84 Hz
Damping : 1.49 %

Mode n°5

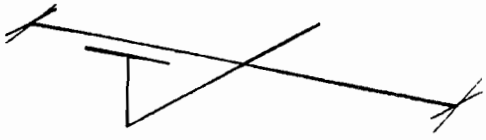

Sine phase resonance
Frequency : 33.375 Hz
Damping : 1.65 / 1.27 %
generalised mass : 0.652 / 0.8 m²Kg

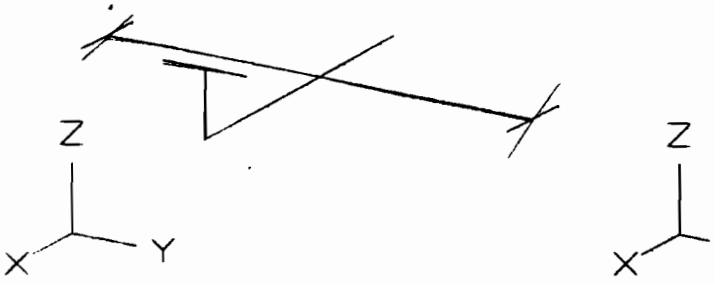

Random MDOF
Frequency : 33.48 Hz
Damping : 1.19 %

Hammer SDOF
Frequency : 34.66 Hz
Damping : 1.89 %

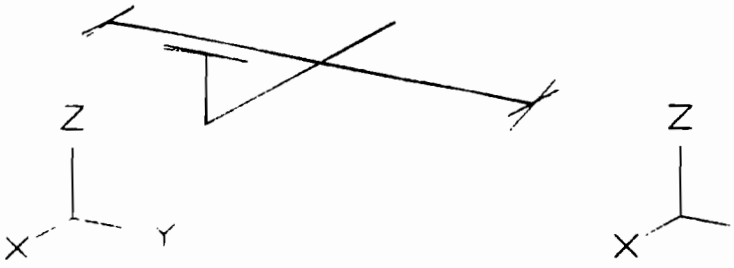

Hammer MDOF
Frequency : 32.33 Hz
Damping : 7.83 %

Mode n°6

Sine phase resonance
Frequency : 34.726 Hz
Damping : 1.03 / 0.80 %
generalised mass : 15.6 / 20.2 m²Kg

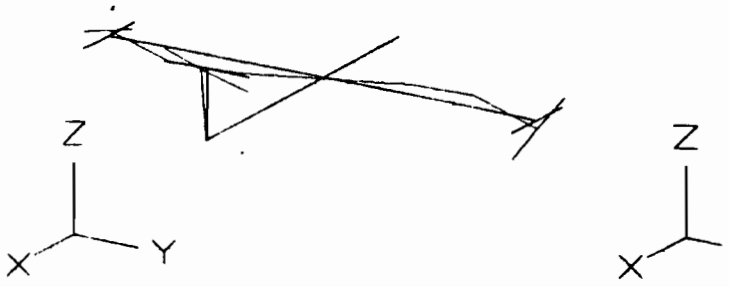

Random MDOF
Frequency : 35.33 Hz
Damping : 1 10 %

Hammer SDOF
Frequency : 35.13 Hz
Damping : 1.08 %

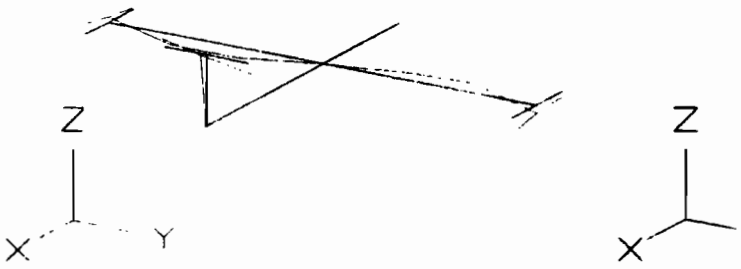

Hammer MDOF
Frequency : 35.12 Hz
Damping : 1.13 %

Mode n°7

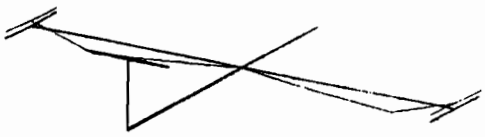

Sine phase resonance
Frequency : 48.07 Hz
Damping : 2.38 / 2.12 %
generalised mass : 9.14 / 10.3 m²Kg

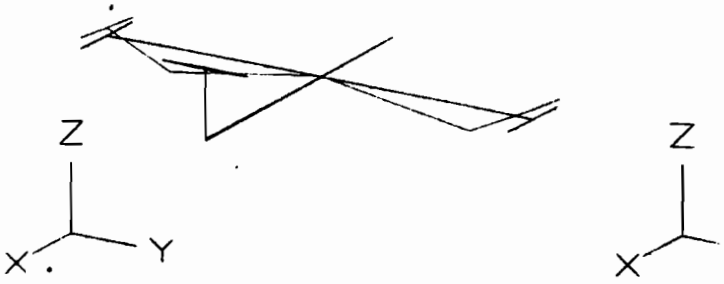

Random MDOF
Frequency : 48.41 Hz
Damping : 2.37 %

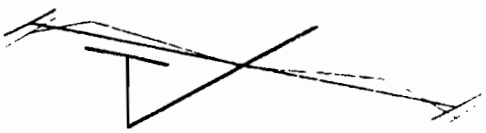

Hammer SDOF
Frequency : 48.49 Hz
Damping : 2.52 %

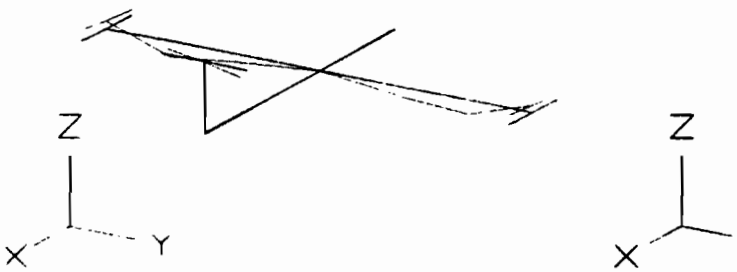

Hammer MDOF
Frequency : 48.47 Hz
Damping : 2.51 %

Mode n°8

Sine phase resonance
Frequency : 49.276 Hz
Damping : 0.54 / 0.53 %
generalised mass : 92 / 94.1 m²Kg

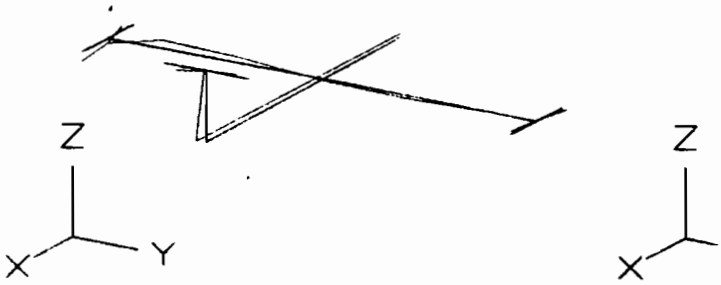

Random MDOF
Frequency : 50.07 Hz
Damping : 1.14 %

Hammer SDOF
Frequency : 49.28 Hz
Damping : 0.50 %

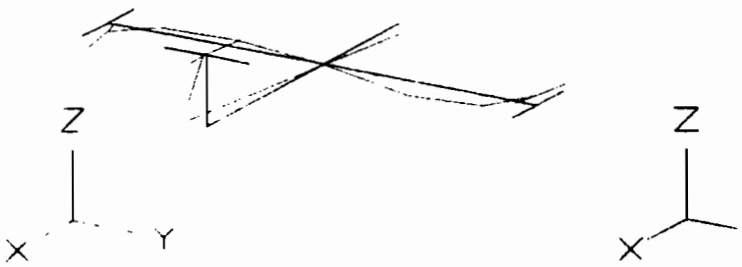

Hammer MDOF
Frequency : 49.25 Hz
Damping : 0.55 %

Mode n°9

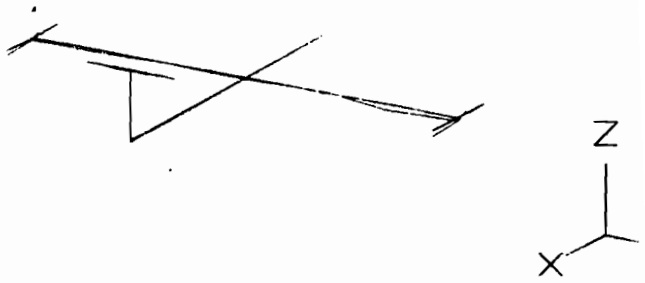

Sine phase resonance
Frequency : ### Hz
Damping : ### / ### %
generalised mass : ### / ### m²Kg

Random MDOF
Frequency : 56.17 Hz
Damping : 0.20 %

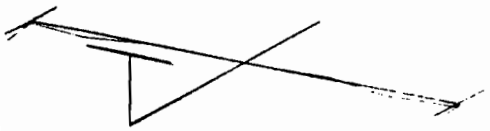

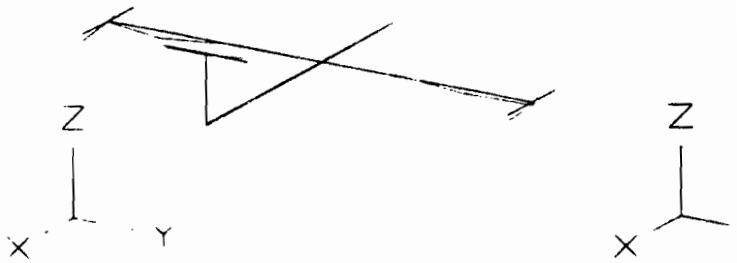

Hammer SDOF
Frequency : 54.43 Hz
Damping : 0.28 %

Hammer MDOF
Frequency : 54.42 Hz
Damping : 0.29 %

Mode n°10

Sine phase resonance
Frequency : 62.443 Hz
Damping : 2.08 / 1.56 %
generalised mass : 18.6 / 26.2 m²Kg

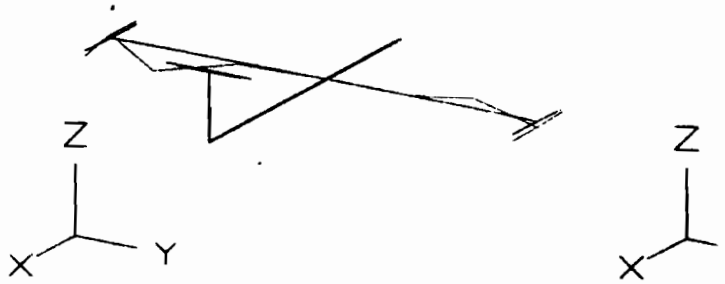

Random MDOF
Frequency : 63.15 Hz
Damping : 0.33 %

Hammer SDOF
Frequency : 62.9 Hz
Damping . 1.72 %

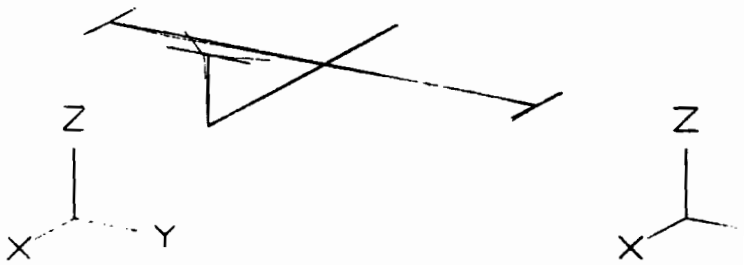

Hammer MDOF
Frequency : 63.01 Hz
Damping : 1.47 %

Mode n°11

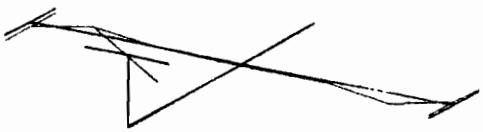

Sine phase resonance
Frequency : 63.888 Hz
Damping : 0.74 / ### %
generalised mass : 38.1 / ### m²Kg

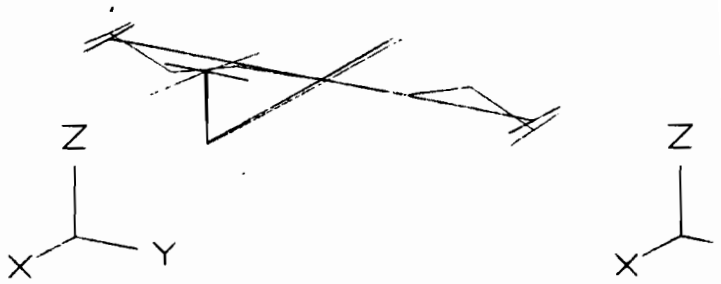

Random MDOF
Frequency : 63.34 Hz
Damping : 1.03 %

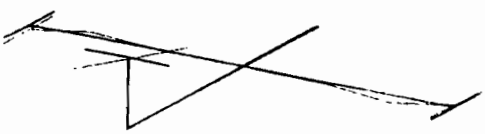

Hammer SDOF
Frequency : 63.29 Hz
Damping : 0.92 %

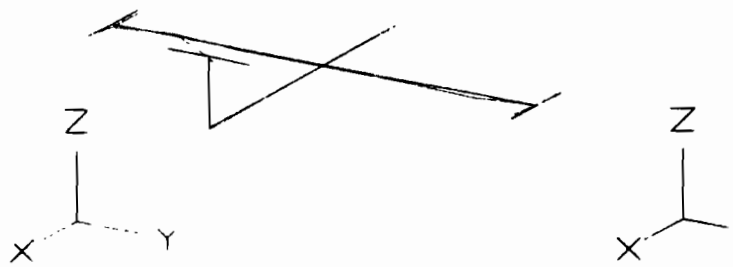

Hammer MDOF
Frequency : 64.74 Hz
Damping : 10.61 %

Mode n°12

7) conclusion

AEROSPATIALE tested three different methods with two types of excitation (shaker and hammer excitations) on this GARTEUR SM-AG 19 testbed.

Analysis of these measurements showed close results in term of frequency and damping between phase resonance method and random excitation MDOF curve fitting method. Nevertheless with hammer excitation, discrepancies in results are noticed due to the lack of energy introduced in the structure by hammer impact.

Up to now, for modal measurements on a complete aircraft structure, we have more confidence in phase resonance method than in other ones to obtain good quality in mode shapes and modal characteristics measurements.

Comparisons with other European companies and laboratories results could modify this point of view and allow us to evaluate the efficiency and the reliability of the different phase separation methods.

This will be helpfull in the future to improve AEROSPATIALE vibration test system and the way to proceed a ground vibration test on aircraft.

Annex 10

SAAB CONTRIBUTION

GVT on GARTEUR SM-AG 19 testbed.

1 Introduction

Ground vibration test (GVT) are used in the certification procedure for aircraft. The tests plays an important role in updating the FE-models. The GARTEUR group decided to compare different modal testing methods used by the different participants throughout Europe. A testbed was made by ONERA and was designed to obtain three close modes. The testbed circulated to each participant during 1995 and 1996. The test request is described in Appendix A.

2 Experimental set-up

A test was made in February 1996 with Saab Military Aircraft GVT system. The system uses a HP 745 I workstation supported by LMS Cada-X software and a 132 channel Difa SCADAS front-end. Ling Dynamic Systems LDS V101/2 shakers were used for excitation and the stinger was a special made rigging screw as shown in figure 3. For excitation in the vertical direction, the shakers were placed directly on different metal cubs as shown in figure 4. For excitation in the horizontal plane, a thin rubber pad was placed between the shaker and the metal cub. The exciter signals were amplified using LDS PA25E power amplifier.

2.1 Testbed

The testbed was a two piece structure (wing and fuselage/tail) with the pieces fixed to each other with four bolts. Figure 1 below shows a sketch of the testbed.

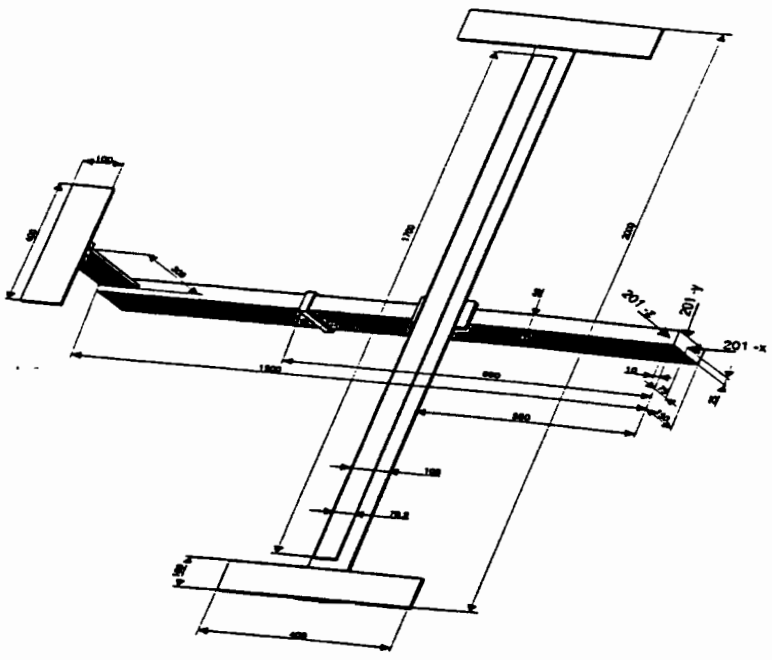

Figure 1 Sketch of testbed

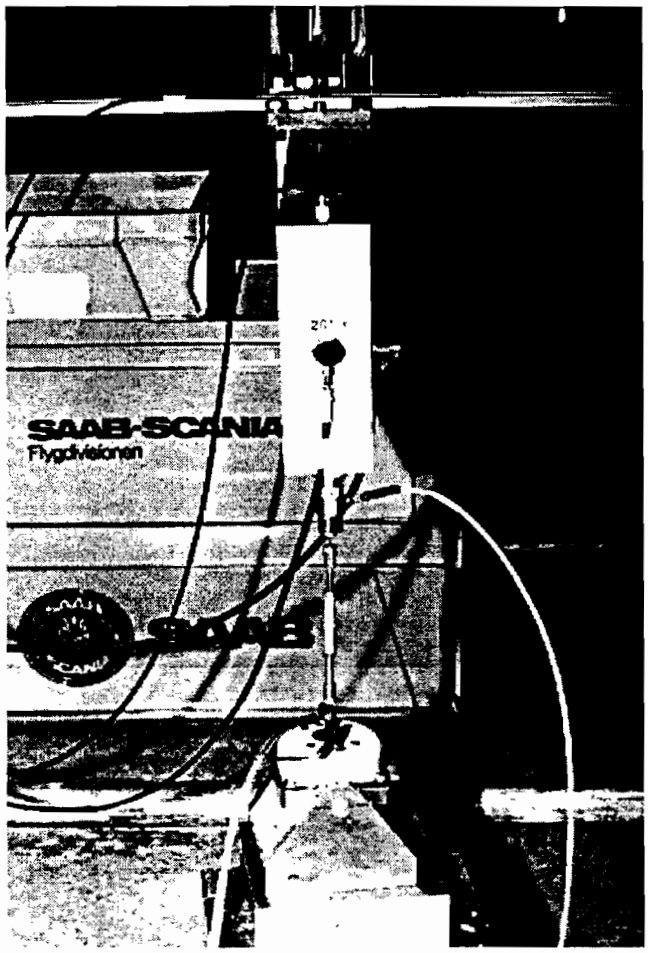

Figure 3 Detailed view of shaker

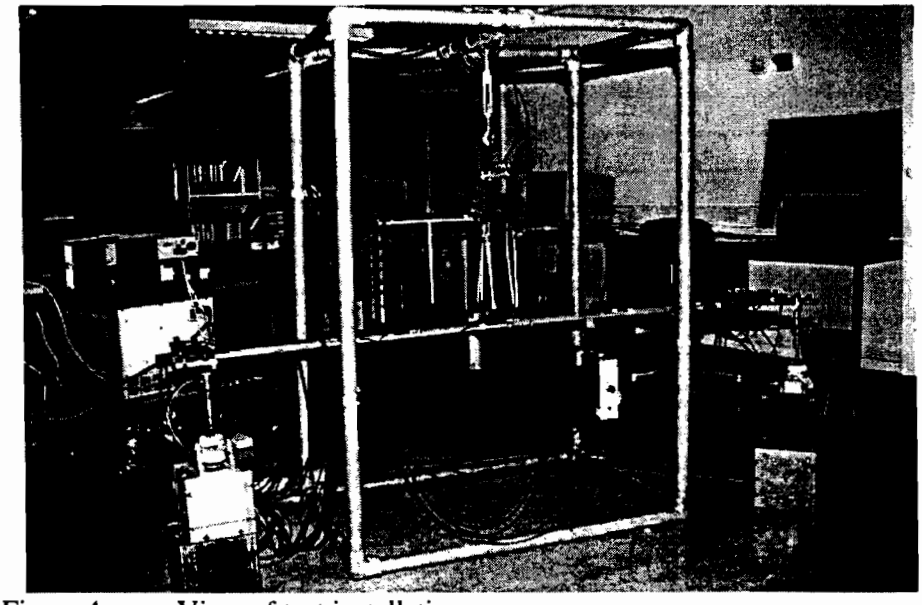

Figure 4 View of test installation

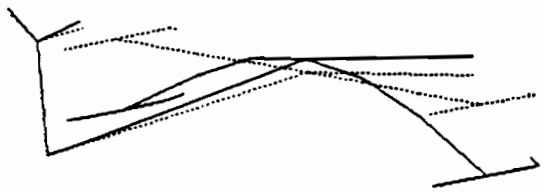

6.48 Hz 0.99 %

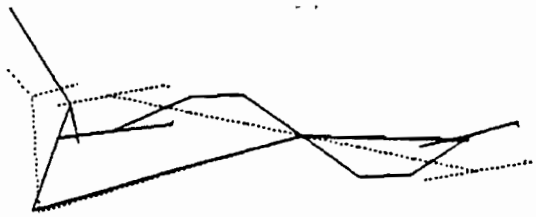

16.33 Hz 1.38 %

33.31 Hz 1.33 %

33.75 Hz 1.40 %

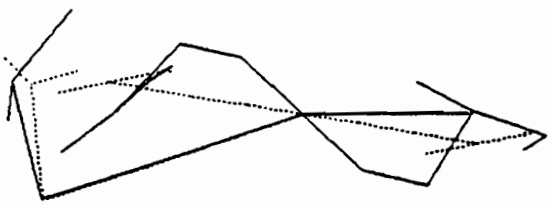

35.73 Hz 0.93 %

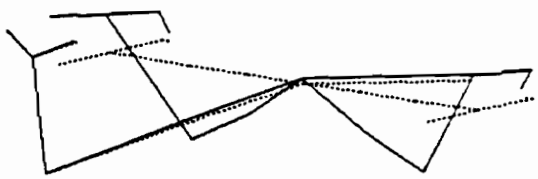

48.85 Hz 2.27 %

49.38 Hz 0.33%

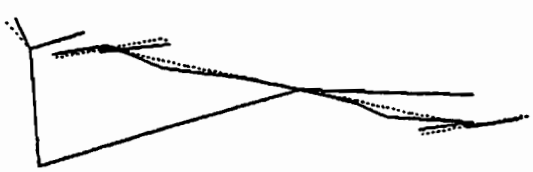

55.18 Hz 0.13 %

Figure 5 Modeshapes, eigenfrequencies and modal dampings of the eight analysed modes

Saab Military Aircraft

Flight Test Department

Test: 4xFRF

FRF

Hv-estimator

Date: 12-06-96

Blocksize: 4096

Number of averages: 2

Resolution: 0.02979[illegible]

Window: uniform

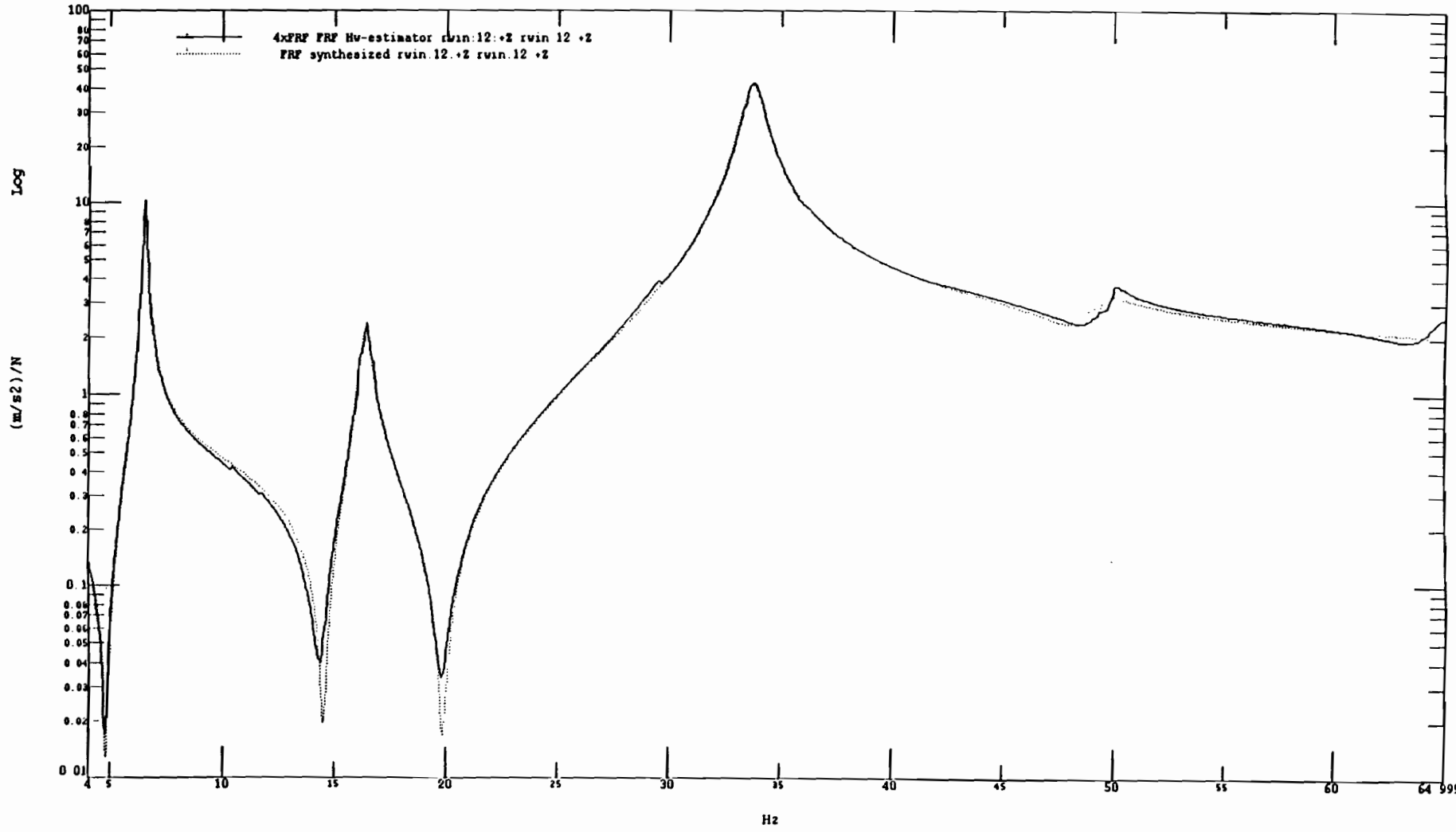

Saab Military Aircraft

Flight Test Department

Test: 4xFRF

FRF

Hv-estimator

Date: 12-06-96

Blocksize: 4096

Number of averages: 2

Resolution: 0.02979[illegible]

Window: uniform

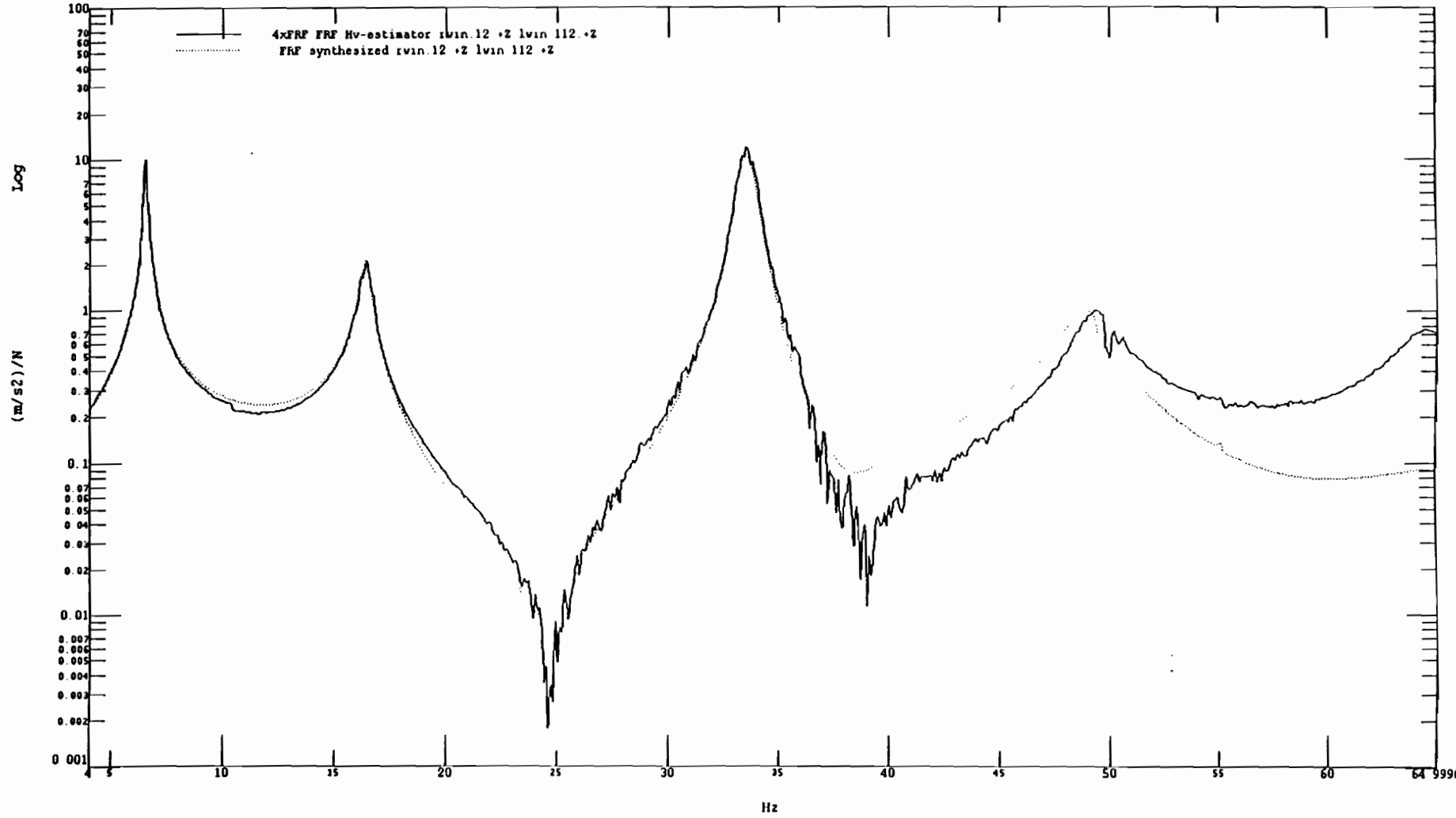

TUFKM-96199
Fig 7.

Saab Military Aircraft

Flight Test Department

Test: 4xFRF

FRF

Hv-estimator

Date: 12-06-96

Blocksize: 4096

Number of averages: 2

Resolution: 0.02979[illegible]

Window: uniform

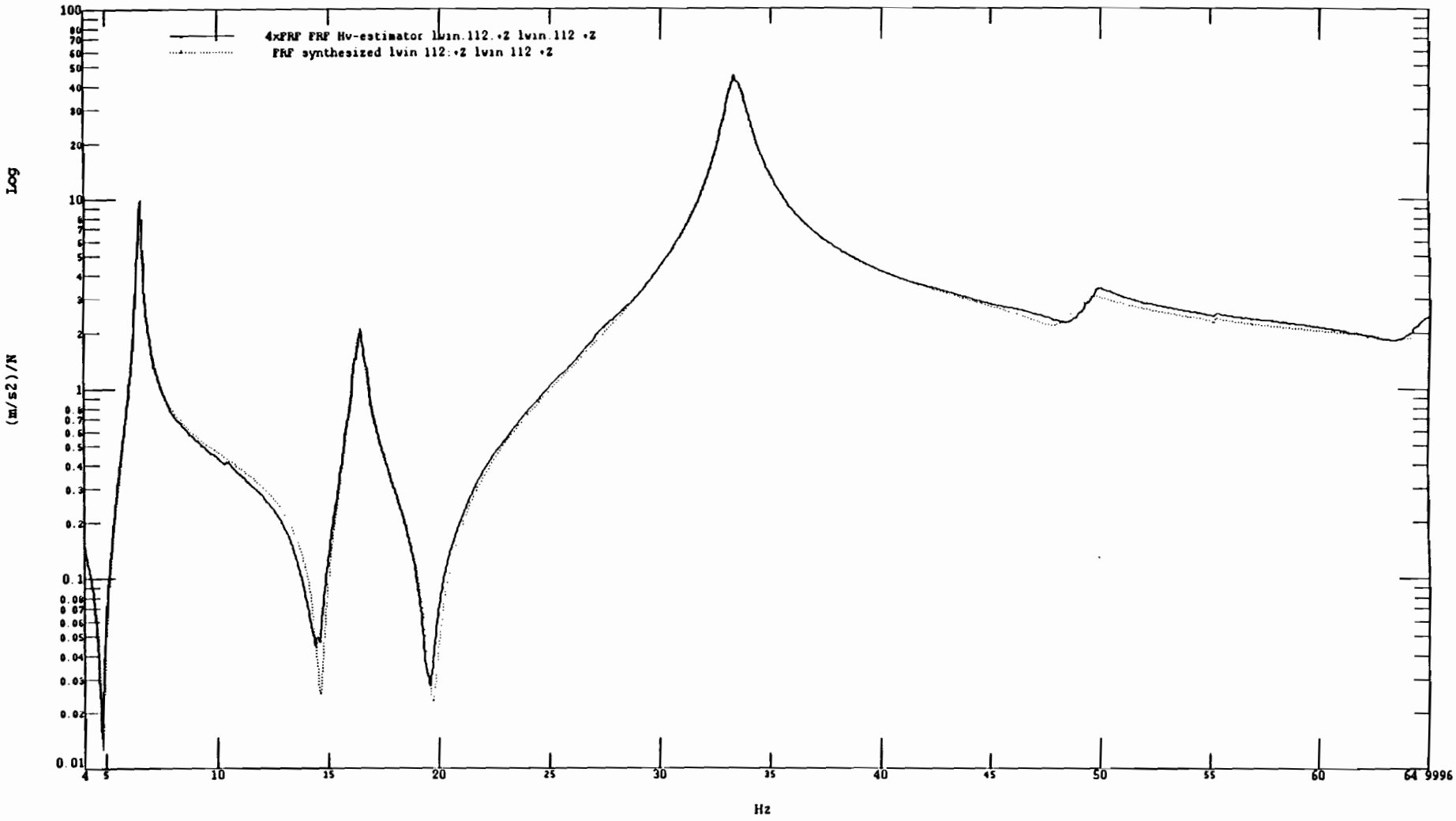

Fig 6

Saab Military Aircraft

Flight Test Department

Test: 4xFRF

FRF

Hv-estimator

Blocksize: 4096

Number of averages: 2

Resolution: 0.029798

Window: uniform

Date: 12-06-96

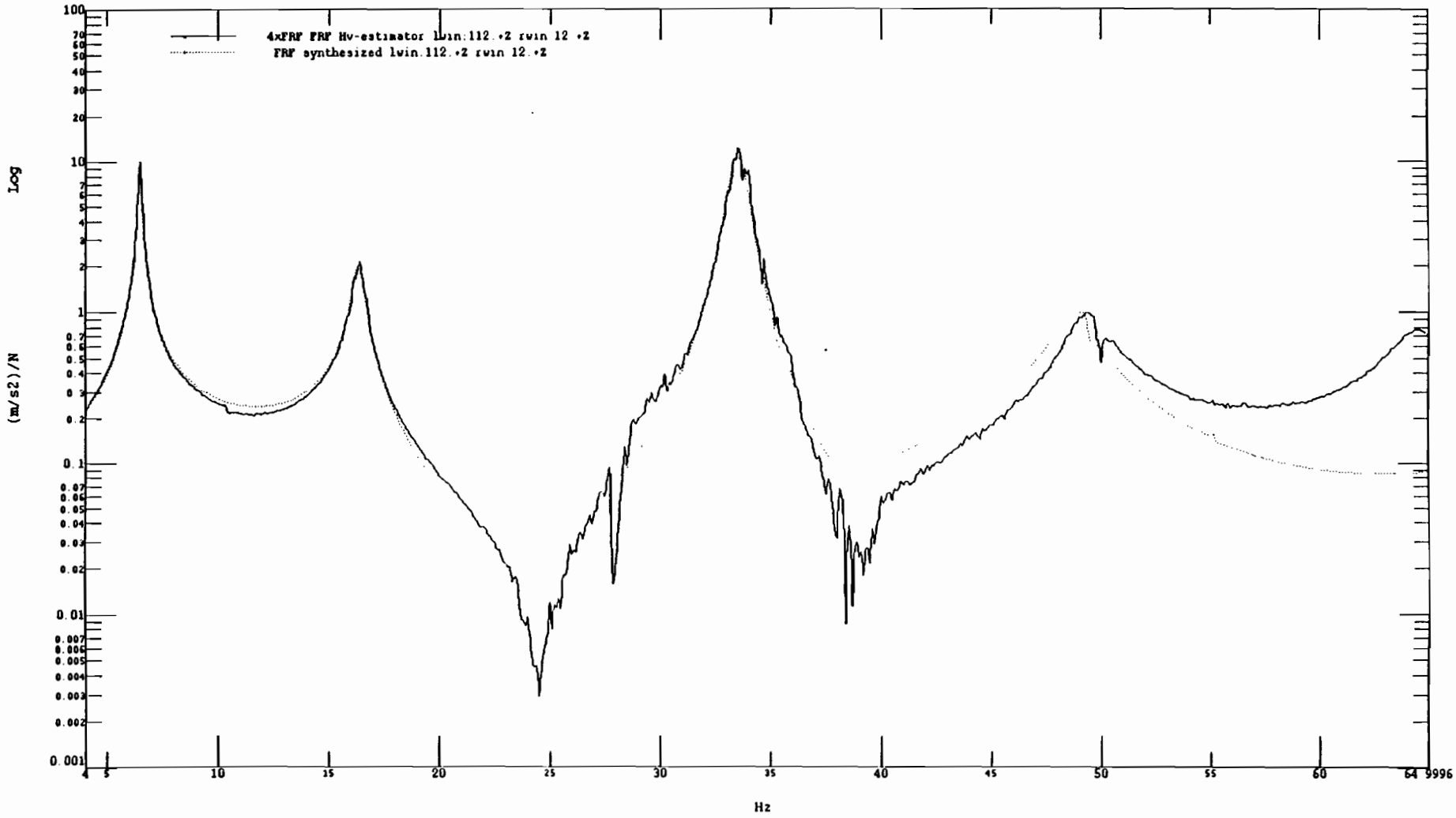

Fig 9

Annex 11

CNAM CONTRIBUTION

GARTEUR SM-AG19
C.N.A.M.
STRUCTURAL MECHANICS AND SYSTEMS LABORATORY.

By Nicole Henriet

September 12, 1996

Contents

List of Tables

List of Figures

Chapter 1

INTRODUCTION

To prove the aeroelastic stability in an airplane, different experimental and numerical methods are used.

Ground Vibration Test (GVT) allow to predict the Dynamic Performances of a structure and/or to check and to update analytical structural models.

The reability of these experimental methods plays a key role in the certification process.

To validate identification methods and their reability the proposed Garteur Action Groupe SM-AG19 expect to make comparative test on a common testbed by means of different GVT methods.

Research institutes and industrial partners group together 12 participants. The documentation for the Garteur SM-AG19 testbed is listed in annex A.

The present document gives a summary of some selected tests with which we try to compare the modal parameters :

- issued from different identification methods.
- given by SOPEMEA
- identified with different softwares

Chapter 2

TEST EQUIPMENT

All the operations about the checkup have been performed :

- degrease the connection plates
- assemble wing and fuselage applying a torque of 15.7mN for the connection screws
- suspend the structure coupling by a hook and the suspension connection piece which is included in the pack on the top of a mezzanine (height : 2.50m)
- stick the 24 accelerometers at the specified locations on a sticky paper glued to the structure (the glue is cyanoacrylate)
- stick 2 force transducers at the points 12 and 112 in the same way as the accelerometers
- suspend 2 vibration exciters in front of the points 12 and 112 of the structure. Each vibration exciter is suspended by 4 bungees on a plate fasten to a three linear axes system screwed on the top of the mezzanine
- fix the 2 complement masses of 200 grs at the drum tips
- perform the horizontability of all suspended parts with a spirit level

Figure 2.1: Test Equipment

Chapter 3

INSTRUMENTATION

See the specifications in annex B.

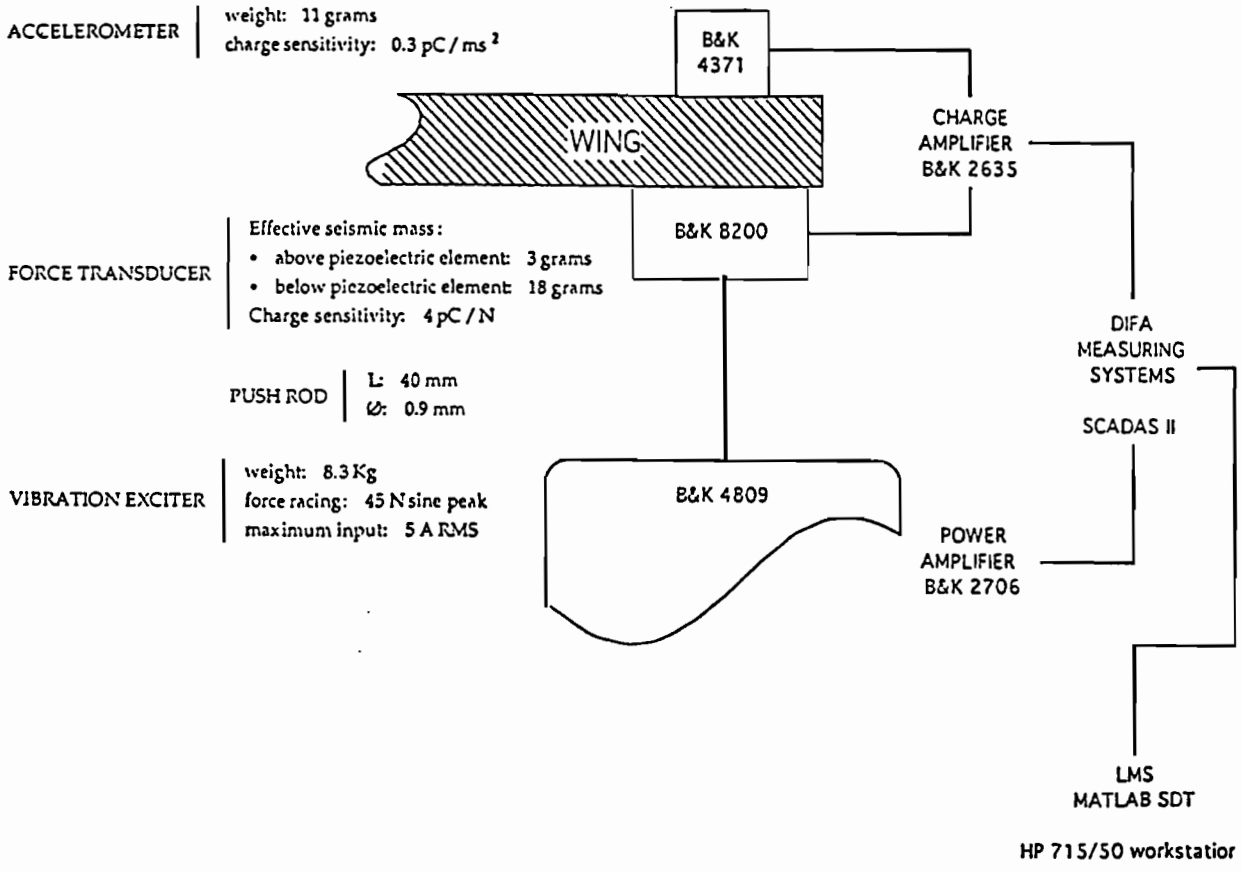

3.1 Exciting part

- 2 vibration exciters of type 4809 with power amplifier model 2706 from Bruel & Kjaer company.
  - Force rating 45 N sine peak
  - Maximum input current 5A RMS
  - Frequency range 10Hz to 20KHz
  - Weight 8.3Kg with a dynamic weight of moving element of 60 grs
- 2 force transducers of type 8200 with charge amplifier model 2635 from Bruel & Kjaer
  - charge sensitivity 4 Pc/N
  - weight 21 grs
    - effective seismic mass above piezoelectric element 3 gr
    - effective seismic mass below piezoelectric element 18 gr
- a push rod of diameter 0.9 mm and lenght of 40 mm is tighten by his extremities with 2 cylinders pieces, screwed at the top with the force transducer and below with the vibration exciter

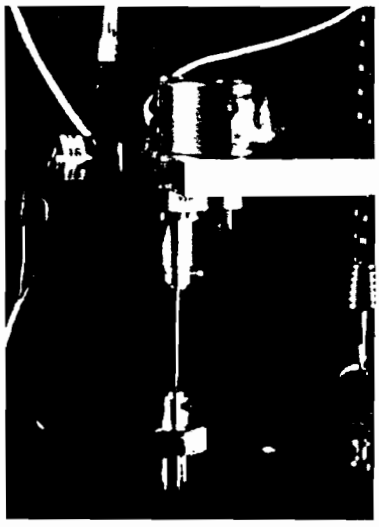

Figure 3.1: Exciting part

Here are some caracteristic dimensions of the test equipment :

- pushrod with the cylinders pieces
  - weight :18 gr
  - lenght :78 mm (pushrod = 30 mm)
- vibration exciter suspension frequency in the vertical axis : $\sim 1Hz$
- airplane suspension frequency in the vertical axis (without the 2 shakers) : $\sim 2Hz$
- airplane suspension lenght

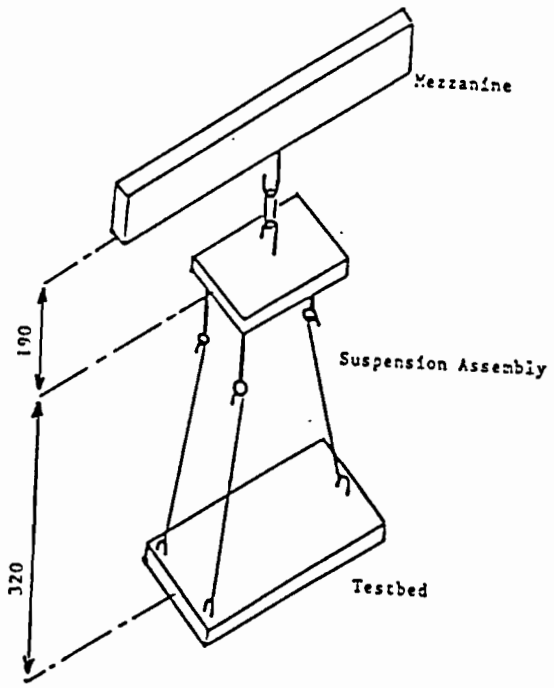

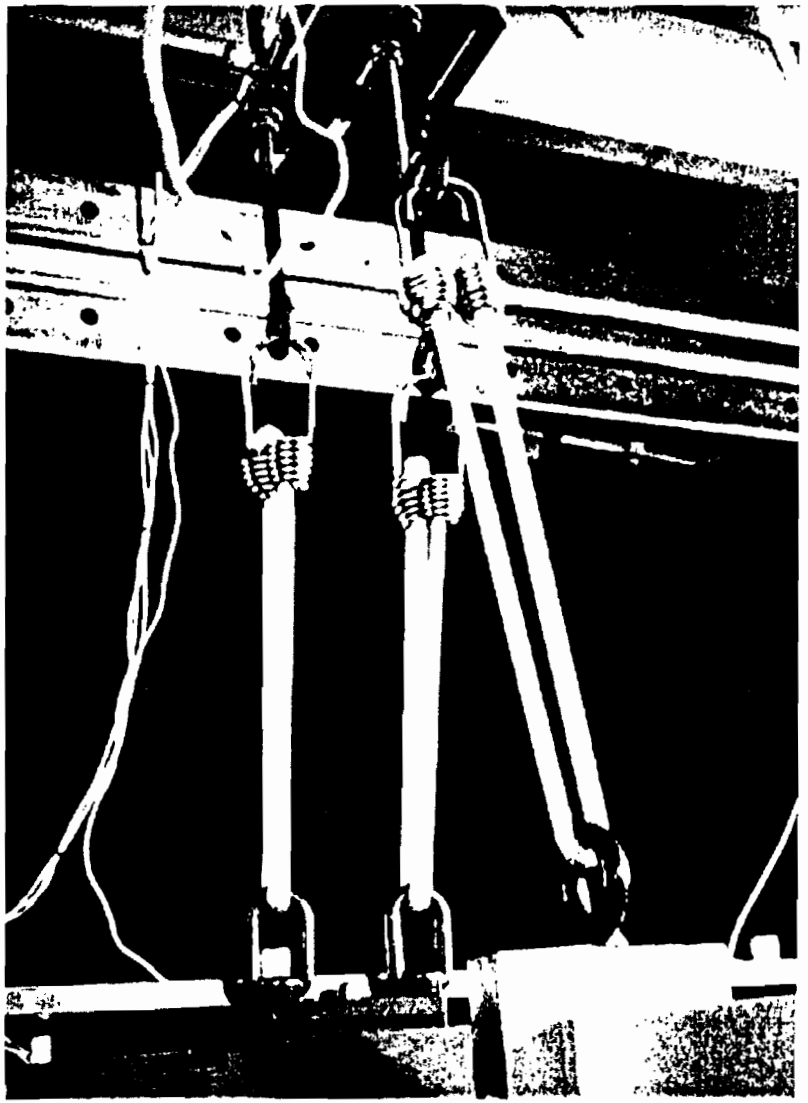

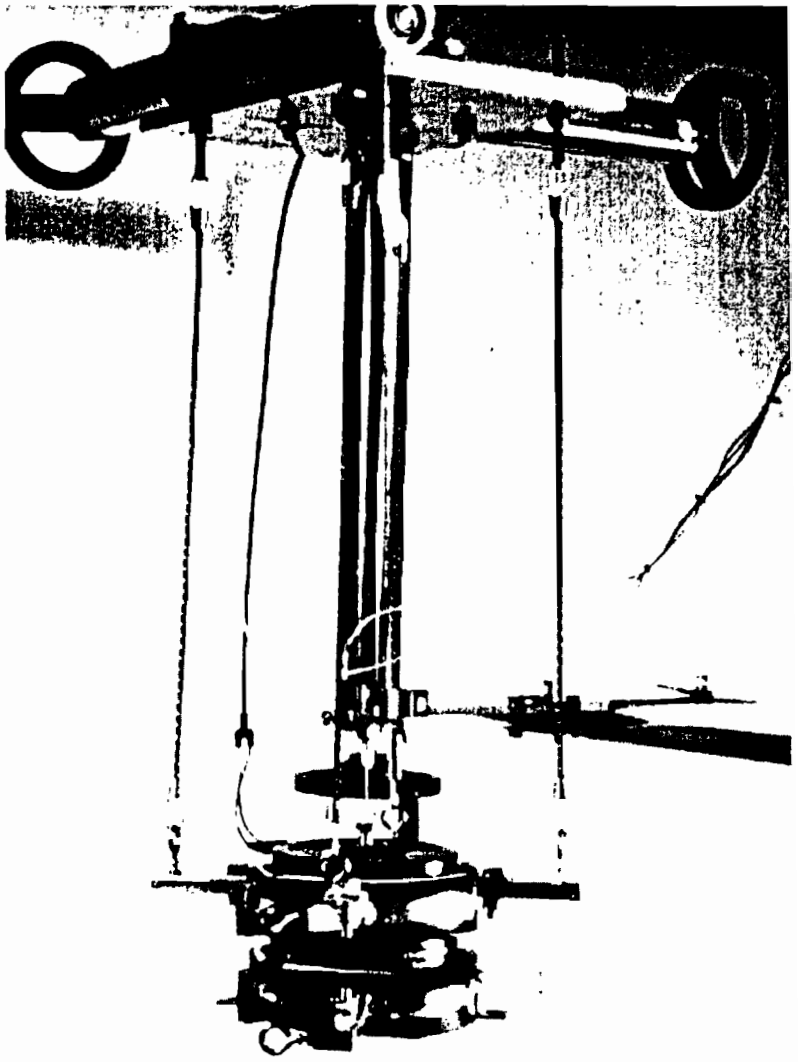

Figure 3.2: Testbed Suspensions

3.2 Response part

- 24 accelerometers type 4371 with charge amplifiers from Bruel & Kjaer
  - charge sensitivity : 9.8 Pc/g
  - weight : 11 gr
  - frequency range : 0.2 - 9100 Hz

3.3 Acquisition part

All the measurements are dealed in a DIFA MEASURING SYSTEM (SCADAS II) which can accept together 4 excitations and 10 response signals.

3.4 Identification

We make the identification using two softwares :

- LMS (Leuven Measurement Systems) modal analysis
- Matlab STRUCTURAL DYNAMICS TOOLBOX (Scientific Software)

on a Hewlett Packard 715/50 station.

Chapter 4

EXPERIMENTAL MEASUREMENTS

We purpose two decorelated random excitation measurement sets at :

- points 12 and 112
- points 01 and 101

The transfer functions were measured 10 by 10 because of the limitations of our hardware in a frequency band of 100 Hz with a low-pass filter ot 80 % and with 50 averages.

Complement mass : The force transducer is sticked to the structure. For this reason and in order to respect the specification. we must include the top seismic mass (18 grams) of the transducer in the determination of the complement mass.

We decide to neglect this 18 grams and to keep the 200 grams complement mass.

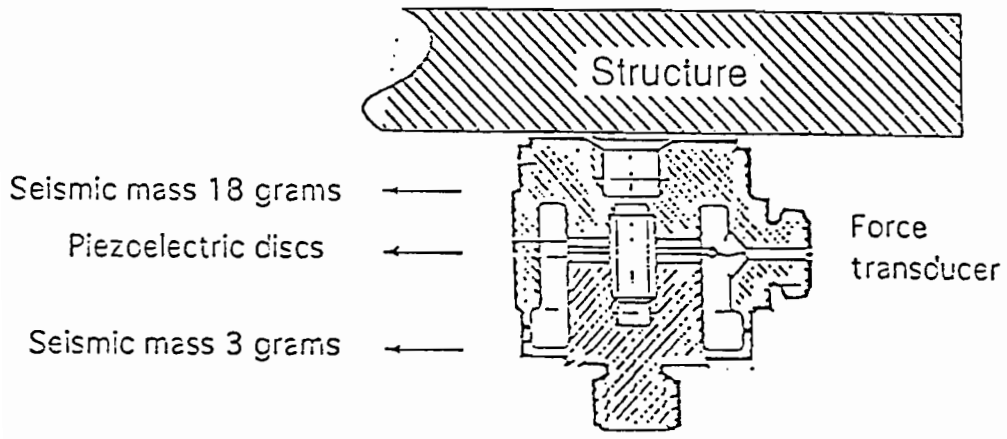

Comment :

- We have some suspension modes in the frequency band of interest.
- The 2 by 2 set transfer functions corresponding to excitation and response at the drum front tips (vertical excitation at points 12 and 112) show :
  - The non symmetry of the structure by the collocated FRF.
  - The reciprocity of the structure by the cross transfers.
- If we remove the 200 grams complement mass, we observe on the two measured FRF 12/112 and 12/12, a shifting forward of the frequencies.

$$\frac{112}{112} \neq \frac{12}{12}$$

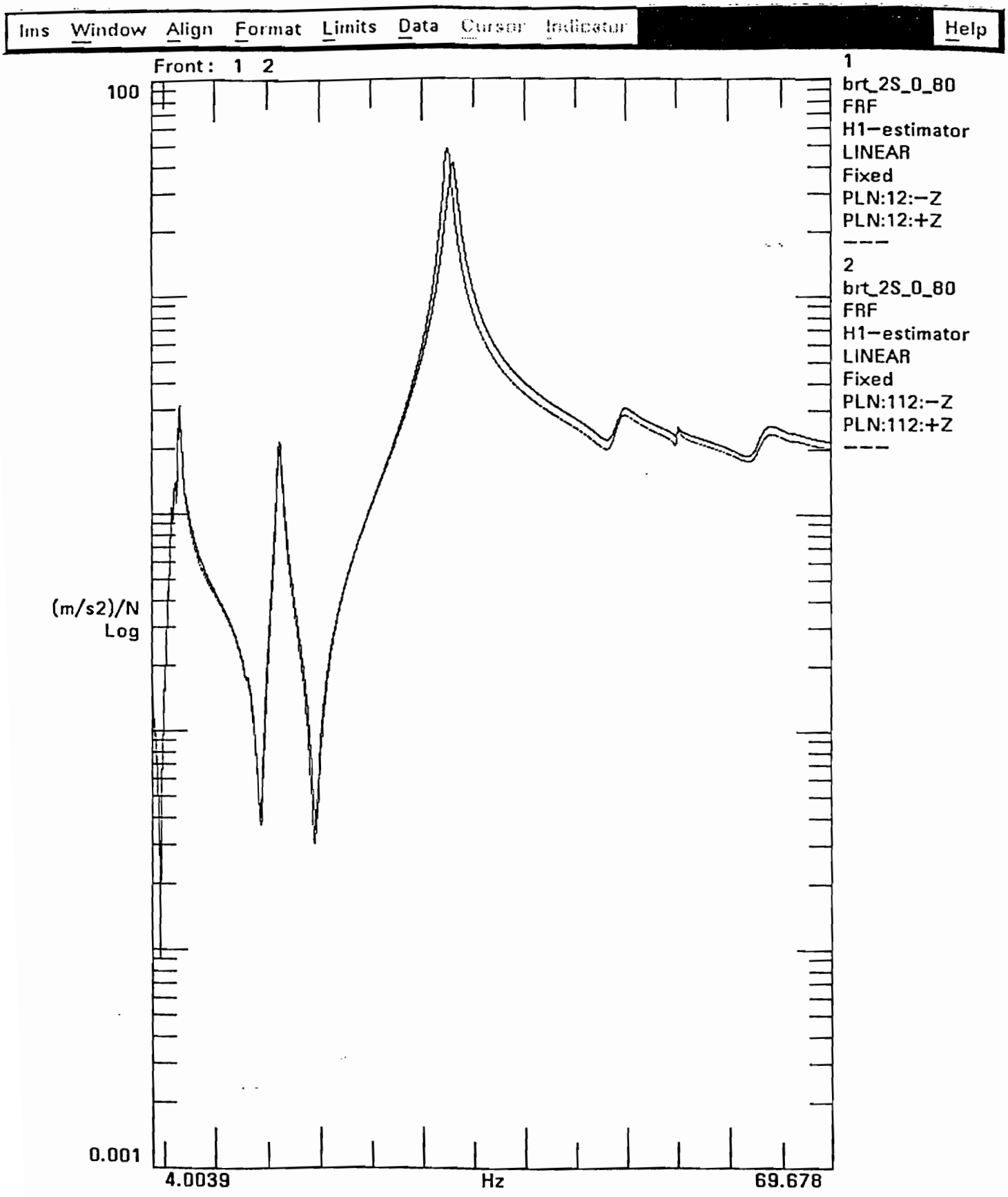

$$\frac{12}{112} = \frac{112}{12}$$

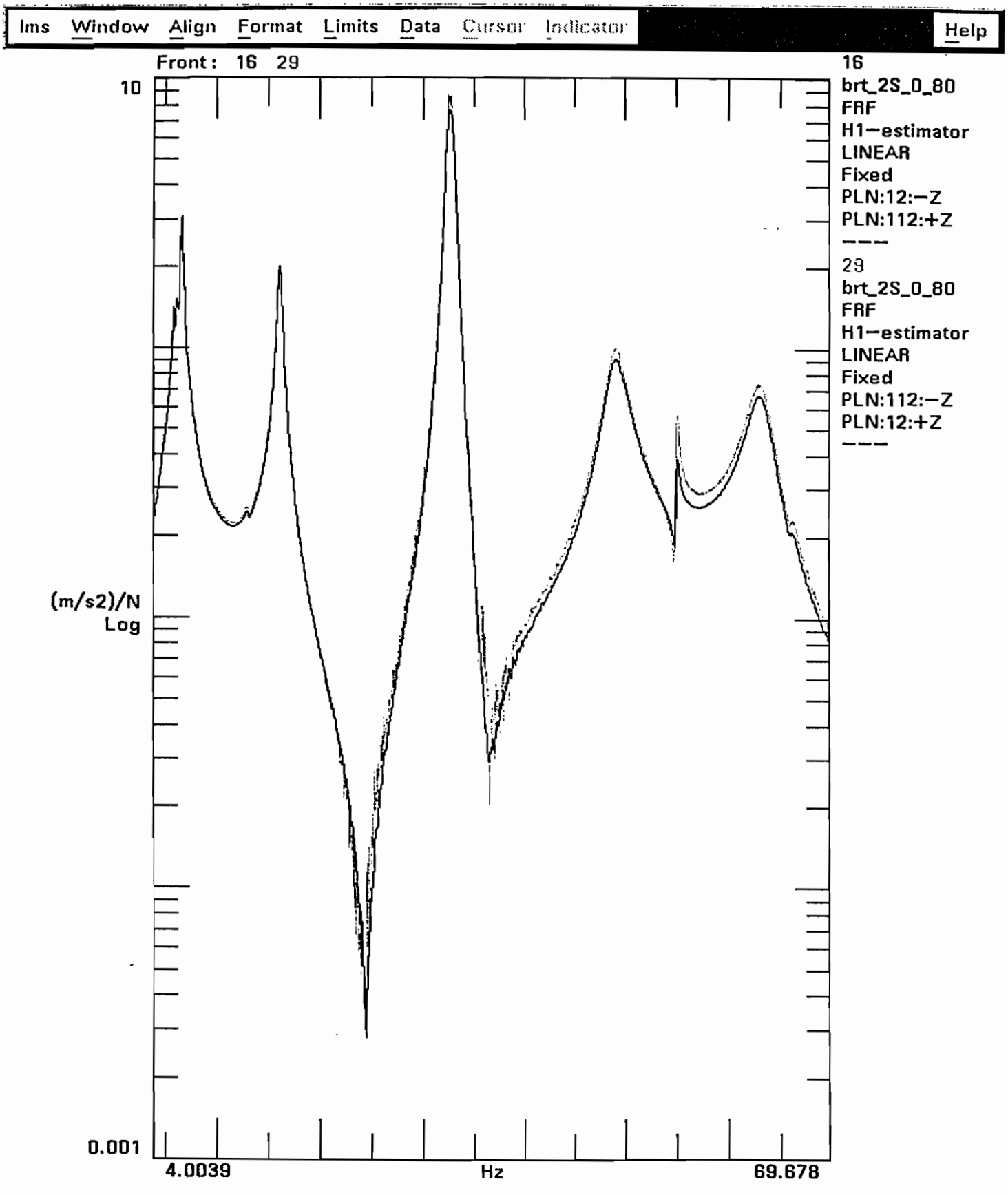

SUPPRESSION OF THE COMPLEMENT MASS

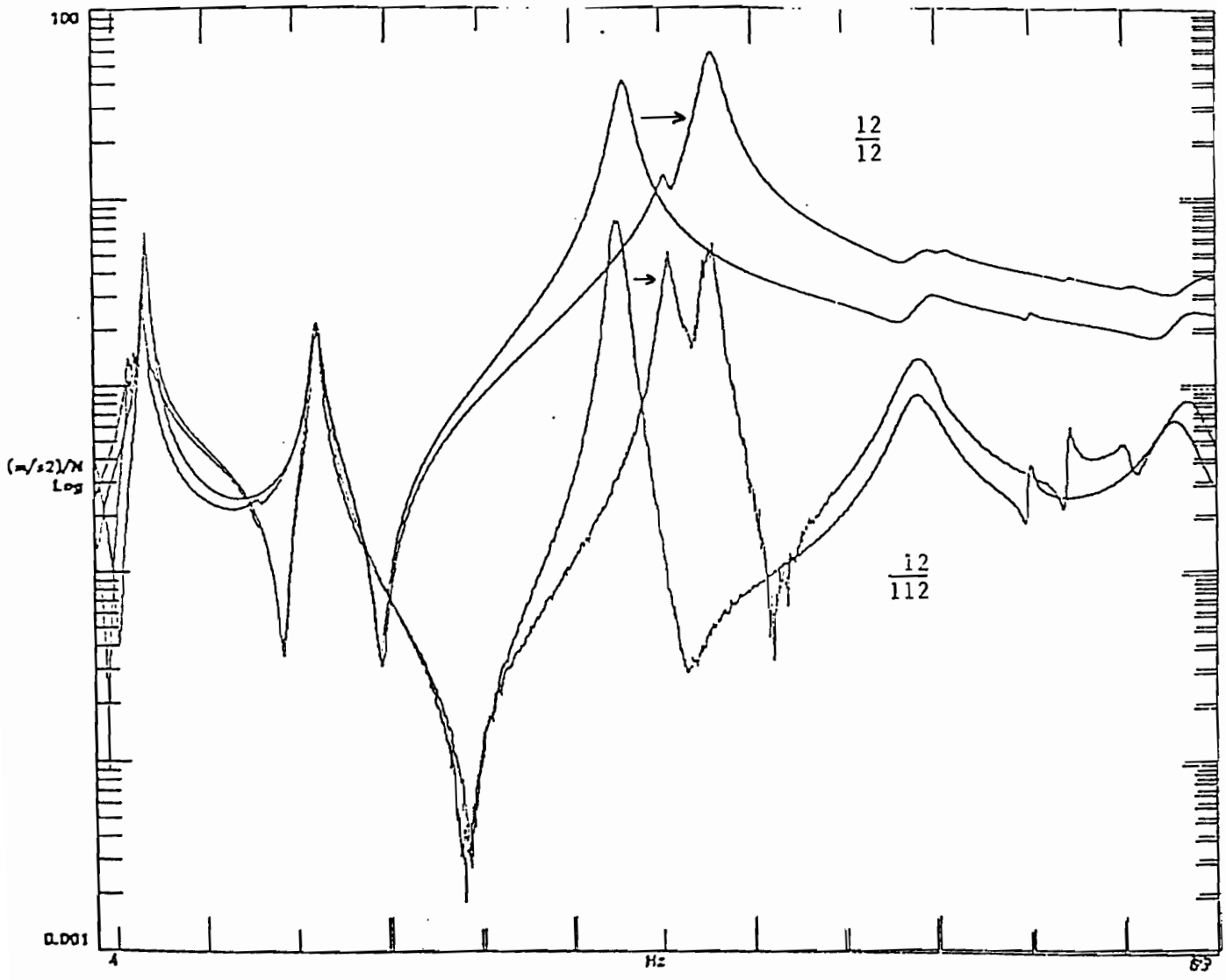

Chapter 5

IDENTIFICATION

We choose 6 frequency bands to identify 9 modes (including 2 suspension modes) in the bands of interest :

4-8 Hz ; 10-20 Hz ; 30-38 Hz ; 43-53 Hz ; 52-58 Hz ; 60-65 Hz.

How the identified modes allow a reconstitution of the measured transfer functions?

Upper and lower residual terms are determined, for each band, by the least squares technique.

Transfert functions are reconstituated by summation on each pole.

The table below presents the comparisons beetween all the results which were available to us.

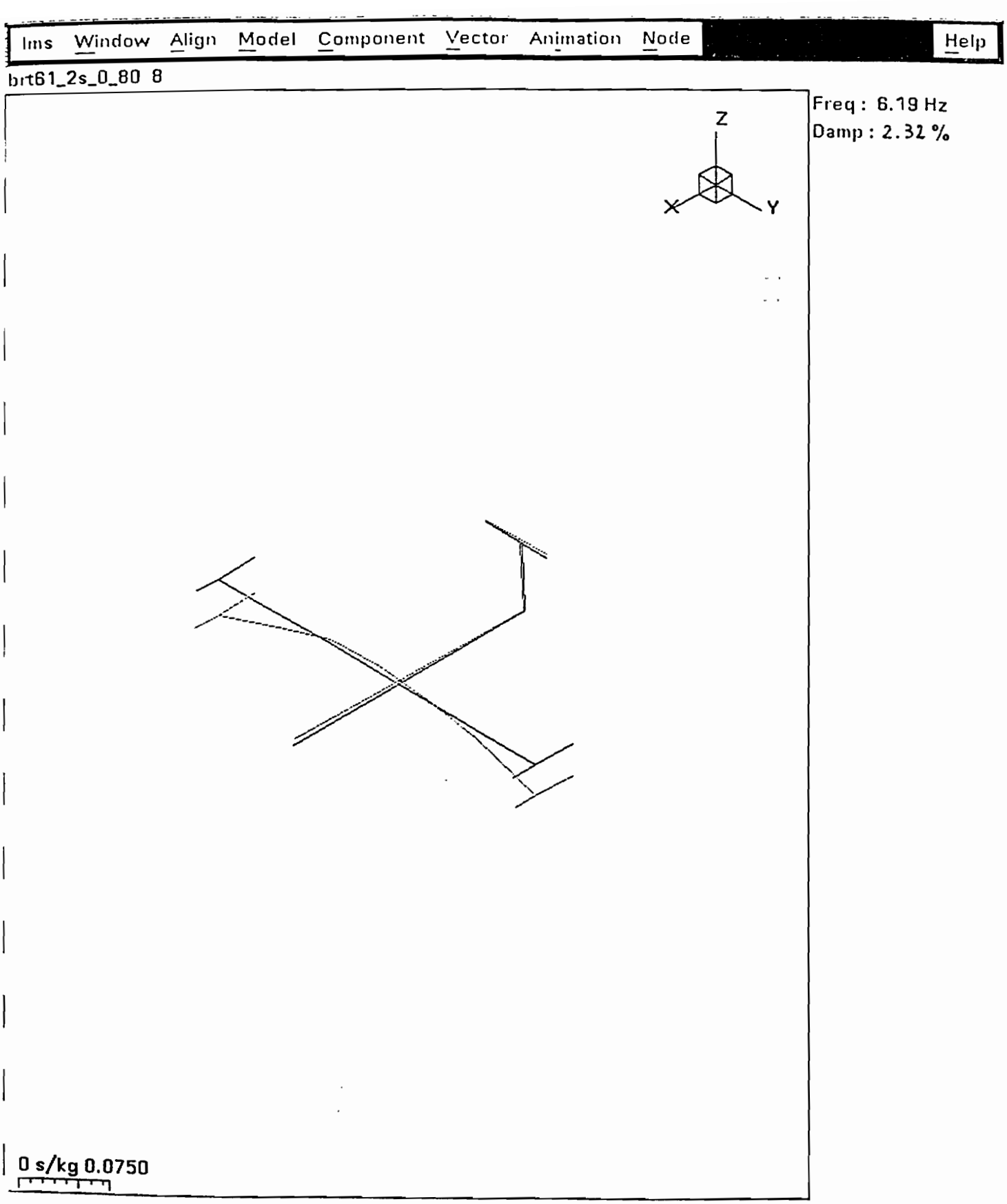
Ims Window Align Model Component Vector Animation Node Help
brt61_2s_0_80 8
Freq : 6.19 Hz
Damp : 2.32 %
Z
X
Y
0 s/kg 0.0750

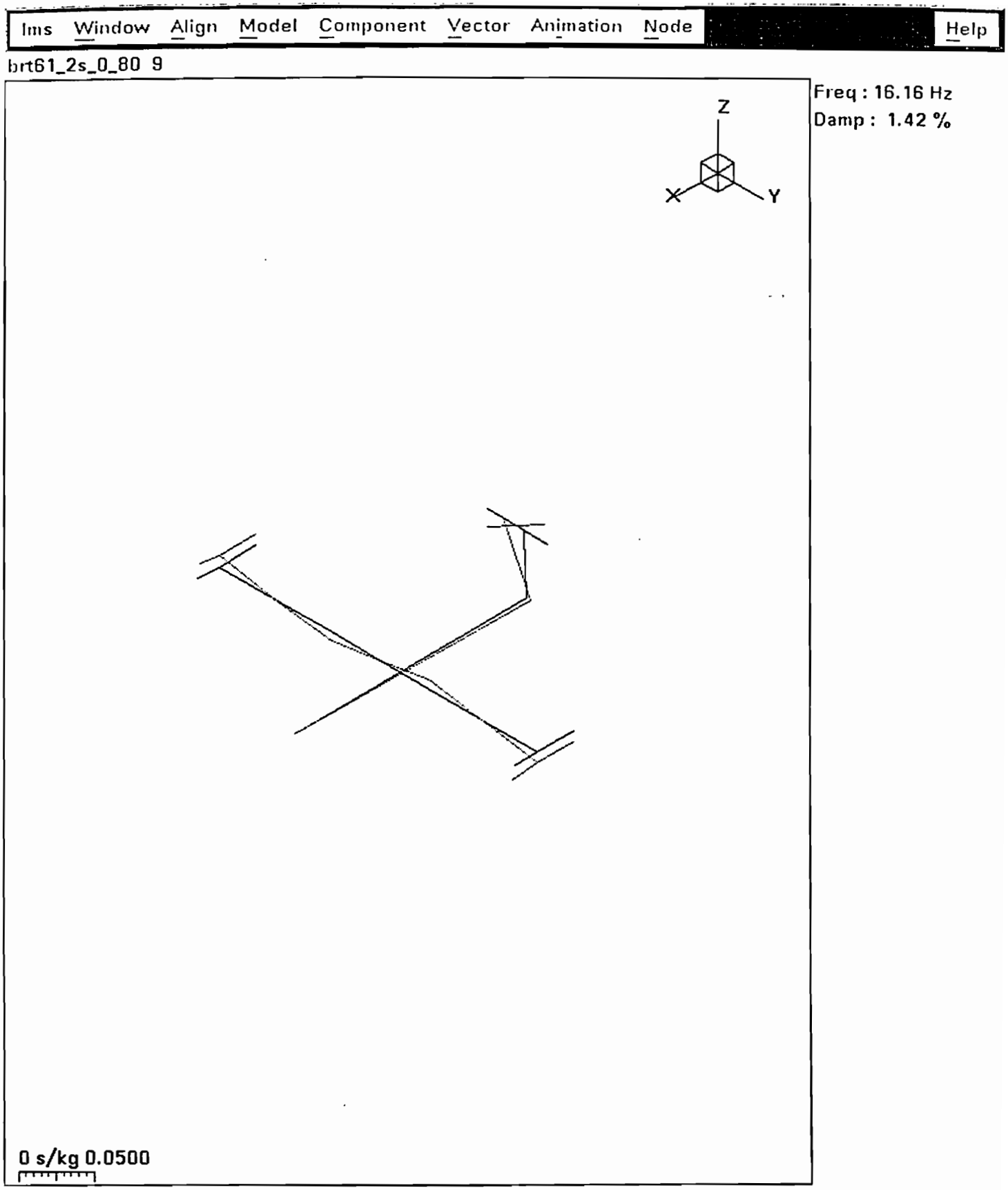
lms Window Align Model Component Vector Animation Node Help
brt61_2s_0_80 9
Freq : 16.16 Hz
Damp : 1.42 %
Z
X
Y
0 s/kg 0.0500

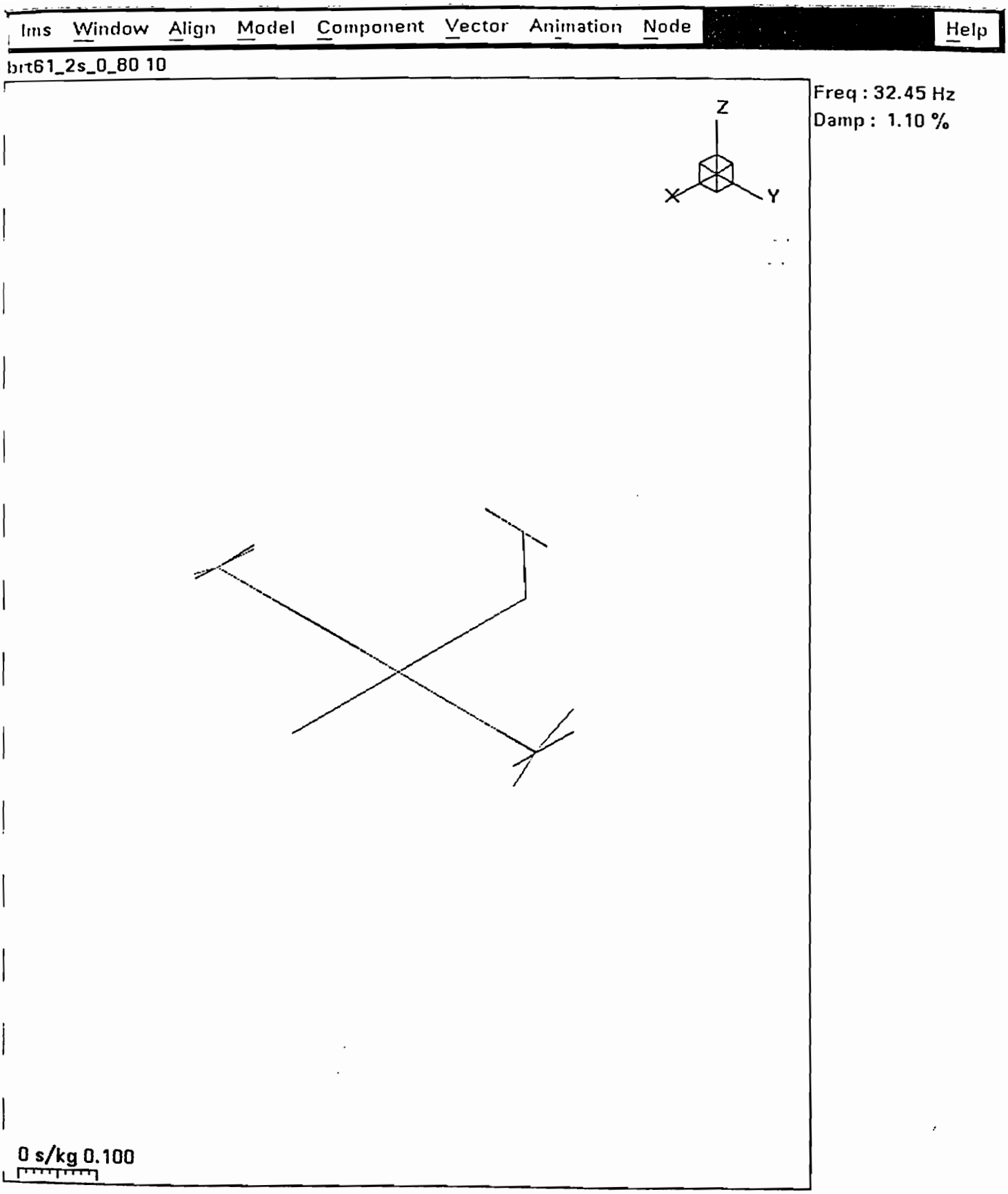
lms Window Align Model Component Vector Animation Node Help
brt61_2s_0_80 10
Freq : 32.45 Hz
Damp : 1.10 %
Z
X
Y
0 s/kg 0.100

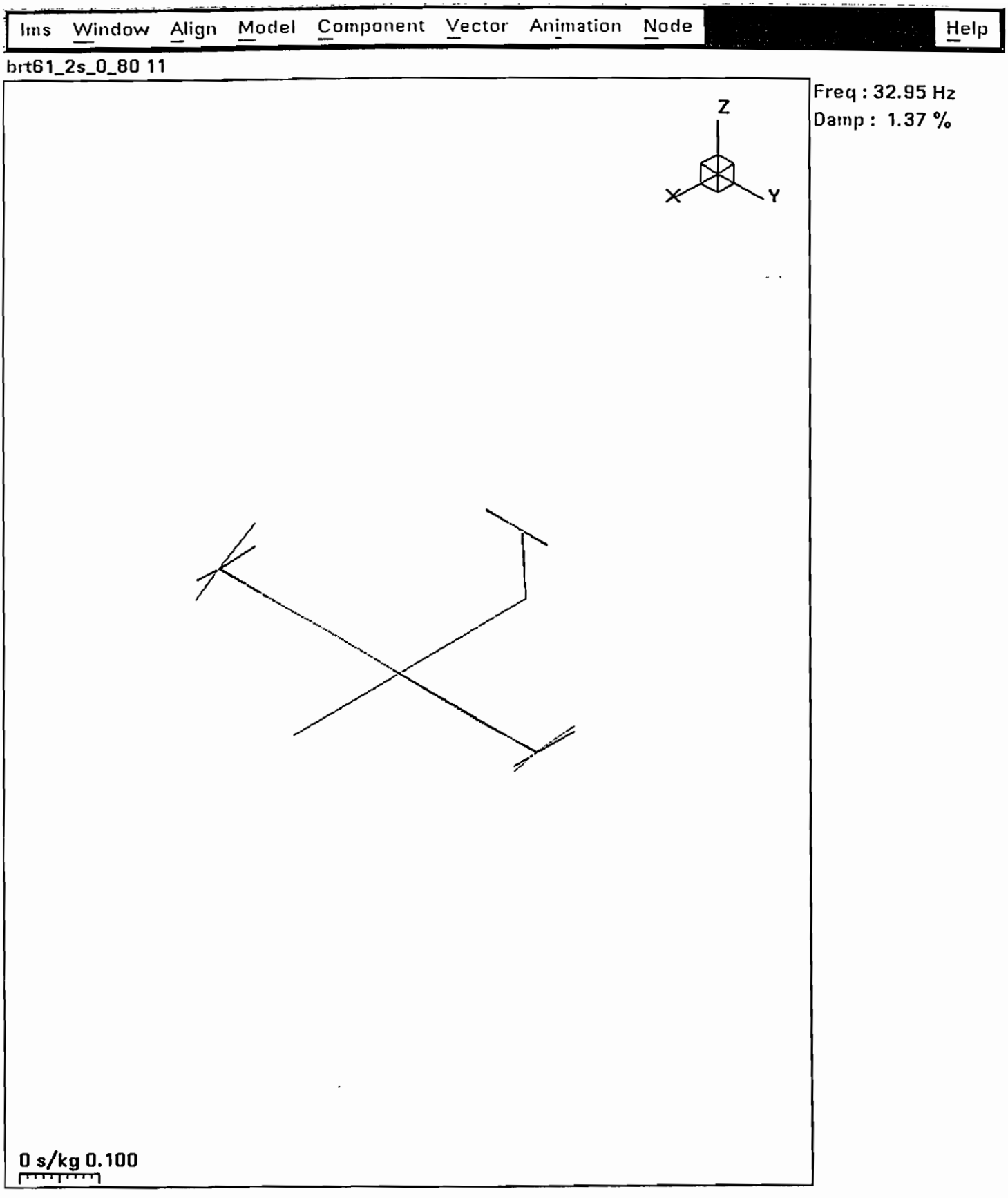
Ims Window Align Model Component Vector Animation Node Help
brt61_2s_0_80 11
Freq : 32.95 Hz
Damp : 1.37 %
Z
X
Y
0 s/kg 0.100

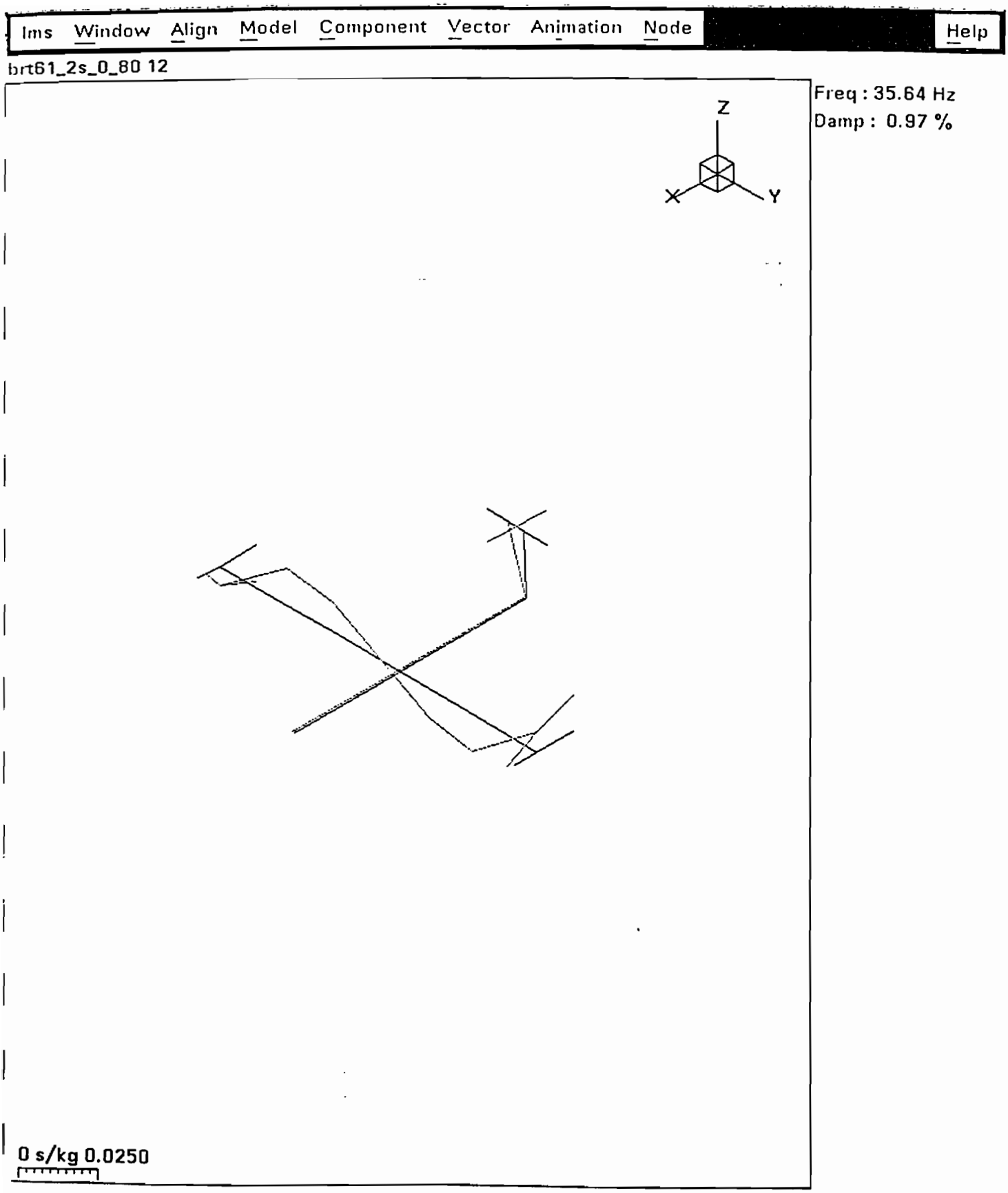
lms Window Align Model Component Vector Animation Node Help
brt61_2s_0_80 12
Freq : 35.64 Hz
Damp : 0.97 %
Z
X
Y
0 s/kg 0.0250

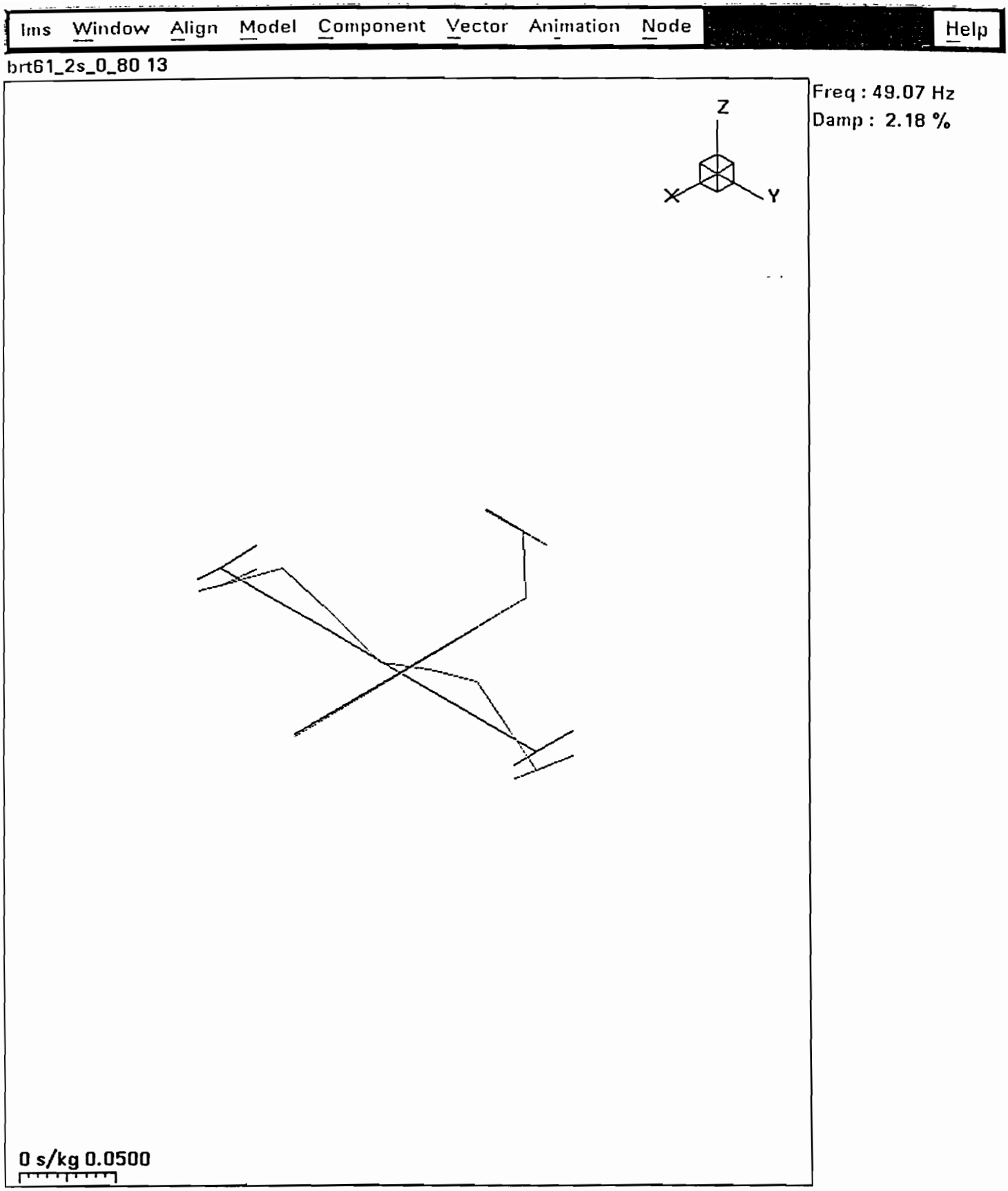
Ims Window Align Model Component Vector Animation Node Help
brt61_2s_0_80 13
Freq : 49.07 Hz
Damp : 2.18 %
Z
X
Y
0 s/kg 0.0500

Ims Window Align Model Component Vector Animation Node Help

brt61_2s_0_80 14

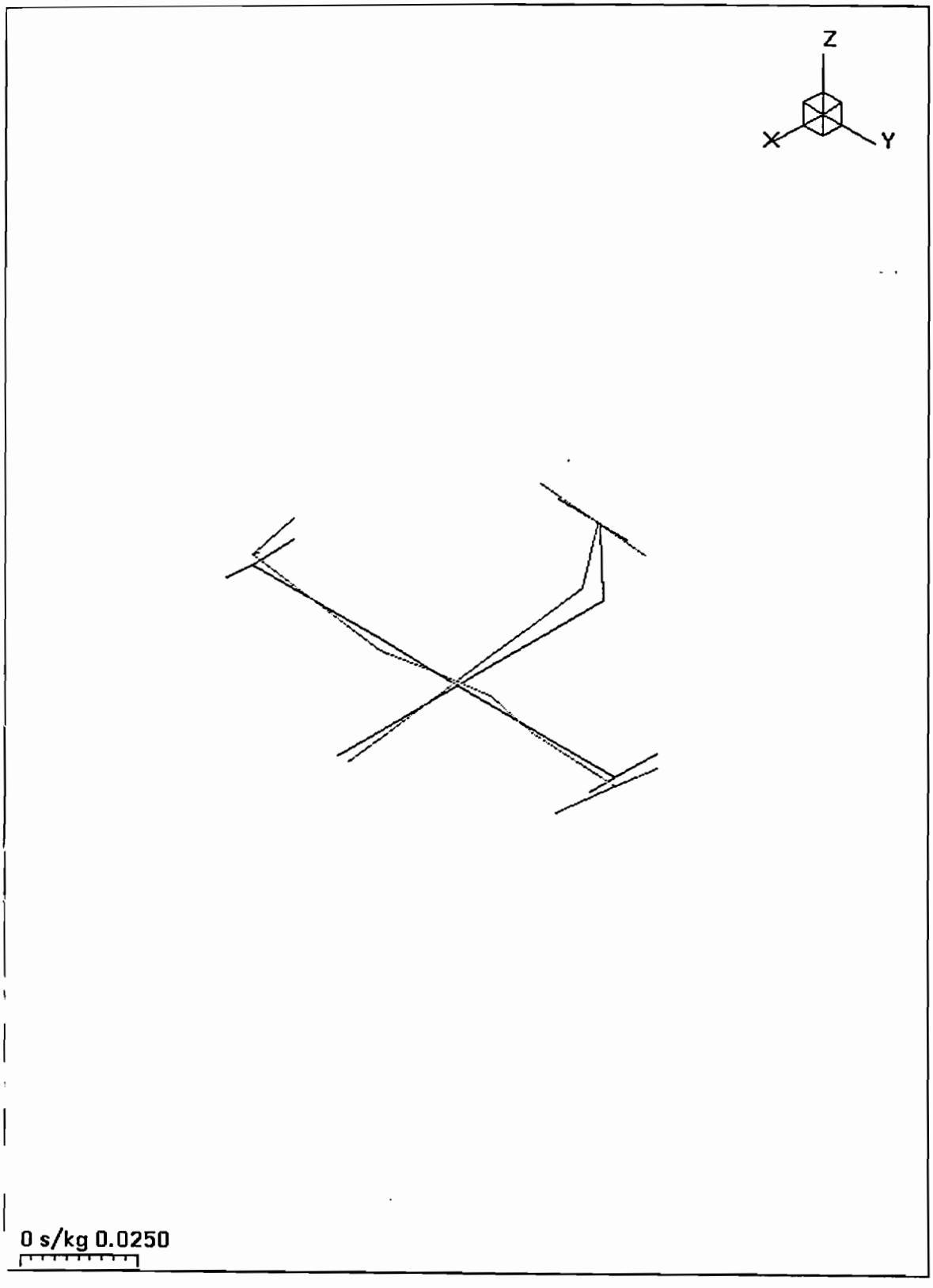

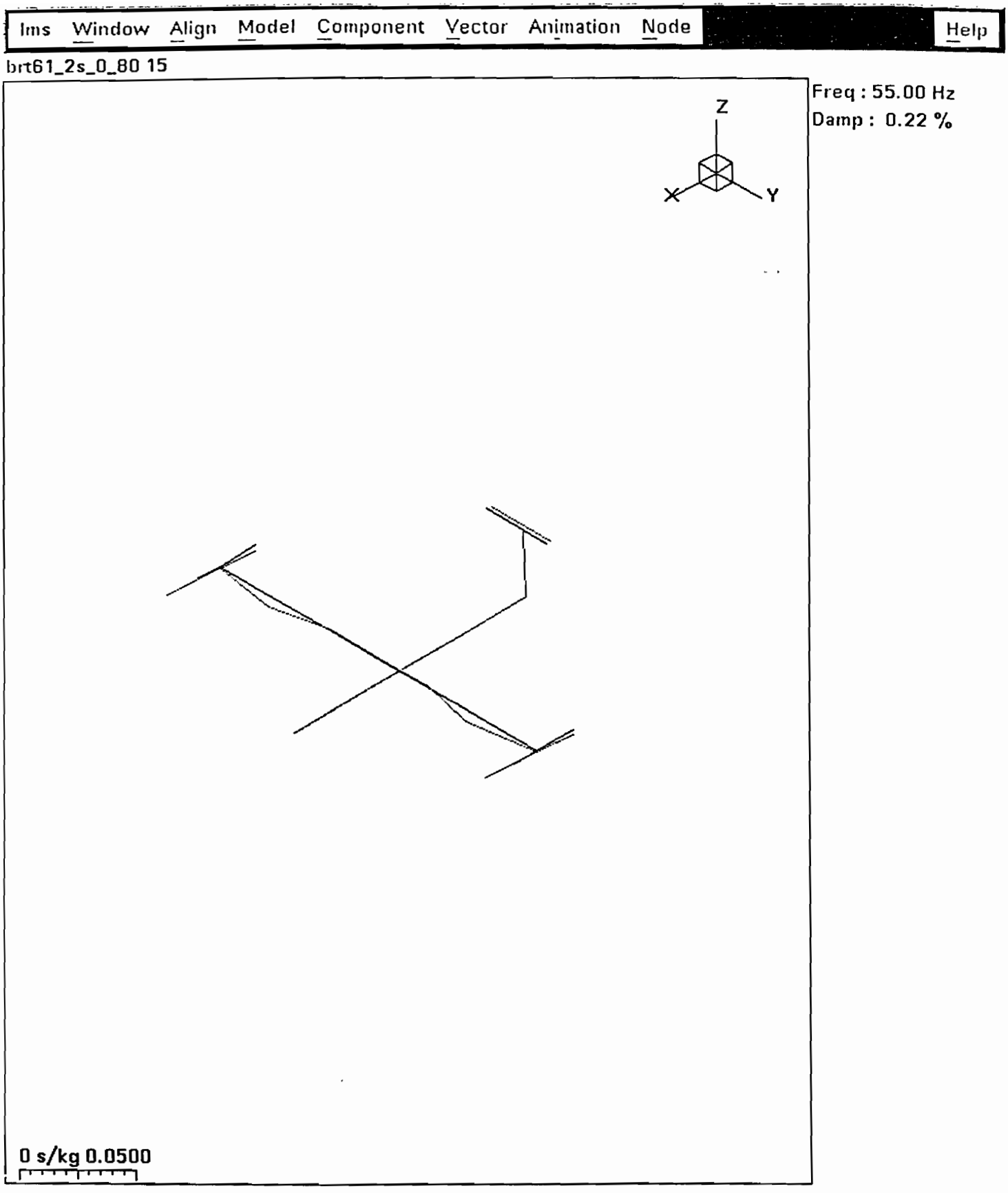
Ims Window Align Model Component Vector Animation Node Help
brt61_2s_0_80 15
Freq : 55.00 Hz
Damp : 0.22 %
Z
X
Y
0 s/kg 0.0500

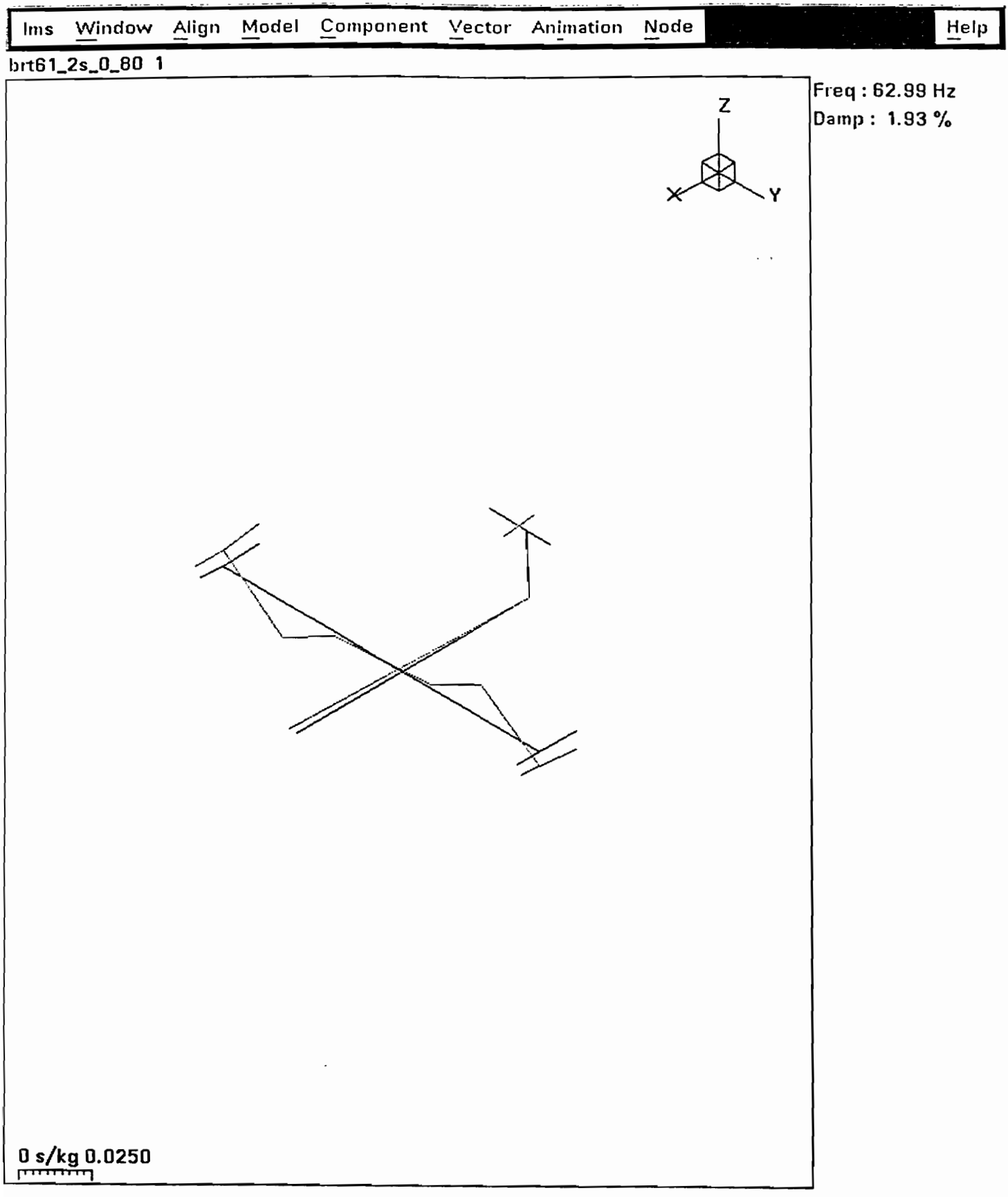
Ims Window Align Model Component Vector Animation Node Help
brt61_2s_0_80 1
Freq : 62.99 Hz
Damp : 1.93 %
Z
X
Y
0 s/kg 0.0250

SOPEMEA		CNAM							
		Actuators : $112/+Z$, $12/+Z$ Mass : 200 gr						Actuators : $101/+Z$, $01/+Z$ Mass : 200 gr	
		4-65 Hz				30-38 Hz		4-65 Hz	
		SDT MATLAB		LMS		LMS		LMS	
PÔLE (Hz)	**DAMPING RATE** (%)	**PÔLE**	**DAMP**	**PÔLE**	**DAMP**	**PÔLE**	**DAMP**	**PÔLE**	**DAMP**
6.97	1.27	6.19	2.13	6.19	2.32			6.18	2.56
16.08	1.36	16.16	1.42	16.16	1.42			16.16	1.42
33.45	1.02	32.45	1.09	32.45	1.10	32.41	1.01	32.45	1.10
33.68	1.47	32.96	1.38	32.95	1.37	32.9	1.2	32.95	1.37
33.94	1.16	35.63	.89	35.64	.97	35.66	.91	35.64	.97
46.08	2.58	49.08	2.18	49.07	2.18			49.07	2.18
48.62	.91	49.56	.5	49.54	.51			49.54	.51
53.58	.56	55.01	.24	55.00	.22			55.00	.22
61.14	2.06	63.03	1.93	62.99	1.93			62.99	1.93

Table 5.1: Comparisons table of results

	6.19 Hz	16.16 Hz	32.45 Hz	32.96 Hz
206/-Z	-2.900e-02	-2.273e-04	-2.512e-02	-2.061e-03
108/-Z	-5.372e-03	-1.017e-01	-6.666e-02	3.642e-02
105/-Z	5.176e-02	-4.840e-02	1.647e-01	4.058e-02
105/-X	-1.336e-04	-2.394e-02	1.068e-01	-1.149e-02
8/-Z	-3.322e-02	1.104e-01	2.790e-01	5.884e-03
5/-Z	3.811e-02	5.101e-02	2.583e-01	1.452e-02
5/-X	1.884e-02	2.497e-02	-1.350e-01	8.433e-03
111/-Z	1.486e-01	1.224e-01	-1.104e+01	-2.326e-01
101/-Z	1.435e-01	1.324e-01	-7.054e-01	-3.719e-02
112/-Z	1.394e-01	1.443e-01	9.712e+00	1.582e-01
112/-X	5.739e-04	-4.080e-02	-2.616e-01	-2.976e-02
11/-Z	1.417e-01	-1.224e-01	1.723e+00	-9.699e-01
1/-Z	1.397e-01	-1.323e-01	-7.095e-02	-6.401e-02
12/-Z	1.363e-01	-1.494e-01	-1.905e+00	8.642e-01
12/-X	2.826e-02	3.750e-02	-2.348e-01	-5.545e-03
201/-X	9.192e-03	-1.693e-04	2.063e-02	1.792e-03
201/-Y	2.031e-02	3.750e-04	-1.250e-01	7.968e-03
201/-Z	-4.043e-02	-1.082e-04	-9.067e-02	-1.102e-02
302/-Y	-8.544e-03	2.646e-01	-5.097e-01	3.681e-02
301/-X	2.092e-02	2.666e-03	3.319e-02	1.119e-02
301/-Z	-1.403e-02	2.156e-01	-7.647e-01	8.218e-02
303/-X	1.583e-02	-2.286e-02	1.669e-01	2.730e-03
303/-Z	-5.826e-03	-2.356e-01	1.035e+00	-5.689e-02
205/-Y	3.895e-03	-5.273e-02	9.747e-02	-3.895e-03

Table 5.2: Mass normalized modeshapes

	35.63 Hz	49.08 Hz	49.56 Hz	55.01 Hz	63.03 Hz
206/-Z	-1.373e-03	1.738e-01	-1.839e-04	1.946e-03	3.586e-03
108/-Z	-2.043e-01	-1.565e+00	-1.542e-02	1.172e-02	-9.907e-02
105/-Z	-2.187e-01	-2.852e+00	-2.725e-02	1.233e-02	-9.083e-01
105/-X	4.114e-02	4.275e-02	-3.098e-02	8.848e-02	6.556e-02
8/-Z	2.001e-01	-1.492e+00	2.213e-02	1.300e-02	1.323e-01
5/-Z	2.154e-01	-2.713e+00	4.024e-02	2.006e-02	9.769e-01
5/-X	-3.725e-02	9.809e-02	3.029e-02	8.984e-02	-6.488e-02
111/-Z	2.523e-01	1.941e+00	2.601e-02	-3.611e-02	5.452e-01
101/-Z	1.349e-01	1.412e+00	1.443e-02	-9.663e-03	4.281e-01
112/-Z	2.566e-02	1.010e+00	2.925e-03	2.074e-02	3.714e-01
112/-X	6.296e-02	-4.961e-02	-6.884e-02	2.290e-01	1.187e-01
11/-Z	-2.212e-01	1.839e+00	-3.467e-02	-4.183e-02	-6.035e-01
1/-Z	-1.184e-01	1.350e+00	-1.839e-02	-5.942e-03	-4.794e-01
12/-Z	-1.664e-02	9.558e-01	-8.360e-03	1.146e-02	-3.968e-01
12/-X	-6.356e-02	2.006e-01	6.633e-02	2.300e-01	-1.434e-01
201/-X	4.099e-04	9.044e-04	8.047e-04	-2.830e-02	-6.861e-03
201/-Y	-1.496e-02	-2.587e-02	-2.208e-02	-9.393e-05	2.658e-01
201/-Z	-2.468e-04	2.553e-01	-8.693e-04	5.542e-03	1.483e-03
302/-Y	-1.190e-01	1.965e-02	4.797e-03	1.132e-03	-4.507e-02
301/-X	3.534e-03	-1.150e-01	-3.549e-02	-3.496e-02	5.451e-01
301/-Z	-2.279e-01	5.766e-02	-4.500e-02	-4.430e-03	9.956e-01
303/-X	1.029e-02	-1.532e-02	3.578e-02	-3.467e-02	-5.895e-01
303/-Z	2.409e-01	5.844e-02	4.667e-02	-6.676e-03	-1.029e+00
205/-Y	-1.855e-02	6.060e-02	4.221e-02	5.423e-04	1.623e-02

Table 5.3: Mass normalized modeshapes

DOF	FE model	Test	CNAM
11 -Z	-1.9425e-01	-2.1084e-01	-1.2245e-01
1 -Z	-2.0671e-01	-2.2120e-01	-1.3232e-01
12 -X	1.0018e-01	6.8343e-02	3.7498e-02
12 -Z	-2.2274e-01	-2.4736e-01	-1.4935e-01
5 -X	6.2270e-02	3.8283e-02	2.4965e-02
5 -Z	2.2410e-02	8.7033e-02	5.1007e-02
8 -Z	1.0906e-01	1.7198e-01	1.1044e-01
111 -Z	1.9425e-01	1.9867e-01	1.2242e-01
101 -Z	2.0671e-01	2.3346e-01	1.3238e-01
112 -X	-1.0018e-01	-3.5782e-02	-4.0803e-02
112 -Z	2.2274e-01	2.4969e-01	1.4435e-01
105 -X	-6.2270e-02	-3.9193e-02	-2.3945e-02
105 -Z	-2.2410e-02	-8.0323e-02	-4.8402e-02
108 -Z	-1.0906e-01	-1.7049e-01	-1.0170e-01
201 -X	7.9818e-12	4.1935e-05	-1.6933e-04
201 -Y	1.9049e-02	-4.3013e-03	3.7497e-04
201 -Z	-4.0715e-12	-1.4436e-03	-1.0822e-04
206 -Z	-2.3427e-12	-1.9260e-03	-2.2734e-04
205 -Y	-1.2461e-01	-8.8705e-02	-5.2732e-02
302 -Y	4.4911e-01	4.3956e-01	2.6463e-01
301 -X	1.9686e-02	7.7945e-02	2.6659e-03
301 -Z	3.7794e-01	3.6447e-01	2.1562e-01
303 -X	-1.9686e-02	-1.7355e-02	-2.2858e-02
303 -Z	-3.7794e-01	-4.3194e-01	-2.3560e-01

Table 5.4: mass normalized modeshape for 16.16 Hz - 1.42 %

Annex 12

INTESPACE CONTRIBUTION

intespace
L'Intelligence de l'Environnement

O/Ref. : DO96.034 DG/ER

Toulouse, August 21 , 1996

GARTEUR - SM-AG 19
MODAL ANALYSIS REPORT

ONERA	**Mr. E. BALMES**	**(2 copies)**
AÉROSPATIALE Toulouse	**Mr. J-P. ESQUERRE**	**(1 copy)**
CNAM	**Mr. N. HENRIET**	**(1 copy)**
DLR	**Mr. M. DEGENER**	**(1 copy)**
DRA	**Mr. W. SKINGLE**	**(1 copy)**
FOKKER Aircraft BV	**Mr. P. SCHIPPERS**	**(1 copy)**
Imperial College	**Mr. A. ROBB**	**(1 copy)**
MANCHESTER University	**Mr. E. COOPER**	**(1 copy)**
NLR AE	**Mr. J. PERSOON**	**(1 copy)**
SAAB SCANIA AB	**Mr. T. ABRAHAMSON**	**(1 copy)**
SOPEMEA	**Mr. B. CARRE**	**(1 copy)**

18, Avenue Edouard-Belin, B.P. 4356, 31029 TOULOUSE CEDEX 4
Tél. (33) 61 28 11 11, Télécopieur : (33) 61 28 11 12
S.A. au Capital de 8 800 000 F - R.C.S. TOULOUSE B 3 26 100 971 - SIRET 326 100 971 00018 - APE 743 B

INTESPACE Research and Development Division	CLASSIFICATION CONTRACT Contract Reference / Contractor

Contractual	Program/Project	Work Package	Task	Imputation
yes	GARTEUR	-	-	J02858

TITLE : GARTEUR SM-AG 19 - Modal Analysis Report

AUTHOR(S) : P-E. DUPUIS

DATE	ISSUE	REFERENCE NUMBER	NUMBER OF		
			Pages	Figures	References
21-08-96	1	DO96.034 DG/ER	33	16	5

SUMMARY :

This document describes first the modal tests performed on GARTEUR SM-AG 19 specimen, then all the parameters issued from the subsequent modal identification and the way used to obtain them.

KEY WORDS		NAME	SIGNATURE
Modal Survey Test . .	Prepared by	P-E. DUPUIS	
	Approval by	L.P. BUGEAT	
	Application authorised by	L.P. BUGEAT R&D Division Manager	

CONTENTS

1 - REASON FOR THE STUDY

This modal test take place in the GARTEUR activity issued from the work of the SM-EG 20 exploratory group [A1]. The goal of the modal test of the GARTEUR SM-AG 19 testbed [R1] is to measure the transfer function between the responses of the accelerometers fixed on the structure and the injected force located at two points. The excitation locations are the outer edge of each wing of the specimen fixing a dummy mass at the opposite side, which gives two test configurations.

The identification task is performed in order to constitute two experimental modal bases, corresponding to the two different configurations, with the eigen frequencies, the damping ratios and the mode shapes of the structure. These identified modal characteristics will be then comparable to the results obtained in different laboratories in Europe.

2 - REFERENCES

2.1. APPLICABLE DOCUMENTS

[A1] "GARTEUR - SM-EG 20 - Proposal for the formation of a GARTEUR action group on ground vibration test techniques", May 3rd, 1995.

2.2. REFERENCE DOCUMENTS

[R1] "Documentation for the GARTEUR SM-AG 19 testbed", ONERA document reference GARTEUR SM-AG 19, test documentation, April 25th, 1995.

[R2] DynaWorks® V3.1, User's Guide, INTESPACE document reference DY31.530_01F/1.3, November 11th, 1994.

[R3] DynaWorks® V4.0, User's Guide, INTESPACE document, issue 1.0, December 21th, 1995.

[R4] PROTO-Dynamique V3.2, User's Guide, INTESPACE document reference DO95.152 EI/ED, July 1st, 1995.

3 - ADMINISTRATIVE DETAILS

3.1. TEST REQUESTED BY

- INTESPACE

3.2. REPRESENTATIVE PRESENT FOR THE TEST

- INTESPACE : P-E. DUPUIS

3.3. DATES

The modal test has been performed from June 5th to 7th, 1996.

3.4. INTESPACE REFERENCE

For the test and the analysis, the reference is J02858.

4 - MODAL TEST

4.1. MATERIAL TESTED

The specimen tested is the GARTEUR SM-AG 19 testbed [R1].

4.2. TEST FACILITY

4.2.1 Site

The modal test takes place at INTESPACE.

4.2.2 Test set-up

The specimen is hanged up to a specific device furnished by ONERA [R1].

4.2.3 Excitation system

The excitation is obtained using an electrodynamics shaker with a maximum force of 200 N. This shaker is mounted on a low frequency suspension in order to mechanically decouple the excitation from the rest of the test set-up. A sweep sine signal from 5 to 65 Hz with a 0.25 octave/minute sweep velocity, is sent to the power amplifier attached to the shaker.

The excitation force is applied to the shaker through an adaptator containing one load cell. Figure 1 presents this test set-up and the excitation principle. Figures 2 and 3 present two examples of excitation.

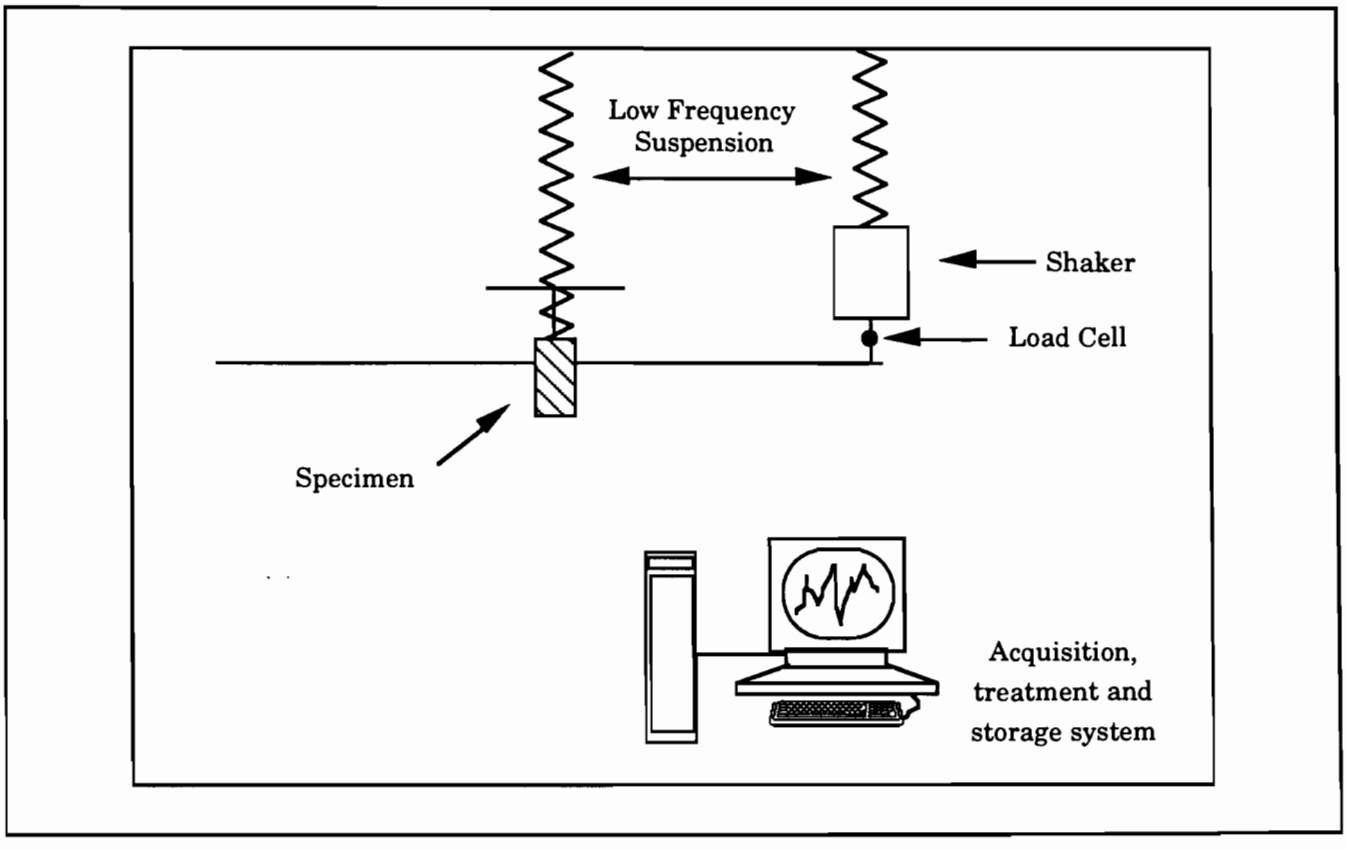

Figure 1 - Test Set-up

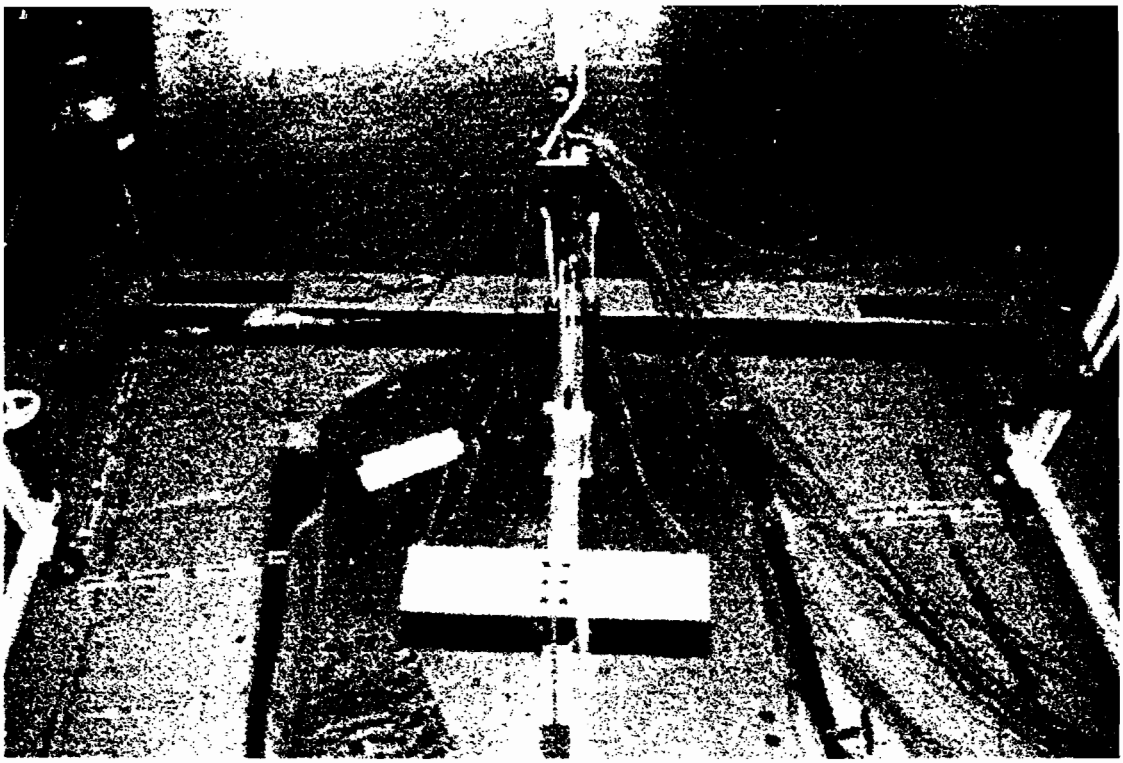

Figure 2 - Specimen with Dummy Mass on left side - Right Excitation

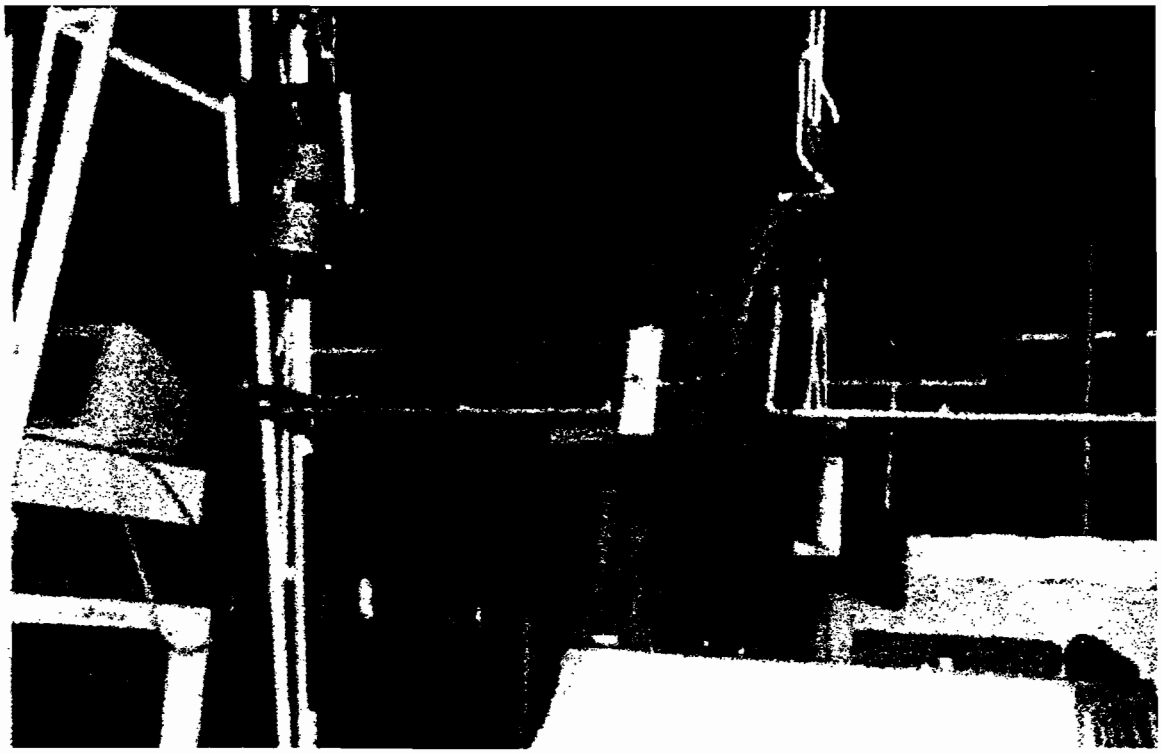

Figure 3 - Specimen with Dummy Mass on right side - Left Excitation

4.3. MEASUREMENT FACILITY

4.3.1 Instrumentation

The specimen is instrumented with 24 accelerometers plus three located on the suspension device. The sensor locations are tabulated and plotted in appendix 1.

4.3.2 Acquisition system

Each accelerometer is connected to an acquisition station which is able to process the 27 accelerometers channels simultaneously. Each channel signal is divided by the load cell signal, thus allowing to generate 27 transfer functions.

4.4. TEST LOG

4.4.1 Sequence

The test sequence is the following :

- configuration of the specimen
- set-up of the excitation system
- excitation and acquisition
- specimen integrity control
- results control (phases coherency, overload detection...)
- run acceptation

This test sequence is respected for each excitation configuration.

4.4.2 Results

For each test, the acquisition software ITS/SAMIX, generates a DynaWorks® 3.1 [R2] neutral file containing each global and filtered signal, and the transfer function obtained between each of the accelerometric channels and the excitation force signal. Table 1 presents the labels of the corresponding files delivered to ONERA.

Tests	N°	Universal files
Run at 1 N, along Z axis, left wing, 5 - 65 Hz	001Z	-
Run at 5 N, along Z axis, left wing, 5 - 65 Hz	004Z	garteur_4Z.dat
Run at 5 N, along Z axis, right wing, 5 - 65 Hz	005Z	garteur_5Z.dat

Table 1 - Tests/Universal Files correspondence

5 - SELECTION OF TEST RESULTS

5.1. PROCEDURE

For one excitation configuration, two excitation force levels were applied : at 1 N and at 5 N, in order to verify the linearity of the response and to determine the level allowing to obtain the best transfer functions, i.e. with the best signal/noise ratio. The transfer overplot allowed to verify that responses were independent from the excitation level on a great part of the frequency range.

The 5 N excitation level, given the best signal/noise ratio, was selected for modal identification.

5.2. TOOL

The software used for the plots and the management of all test data is DynaWorks® version 4.0 [R3].

5.3. RESULTS

The transfer functions obtained are written in an archive base which is used for the identification described in the next chapter.

6 - MODAL IDENTIFICATION

6.1. TOOL AND METHOD

The identification task is performed with DynaWorks® version 4.0 [R3] software which includes the identification method developed by the Professor LINK (University of Kassel, Germany).

The modal parameters of the fundamental equation of motion are adjusted to measured frequency responses by curve fitting algorithms which minimize the least square deviation of measured and recalculated response.

The influence of out of range modes is taken into account through the use of residual correction terms.

6.2. MODE SHAPES IDENTIFICATION

The modal parameters are identified using all the available responses.

The mode shapes are identified on the experimental geometry defined in the previous chapter. This allows the generation of 10 modal vectors with 21 components each (21 degrees of freedom).

The resulting mode shapes are stored in a temporary modal base with all the modal results (modal parameters, bandwidth used...) related to the two tests.

7 - COHERENCY CONTROL OF THE MODAL DATABASE

This last step is essential : it allows the elimination of numerical modes or modes which are not well identified in order to build a final modal base with physical modes which allows a good representation of the dynamic behaviour of the structure. This "sorting" is based on three main criteria.

The first one consists in visualisation of the mode shapes on the experimental structure, in order to point out incoherencies due to identification errors. This allows also the detection of sensors with wrong polarity (corresponding to "opposite" behaviour compared to the other sensors).

The second criteria consists in the computation of the MAC matrix (Modal Assurance Criterion) which allows the quantification of the geometrical independence between modes shapes. This correlation is achieved through the following definition :

$$\text{For two modes } \phi_1 \text{ and } \phi_2\text{, the MAC is : } \quad MAC(\phi_1,\phi_2) = \left\| \sum_{j=1}^{21} \phi_{1j}\phi_{j2} \right\|^2 / \left(\sum_{j=1}^{21} \phi_{1j}\phi_{j1} \sum_{j=1}^{21} \phi_{2j}\phi_{j2} \right)$$

This value is a kind of scalar product or coherency computation in FRF estimation. If MAC takes on a value near zero, that means that the modes shapes are linearly independent. This can be used as an approximation of an orthogonality check. This is a geometrical orthogonality check.

The last criteria, maybe the most physical one, is the response synthesis. It is possible to synthesise with modal superposition, transfer functions built on the modal data identified. By this way, for a given sensor, the comparison between a synthesised transfer and the initial measured one, can quantify the representativity of the dynamic response built on these identified data.

After the coherency control of the modal base, 10 modes have been identified for the two configurations :

Mode N°	Frequencies (Hz)	Viscous damping (%)	Comments
1	6.1	4.1	
2	7.7	2.9	
3	16.3	1.1	
4	33.7	1.0	
5	36.0	0.7	
6	40.7	0.9	
7	49.6	3.4	
8	50.3	0.9	
9	56.7	0.1	
10	64.0	0.4	

Table 2 - Identified Modes for Left Excitation (004Z)

Mode N°	Frequencies (Hz)	Viscous damping (%)	Comments
1	6.2	3.8	
2	7.3	4.2	
3	16.3	1.2	
4	33.3	0.7	
5	35.8	1.0	
6	41.4	0.8	
7	49.4	3.2	
8	50.0	0.4	
9	56.7	0.2	
10	63.9	1.3	

Table 3 - Identified Modes for Right Excitation (005Z)

The identified modal base is then exported, under SDRC dataset 55 universal file format, to PROTO-Dynamique [R4] software which works in a matrix environment and includes a lot of tools for test-analysis comparison and optimisation.

The MAC matrix computed on this base points can be represented as plotted in Fig. 4a and 4b. The four main values are tabulated for each mode in appendix 3.

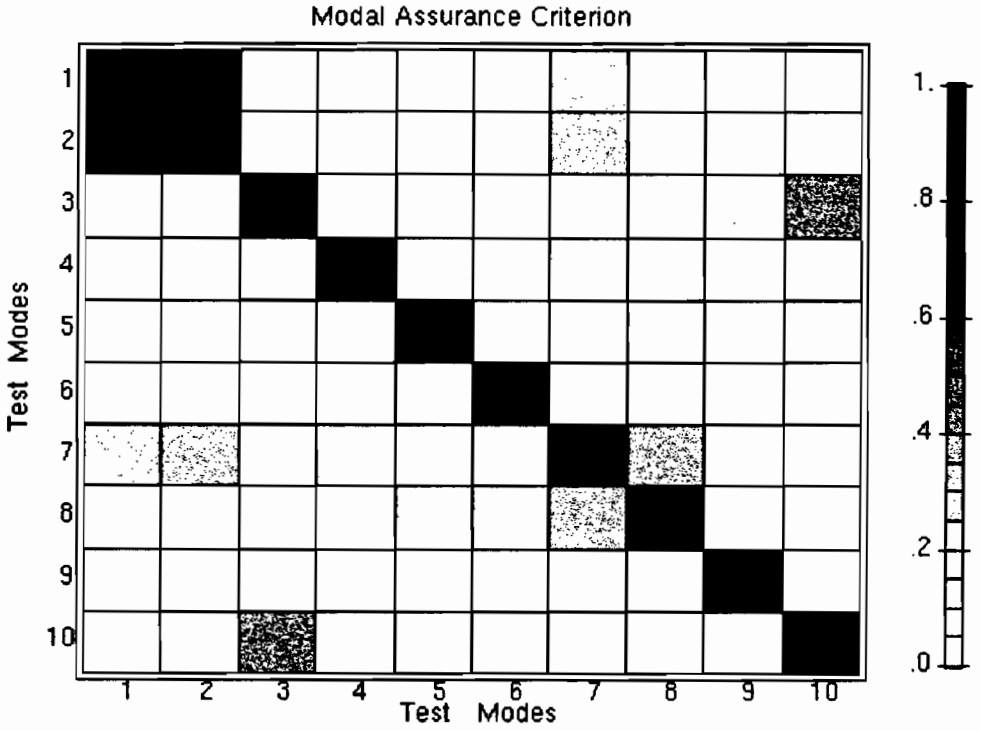

a - Left Excitation (004Z)

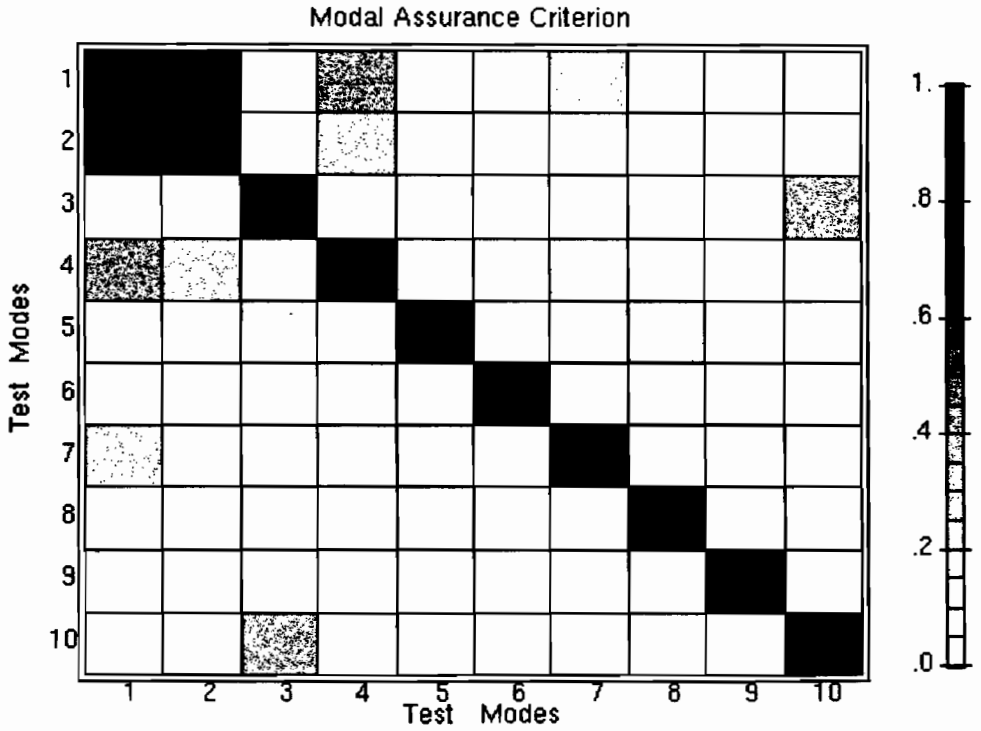

b - Right Excitation (005Z)

Figure 4 - MAC Matrix between Identified Modes

The comparison of results show a very good coherency between the two runs.

In appendix 2 are plotted the three first modes for each configuration.

In appendix 4 are plotted the response curves compared to the corresponding synthesis ones. The results show a very good coherency of the modal base and its ability to represent the dynamic behaviour of the specimen.

8 - CONCLUSION

Two modal tests have been performed on the GARTEUR SM-AG 19 testbed corresponding to two configurations.

DynaWorks® software has been used to compare and to manage the data in a first step and to perform the modal identification in a second step.

This identification points out 10 modes for each configuration, in the 5-65 Hz analysis bandwidth. The consistency of the identified modal base (eigen frequencies, damping ratios and mode shapes) have been checked through geometric orthogonality tests, through mode shapes visualisation on an experimental model previously built, and through response synthesis.

These criteria have pointed out the coherency of the modal base and its ability to represent the dynamic behaviour of the specimen.

This modal base can be now compared to the results obtained by the other partners.

Appendix 1

Nodes of the experimental model

Node	X (cm)	Y (cm)	Z (cm)	Instrumented dofs
1	0	-95	0	Z+
2	0	-90	0	
3	0	-80	0	
4	0	-70	0	
5	0	-60	0	X+ Z+
6	0	-50	0	
7	0	-40	0	
8	0	-30	0	Z+
9	0	-20	0	
10	0	-10	0	
11	-20	-95	0	Z+
12	20	-95	0	X+ Z+
101	0	95	0	Z+
102	0	90	0	
103	0	80	0	
104	0	70	0	
105	0	60	0	X+ Z+
106	0	50	0	
107	0	40	0	
108	0	30	0	Z+
109	0	20	0	
110	0	10	0	
111	-20	95	0	Z+
112	20	95	0	X+ Z+
201	60	0	-9.6	X+ Y+ Z+
202	0	0	-9.6	
203	-40	0	-9.6	
204	-75	0	-9.6	
205	-90	0	-9.6	Y+
206	0	0	0	Z+
301	-90	-20	28.5	X+ Z+
302	-90	0	28.5	Y+
303	-90	20	28.5	X+ Z+
999	-	-	-	X+ Y+ Z+

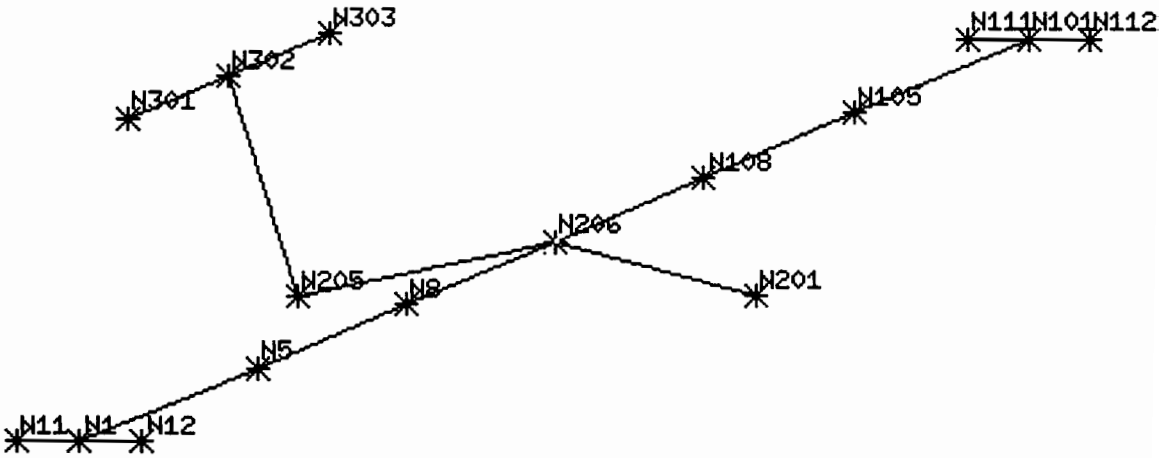

Instrumented DOFs

Appendix 2

Mode shapes visualisation

_____ : mode shape

\- - - - - - - - - - : undeformed structure

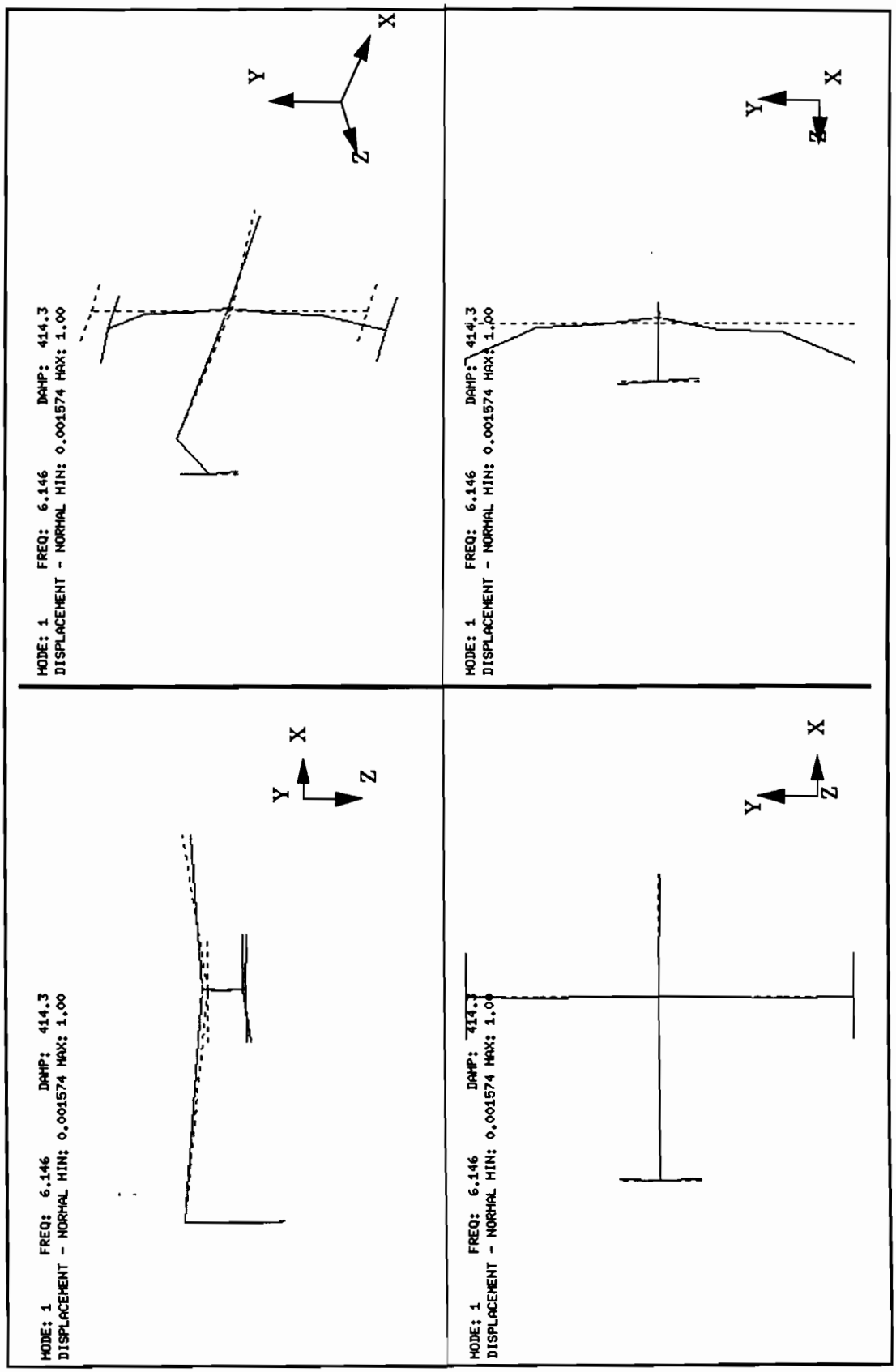

Run 004Z

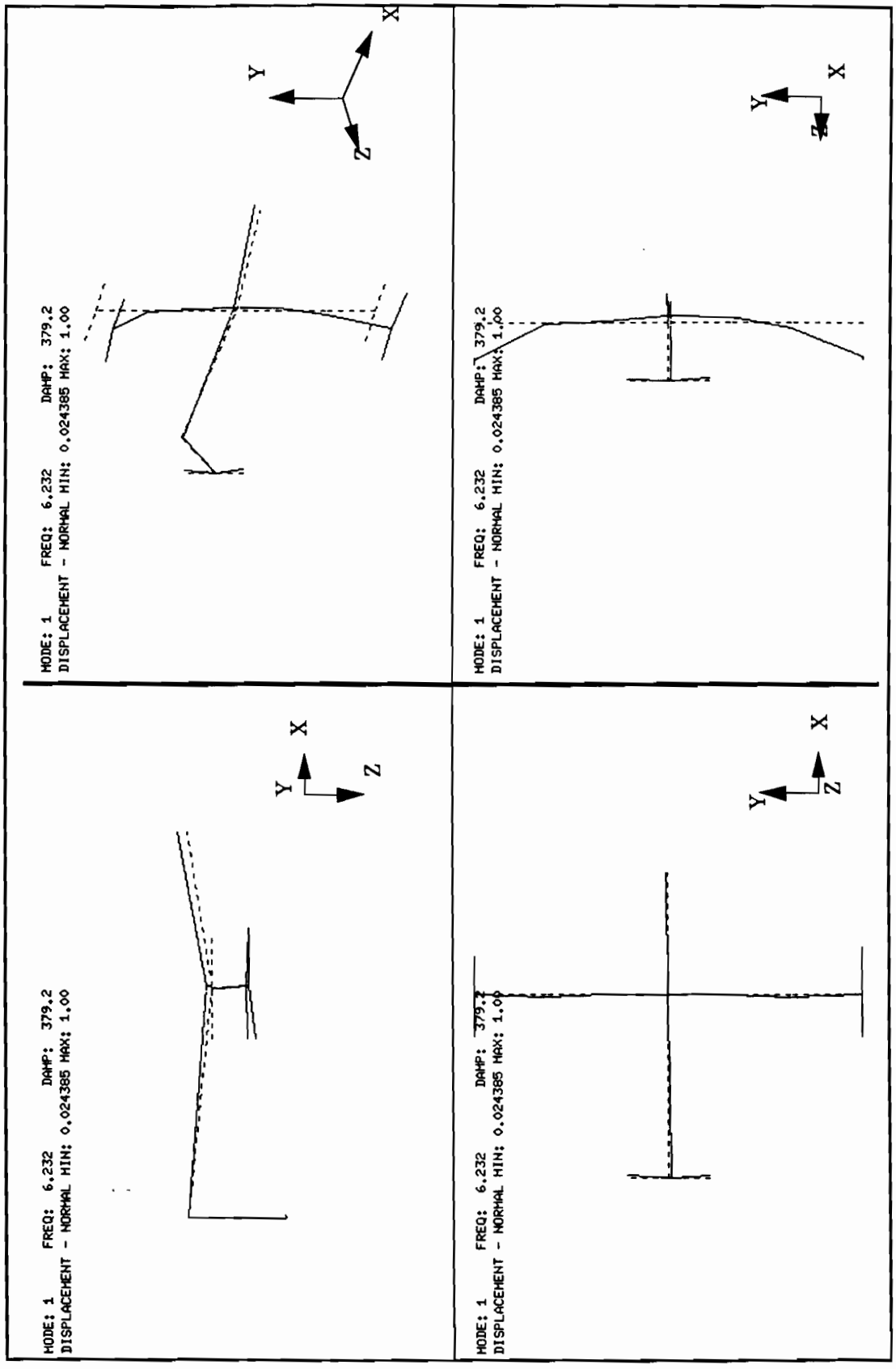

Run 005Z

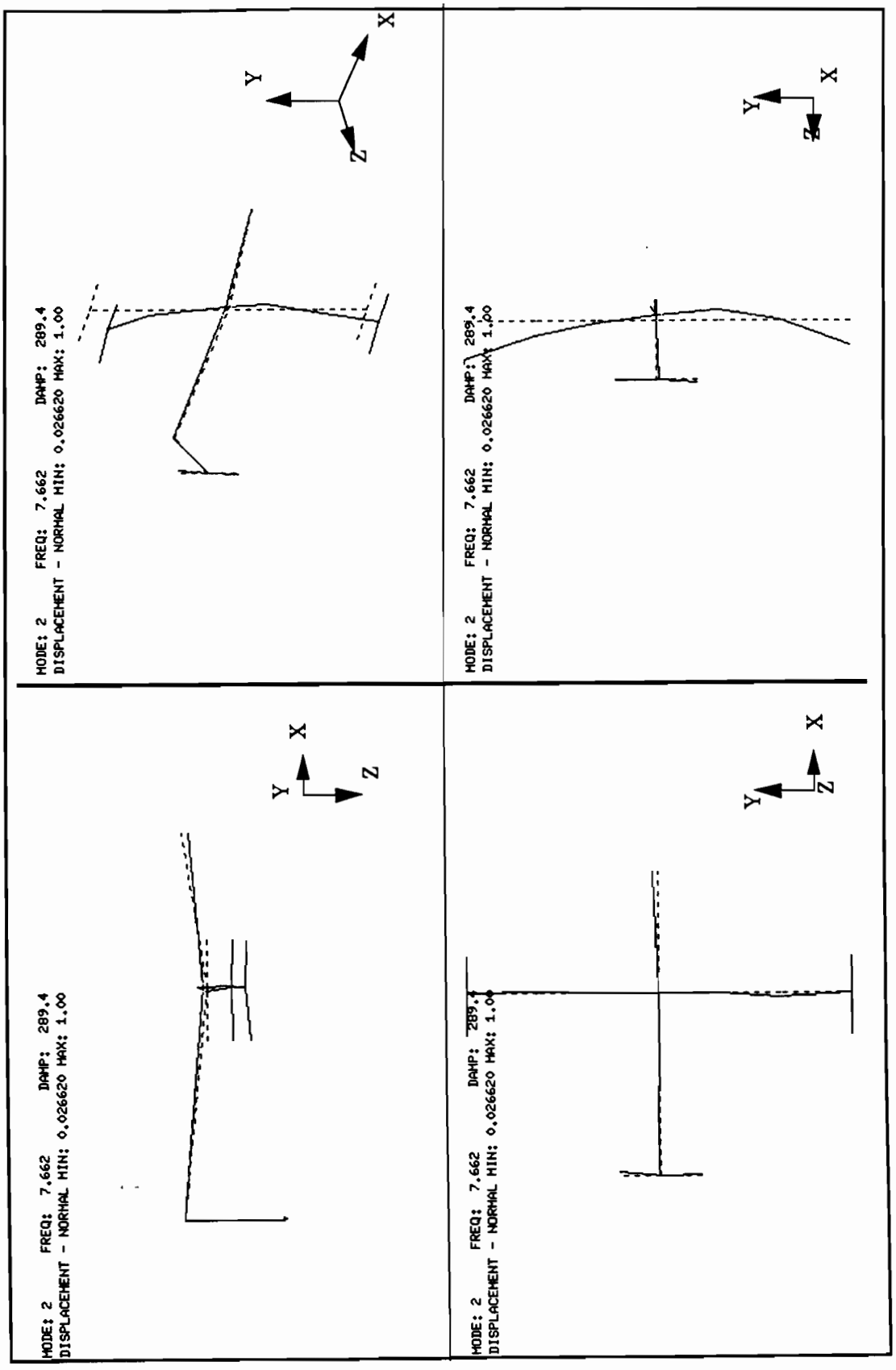

Run 004Z

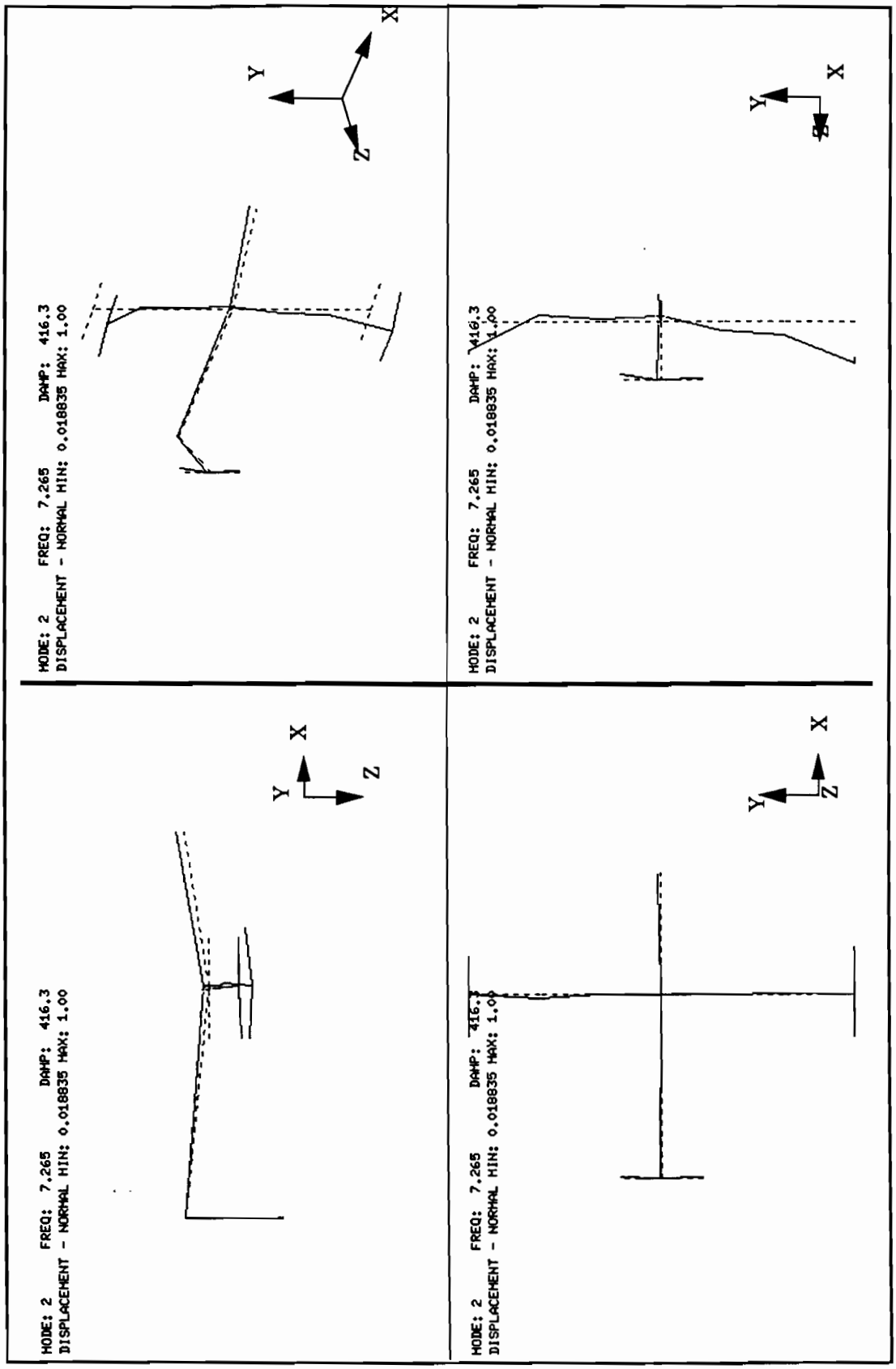
MODE: 2 FREQ: 7.265 DAMP: 416.3
DISPLACEMENT - NORMAL MIN: 0.018835 MAX: 1.00
X
Y
Z

Run 005Z

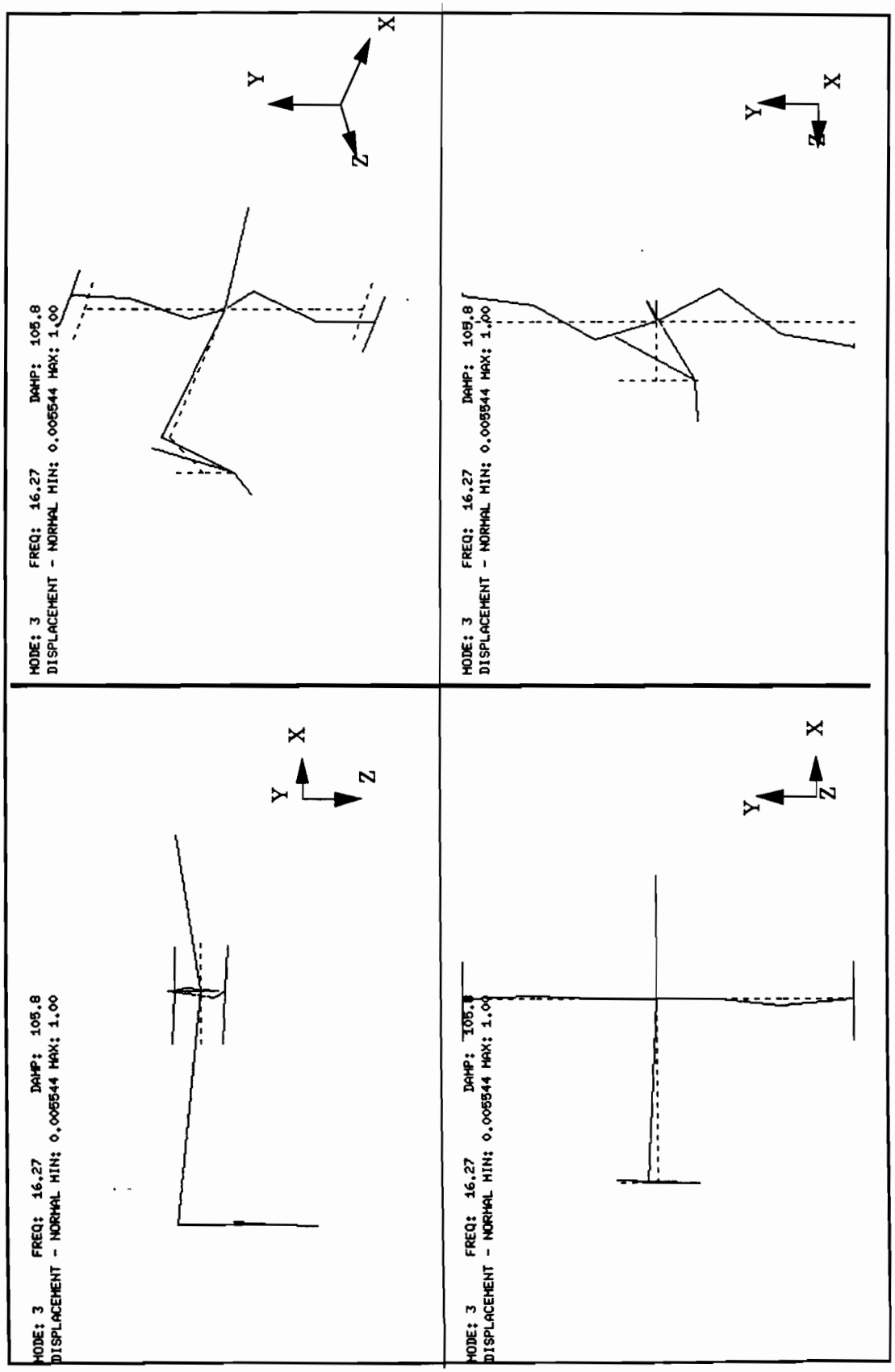

Run 004Z

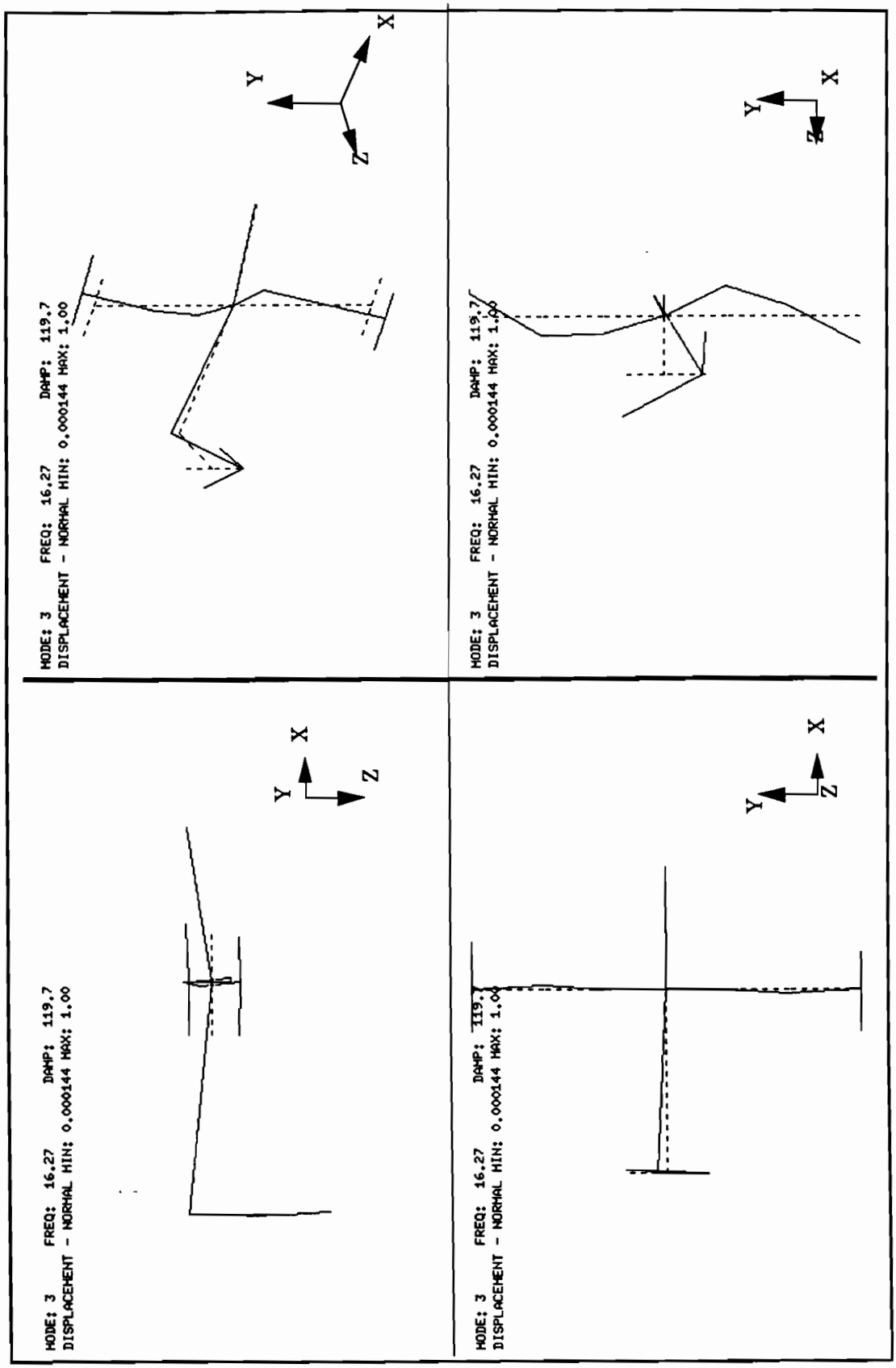

Run 005Z

Appendix 3

MAC matrices

MODAL ASSURANCE CRITERION

Structure: garteur
Model : initial
Test : garteur_4Z

Test Mode	Test Mode (value)	Test Mode (value)	Test Mode (value)	Test Mode (value)
1	1 (1.00)	2 (0.86)	7 (0.25)	8 (0.08)
2	2 (1.00)	1 (0.86)	7 (0.31)	10 (0.06)
3	3 (1.00)	10 (0.42)	5 (0.05)	4 (0.02)
4	4 (1.00)	7 (0.13)	8 (0.09)	5 (0.06)
5	5 (1.00)	8 (0.14)	4 (0.06)	3 (0.05)
6	6 (1.00)	8 (0.17)	7 (0.02)	4 (0.02)
7	7 (1.00)	8 (0.33)	2 (0.31)	1 (0.25)
8	8 (1.00)	7 (0.33)	6 (0.17)	5 (0.14)
9	9 (1.00)	2 (0.02)	3 (0.01)	10 (0.01)
10	10 (1.00)	3 (0.42)	2 (0.06)	5 (0.05)

MODAL ASSURANCE CRITERION

Structure: garteur
Model : initial
Test : garteur_5Z

Test Mode	Test Mode (value)	Test Mode (value)	Test Mode (value)	Test Mode (value)
1	1 (1.00)	2 (0.92)	4 (0.40)	7 (0.25)
2	2 (1.00)	1 (0.92)	4 (0.27)	7 (0.10)
3	3 (1.00)	10 (0.37)	4 (0.07)	7 (0.06)
4	4 (1.00)	1 (0.40)	2 (0.27)	7 (0.11)
5	5 (1.00)	8 (0.19)	7 (0.13)	4 (0.10)
6	6 (1.00)	4 (0.03)	7 (0.01)	9 (0.01)
7	7 (1.00)	1 (0.25)	5 (0.13)	4 (0.11)
8	8 (1.00)	5 (0.19)	7 (0.04)	10 (0.04)
9	9 (1.00)	6 (0.01)	4 (0.01)	10 (0.01)
10	10 (1.00)	3 (0.37)	8 (0.04)	4 (0.02)

Appendix 4

Synthesised transfers compared to the measured ones

_____ : Measured transfers

_ _ _ _ _ _ _ _ _ _ _ _ _ _ _ : Synthesised transfers

The transfers presented are available in the files :

J96000000004Z_0
J96000000005Z_0

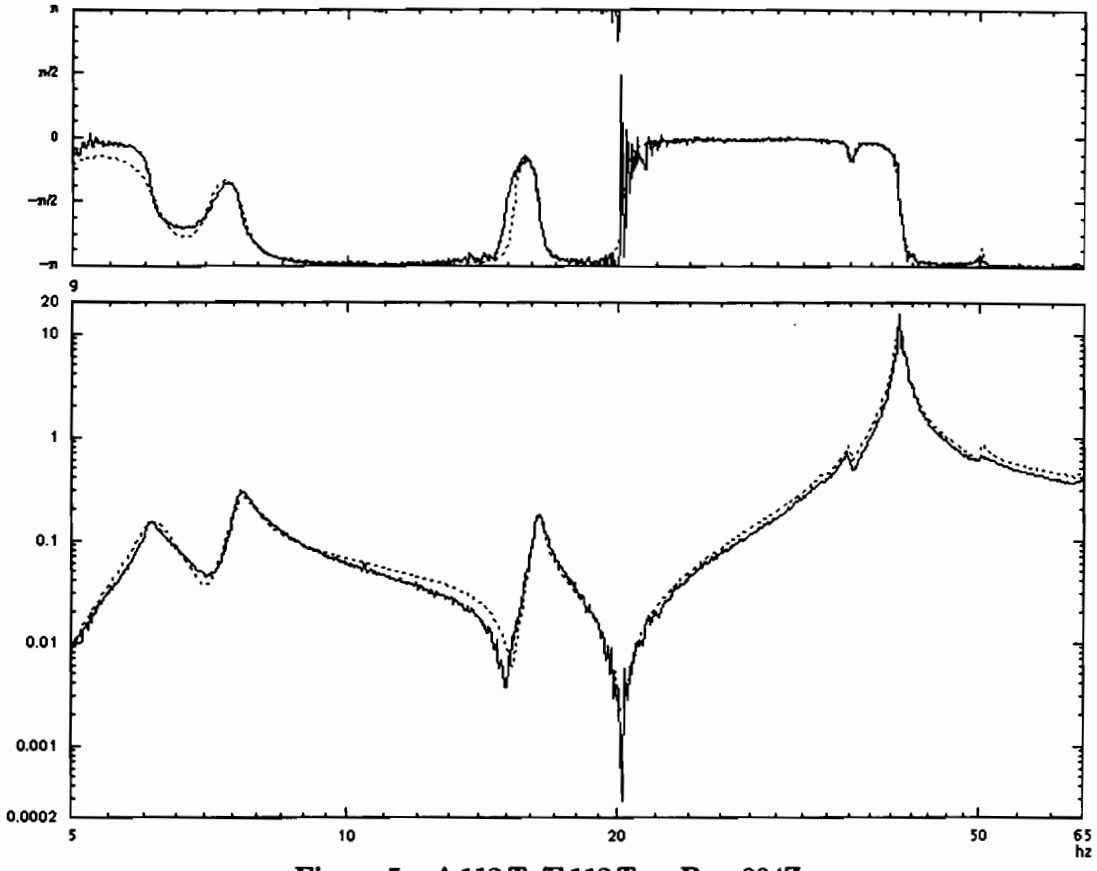

Figure 5 - A 112 Tz/F 112 Tz - Run 004Z

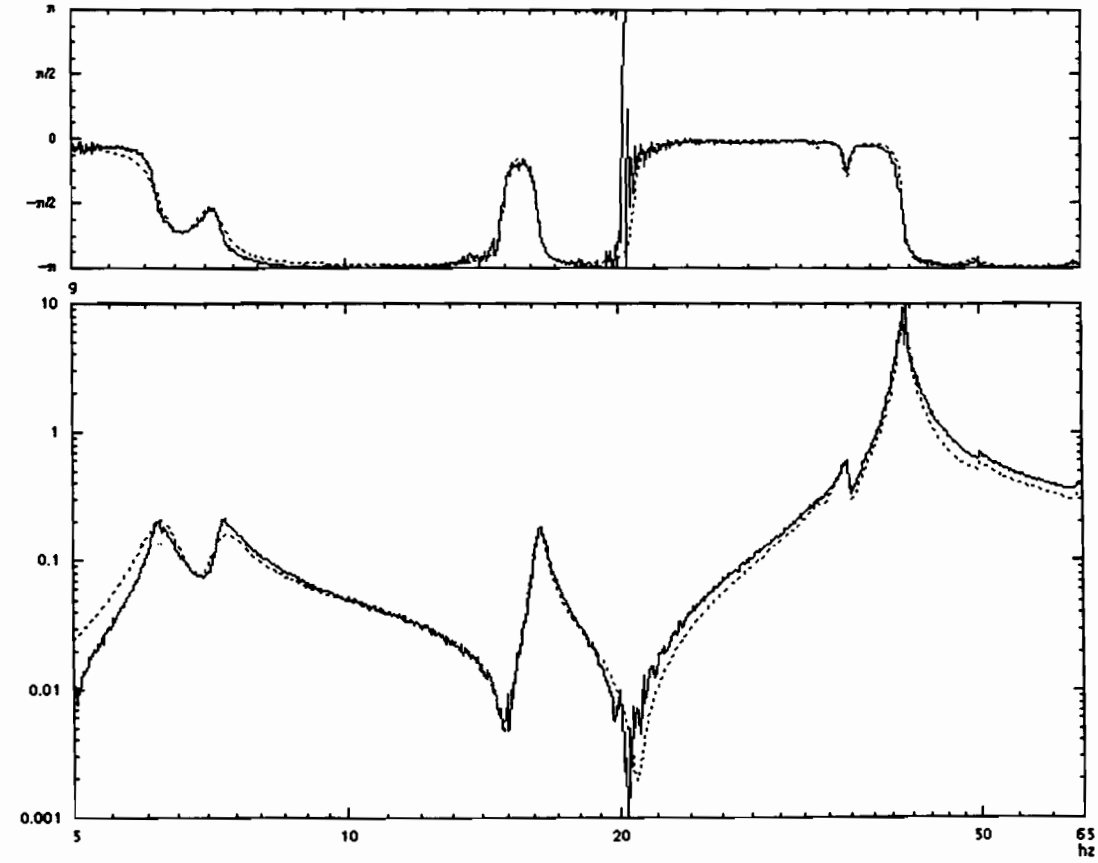

Figure 6 - A 12 Tz/F 12 Tz - Run 005Z

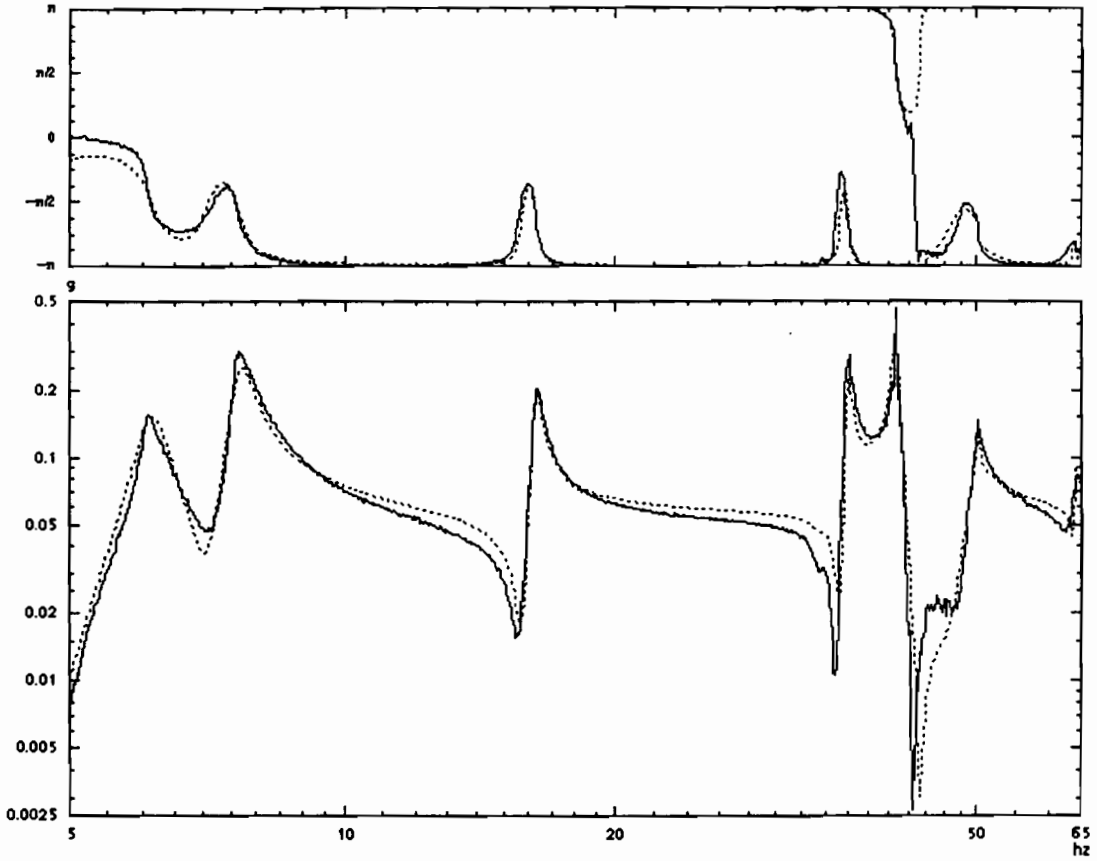

Figure 7 - A 101 Tz/F 112 Tz - Run 004Z

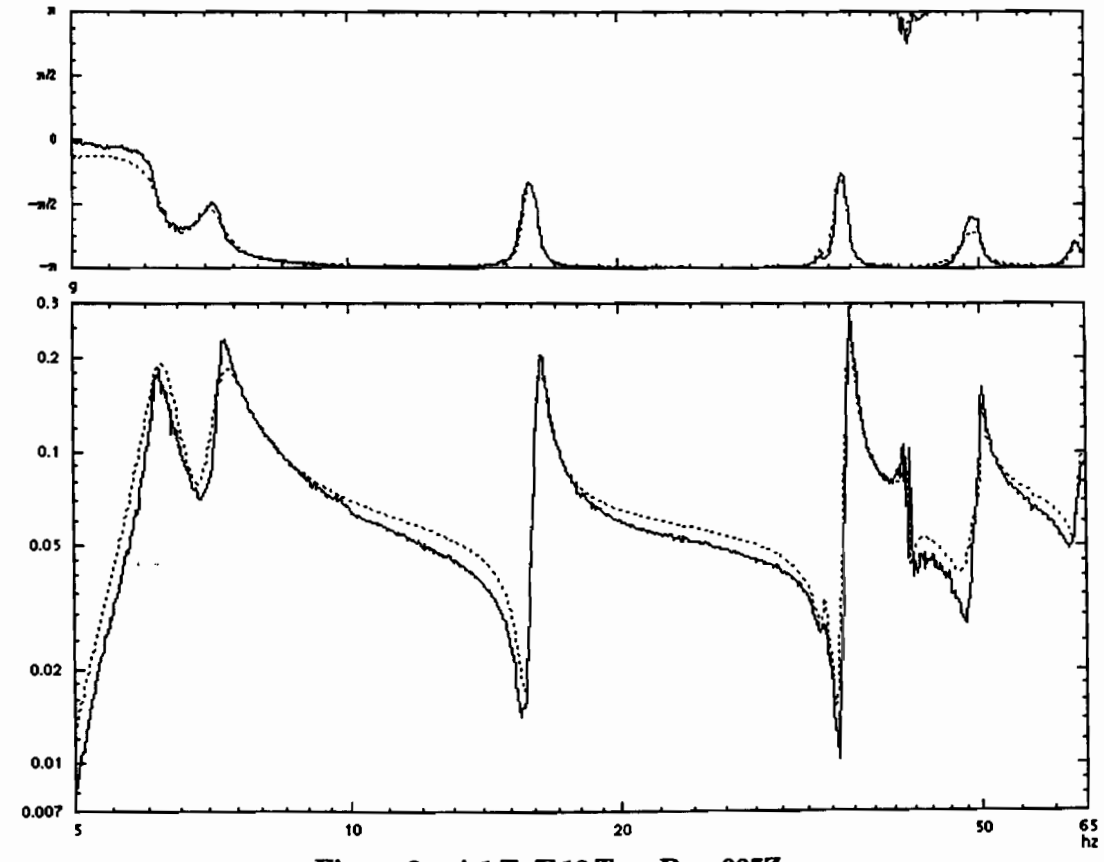

Figure 8 - A 1 Tz/F 12 Tz - Run 005Z

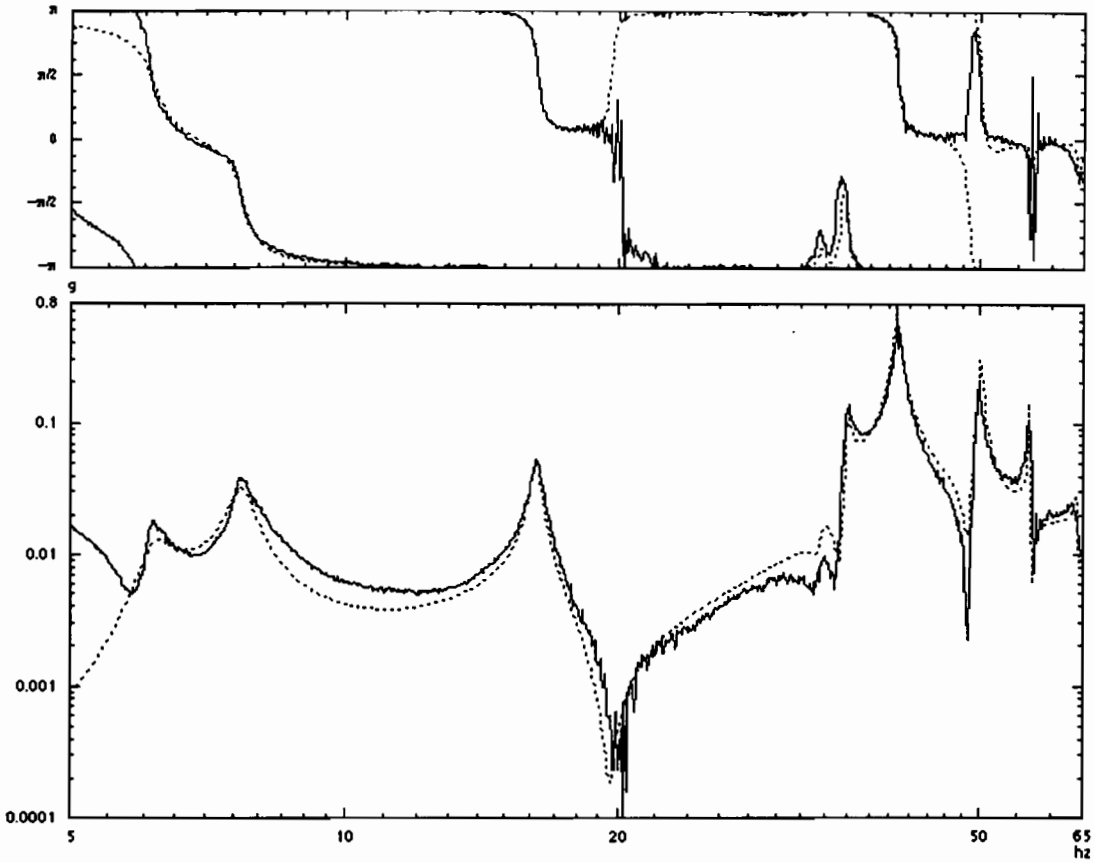

Figure 9 - A 112 Tx/F 112 Tz - Run 004Z

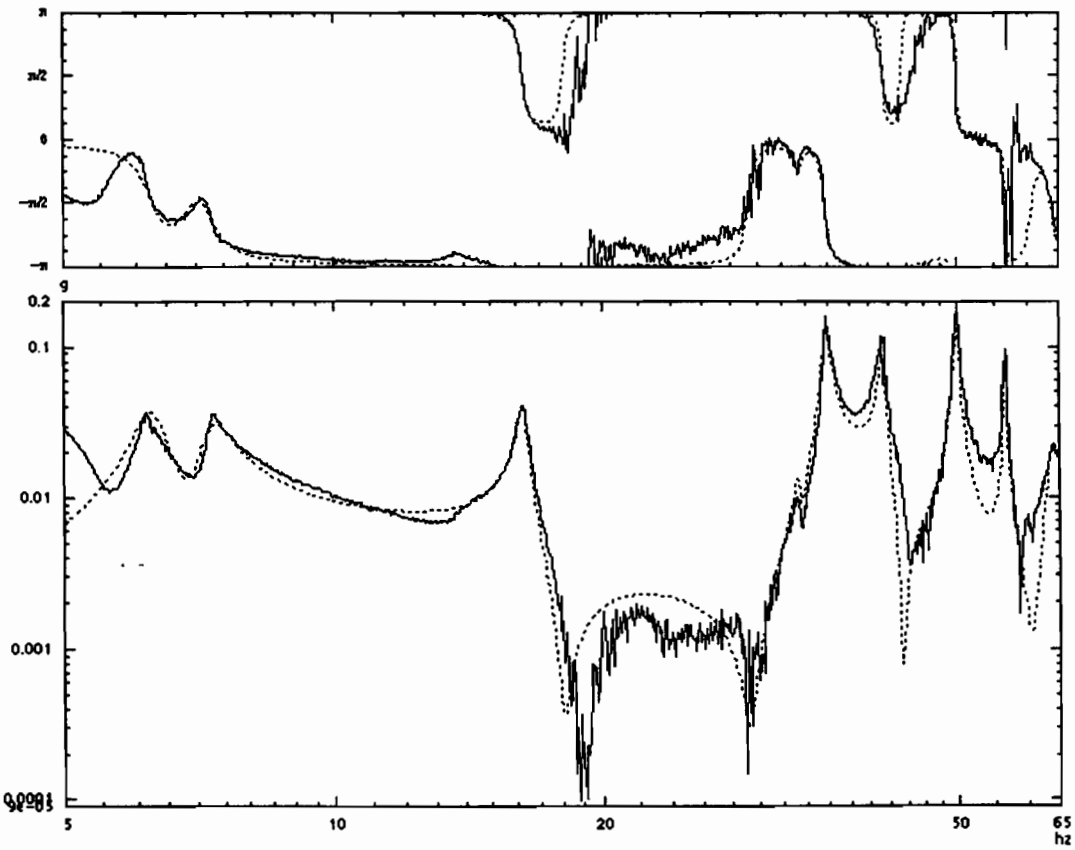

Figure 10 - A 12 Tx/F 12 Tz - Run 005Z

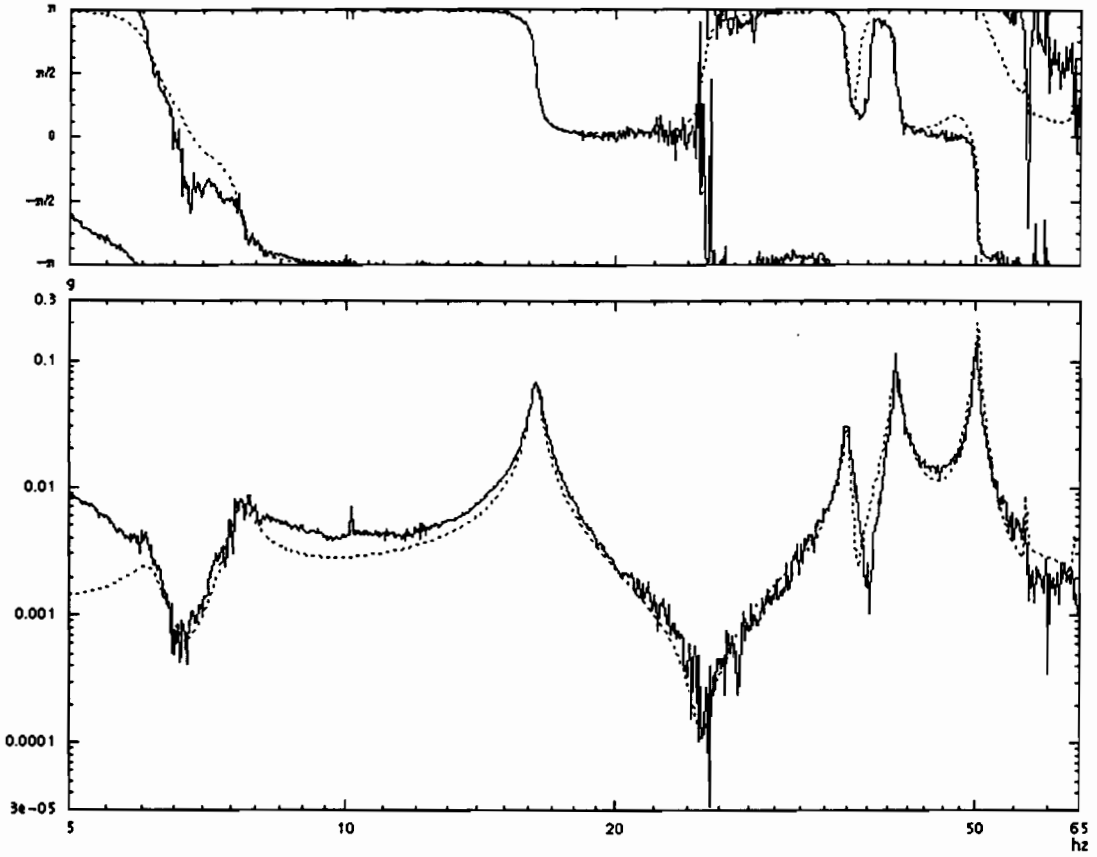

Figure 11 - A 205 Ty/F 112 Tz - Run 004Z

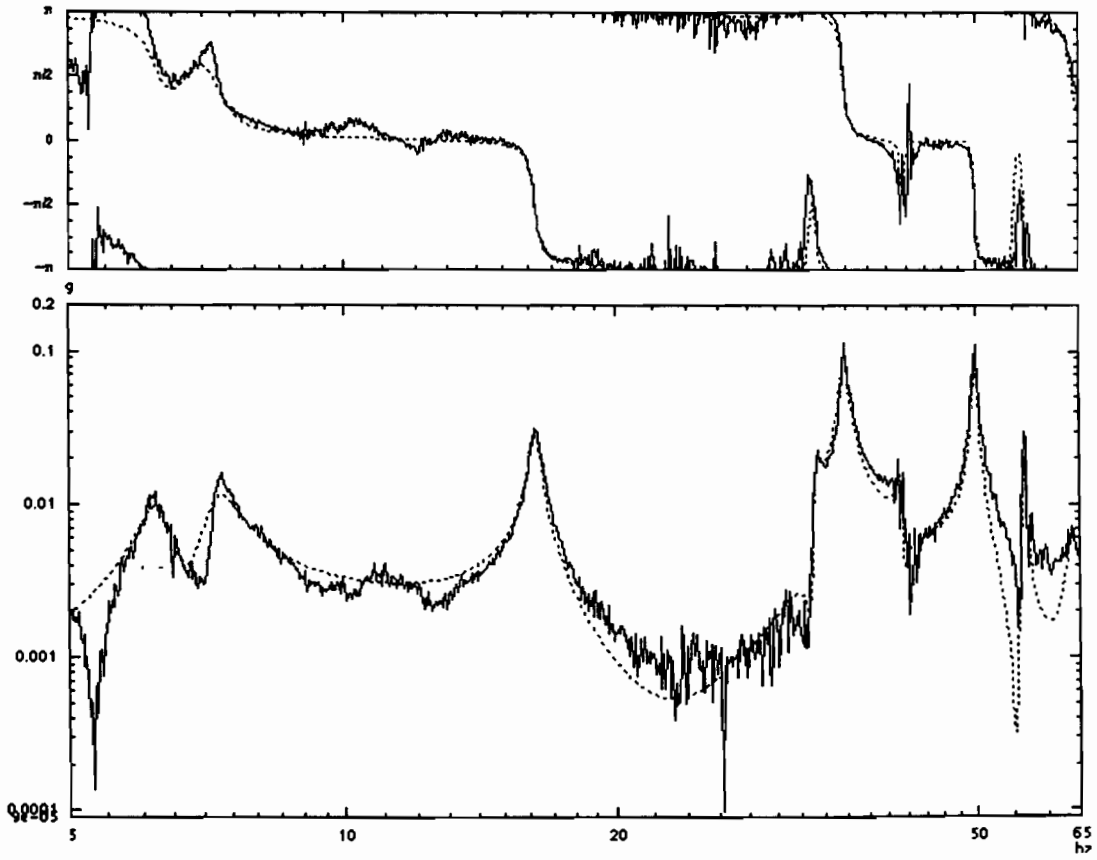

Figure 12 - A 105 Tx/F 12 Tz - Run 005Z

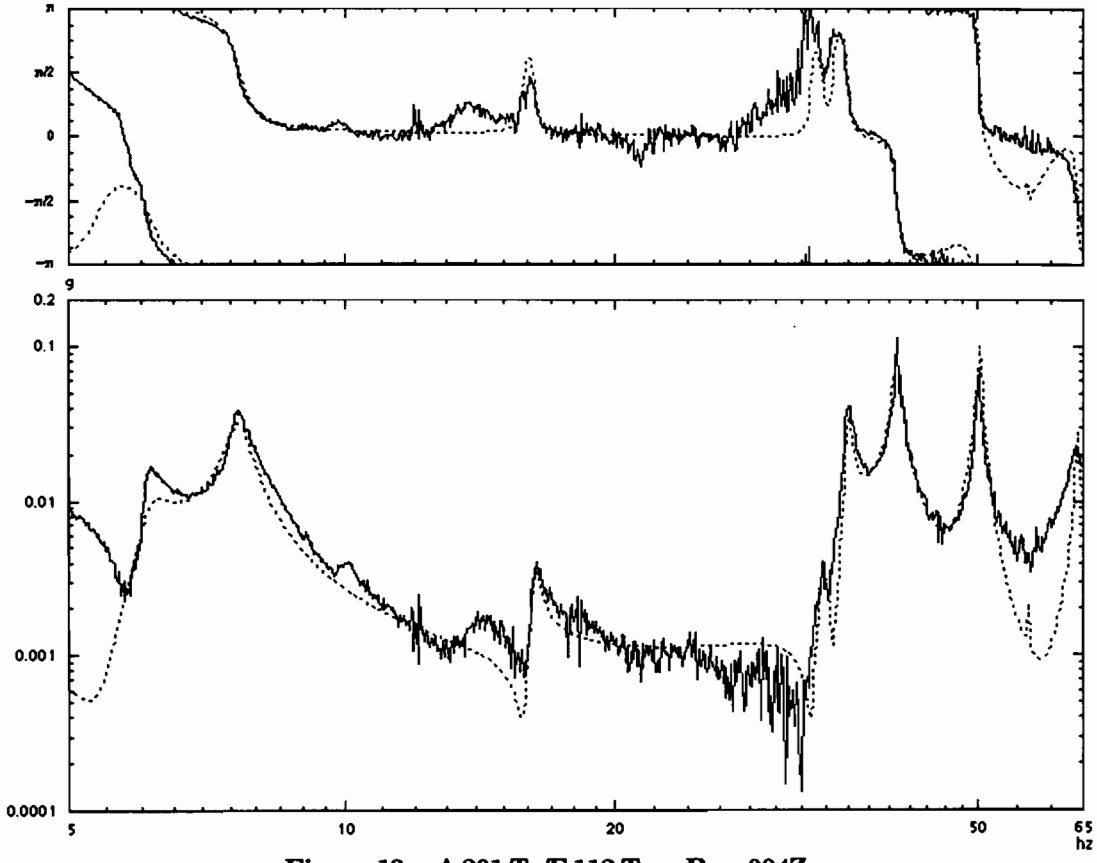

Figure 13 - A 201 Ty/F 112 Tz - Run 004Z

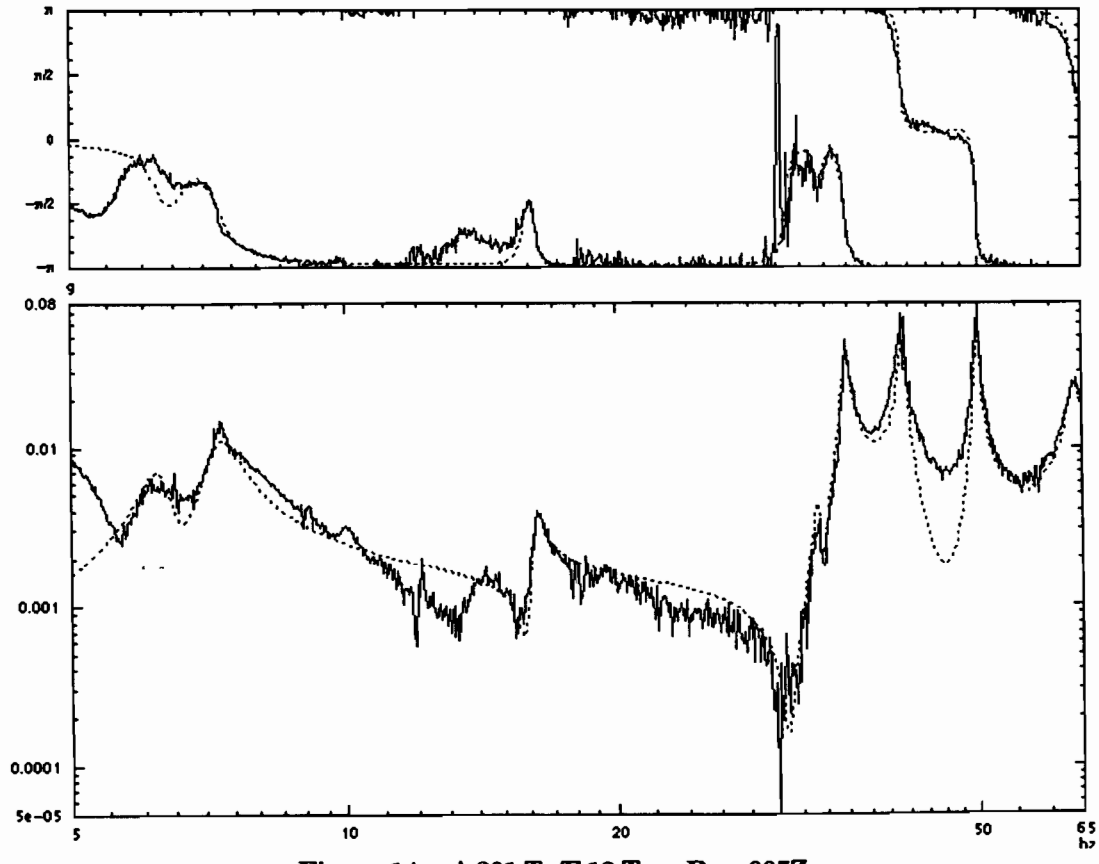

Figure 14 - A 201 Ty/F 12 Tz - Run 005Z

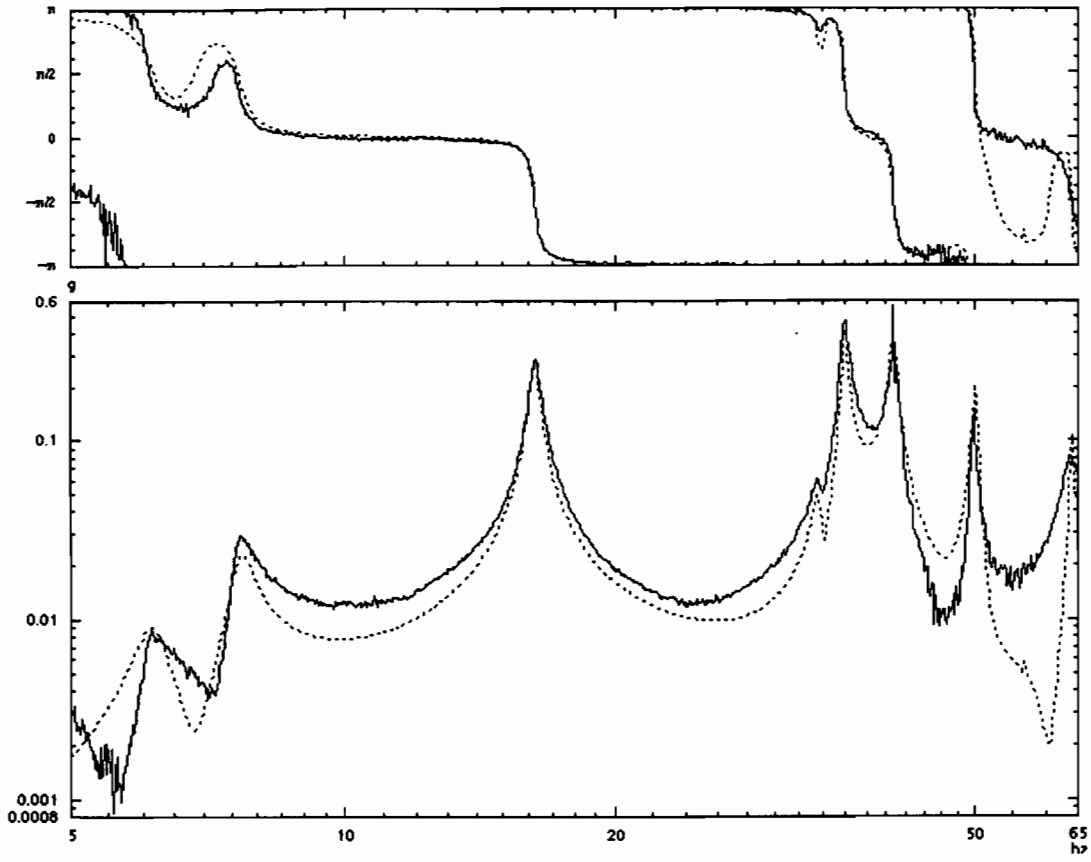

Figure 15 - A 301 Tz/F 112 Tz - Run 004Z

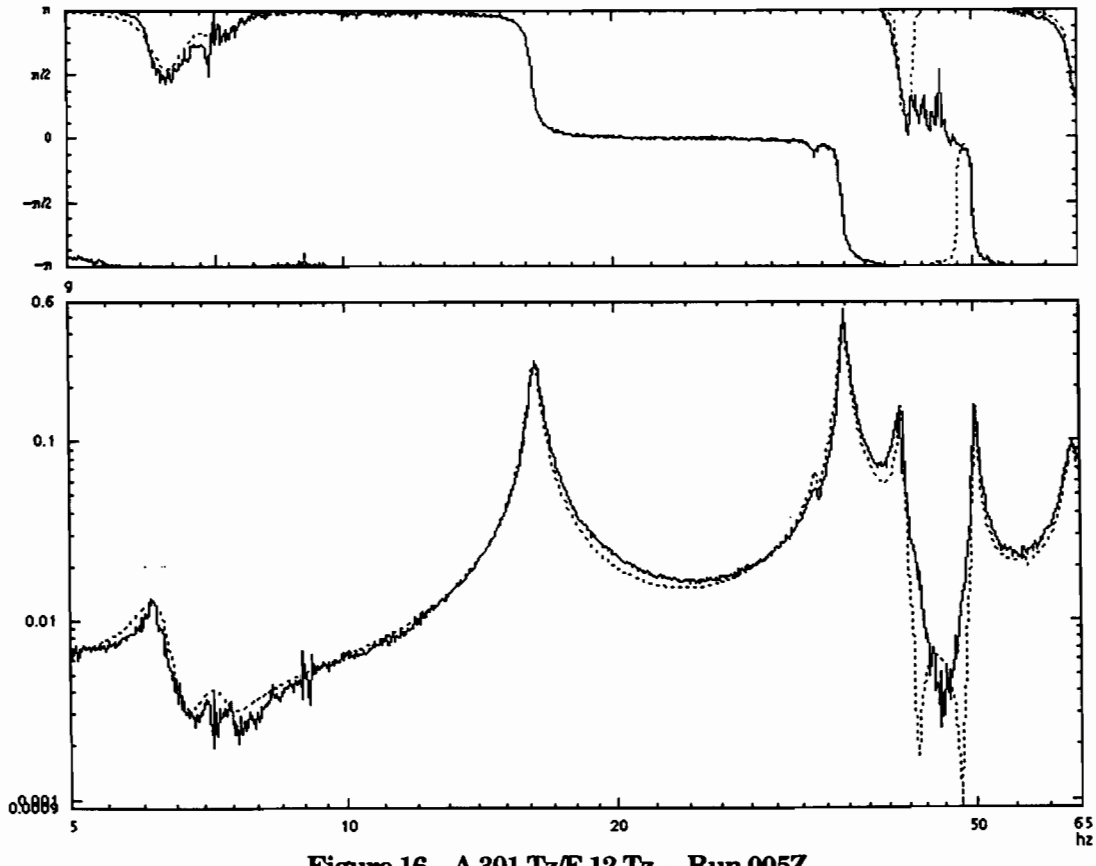

Figure 16 - A 301 Tz/F 12 Tz - Run 005Z

Annex 13

IMAC (USA) PUBLICATION

GARTEUR GROUP ON GROUND VIBRATION TESTING. RESULTS FROM THE TEST OF A SINGLE STRUCTURE BY 12 LABORATORIES IN EUROPE.

Etienne Balmès
DRET / AC, ONERA, Structures Department
B.P.72, 92322 Chatillon Cedex, FRANCE

ABSTRACT

In an effort to assess state of the art methodologies for the experimental determination of modal characteristics, 12 European groups, most of them working in the area of aircraft ground vibration tests for flutter certification, participated in a GARTEUR action group whose main activity was to have independent tests of a single representative structure. Design considerations for the common structure are first detailed. Estimates of frequency response functions and modal characteristics are then compared and show a level of consistency that is much higher than those reported in previous similar exercises.

1. INTRODUCTION

In the certification of new aircraft, Ground Vibration Tests (GVT) play an important role for the verification or updating of analytical models, allowing more accurate aeroelastic predictions. Facing the risk of flutter, a high level of quality and reliability in obtaining the modal characteristics of the aircraft has to be achieved during the GVT.

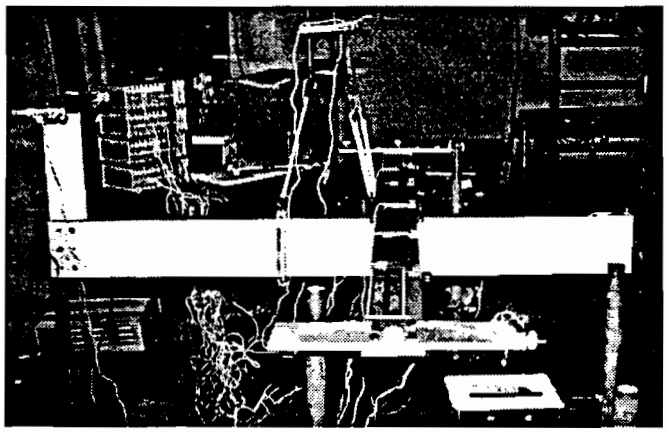

Figure 1: Common testbed of the GARTEUR SM-AG-19.

Following a series of previous Round Robin surveys held in the early 60s [1] and late 70s [2], a Structures and Materials Action Group SM-AG-19 of GARTEUR (Group for Aeronautical Research and Technology in Europe) was initiated in April 1995 with the major objective to compare a number of current measurement and identification techniques applied to a common structure. The testbed (see figure 1) was designed and manufactured by ONERA (France) and investigated by various companies, research centers and universities from France (ONERA, SOPEMEA, Aérospatiale, Intespace, CNAM), Germany (DLR), the Netherlands (NLR, Fokker), Sweden (Saab) and the United Kingdom (DRA, Manchester University, Imperial College).

More specifically, the objectives of the GVT tests were to evaluate the efficiency and reliability of test methods and to identify the cause of discrepancies between measured frequency responses or identified modal parameters. Each participant was required to provide:

- a set of 4 transfer functions corresponding to excitation and response of the left and right wing tip body (called *drums* in the rest of the paper) in the 4-60 Hz band. Although not required, most participants provided a 2 input 24 output set of transfer functions.
- estimated modal parameters (modeshape, frequency, damping factor, and modal mass) at 24 reference accelerometer locations.

The present paper outlines the activity of SM-AG-19 and compares data provided by the participants. Design considerations for the testbed are discussed in section 2. Frequency response measurements are compared in section 3 and modal parameters in section 4. In the comparisons, participants are identified by letters in chronological testing order. Some data sets obtained in a configuration differing from the test guidelines (see more details in section 2) are not comparable and are thus not included.

2. DESIGN CONSIDERATIONS

Specifications for the testbed were

- a group of 3 very close modes to make the problem difficult.
- 5 to 60 Hz, 50-100 kg, 2 by 2 m to make the testbed suitable for instrumentation designed for aircraft.
- a joint at the wing/fuselage connection for transportation but limiting variability from assembly to assembly.
- damping treatment to limit the effect of dissipation linked to instrumentation.
- suspension by a common set of bungees to have similar boundary conditions.
- 24 common sensor and 2 common shaker locations to allow direct comparisons.

The most difficult design criterion was the presence of 3 very close modes. On such a simple structure, close modal spacing can only be achieved by using modes of a different nature (bending modes in different directions, torsion modes, wing modes vs. tail modes). The relatively massive fuselage induces a near decoupling of torsion modes for each half wing, so that the first two torsion modes come as a pair. The design thus mostly adjusted the drum mass to put the frequency of the 2 torsions close to another mode (the 3 node bending eventually). As shown in figure 2, Nyquist plots of the final testbed show near the resonance a single lobe or three very coupled circles depending on the sensor.

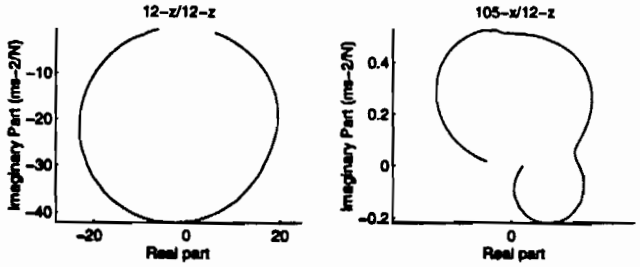

Figure 2: Nyquist plots near the resonance. A single circle is found on some transfer functions while the three modes are always very coupled.

To measure force, participants used load cells or electrical impedance (force/current factor on a current driven shaker). With the second technique, the moving mass, stiffness and damping of the shaker becomes part of the measured structure. On an aircraft the moving masses are so small that the effect is negligible, but for this small testbed a way to compensate for the added mass was needed. The design thus placed a 200g compensation mass at each drum tip (as shown in Fig. 3). In a case where additional mass was known to be added, the nominal mass could thus be replaced by a smaller one to physically compensate for the effect (the fact that the mass position does not exactly coincide with the expected shaker position was not taken into account).

Figure 3: Shaker attachments on the axes of the accelerometer (A) or the compensation mass (B).

The mass sensitivity, of the torsion modes in particular, significantly helped the design but was also one of the major sources of variations in the results of different tests. Inappropriate mass compensation was used for some tests so that not all data sets could be included in the comparisons of sections 3 and 4. Some groups also positioned their shaker on the mass axis rather than on the accelerometer axis (positions A and B in figure 2). The resulting data sets from different groups are clearly different (see following sections).

Sufficient damping levels were obtained through the use of a viscoelastic layer with an aluminum constraining layer. The viscoelastic used is the 3M acrylic viscoelastic polymer ISD 112 in the form of a 76 mm by 50 μm roll. A sample roll (Ref: SJ 2015 Type 1202) was provided by 3M Laboratories (Europe), Hansastr. 9, 41453 Neuss, Germany. This viscoelastic is particularly well suited for the testbed operating range of 5-50 Hz and 20 C where the loss factor is near its peak of 0.9.

Significant levels of shear strain are obtained in the viscoelastic through the use of a 1.1 x 76.2 x 170 mm constraining layer covering the complete viscoelastic treatment. The ISD 112 being pressure sensitive, the bonding was obtained easily and 3M confirmed that only extreme conditions should damage it. In a wing only test, damping factors increased significantly (from 0.28% to 1.1% in bending at 9 Hz and from 0.15% to 0.86% in torsion at 27 Hz) with the added treatment. Tests done on different days gave very similar results.

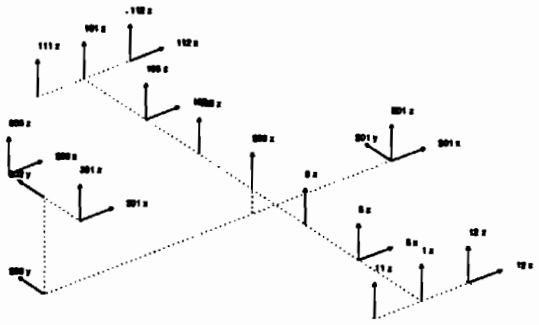

Figure 4: 24 common accelerometer locations. Nominal excitation locations are 12-z and 112-z.

Table 1 : Check of the sensor placement using the MAC comparison of a set of experimental modes with themselves.

Mode	1	2	3	4	5	6	7	8
1	100.0	0.0	0.2	1.6	0.5	18.1	0.0	0.1
2	0.0	100.0	0.5	0.2	0.0	0.1	0.1	0.0
3	0.2	0.5	100.0	0.3	11.8	1.7	0.5	0.1
4	1.6	0.2	0.3	100.0	1.1	1.8	0.1	2.0
5	0.5	0.0	11.8	1.1	100.0	0.8	21.3	0.0
6	18.1	0.1	1.7	1.8	0.8	100.0	0.5	0.4
7	0.0	0.1	0.5	0.1	21.3	0.5	100.0	0.4
8	0.1	0.0	0.1	2.0	0.0	0.4	0.4	100.0

The common 24 sensor locations, shown in figure 4, were chosen by hand early in the design process. As shown in table 1 by the off-diagonal terms of the Modal Assurance Criterion (MAC [3]) comparison of an experimental mode set with itself, this set of

sensors has problems distinguishing mode pairs 1-6, 3-5 and 5-7. The fact that modes 3-5 are very close in frequency is an additional difficulty. No simple weighting of the sensors seems to significantly improve the geometrical independence of these 3 mode pairs.

Figure 5 shows the 9 modeshapes measured by participant C. The second mode was used as a check of proper assembly. As will be shown in section 4, it was effectively the most consistently estimated mode. *A posteriori*, it should be said that this choice was not ideal since this mode was among the least sensitive to perturbations and thus not informative on the fact that the test configuration specification was met.

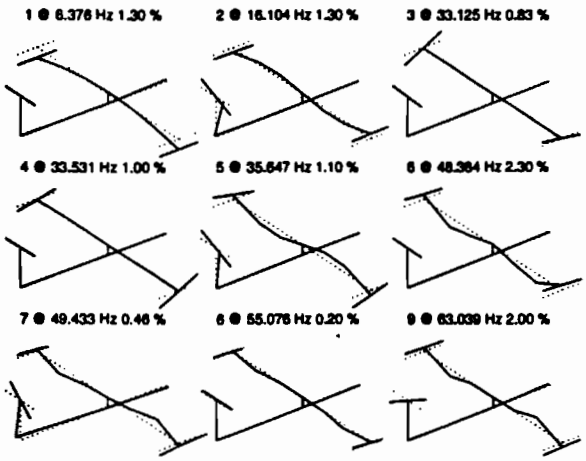

Figure 5. Set of modes measured by participant C.

For all tests, the structure was suspended using bungees linked to a small plate common to all the participants (as shown in figure 1). The participants were however free to attach the plate in any appropriate manner. Some fixed the plate to a hard point while others used pendulums of various lengths. Table 2 shows however no direct relation between pendulum length and estimated rigid body heave mode.

Table 2 : Length of suspension pendulum (length of bungees not included) and estimated frequency of heave mode.

Set	B	C	E-F	G	H	I
Length (m)	12.0	0.0	2.6	0.7	0.4	0.9
Freq (Hz)	1.88	1.8	2.7	2.2	2.6	2.4

3. COMPARISON OF MEASURED FRF

The participants were required to provide a 2 by 2 set of transfer functions with 2 collocated transfers (point mobilities) at the drum tips (12z and 112z) and 2 cross transfers (12z to 112z, 112z to 12z). The collocated transfers are expected to be equal because of the symmetry of the structure, and the cross transfers because of reciprocity.

Figures 6 shows a comparison of the 112z collocated transfers measured by a number of participants. General trends are clearly common to all measurements. Above 40 Hz, the response is however dominated by modes near 34 Hz so that it is hard to see how coherent the measurements are. Tests B and J show significant discrepancy near 35 Hz, these are however easily explained by the selection of inappropriate compensation masses.

The collocated transfers 12z are slightly different from those of figure 6 because the structure is not really symmetric (manufacturing tolerances led to a non symmetric wing), but otherwise show little more information.

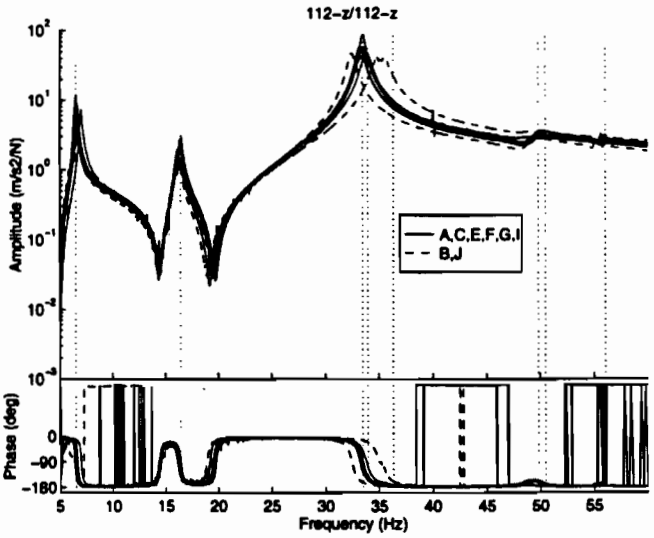

Figure 6. Collocated transfer function at left drum (112z).

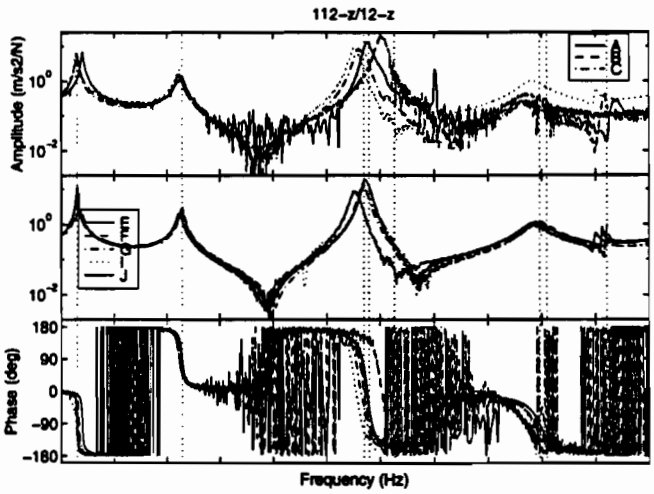

Figure 7. Cross transfer 112z to 12z. Amplitude plots are separated in two groups depending on shaker position (A and B in figure 3).

The required cross transfers (12z to 112z shown in figure 7) are much more informative. Some data sets are very noisy and/or show quantization errors. Data set A has for example a fairly high noise floor, which masks the anti-resonances of cross transfers. It must be noted however that the groups who provided noisy data sets do not use FRF data for identification purposes.

Resonance frequencies show significant variability from test to test. For example, the resonance of the first mode goes from 6.4 to 7 Hz. These variations are coherent with the modal results

given by the participants. Despite frequency shifts, the general trends (positions of resonances and anti-resonances) are well preserved in all data sets. Sets B and J have again the resonances of the torsion modes shifted up and down respectively.

Figure 7 distinguishes sets ABC from sets EFGJ based on where the shaker was attached (positions A and B of figure 4). Above 35 Hz, the two sets show a significant difference in the level of response. Within each set, the responses are however coherent.

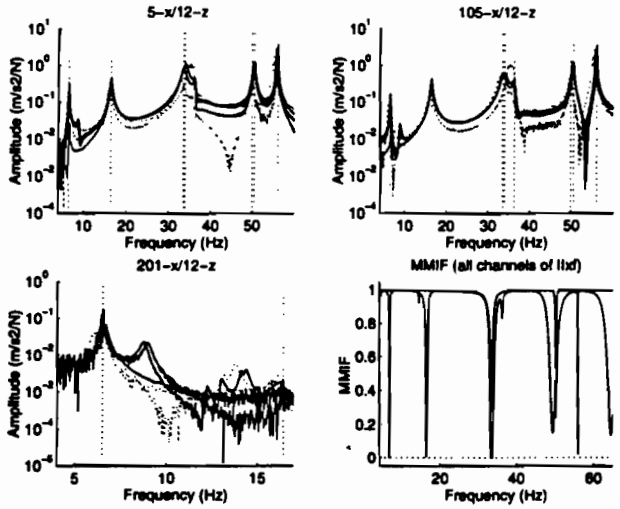

Figure 8. A-B cross transfers 12z to 5x and 105x. C low frequency range of 201x/12z. D Multivariate Mode Indicator Function [4] for inputs 12z and 112z

Figure 8a and 8b show transfers between drum excitation and the in plane mid wing sensor. Sets AC which are very noisy for these sensors have been removed. Sets B,J are shown in dotted lines and one sees the frequency shifts near 35 Hz. Set J significantly differs from other sets which may account for the discrepancies seen for modeshapes (see section 4).

Sensors 5x, 105x and sensor 201x even more (figure 8c) indicate the presence of many suspension modes in the 5-15 Hz range. These modes are hardly seen in the response of vertical sensors except for group J which was unlucky enough to have the frequency of 2 suspension modes coincide with the 2 node bending.

Drops in the second mode indicator function of figure 8d clearly indicate the presence of the two torsions (33.8 Hz) and tail torsion (49.4 Hz). The 3 node bending (35.7 Hz) is however not very well excited (the minimum of the MIF is above 0.8) which shows that these shaker positions are not suited for a force appropriation of this mode.

One should also note that the force measurement technique (groups ACG use current, others use load cells) or the input signal used (participants used stabilized and swept sine, single and multiple input broadband signals) do not appear to have any significant influence. Noise levels seem to be inversely proportional to how much use was made of them for identification purposes. Even for groups using identification, responses to non reference inputs were used to identify some modes (3 bending and in plane modes in particular).

As a check for the variability of results, the test was performed at ONERA in the middle and the end of the testing period. The two tests differ by shaker stinger, shaker suspension, testbed bungees, excitation level. The results shown in figure 9 are thus a case where a marginal evolution of test conditions leads to visible differences in the test response. The change in noise level is related to a change in the algorithm used to detect stabilization in a stepped sine but shifts of resonance frequencies are clearly apparent. It is not possible to tell whether these are due to modifications of the structure or the test set-up but they are significant and of the same order as variations seen between results of different participants. Further tests will be performed to clarify this issue.

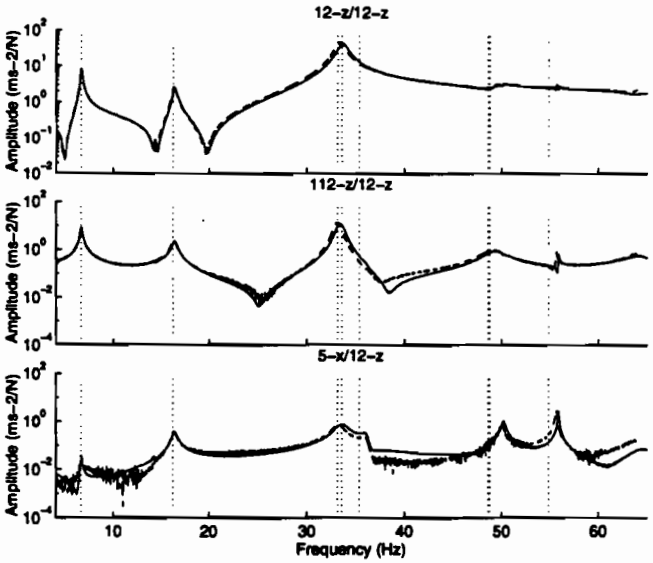

Figure 9. Comparison of two tests performed by ONERA.

4. COMPARISON OF MEASURED MODES

The second part of the exercise was to provide estimates of modal characteristics: frequency, damping ratio, modeshape and modal mass.

Participants ACEGH provided results obtained using force appropriation methods, while other results are based on model identification from measured transfer functions. The results shown do not indicate any influence of the method used on the results obtained.

Figure 10 shows the typical spread of identified modes to be close to 4 %. Many frequency discrepancies can be related to structural modifications linked to the instrumentation or selection of compensation masses. For example, an insufficient compensation mass leads for test B to the high frequency estimate of the 2 torsion modes (33.45 and 33.89 Hz). No simple explanation of the high variability of mode 1 frequencies was however found.

For damping ratios, the typical spread is closer to 30%. Modes 7 and 8 show the highest variations but also have the lowest damping values. This only confirms the fact that very lightly damped modes are difficult to characterize. In particular, instrumentation is likely to contribute most of their damping so

that one should not expect their damping values to stay constant. This expected sensitivity was the main reason to design a damping treatment to increase the overall damping of the testbed.

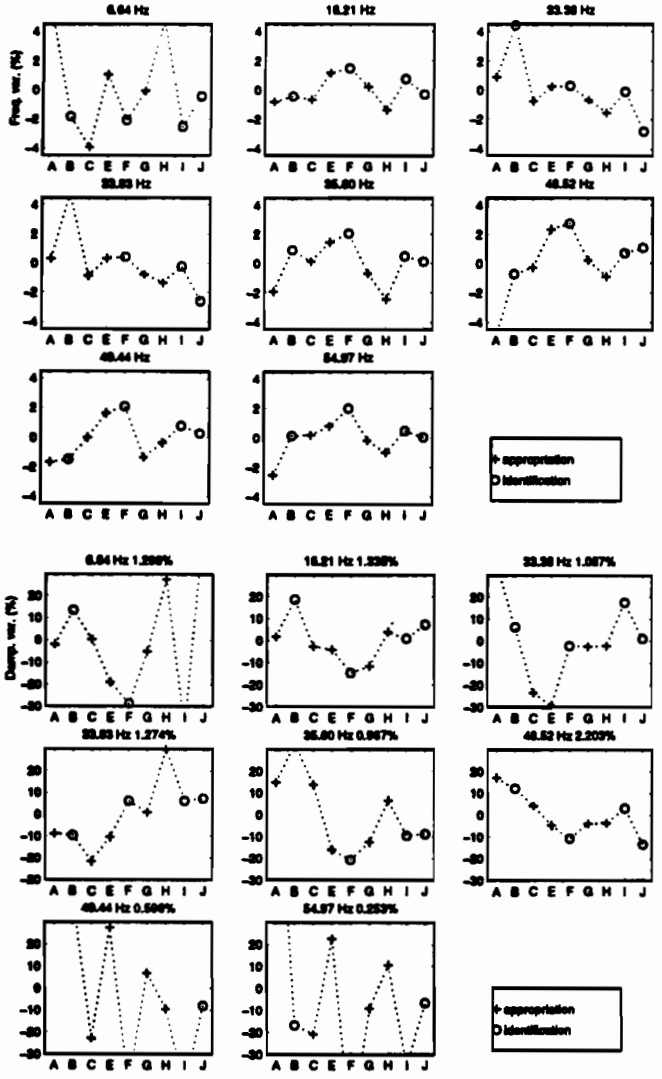

Figure 10. Variations in estimated modal frequencies and damping ratios.

Another question of interest is the sensitivity of the results to the method used. The plots do not indicate any particular trend that would be characteristic of either identification or force appropriation. To confirm that the variability of results is indeed linked to changes in the structure/test setup and not the method, the IDRC [5] identification method was used on available data sets to provide independent estimates of modal frequencies.

For the three close modes, figure 11 shows that the only visible frequency variations from the participants results are found for the 3 node bending for groups ACEG. These groups used force appropriation and good appropriation of the 3 node bending cannot be achieved with the drum tip shakers only. These groups thus had to use another shaker and, given the modification of the test setup, variations of frequencies are expected. Group C, who attached the shaker to the fuselage, minimized this effect and the frequency difference is low. The FRFs of this group to the 2 reference inputs are not however consistent (resonance frequencies shift when the input is changed). The identification was thus performed on a single excitation which may explain the relatively poor MAC comparison of torsion modeshapes. On real aircraft, dependence on input location is often linked to the presence of non linearities. On the considered testbed it is more likely that the instrument loading changed between tests.

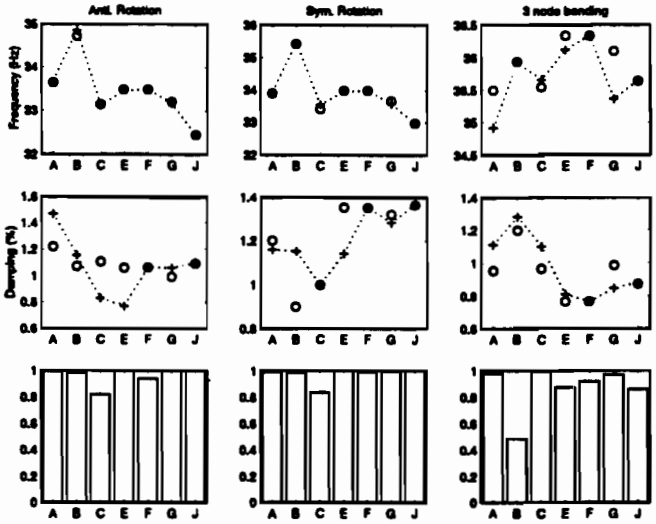

Figure 11. Comparison of the 3 close modes given by the groups with results independently identified from their FRF data (IDRC method).

The participants were all asked to compare their results with those of test A. This test however happens to have rather different modes 4 and 5 so that set C will be used as reference here. The MAC comparisons shown in figure 12 indicate a very good overall correlation. A few poor modes (mode 2 set E, 7 set F, 8 set H) are really exceptional errors of these groups. The only real difficulties are linked to the three closely spaced modes (modes 3-5).

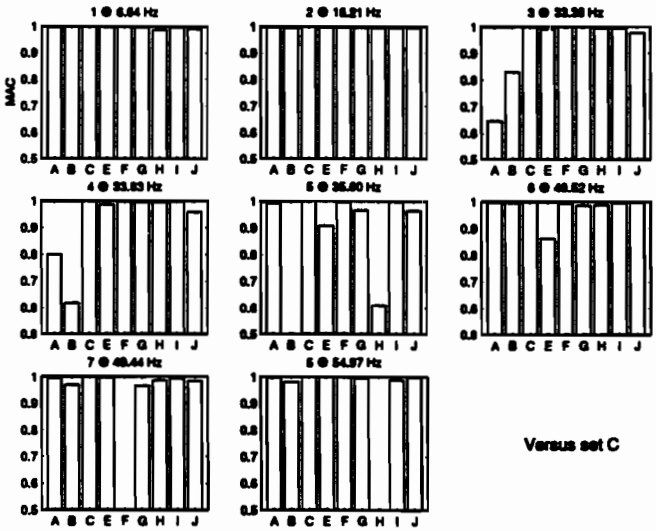

Figure 12. Diagonal MAC values for comparison of different test modeshapes with those of test C.

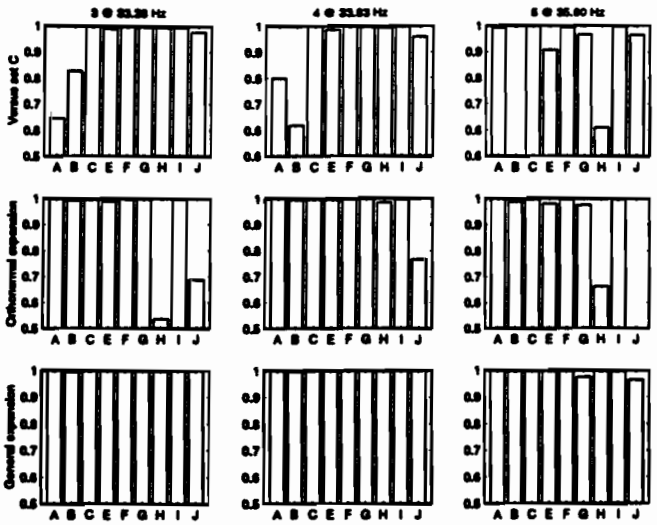

Figure 13. a) MAC comparison with test C
b) Comparison after orthonormal expansion
c) Comparison after general expansion.

It is well known that modes that are close in frequency can be very sensitive to small modifications of the structure. The symmetric and antisymmetric torsions (modes 3-4) and the 3 node bending (mode 5) are very sensitive to mass stiffness modifications. Since the instrumentation of each participant is expected to vary, non-negligible perturbations are expected. Such perturbations however will only induce recombination of modes that are close in frequency (this is the case of modes 3-5). It could be further argued that the recombination should be almost orthogonal since orthogonality conditions always exist even for modes with equal frequencies.

A general linear combination and an orthogonal linear combination of the basis of the modeshapes 3-5 is done to improve the match between each set and set C. The resulting comparison of modeshapes (shown in Fig. 13) shows a very significant improvement over the results of Fig. 12. Even for the orthonormal expansion, only sets H and J have difficulties which may be explained by a poor orthogonality and/or normalization of the results given by these groups.

Modal masses are the last step of the comparison. Rather than comparing modal masses which would be sensitive to the choice of a particular scaling sensor, it is preferred here to consider mass normalized modeshapes such that the reconstructed FRF are given by

$$H_{kl} = \sum_{j=1}^{N} \frac{\left(c_k\phi_j\right)\left(\phi_j^T b_l\right)}{s^2 + 2\zeta_j\omega_j s + \omega_j^2} \qquad (1)$$

where c_k and b_l are used here to represent the extraction of the proper component of the measured modeshape. When the scaled modeshapes are known at the 24 sensors, the scaling error can be measured using the scaling coefficient f

$$f_{AB} = \frac{\left(c_k\phi_j\right)^T_{\text{Test A}}\left(c_k\phi_j\right)_{\text{Test B}}}{\left(c_k\phi_j\right)^T_{\text{Test A}}\left(c_k\phi_j\right)_{\text{Test A}}} - 1 \qquad (2)$$

which should be close to 0. Table 3 shows the values of coefficient f_{AB} for a comparison with the 8 modes of set C. The scaling coefficient is only appropriate if the modeshapes are similar, so that scaling coefficients corresponding to low MAC values are shaded in the table and should not be considered for the comparison. The table clearly indicates that typical mass normalization errors are below 10%.

Table 3 : scale factor (2) and variation in estimated damping (in %) for a comparison of mass normalized modes given by different groups. Shaded elements correspond to low MAC (see Fig. 12).

Mode	A		C		E		F		G	
In %	f	$\Delta\zeta$	f	$\Delta\zeta$	f	$\Delta\zeta$	f	$\Delta\zeta$	f	$\Delta\zeta$
1	-3	-2	0	0	9	-19	3	-29	3	-5
2	-7	5	0	0	5	-2	8	-12	-4	-9
3	-21	77	0	0	5	-7	6	28	0	28
4	-175	16	0	0	0	14	7	35	6	28
5	7	1	0	0	2	-26	12	-30	3	-23
6	-6	12	0	0	-8	-9	20	-15	-3	-8
7	-6	98	0	0	10	65	-96	-28	-6	38
8	-4	180	0	0	-17	55	7	-56	-1	15

Most identification methods tend to preserve the response at resonance ($s = i\omega_j$). From (1), an error on the damping ratio ζ_j would thus tend to be compensated by an error in the same direction on the modal mass. The damping variations shows in the table are clearly much more significant than the modal mass variations so that the variations cannot be attributed to bad identification. It seems that damping changed from test to test, while modal mass was properly identified and is, as expected, independent of the damping level.

Figure 14 shows for groups CEG, the absolute value of the mass normalized modeshapes $c_k\phi_j$ at the 24 sensors. The overall comparison is very good. One can note the dissymetry of the torsion modes 3 and 4 (the pairs of high peaks correspond to right and left vertical sensors at drum tips). For modes 5 and 6, the low MAC (below 0.9) shown in figure 12 now appears as variations in the wing (mode 5) and tail (mode 6) motion.

One can again try to see if the results found depend on the parameter extraction method used. For mode 2, the IDRC identification algorithm was again used on data sets EFGJ. The resulting mass normalized modeshape is shown in figure 15 where only very minor variations are seen (the error on sensor 20 group E is just a calibration problem). For sets ABC, the results are also very similar but an identical scale difference is found which is easily explained by the fact that these groups excited at point B (see figure 3).

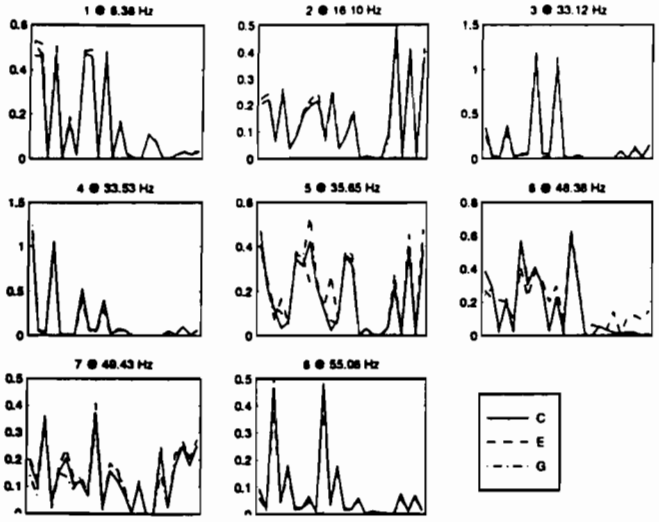

Figure 14. Mass normalized modeshapes given by participants at the 24 sensors.

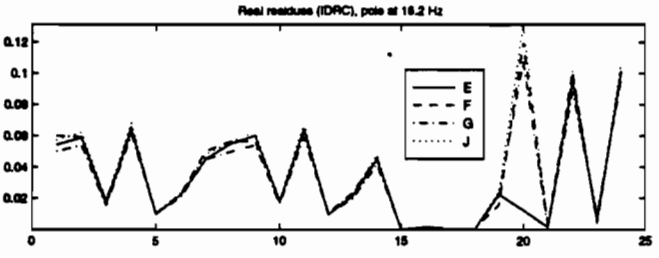

Figure 15. Mass normalized shape of mode 2 found by IDRC identification using different data sets.

5. CONCLUSIONS

Although the methods and hardware used by different participants were widely different, the results compare very well. Force measurement techniques through load cell or current measurements did not lead to any visible modification of the frequency responses.

Force appropriation and identification methods led to very similar modeshape estimates. Identification results were however generally given as complex modes. Simple methods were used to determine normal modes but vector normalization was often lost in this process. Variability in frequencies were of the order of 4%, in damping of the order of 30%. Variability in estimated modal masses were, for the groups who provided mass normalized normal modes, below 10% which leads to think that damping truly varied significantly from test to test while participants were able to properly identify mass normalized modeshapes.

The force appropriation of certain modes implies the use of additional shakers which, for this small testbed, introduces modifications linked to instrument loading. The testbed is mostly linear, has only one difficulty with closely spaced modes and uses a small number of sensors. None of the main reasons that make force appropriation useful are met. The results still compare extremely well.

Many of the important variations between the various test results could be traced back to inappropriate mass compensation of the shaker moving mass, or mass and stiffness loading of the structure by instruments or suspension. For tests performed a year apart by the same team, visible variations were found without having the possibility to determine if these were due to changes in the structure or the test conditions. This highlights the difficulty of obtaining the desired test conditions or simply characterizing the effect of the actual instrumentation.

Future group activities will be to compare identification results on a common data set, in an exercise similar to the SVIB Round Robin [6] but based on actual test data, and to analyze strategies considered for shaker and sensor placement.

6. REFERENCES

[1] Remmers, G.M., Belsheim, R.O. "Effects of technique on reliability of mechanical impedance measurement," *Shock and Vibration Bulletin*, 34-3, 1964

[2] Ewins, D.J., Griffin, J., "A State of the Art Assessment of Mobility Measurement Techniques – Results for the Mid-Range Structures (30-3000 Hz)," *Journal of Sound and Vibration*, 1981, 78-2, p. 197-222

[3] Avitabile, P., O'Callahan, J., Milani, J., "Model Correlation and Orthogonality Criteria," *IMAC*, 1988, pp. 1039-1047

[4] Williams, R., Crowley, J., Vold, H., "The Multivariate Mode Indicator Function in Modal Analysis," *IMAC*, 1985, p. 66-70

[5] Balmès, E., "Frequency domain identification of structural dynamics using the pole/residue parametrization," *IMAC*, 1996, p. 540-546

[6] Ahlin, K., "Round Robin Exercise on Modal Parameter Extraction," *IMAC*, 1996, pp.

Annex 14

IMAC (JAPAN) PUBLICATION

Nationaal Lucht- en Ruimtevaartlaboratorium
National Aerospace Laboratory NLR

NLR TP 97086

A ground vibration test on the GARTEUR SM AG-19

A.J. Persoon and E. Balmes

Contents

(11 pages in total)

A GROUND VIBRATION TEST ON THE GARTEUR TESTBED SM AG-19

Albert J. Persoon - National Aerospace Laboratory (NLR),
Anthony Fokkerweg 2, 1059 CM Amsterdam, The Netherlands

and

Etienne Balmès - Office Nationale d'Etudes et Recherches Aérospatiales (ONERA)
29 Avenue de la Division Leclerc, 92322 Chatillon Cedex, France

Abstract

In april 1995 a Structures and Materials Action Group (SM AG-19) of GARTEUR (Group for Aeronautical Research and Technology in Europe) started an activity with the major objective to compare a number of current measurement and identification techniques applied to a common testbed. Twelve European groups participated, most of them involved in ground vibration testing of aircraft for flutter clearance purposes.

It seldom occurs in practice that a ground vibration test is repeated by a third-party and can therefore be considered as an unique opportunity to validate the results of each individual test setup.

This paper addresses the variability of the measured data and analysis results. Further this paper deals with the identification and comparison of the modal parameters of this testbed, where three closely spaced modes were incorporated as a "hidden" vibration problem.

1. Introduction

In the certification process of new aircraft, a ground vibration test (GVT) plays an important role for the verification or updating of analytical models. Facing the risk of flutter, high quality GVT results has to be achieved to model the vibrational characteristics of an airplane structure being a basis for reliable flutter predictions.

In April 1995 an Action Group (SM AG-19) of GARTEUR started its activities with the major objective to compare a number of current measurement and identification techniques applied to a common testbed designed and manufactured by ONERA [Ref. 1]. The various companies, research centers and universities in Europe participating were ONERA, SOPEMEA, AEROSPATIALE, CNAM and INTESPACE from France, DLR from Germany, NLR and Fokker from the Netherlands, SAAB from Sweden and finally DRA, University of Manchester and the Imperial College from the United Kingdom.
More specifically, the objectives of the GVT tests were to evaluate the reliability of test methods and to compare modal parameters extracted from different identification techniques.

This paper deals with the identification of modal parameters of the testbed (Fig. 1) but does not intent to evaluate a specific test setup, data reduction or identification technique as there was a variety in test equipment and software used by the various participants.

2. Requirements and recommendations for the ground vibration test

The ground vibration test on the testbed aimed to measure transfer functions between the response of the structure and the applied excitation forces and to determine the natural frequencies and mode shapes with related parameters. Each participant was requested to provide at least (i) a reference set of four transfer functions corresponding to excitation and response of the left and right wingtip body, and (ii) the mode shapes of the testbed in a 4-65 Hz band. It was further agreed between the participants that the mode shapes would be based on 24 accelerometer positions (Fig. 2) recommended by ONERA. Attachment of two electrodynamic shakers was foreseen at position 12z and 112z (Fig. 2) close to additional wing tip masses of 200g each, which were installed to introduce a "hidden" vibration problem of three closely spaced natural frequencies with their mode shapes.

The aluminium testbed with dimensions of 2m (span) and 1,5m (length of fuselage) and a mass of 45 kg was suspended by a common set of bungees in order to obtain similar boundary conditions for each participant. The bungees were linked to a plate and the participants were free to fix this plate in any appropriate manner. To the participants it was further recommended to detect at least the highest rigid body frequency (the heave mode) and to measure the second mode shape of the testbed being the fuselage torsion mode (f = 16,17 Hz with a damping factor of 1,45 %) as a check of proper assembly of the testbed. Apart from that the participants were free to perform the ground vibration test following their own view and experiences to identify the vibration modes and the related modal parameters (frequencies, damping factors and modal mass).

3. Equipment setup

An interesting aspect in this GARTEUR activity was the use of different measuring equipment, data reduction- and analysis techniques by the various participants.
Besides commercially available equipment also "in-house made" equipment was used like accelerometers, conditioners or filters. Most of the participants used front-end type multi-channel measuring systems with software of different suppliers like CADA-X (Leuven Measurement Systems), the Structural Dynamics Toolbox for use with Matlab (Scientific Software Group) or "in-house made" software.

Excitation of the testbed was performed in various ways. The participants used different shaker positions but also mounting of the shakers was quite different (again Fig. 1). Most of the participants were able to use uncorrelated band limited noise showing the symmetrical and anti-symmetrical frequencies simultaneously in the transfer functions; otherwise correlated excitation signals were applied by which the shakers act in-phase or in counter- phase. The excitation forces were measured by load cells or by the current through the shakers. The latter procedure needed a compensation for the moving mass of the shakers because of the relative low mass of the testbed. A typical equipment setup of one of the participants for this testbed is presented in Figure 3.

4. The ground vibration test in practice

In spite of the recommendations and requirements for the ground vibration tests, given by ONERA, some "shortcomings" occurred in the test setup of various participants. Inappropriate mass compensation at the wingtips (to compensate for the moving mass of the shakers) was a major source, but also the position of the shakers at the wingtips as clearly shown in Figure 4. For that reason, ONERA was not able to include all data sets in one comparison but had to make a selection between two representative groups of participants [Ref. 1]. The final results however appeared to be consistent and differences in natural frequencies, especially in the 30-35 Hz band where the presence of mass is of a substantial influence on the three closely spaced modes (see section 5), could be easily explained. Finally the test setup of some participants suffered from suspension modes appearing in the transfer functions.

5. Presentation of some typical results

5.1 Transfer functions

Using uncorrelated noise as excitation of the testbed transfer functions like those presented in Figure 5 were obtained. These include both the symmetrical and antisymmetrical behaviour of the testbed. Observation shows that the natural frequencies around 35 Hz are sensitive for a different mass compensation (see Fig. 4b and Fig. 4d) resulting in a slight frequency shift. The 180 deg phase difference is explained by the way of mounting the loadcell (upside down, -z) by one of the participants.

The presence of closely spaced modes is well illustrated in Figure 6. When measuring the transfer between excitation and response on both wings (105z and 5z, Fig. 2) a single circle is the result showing no indication of a hidden vibration problem. By measuring the response on one of the wing tip bodies (12z) however, the closely spaced modes (as coupled circles) become visible (Fig. 6b).

5.2 Frequencies, damping factors and mode shapes

Analysis of the closely spaced modes took place in different ways depending of the software used by the participants. An example is shown in Figure 7.
Applying a multi degree of freedom curve fitter on the data and creating a stabilization diagram, the evaluation of frequency

and damping (poles) is shown with an increasing number of computational modes (up to 32). Once stabilized the poles are marked by "S" and the residuals are determined, resulting in a mode shape and presented in an animated display. The three closely spaced modes (Fig. 7) were identified as an antisymmetrical and symmetrical rotation of the wing tip bodies and a three node bending of the wing. The results fairly match the finite element analysis of the testbed (Fig. 8) performed by DLR (Germany) in an earlier stage to provide proper accelerometer positions and exciter locations for the ground vibration test [Ref. 2]. Finally a representative overview of all mode shapes measured in the 4-65 Hz band is presented in Figure 9.

5.3 Modal mass

It is well known that the modal (or generalized) mass is a relevant parameter in aeroelastic (flutter) prediction methods. An inaccurate determination of the modal mass may lead to unreliable computations on the flutter speed of an aircraft. This GARTEUR activity was an excellent opportunity to compare modal mass results determined by the participants (section 6). Also some checks on the data processing software were performed indicating the importance of an accurate measurement of damping factors and mode shapes.

A relatively simple check is the determination of the modal mass of the heave mode (f = 1,8 Hz) by which the testbed is considered to behave rigid in its suspension (Fig. 10a). In that case, the weight of the model (around 44,8 kg) should be equal to the computed modal mass. The data processing computing of one of the participants yielded results (Fig. 10b) in which the modal mass ranges from 45,2 kg (+ 1%) to 50,7 kg (+ 13%) depending of the damping. The same participant did a further check for the second mode shape of the model using the technique of added masses (Δm) by measuring the frequency shift (Δf) after re-adjusting the 90 deg phase criterion during a sine dwell. The result (Fig. 11) should be a straight line if the mode shape is not influenced by added masses placed at locations 112z and 12z. Comparable results with the computation (17,9 kg) are obtained (Fig. 12). The next section however will show that the modal mass determination still remains a subject of investigation because of its variability.

6. Comparison of results

Considerable effort was put into the comparison of test results of the various participants carried out by ONERA [Ref. 1] concerning natural frequencies and damping factors and by DLR [Ref. 2] concerning the modal mass. The results are presented in Figure 13 and Figure 14. Here the participants are identified as A to J in chronological order of testing. Figure 13a shows the variation of identified frequencies to be close to only 4%. The "discrepancies" can be easily related to inappropriate selection of compensation masses or shaker position. The unexpected variability of the first mode (wing bending) around f = 6.5 Hz could be possibly explained by interaction with the rigid heave mode which varied between 1.8 and 2.7 Hz as measured by various participants.

For the damping ratios (Fig. 13b), the variability is close to 30%. Modes 7 and 8 show the largest variation but have the lowest damping ratio (coplanar modes, 0.2% - 0.6%). This confirms the fact that lightly damped modes are difficult to characterize. The plots do not indicate any particular trend that would be characteristic for either the method of identification or force appropriation.

Finally the modal (or generalized) mass comparison is presented in Figure 14. The values calculated from mass normalized mode shapes show similar trends but scatter occurs at all modes. This fact confirms general experiences in determining the modal mass of a real aircraft. The modal mass computation for mode 3 and 4, being the closely spaced rotational wingtip body modes, shows the lowest values. It is however the opinion of the authors that the scatter of the data should be lesser for a rather linear structure like this testbed. Further investigation on modal mass measurement is therefore recommended.

7. Conclusions

- The present GARTEUR activity (SM AG-19) has clearly shown that different test setups and the variety in hard- and software applied by the various participants, have resulted in a consistent set of data.
- The technique of force measurements by load cells or by electrical current through a shaker showed similar transfer functions and led to comparable mode shape results.
- Analysis of the variability of the test results showed an amount of only 4% in natural frequencies and around 30% in damping factors.
- Variation in results of the natural frequencies could be easily traced back to "shortcomings" in the test setups as applied by the participants.
- The modal mass measurements showed similar trends but are affected by scatter of the data.
- The determination of the modal mass of this testbed requires therefore further investigation.
- The present activity has highlighted the reliability of the various test- and identification methods of this ground vibration test performed by the GARTEUR participants.

8. References

1. Balmès, E. "GARTEUR Group on Ground Vibration Testing. Results from the test of a single structure by 12 laboratories in Europe", paper presented at IMAC, Febr. 1997, USA.
2. Degener, M. "Ground Vibration tests on an Aircraft Model Performed as Part of a European Round Robin Exercise", paper presented at the International Forum on Aeroelasticity and Structural Dynamics, July 1997, Rome, Italy.

9. About GARTEUR

The Group for Aeronautical Research and Technology in Europe (GARTEUR) was formed in 1973 by representatives of the government departments responsible for aeronautical research in France, Germany and the United Kingdom. The Netherlands joined in 1977 and Sweden in 1992.

The aim of GARTEUR is, in the light of the needs of the European Aeronautical Industry, to strengthen collaboration in aeronautical research and technology between countries with major research and test capabilities and with government-funded programmes in this field.

The cooperation in GARTEUR is concentrated on pre-competitive aeronautical research. Potential research areas and subjects are identified by Groups of Responsables and investigated for collaboration feasibility by Exploratory Groups. If the subject is feasible, an Action Group is established.

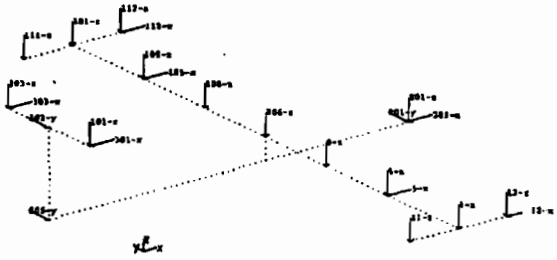

Fig. 2 The 24 accelerometer positions and directions

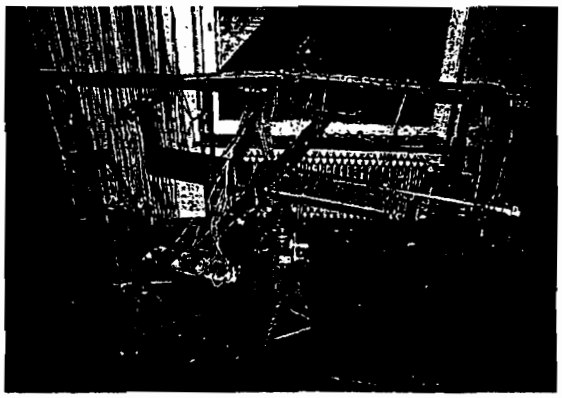

a) by DLR (Germany)

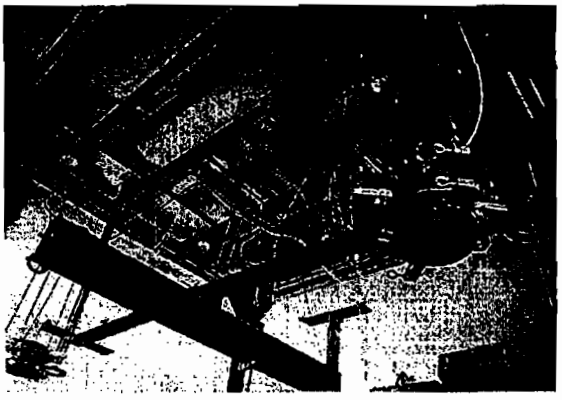

b) by CNAM (France)

Fig. 1 Variety in the test setup

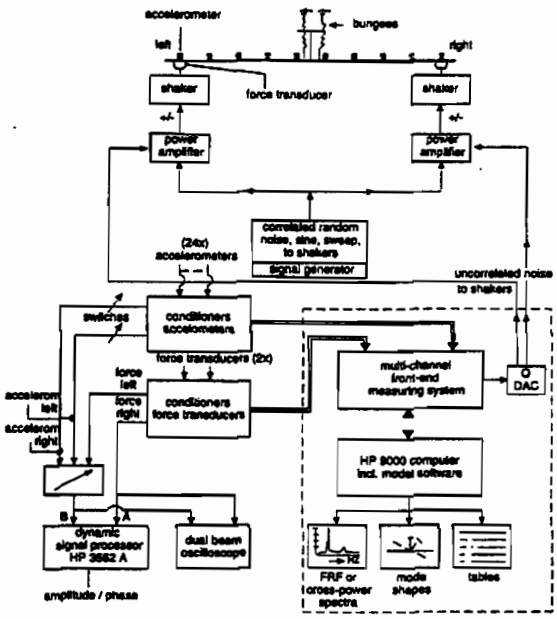

Fig. 3 Example of equipment setup

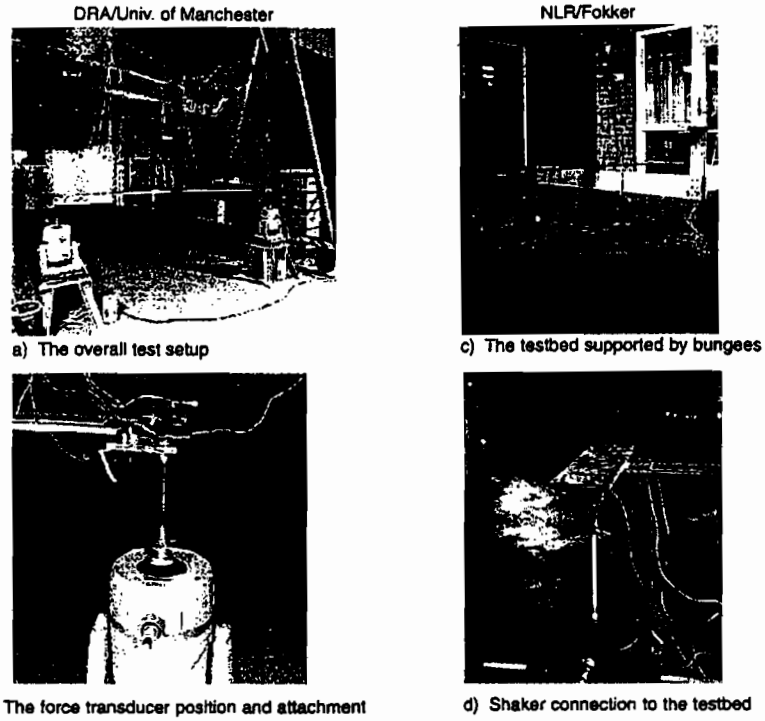

a) The overall test setup

c) The testbed supported by bungees

b) The force transducer position and attachment

d) Shaker connection to the testbed

Fig. 4 Variety in mounting the shakers and compensation of tipmasses

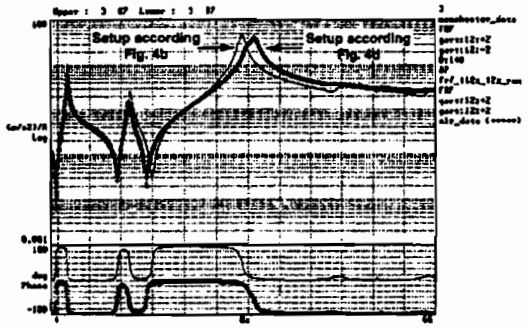

a) Driving point measurement (12z/12z)

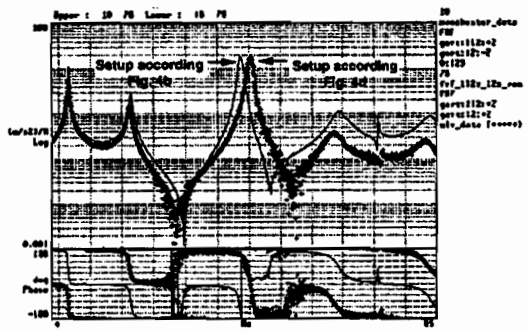

b) Cross transfer (112z/12z)

Fig. 5 Effect of tipmasses and shaker position on transfer functions

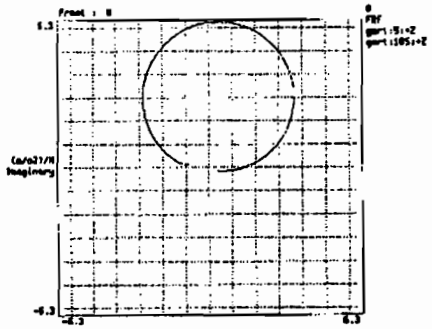

a) Excitation on wing (105z) and response on wing (5z)

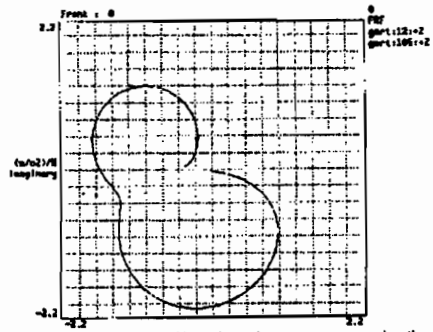

b) Excitation on wing (105z) and response on wingtip body (12z)

Fig. 6 Nyquist diagrams in the 30-35 Hz band

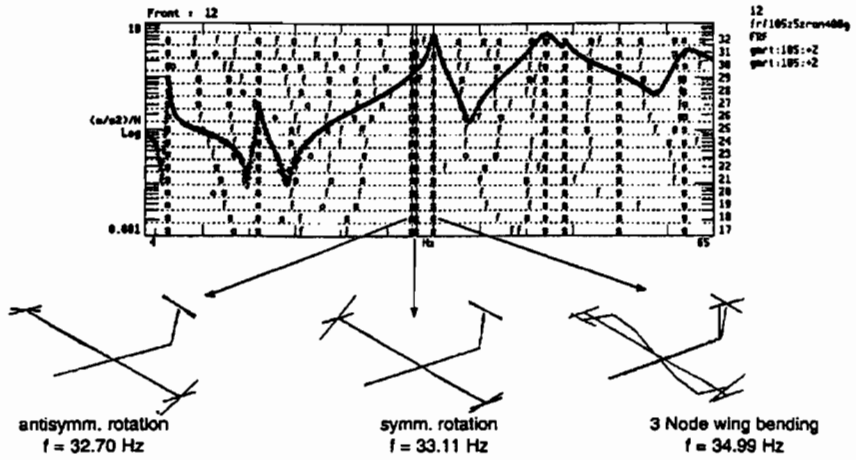

Fig. 7 The "hidden" vibration problem of three closely spaced modes

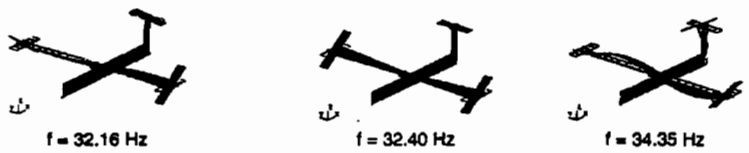

Fig. 8 The closely spaced modes from computations (including the masses of accelerometers) performed by DLR (from ref. 2)

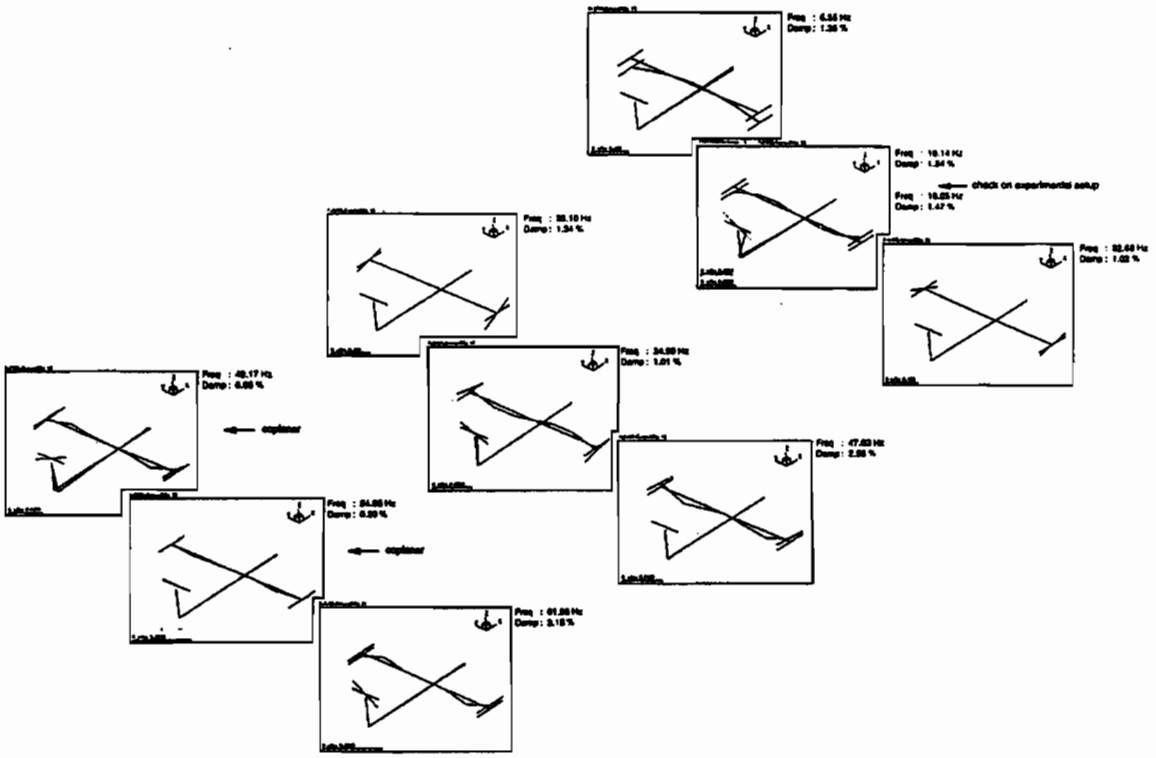

Fig. 9 The mode shapes of the testbed in the 4-65 Hz band as measured by one of the participants

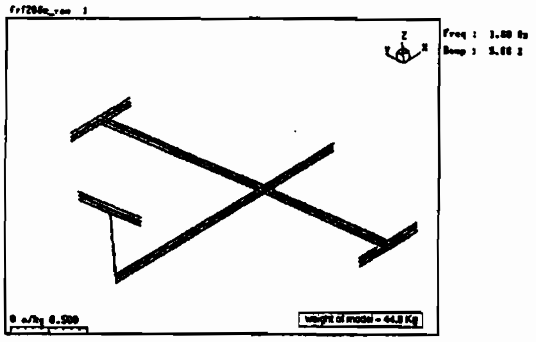

a) Heave mode of the testbed

Generalized modal parameters when scaled as
UNITY COMPONENT for identifier "gart:206:+Z"

No	mode no	freq Hz	damping (%)	mass kg	damping kg/s	stiffness kg/s2
1	1	[illegible]	[illegible]	[illegible]	[illegible]	[illegible]
2	2	[illegible]	[illegible]	[illegible]	[illegible]	[illegible]

b) Computation of the modal mass

Fig. 10 The modal mass of the heave mode

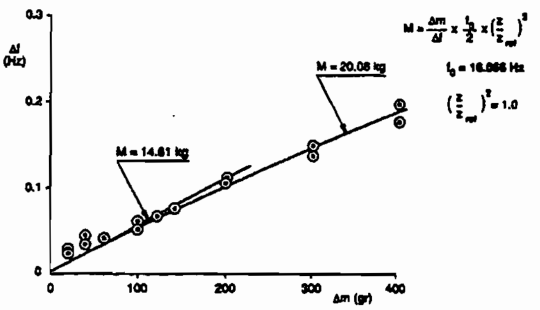

Fig. 11 Determination of modal mass of the fuselage torsion mode (pos.: 112z/12z) by added masses at a sine dwell

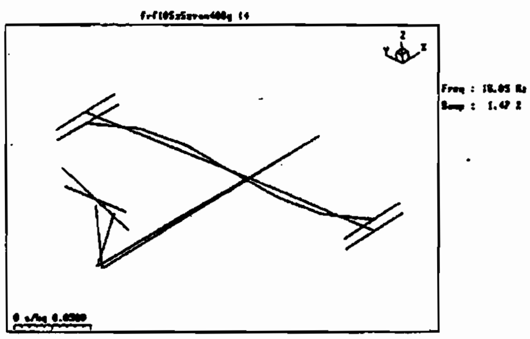

a) Fuselage torsion mode of testbed

Generalized modal parameters when scaled as
UNITY COMPONENT for identifier "gart:112:+Z"

No	mode no	freq Hz	damping (%)	mass kg	damping kg/s	stiffness kg/s2
1	2	16.85	1.47	1.73e+01	5.31e+01	1.82e+05

b) Computation of modal mass

Fig. 12 The modal mass of the fuselage torsion mode

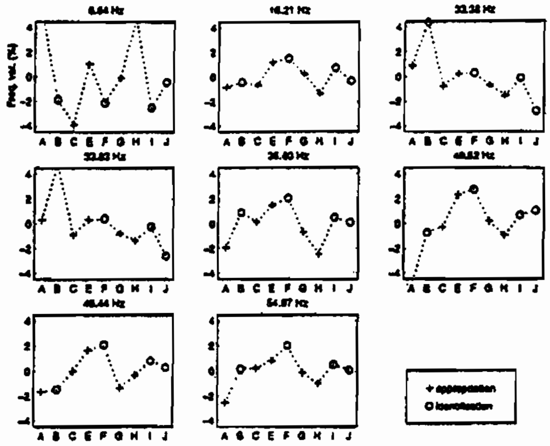

a) Modal frequencies

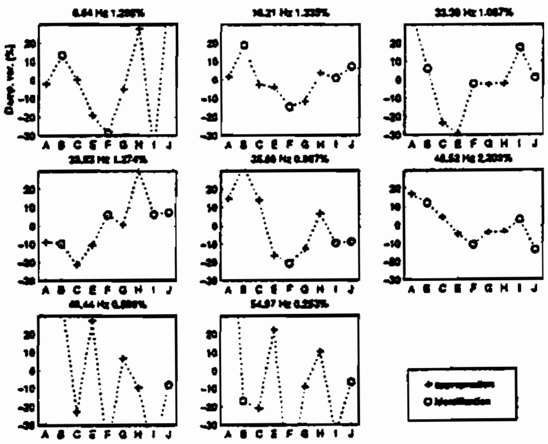

b) Damping ratios

Fig. 13 Variations in estimated modal frequencies (a) and damping ratios (b) (from ref. 1)

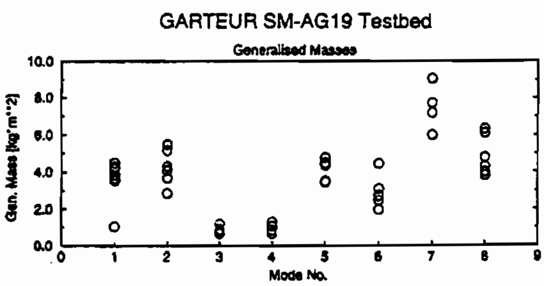

Fig. 14 Comparison of modal mass results (from ref. 2)

Annex 15

INTERNATIONAL FORUM ON AEROELASTICITY AND STRUCTURAL DYNAMICS PUBLICATION

GROUND VIBRATION TESTS ON AN AIRCRAFT MODEL PERFORMED AS PART OF A EUROPEAN ROUND ROBIN EXERCISE

Manfred Degener
DLR - Deutsche Forschungsanstalt für Luft- und Raumfahrt
Institute of Aeroelasticity
Bunsenstrasse 10, D-37073 Göttingen, Germany
email address: Manfred.Degener@dlr.de

Abstract. To analyse the different test methods and to evaluate the discrepancies between test facilities and analysis methods, an Action Group on 'Ground Vibration Test Techniques' was established by GARTEUR. Twelve members from the industry, universities and research institutes of the five GARTEUR member countries participated in the Action Group.
The group members agreed to design and manufacture a common testbed, which should be representative of typical aircraft structures. Modal parameters as well as frequency response functions were to be measured by each participant using his own test facility and evaluation methods.
This paper describes the ground vibration test performed on the test structure by DLR. Modal parameters were evaluated using the phase resonance method with appropriate exciter forces as well as phase separation techniques applied to the measured frequency response functions. The test results are compared with the analytical predictions of a respective Finite Element analysis. The Finite Element model was also used to calculate optimum exciter positions based on different algorithms.
The test results of the GARTEUR Action Group members are correlated in detail. The coincidence and differences in frequencies, mode shapes, damping values, and generalised masses are analysed. Improvements in ground vibration testing are discussed with respect to the increasing aeroelastic demands of future aircraft projects, which will require an increase in measuring accuracy as well as a reduction of cost and time.

Key words: GARTEUR, Ground Vibration Test, Modal Analysis, Phase Resonance, Phase Separation

1. Introduction

Ground vibration tests play a key role in the certification process of each new airplane. These tests provide the experimental data base to be used directly for the flutter predictions and for the validation and update of the analytical structural model. With respect to the flutter risk, the highest level of security and reliability has to be achieved, which requires high-quality ground vibration test results. Various test methods like the phase resonance method and phase separation techniques in time and frequency domain are commonly used to identify the structural modal parameters.
Various test and identification methods using different excitation signals and excitation points are applied. To evaluate the efficiency and reliability of these test techniques a GARTEUR Action Group was established. A common testbed was designed and manufactured, which was to be tested by each group member. A critical review of the different test and analysis methods, more than the selection of the 'best' method, was to be performed. The aim was to define the application field of each one and evaluate both the accuracy of results and the easiness of implementation.

2. The GARTEUR Participants

GARTEUR (Group for Aeronautical Research and Technology in Europe) was formed in 1973 by representatives of the Government departments responsible for aeronautical research in France, Germany and the United Kingdom. The Netherlands joined in 1977, and Sweden joined in 1991. According to its MoU, the mission of GARTEUR is to mobilize, for the mutual benefit of the member countries, their scientific and technical skills, human resources and facilities, in the field of aeronautical research and technology. The scientific and technical substance of GARTEUR is embodied in the Action Groups, which organize and execute the collaborative research work.
Initiated by ONERA, the Action Group SM-AG19 on 'Ground Vibration Test Techniques' was established by the GARTEUR Executive Committee in March 1995. The action group members were from industry, universities and research institutes of five European countries. The participating laboratories are listed in *Table 1.*

3. The Testbed

3.1. Design

The Action Group members agreed to design and manufacture a common test article, which should be representative of typical aircraft structures. The test article was also easily to be shipped to the test

France	Aérospatiale, Toulouse CNAM, Paris Intespace, Toulouse ONERA, Châtillon SOPEMEA, Vélizy
United Kingdom	DRA, Farnborough Imperial College, London University of Manchester
The Netherlands	Fokker, Schiphol NLR, Amsterdam
Sweden	SAAB, Linköping
Germany	DLR, Göttingen

Table 1. GARTEUR Participants

facilities of the different participants and should ensure a perfect structural repeatability.
For this purpose the following design requirements were proposed:

- general shape: aluminium beam assembly representing a fuselage with wings and tail
- dimensions of ca. 2 by 2 m and a mass of between 50 and 100 kg
- frequency range 5 to 65 Hz
- damping treatment by constrained viscoelastic layers to get realistic damping values and to limit the effect of instrumentation dissipation
- no specific nonlinear elements
- low frequency suspension by a set of common bungees in order to provide similar boundary conditions
- at least 3 modes within 1 Hz frequency bandwith to simulate the difficulties encountered in real aircraft

The final design of the testbed shown in *Figure 1* had a fuselage length of 1.5 m and a wing span of 2 m. The cross section of the fuselage beam was 50 x 150 mm, while the wing and tail beams had 10 x 100 mm cross sections. The total mass of the model was 44 kg.

3.2. Common Test Setup

A common test setup was defined with respect to the suspension of the model, measurement points and exciter locations.
To simulate the free-free boundary conditions, the aircraft model was suspended by a set of three bungee cords. Some participants used a crane to suspend testbed and bungees, while other participants connected the bungees to a frame-type support structure in order to avoid noisy measurement signals due to crane rope vibrations. The heave mode frequency of the testbed was below 2 Hz. This frequency was well separated from the elastic modes of the structure and confirmed the suitability of the suspension.

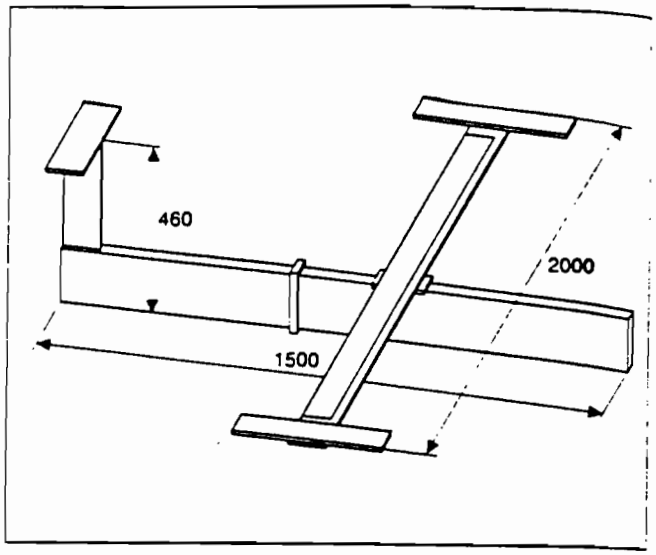

Figure 1. Testbed Design

A common accelerometer plan to be used by each participant was defined by the Action Group in order to facilitate the comparison of the test results. 24 accelerometers were used for this purpose as shown in *Figure 2*.
Two common shaker locations (12-z and 112-z) at the wing tips were required to allow direct comparison of transfer function measurements. Each participant was free to use additional excitation points to obtain better results or to improve mode phase purity.

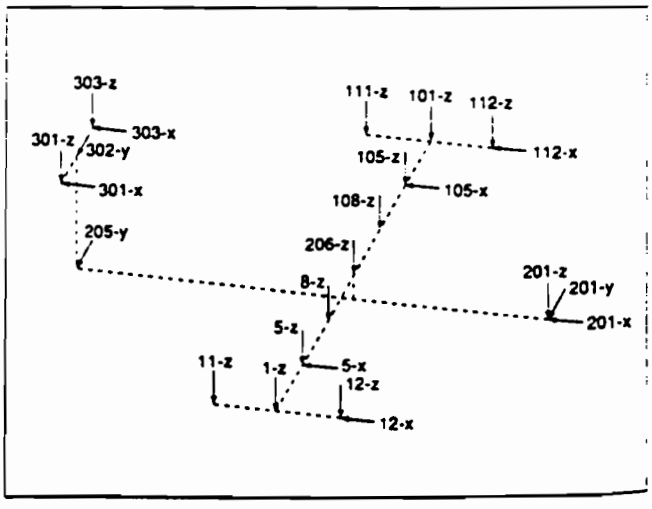

Figure 2. Test Setup

4.1 Test Setup

Apart from the common test setup, each participant was free in its own test performance. The DLR ground vibration test setup is shown in *Figure 3*. The suspension bungee cords were connected to a stiff beam supported by two tripods. By this frame-type suspension the use of a crane could be avoided. The support structure was also used conveniently to carry the accelerometer cables, thus minimising the mass and damping influence of the test equipment.
The common accelerometer plan with 24 measurement points was modified by 18 additional accelerometers to enable a better identification of fuselage rotation and wing torsional deformations as indicated by Finite Element predictions.
To obtain optimum phase purity for each mode, a total of 8 shaker locations was applied. The test structure was also used for a cooperative study on optimum exciter positions performed by the Italian Aerospace Research Center CIRA and DLR. By means of a genetic algorithm optimum exciter configurations were calculated based on Finite Element predictions and experimentally verified [1].

4.2. Test Methods

Both phase resonance and phase separation methods can be applied by the DLR vibration test facility [2]. For phase resonance testing, phase purity has to be achieved by force appropriation in order to compensate the internal damping forces. The experimental identification of the normal modes is supported by calculation of phase purity via the

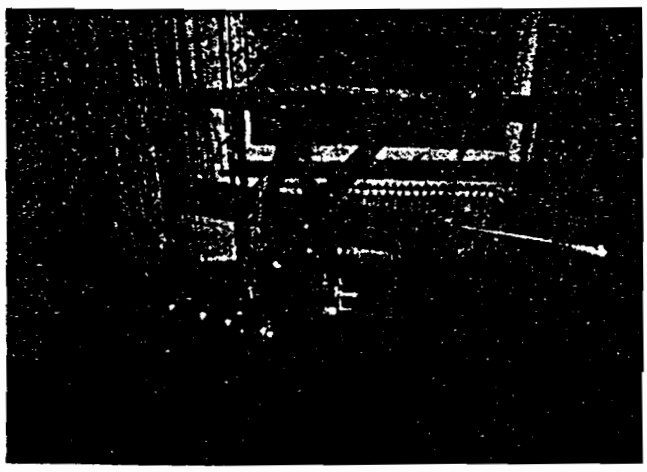

Figure 3. Ground Vibration Test

2	Fuselage Rotation	16.1 Hz
3	Antisymmetric Wing Torsion	33.1 Hz
4	Symmetric Wing Torsion	33.5 Hz
5	3N Wing Bending	35.6 Hz
6	4N Wing Bending	48.4 Hz
7	Inplane Wing vs. Fuselage	49.4 Hz
8	Symmetric Inplane Wing Bending	55.1 Hz
9	5N Wing Bending	63.0 Hz
10	Tail Torsion	66.5 Hz

Table 2. Normal Modes of GARTEUR Testbed

following Mode Indicator Function *MIF*:

$$MIF = 1 - \frac{\sum |u_i'||u_i|}{\sum |u_i|^2} \quad , \quad 0 \le MIF \le 1. \qquad (1)$$

The summation is performed over all measurement responses u_i. In case of a normal mode, all real parts u_i' vanish and the Mode Indicator Function assumes a value of $MIF = 1$. The Mode Indicator Function has proved to efficiently identify and isolate the normal modes of even very complex structures. Furthermore, it provides a sharp criterion for the achieved degree of phase purity.
Damping values and generalised masses were determined by evaluation of the structural responses measured at several frequencies near resonance. Different evaluation methods are applied in order to increase measurement reliability.
Phase separation methods were applied to the frequency response functions measured by excitation of the common shaker locations (vertical excitation at nodes 12-z and 112-z).

4.3. Finite Element Analysis

A NASTRAN Finite Element model was designed to compare the test results with analytical predictions. The calculated mode shapes were used to optimise the measurement point plan.
The model was mainly described by plate elements. 2550 degrees of freedom were taken into account. For correlation purposes the model was reduced to 183 degrees of freedom. The reduced mass matrix was used to perform an orthogonality test of the measured modes. These were expanded to the analytical degrees of freedom by suitable interpolation.

4.4. Test Results

One part of the GARTEUR exercise was to provide estimates of modal characteristics, i.e. frequencies, mode shapes, damping ratios and generalised masses in the frequency band up to 65 Hz. 9 normal

Mode	1	2	3	4	5	6	7	8	9	10
1	100	0	1	2	1	0	1	4	0	0
2	0	100	3	4	10	2	2	2	8	18
3	1	3	100	5	7	1	10	10	2	6
4	2	4	5	100	9	0	0	11	0	3
5	1	10	7	9	100	3	7	1	4	11
6	0	2	1	0	3	100	3	1	3	0
7	1	2	10	0	7	3	100	3	6	3
8	4	2	10	11	1	1	3	100	1	0
9	0	8	2	0	4	3	6	1	100	3
10	0	18	6	3	11	0	3	0	3	100

Table 3. Orthogonality Test

Mode	f [Hz]	A	B	C	E	F	G	H	I	J
1	6.64	5.1	-1.8	-3.9	1.0	-2.1	-0.1	4.7	-2.5	-0.4
2	16.21	-0.8	-0.4	-0.7	1.2	1.5	0.2	-1.4	0.7	-0.3
3	33.38	0.9	4.4	-0.8	0.2	0.3	-0.7	-1.5	-0.1	-2.8
4	33.83	0.3	4.8	-0.9	0.3	0.4	-0.8	-1.4	-0.2	-2.6
5	35.60	-1.9	0.9	0.1	1.4	2.1	-0.7	-2.5	0.5	0.1
6	48.52	-5.0	-0.7	-0.3	2.3	2.7	0.2	-0.9	0.7	1.1
7	49.44	-1.7	-1.5	0.0	1.6	2.1	-1.3	-0.3	0.8	0.3
8	54.97	-2.5	0.1	0.2	0.8	2.0	-0.2	-1.0	0.5	0.1
9	62.84	-2.7	1.6	0.3	-.-	2.7	1.6	-0.6	-.-	0.3
10	66.57	-.-	-.-	-0.1	-.-	4.1	-.-	-4.0	-.-	-.-

Table 4. Frequencies (Mean Values) and Deviations [%]

modes were identified by DLR in this frequency range. The 10th mode at 66 Hz was also included in the measurements. This seemed to be convenient, because there was a distinct frequency separation to the following higher modes. The 11th mode appeared at 103 Hz.

Table 2 summarises the first 10 modes as measured by DLR. The measurements were performed utilising the phase resonance method. Appropriate exciter positions were chosen to improve phase purity by optimising the respective *MIF* values. By choosing optimum shaker locations, the number of exciters could be kept small. 7 modes could be measured by a single exciter, only modes 3, 4 and 10 required two exciters. Most shaker locations were applied at the fuselage in order to reduce the influence of covibrating exciter masses. High phase purity could be achieved for all modes. The *MIF* values were between 0.93 and 0.99.

A modal identification was also performed from the transfer functions measured for the common excitation points of the left and right wing tip body. The modal parameters were evaluated by means of the phase separation method *ISSPA* [3]. The modal results were very close to the phase resonance measurements, except of Mode 7 (Inplane wing Bending vs. Fuselage). For this mode the two exciter locations at the wing tips did not seem to be suitable.

By means of the analytical mass matrix an orthogonality test was performed for the measured modes as shown in *Table 3*. Except of Modes 2 and 10, which show a coupling factor of 18%, all other modes are almost orthogonal with respect to the analytical mass matrix. This confirms the accuracy of the measurement as well as the reliability of the analytical model for the investigated frequency range.

5. Comparison of Test Results

As stated above, each participant in the GARTEUR exercise was required to provide for the frequency band up to 65 Hz:

- a set of transfer functions corresponding to excitation of the left and right wing tip body
- modal parameters (frequencies, mode shapes, damping values, and modal masses)

The measurement of the transfer functions, the applied excitation signals, and the comparison of the results is discussed in detail in [4] and [5]. The aim of this paper is focussed on the comparison of the results of the second task, i.e. the estimation of the modal parameters. Data sets of 9 participants were provided for comparison. The correlations are further restricted to the lowest 8 modes, because Modes 9 and 10 were not analysed by all participants. The test results of the participants are listed in chronological order, i.e. the tests started with Participant A and ended with Participant J.

All participants were able to evaluate frequency response function. 5 participants (A,C,E,G,H) additionally used the phase resonance method with tuned exciter configurations. It is interesting to note, that those participants, who applied both methods, provided the phase resonance results for the exercise.

5.1. Frequencies and Mode Shapes

The measured frequencies are listed in *Table 4*. The deviations between the different participants are rather small and may be attributed to differencies in the test setup. This is confirmed by the fact, that the relative frequency spacing is almost identical for all participants. Surprisingly, the largest scattering was measured for the first mode. A clear explanation was not found for this fact.

Mode	f [Hz]	A	B	C	E	F	G	H	I	J	FE
1	6.64	100	100	100	100	100	100	99	100	100	100
2	16.21	100	100	100	100	100	100	100	100	100	99
3	33.38	80	92	100	100	100	100	100	100	99	88
4	33.83	90	78	100	99	100	100	100	100	98	93
5	35.60	99	69	100	96	99	97	79	100	99	97
6	48.52	100	100	100	92	100	99	100	100	100	98
7	49.44	100	98	100	100	17	99	100	100	99	93
8	54.97	100	99	100	100	100	100	59	100	100	89

Table 5. MAC Values for Measured Modes

The correlation of mode shapes was performed in a first attempt by means of the Modal Assurance Criterion *MAC*. For this purpose a reference mode was defined as the mean value of the individual test results. Because some participants failed to measure all modes correctly, the participant with the largest deviation was not taken into account for the respective reference mode, which was calculated from the 8 remaining data sets.

The resulting *MAC* matrix is given in *Table 5*. The last column of the table includes the correlation of the Finite Element model with the reference mode. For most of the analytical modes the correlation is very good. Some poor *MAC* values can be assigned to structural unsymmetries of the testbed, as discussed later, whereas the analytical model is a symmetric one.

Besides a very few poor correlation values (e.g. Mode 7 of Participant F and Mode 8 of Participant H) most *MAC* values showed a good measurement consistency. Nevertheless, in order to obtain a more detailed understanding of the remaining differencies in the mode shape measurements, the individual modes were plotted within one respective figure as shown in *Figure 4*. For this purpose all modal vectors were normalised to the same unit length. The ordinate values given in *Figure 4* correspond to this normalisation.

For ease of understanding, the measurement points listed on the abscissa have been arranged following the geometry of the testbed. The first five measurement points are the inplane wing accelerometers. The next block of data shows the vertical accelerometers on the wings including the wing tip bodies. The remaining fuselage and tail accelerometers are plotted at the right hand side of each figure.

Following remarks and comments can be given to the individual modes:

- *Mode 1*:

The first mode is the fundamental 2N wing bending. The mode shapes are very similar and the data scattering is very small.

- *Mode 2*:

The fuselage rotational Mode 2 is obviously the mode with the greatest conformity. The first two modes did not cause any problems for the participants.

- *Mode 3*:

Mode 3, the 'antisymmetric' wing torsion mode, is the first of three very closely spaced modes. Obviously, in spite of its basic symmetric design, the aircraft model shows some significant unsymmetries in the dynamic behaviour. 7 participants measured much higher torsional deflections on the left wing than on the right wing.

- *Mode 4*:

Consequently, the 'symmetric' torsion Mode 4 shows a similar structural unsymmetric mode shape. In this case the torsional amplitudes at the right wing are very similar for the same participants as for the last mode, but there is some scattering for the left wing. The torsional mode shapes of data sets A and B show large deviations from those of the other participants. This is also expressed by the *MAC* values of *Table 5*, which are between 78% and 92%.

- *Mode 5*:

The fundamental antisymmetric 3N wing bending mode is closely spaced to the torsional modes. The vertical displacements of all data sets have a quite similar mode shape pattern. Not satisfying is the measurement accuracy of the bending/torsion coupling. Not even the sign of the torsion angle is identical for all data sets.

- *Mode 6*:

Most participants had provided very similar data for the second symmetric wing bending mode. Only participant E shows some significant deviations, although the *MAC* value of 92% is still large.

- *Mode 7*:

The measurement of Participant F seem to be an exceptional error. The other data are quite similar, but there is some scattering for the vertical wing bending displacements.

- *Mode 8*:

For the last mode Participant H failed to analyse the mode correctly. One explanation for erroneous results may be the restriction to the two common shaker locations, which were not suitable to excite all modes sufficiently.

Summarising, the comparison of the test results show, that most participants provided very similar results for most of the mode shapes especially for well separated frequencies. On the other hand, for the three closely spaced Modes 3, 4, and 5,

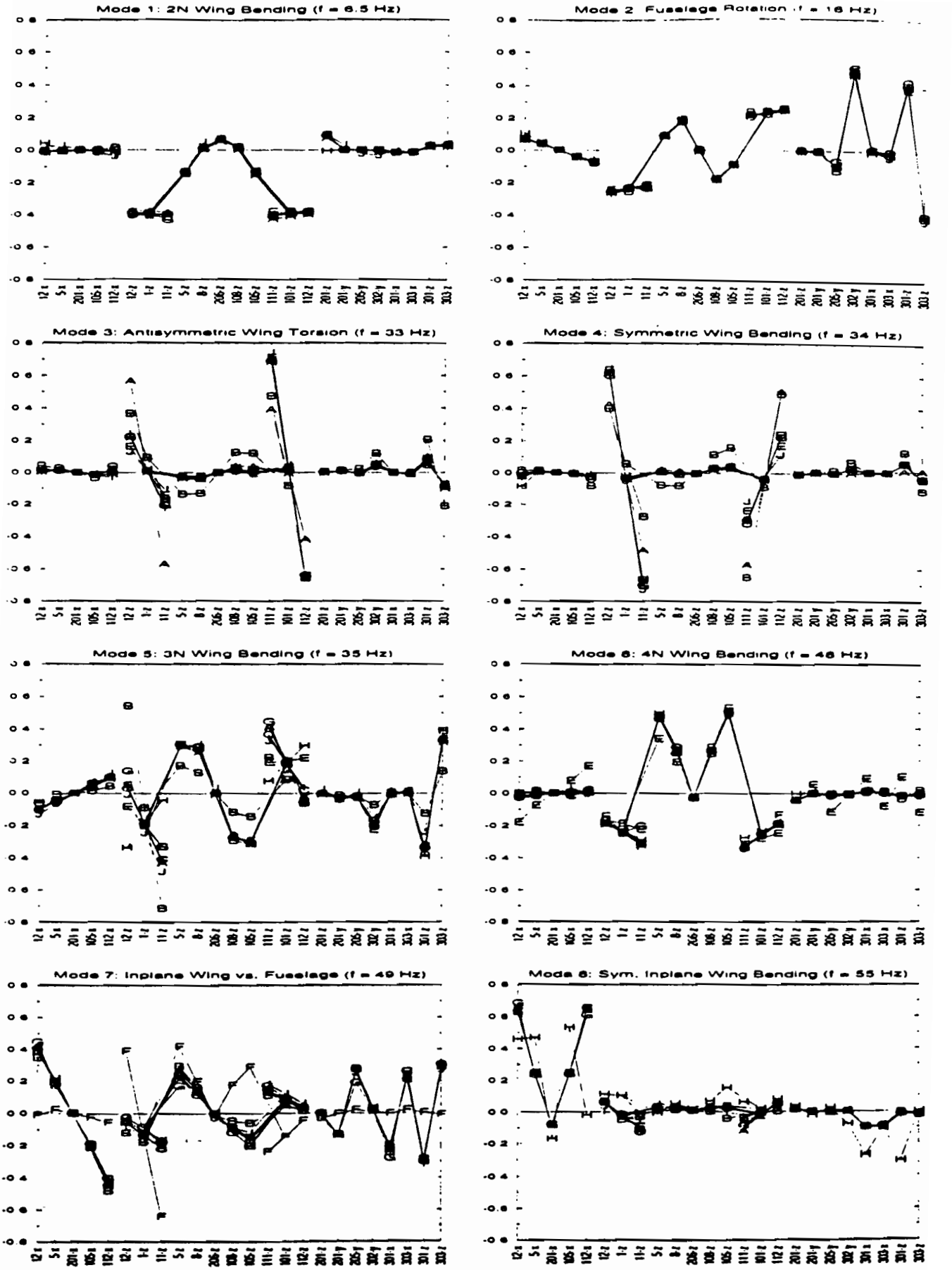

Figure 4. Measured Mode Shapes

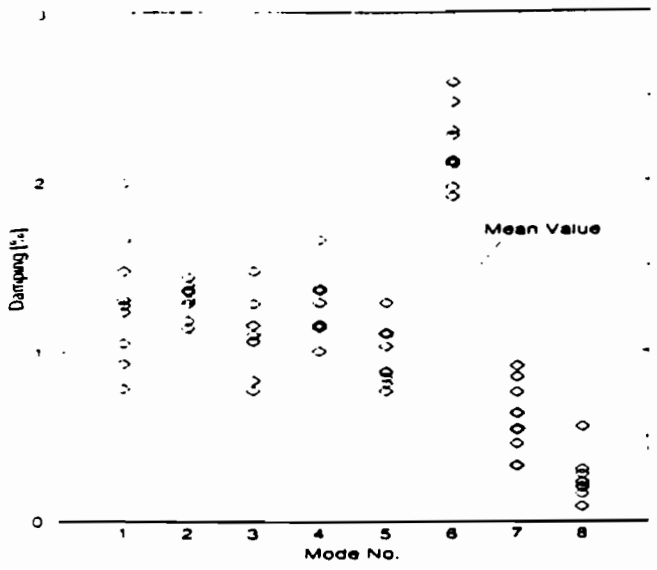

Figure 5. Damping Values

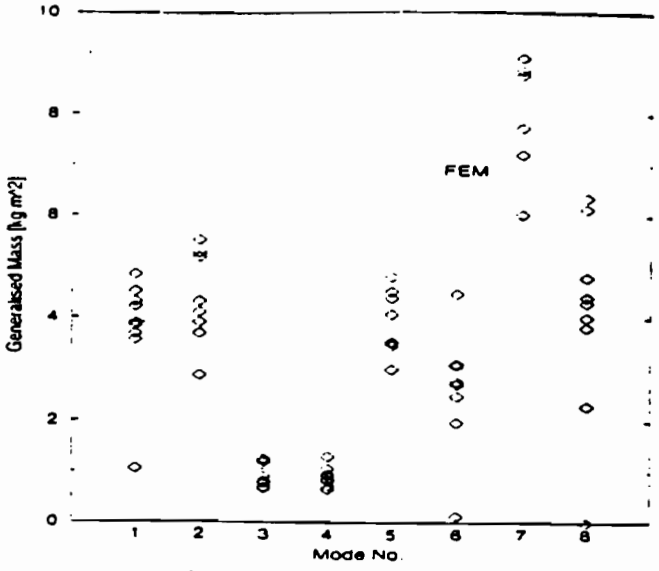

Figure 6. Generalised Masses

there are large deviations in the bending/torsion coupling deformations.
Comparing the mode shapes and the respective deviations as shown in *Figure 4* with the MAC values of *Table 5*. it becomes evident. that the Modal Assurance Criterion is a rather rough correlation tool. Even for large MAC values, there may be significant scattering in the corresponding data sets.

5.2. Damping Values

Correct damping measurement is an important experimental task. because damping values are not predicted by the analytical model. In order to obtain realistic damping values. the GARTEUR aircraft model was equipped with constrained viscoelastic damping layers on the upper wing surface. By this means the very low material damping could be increased significantly.
Figure 5 shows the damping values measured for the first 8 modes of the testbed. The dotted line indicates the mean values. The deviations in the data sets may be attributed to the different instrumentation setups. As for the frequency measurements. the greatest deviations can be observed for the first bending mode. Taking into account the small model size and the rather low damping, the test results seem to be acceptable.

5.3. Generalised Masses

The determination of generalised (or modal) masses is the most crucial task in ground vibration testing. It is influenced by correct measurement of vibration amplitudes, exciter forces and damping values.

Consequently, the largest deviations of the measured modal parameters occured for the generalised masses. which are given in *Figure 6*. It has to be noted. that a number of unrealistic large values are not included in the figure. Surprisingly, the best coincidence was found for the three closely spaced Modes 3. 4, and 5.
For comparison. the generalised masses as calculated by the Finite Element model (FEM) are also included in *Figure 6*. In general. the values should be close to the measured ones due to the reliability of the model. Only in cases of unsymmetry, e.g. for the torsional modes. the predicted values differ from the measured ones.
It seems to be worthwhile. to further investigate the determination of the generalised masses and to look for methods of improvement. A useful approach would be the use of a common set of frequency response functions in order to compare and explain the differencies in the evaluation methods.

6. Conclusions

A survey of ground vibration test techniques applied in different European laboratories was performed by the GARTEUR Action Group SM-AG19. A common testbed was manufactured and investigated. Due to the sophisticated design of the testbed, no obvious influence of the test sequence chronology was observed and a comprehensive data base for correlation and evaluation of test methods was obtained.
Both phase resonance and phase separation techniques yielded consistent data if applied conveniently. The accuracy of the modal data depends

significantly on the suitability of the excitation points. Each mode must be recognizable in the structural response to be evaluated reliably.

Good coincidence of test results (frequencies and mode shapes) was found for all well separated modes. Some problems occured in case of frequency clusters especially for bending/torsion coupling. This may become important for flutter analysis of real aircraft. While deviations in the damping values may be attributed to the test setup, the evaluation of generalised masses requires further investigation.

For real aircraft structures improvements in the measurement accuracy and reduction of the time schedule seem to be possible, if optimum shaker positions can be applied during the test. For this purpose use should be made of the predictions of the Finite Element analysis. A close cooperation between Finite Element designers and test engineers is also important for data evaluation, correlation, and updating of the mathematical model. Combining phase resonance and phase separation techniques seems to be most promising for ground vibration test performance in order to obtain the maximum benefit from the respective advantages of each method.

References

1. Bifulco, A., Degener, M.: *Theoretical Prediction and Experimental Verification of Optimum Exciter Configurations for Modal Testing*. Proceedings of the Conference on Identification in Engineering Systems, University of Wales Swansea, UK, March 27 - 29, 1996.
2. Degener, M.: *Ground Vibration Testing for Validation of Large Aircraft Structural Dynamics*. Proceedings of the International Forum on Aeroelasticity and Structural Dynamics 1995, Manchester, UK, June 26 - 28, 1995.
3. Link, M.: *Theory of a Method for Identifying Incomplete System Matrices from Vibration Test Data*. Zeitschrift für Flugwissenschaften und Weltraumforschung, Vol.9, No.2, 1985, pp.58-67.
4. Balmès, E.: *Garteur Group on Ground Vibration Testing. Results from the Test of a Single Structure by 12 Laboratories in Europe*. Proceedings of IMAC-XV, Orlando, Florida, USA, February 3 - 6, 1997.
5. Persoon, A.J., Balmès, E.: *A Ground Vibration Test on the Garteur Testbed SM AG-19*. Proceedings of IMAC-XV Japan, Tokyo, Japan, September 1 - 4, 1997 (also published as NLR Technical Publication TP 97086 L).